Faculdade de Engenharia da Universidade do Porto

Modeling of Biomass Gasification: Comparison with Semi-Industrial Gasifier and In Depth Analysis on Process Difficulties

Nuno Tiago Dinis Couto

Tese Submetida à Universidade do Porto com vista à obtenção do grau de Doutor em Engenharia Mecânica

Orientador: Prof. Dr. Abel Ilah Rouboa

Co-orientador: Prof. Dr. José Luís Alexandre

Co-orientador: Dr. Valter Bruno Silva

Setembro de 2017

Resumo

Encontrar novas formas de combater o aquecimento global e alterações climáticas tem sido um dos focos principais da comunidade científica. Investigadores acreditam que a resposta reside em promover fontes de energia renovável, particularmente biocombustíveis sólidos e resíduos renováveis. A gasificação recebeu um interesse renovado na conversão termoquímica da biomassa devido ao seu desempenho ambiental e à sua forte portabilidade. No entanto, apesar das suas várias vantagens, o estado de desenvolvimento desta tecnologia pode ser, quanto muito, caracterizado como um nicho limitado. Para estimular incentivos financeiros adicionais, bem como o interesse cientifico, para impulsionar o uso comercial da tecnologia há vários obstáculos tecnológicos que devem ser resolvidos, nomeadamente o *scale-up*, produção de alcatrão e CO_2, limpeza do gás e a fraca competitividade económica. Uma das maiores ferramentas disponíveis para auxiliar os investigadores nesse sentido é a simulação numérica. Esta ferramenta permite cortar custos (uma vez que são necessárias menos actividades experimentais), diminuir o ciclo de projecto necessário (normalmente é preciso menos tempo para simular um processo do que para testá-lo) e aumentar o conhecimento sobre o próprio processo (uma vez que é mais fácil isolar parâmetros e testar qual é realmente a sua influência). A capacidade do modelo numérico em encontrar soluções para as principais dificuldades desta tecnologia foi testada nesta tese. Para o fazer, resultados numéricos foram comparados e validados com resultados experimentais (obtidos numa central em escala piloto) e com literatura disponível. Os resultados de substratos portugueses, bem como de resíduos sólidos urbanos, foram investigados.

Palavras-chave: Simulação numérica; Biomassa; Resíduos sólidos urbanos; Gasificação; Optimização.

Página em branco

Abstract

Finding new ways to fight global warming and climate change has been one of the main focuses of the current scientific community. Researchers believe the answer relies on promoting renewable energy sources with special attention given to solid biofuels and renewable waste. Gasification has recently received renewable interest in the thermochemical conversion of biomass due to its environmental performance and high portability component. However, despite its many advantages, the stage of development of biomass gasification can best be characterized as one of limited niche development. To stimulate further financial incentives as well as research interest to push for the commercial use of biomass gasification there are several technology setbacks that must be addressed, namely the scaling up, tar and CO_2 production, gas cleaning and increase the economic competitiveness. Perhaps the greatest tool available to assist researchers with this regard is numerical simulation. This tool allows cutting costs (since less experimental activities are required), decreasing the necessary design cycle (it typically takes far less time to compute a process than to actually test it) and allows an enormous amount of physical insight on the process itself (since its far easier to isolate parameters and to test what the influence of all the desired conditions actually is). Numerical model's ability to address and possibly find solutions to biomass gasification's main technology setbacks was tested in this thesis. To do so, numerical results were compared and validated with experimental results (from a pilot scale plant) and available literature. Results from common Portuguese biomass substrates as well as municipal solid wastes were investigated.

Keywords: Numerical simulation; Biomass; Municipal solid wastes; Gasification; Optimization.

Página em branco

Acknowledgements

There are so many people who deserve a “thank you” for their insight and encouragement during the course of the last four years.

Firstly, I would like to express my sincere gratitude to my supervisor Prof. Dr. Abel Rouboa and my co-supervisors, Dr. Valter Silva and Prof. Dr. José Alexandre for the continuous support of my Ph.D. study and related research, for their patience, motivation, and immense knowledge. Their guidance helped me during the research time and writing of this thesis. I could not have imagined having a better supervisor and mentor team for my Ph.D. study.

To Prof. Dr. Eliseu Monteiro for his help and experience related to the combustion and gasification processes.

To Prof. Dr. Paulo Brito from the Polytechnic Institute of Portalegre for the experimental data used in this thesis.

A special thanks to my family. Words cannot express how grateful I am to my parents and my maternal grandparents for all of the sacrifices that they have made on my behalf.

To all the friends who have supported me or helped in any way in recent years.

Finally, I would like to express my gratitude to the Portuguese Foundation for Science and Technology (FCT) for the support to the grant SFRH/BD/86068/2012.

Página em branco

List of Publications

The presented thesis is based on work presented in the following papers:

I. **N. Couto**, V. Silva, J. Cardoso, A. Rouboa. 2nd law analysis of Portuguese municipal solid waste gasification using CO2/air mixtures. Journal of CO2 Utilization 20 (2017) 347-356.
https://doi.org/10.1016/j.jcou.2017.06.001

II. **N. Couto**, V. Silva, E. Monteiro, A. Rouboa. Exergy analysis of Portuguese municipal solid waste treatment via steam gasification. Energy Conversion and Management 134 (2017) 235-246.
https://doi.org/10.1016/j.enconman.2016.12.040

III. **N. Couto**, V. Silva, E. Monteiro, A. Rouboa, P. Brito. An experimental and numerical study on the Miscanthus gasification by using a pilot scale gasifier. Renewable Energy 109 (2017) 248-261.
https://doi.org/10.1016/j.renene.2017.03.028

IV. V. Silva, **N. Couto**, D. Eusébio, A. Rouboa, P. Brito, J. Cardoso, M. Trninic. Multi-stage optimization in a pilot scale gasification plant. International Journal of Hydrogen Energy 42 (2017) 23878-23890.
https://doi.org/10.1016/j.ijhydene.2017.04.261

V. **N. Couto**, V. Silva, A. Rouboa. Thermodynamic evaluation of Portuguese municipal solid waste gasification. Journal of Cleaner Production 139 (2016) 622-635.
http://dx.doi.org/10.1016/j.jclepro.2016.08.082

VI. **N. Couto**, V. Silva, A. Rouboa. Assessment on steam gasification of municipal solid waste against biomass substrates. Energy Conversion Management 124 (2016) 92-103.
doi:10.1016/j.enconman.2016.06.077

VII. **N. Couto**, E. Monteiro, V. Silva, A. Rouboa. Hydrogen-rich gas from gasification of Portuguese municipal solid wastes. International Journal of Hydrogen Energy 41 (2016) 10619-10630.
doi:10.1016/j.ijhydene.2016.04.091

VIII. **N. Couto**, V.B. Silva, C. Bispo, A. Rouboa. From laboratorial to industrial gasification: Analysis of the scale-up phenomenon. Energy Conversion Management 119 (2016) 177-186.
doi:10.1016/j.enconman.2016.03.085

IX. **N. Couto**, V.B. Silva, A. Rouboa. Municipal solid waste gasification in semi-industrial conditions using air-CO2 mixtures. Energy 104 (2016) 42–52.
doi:10.1016/j.energy.2016.03.088

X. **N. Couto**, V.B. Silva, E. Monteiro, A. Rouboa. Assessment of Municipal Solid Wastes Gasification in a Semi-industrial Gasifier using Syngas Quality Indices. Energy 93 (2015) 864-873.
doi:10.1016/j.energy.2015.09.064

XI. **N. Couto**, V.B. Silva, E. Monteiro, S. Teixeira, R. Chacartegui, K. Bouziane, P. Brito, A. Rouboa. Numerical and Experimental Analysis of Municipal Solid Wastes Gasification Process. Applied Thermal Engineering 78 (2015) 185-195.
doi:10.1016/j.applthermaleng.2014.12.036

XII. **N. Couto**, V.B. Silva, E. Monteiro, P. Brito, A. Rouboa. Using an eulerian-granular 2-D multiphase CFD model to simulate oxygen air enriched gasification of agroindustrial residues. Renewable Energy 77 (2015) 174-181.
doi:10.1016/j.renene.2014.11.089

XIII. V.B. Silva, **N. Couto**, E. Monteiro, P. Brito, A. Rouboa, Analysis of syngas quality from Portuguese biomasses: An experimental and numerical study. Energy & Fuels 28 (2014) 5766-5777.
http://pubs.acs.org/doi/abs/10.1021/ef500570t

Author's Contribution

The papers are co-authored. The author of the thesis has performed the following work for the presented papers:

Paper I. Co-developed the numerical model used in the simulations. Developed and implemented the exergy analysis presented in the paper. Ran all the simulations used in the paper. Responsible for writing the paper and creating all the Figures and Tables presented.

Paper II. Co-developed the numerical model used in the simulations. Developed and implemented the exergy analysis presented in the paper. Ran all the simulations used in the paper. Responsible for writing the paper and creating all the Figures and Tables presented except for the exergy efficiency optimization section.

Paper III. Co-developed the numerical model used in the simulations. Ran all the simulations used in the paper. Responsible for writing the paper and creating all the Figures and Tables presented.

Paper IV. Co-developed the numerical model used in the simulations. Ran all the numerical simulations used in the paper. The author was directly involved in co-authoring and revising paper with interpretation of the results and discussion.

Paper V. Co-developed the numerical model used in the simulations. Developed and implemented the exergy analysis presented in the paper. Ran all the simulations used in the paper. Responsible for writing the paper and creating all the Figures and Tables presented.

Paper VI. Co-developed the numerical model used in the simulations. Ran all the simulations used in the paper. Responsible for writing the paper and creating all the Figures and Tables presented.

Paper VII. Co-developed the numerical model used in the simulations. Ran all the simulations used in the paper. The author was directly involved in co-authoring the writing of the paper and all the Figures and Tables presented.

Paper VIII. Co-developed the numerical model used in the simulations. Ran all the simulations used in the paper. Responsible for writing the paper and creating all the Figures and Tables presented except for the uncertainty analysis section.

Paper IX. Co-developed the numerical model used in the simulations. Ran all the simulations used in the paper. Responsible for writing the paper and creating all the Figures and Tables presented.

Paper X. Co-developed the numerical model used in the simulations. Ran all the simulations used in the paper. Responsible for writing the paper and creating all the Figures and Tables presented.

Paper XI. Co-developed the numerical model used in the simulations. Ran all the simulations used in the paper. The author was directly involved in co-authoring and revising paper with interpretation of the results and discussion.

Paper XII. Co-developed the numerical model used in the simulations. Ran all the simulations used in the paper. The author was directly involved in co-authoring and revising paper with interpretation of the results and discussion.

Paper XIII. Co-developed the numerical model used in the simulations. Ran all the simulations used in the paper. The author was directly involved in co-authoring and revising paper with interpretation of the results and discussion.

Additional Publications and Presentations

To avoid making this thesis too exhausting only a select number of scientific papers were chosen to appear, it stays here nevertheless, the list of work produced throughout the thesis where the author intervened.

Journal Papers

XIV. **N. Couto**, V.B. Silva, E. Monteiro, P. Brito, A. Rouboa. Modeling of Fluidized bed gasification: Assessment of zero-dimensional and CFD approaches. Journal of Thermal Science 24 (2015) 378-385.
doi:10.1007/s11630-015-0798-7

XV. A.F.L. Teixeira, **N.T.D. Couto**, S.C.F. Teixeira. Syngas combustion analysis using an experimental and numerical approach, American Society of Mechanical Engineers, Power Division (Publication) POWER 2 (2014).
doi:10.1115/POWER2014-32092

XVI. **N. Couto**, **V.B. Silva**, E. Monteiro, P. Brito, A. Rouboa. Experimental and Numerical Analysis of Coffee Husks biomass Gasification in a Fluidized bed Reactor. Energy Procedia 36 (2013) 591-595.
doi:10.1016/j.egypro.2013.07.067.

XVII. **N. Couto**, **V.B. Silva**, E. Monteiro, A. Rouboa. Hazardous waste management in Portugal: An overview. Energy Procedia 36 (2013) 607-611.
doi:10.1016/j.egypro.2013.07.067

XVIII. **N. Couto**, **V.B. Silva**, E. Monteiro, A. Rouboa, K. Bouziane. Influence of the biomass gasification processes on the final composition of syngas. Energy Procedia 36 (2013) 596-606.
doi:10.1016/j.egypro.2013.07.068

XIX. **V. B. Silva**, **N. Couto**, A. Rouboa, J. L. Alexandre, Syngas Combustion: Analysis of Exergy Losses. Advanced Science Letters 19 (2013) 609-614.
http://dx.doi.org/10.1166/asl.2013.4727

XX. **V. B. Silva**, **N. Couto**, A. Rouboa, J. L. Alexandre. Analysis of the Pine Biomass Gasification to Obtain H_2 Enriched Syngas. Advanced Science Letters 19 (2013) 946-949.
http://dx.doi.org/10.1166/asl.2013.4837

Conferences and Presentations

XXI. **N. Couto**, V. Silva, D. Eusébio, P. Brito, A. Rouboa. A Dual-Stage Approach to Simulate Portuguese Substrates for Gasification Purposes. 2nd International Workshop on CFD and Biomass Thermochemical Conversion. September 9th, 2016, Leipzig.

XXII. **N. Couto**, V.B. Silva, A. Rouboa. Hydrogen production optimization from Portuguese municipal solid waste gasification. AEM2016, University of Surrey, Guildford, England.

XXIII. **N. Couto**, V.B. Silva, A. Rouboa. H_2-rich gas from steam gasification of Portuguese MSW. AEM2016, University of Surrey, Guildford, England.

XXIV. **N. Couto**, V.B. Silva, D. Eusébio, A. Rouboa. Analysis of Vineyard Pruning Residues Potential as a Function of Syngas Quality Indices. ICNAAM, Greece, 2015.

XXV. E. Monteiro, **N. Couto**, V. Silva, A. Rouboa, P. S. D. Brito. Modeling of Fluidized Bed Biomass Gasification: Comparison of Zero-Dimensional and CFD Simulations. ICNAAM, Greece, 2015.

XXVI. **N. Couto**, V. B. Silva, E. Monteiro, A. Rouboa. 3D CFD methodology applied to gasification of Portuguese agroindustrial residues. 6th International Congress of Energy and Environment Engineering and Management (CIIEM15), Paris 2015.

XXVII. **N. Couto**, V. B. Silva, E. Monteiro, A. Rouboa. Modeling of solid waste gasification using eulerian-eulerian approach in semi-industrial reactor. 6th International Congress of Energy and Environment Engineering and Management (CIIEM15), Paris 2015.

XXVIII. A.F.L. Teixeira, **N.T.D. Couto**, S.C.F. Teixeira, Syngas combustion analysis using an experimental and numerical approach, USA, ASME 2014.

XXIX. **N. Couto**, V.B. Silva, E. Monteiro, P. Brito, A. Rouboa, Experimental and Numerical Analysis of Coffee Husks biomass Gasification in a Fluidized bed Reactor, Lebanon, Terra Green 2013.

XXX. **N. Couto**, V.B. Silva, E. Monteiro, A. Rouboa, Hazardous waste management in Portugal: An overview, Lebanon, Terra Green 2013.

XXXI. **N. Couto**, A. Rouboa, V.B. Silva, E. Monteiro, K. Bouziane, Influence of the biomass gasification processes on the final composition of syngas, Lebanon, Terra Green 2013.

Nomenclature

A, B	Calibration constants
A_i	Pre-exponential factor, $1/s$
$C_{1\varepsilon}$, $C_{2\varepsilon}$, $C_{3\varepsilon}$	Constants
C_p	Specific heat, J/kgK
E_i	Activation energy, J/mol
G_k	Turbulence kinetic energy generation due to the mean velocity gradients, kg/ms^3
G_b	Turbulence kinetic energy generation due to buoyancy, kg/ms^3
h_q	Specific enthalpy of phase, J/kg
h_{pq}	Heat transfer coefficient between the fluid phase and the solid phase, J/kg
k	Thermal conductivity, W/mK
Nu	Nusselt Number
$\dot{m}$	Biomass flow entering into the gasifier, kg/s
M	Total mole flow of carbon in the syngas components, mol/s
M_i	Molecular weight of each the species, kg/mol
M_c	Molecular weight, kg/mol
$M_{w,i}$	Molecular weight of i component, kg/mol
p	Gas pressure, Pa
Pr	Prandtl Number
p_s	Particle phase pressure due to particle collisions, Pa
$\vec{Q}_{pq}$	Heat transfer between pth and qth phases, W
$\vec{q}_q$	Heat flux, W/m^2

q^{th}	Specific enthalpy, J/kg
R	Universal gas constant, J/kgK
R_i	Net generation rate of specie i due to homogeneous reaction, mol/Ls
Re	Reynolds Number
R_c	Reaction rate, mol/Ls
S_i	Source term of the species i production from the solid heterogeneous reaction, mol/m^3
S_k	User-defined source terms, kg/ms^3
S_q	Source term due to chemical reactions, mol/m^3
S_ε	User-defined source terms, kg/ms^4
T	Temperature, K
t_s	Particle phase stress tensor, Pa
U	Mean velocity, m/s
v	Instantaneous velocity, m/s
X_C	Carbon fraction in the biomass
Y	Mass Fraction
Y_M	Contribution of the fluctuating dilatation in compressible turbulence to the overall dissipation rate, kg/ms^3

Other Symbols

α	Volume fraction
β	Gas-solid interphase drag coefficient
γ_c	Stoichiometric coefficient
γ_{Θ_a}	Collisional dissipation of energy, W

ε	Dissipation rate, J/kgs
ρ	Density, kg/m^3
ϕ_{ls}	Energy exchange between gas and solid phases, W
k_{Θ_a}	Diffusion coefficient, m^2/s
$k_{\Theta_a}\nabla(\Theta_s)$	Diffusion energy, W
$\left(-p_s\bar{I}+\bar{\tau}_s\right):\nabla(\vec{v}_s)$	Generation of energy by the solid stress tensor, W
τ	Tensor stress, Pa
μ	Viscosity, kg/ms

Abbreviations

ANOVA	Analysis Of Variance
BOE	Barrels of Oil
CC	Carbon Conversion
CDMR	CO_2-to-MSW Ratio
CFD	Computational Fluid Dynamics
CGE	Cold Gas Efficiency
CPLF	Composite Packaging for Liquid Foods
DoE	Design of Experiments
EU	European Union
ER	Equivalence Ratio
EPA	Environmental Protection Agency
GGE	Greenhouse Gas Emissions
GHG	Greenhouse Gas
IPCC	Intergovernmental Panel on Climate Change

LIPOR	Intermunicipal Waste Management of Greater Porto
MSW	Municipal Solid Wastes
PEHD	Polyethylene High-Density
PERSU	Plano Estratégico para os Resíduos Urbanos
PET	Polyethylene Teraphthalate
PMSW	Portuguese Municipal Solid Wastes
POE	Propagation of Error
RDF	Refuse Derived Fuel
RSM	Response Surface Methods
SBR	Steam-to-Biomass Ratio
SIMPLE	Semi-Implicit Method for Pressure Linked Equations
SMSS	Sequential Model Sum of Squares
TCE	Tons of Carbon Equivalent
TOE	Ton of Oil Equivalent
WTE	Waste-to-Energy

Subscripts

g	Gas Phase
s	Solid Phase
i	Component

Table of Contents

List of Figures

List of Tables

Introduction

Climate change is one of the greatest environmental, social and economic threats of our time. According to the IPCC, greenhouse gas emissions have increased since the pre-industrial era at an alarming rate and are now the highest in history [1]. In fact, the concentration of carbon dioxide in the atmosphere (the main culprit of global warming) is now 1.5 times higher when compared to the pre-industrial era values. As a result, earth's average surface temperature has increased by around 0.6 ºC from the beginning of the 20th century and is expected to reach 1 ºC by 2035 [2]. Current projections point that if no additional mitigation efforts are implemented the estimated warming in 2100 will be in the range between 2.5 ºC to 7.8 ºC (when compared with the pre-industrial levels). According to the scientific community, consequences of temperatures at or above 4 degrees Celsius include: significant species extinction; extreme weather events; enormous risks to global and regional food security; consequential constraints on common human activities; increased likelihood of triggering tipping points and limited potential for adaptation in some cases [1].

Preventing this catastrophic outcome is a key priority for the European Union. Europe is making significant efforts to substantially reduce its GGE by encouraging other countries and regions to follow their example. Latest reports from Eurostat [3], show that in 2014, greenhouse gas emissions in the EU-28 were down by 22.9 % when compared with 1990 levels, putting it on track to surpass its 2020 target, which is to reduce GGE by 20 %. EU's long-term goal is to reduce its emissions by 80-95 % when compared to 1990 levels.

Renewable energy sources represent a cornerstone of EU's energy policy in achieving this goal [4]. Utilization of renewable sources helps fulfilling the energy demand while

mitigating the environmental problems. In 2014, the contribution of renewable energy to the total primary energy production from all sources in the EU-28 was 25.4 % (representing 196 million TOE). Among renewable sources, the most important ones were solid biofuels and renewable waste, accounting for just under two thirds of primary renewables production [3].

Biomass is one of the renewable energy resources with the greatest potential for development since it can be easily stored and transported, can also be converted into biofuels thus increasing its applicability and perhaps more importantly it can contribute significantly to energy independence of the region along with associated economic and environmental benefits. In fact, biomass utilization represents a crucial component in Portugal's strategic plan in reducing its foreign energy dependence. Portuguese biomass resources are diverse but an important contribution can be found from agricultural-related residues. Coffee husks, forest and vineyard pruning residues are largely available and have attractive low costs [5].

Among biomass sources, MSW are the largest volume of residues produced worldwide [6]. The world is going through an intense process of urbanization and MSW, one of the most important by-products of an urban lifestyle, is growing at an even higher rate. According to the latest reports [7], in just 10 years the production of MSW increased from 680 to 1,300 million tons per year, which represents an average increase of 0.64 to 1.2 kg of MSW per person per day. Current projections estimate an increase to 1.42 kg of MSW per person per day by 2025, which would translate into an annual generation of 2,200 million tons.

The treatment of these residues is quite expensive and often represents the single largest budgetary item of a city. Worldwide MSW management costs from 2012 exceeded 190,000 million euros and are expected to reach 350,000 million by 2025 [7]. Of all methods of

waste disposal, landfill is still the most used today, although it is becoming less and less popular due to the lack of available land and due to the emission of CH_4 and other landfill gases, which can cause numerous contamination problems [8]. Incineration has gained ground over landfills since it can reduce the solid waste volume, decreasing the space it takes up and reducing the stress on already overflowing landfills. However, waste incineration is expensive and poses challenges of air pollution and ash disposal [8].

With applications going back as far as the 19^{th} century, gasification has received renewable interest in the thermochemical conversion of biomass for being CO_2-neutral, having a high potential, improving security of supply while being able to provide power, chemicals and fuels. Furthermore, gasification is becoming an increasingly attractive technology to treat MSW with fewer emissions than other methods of treatment [9]. It has been mostly used in WTE plants, and one of its most promising results was achieved for the production of H_2-rich gas [10].

However, despite its many advantages and increase research, the stage of development of biomass gasification can best be characterized as one of limited niche development [11]. To stimulate further financial incentives as well as research interest to push for the commercial use of biomass gasification there are several technology setbacks that must be addressed, namely the scaling up [12], tar and CO_2 production [13], gas cleaning and increase the economic competitiveness [11].

Researchers have been trying to address these issues, mostly using laboratory scale gasifiers (due to lower operating costs [14]), being the work carried out on industrial gasifiers extremely limited (due to the high cost of a gasification plant, which can reach tens of millions of euros [15]). This is a major concern since the hydrodynamics from a small reactor change drastically in a larger reactor, meaning that the information gathered

in laboratory scale reactors can be of little to no help when building a commercial size reactor that can be tens or even hundreds of times larger [16].

Mathematical models are being employed to work around this exact problem. By allowing for a simplified representation of reality they provide the ability to better understand the physical and chemical mechanisms inside the reactor without major investments nor time consuming experiments [16]. Different modeling approaches have been used by different researchers depending on the degree of complexity they are willing to endure. Equilibrium models are a popular method since they provide a quick way to calculate the maximum yield of a desired product [16]. However, since they don't take hydrodynamics, transport process or reaction kinetics into account results sometimes lack meaningful information. These setbacks led to the development of kinetic models, being much more accurate but also computationally expensive [17].

Increase in computational power is gradually replacing empirical or semi-empirical models with CFD to study biomass and waste gasification. These models can provide crucial insights into the flow field inside the reactor and can lead to a better understanding and improve performance of the operation while indicating solutions to potential problems. However, due to the extreme complexity in creating a realistic model, this application is still in a developing stage and more studies are needed [18].

The gasification process is characterized by a multiphase flow containing solid and gas phases (in a slagging gasifier liquids can also be present). The solid particles can have a wide range of sizes and shapes (especially when we consider solid wastes) and their organic components are consumed while passing through the reactor. Correctly modeling the interaction between phases is crucial since they exchange heat by convection, mass over the heterogeneous chemical reactions, and momentum due to the drag between gas and solid

phase [19]. In most cases this can become extremely complex since the user needs to have a complete knowledge of all relevant phenomena (i.e. mass transfer rates, solid properties, heat transfer rates, reaction rates, equation of state data and gas viscosities, to name a few) which unfortunately is rarely available [20]. Modeling of these phenomena, on top of all the other necessary steps to create a realistic model with the ability to correctly predict the gasification process, has proved to be a daunting process to most researchers.

Thesis Outline

The focus of this thesis is to address and possibly promote solutions to biomass gasification's main technology setbacks. To do so, I've drawn from my own previous studies and use them as stepping stones to deepen the literature on the subject. Therefore, the presented thesis was compiled as a collection of scientific research papers that have been written throughout the years. Still, to avoid repetition and to make the document stand on its own, the remaining of the work is presented as a continuous effort.

That being said, chapter 2 compiles all of the key information related to feedstock materials, experimental data and data regarding LIPOR's partnership. Chapter 3 and chapter 4 expose the key features of the mathematical and thermodynamic models, respectively. In chapter 5 all the main results are displayed, starting with model validation, assessing operational conditions, analyzing syngas quality indices and performing first and second law analysis on MSW gasification. Finally a multi-stage optimization is explored as well as the haunting scale-up phenomenon. At the end, some possible applications for MSW gasification using different gasifying agents are discussed. Recommendation for future work and main conclusions of this work are presented in Chapter 6. Furthermore, all the major scientific publications this thesis is based on are displayed at the end for consultation purposes.

2. Material and Methods

2.1.Feedstock Material

Given the growing concerns about climate change, namely heavy dependence on fossil fuels and rising energy costs, many countries, in particular Portugal, have been promoting renewable energy sources. The use of biofuels comes forward as a contributing solution, since it leads to globally lower emissions when compared to using fossil fuels, and one of the breakthroughs of European Union legislation was the approval of so-called "energy crops" for biofuel production [21]. Portuguese biomass resources are diverse but an important contribution can be found from agricultural-related residues. Coffee husks, forest and vineyard pruning residues are largely available and have attractive low costs [5].

Portuguese forest covers 3.2 million ha, which corresponds to 35.4 % of the national territory and is the basis of an economic sector that generates about 113,000 direct jobs (2 % of the workforce) [22].

The wine sector is one of the most important in the Portuguese economy, contributing very significantly to the final value of agricultural production and exportation, with a remarkably high contribution to the balance of trade; in fact, it is one of the few agri-food sectors with a positive trade balance. There is a great interest by Portuguese entities to study the best ways to valorize the residues and sub-products generated by this industry [22].

When processed, coffee generates a significant amount of agricultural wastes. Coffee husks, comprised of dry outer skin, pulp and parchment, are probably the major residues from the handling and processing of coffee. One of the main problems facing industries nowadays is how to dispose of these residues (there are more than two million tons

produced yearly [23]), since they contain some amount of caffeine, polyphenols and tannins, which makes them toxic in nature.

The total primary energy demand in Portugal amounted to 243,311 GWh in 2014 [24]. According to Ferreira *et al.* [25], forest and pruning residues alone can potentially produce 13,768 GWh per year (about 5.7 % of the total primary energy demand in the country). Additionally, the energy production from bioresources (biomass, solid urban waste, and biogas) was 29,400 GWh in 2014. Previous data showed that both forest and pruning residues can play an important role in the Portuguese energy scenario.

Prior to the actual gasification process, biomass analysis was carried out in the Laboratory of Chemistry of the High School of Technology and Management located in Portalegre, Portugal, since biomass characteristics can provide valuable information on how the gasification process will occur. This kind of analysis also provides crucial data to feed into the implemented numerical model.

The instruments used in the performed analysis are as follows:

- Thermal Gravimetric Analysis - Data for proximal analysis (Figure 2.1a);
- Elemental Analysis - Determination of biomass composition with respect to the percentage of C, H, N and O (Figure 2.1b);
- Humidity - Sample moisture content assessment (Figure 2.1c);
- Calorific Value - Appraisal of energy contained in biomass (Figure 2.1d).

From the tests carried out it was possible to compile the main biomass properties, available in Table 2.1.

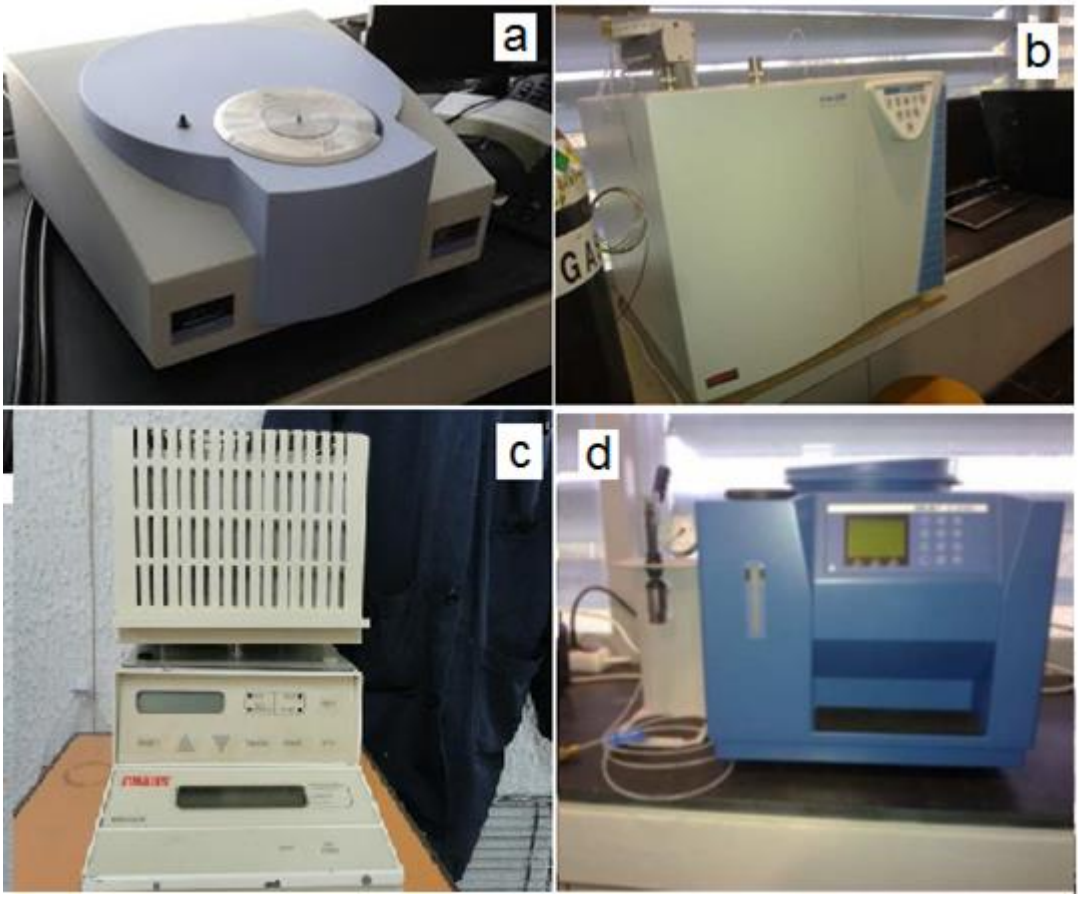

Figure 2.1 - Photographs of a) Simultaneous Thermal Analyzer (STA) 6000, b) Elemental Analyzer Flash 2000, c) MB200 Moisture Analyzer and d) Calorimeter (IKA C200).

Table 2.1 - Biomass properties.

Substrate properties	**Forest residues**	**Coffee husk**	**Vines pruning**
Elementary analysis (dry ash free)			
N (%)	2.4	5.2	2.6
C (%)	43.0	40.1	41.3
H (%)	5.0	5.6	5.5
O (%)	49.6	49.1	50.6
Humidity (%)	11.3	25.3	13.3
Density (kg/m^3)	650	500	265
Lower heating value (MJ/kg biomass)	21.2	20.9	15.1
Proximal analysis (%)			
Ash	0.2	2.5	3.1
Volatile matter	79.8	83.2	83.6
Fixed carbon	20.0	14.3	13.3

2.2.Experimental Setup

Gasification tests were performed in a semi-industrial gasification plant (Figure 2.2), installed in the Industrial Park of Portalegre, Portugal. The plant is based on fluidized bed technology, with a processing capacity of approximately 100 kg/h, operating between 750 ° and 850 °C.

Figure 2.2 - Photograph of the semi-industrial gasification plant in Portalegre, Portugal.

Figure 2.3 depicts a diagram of the biomass gasification unit used in the experiments.

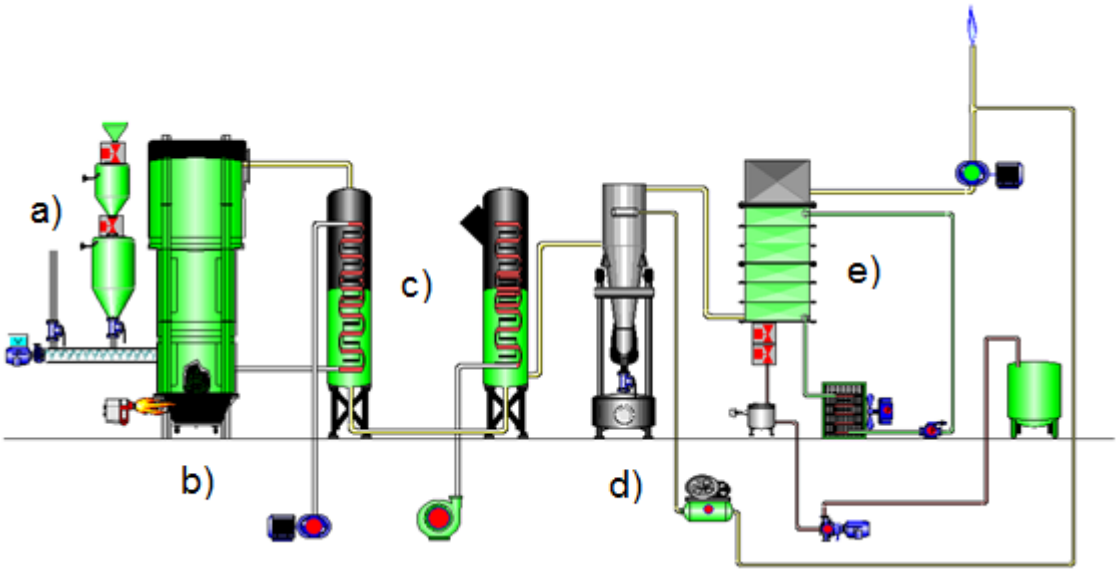

Figure 2.3 - Schematics of the gasification plant.

The main components of the unit are as follows:

a) Biomass feed system with two storage silos to allow the loading of biomass into the reactor using an Archimedean screw variable and controllable speed, in which the silos also act as buffers to prevent the entry of air through the biomass feed system;

b) Fluidized bed reactor as a tubular reactor of 0.5 m in inner diameter and slightly over 4.0 m in height, internally lined with refractory ceramic material; biomass enters the reactor at 0.5 m from its base, whereas preheated air is admitted from the base by means of a set of diffusers (usually at 300 ºC), providing a flow of about 70 m^3/h; three temperature sensors are installed inside in order to monitor and control the gasification temperature and ensure syngas leaves the reactor at 600 °C; the reactor operates with a negative pressure gradient produced by the vacuum pump installed at the end of the process line; monitoring the temperature inside the reactor is a key factor for the success of the gasification process, and its control is achieved by adjusting the amount of air admitted to the reactor;

c) Gas cooling system comprising two heat exchangers; the first cools the synthesis gas to about 300 °C using a co-current air flow entering the unit and the second further cools the synthesis gas to about 150 °C by forced flow of air from the exterior;

d) Cellulosic bag filter which removes carbon particles and ash produced in the gasification process and is cleaned by injecting pressurized synthesis gas; carbon particles are collected at the bottom of the filter and stored in a warehouse;

e) The condenser, where condensed liquids are removed by cooling the syngas to room temperature, through a third heat exchanger.

2.3.Analysis Procedures

Syngas analysis was performed on a gas chromatograph Varian 450 TCD-GC (Figure 2.4a) with two detectors which reveal the presence of H_2, CO, CO_2, CH_4, O_2, N_2, C_2H_6, C_2H_4 using He as carrier gas. The samples for analysis were obtained from Tedlar bags (Figure 2.4b) at the condenser outlet once the gasification of a given raw material composition had reached steady state. The collected gas samples were then injected (up to 1 hour after sampling) directly from the chromatograph sampling bags using a peristaltic pump equipped with a Marpren tube. Chromatographic peaks for different gases were identified based on their retention times by comparison with those of the same reference gas chromatogram provided by the manufacturer. The molar percentage of the gas composition was calculated from the peak area of the chromatographic signal.

Figure 2.4 - Photographs of a) Varian Bruker 450 GC gas chromatograph, b) system for injection of samples into the gas chromatograph and bags for gaseous sample collection.

2.4.Uncertainty Analysis

Errors and uncertainties in experimental results can arise from various factors, such as instrument selection, condition, calibration, observation, reading, surroundings and test planning [26]. In the experiments of biomass gasification, temperatures, flow rates and pressure drops were measured with appropriate instruments. The following is a compilation of the major uncertainties in the process made available by Portalegre's team [27].

- Total Uncertainties in Reactor Temperatures

For the gasification process, the average uncertainties resulting from temperature measurement are classified as follows:

- Average uncertainty resulting from the thermocouple fabrication process ± 0.3 %;
- That arisen from connecting devices and thermocouple settling ± 0.5 %;
- The average uncertainty as a result from the interaction of the thermocouples with the SCADA system ± 0.02 %.

Individual uncertainties such as those mentioned above can be combined together as the root the sum of the squares of each uncertainty, like so:

$$Combined\ uncertainty = \sqrt{a^2 + b^2 + c^2 + \cdots} \quad (2.1)$$

The combined uncertainty for reactor temperatures is ± 0.58 %.

- Total Uncertainties in Pressure Drops

During the gasification process, the average uncertainties resulting from pressure drop measurement are taken as the average uncertainty associated to the fabrication process and to the connecting devices of pressure transducers, which is ± 0.75 %.

- Total Uncertainties in Biomass Flow Rates

The average uncertainties arisen from flow rate measurement are listed below:

- The average uncertainty arisen from time recorder ± 1 %;
- That resulting from balance instrument vibration ± 0.015 %;
- That arisen from weighing biomass ±1 %;
- That as a result from wet feed rate of biomass assessment ± 0.25 %.

- Total Uncertainties in Air Flow Rate

The average uncertainty resulting from air flow rate calculation is ± 1.2 %.

- Total Uncertainties in Syngas Outflow Rate

The analysis of gasification gas and determination of molar percentage composition were performed as explained in depth in section 2.3. Taking those considerations into account, the average uncertainty associated to volumetric gas flow rate calculation is ± 1.75 %.

The results are consistent with the scarce literature on biomass gasification uncertainty analysis [28].

2.5.Portuguese Municipal Solid Waste Evolution

Before the late nineteens Portugal's situation regarding solid waste management was dramatic with 76 % going to open landfills and 14 % going to controlled landfills. Due to

an overwhelming change in public opinion, caused by landscape and soil degradation as well as disease spreading in local populations, national governments were forced to implement the first National Waste Management Plan (PERSU) [29]. Since then, Portugal has been slowly reversing the previously stablish trend. Figure 2.5 presents the development of MSW generation and respective final destination in Portugal from 2001 to 2010.

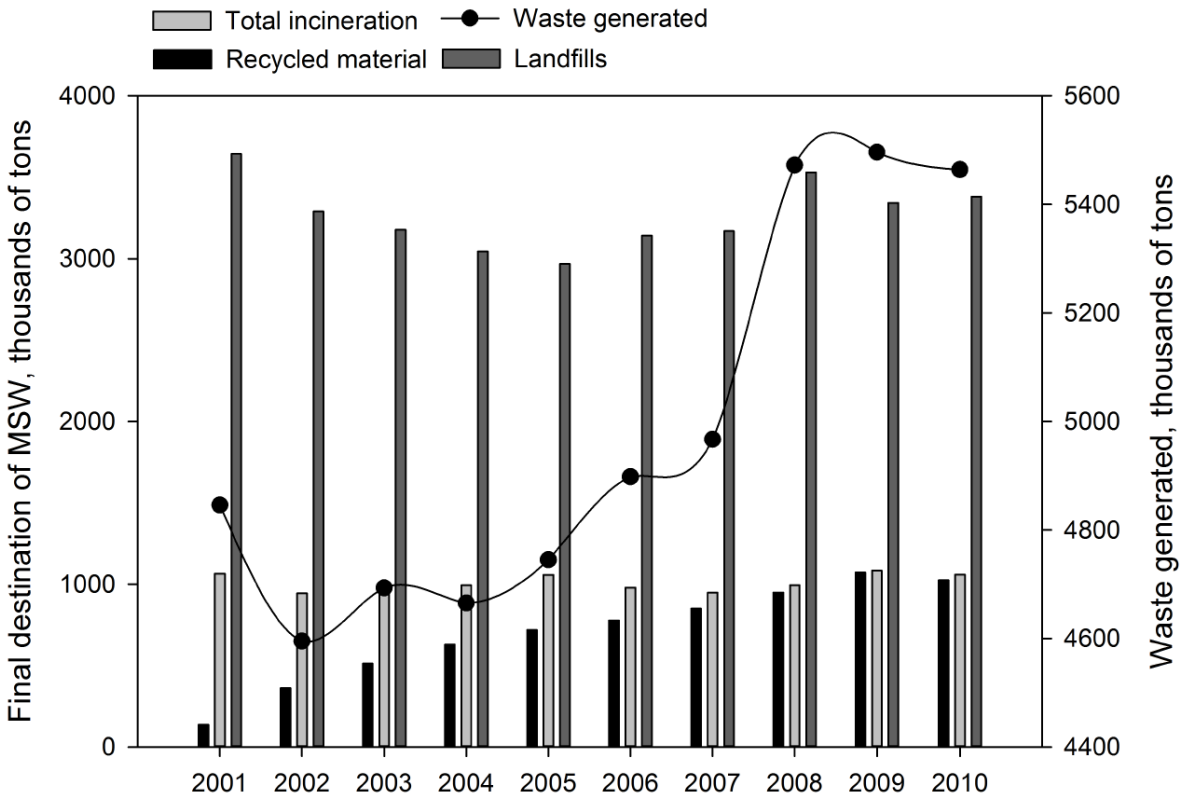

Figure 2.5 - MSW generation and final destination in Portugal from 2001 to 2010.

Despite decreasing landfills from over 75 % to 60 % the strategy aimed at the total eradication of open dumps failed. In February 2007, PERSU II was ratified to target the period between 2007 and 2016. The new national plan tried to carry on the previous waste management policy, taking into account new requirements formulated at national and EU level, in particular by ensuring compliance with Community targets for diverting

biodegradable municipal waste from landfill, while trying to remedy the limitations mentioned on the implementation of PERSU I.

Still, according to the European Environment Agent [30], Portugal needs to intensify the implementation of the plan while adding considerable efforts to fulfil the EU targets. Gasification is becoming an increasingly attractive technology to treat MSW, through clean gas production, and thus becoming a valuable root to achieve those targets.

2.5.1. MSW Characterization and LIPOR's Sorting Plant

Since model accuracy depends on using realistic data, the characterization and analysis of Portuguese MSW was carried out using data from the Oporto metropolitan area obtained from LIPOR, the entity responsible for the management, treatment and recovery of solid waste municipal produced in the city. Based on modern municipal waste management concepts that stand for the implementation of integrated systems and reduction of waste disposal in landfills, LIPOR has developed an integrated strategy for the recovery, treatment and confinement of municipal waste, based on three main areas: multi-material recovery, organic recovery and energy recovery, which are complemented by a landfill where rejected and previously prepared waste is sent to.

Every year, LIPOR treats about 500,000 tons of municipal waste that are produced by roughly 1 million inhabitants. Early estimates from 2016 indicate that 240,648 tons of wastes were produced in the first half of the year. Although premature, this represents an increase in 2.7 % when compared to the same period from previous year. After years of undefined trends, these figures seem to indicate a return to the increasing trend in municipal waste production that occurred during the period between 2002 and 2010 (up to 18 %), which can be explained by the improvement of the macroeconomic situation of the country, which increased the level of consumption and, consequently, the production of waste.

During the management and treatment of collected MSW, samples were acquired for posterior physical characterization. Table 2.2 describes the obtained samples.

Table 2.2 - Physical characterization of the MSW in Oporto in 2014.

Category	**Weight (%)**
Putrefied residues	37.57
Paper	6.16
Cardboard	4.31
Composites	6.39
Textiles	7.74
Sanitary textiles	8.72
Plastics	12.10
Combustive non specified	0.93
Glass	5.53
Metals	2.45
Non-combustive non specified	0.50
Hazardous residues	0.01
Fine elements	7.59

To better understand how the physical characterization was obtained as well as the steps necessary to formulate the chemical composition used in the simulations it is best to understand how the sorting process works. The following is a summarized step-by-step process of LIPOR's sorting plant (full process description can be viewed at [31]):

- The materials from the Ecocontainer, the door-to-door packaging collection, the Ecofone and other special circuits are discharged in the Sorting Plant reception area. These discharges are subject to an inspection, to record its quality. The materials are placed in the pre-sorting cabin, where pre-sorting is done, resulting in 3 streams: large film, large rejected and other materials of large dimension. After passing the pre-sorting cabin, the materials are forwarded to a "bag-opener", to homogenize the material.
- The materials, after passing through the "bag-openers" (so the material homogenate), are forwarded to the ballistic sorter. Ballistic sorting equipment is a

device that allows the sorting of material in 3 fractions: thin, rolling and flat. The equipment is assembled with a pre-defined inclination, and consists of a set of perforated bars, which in a continuous movement, sorts the materials.

- The materials, which in the ballistic section followed the rolling's path, are forwarded to the respective hopper. Before they get to the rolling hopper, the materials go through two automatic sorting systems: an automatic vacuum system that sucks all the light and flexible materials; and an electromagnet, which sorts all ferrous metals and forward them through a hopper, to a metal baler, where they are pressed and sent to recycling industries.
- The escalators sent to the respective hopper, are transported to the rolling sorting cabin. The sorting cabin consists of two rows of parallel sorting, where is sorted sequentially 4 materials (PET, PEHD, Mixed Plastics and CPLF). The materials follows to Foucault currents, where aluminum is sorted by a magnetic flux process that allows automatic sorting of the material. The remaining material is considered process rejected.

From the described pre-treatment of MSW done by LIPOR, a refuse derived fuel simply containing cellulosic materials and plastics is obtained (comprised of putrefied wastes, paper, wood wastes, and plastic residues). The remaining MSW components follow another route for valorization or elimination, as described above. It has been shown that the plastic residues are mainly composed of polyethylene, polystyrene, and polyvinyl chloride [32] while cellulosic materials are composed of cellulose, hemicelluloses, and lignin [33].

Since the ultimate analysis from LIPOR does not distinguish between cellulosic materials, their composition was presupposed to be similar to the one found by Onel *et al.* [34], where the cellulosic material comprises cellulose, hemicellulose and lignin. Regarding the plastics

group, LIPOR report shows the relative quantities of each monomer in the MSW. Therefore, it was possible to take into account different monomers for the plastics group as shown in Table 2.3.

Table 2.3 - Chemical composition of the MSW in Oporto in 2014.

Category	**Weight (%)**	**Chemical formula**
Cellulosic material	85.42	*
Polyethylene	10.99	$(C_2H_4)_n$
Polyethylene terephthalate	2.02	$(C_{10}H_8O)_n$
Polypropylene	0.81	$(C_3H_6)_n$
Polystyrene	0.76	$(C_8H_8)_n$

*It was considered the proportion of cellulose, hemicellulose and lignin found in [34].

3. Mathematical Model

Experimental studies conducted in pilot scale or industrial reactors like the one presented in the previous section are fairly absent from the available literature. The reason why is due to the difficulty in regulating operating parameters but primarily due to the high cost of a gasification plant, which can reach tens of millions of euros depending on the generated power [15].

Mathematical models, with the ability to theoretically simulate any physical condition, allow studying the gasification process without resorting to major investments and/or the need for long waiting periods (with all the bureaucratic and logistical problems associated). However, due to the extreme complexity of the gasification process, largely due to the chemical and physical interactions that occur throughout, the ability of numerical models to correctly predict experimental data collected from pilot scale or industrial reactors is usually very limited. In fact, the lack of reliable models was the main motivation for the first draft of our developed model early in the decade [35].

3.1.Gas-Solid Interaction

When modeling bubbling fluidized-bed reactors, like the one described, the two-phase flow theory of fluidization is usually applied for the description of the process hydrodynamics. Because of this, correctly modeling the interaction between gas and solid phases is crucial since they exchange heat by convection, mass over the heterogeneous chemical reactions, and momentum due to the drag between gas and solid phase. The main equations governing both phases are depicted in Table 3.1.

Table 3.1 - Governing equations for gas and solid phases.

Gas Phase	Solid Phase
Energy:	
$\frac{\partial(\alpha_g \rho_g h_g)}{\partial t} + \nabla \cdot (\alpha_g \rho_g \vec{u}_g h_g) = -\alpha_g \frac{\partial(p_g)}{\partial t} +$ $\bar{\bar{\tau}}_g : \nabla(\vec{u}_g) - \nabla \vec{q}_g + S_g + \sum_{g=1}^{n} (\vec{Q}_{sg} + \dot{m}_{sg} h_{sg})$	$\frac{\partial(\alpha_s \rho_s h_s)}{\partial t} + \nabla \cdot (\alpha_s \rho_s \vec{u}_s h_s) = -\alpha_s \frac{\partial(p_s)}{\partial t} + \bar{\bar{\tau}}_s : \nabla(\vec{u}_s) -$ $\nabla \vec{q}_s + S_{ps} + \sum_{s=1}^{n} (\vec{Q}_{sg} + \dot{m}_{sg} h_{sg})$
Mass:	
$\frac{\partial(\alpha_g \rho_g)}{\partial t} + \nabla \cdot (\alpha_g \rho_g \vec{u}_g) = -M_C \sum \gamma_C R_C$	$\frac{\partial(\alpha_s \rho_s)}{\partial t} + \nabla \cdot (\alpha_s \rho_s \vec{u}_s) = M_C \sum \gamma_C R_C$
Momentum:	
$\frac{\partial(\alpha_g \rho_g \vec{u}_g)}{\partial t} + \nabla \cdot (\alpha_g \rho_g \vec{u}_g \vec{u}_g) = -\alpha_g \nabla p_g +$ $\alpha \rho_g g + \beta(u_g - u_g) + \nabla \cdot \alpha_g \bar{\bar{\tau}}_g + S_{sg} U_S$	$\frac{\partial(\alpha_s \rho_s \vec{u}_s)}{\partial t} + \nabla \cdot (\alpha_s \rho_s \vec{u}_s \vec{u}_s) = -\alpha_s \nabla p_s + \alpha \rho_s g +$ $\beta(u_s - u_s) + \nabla \cdot \alpha_s \bar{\bar{\tau}}_s + S_{sg} U_S$

3.1.1. Granular Eulerian Model

According to Goldschmidt *et al.* [36], two phase flows can be modeled using two different approaches: the Eulerian-Lagrangian and the Eulerian–Eulerian models. With considerable similarities, the fundamental difference between them lies in the way the particles are treated. The former describes the solid phase at the particle level while the latter treats the particles as continuum. In industrial applications, typically comprised of millions of particles, following individual particles becomes excessively time consuming and for this reason the Lagrangian approach tends to be less used [37].

The Eulerian approach not only requires lower computational resources and calculation times, but also allows a detailed analysis of the disperse phase flow field, which is convenient for engineering design applications. For this reason the Granular Eulerian model was applied to our model.

Granular Eulerian model is described by the following conservation equation for granular temperature:

$$\frac{3}{2}\left[\left(\frac{\partial(\rho_s\alpha_s\Theta_s)}{\partial t}\right)+\nabla\cdot(\rho_s\alpha_s\vec{v}_s\Theta_s)\right]$$

$$=(-p_s\bar{I}+\bar{\tau}_s):\nabla(\vec{v}_s)+\nabla\cdot\left(k_{\Theta_a}\nabla(\Theta_s)\right)-\gamma_{\Theta a}+\phi_{ls} \tag{3.1}$$

This expression is obtained from the kinetic theory of gases. The term $(-p_s\bar{I}+\bar{\tau}_s):\nabla(\vec{v}_s)$ describes the generation of energy by the solid stress tensor, ϕ_{ls} stands for the energy exchange between fluid and solid phase, $\gamma_{\Theta_a}$for the collisional dissipation of energy and $k_{\Theta_a}\nabla(\Theta_s)$ for the diffusion energy, in which $k_{\Theta_a}$is the diffusion coefficient.

3.2.Turbulent Model

In turbulent flows, like the one being studied, transported quantities like momentum, energy and species concentration tend to fluctuate. Modeling said fluctuations can be too computationally expensive, which is why instantaneous governing equations are usually replaced with their time-averaged, ensemble-averaged, or otherwise manipulated to remove the small time scales.

The standard k-ε model was used to simulate the turbulent flow due to its suitability for a wide range of wall-bounded and free-shear flows. The model is the simplest turbulence two-equation model in which the solution of two separate transport equation allows the turbulent velocity and length scales, which are to be independently determined. Turbulence kinetic energy (k) and dissipation rate (ε) are respectively given by:

$$\frac{\partial}{\partial t}(\rho k)+\frac{\partial}{\partial x_i}(\rho k u_i)=\frac{\partial}{\partial x_j}\left[\left(\mu+\frac{\mu_t}{\sigma_k}\right)\right]G_k+G_b-\rho\varepsilon-Y_M+S_k \tag{3.2}$$

$$\frac{\partial}{\partial t}(\rho\varepsilon)+\frac{\partial}{\partial x_i}(\rho\varepsilon u_i)=\frac{\partial}{\partial x_j}\left[\left(\mu+\frac{\mu_t}{\sigma_\varepsilon}\right)\right]+C_{1\varepsilon}\frac{\varepsilon}{k}(G_\varepsilon+C_{3\varepsilon}G_b)-C_{2\varepsilon}\rho\frac{\varepsilon^2}{k}+S_\varepsilon \tag{3.3}$$

To determine the turbulence kinetic energy as well as the dissipation rate, the following constants were assumed: $G_k=1.0$ and $G_\varepsilon=1.3$ stand for the turbulent Prandtl numbers for

k and ε, respectively, $C_{1\varepsilon} = 1.44$, $C_{2\varepsilon} = 1.92$, and $C_{3\varepsilon} = 0$ are default constants commonly used in Fluent and S_k and S_ε for user-defined source terms.

3.3.Chemical Reaction Model

In this study, two different chemical reaction models were used in the simulation: the finite-rate/Eddy-dissipation model was used to describe homogeneous reactions while the Kinetic/Diffusion Surface Reaction Model was employed for heterogeneous ones. The main distinction between these two models is associated to how the carbon species are treated. The homogeneous gas reaction assumes the carbon species gasified straightaway, and that the carbon is treated as a gas, while heterogeneous particle-gas reaction treat carbon as solid particles and they go through finite-rate reaction via a typical reaction at particle surface. Table 3.2 presents the main reactions as well as the corresponding reaction rates for these 2 models. Shown reactions can slightly change if different gasifying agents other than air are considered. Previously published models using steam [38] and carbon dioxide [13] address those exact changes.

Table 3.2 - Chemical reaction model.

Reactions	Reaction Rate	Ref.
Homogeneous Reactions:		
$CO + 0.5O_2 \rightarrow CO_2$	$r_1 = 1.0 \times 10^{15} exp\left(\frac{-16000}{T}\right) C_{CO} C_{O_2}^{0.5}$	[39]
$CO + H_2O \rightarrow CO_2 + H_2$	$r_2 = 5.159 \times 10^{15} exp\left(\frac{-3430}{T}\right) T^{-1.5} C_{O_2} C_{H_2}^{1.5}$	[39]
$CO + 3H_2 \leftrightarrow CH_4 + H_2O$	$r_3 = 3.552 \times 10^{14} exp\left(\frac{-15700}{T}\right) T^{-1} C_{O_2} C_{CH_4}$	[39]
$H_2 + 0.5O_2 \rightarrow H_2O$	$r_4 = 2780 exp\left(\frac{-1510}{T}\right)\left[C_{CO} C_{H_2O} - \frac{C_{CO_2} C_{H_2}}{0.0265 exp\left(\frac{3968}{T}\right)}\right]$	[39]
$CH_4 + 2O_2 \rightarrow CO_2 + 2H_2O$	$r_5 = 3.0 \times 10^5 exp\left(\frac{-15042}{T}\right) C_{H_2O} C_{CH_4}$	[39]
Heterogeneous Reactions:		
$C + 0.5O_2 \rightarrow CO$	$r_6 = 596 T_P exp\left(\frac{-1800}{T}\right)$	[39]
$C + CO_2 \rightarrow 2CO$	$r_7 = 2082.7 exp\left(\frac{-18036}{T}\right)$	[39]
$C + H_2O \rightarrow CO + H_2$	$r_8 = 63.3 exp\left(\frac{-14051}{T}\right)$	[39]

3.4.Model Expansion for MSW

In the above sub-section the mathematical treatment for the devolatilization phenomenon was purposely not address. The reason why being that the devolatilization section was only properly included when the model was expanded to handle the heterogeneity of MSW. Until that point, a single rate model, developed by Badzioch and Hawsley [40], was assumed which computed reliable devolatilization rates in a simple way.

To cope with the heterogeneity of said substrate a pyrolysis model with secondary tar generation was implemented. MSW is mainly composed by cellulosic and plastic components, and while cellulosic material can be divided in cellulose, hemicellulose and

lignin [34], plastics are comprised of polyethylene, polystyrene, and polypropylene, among others. To distinguish the several components that comprise the MSW, the pyrolysis reactions of cellulosic and plastic groups are considered individually and following an Arrhenius kinetic expression, as shown in Table 3.3.

Table 3.3 - Devolatilization model.

Reactions	Reaction Rate	Ref.
$Cellulose \rightarrow \alpha_1 volatiles + \alpha_2 TAR + \alpha_3 char$	$r_9 = A_i exp\left(\frac{-E_i}{T_s}\right)(1-a_i)^n$	[39]
$Hemicellulose \rightarrow \alpha_4 volatiles + \alpha_5 TAR + \alpha_6 char$	$r_{10} = A_i exp\left(\frac{-E_i}{T_s}\right)(1-a_i)^n$	[39]
$Lignin \rightarrow \alpha_7 volatiles + \alpha_8 TAR + \alpha_9 char$	$r_{11} = A_i exp\left(\frac{-E_i}{T_s}\right)(1-a_i)^n$	[39]
$Plastics \rightarrow \alpha_{10} volatiles + \alpha_{11} TAR + \alpha_{12} char$	$r_{12} = \left[\sum_{i=1}^{n} A_i exp\left(\frac{-E_i}{RT}\right)\right]\rho_v$	[39]
$Primary\ TAR \rightarrow volatiles + SecondaryTAR$	$r_{13} = 9.55 \times 10^4 exp\left(\frac{-1.12 \times 10^4}{T_g}\right)\rho_{TAR1}$	[39]

3.5.Numerical Procedure

Fluent, a finite volume method based CFD solver, was employed in this work to solve the stated problem. Regarding the geometry modelling there are some simplifications that one can make in order to make the computation less expensive. Since the described reactor type is cylindrical, one can use a 2D axisymmetric problem setup. Figure 3.1. displays the reactor schematics.

Mesh was built using GAMBIT software and the size of the cell in both the x- and y-directions was specified with a 1:1 ratio. The time step was decreased with decreasing cell size to help maintain numerical stability. To select the optimum number of cells, grid independence studies were performed.

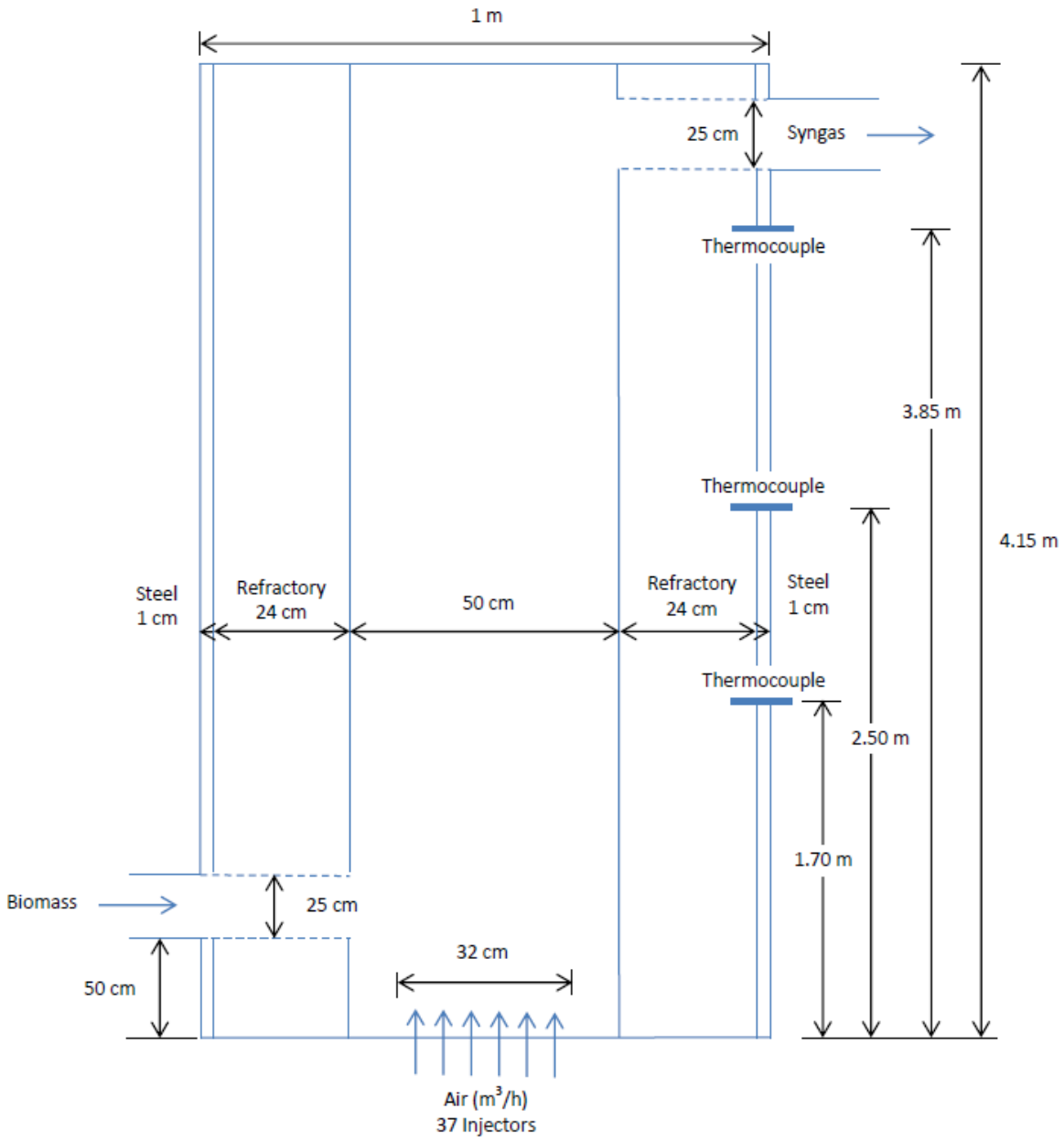

Figure 3.1 - Gasifier schematics.

The simulations are carried out on 4 different grids with increasing grid density in order to ensure a grid-independent solution. Table 3.4 displays the main mesh characteristics.

Molar fraction compositions for CH_4, CO, CO_2 and H_2 at gasifier outlet are compared for the described grids. The grid-independent solution is illustrated in Figure 3.2.

Table 3.4 - Mesh characteristics.

Mesh	$x \times y$	Number of Elements
1	80 x 664	53,120
2	90 x 747	67,230
3	100 x 830	83,000
4	110 x 913	100,430

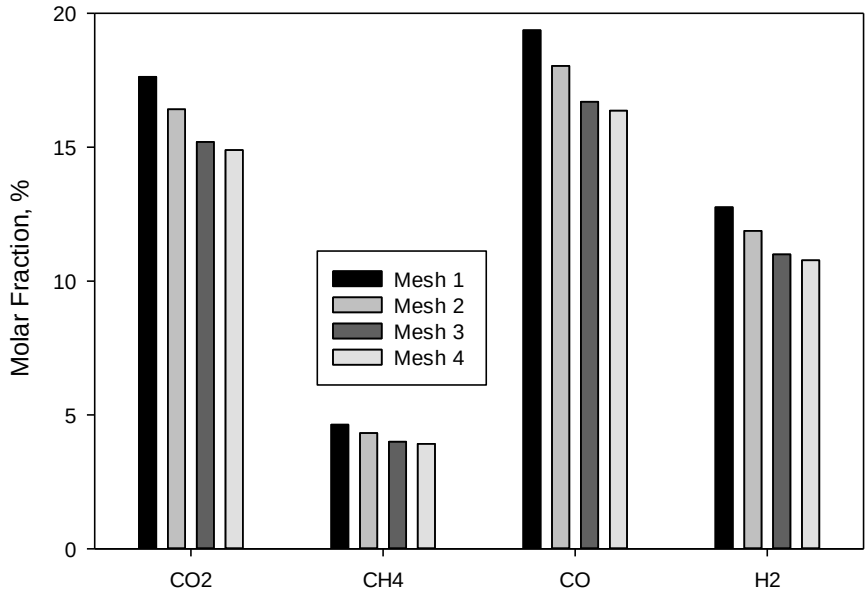

Figure 3.2 - Grid independence study for the described meshes.

The simulation results for the various meshes are found to be in good agreement with each other. As can be seen, the grids exceeding 83,000 cells reveal a variation in parameter convergence less than 3%. Consequently, the grid with 83,000 cells is recommended to use for accurate calculations. Unsurprisingly, the chosen cell size was about twelve times larger than the average particle size which was shown to be able to effectively capture the hydrodynamics in fluidized bed gasifier [41].

In order to avoid poor convergence, an unsteady model was used with a time step size of 1.0^{-4}s and the gasification time of the biomass was resolved by 400,000 time steps.

In such a complex model is sometimes difficult to define a good initial condition. For this reason, the process was first simulated considering only flow and non-reacting heat transfer (also known as “cold flow”) and after reaching conversion reactive multiphase flow was added.

Substrate and air inlet were defined as “velocity inlets”. Each velocity-inlet surface was identified by mass fractions, temperature, and a velocity magnitude. The flow direction was kept normal to the surface. Turbulence of the inlet surfaces were detailed by turbulence intensity and hydraulic diameter. Outlet was set as the pressure outlet, specified by a gauge pressure value of zero.

For the pressure–velocity coupling, the widely used SIMPLE algorithm was enabled. For all simulations presented in this paper, a First Order Upwind Scheme was used for all equations. The Standard scheme was used for interpolation methods of pressure. This means that the solution approximation in each finite volume was presumed to be linear, leading to less computational expenses. In order to properly justify using a first order scheme, it was necessary to make sure that the grid used in this work had adequate resolution to accurately capture the physics occurring within the domain. In other words, the results needed to be independent of the grid resolution. Nonetheless, for better accuracy, this was later changed to the second-order upwind scheme.

Similarly, the under-relaxation factors were initially set at 0.5 (except for turbulent viscosity, pressure, and body forces, which were kept the same as default), and were then gradually conveyed to their default values with convergence. Convergence criteria were set that normalized residuals for all equations must fall under 10^{-6}.

4. Thermodynamic Methodology

Thermodynamic analyses are used to evaluate how energy streams affect the overall performance of a given system. Through mathematical models, these analyses can help determining the effects of parameters on the system's optimal operating point. In this particular study the goal is to use first and second law analysis to improve MSW conversion from an efficiency and ecofriendly standpoint. In order to simplify the analysis the following assumptions were made [42]:

- Steady State;
- Kinetic and potential energy ignored;
- Ideal gas principles apply for the gases;
- Syngas is only formed with H_2, CO, CO_2, N_2, C_nH_m and it is at chemical equilibrium;
- Heat losses from the components are neglected;
- T_0 is 25 ºC and P_0 101.325 kPa;
- Ash residues are negligible;
- Gasifier is isothermal and at equilibrium condition.

4.1.Energy Analysis

The overall energy balance can be expressed as the total energy input rate equal to total energy output rate ($E_{in} = E_{out}$), with all energy terms being:

$$\dot{Q} + \sum \dot{m}_{in} h_{in} = \dot{W} + \sum \dot{m}_{out} h_{out} \quad (4.1)$$

Where $\dot{Q}$ is the heat rate, $\dot{W}$ is the work rate and h is the specific enthalpy. Applying this concept to the current study, energy transferred as heat can be written as:

$$\dot{Q}_{MSW} + \dot{Q}_{heated\ air} = \dot{Q}_{syngas} + \dot{Q}_{tar} + \dot{Q}_{system} \quad (4.2)$$

The fuel's energy input can be calculated as:

$$\dot{Q}_{MSW} = \dot{m}_{MSW} \times LHV_{MSW} \tag{4.3}$$

Where LHV is the lower heating value and $\dot{m}_{MSW}$ is the mass flow rate for MSW. As long as there is no condensation occurring, the power of supplied air can be given by:

$$\dot{Q}_{air} = \dot{m}_{air} \sum_{1}^{j} w_j \, c_{p,j}(T - T_0) \tag{4.4}$$

Where w_j is the mass fraction and $c_{p,j}$ the specific heat of a component, T and T_0 represent preheat gas temperature and ambient temperature, respectively. To calculate the energy associated with the produced syngas one can use:

$$\dot{Q}_{syngas} = \dot{m}_{syngas} \times LHV_{syngas} \tag{4.5}$$

Similarly, tar content energy can be obtained by simply:

$$\dot{Q}_{tar} = \dot{m}_{tar} \times LHV_{tar} \tag{4.6}$$

So, in order to calculate the cold gas energy efficiency one can simply put it:

$$\eta_{coldgas} = \frac{\dot{Q}_{syngas}}{\dot{Q}_{MSW} + \dot{Q}_{air}} \tag{4.7}$$

4.2.Exergy Analysis

Exergy analyses are far superior to energetic ones, since energetic analyses do not take into consideration irreversibilities that occur in every thermodynamic process. In this work the same methodology to calculate exergy used by Zhang *et al.* [43] was employed. Exergy rate can be defined by the sum of the chemical exergy rate and the physical exergy rate:

$$Ex = Ex_{ch} + Ex_{ph} \tag{4.8}$$

Where the chemical and physical exergy can be written, respectively as:

$$Ex_{ch} = \sum_{i} n_i \left(e_{0_i} + RT_0 ln \frac{n_i}{\sum n_i} \right) \tag{4.9}$$

$$Ex_{ph} = \sum_i n_i \left[(h - h_0) - T_0(s - s_0)\right] \tag{4.10}$$

Where n_i is the molar yield of gas component i (mol/kg), R is the ideal, or universal, gas constant and e_{0_i} is the standard chemical exergy of a pure chemical compound i and it can be found in [43]. Also, s and h are entropy and enthalpy of a system at given temperature and pressure, and h_0 and s_0 are enthalpy and entropy of a system at the environmental temperature and pressure, respectively.

In order to calculate the exergy of MSW with less complexity, taking into account its heterogeneous, the introduced correlation by Szargut and Styrylska [44] was used:

$$Ex_{MSW} = \dot{m}_{MSW} \beta LHV_{MSW} \tag{4.11}$$

The formula of correlation factor β is given by:

$$\beta = \frac{1.0412 + 0.2160\left(\frac{H}{C}\right) - 0.2499\left(\frac{O}{C}\right)\left[1 + 0.7884\left(\frac{H}{C}\right)\right] + 0.0450\left(\frac{N}{C}\right)}{1 - 0.3035\left(\frac{O}{C}\right)} \tag{4.12}$$

Where O, C, H and N are the weight fractions of oxygen, carbon, hydrogen and nitrogen in the MSW, respectively.

Similarly, in this work the tar chemical exergy is simulated with help of another correlation for liquid fuels [45]:

$$Ex_{tar} = \dot{m}_{tar} LHV_{tar} \left(1.0401 + 0.1728\left(\frac{H}{C}\right) + 0.0432\left(\frac{O}{C}\right) + 0.2196\left(\frac{S}{C}\right)\left[1 - 2.0628\left(\frac{H}{C}\right)\right]\right) \tag{4.13}$$

Using the previous equations the exergy balance simply becomes:

$$\sum_{in} Ex_{in} = \sum_{out} Ex_{out} + \dot{I} \tag{4.14}$$

$\dot{I}$ Represents the internal exergy destruction rate due to irreversibility (unlike energy, exergy can actually be destroyed). The *in* and *out* subscripts stand for inlet and outlet, respectively.

Using the same principal as in the energy analysis, syngas exergy efficiency can be calculated as being:

$$\varepsilon_{syngas} = \frac{Ex_{syngas}}{Ex_{MSW} + Ex_{air}} \tag{4.15}$$

Similarly, tar content exergy efficiency can be written as:

$$\varepsilon_{tar} = \frac{Ex_{tar}}{Ex_{MSW} + Ex_{air}} \tag{4.16}$$

5. Results and Discussion

5.1.Model Validation

5.1.1. Validation for Semi-Industrial Conditions

The numerical model presented in Chapter 3 is the result of continuous improvement on the described set of phenomena that includes fluid flow, heat transfer, and chemical reactions necessary for modeling the gasification process. At the same time, the software related parameters have been optimized to mimic similar conditions to those found in experimental activities and thus obtaining more realistic results.

The model was first applied to the study of Portuguese biomass gasification [46]. To validate the numerical model a wide range of operational conditions were tested in the described plant for several Portuguese biomass substrates. Table 5.1 shows 9 operating conditions for 3 distinct substrates (representing just a fraction of the overall conducted runs used to validate the numerical model).

Table 5.1 - Operating conditions for validation proposes.

Experimental Conditions	**Forest Residues**			**Coffee Husk**			**Vines Pruning**		
Run	**1**	**2**	**3**	**4**	**5**	**6**	**7**	**8**	**9**
Temperature (ºC)	815	815	790	815	790	790	790	790	815
Admission Biomass (kg/h)	63	74	63	28	28	41	25	55	55
Air Flow Rate (Nm^3/h)	94	98	98	75	72	80	52	40	40
Test Results									
Syngas NHV (MJ/Nm^3)	5.16	5.02	4.93	3.34	3.20	3.07	1.99	3.46	4.02
Cold Gasification Efficiency	0.41	0.30	0.37	0.60	0.47	0.42	0.55	0.45	0.49

Figure 5.1 compares modeled and measured gas composition for the described operating conditions. Presented results show that the developed numerical model has the ability to predict the obtained synthetic gas composition within a satisfactory margin of error of 20%, commonly found in similar studies [47]. The biggest deviation was observed for CH_4,

which was expected since smaller fractions tend to produce higher relative errors. Furthermore, all light hydrocarbons and tar can lump into CH_4, which can explain the disagreement sometimes found [46].

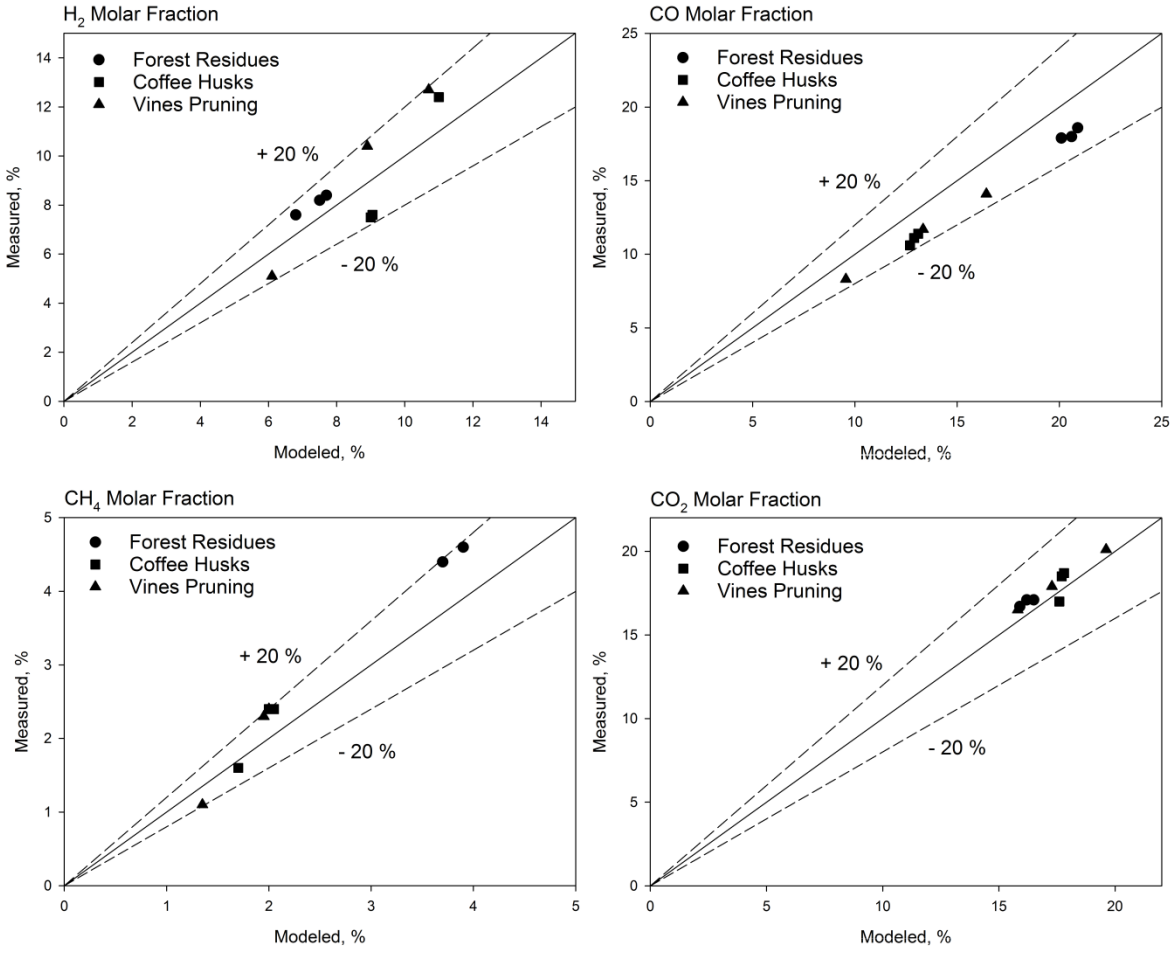

Figure 5.1 - Comparison between modeled and measured syngas composition for biomass substrates.

In order to further validate the numerical model, the temperature distribution inside the reactor was studied using the three thermocouples previously mentioned. A comparison between the numerical model and experimental results is displayed in Table 5.2.

Table 5.2 - Temperature distribution for experimental and numerical results (Runs 1, 4 and 7 from Table 5.1).

Runs	Type	T1	T2	T3
1	Numerical	822	620	468
	Experimental	815	596	450
4	Numerical	835	603	465
	Experimental	815	581	440
7	Numerical	812	607	455
	Experimental	790	568	422

T1, T2 and T3 are located at 1.70, 2.50 and 3.85 m from the bottom. From the view point of the oxidizer, several stages can be differentiated: drying, devolatilization, volatile matter combustion and char gasification. Since there are only 3 thermocouples, it is impossible to determine where each reaction zone can be found, but since the first thermocouple is located 1.70 m above the air inlet, it is safe to assume that most stages are completed at that point and that gasification is the only process remaining. Therefore, it comes with no surprise that the temperature inside the reactor appears to drop almost linearly until it reaches syngas outlet, which can be attributed to exothermic reactions (namely combustion) occurring near the biomass inlet and producing heat, and then through the reactor length the heat is being consumed by the gasification reactions. Even though no results for temperature distribution in a pilot scale up-flow atmospheric fluidized bed gasifier can be found in the literature, the findings from the very scarce sources available on the subject show consistency with obtained results [48, 49].

Overprediction in the temperature profile can be caused by considering the particle phase as continuum, leading to calculation errors for mass and energy transfers between phases, which were also found in the literature [50].

As previously mentioned, the model had to undergo a restructuring on the devolatilization section in order to cope with the heterogeneity of MSW [51]. Ideally one would like to

validate the new upgraded model with the experimental set-up used earlier. However, due to unfortunate logistical and bureaucratic setbacks this was not possible. To work around the problem it was decided to validate the upgraded model using data collected from the literature [52]. Table 5.3 shows the operating conditions for 9 experimental runs used to validate the numerical model.

Table 5.3 - Operating conditions for the experimental gasification runs.

Run	**1**	**2**	**3**	**4**	**5**	**6**	**7**	**8**	**9**
Temperature (ºC)	493	705	602	507	687	593	516	691	507
MSW Admission (kg/h)	2.3	3	3	3	4	4	4	6	6
ER	0.5	0.4	0.4	0.4	0.3	0.3	0.3	0.2	0.2
Preheated Air (ºC)	290	352	296	281	352	307	282	352	279

Figure 5.2 matches the composition of obtained gas that is estimated by the model with that measured in the experiments. Comparison between Figures 5.1 and 5.2 shows that the upgrade done to the model allowed a more complex system to perform in a similar fashion and in some cases to predict syngas composition slightly better. This was due to a more realistic devolatilization model and the inclusion of light hydrocarbons. Nevertheless, some differences can be observed due to some simplifying assumptions followed by the model, which are explained in detail in [46].

Having a model not only able to correctly predict trends but also the overall compositions, gives the user the ability to forecast scenarios while minimizing costs. This can become extremely time-efficient since it can eliminate or at least greatly diminish the necessary experimental runs with all the bureaucratic and logistical problems associated with it.

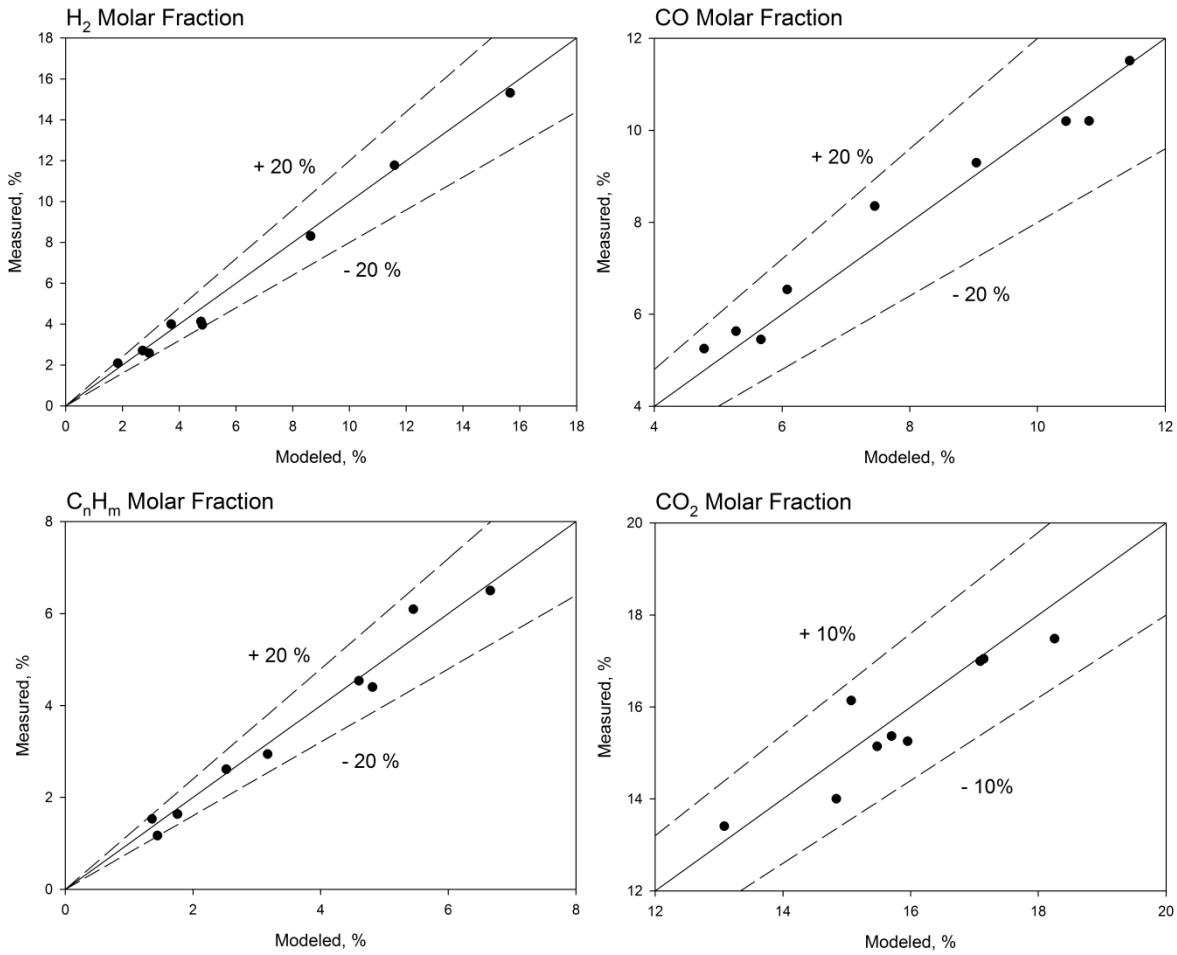

Figure 5.2 - Comparison between modeled and measured syngas composition for MSW.

5.1.2. Validation for Laboratory Conditions

To validate the use of the developed model in the study of the scale-up phenomenon, it is necessary to evaluate its performance under laboratorial and pilot scale experimental conditions. Accordingly, the numerical model was first validated using experimental results (Figure 5.1) collected from the performed runs. Since no results were gathered in laboratorial scale reactor data available in the literature was needed. The work from Campoy *et al.* [53] was used to validate the model in laboratorial scale conditions since extensive information not only on the gasification process and biomass substrate used but

also regarding reactor geometry, necessary to build the numerical model, was available. Table 5.4 shows the gasification conditions selected for the model validation.

Table 5.4 - Experimental gasification conditions used for the model validation.

Gasification Run	Biomass feeding rate (kg/h)	Flux of air (Nm^3/h)	Oxygen flow rate (Nm^3/h)	Steam flow rate (kg/h)	Gasification Temperature (ºC)
1	12.2	17.0	0.0	2.5	804
2	12.2	17.0	0.0	5.1	789
3	15.0	17.0	0.0	3.2	786
4	10.0	9.1	1.2	5.6	790
5	16.2	10.6	1.4	4.7	781
6	12.0	7.7	1.0	6.5	765

Syngas molar fractions for both experimental and numerical results are depicted in Figure 5.3.

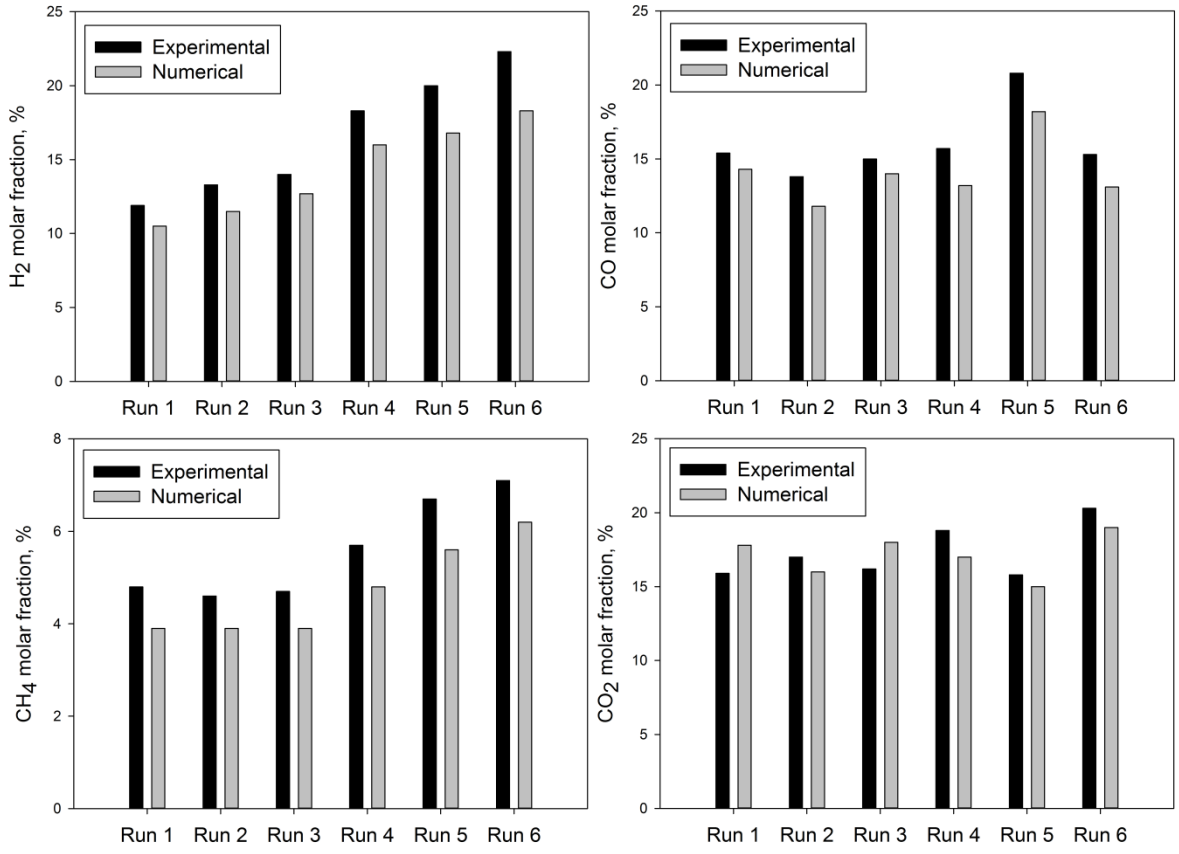

Figure 5.3 - CFD and experimental molar fractions for the 6 gasification runs defined in Table 5.4.

Results from the numerical model show a very reasonable agreement with the experimental data at laboratory scale reactor. Similar errors were found for additional runs. Again, variation can be explained due to the complexity of a gasification system. In depth analysis on the presented results can be seen in [53]. Range of errors between laboratory-scale and industrial was quite similar.

5.2.Assessment of Operational Conditions

After validating the numerical model and reaffirming the reliance on experimental results, it is now possible to study the influence of several operating parameters on the final composition of the gas produced in pilot scale conditions.

5.2.1. Effect of Equivalence Ratio

Equivalence ratio is one of the most significant parameters which have effect on the gasification process including syngas composition. ER is the ratio of the actual air/fuel ratio to the stoichiometric air/fuel ratio. The ratio was kept between 0.15 and 0.35 since all of the experiments conducted to validate the model fell in this range and also because the ER values most suitable for gasification range between 0.2 and 0.4. The model predictions about the influence of ER on syngas molar fraction and hydrogen yield are shown in Figure 5.4.

It can be observed that when ER rose, the CO_2 content increased, while CO and H_2 content decreased. With an increase in O_2 content combustion reactions (that consume CO and H_2 to produce CO_2) will be promoted, since O_2 is more reactive to carbon than steam or CO_2. Although to a smaller degree, ER negatively affects C_nH_m content by enhancing steam reactions at higher temperatures leading to methane decomposition [54].

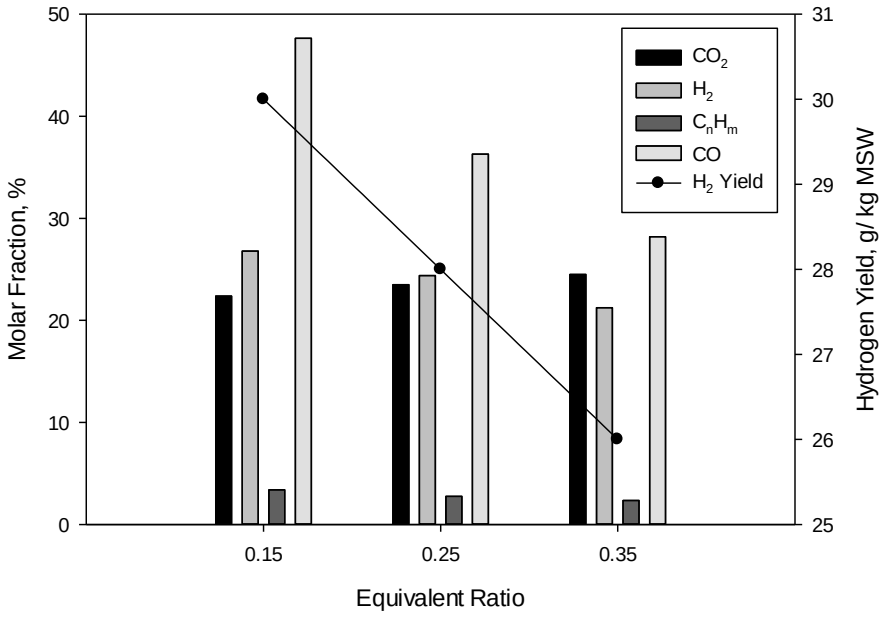

Figure 5.4 - Influence of ER on syngas molar fraction and hydrogen yield. Dry and N_2-free basis. (Operating conditions: Temperature - 700 ºC; MSW admission - 25 kg/h).

Increasing ER by raising the air flow rate also causes more N_2 to enter the reactor, causing the produced gas to be more diluted in N_2 and a poorer gas. The fact that CO and H_2 content decrease with ER can also be explained by a shorter residence time, seeing that, as air flow rate increases, it is no longer sufficient for CO and H_2 formation reactions to occur. The influence of ER on tar content and gas yield is shown in the Figure 5.5. A decrease in tar release around 68 % with the rise of ER to 0.35 is observed. Gas yield on the other hand increased with the rise of ER. Oxidation reactions are exothermic and therefore lead to an increase in temperature inside the reactor. This increase in temperature enhances steam reforming reactions, which in turn promote carbon conversion [55]. This leads to increase in gas yield, which is known for improving tar decomposition.

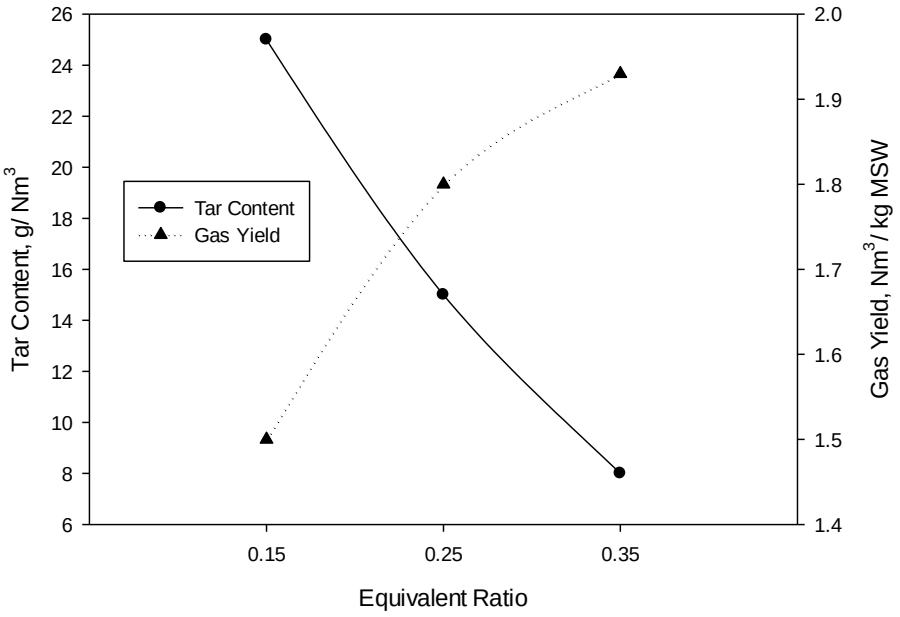

Figure 5.5 - Influence of ER on tar content and gas yield. Dry and N_2-free basis. (Operating conditions: Temperature - 700 ºC; MSW admission - 25 kg/h).

5.2.2. Effect of Steam to Biomass Ratio

As the gasification medium is a very important parameter in governing the gas yield and composition, the effect of using steam instead of air was also studied. The steam to biomass ratio is defined as the steam mass flow rate divided by the biomass mass flow rate in dry basis. The use of steam as a gasifying agent increases the partial pressure of H_2O inside the gasification reactor which favors the water gas, water-gas shift and steam reforming reactions, leading to increased H_2 production [56]. The SBR was varied over a range of values from 0 to 1.5 by holding the other variables constant. This range was selected based on previous findings from our research team using the same facilities but for a different biomass substrate. Figure 5.6 shows the syngas molar fractions as a function of the SBR.

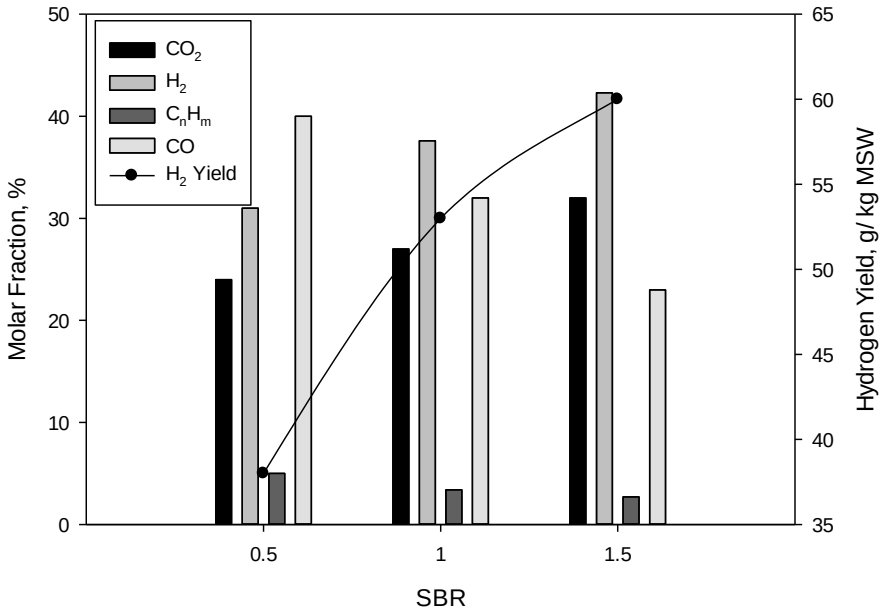

Figure 5.6 - Influence of SBR on syngas molar fraction and hydrogen yield. Dry and N_2-free basis. (Operating conditions: Temperature - 700 ºC; MSW admission - 25 kg/h).

The presence of steam in gas-phase reactions will mostly favor char and tar steam reforming as well as water-gas shift reaction, which in turn will lead to an increase in CO_2 and H_2 content at the expense of CO and C_nH_m. In fact water-gas shift reaction will be the dominant reaction and CO will be consumed to produce CO_2 and H_2. These results are consistent with the current literature [55].

Moreover, it can be found from Figure 5.7 that with the introduction of steam, tar content remarkably decreases, which is attributed to steam reforming of the tar with an increased partial pressure of steam. This promotion of the steam reforming reactions led to a rapid increase of dry gas yield as shown in the Figure 5.7, which agrees with the reduction of tar. The results obtained agree with those found in literature [57, 58].

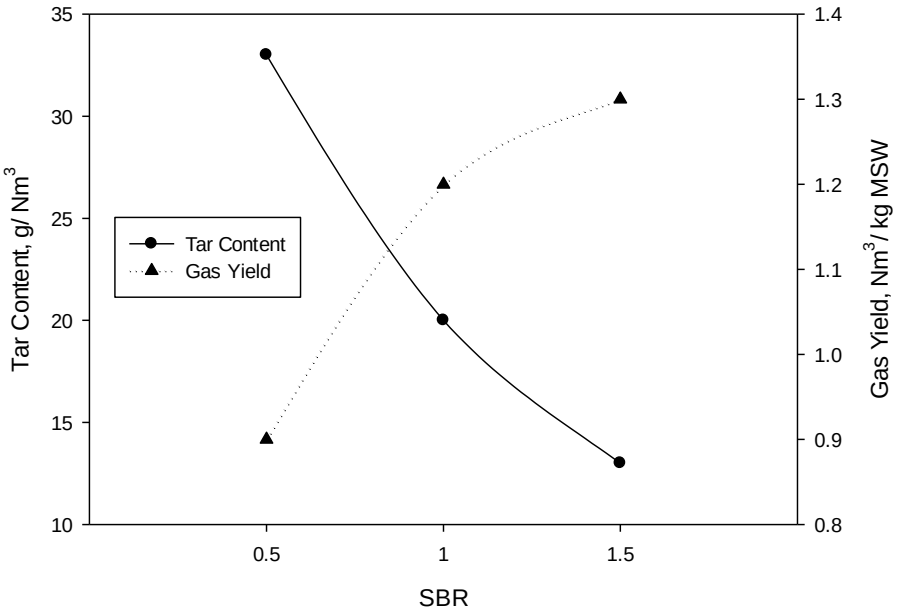

Figure 5.7 - Influence of SBR on tar content and gas yield. Dry and N_2-free basis. (Operating conditions: Temperature - 700 ºC; MSW admission - 25 kg/h).

5.2.3. Effect of Carbon Dioxide to MSW Ratio

Although poorly studied, the addition of carbon dioxide as a gasifier agent has been showing promising results. Not only uses an unwanted end product of various industrial processes instead of steam (which is becoming an increasingly rarer resource) but also enhances both char gasification and pyrolysis and has the ability to act as a catalyst enhancing thermal cracking of volatiles leading to tar mitigation.

The effect of carbon dioxide as a gasifying agent was studied using CO_2-to-MSW ratio (which we will refer from now on "CDMR" for simplicity). The CDMR was varied over a range of values from 0 to 1 by holding the other variables constant. To the best of our knowledge this ratio is yet to be addressed in the current literature, although some work has been made using CO_2-to-biomass [59-61]. Figure 5.8 shows the syngas molar fractions as a function of CDMR.

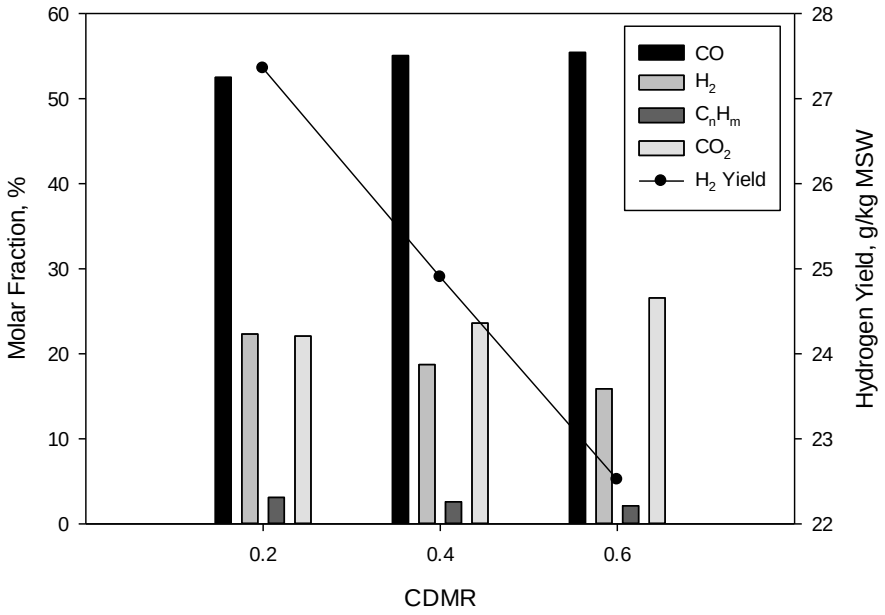

Figure 5.8 - Influence of CDMR on syngas molar fraction and hydrogen yield. Dry and N_2-free basis. (Operating conditions: Temperature - 700 ºC; MSW admission - 25 kg/h).

Results show that increasing CDMR leads to higher levels of CO and CO_2 and lower levels of H_2 and C_nH_m. This is explained by higher CO_2 content mainly promoting Boudouard and reverse water-gas shift reactions which leads to CO content increasing while H_2 decreases. C_nH_m molar fraction slightly decreases due to being consumed via CH_4 reforming to produce CO and H_2 [62]. CO_2 content increases since a considerable fraction of the gasifying agent leaves the reactor unreacted.

CO_2 addition is also responsible for decreasing one of the major concerns related to MSW gasification, tar formation [63]. Figure 5.9 shows CDMR influence on tar content and gas yield.

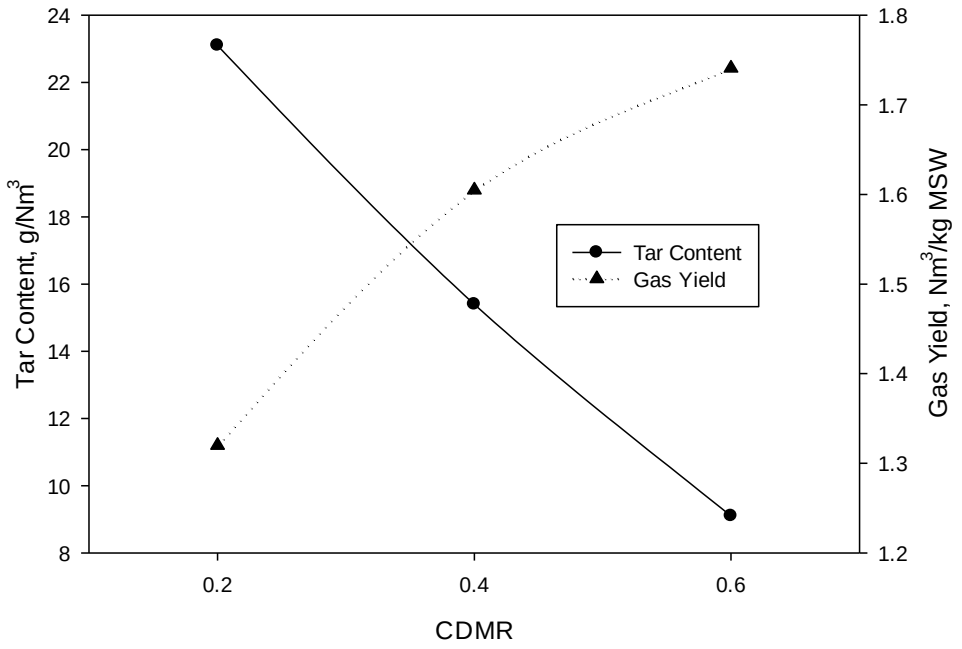

Figure 5.9 - Influence of CDMR on tar content and gas yield. Dry and N_2-free basis. (Operating conditions: Temperature - 700 ºC; MSW admission - 25 kg/h).

Results show that increasing CDMR positively influences the gas yield and negatively influences the tar content. Since CO_2 addition enhances both char gasification and pyrolysis, which leads to increase in carbon conversion, gas yield is expected to increase. The catalyst effect of CO_2 enhances thermal cracking of volatiles leading to a substantial decrease in tar content. In fact, some authors found tar mitigation up to 50% when CO_2 was added [64].

Despite no results in the literature were found for MSW, those available for biomass are in agreement with the obtained results [59-61]. Since the municipal wastes considered consist of over 85% of cellulosic material is safe to say that the trends for MSW will be similar to the biomass.

5.2.4. Effect of Reactor Temperature

Gasification temperature is one of the most influential factors affecting the product gas composition and respective properties. The main reactions of the gasification process are endothermic and thus strengthened by increasing temperature. Since the water gas, water gas shift, steam reforming and Boudouard reactions occur simultaneously, the contents and ratios of H_2, CO, CO_2 and C_nH_m in the product gas are affected by temperature and partial pressures of reactants. As shown in Figure 5.10, higher temperatures considerably resulted in higher H_2 contents.

At temperatures above 750 °C, the endothermic nature of the H_2 production reactions (steam reforming and water-gas reactions) results in an increase in H_2 content and a decrease in C_nH_m content with an increase in temperature. At temperatures above 850 °C, both steam reforming and the Boudouard reactions dominate, resulting in increases in CO content. It can be concluded that Boudouard reactions, carbon gasification reaction, together with the secondary cracking reactions of tar, were the main factors responsible for the increase in H_2 and CO contents.

Moreover, high temperature also favors destruction and reforming of tar leading to a decrease in tar content and an increase in gas yield because of higher conversion efficiency as it can be observed in the Figure 5.11. The results obtained are also confirmed in the literature [65, 66].

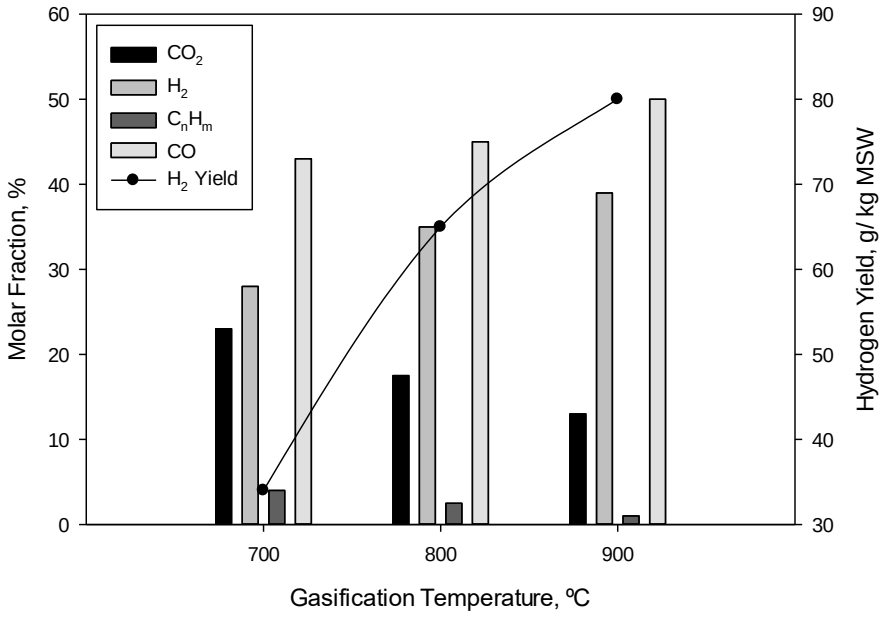

Figure 5.10 - Influence of temperature on syngas molar fraction and hydrogen yield. Dry and N_2-free basis. (Operating conditions: ER - 0.25; SBR - 1; CDMR - 0.4; MSW admission - 25 kg/h).

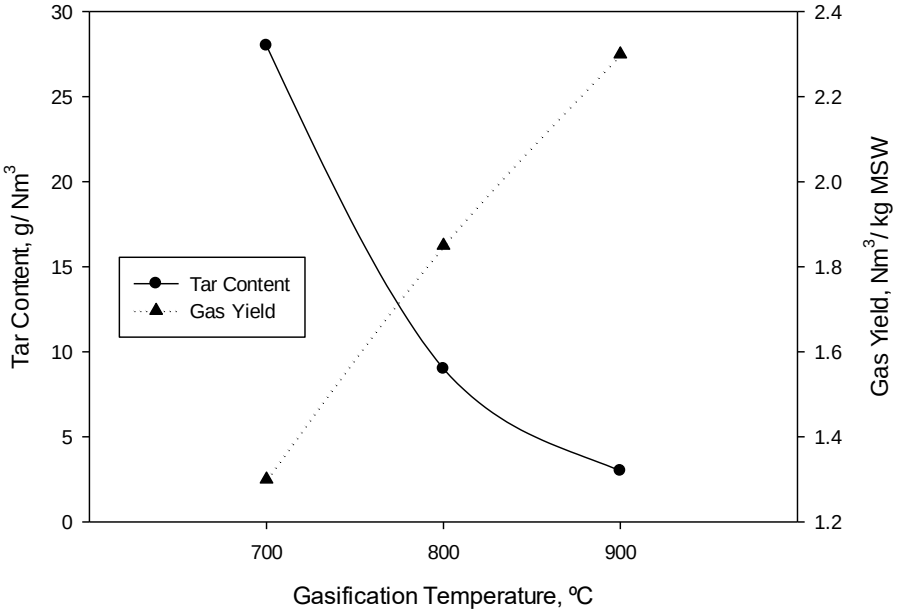

Figure 5.11 - Influence of temperature on tar content and gas yield. Dry and N_2-free basis. (Operating conditions: ER - 0.25; SBR - 1; CDMR - 0.4; MSW admission - 25 kg/h).

5.2.5. Effect of Catalysts for MSW Gasification

The use of catalysts in biomass gasification may not be essential, but it can help under certain conditions being the tar formation one of the major issues. In fact, during MSW gasification process tar is formed and some catalysts can be used to eliminate or at least greatly diminished the tar produced. The choice of a catalyst for reforming reactions is to be made keeping in mind their purpose and practical use. Earth metal catalysts such as dolomite had attracted much interest in this regard, because it is inexpensive and abundant and can notably reduce the tar content of the product gas from a gasifier [67]. Ni-based catalysts are highly effective as a reforming catalyst for reduction of tar as well as for correction of the CO/H_2 ratio through methane conversion. Nickel is relatively inexpensive and commercially available though not as cheap as dolomite. Simulations were performed considering 3 different scenarios: no catalyst, using dolomite and using NiO catalyst such as in Jingbo *et al.* [55]. Figure 5.12 shows this comparison for ER equal to 0.25, SBR equal to one and CDMR equal to 0.4.

As far as the composition of the produced gases is concerned, hydrogen remarkably increases (the production is more than twice and three times using dolomite or NiO/MD, respectively). NiO/MD led to the lowest hydrocarbons (C_nH_m), with reductions around 50 %, and to the highest H_2 contents. Both of these factors indicate that dolomite and NiO/MD are active for tar destruction but not for methane reforming, as is to be expected. There is also an increase in the production of CO and the decrease of CO_2.

Dolomite usually shows some catalytic effect in promoting hydrocarbons destruction by cracking reactions, steam reforming reactions and CO_2 reforming reactions. Thus, CO and H_2 contents are expected to increase, as shown in Figure 5.13.

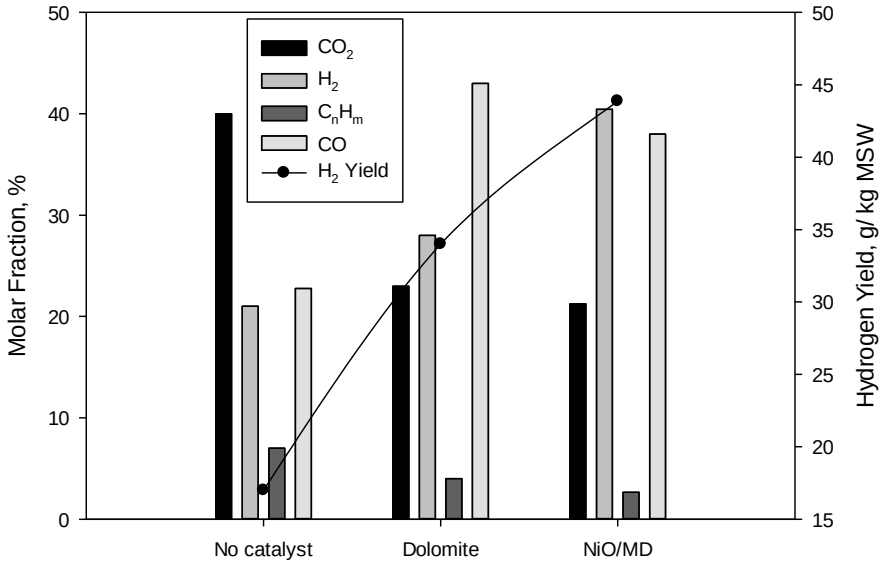

Figure 5.12 - Influence of catalyst type on syngas molar fraction and hydrogen yield. Dry and N_2-free basis. (Operating conditions: ER - 0.25; SBR - 1; Temperature - 700 ºC; CDMR - 0.4; MSW admission - 25 kg/h).

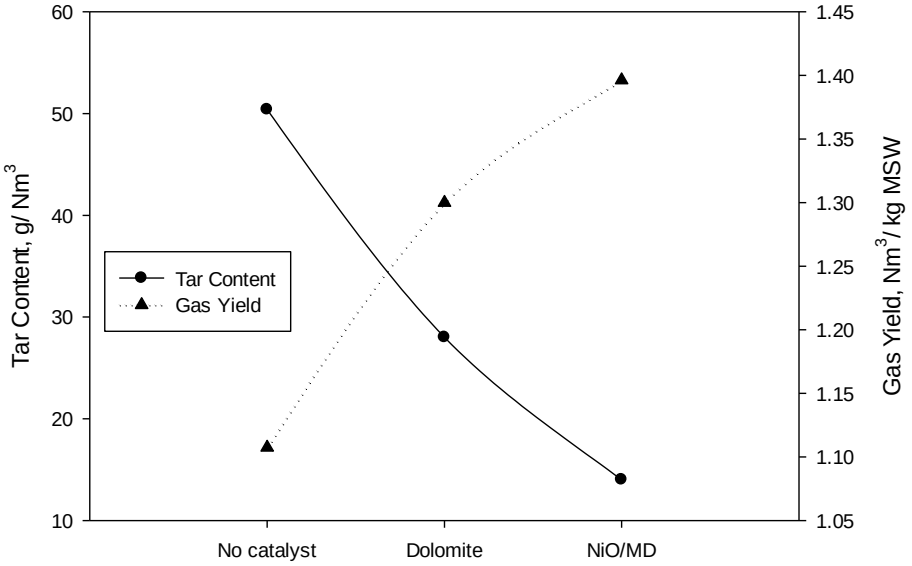

Figure 5.13 - Influence of temperature on tar content and gas yield. Dry and N_2-free basis. (Operating conditions: ER - 0.25; SBR - 1; Temperature - 700 ºC; CDMR - 0.4; MSW admission - 25 kg/h).

Figure 5.13 shows the results obtained under the same conditions save for the nature of the bed inventory material. A remarkable difference in the results is immediately apparent when some catalyst is introduced in the reactor bed: the production of gas increases by more than 20 % using dolomite and by more than 30 % using NiO/MD, with a consequential and also remarkable reduction in tar content by 2 fold (dolomite) and 4 fold (NiO/MD).

5.2.6. Effect of Biomass Substrate

To assess the potential of Portuguese municipal residues a comparison was made with 3 characteristic biomass substrates previously studied. Coffee husks [46], forest residues [68] and vines pruning residues [69] were studied using the described pilot-scale thermal gasification plant, for which relevant energetic as well as economic benefits were found. Figure 5.14 shows the syngas molar fractions for all four fuels.

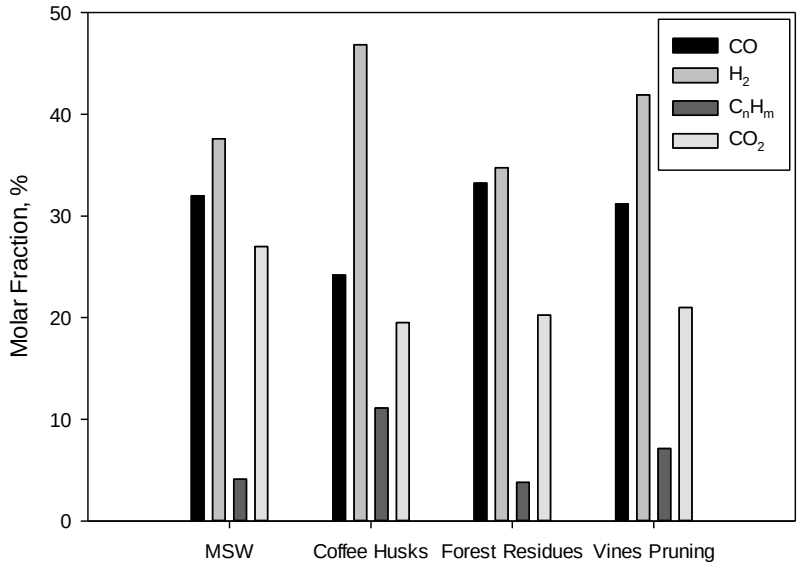

Figure 5.14 - Influence of substrate type on syngas molar fraction and hydrogen yield. Dry and N_2-free basis. (Operating conditions: ER - 0.25; SBR - 1; Temperature - 700 ºC; CDMR - 0.4; MSW admission - 25 kg/h).

For this particular set of operating conditions coffee husks presents both the highest H_2 and C_nH_m molar fractions, while forest residues presents both the highest CO and CO_2 molar fractions. This can be explained by the chemical composition of each fuel. In fact, biomasses with a low C:H ratio and low O_2 content are responsible for maximum H_2 and CH_4 yields while biomasses with low O_2 content and high C:H ratio are responsible for maximum CO and CO_2 yields. This is consistent with the work of Louw *et al.* [70].

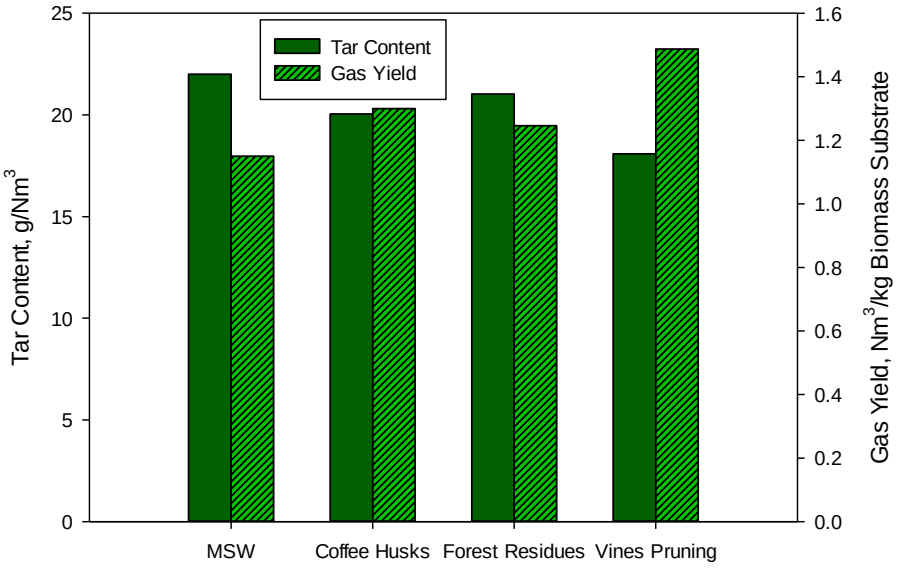

Figure 5.15 - Influence of substrate type on tar content and gas yield. Dry and N_2-free basis. (Operating conditions: ER - 0.25; SBR - 1; Temperature - 700 ºC; CDMR - 0.4; MSW admission - 25 kg/h).

Figure 5.15 shows the influence of substrate type on tar content and gas yield. Vines pruning presents both the highest gas yield and the lowest tar content while MSW presents both the lowest gas yield and the highest tar content. This can be explained by higher volatile content leading to an increase in residence time that in turn will favor gasification reactions which leads to a higher gas yield [71]. Moreover, promoting gas yield is known for improving tar decomposition. This is consistent with the literature on the subject [72].

Since MSW has the lowest volatile content from the studied fuels [46], it comes with no surprise that it also presents the highest tar content.

5.3.Syngas Quality Indices

Syngas quality indices such as H_2/CO and CH_4/H_2 ratios are very important for choosing the correct application for each produced syngas. For domestic purposes a higher CH_4/H_2 ratio is preferable. For the chemical industry H_2/CO ratio as well as the sum of H_2 and CO gas percentages are two important measures of syngas quality [73]. A syngas with a high percentage of CO+H_2 has strong reducing power, while a high value of the ratio H_2/CO indicates a syngas useful for chemical syntheses [73]. In fact, H_2/CO ratio higher than 1.70 should be presented in syngas to make it useful for chemical industries to syntheses products such as methanol and virgin naphtha. Whereas such a ratio is easily obtained by gasifying methane, it is not possible by gasifying other wastes. Increase in H_2/CO ratio can only be accomplished by an injection of water [73]. Figure 5.16 shows the influence of gasification temperature and ER on syngas CH_4/H_2 molar ratio.

From Figure 5.16 is clear that CH_4/H_2 ratio sharply decreases with gasification temperature. This can be easily explained referring that, according to Le Chatelier´s principle, increasing temperature will promote higher levels of H_2. And on the other hand, due to the strengthening of the endothermic steam-methane reactions a decrease in CH_4 fraction is also expected. It is also clear that influence of gasification temperature diminishes with higher temperature simply because within the temperature range studied, decrease in CH_4 is somewhat constant while at higher temperature endoenergetic reactions will favor CO formation instead of H_2. This phenomenon will be further explained later in this section. Influence of ER on CH_4/H_2 ratio is very small since it decreases both species in the same way, although since H_2 fraction is much larger is easy to detect smaller changes than CH_4.

Since MSW intake virtually has no impact on CH_4/H_2 ratio no graph is presented on the subject.

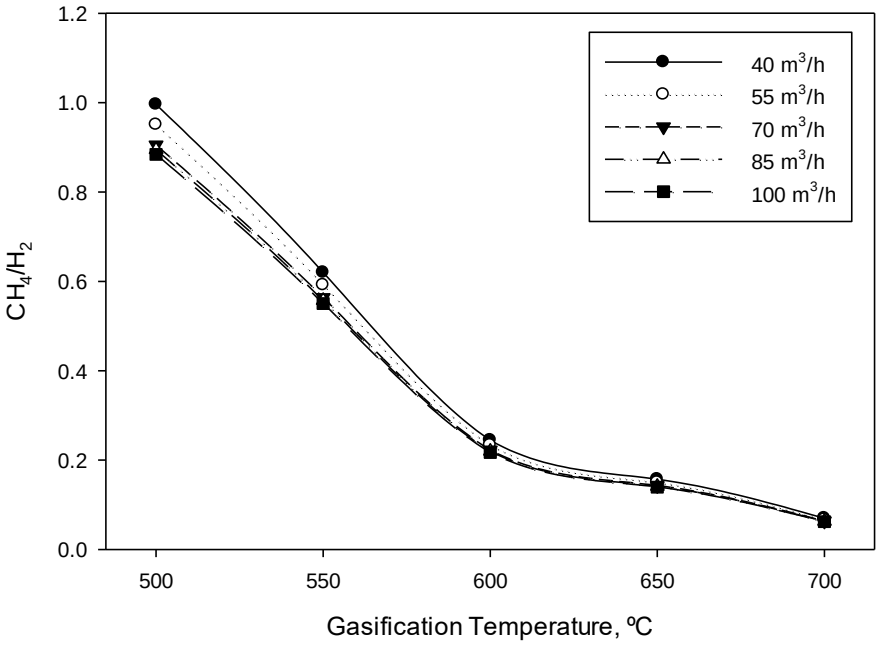

Figure 5.16 - Syngas CH_4/H_2 molar ratio as a function of the temperature and air flow rate (MSW feeding rate = 25 kg/h).

Figure 5.17 shows the influence of gasification temperature, ER and MSW admission on syngas H_2/CO molar ratio. Figure 5.17a uses operating conditions MSW feeding rate equal to 25 kg/h while Figure 5.17b uses constant air flow (40 m^3/h) to study gasification temperature and MSW admission.

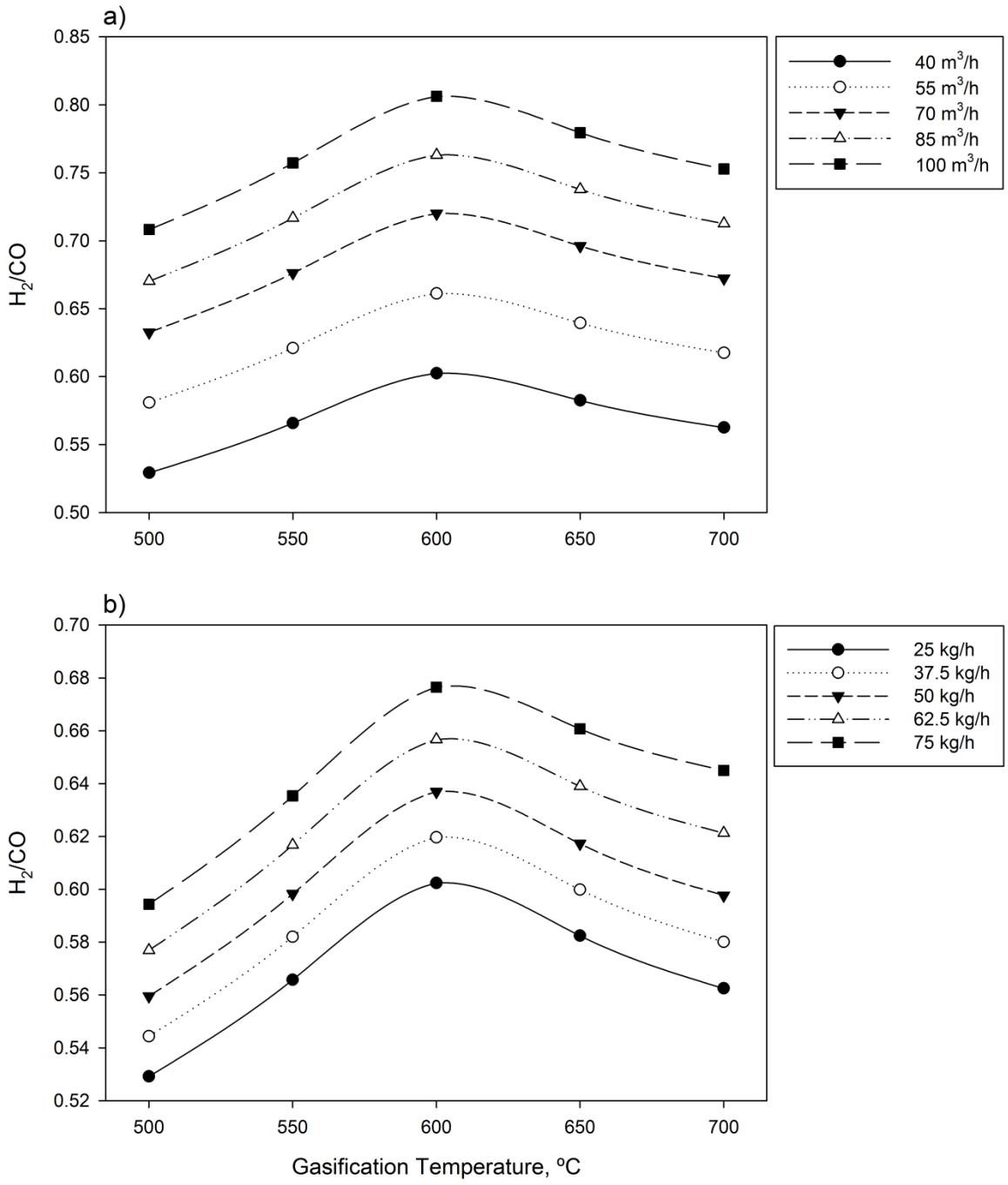

Figure 5.17 - Syngas H_2/CO molar ratio as a function of the temperature and a) air flow rate (MSW feeding rate = 25 kg/h) and b) MSW admission (operating conditions: Air flow rate = 40 kg/h).

From analyzing Figure 5.17 it can be seen that at low temperatures, gasification temperature has a positive influence on H_2/CO ratio but at higher temperatures the opposite trend occurs. This is due to the fact that at low temperatures H_2 production is enhanced by primary water-gas reaction as well as steam-methane reforming reactions while at higher temperatures primary water-gas as well as Boudouard reaction will favor more CO production. At the same time, by reverse water-gas shift reaction, H_2 is actually converted to CO and a faster growth rate is observed in CO than H_2. This is consistent with [74].

A low ER ensures high syngas quality due to higher values of the combustible gases. Nevertheless, when the ER is too low, the gasification agent cannot supply enough oxygen to convert char into CO or CO_2. Like was previous mentioned, increase in ER favors the partial combustion of char, CO and H_2.

As was to be expected MSW admission has a positive effect on H_2/CO ratio simply because MSW admission barely has any effect on H_2 fraction while having a negative effect on CO, and therefore affecting positively the H_2/CO ratio.

Even though data regarding similar operating conditions as well as reactor dimensions are very limited in the literature, results from both CH_4/H_2 and H_2/CO indices appear to follow the common trend among them [52, 75, 76].

Obviously results will always slightly diverge not only due to different gasifier geometries and operating conditions but, equally important, different MSW material properties.

To complete the study on syngas quality and the gasification performance it is necessary to study both carbon conversion as well as cold gas efficiency.

The carbon conversion defines the fraction of carbon from MSW converted to carbon in syngas composition. It gives an indication of the amount of unconverted material and provides a measure of chemical efficiency of the process. It can be given by:

$$Carbon\ Conversion = \frac{12 \times M}{X_c \times m} \quad (5.1)$$

Where M is the total mole flow of carbon in the syngas components X_C is the carbon fraction in the MSW and m is the MSW flow into the gasifier.

CGE can be defined as the percentage of the heating value of MSW converted into the heating value of the product gas. It can be computed as follows:

$$CGE = \frac{Gas\ Yield\ \times HHV\ of\ Syngas}{HHV\ of\ Fuel + Heat\ Addition} \quad (5.2)$$

Figures 5.18 and 5.19 describe the influence of gasification temperature as well as ER on CC and CGE, respectively.

According to Figure 5.18 and 5.19, gasification temperature appears to have a positive effect on both carbon conversion and cold gas efficiency. Increase of CO and H_2 content with temperature can explain this trend. At lower temperatures the system efficiency as well as carbon conversion showed a relatively small growth with rising temperature, because of the sustained decrease in CH_4 molar fraction. This is consistent with [75, 76].

Increase on ER has negative effects in both carbon conversion and cold gas efficiency. This has to do with higher levels of CO_2 being produced with ER. Also it is expected that CGE should decrease with ER since the combustible gases decrease with ER.

According to Arena and Gregorio [77] the typical ranges of variation on process performance parameters in air or oxygen-enriched air gasification of municipal solid waste are: 90 to 99 % carbon conversion efficiency; 50 to 80 % cold gas efficiency; 4 to 7 MJ/Nm^3 syngas low heating value. It can be noted that all the results presented so far fall within the range. Again, some minor discrepancies may be found but the errors can be assumed as very reasonable for such a complex system.

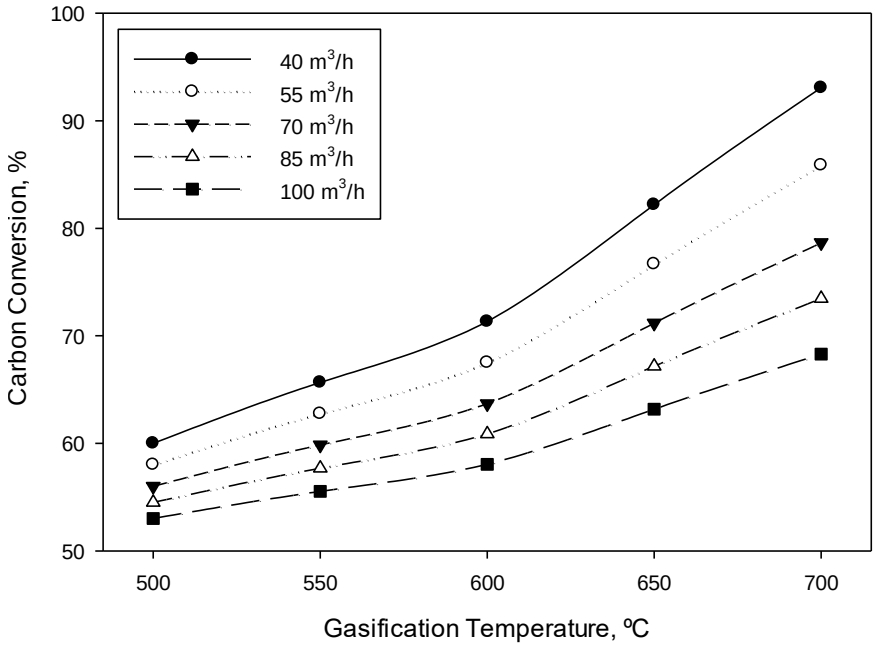

Figure 5.18 - Carbon Conversion as a function of the temperature and air flow rate (operating conditions: Air flow rate = 40 kg/h).

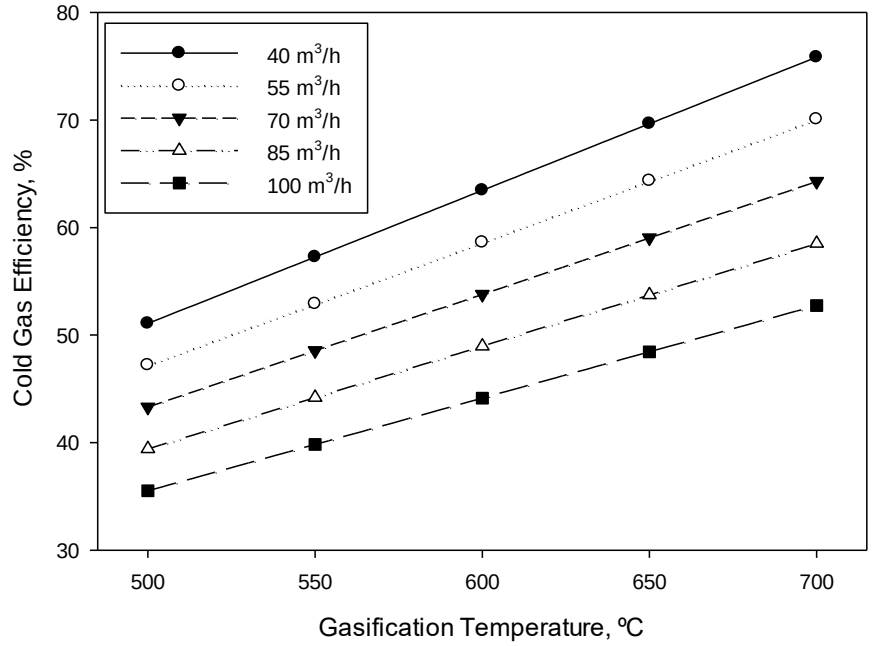

Figure 5.19 - Cold Gas Efficiency as a function of the temperature and air flow rate (operating conditions: Air flow rate = 40 kg/h).

5.4.Thermodynamic Evaluation

5.4.1. Energy Values

Based on 1 kg MSW, the energy values of syngas and tar from air gasification at different gasification temperatures and ER values are calculated and analyzed.

5.4.1.1.Syngas Energy Values

The energy values of syngas components at various ER values are shown in Figure 5.20. As stated, by increasing ER, more active combustion reactions, such as the partial combustion of char, CO and H_2 will occur leading to higher levels of CO_2 and H_2O at the cost of CO and H_2 [78]. C_nH_m presents a very low molar fraction level and it decreases slightly with increase of ER due to strengthening of steam reforming reaction. N_2 is expected to increase simply because additional air is entering the gasifier.

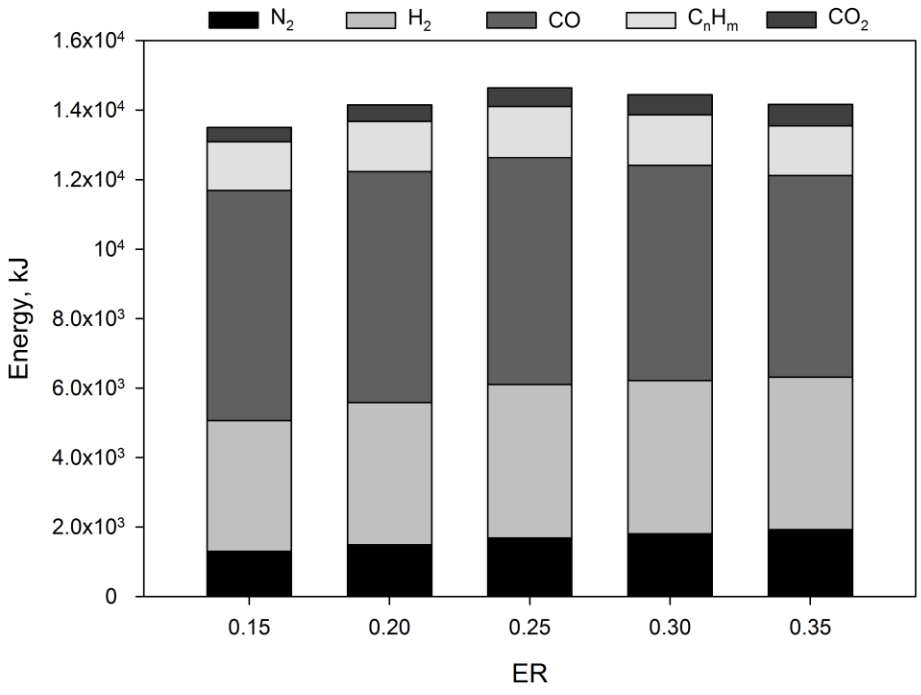

Figure 5.20 - Energy values of gas components at various ER values.

From Figure 5.20 one can see that when ER was increased from 0.15 to 0.25 syngas total energy value increased from 13,507 kJ to 14,642 kJ and then decreased to 14,169 kJ when ER was further increased to 0.35. This can be explained by the initially increase in the gross heat of combustion contained in syngas when air is added due to conversion of solid carbon. At the solid carbon boundary, addition of further air leads to a decrease in the combustion energy and an increase in sensible energy of the gas. This is consistent with the current literature [43, 63].

Current literature agrees that reactor temperature is one of the most influential factors affecting the product gas composition and related properties [79]. It is thus imperative to analyze its influence on syngas energy values as well.

Figure 5.21 shows the effects of reactor temperature on the total syngas energy. Since syngas energy values are determined by its enthalpy and molar yield (as shown in chapter 4) they are expected to increase with increasing temperature. In fact, when the reactor temperature was increased from 700 to 900 ºC the total energy of syngas increased from 13,507 to 18,219 kJ.

Comparing both parameters, one can see that the effect of reactor temperature on the total syngas energy (34.9 %) was much greater than that of ER (8.4 %). This is consistent with the current literature [39]. One can notice that energy values follow a similar pattern to that found for syngas composition. This has to do with energy values being determined by the temperature and yield of each individual gas component.

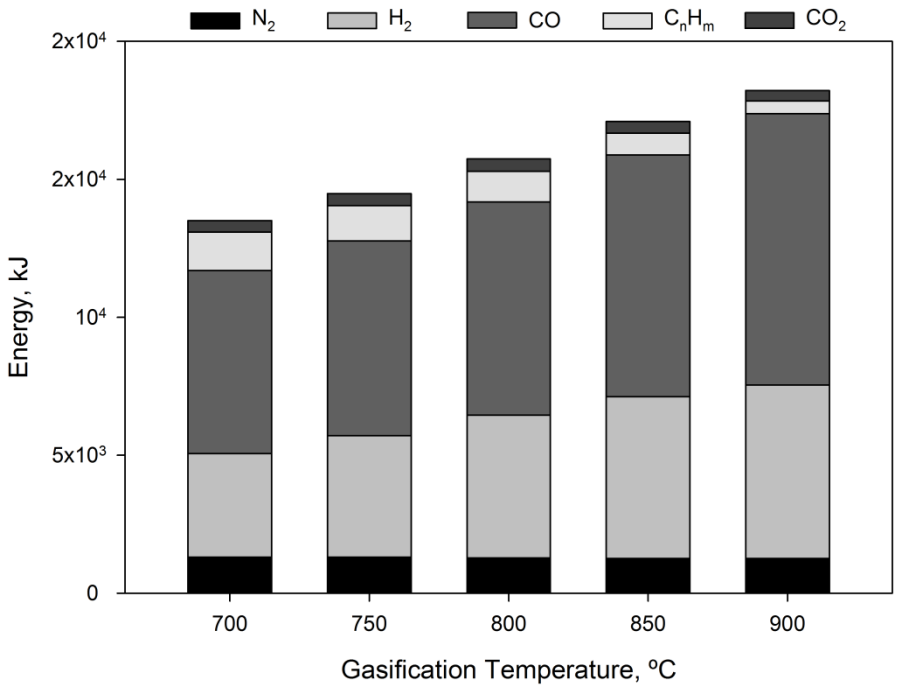

Figure 5.21 - Energy values of gas components at various reactor temperatures.

5.4.1.2.Tar Energy Values

Although attempts have been made to suppress tar production from the gasification process it is still one of the main concerns keeping the technology from being widely use and commercially successful. Because of this, it is a necessity to increase the efforts on studying this undesired by-product and ways to suppress or at least greatly diminished it. A main absence can be found on the current literature for thermodynamic analysis of tar production, especially for industrial conditions. Figure 5.22 exhibits tar energy values at different reactor temperatures and ER values.

Contrary to syngas, both gasification temperature and ER present the same trend when it comes to tar energy values. This is mainly due to increases in gasification temperature and ER leading to lower tar yields. Although higher gasification temperatures are known for increasing physical energy, a dramatically reduction in tar yield will lead to a decrease in the total physical energy of tar content. This decrease in tar yield was already explained and

it is due to the enhancement of tar cracking reaction at elevated temperatures. This is consistent with the current literature [80, 81].

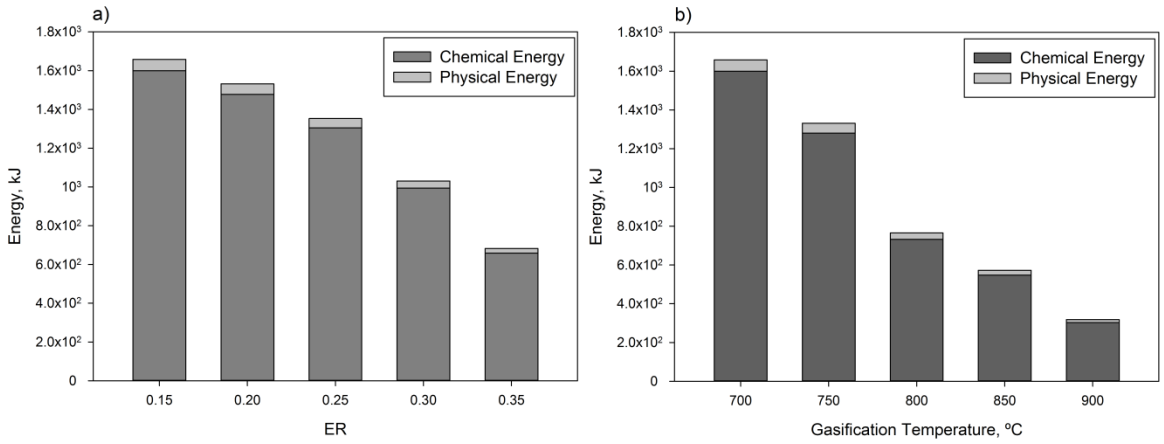

Figure 5.22 - Energy values of tar content at various a) ER values and b) reactor temperatures.

5.4.2. Exergy Values

Based on 1 kg MSW, the exergy values of syngas and tar from air gasification at different gasification temperatures and ER values are calculated and analyzed.

5.4.2.1.Syngas Exergy Values

Following the sequence establish in the previous chapter, Figure 5.23 presents the exergy values of gas components at various ER values and temperatures. Regarding calculations, exergy values primarily differ from the energy values due to the inclusion of entropy.

After careful examination, one can see that Figure 5.23 shares great similarities with Figures 5.20 and 5.21. In fact, exergy values are lower than energy values while sharing the same trends. This can be easily understood since both physical and chemical exergy values tend to be lower than the corresponding energy values. This is consistent with the current literature [78, 82]. Similarly to Figure 5.20, Figure 5.23a also presents a maximum value for ER = 0.25. According to Prins *et al.* [83], and clearly witness in the presented results, past this maximum ER value, both energy and exergy values decrease due to a decrease in

both chemical energy (and exergy) which is not fully compensated for by the increases in the physical energy (and exergy).

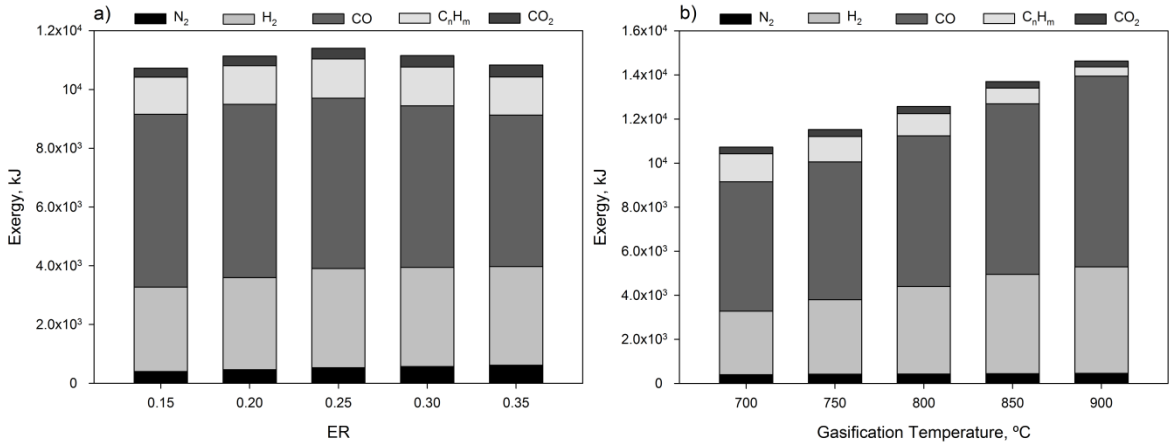

Figure 5.23 - Exergy values of gas components at various a) ER values and b) reactor temperatures.

Regarding influence of reactor temperature, when temperature was increased from 700 to 900 ºC, exergy values went from 10,727 to 14,632 kJ (increase over 36 %). This is a clear statement on the effect gasification temperature has over ER, which only gained 6.3 % (from 10,727 to 11,407 kJ) when ER was increased from 0.15 to 0.25.

5.4.2.2.Tar Exergy Values

Figure 5.24 exhibits tar exergy values at various ER values and temperatures. When ER is increased from 0.15 to 0.35, exergy values decline from 1,611.75 to 663.61 kJ. Similarly, increase in gasification temperature leads to a drastic reduction in exergy values from 1,611.75 to 307.40 kJ. These trends can be explained by the promotion of gas yield by both ER and gasification temperature leading to tar decomposition [84]. This is consistent with the current literature [80].

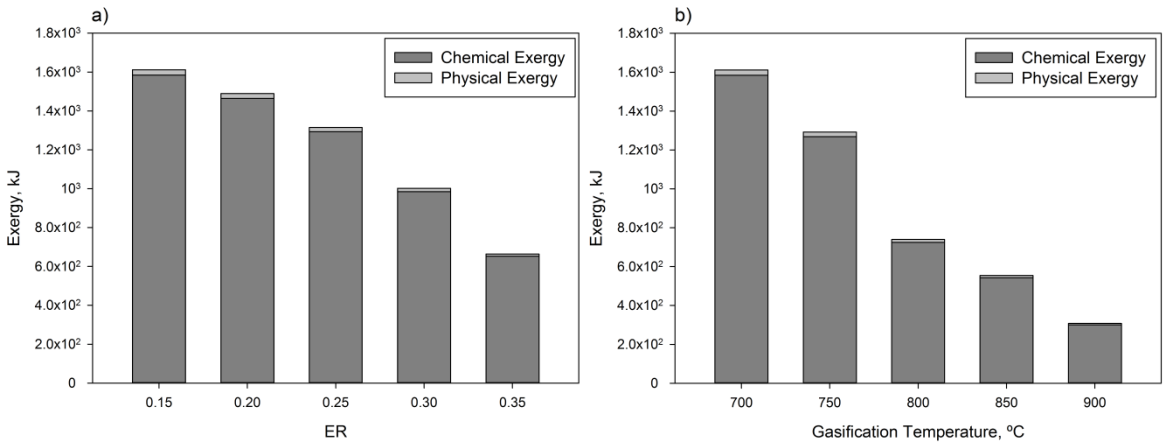

Figure 5.24 - Exergy values of tar content at various a) ER values and b) reactor temperatures.

5.4.3. Process Efficiency

Most of the scientific community defines the efficiency of given process as the ratio of desired output over input. Regarding gasification process, its efficiency is usually defined by the cold gas efficiency. Despite being an important parameter it has some shortcomings, especially neglecting the energy in the unconverted char as well as the sensible heat of the produced gas and in particular, the increase in entropy due to conversion of a solid fuel into gaseous compounds [83]. Because of this it is imperative to also study exergy efficiencies since they avoid said drawbacks. Figure 5.25 shows the energetic and exergetic efficiencies of gas components and tar content at various ER values and reactor temperatures.

After careful analysis one can see that both energy and exergy efficiencies follow the same trend presented by their respective values. This is expected since efficiency values are mostly determined by their energy/exergy values [80]. Efficiency based on LHV is higher than both exergy efficiencies. This was already addressed and is due to increase in entropy being disregarded in the energy efficiency. Obviously chemical and physical exergy based efficiency is higher than just chemical exergy based efficiency since physical exergy presents a positive value [85].

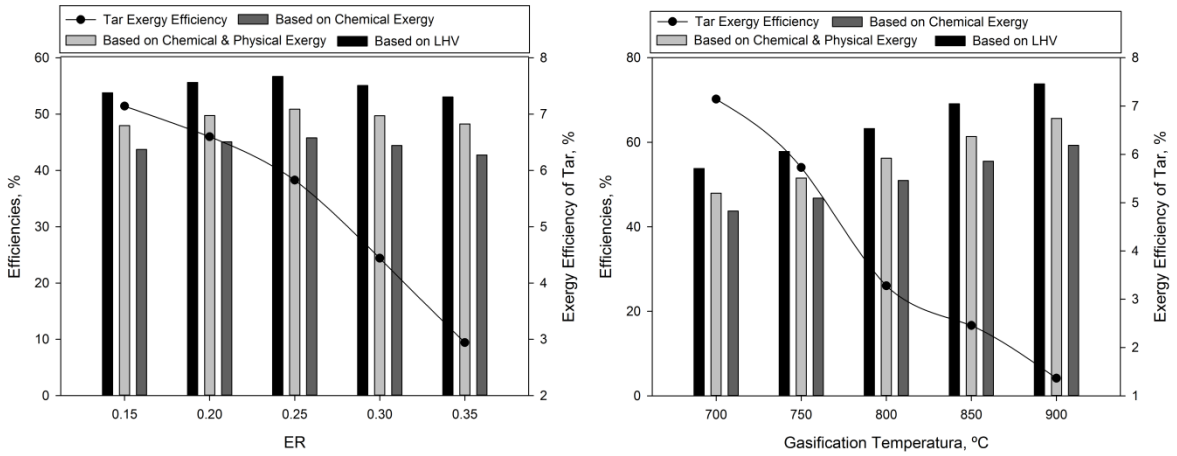

Figure 5.25 - Comparison between gasification efficiencies at various a) ER values and b) reactor temperatures.

Regarding ER influence on gasification efficiencies, when ER was increased from 0.15 to 0.25 LHV based efficiency increased from 53.8 to 56.7 %, chemical exergy based efficiency rose from 43.7 to 45.8 % and chemical and physical exergy based efficiency increased from 48 to 50.9 %. After 0.25 all efficiencies decreased almost linearly. According to Double and Bridgwater [86], this point represents the optimum point of operation for an air-blown biomass gasifier, giving an excellent indication where the gasifier should operate to be at the highest efficiency level possible. This is consistent with the current literature [15, 83].

Reactor temperature influence on the other hand presents a very different tendency. In fact, when temperature was increased from 700 to 900 ºC, LHV based efficiency increased from 53.8 to 73.8 %, chemical exergy based efficiency rose from 43.7 to 59.3 % and chemical and physical exergy based efficiency increased from 48 to 65.7 %. Indeed all studied efficiencies steadily rose within the studied range at a much higher rate when compared to ER. This is due to increase in gasification temperature promoting both endothermic reactions and gas yield. This is consistent with the current literature [15, 81].

Tar exergy efficiencies follow a very close trend to tar exergy values presented in Figure 5.24. Both ER and reactor temperature led to a drastically decrease in tar efficiency. When ER was increased from 0.15 to 0.35 tar efficiency decreased from 7.2 to 2.9 %. Conversely, when temperature was increased from 700 to 900 ºC tar efficiency decreased from 7.2 to 1.4 %. This was already explained and has to do with the fact that higher gasification temperatures dramatically reduce tar yields. This is consistent with the current literature [80, 87].

To better understand the gasifier's overall energy flow a Sankey diagram was created. These diagrams are great visualization process tools and in this particular case were used to map energy consumption and corresponding transformation from source (MSW and air) to end use (syngas and tar). Figure 5.26 displays the created Sankey diagram for the optimal set of operational conditions found in the thermodynamic analysis.

Even with a simplified diagram one can clearly see the overall energy flow thus quickly identifying system's efficiency (instead of power one could display the same diagram in terms of efficiency) and the overall losses. Ideally one would apply these diagrams to the entire plant to identify the sectors with the highest potential for improvement as well as identifying measures to reduce GHG emissions [88].

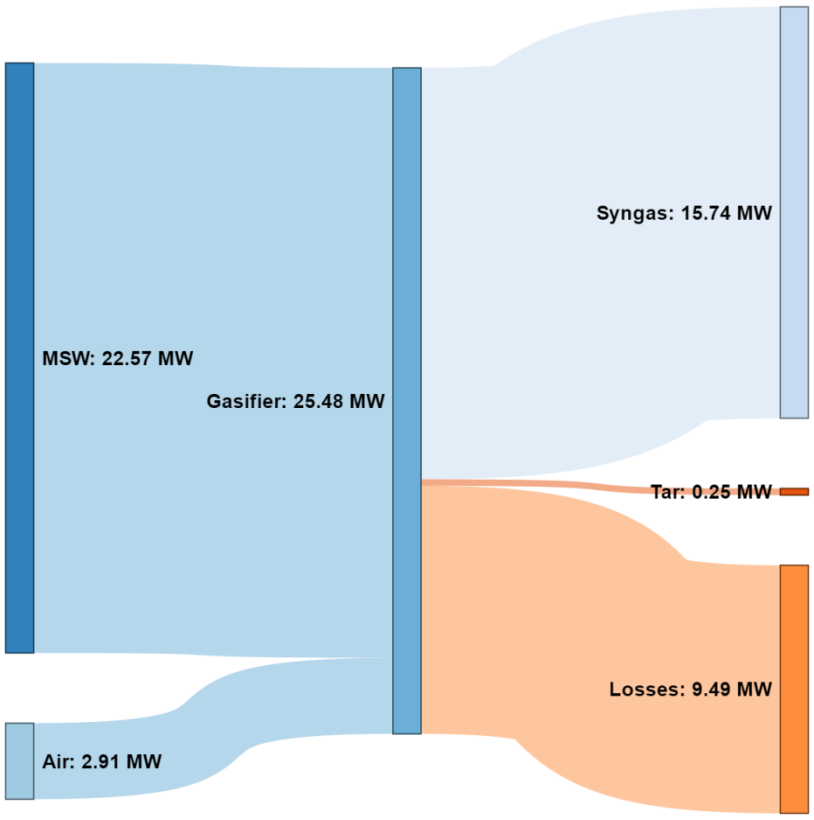

Figure 5.26 - Sankey diagram (Operational conditions: ER - 0.25; Gasification temperature - 900 ºC).

5.5.Multi-Stage Optimization in a Pilot Scale Gasification Plant

Optimized operation conditions for complex systems can be attained by using advanced combinations of numerical and statistical methodologies such as design of experiments and response surface methods [89, 90]. DoE deals with several factors where all of them are varied altogether, instead of one at a time [89]. The great advantage of implementing this strategy is its success to consider multiple interactions between the factors. Furthermore, it also significantly reduces the number of runs necessary to extract meaningful information from data. Few works are found in the literature devoted to the use of DoE and RSM to analyze and optimize the operating conditions in gasification related processes [91-95]. Carpenter *et al.* [91] performed a total of 22 statistically designed experimental conditions to study the effects of fluidized bed temperature, the temperature of the secondary thermal

cracker, and steam-to-biomass ratio on the gasification of four feedstocks. The authors concluded that there were significant differences between the feedstocks studied in terms of light gases formed. Karimipour *et al.* [92] applied RSM to the fluidized bed gasification of lignite coal considering as input factors coal feed rate, coal particle size and steam/O_2 ratio and as responses the quality of syngas evaluated based on five indices including carbon conversion, H_2/CO ratio, CH_4/H_2 ratio, gas yield, and gasification efficiency. They were able to find the best operating conditions to achieve syngas with a desired quality for different applications. To assess the combined effects of the operating variables on high-pressure coal gasification, Fermoso *et al.* [93] used a face centered central composite design based on RSM. Results revealed the effects of interaction between the tested variables, which would not have been possible by a traditional method. Silva and Rouboa [94] combined a thermodynamic dual stage model with RSM to optimize both hydrogen generation and cold gas efficiency by using forest residues for gasification. By using the operational conditions and desirability functions they were able to find the optimal conditions to achieve considerable economical energy savings without reducing the hydrogen generation. Coetzer and Keyser [95] used the method of factorial experimental design on the input factors of interest from a full-scale test gasifier concerning the Sasol-Lurgi coal gasification process. They developed empirical models (by using RSM) able to fit experimental data under different data sets. They concluded that the factorial experimental design combined with response surface analysis could be applied to a full-scale production process.

Because experimental runs conducted on industrial gasification plants or even on pilot scale gasification plants are very expensive, predictable models able to simulate the syngas composition and other responses of interest are required. Accurate predictions by

gasification models require the simulation of different kinetic and hydrodynamic phenomena while taking into account complex chemistry. There are few reports on the literature combining advanced statistical strategies with predictive models applied to gasification processes to find the most efficient combination of process variables that might be used during normal operation. Even fewer reports are found considering strategies to ensure a sustainable gasifier operability and throughput with minimal variations on the syngas generation (robust process) [47, 96]. Silva and Rouboa [47] coupled the results obtained from a 2D Eulerian–Eulerian biomass gasification model developed under the CFD framework with RSM to find the best operating conditions to generate syngas for different applications. Later, they proceed to do a multiple optimization coupling each one of the studied responses with the minimization of the error propagation. The authors were able to find the operation conditions that guaranteed both the best response and minimal variations caused by input factors.

5.5.1. Empirical Model Validation

Guidelines from good statistical practices suggest that an empirical model should be kept as simple as possible. Additional terms should be only included if they would be able to explain variation beyond what's already accounted for [97]. A very expedite tool to select how far one should go on adding polynomial terms to the empirical model is the sequential model sum of squares. SMSS provides the p-values for the model's term sources. Table 5.5 depicts the SMSS results for hydrogen generation. Similar analysis was carried out for all the other studied responses.

From Table 5.5, one can conclude that both linear (A, B and C) and quadratic (A^2, B^2 and C^2) terms can explain the process variation showing the smallest p-values. The table also

depicts another statistical measure, the F value. Larger values of F imply more significant factors similarly to small p-values. When p-values are larger than 0.1 the terms are not by themselves considered as significant. The cubic terms are aliased so they should not be included. Quadratic model also includes linear and interaction terms (AB, BC, etc.), so this solution should be the one selected.

Table 5.5 - Sequential model sum of squares (hydrogen generation).

Source	**Sum of Squares**	**F Value**	**p-value Prob > F**
Mean vs Total	1539.22		
Linear vs Mean	586.25	466.92	< 0.0001
2FI vs Linear	3.72	4.2	0.0185
Quadratic vs 2FI	5.81	348.42	< 0.0001
Cubic vs Quadratic	0.073	4.85	0.0127
Residual	0.021		
Total	2135.09		

The development of the empirical model is based on Eulerian-Eulerian simulations under the CFD framework. Computer based simulations will always provide the same solution at certain operating conditions implying that the concept of replicates becomes meaningless. At these circumstances, the use of some statistical measures such as lack of fit do not bring any data of interest for analysis purpose.

However, measures such as R^2, R^2_{adj} and R^2_{pred} are still useful. The R^2 measures how well the model is able to fit correctly the experimental data or the computed based simulations as in the present case. The R^2 value can sometimes be misleading causing overfitting the data. The R^2_{adj} counteracts this overfitting giving a more reliable tool to evaluate the data fitting quality.

The R^2_{pred} measures how well the model is able to re-fit the data when one point is missing. When these measures are close enough a high quality fit is expected. Table 5.6 shows the

result of these additional measures. R^2 presents the highest value for the cubic model as expected. Indeed, adding additional terms will inflate the R^2 value. Also, the cubic model is aliased so it cannot be considered as a feasible option. Once again, the quadratic model stands out as the most valuable option with considerable high values for all the R^2 measures.

Table 5.6 - Model summary statistics.

Source	R^2	R^2_{adj}	R^2_{pred}
Linear	0.9838	0.9817	0.9774
2FI	0.9901	0.9871	0.983
Quadratic	0.9998	0.9998	0.9996
Cubic	1	0.9999	0.9997

After selecting the empirical model and before applying it to generate the response surface, it is important to proceed to the analysis of variance and confirm if all terms should be or not included. Myers and Montgomery [98] suggest that in response surface work it is customary to fit the full model. Anderson and Whitcomb [99] state that insignificant terms will not create much impact, so they could be excluded from the model. From Table 5.7, and following Anderson and Whitcomb suggestion, terms AB and A^2 were removed by using a backward reduction algorithm.

The final empirical model to predict the hydrogen generation and shown in coded form is as follows:

$$H_2 = 6.99 - 0.24A - 0.71B + 5.66C - 0.20AC - 0.52BC - 0.13B^2 + 0.97C^2 \qquad (5.3)$$

The coded equation is useful for identifying the relative impact of the factors with their respective coefficients. Positive coefficients mean that increasing the factor leads to a response increase. By default, the high levels of the factors are coded as +1 and the low levels of the factors are coded as -1.

Table 5.7 - ANOVA data.

Source	Sum of Squares	F Value	p-value Prob > F
Model	595.78	11911.5	< 0.0001
A- MSW Feeding Rate	1	179.71	< 0.0001
B - Air Flowrate	8.95	1609.81	< 0.0001
C - Temperature	576.3	103700	< 0.0001
AB	0.016	2.9	0.1066
AC	0.47	84.94	< 0.0001
BC	3.23	581.99	< 0.0001
A^2	0.012	2.24	0.1528
B^2	0.11	19.03	0.0004
C^2	5.69	1023.98	< 0.0001

The last step to conclude about the model adequacy is to diagnose the residual for abnormalities. Basically, differences (residues) between experimental data and the computed model are analyzed to verify if the residuals are pure noise or if there are other reasons behind the residuals patterns. Figure 5.27 depicts the normal probability as a function of internal studentized residuals. As it can be seen from Figure 5.27, only minor deviations are found confirming the assumption of normality.

Also, a very helpful diagnostic can be found by plotting the residuals as a function of the predicted response. Figure 5.28 displays a random scatter which again confirms the usefulness of the developed empirical model. Furthermore, this indicates that is not necessary to consider transforming the responses by using other mathematical functions such as log or square-root. The same procedure was followed considering the other responses. All of them presented minor deviations from normality and constancy of variance and can be accepted as suitable to describe the behavior of the corresponding responses in the experimental design space.

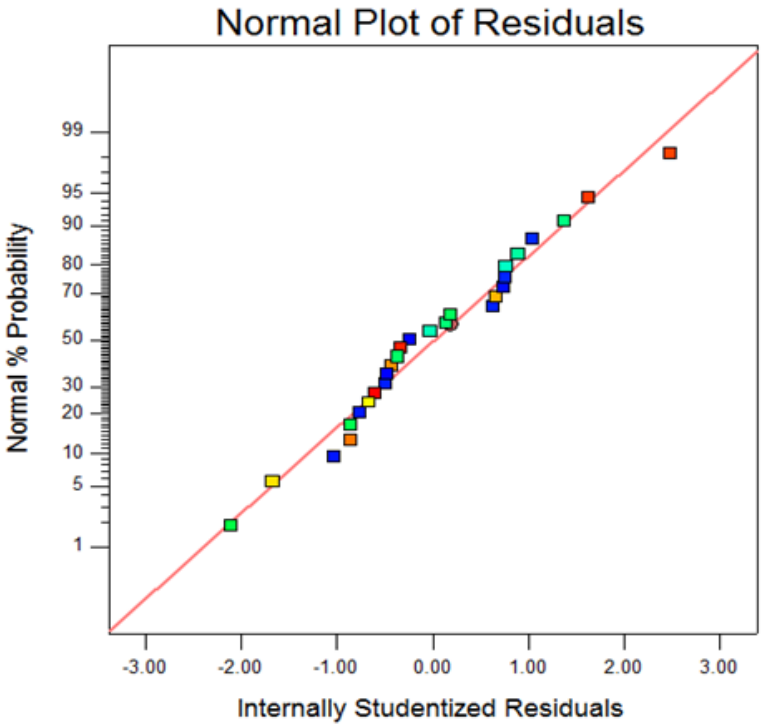

Figure 5.27 - Normal plot of residuals.

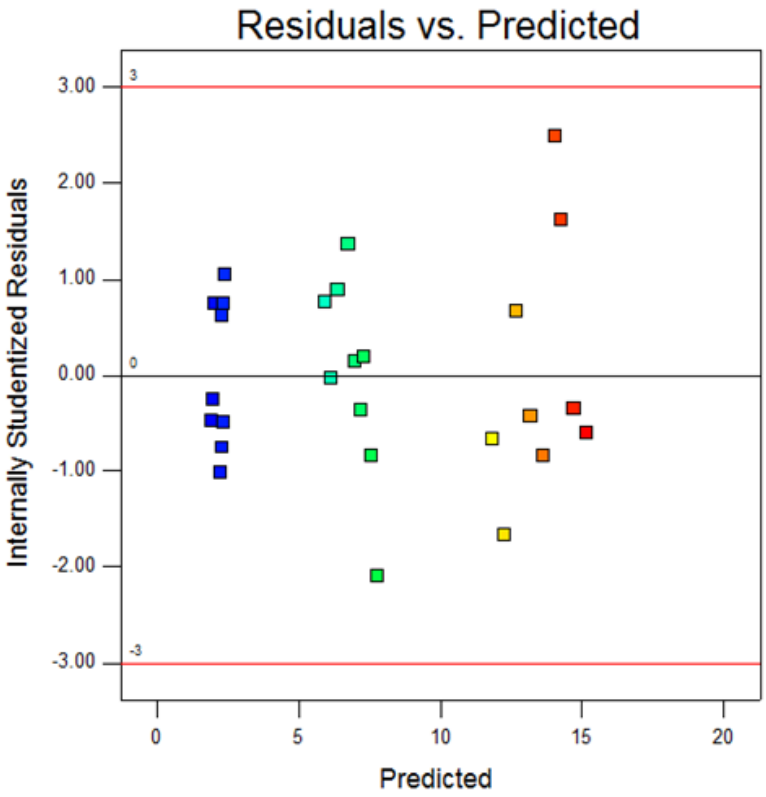

Figure 5.28 - Residuals as a function of the predicted response.

5.5.2. Single Response Optimization

When 3 factors (or more) are studied and it is impossible to depict all factors at once in a graph, it is always interesting to present the perturbation plot. Figure 5.29 displays the effect of changing each one of the selected factors (MSW feeding rate (A), air flowrate (B), and gasification temperature (C)) on the hydrogen generation keeping all other operating conditions constant. The curvatures of each of the three factors from the center point dictate their significance. In this particular case, the sharp curvature of the gasification temperature (C) shows that the response "hydrogen molar fraction" is highly sensitive to this variable. On the other hand, the comparatively low curvatures from both MSW feeding rate (A) and air flowrate (B) shows less sensitivity of hydrogen production towards the change in these two factors. By using the perturbation plot as a departure point, the axis for contour or 3D response surface plots can be easily defined keeping the analysis with the most interesting factors for the process.

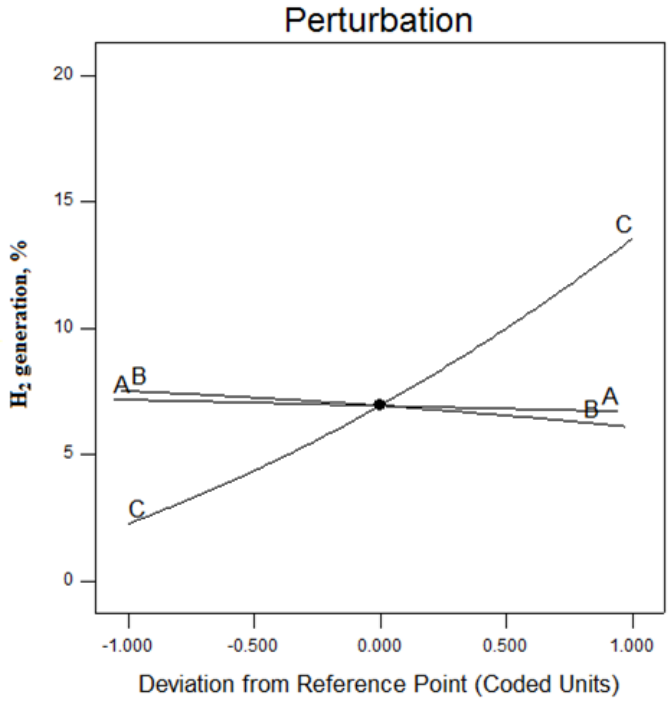

Figure 5.29 - Perturbation plot for hydrogen generation.

Figure 5.30 shows the response contour plots as a function of the most significant factors after running an optimization algorithm for a single response.

Figure 5.30a shows how the studied factors affect hydrogen generation (MSW feeding rate was kept at a constant value of 25 kg/h). Once again, the selected factors to appear in the plot axis are in agreement with the perturbation plot, where large coefficients imply more significant factors. Investigated parameters appear to provoke opposite effects on hydrogen fraction; on one hand H_2 increased (over 6 times) when temperature was increased from 500 to 700 ºC, while on the other hand H_2 decreased (around 16 %) when air flowrate was increased from 40 to 100 m^3/h. Increase in air flowrate will mostly promote oxidizing reactions which explains why hydrogen fraction decreases since these reactions promote both CO_2 and H_2O at the expense of CO and H_2 [78]. Besides, since hydrogen generation reactions are mostly from endothermic nature, an increase in temperature will promote more hydrogen in the syngas mixture, in accordance with Le Chatelier's principle. The operating conditions able to maximize this particular response through the optimization procedure were about 700 ºC and 40 m^3/h. Both the obtained maximum value as well as the overall trends are in agreement with available literature as well as previously attained experimental results [13, 65, 66].

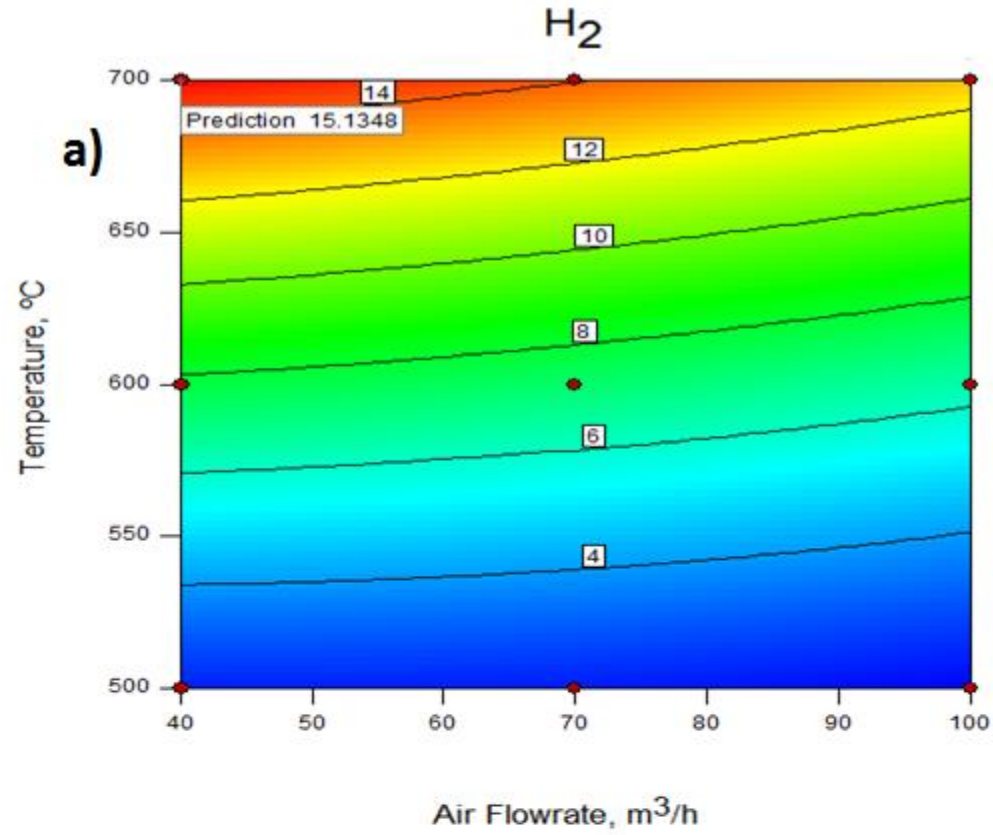
H2
a)
Prediction 15.1348
14
12
10
8
6
4
700
650
600
550
500
Temperature, °C
40
50
60
70
80
90
100
Air Flowrate, m3/h

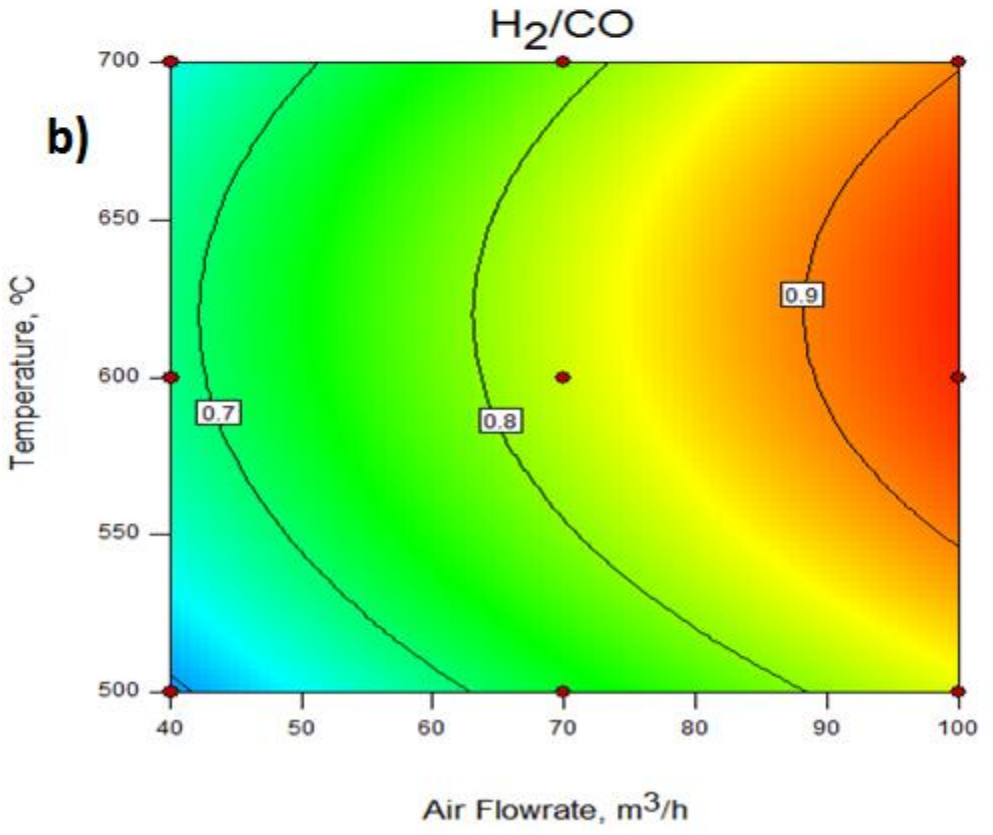
H2/CO
b)
0.7
0.8
0.9
700
650
600
550
500
Temperature, °C
40
50
60
70
80
90
100
Air Flowrate, m3/h

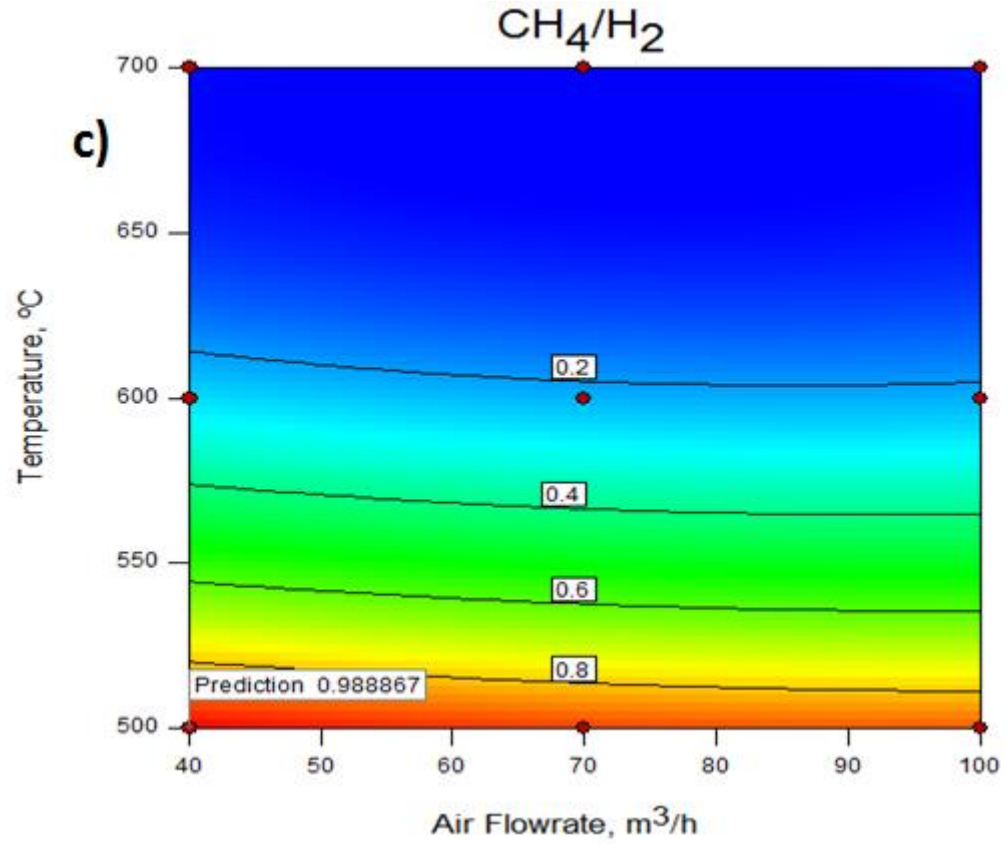
c)
CH_4/H_2
Temperature, °C
700
650
600
550
500
0.2
0.4
0.6
0.8
Prediction 0.988867
40
50
60
70
80
90
100
Air Flowrate, m^3/h

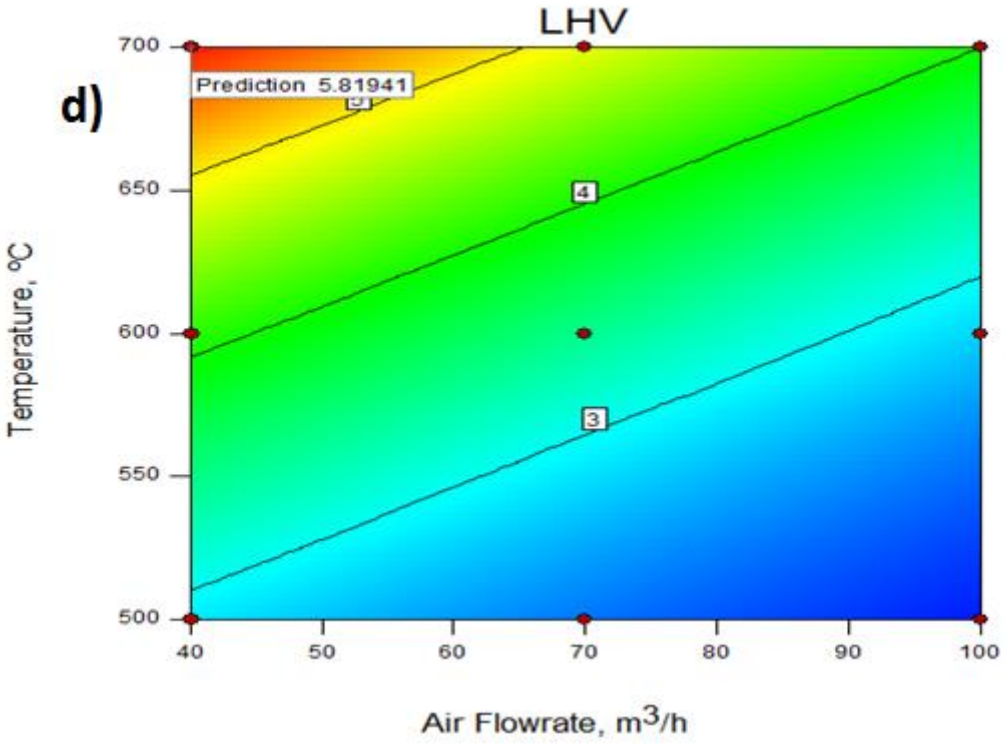
d)
LHV
Temperature, °C
700
650
600
550
500
Prediction 5.81941
5
4
3
40
50
60
70
80
90
100
Air Flowrate, m^3/h

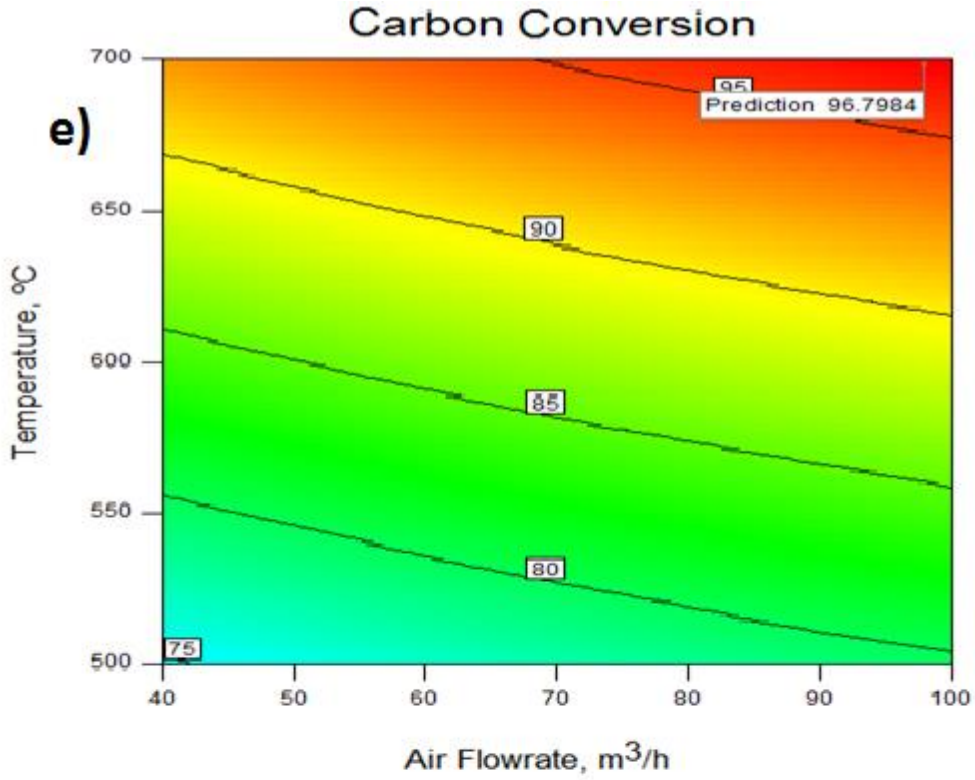
Carbon Conversion
e)
Prediction 96.7984
95
90
85
80
75
Temperature, °C
700
650
600
550
500
40
50
60
70
80
90
100
Air Flowrate, m3/h

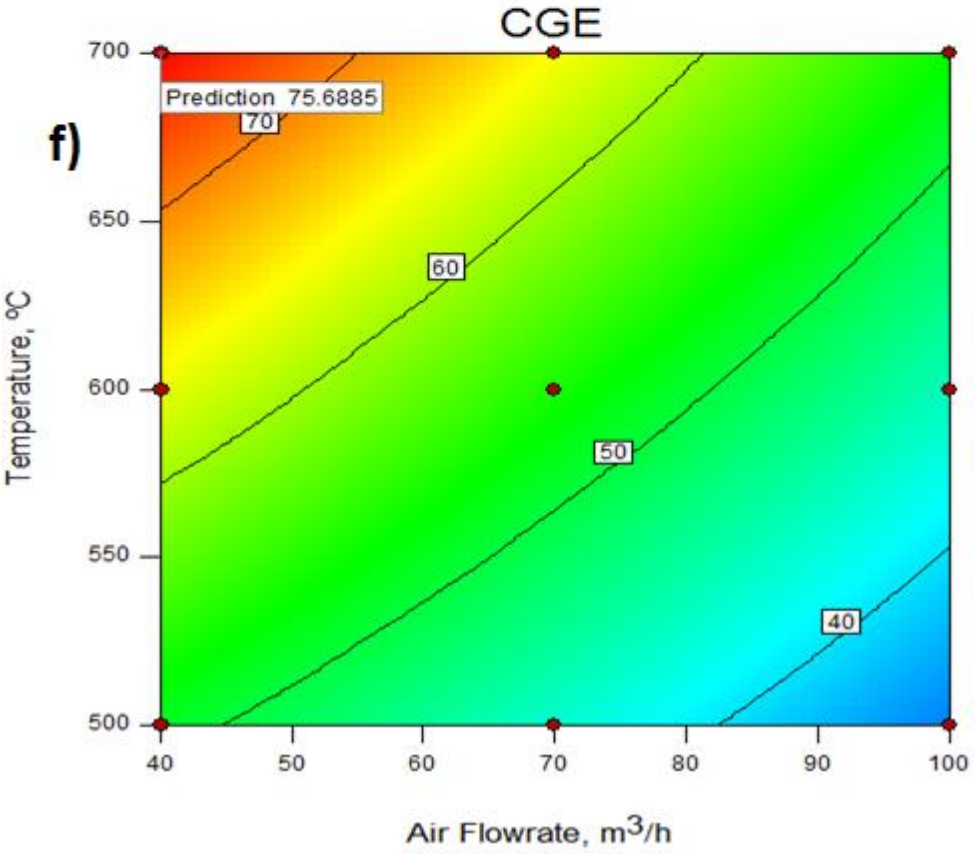
CGE
f)
Prediction 75.6885
70
60
50
40
Temperature, °C
700
650
600
550
500
40
50
60
70
80
90
100
Air Flowrate, m3/h

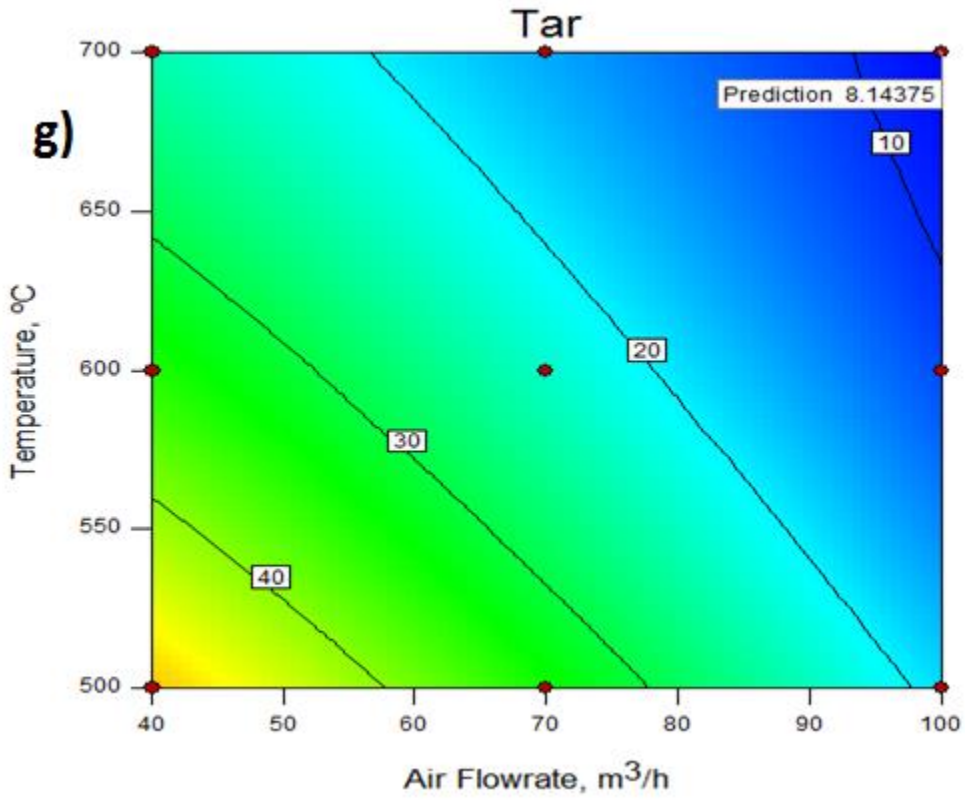

Figure 5.30 - Contour response plots for a) H_2 generation; b) H_2/CO ratio; c) CH_4/H_2 ratio; d) LHV; e) Carbon conversion; f) Cold gas efficiency and g) Tar generation.

In Figure 5.30b H_2/CO ratio appears to be more sensible with air flowrate variation. Although an increase in air flowrate decreases both CO and H_2, the increase of steam inside the reactor strengthens the water-gas shift reaction encouraging CO consumption and H_2 generation. Furthermore, this steam surplus decreases bed temperature thus preventing CO formation [100]. Regarding the influence of gasification temperature on the H_2/CO ratio, it has a positive effect when temperature is first increased but that trend reverses once temperature reaches about 620 ºC. Since hydrogen production reactions are mainly promoted at lower temperatures the ratio first presents a strong increase. However, since carbon monoxide is mainly promoted at higher temperatures the trend quickly reverses. This is consistent with available literature [74]. Optimal operating conditions to maximize

this ratio were found at: MSW feeding rate = 75 kg/h; Air flowrate = 100 m^3/h; and temperature = 621 ºC. Absolute values are extremely hard to validate since there are many parameters that greatly impact these ratios (reactor dimensions and feedstock properties, just to name a few) one cannot pinpoint experimental data from the current literature but the overall trends follow the obtained results [52, 65].

CH_4/H_2 ratio appears to be highly dependent on the temperature variation, Figure 5.30c. As temperature rises, endothermic reactions (mainly steam reforming and water-gas reactions) will be promoted leading to an increase in H_2 content at the expense of CH_4. Air flow rate has a much smaller effect on CH_4/H_2 ratio since it decreases both species similarly. These results are consistent with the current literature [101]. Near unity ratios were found in the 500 ºC range (at a MSW feeding rate of 75 kg/h and an air flowrate of 40 m^3/h). While MSW isn't particularly known for high CH_4/H_2 ratios, at low temperatures pyrolysis has a predominant role in gasification leading to an overall higher ratio [102].

Figure 5.30d highlights that gasification temperature has a positive influence on LHV while air flowrate has the exactly opposite effect. This is expected since the former promotes the formation of combustible gases (responsible for the syngas calorific value) while the latter prevents it. Overall calorific values for this particular waste are on the lower-hand (2 – 6 MJ/Nm^3) but within what is commonly found on the literature for MSW gasification using air as a gasifying agent (4 – 7 MJ/Nm^3) [103].

From Figure 5.30e, it can be seen that both gasification temperature and air flowrate have a strong (positive) effect on carbon conversion (a value of MSW feeding rate = 27.5 kg/h was obtained at the maximum carbon conversion point). This can be explained with temperature favoring tar reforming leading to overall higher conversion [66]. Similarly, since oxidation reactions are exothermic (meaning they release energy into the reactor) leads to steam

reforming reactions being promoted which in turn promotes carbon conversion [104]. The obtained values are also within the typical ranges for this kind of wastes [103].

Cold gas efficiency is mostly dictated by gas yield and syngas calorific value. While both gasification temperature and air flowrate promote gas yield (by enhancing reforming reactions) only temperature has a positive impact on the calorific value, thus explaining why parameters display opposed trends. Most commercial-size reactors found in the literature operating with MSW and using air or oxygen-enriched air as gasifying agent have a CGE of at least 50 % and in some cases slightly exceeding 80 % [103], which is consistent with the obtained results. If one pays close attention to contour plots for carbon conversion and tar content (figure 5.30g) one will surely notice that they are the reverse of one another. This is to be expected since an increase in temperature (which both parameters lead to) enhances reforming reactions which in turn promotes carbon conversion which is known for improving tar decomposition. This is consistent with the available literature [65, 66]. A minimal value of 8.1 g/Nm^3 was found at the highest values of temperature and air flowrate (MSW feeding rate = 25 kg/h).

5.5.3. Desirability Function

So far, the previous analysis was performed considering a single response. However, an industrial environment requires the ability to lead with several restrictions and multiple goals. Sometimes, it is necessary to find a commitment between yields and energy savings or other responses of interest. To cope with several goals, one should combine all goals into a unique function, also known as an objective function. Derringer *et al.* [105] suggests the use of the desirability concept as a way to measure the success of combing multiple responses. Desirability can be computed as follows:

$$D = \left(\prod_{i=1}^{n} d_i \right)^{\frac{1}{n}} \tag{5.4}$$

Where d_i is the desirability of each response and D is the overall desirability. D ranges from 0 to 1 (1 being the most desirable condition). Prior to computing desirability values, it is necessary to define the goals for each one of the selected responses (maximize, minimize, bounded between certain values or even equal to a fixed value) and also different weights in the case of some variables must be more important than others. Table 5.8 shows the goals for each one of the responses at different simulation scenarios. The imposed goals are based in typical working responses at industrial conditions. Figure 5.31 shows the optimal operating conditions and response values considering a complex study of 7 different responses. The purpose of this kind of methodology is quite obvious in an industrial environment. It is important to notice that the optimal operating conditions are now different from those found for single response optimization. Also, it is possible to tailor the required responses changing the input conditions.

Table 5.8 - Optimization scenarios based on different combined response targets.

Response	**Optimization 1**	**Optimization 2**
H_2, %	Maximize	Maximize
H_2/CO	Maximize	Maximize
CH_4/H_2	Minimize	Minimize
LHV, MJ/Nm^3	Maximize	4-7
Carbon Conversion, %	Maximize	>90
Cold Gas Efficiency, %	Maximize	50-80
Tar, g/Nm^3	Minimize	<10

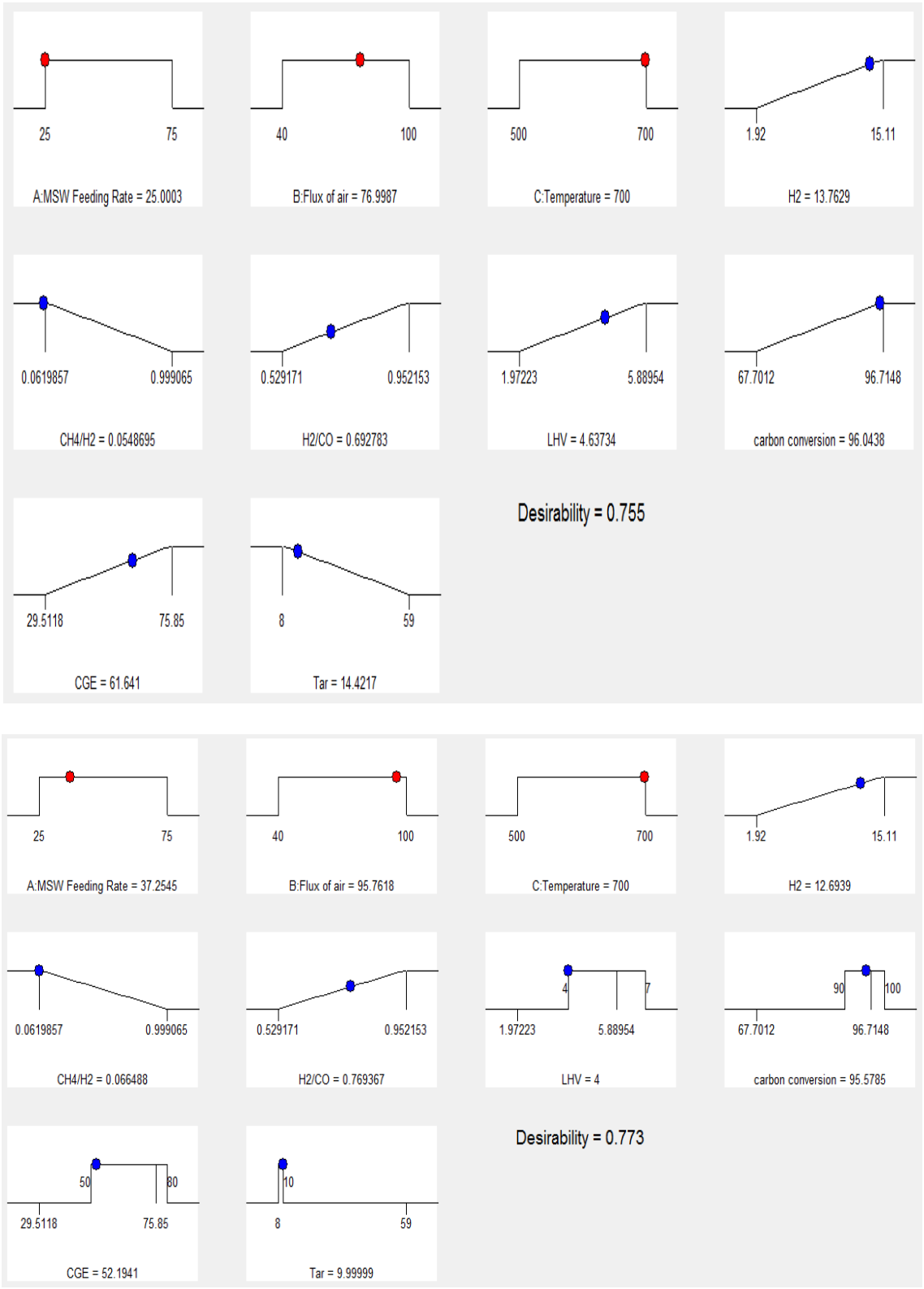

Figure 5.31 - Optimal operating conditions and corresponding responses based on scenarios described in table 9: a) optimization 1; and b) optimization 2.

5.5.4. Robust Operating Conditions

When a single optimization is carried out it is possible to obtain the desired target (maximum, minimum or value within a range) at multiple points of operation. However, some of these points might set the process on a sharp peak of response. At these circumstances, one should select the operating conditions more robust to variation transmitted from input factors. These conditions can be found applying a mathematical tool named propagation of error. POE can be defined as the square root of the variance of the selected response. To proceed with POE, the standard deviation from each one of the studied input factors is needed. Data was obtained considering historical data from experiments gathered at the pilot scale gasification plant presented in Chapter 2. Standard deviations from the selected input factors can be found in Table 5.9.

Table 5.9 - Standard deviation for input factors.

Input Factor	**Standard Deviation**
MSW feeding rate, kg/h	8
Air flowrate, m^3/h	15
Temperature, ^oC	5

Unfortunately, the setting of factors that meet the maximum of response are not at minimum POE. Once again, this problem (multi-optimization) can be overtaken taking advantage of using the desirability function where the response is maximized and POE is minimized. Figure 5.32 shows the 3D plot of hydrogen generation as a function of temperature and air flowrate a) at the optimal condition; b) combining the optimal and robust conditions.

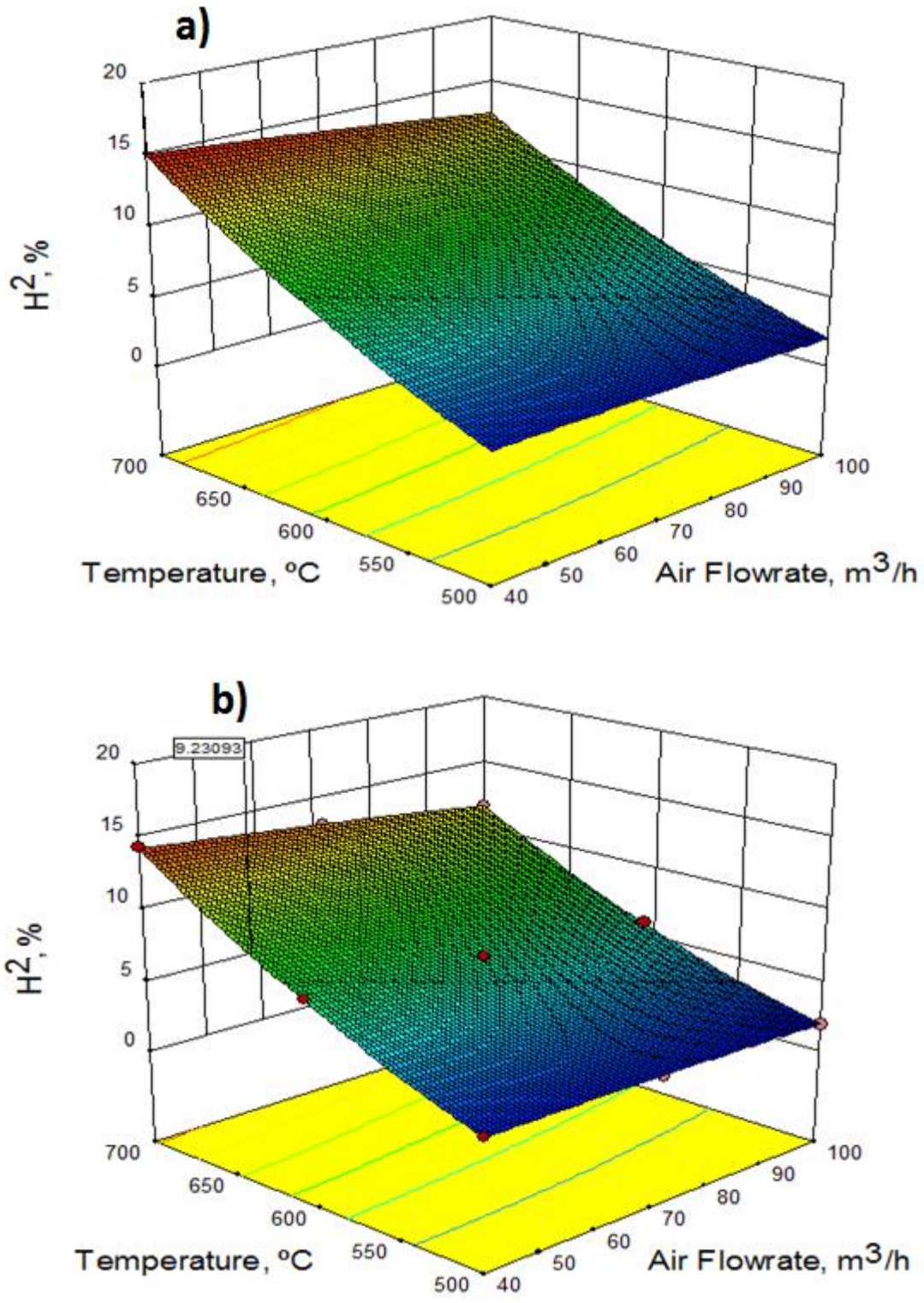

Figure 5.32 - Hydrogen generation as a function of the temperature and air flowrate for a) single optimization; b) optimization combined with POE.

From Figure 5.32, it can be observed that combining the optimization procedure with robust conditions implies a decrease on hydrogen generation from 15 % to about 9 %. Also, the MSW feeding rate changes from 25 kg/h in Figure 5.32a to 75 kg/h in Figure 5.32b. Obviously, other results can be obtained considering different weights for each one of the studied responses. Also, considering that this approach is a numerical methodology it could be possible to attain similar results considering a different set of factors. This kind of information combined with acquired experience of operating a gasifier allows taking reliable and smart decisions considering a wide range of goals.

A similar approach was performed for the other responses of interest and is given in Table 5.10.

Table 5.10 - Combined optimization for single responses.

Response	**Factors SO/SO+POE**			**Single Optimization (SO)**	**SO + POE**
	MSW Feeding Rate, kg/h	**Air Flowrate, m^3/h**	**Temperature, ºC**		
H_2/CO	75/25	100/100	621/610	0.94	0.80
CH_4/H_2	75/75	40/100	500/545	0.99	0.55
LHV, MJ/Nm^3	25/75	40/40	700/682	5.81	4.92
Carbon Conversion, %	27.5/27.5	100/100	700/700	96.80	96.80
CGE, %	25/30	40/40	700/600	75.70	62.80
Tar, g/Nm^3	25/25	100/100	700/700	8.10	8.10

From table 5.10, it can be observed that both carbon conversion and tar responses show the same set of operating conditions for single and combined optimization. This means that it is possible to achieve the maximum performance of this response at the most stable operating conditions.

5.5.5. Improving System's Capability towards Six Sigma Standards

The tolerance intervals (95 %) for hydrogen generation (combined optimization) are in the range 8.89 - 9.60. At industrial level, it is sometimes necessary to shorten these intervals and guarantee narrower boundaries and consequently less variation on the final syngas responses. We can assess and establish targets and tolerances for the selected responses by using a mathematical approach. To improve the system capability, Cpk, a mathematical model of the process is needed which can be obtained by the developed empirical model of the response surface method. Also, additional data from the design of experiments is needed: input factors, corresponding ranges and standard deviation and responses data. To end the process it is necessary to provide the response specifications. In this particular case, the new range will be 9 - 9.5. These new specifications narrow the former confidence/tolerance intervals obtained by coupling the selected response and corresponding POE. In such manner, the Cpk and 6 sigma level are increased about 20 %. The new operating conditions are: MSW Feeding Rate = 72 kg/h; Air Flowrate = 40 m^3/h; Temperature = 622 ºC.

At this level, the response interval can be accepted and assume that the response is satisfactory or decisions have to be taken to improve the process. Improvements can be attained: by reducing the standard deviation of the input factors with improved control devices and methods; by changing the intervals of the selected inputs or changing for different inputs; by changing the process design; by accepting the occurrence of some deviations; or then by refusing the opportunity to produce the syngas for certain applications that require minimal variation at this kind of response.

One possible solution is to control the inputs more effectively. Figure 5.33 shows that the most variation transmitted to the response comes from the input factors B and C. Improving

input factor A does not bring any advantage to the process, so our focus should be in input factors B and C. Some of the transmitted variation is also due to model development.

A similar approach can be followed for each single response or considering a combined optimization including all the responses.

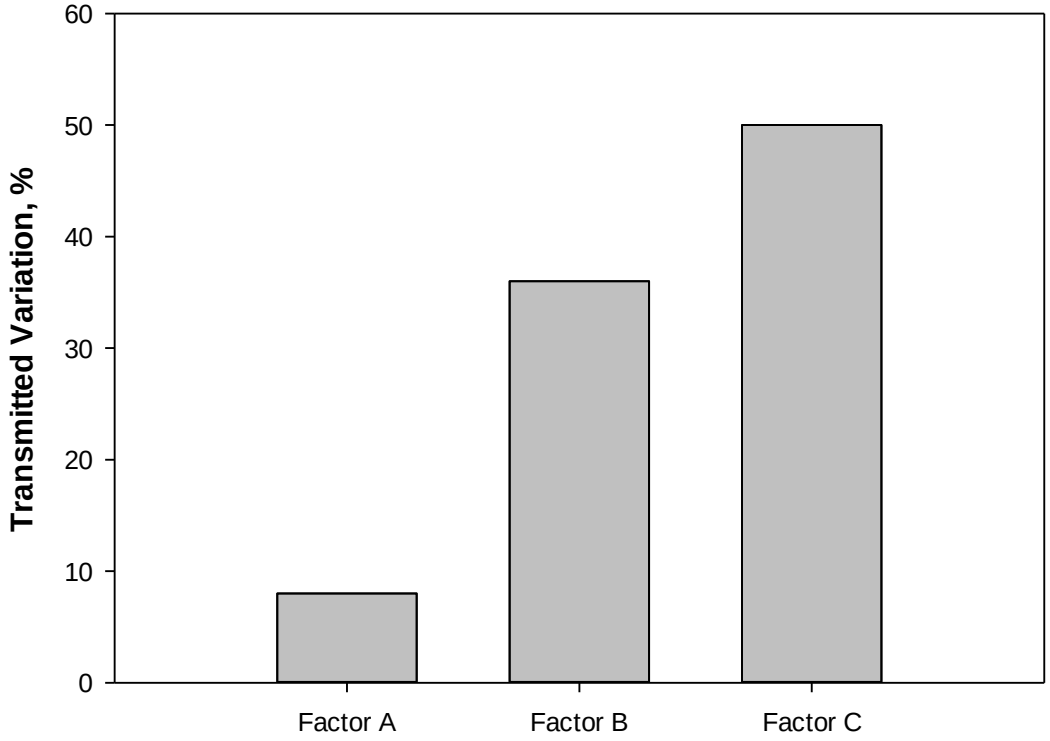

Figure 5.33 - Transmitted variation to the response from input factors.

5.6.Scale-up Analysis

At this time the model has been validated for both pilot and laboratorial scale conditions and presented similar relative errors and capability in correctly predicting trends for different operating conditions. This means that it is now possible to compare both reactors using the same biomass type as well as operating conditions without the influence of the model being responsible for the variation in results.

According to Knowlton *et al.* [106] one of the major concerns regarding biomass gasification is the scale-up effect. The nonlinear hydrodynamic behavior combined with complex chemistry schemes can greatly impact the gas-solid flow [14]. Because of this, larger particles are more difficult to scale-up than smaller ones. Although trends were similar between reactors there were significant differences regarding gasification products. Table 5.11 summarizes some of most relevant findings.

Table 5.11 - Most relevant findings regarding gasification products for different reactors.

Gasification Product	**Findings**
Residence Time	Residence time was shorter for laboratory-scale reactor
Gas composition	Syngas obtained in laboratorial runs presented higher levels of CH_4 and CO_2 and lower levels of CO and H_2
Gas yield	Gas yield was higher in semi-industrial reactor
Temperature	Temperature was higher in semi-industrial reactor

In fact, laboratory scale reactor led to a syngas with higher levels in CO_2 and CH_4 and lower CO and H_2 ones. This has to do with higher residence time in semi-industrial reactor will favor gasification reactions thus leading to a syngas with higher calorific value [107]. Moreover, the increase in residence time promotes gasification reactions and carbon conversion leading to higher gas yield [71].

Scale-up effects can also be seen in other gasification parameters such as syngas calorific value and biomass type. Figure 5.34 shows the scale-up effects in syngas calorific value for the two studied biomass substrates.

Generally, biomass with higher heating value will produce syngas with higher heating value as well [108]. So, it comes with little surprise that syngas with higher heating value was produced by forest residues, a more energetic substrate.

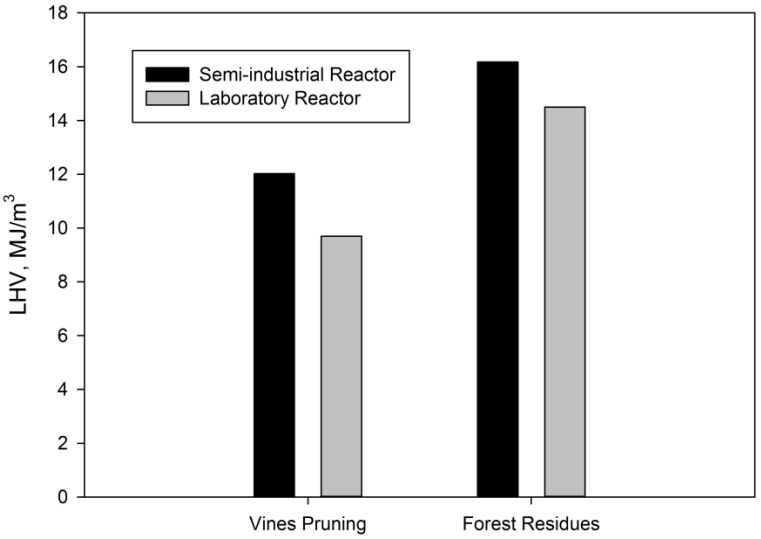

Figure 5.34 - Effect of scale-up on syngas low heating value for all studied biomass types. (Operating conditions were 800 ºC gasification temperature and 21% oxygen content).

Effects of scale-up on syngas composition were already studied but in a summarized manner due to shorter residence time, laboratory scale reactor led to a produced gas with higher CO_2 and CH_4 and lower CO and H_2 content [109]. Being the later 2 the ones with the most influence in the syngas calorific content.

So far the influence of biomass type on scale-up effects in biomass gasification hasn't been properly explained in literature. There are several biomass properties that can influence scale-up, namely chemical structure, volatile content, size particle, just to name a few.

Some studies on co-gasification showed that coal mixed with pine presented an increase in gas yield due to the higher volatile content of pine [110]. Increase in gas yield is related to tar decomposition into smaller and gaseous molecules. According to Aljbour and Kawamoto [111] a reduction in tar production by increasing the residence time was observed. So, it is possible to say that higher volatile content will lead to an increase in the residence time that in turn will favor gasification reactions [107]. Well, since vines pruning

has the highest volatile content of the two [110] it comes with no surprise that it also presents the biggest difference between both reactors as seen in Figure 5.34.

Particle size can play a very important role in the scale-up effects. As previously stated, different size particles scale-up differently. In fact, larger particles are more difficult to scale-up than smaller ones. Also, according to [106], scale-up becomes more complex by needing to know how the particle density in the fluidized bed reactor changes with diameter. So a larger particle or denser biomass type will be harder to scale-up and it will also be harder to correctly predict the biomass gasification process than in a smaller one with less density. This can be explained by smaller particles, due to their larger surface areas per mass unit, can facilitate faster gasification rates [112]. Regarding produced gas composition from smaller biomass particles, Rapagna *et al.* [113] found that smaller particles led to a syngas with higher CO and H_2 contents. Because of this smaller particles can result in higher gas energy content [114]. So, again, it comes with no surprise that forest residues, which has a smaller particle than vines pruning [115], has a syngas with higher gas calorific content.

Numerical modeling has great potential in predicting scale-up effects on the gasification process. However, at this point in the development of numerical models the use of CFD alone to scale-up a new process must be used with caution. Extensive experimental work is still required for successful scale-up.

5.7.MSW Gasification: Possible Applications

MSW as well as other biomass substrates can help to replace or at least diminish the use of fossil fuels. Not only does it have a LHV nearly as high as most conventional biomass feedstocks but also has a pre-existing collection/transportation infrastructure that does not exist for conventional biomass resources [116].

Alongside LHV there are other gasification products that dictate the best use for a particular produced syngas. In Table 5.12 desirable syngas characteristics for the various options are summarized.

According to Table 5.12, as well as the results from sections 5.2 and 5.3, it can be seen that the optimal application for the syngas obtained from LIPOR's MSW (with corresponding operating conditions) is synthetic fuels. In fact there is substantial work on the subject [117-119]. According to [120], a metric ton of USA MSW can produce up to 145 liters of ultra clean diesel fuel or up to 165 liters of ultra clean gasoline.

Table 5.12 - Desirable Syngas Characteristics for Different Applications [121].

Product		**H_2/CO**	**hydrocarbons**	**LHV**	**Temperature, ºC**
Synthetic Fuels		0.6	Low	Not Important	300-400
Methanol		2	Low	Not Important	100-200
Hydrogen		high	Low	Not Important	100-200
Fuel Gas	**Boiler**	Not important	High	High	250
	Turbine	Not important	High	High	500-600

Materials of biological nature can help to replace natural gas and fuels made from fossil. This can be of great help to the reduction of greenhouse gas. By converting MSW (along with all the other organic matter) it is possible to eliminate the increase of carbon dioxide which would otherwise occur by burning fossil fuels.

Generally, requirements for syngas characteristics for fuels and chemical synthesis applications are far more critical than for hydrogen and fuel gas applications. Syngas with low quantities of inerts such as N_2 can in fact be extremely beneficial for fuels and chemicals synthesis since it considerably reduces the size and cost of downstream equipment. Also higher temperatures can benefit production of fuels, chemical synthesis and hydrogen. In fact, at temperatures over 1,200 °C little or no tar, methane, or higher

hydrocarbons are formed, while syngas (H_2 and CO) production is maximized. If higher temperatures cannot be achieved inside the gasifier, tar cracking might be required. Typically, though, this is not the case and therefore gas cleanup is somewhat minimal for synthesis applications [121].

Other operating parameters like gasification pressure as well the oxidant used, can have a great degree of influence on the optimal syngas output. High pressures, over 20 bar, can be advantageous for fuel and chemical synthesis. On the other hand, air can have a detrimental effect to synthesis processes due to nitrogen diluting the product gas. Changing steam to oxygen ratio input can be used to adjust the H_2/CO ratio in order to match desirable syngas characteristics [121].

Even though guidelines from Table 5.12 can give a good indication on optimal syngas use, it should not be interpreted as strict requirements. Supporting process equipment such as scrubbers, compressors, coolers, etc. can be used to adjust the condition of the product syngas to match those optimal for the desired end-use [121].

To the best of our knowledge there is limited data regarding syngas quality indices for MSW. Also, data regarding syngas obtained from MSW using a pilot scale thermal gasification plant is very limited. The majority of the literature shows syngas compositions obtained in a laboratory or small-scale gasifier. These two factors combine make the results presented in this thesis very significant to MSW gasification in semi-industrial conditions.

5.7.1. Applications for MSW Gasification with CO_2

Due to its characteristics, syngas from MSW has been used both for fuel gas and synthetic fuel application, although mainly for the latter than the former in recent years [122]. Syngas composition for fuel gas applications does not require very strict specifications as long as a

high enough heating value is supplied through combustible gases, whereas chemical and fuel production require not only high H_2 content but also low CO_2 and CH_4 content.

On the other hand, biomass gasification with CO_2 as its gasifying agent can be used for an extremely wide variety of applications [61, 123] due to the ability to tailor H_2/CO ratio via CO_2 injection. As observed by Butterman and Castaldi [123], the H_2/CO ratio has a clear impact on the optimal application for a given substrate. Higher H_2/CO ratios allow for the operation of solid oxide fuel cells [124] while mid H_2/CO ratios are more appropriate for FT synthesis of liquid fuels. Mid-to-lower ratios are mainly suitable for catalyst-based FT synthesis whereas very low ratios are particularly suitable for the production of a specific biomass-derived liquid chemical [125] which can be obtained by CO_2 injection during thermal processing.

This means that CO_2 gasification decreases substrate influence on the produced gas and, at the same time, is able to ensure the production of a syngas that can meet the requirements of a particular chosen industrial application [123]. In addition to improving the gas obtained, adding CO_2 to the gasification process can reduce two major concerns related to municipal solid waste gasification, namely tar formation and CO_2 production.

5.7.2. Assessment of Steam Gasification in the Treatment of PMSW

Even though the results from PMSW are not on par with those from other studied fuels, gasification can still be an advantageous alternative when handling municipal wastes. By allowing a safe residue disposal via an optimal route for waste-to-energy, steam gasification of MSW becomes a very attractive process and the pre-existing collection and transportation infrastructure that is currently available does not exist for the compared biomass resources, rendering it an even more interesting process [116].

There are two other relevant concerns that further increase the interest on MSW gasification in relation to biomass substrates, namely the undefined availability of sustainable biomass resources, seasonal availability and local energy supply [126] that can lead to great uncertainty on the overall availability and sustainability of biomass as a resource; and the fact that waste production is becoming one the main concerns of the 21st century seeing that, according to the latest report regarding MSW production [7], approximately 1,300 million tons of MSW were produced in 2012, a value which is projected to double by 2025. Overcoming these issues justifies the need for studying gasification for MSW treatment.

Steam gasification is an effective process of renewable H_2 generation, capable of producing the highest yield of H_2 from biomass while simultaneously offering a cleaner product with minimal environmental impact. In fact, according to Nipattummakul *et al.* [127], it is an effective mode of producing renewable H_2 without leaving any carbon footprint in the environment.

Hydrogen can play a key role in the replacement of fossil fuels [128]. It exhibits excellent properties both as fuel and as an energy carrier, and when generated via combustion of renewable resources, it significantly reduces pollutant emissions. However, the majority of H_2 is produced from fossil fuels, while only 4 % is produced from renewable sources [128]. Due to the negative effect that fossil fuels have on the environment as well as their negative economic impact on importing countries, it is crucial to look for an alternative source of H_2 generation. It follows that if MSW were to be used for H_2 production, not only would it protect the environment, but it would also provide a sustainable source of H_2.

In this section, previously obtained results are analyzed in an economic perspective in a framework of hydrogen production through RDF gasification. To assess the potential of

this system it is necessary to compare it with conventional management practices such as landfills. Some of the considerable costs and benefits associated with RDF production and utilization are summarized in Table 5.13 (detailed explanation on these considerations can be found in the work of Reza *et al.* [129]).

Table 5.13 - Considerable costs and benefits associated with RDF production and utilization.

Associated Costs	**Associated Benefits**
Operational costs	Fuel savings
Plant construction and land cost	Reduction of landfilling expenses
Additional costs for hydrogen production	Recovered material
Transportation costs	Employment impact

Processing and converting MSW to RDF has both costs and benefits. On one hand, it consumes energy and produces emissions. On the other hand, recovered materials, such as ferrous metals, can be sent to a secondary market for sale thus decreasing the cost for processing and converting. On top of that, by choosing this technology over landfills, only a small percentage of waste ends up being deposited resulting in at least 60 % landfill reduction.

According to Zhang *et al.* [130], approximately 28,500 tons of MSW can occupy 1 ha of land. Therefore, by applying this technology to 2.72 million tons of MSW (Portuguese production of MSW sent to landfills in 2012 [131]), over 57 ha of land can be saved from landfilling each year. This reduction can be extremely beneficial not only in financial savings but most important in a substantial decrease in air emissions.

A 2012 EPA study commissioned by the American Chemistry Council's Plastics Division and conducted by RTI International [132], estimated that gasification results in a net carbon emission savings of 0.3 - 0.6 tons of carbon equivalent per dry ton of MSW when compared to landfill disposal. This net savings is due mainly to the energy produced

through gasification because even in the scenario with the landfill recovering energy, the gasification facility produces energy in a much more efficient way [134].

The following analysis is based on the results presented in [38] for MSW applied to the gasification plant described in Chapter 2. Chosen operational conditions are: SBR of 1.5; gasification temperature of 750 ºC and MSW feed rate of 50 kg/h. The higher feed rate (half of full capacity) was selected since, from experimental analysis, this feed corresponds to the optimal operating condition (more stable gasification results). Also, from previous studies [134] we know that hydrogen production isn't seriously affected by operating at higher MSW feed. Considering a syngas composition comprising 36.2 % of H_2 and a 1.51 m^3 of syngas produced per kg of RDF, which in turns, gives 0.55 m^3 of H_2 per kg of RDF. Considering that 1 m^3 of H_2 can translate to roughly 0.002 barrels of oil [135], one can estimate both the number of barrels of crude oil saved and the annual savings from the collected data.

With the Oil Brent Price currently around 45 €, Portugal spends on average 4,971 million € a year on international transactions, importing close to 110 million crude oil Brent Barrels, although the yearly budget used to be much higher when the price per barrel was over 100 €. By resorting to MSW gasification with steam, and considering the conditions described above, an estimated expense of about 81.5 million € could be avoided, which represents a global decrease of 1.8 million crude oil Brent Barrels imported.

Table 5.14 shows several parameters taken into account to perform this economic evaluation. The capital cost of a gasification plant of 50 kg/h identical to the one previously described is around 450,000 € that are linear amortized in its life time of 20 years with residual value of zero. Assuming a cost of 20 €/ton of RDF (commonly found in similar situations [136]) the minimum cost for hydrogen production is close to 2.66 €/kg.

Considering an annual hydrogen production of 216,342 cubic meters from 660 tons of MSW (which are converted to 396 tons of RDF) one can expect to save 432 barrels of crude and avoid almost 232 cubic meters of landfill a year. On top of that one can expect to recover at last 66 kg (10% of the total MSW) which, as stated, can be sent to a secondary market for sale. Estimating a net carbon emission savings of 0.45 TCE per dry ton of MSW one can estimate reduction of 297 TCE per year.

Considered benefits and costs have been calculated based on actual data from Portalegre's plant, expert judgments, and construction and operation costs of analogous waste treatment plants in Europe. Although at different scales and applications, existing economic studies corroborate the obtained data [129, 132, 137-139].

There are several sources that are currently being used for H_2 production. Figure 5.35 depicts energy efficiency and H_2 production cost for the main processes and compares it with obtained results for MSW gasification.

Out of all presented methods, MSW gasification appears to be very well balanced, displaying an average efficiency and a low production cost, and is the only process with a renewable source, since all other relevant methods depend on fossil fuels.

Although hydrogen production cost for this particular study was slightly higher than expected it is crucial to mention that the comparison was made with large facilities, some having an annual H_2 production which exceeds the production of the studied process by a factor of more than 100. While this makes the comparison between the data difficult, they certainly allow for an optimistic prediction.

Table 5.14 - Economic and environmental impact from the conducted simulations.

Operational Costs		
RDF feed	396	ton/year
RDF costs	20	€/ton
Total RDF costs	7,920	€/year

Dolomite feed	3.3	ton/year
Dolomite costs	55	€/ton
Total dolomite costs	181.5	€/year

Electricity costs	2,059	€/year
Personnel costs	41,328	€/year
Maintenance costs	10,890	€/year

Plant Construction and Additional Costs		
Fluidized Bed Gasification Plant 50 kg/h	450,000	€

Associated Benefits		
Fuel Savings	432.68	boe/year
Landfill Reduction	231.58	m^2/year
Emission reduction	297	TCE/year
Recovered material	66	kg/year

Hydrogen Production		
Syngas production (1.51 m^3/kg RDF)	597,960	m^3/year
Hydrogen production	216,342	m^3/year

Operational Result		
Total production costs	62,379	€/year
Linear amortization (20 years)	22,500	€/year
Total production benefits	33,108	€/year
Total hydrogen production costs	2.66	€/kg

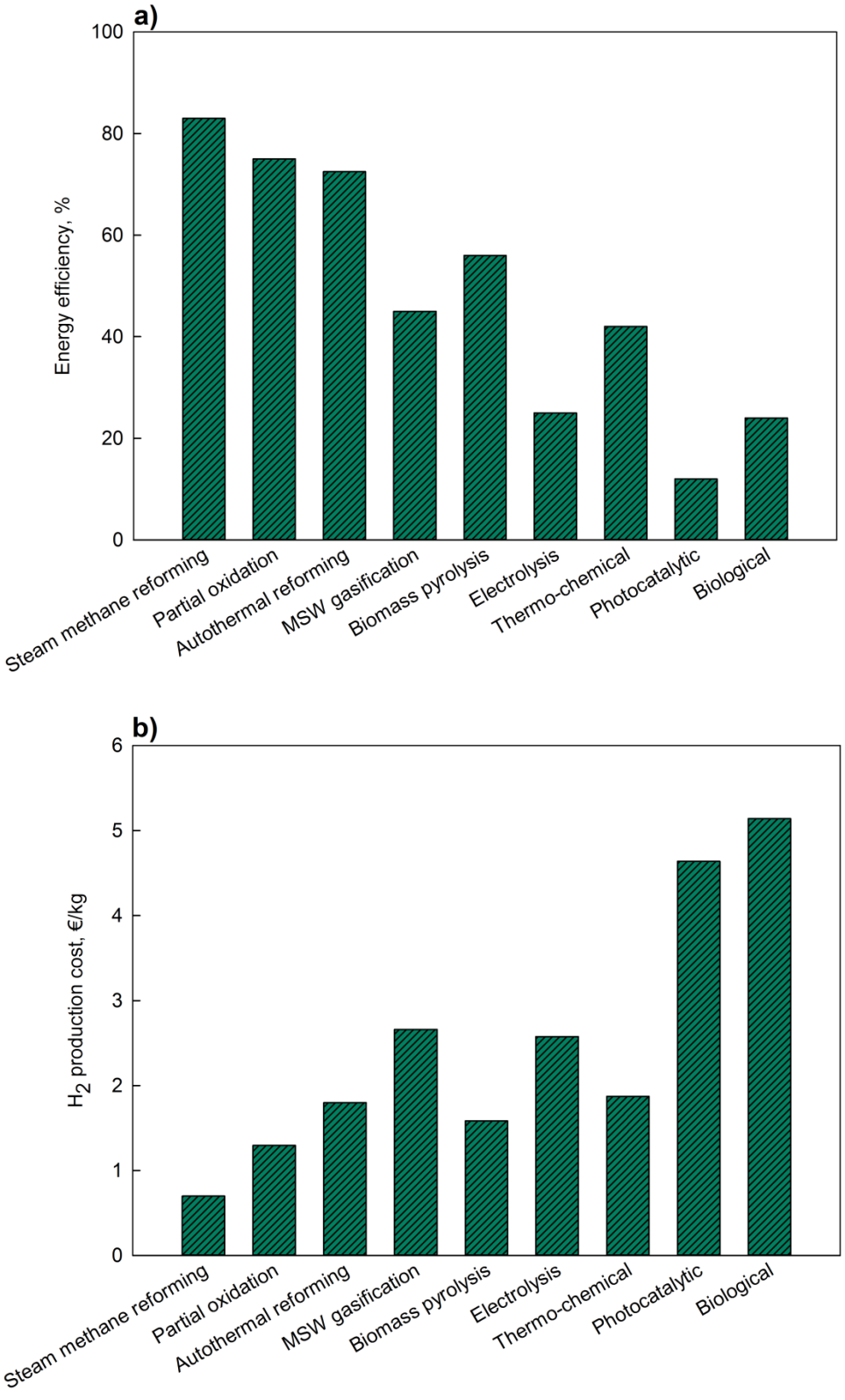

Figure 5.35 - Comparison between H_2 production methods for a) Energy production and b) H_2 production cost [109].

In fact, one can only assume that with a bigger installation the average hydrogen production costs would only decrease. According to Farver and Frantz [133], larger facilities of over 100 metric tons of MSW per day are predicted to be more profitable but as yet do not exist.

This also brings us to a very important aspect, which is the learning effect. The economic analysis is presented based on current or recent costs. However, learning effects reduce these costs as more units are built and experience is accumulated [140]. The impact on total plant costs can be significant. According to the International Energy Agency [141], for emerging technologies, a 50 % reduction of total plant costs may be achieved after the installation of 10 plant units.

This data is of utmost importance considering the Portuguese economic overview. Portugal is a country poor in energy resources of fossil origin and with a recorded energy dependence on imports of energy products of 79.4 % in 2012, which translates into an expense of over 7,000 million euros to meet power requirements. In order to reduce energy dependency and secure the national supply, it is necessary to increase the relative weight of primary energy produced in Portugal.

Considering the latest national report, in 2012, 4.53 million tons of MSW were produced in Portugal [131]. According to Teixeira *et al.* [8], most of the MSW in Portugal is sent to landfill and incineration continues to be the most common method of thermal treatment for waste-to-energy facilities. The state of development of gasification technology and its increasing adoption rate, along with environmental restrictions and laws, shows that gasification is a viable and cleaner alternative for MSW conversion to energy.

Although quantifying the global volume of harmful emissions saved from reducing the total amount of municipal solid waste going to landfill is extremely difficult it is unquestionably that reducing methane, volatile organic compounds, and hazardous air pollutants (such as

benzene, toluene, ethylbenzene, etc.) will have a positive effect on environmental and human health.

In fact, reduction of MSW sent to landfills in one of the greatest benefits of hydrogen production from MSW gasification. Transportation costs and tipping fees are growing increasingly expensive as more landfills are closed while few are opened. This type of relief to a constrained landfill system holds enormous promise, particularly for Azores and Madeira (islands that are part of the national territory) with limited landfill space and regions of the country with high tipping fees for waste disposal.

These results show the potential benefits of MSW gasification, not only at an environmental level, but also on an economic one. However, these figures should be regarded only as indicative and an economic viability study must be carried out with the valuable assistance of numerical simulation.

6. Conclusions & Future Work

Accelerated population growth combined with high socioeconomic development and rapid urbanization has led to one of the greatest challenges facing modern society, the management of municipal solid waste. Not only does its incorrect management negatively impact public health and the environment but its treatment usually represents the single largest budgetary item of a city. As a possible solution to this problem, gasification of MSW from Portugal, in particular from the Oporto metropolitan area, was investigated.

A previously developed numerical model was employed and its results validated using data collected from the literature, and then expanded to predict process results using a pilot scale gasifier. Chosen limits for the several studied parameters were selected based on previous studies and available literature. The following conclusions can be drawn from the obtained results:

- The increase of ER has a negative effect on H_2 production because the oxidation reactions are favored when the reaction medium had higher contents of oxygen. On the other hand, the increase of ER has a positive effect on the reduction of tar content with increased gas yield.
- The use of steam as a gasifying agent in gas-phase reactions results in the decomposition of hydrocarbons and increasing contents of H_2. The introduction of steam also leads to more tar participating in steam reforming, which led to a rapid increase of gas yield and tar reduction because of higher conversion efficiency.
- The reactor temperature had a significant influence on the syngas compositions, since the main reactions of the gasification are endothermic. Higher temperature contributes to higher hydrogen content. Moreover, high temperature also favors destruction and

reforming of tar leading to a decrease in tar content and an increase in gas yield because of higher conversion efficiency.

- CO_2 as a gasifying agent has a strong influence on syngas composition. With higher CO_2 content, Boudouard and reverse water-gas shift reactions are promoted leading to higher CO content while H_2 presented lower content. Results show that increasing CO_2-to-MSW ratio positively influences gas yield while negatively influences the tar content. This is related to enhancement in char gasification and pyrolysis as well as enhancement in thermal cracking of volatiles.
- Catalysts can significantly increase the content of hydrogen while decreasing tar yield in the gasification of MSW. With the presence of NiO/MD catalysts, the tar was almost eliminated and gas yield increased remarkably. Particularly, the content of hydrogen in the generated gas increased to 40%. Therefore, the NiO/MD is a promising catalyst for the application of hydrogen production from MSW steam gasification.
- MSW was also compared with previously studied Portuguese biomass substrates. Results shown that MSW produced lower H_2 and C_nH_m due to low C:H ratio and low O_2 content. On the other hand due to low volatile content it also presented high tar content and lower gas yield than the other studied fuels.

Energetic and exergetic efficiencies of gas components and tar content at various ER values and reactor temperatures were also studied. The set of operational conditions that promoted the highest overall efficiency were found at 0.25 and 900 ºC. In this particular point a Sankey diagram was created for visualization purposes.

A 3^k full factorial design with 27 runs generated by a 2D Eulerian-Eulerian multiphase CFD model was used to proceed a single optimization based on the response surface

method to target the best operating conditions for 7 different responses that quantitatively determine the gasifier performance. Using such approach, the best conditions for MSW feeding rate, air flowrate and temperature were found. Also, it was possible to define the full behavior of these factors under the design space considering all the responses in a single and combined ways. A similar study was performed considering the normal response values in industrial environment and making use of the desirability function it was possible to get the best conditions that respected those targets. A procedure to combine both optimized and robust conditions was followed by combining response surface and propagation of error methods. In such manner, each response was obtained ensuring a stable syngas generation. Finally, and by using empirical equations from the response surface method combined with narrower specifications for each response was possible to improve the process Cpk and six sigma standards. One feasible solution to get further improvements suggests the standard deviation reduction by more restrictive control procedures on the input factors.

The scale-up of a new fluidized bed process is one of the most difficult types of scale-up. However, the use of techniques based on experience and design models can minimize risk and uncertainty. Computation Fluid Dynamics has potential in predicting the effect of scale on biomass gasification. In order to test the true potential of numerical models to predict the effects of scale-up, a two-dimensional model was build using data from a semi-industrial gasification plant. Height/cross section ratio between both reactors was chosen according to previously relevant studies. Influence of gasification temperature, oxygen content and biomass type on different reactors size was studied. Bigger reactors led to syngas with higher contents in CO and H_2 due to residence time in those reactors being longer. In fact, residence time showed to be a major influence on the scale-up effects. Influence of biomass

type in different reactors was yet to be properly addressed on the current literature. An attempt on answering was made. Volatile content as well as particle size showed a considerable influence on the obtained results.

By applying a robust and proven numerical model to the thermodynamic analysis of MSW gasification the work presents a set of interesting results on the optimal operating point of an industrial size system. The pre-existing collection and transportation infrastructure that is currently available for municipal waste combined a safe residue disposal via an optimal route for waste-to-energy with the possibility for efficiency optimization as shown in this thesis makes the gasification of MSW in Portugal a very attractive process.

Finally, the influence of steam gasification on both harmful emissions avoided and annual savings was studied. By resorting to MSW gasification with steam, an estimated annual savings of about 81.5 million euros could be attained, which represents a global budget decrease of 1.63 %, and an average of over 57 ha land can be saved from landfilling each year. Although purely indicative, these figures present very promising estimates for the future.

Having exhausted the study on Eulerian-Eulerian models of fluidized-bed gasification the plan is to move to more advanced models (namely hybrids between Eulerian-Eulerian and Eulerian-Lagrangian). Furthermore, the scale-up phenomenon will be further investigated by performing experimental runs on different size reactors. Finally, interaction between technologies is the next major step in our work.

References

[1] IPCC, Climate Change 2014: Synthesis Report. Contribution of Working Groups I, II and III to the Fifth Assessment Report of the Intergovernmental Panel on Climate Change, in: C.W. Team, R.K. Pachauri, L.A. Meyer (Eds.) Geneva, Switzerland, 2014.

[2] Herbert GM, Krishnan A. Quantifying environmental performance of biomass energy. Renew Sust Energ Rev 59 (2016) 292-308.

[3] Eurostat, Greenhouse gas emission statistics. http://ec.europa.eu/eurostat/statistics-explained/index.php/Greenhouse_gas_emission_statistics, last access in September 26th 2017.

[4] Vávrová K, Knápek J, Weger J. Short-term boosting of biomass energy sources – Determination of biomass potential for prevention of regional crisis situations. Renew Sust Energ Rev 67 (2017) 426-36.

[5] Silva V, Monteiro E, Couto N, Brito P, Rouboa A. Analysis of Syngas Quality from Portuguese Biomasses: An Experimental and Numerical Study. Energ Fuel 28 (2014) 5766-77.

[6] Achillas Ch, Vlachokostas Ch, Moussiopoulos N, Banias G, Kafetzopoulos G, Kara-Giannidis A. Social acceptance for the development of a waste-to-energy plant in an urban area. Resources, Conservation and Recycling 55 (2011) 857-63.

[7] Hoornweg D, Bhada-Tata P. WHAT A WASTE, A Global Review of Solid Waste Management. 15 (2012). Urban Development Series Knowledge Papers. http://siteresources.worldbank.org/INTURBANDEVELOPMENT/Resources/336387-1334852610766/What_a_Waste2012_Final.pdf, last access in September 26th 2017.

[8] Teixeira S, Monteiro E, Silva V, Rouboa A. Prospective application of municipal solid wastes for energy production in Portugal. Energ Policy 71 (2014) 159-68.

[9] Al-Hamamre Z, Al-Mater A, Sweis F, Rawajfeh K. Assessment of the status and outlook of biomass energy in Jordan. Energ Convers Manage 77 (2014) 183–92.

[10] Zheng X, Chen C, Ying Z, Wang B. Experimental study on gasification performance of bamboo and PE from municipal solid waste in a bench-scale fixed bed reactor. Energ Convers Manage 117 (2016) 393–9.

[11] Kirkels AF, Verbong G. Biomass gasification: Still promising? A 30-year global overview. Renew Sust Energ Rev 15 (2011) 471-81.

[12] Couto N, Silva V, Bispo C, Rouboa A. From laboratorial to pilot fluidized bed reactors: Analysis of the scale-up phenomenon Energ Convers Manage 119 (2016) 177-86.

[13] Couto N, Silva V, Rouboa A. Municipal solid waste gasification in semi-industrial conditions using air-CO2 mixtures. Energ 104 (2016) 42-52.

[14] Eaton AM, Smoot LD, Hill SC, Eatough C.N. Components, formulations, solutions, evaluation, and application of comprehensive combustion models. Prog Energ Combust 25 (1999) 387-436.

[15] Alauddin Z, Lahijani P, Mohammadi M, Mohamed A. Gasification of lignocellulosic biomass in fluidized beds for renewable energy development: A review. Renew Sust Energ Rev 14 (2010) 2852-62.

[16] Patra TK, Sheth PN. Biomass gasification models for downdraft gasifier: A state-of-the-art review. Renew Sust Energ Rev 50 (2015) 583-93.

[17] Loha C, Gu S, Wilde J, Mahanta P, Chatterjee P. Advances in mathematical modeling of fluidized bed gasification. Renew Sust Energ Rev 40 (2014) 688-715.

[18] Singh R, Brink A, Hupa M. CFD modeling to study fluidized bed combustion and gasification. Applied Thermal Engineering 52 (2013) 585-614.

[19] Nguyen T, Seo M, Lim Y, Song B, Kim S. CFD simulation with experiments in a dual circulating fluidized bed gasifier. Comput Chem Eng 36 (2012) 48-56.

[20] Bell D, Towler B, Fan M. Chapter 3 - Gasification Fundamentals, in: Coal Gasification and Its Applications, William Andrew Publishing, Boston, (2011) 35-71.

[21] http://www.biofuelstp.eu/biofuels-legislation.html, last access in September 26th 2017.

[22] Couto N, Silva V, Rouboa A. Assessment on steam gasification of municipal solid waste against biomass substrates. Energ Convers Manage 124 (2016) 92–103.

[23] Fan L, Pandey A, Mohan R, Soccol CR. Acta Biotechnol 20 (2000) 41-52.

[24] http://www.pordata.pt, last access in September 26th 2017.

[25] Ferreira S, Moreira N, Monteiro E. Bioenergy overview for Portugal. Biomass Bioenerg 33 (2009) 1567–76.

[26] Holman JP. Experimental Methods for Engineers, 4th edn. McGraw-Hill, New York, USA, 1984.

[27] Monteiro E. Personal communications. November 23, 2015.

[28] Dogru M, Midilli A, Howarth C. Gasification of sewage sludge using a throated downdraft gasifier and uncertainty analysis. Fuel Process Technol 75 (2002) 55-82.

[29] Magrinho A, Ddilet F, Semiao V. Municipal solid waste disposal in Portugal. Waste Manage 26 (2006) 1477-89.

[30] EEA Report No 2/2013. Portugal – municipal waste management. Available online: http://www.eea.europa.eu/publications/managing-municipal-solid-waste,

last access in September 26th 2017.

[31] LIPOR, 2016. Sorting Plant Description. Available online: http://www.lipor.pt/pt/residuos-urbanos/valorizacao-multimaterial/descricao-do-processo/ last access in September 26th 2017.

[32] Scott D, Czernik S, Piskorz J, Radlein D. Fast pyrolysis of plastic wastes. Energ Fuel 4 (1990) 407-11.

[33] Baliban R, Elia J, Floudas C. Toward novel biomass, coal, and natural gas processes for satisfying current transportation fuel demands, 1: process alternatives, gasification modeling, process simulation, and economic analysis. Ind Eng Chem Res 49 (2010) 7343-70.

[34] Onel O, Niziolek AM, Hasan M, Floudas CA. Municipal solid waste to liquid transportation fuels - part I: mathematical modeling of a municipal solid waste gasifier. Comput Chem Eng 71 (2014) 636-47.

[35] Couto N, Silva V, Monteiro E, Brito P, Rouboa A. Experimental and Numerical Analysis of Coffee Husks Biomass Gasification in a Fluidized Bed Reactor. Enrgy Proced 36 (2013) 591-5.

[36] Goldschmidt M, Kuipers J, Swaaij W. Hydrodynamic modelling of dense gas-fluidised beds using the kinetic theory of granular flow: effect of coefficient of restitution on bed dynamics. Chem Eng Sci 56 (2001) 571-8.

[37] Cornejo P, Farías O. Mathematical Modeling of Coal Gasification in a Fluidized Bed Reactor Using a Eulerian Granular Description, in: International Journal of Chemical Reactor Engineering, 2011.

[38] Couto N, Silva V, Rouboa A. Assessment on steam gasification of municipal solid waste against biomass substrates. Energ Convers Manage 124 (2016) 92-103.

[39] Couto N, Monteiro E, Silva V, Rouboa A. Hydrogen-rich gas from gasification of Portuguese municipal solid wastes. Int J Hydrogen Energ 41 (2016) 10619-30.

[40] Badzioch S, Hawksley P. Kinetics of Thermal Decomposition of Pulverized Coal Particles. Ind Eng Chem Proc DD 9 (1970) 521-30.

[41] Gelderbloom S, Gidaspow D, Lyczkowski R. CFD Simulations of bubbling/collapsing fluidized beds for three Geldart Groups. AIChE Journal 49 (2003) 844-58.

[42] Pellegrini L, Oliveira S. Exergy analysis of sugarcane bagasse gasification. Energ 32 (2007) 314-27.

[43] Zhang Y, Zhao Y, Gao X, Li B, Huang J. Energy and exergy analyses of syngas produced from rice husk gasification in an entrained flow reactor. J Clean Prod 95 (2015) 273-80.

[44] Szargut J, Styrylska T. Approximate evaluation of the exergy of fuels. Brennst Warme Kraft 16 (1964) 589–96.

[45] Stepanov VS. Chemical energy and exergy of fuels. Energy 20 (1995) 235–42.

[46] Silva V, Monteiro E, Couto N, Brito P, Rouboa A. Analysis of Syngas Quality from Portuguese Biomasses: An Experimental and Numerical Study. Energ Fuel 28 (2014) 5766-77.

[47] Silva V, Rouboa A. Combining a 2-D multiphase CFD model with a Response Surface Methodology to optimize the gasification of Portuguese biomasses. Energ Conv Manage 99 (2015) 28-40.

[48] Kim Y, Yang C, Kim B, Kim K, Lee J, Moon J, Yang W, Yu T, Lee U. Air-blown gasification of woody biomass in a bubbling fluidized bed gasifier. Appl Energ 112 (2013) 414-20.

[49] Liu H, Elkamel A, Lohi A, Biglari M. Computacional fluid dynamics modeling of biomass gasification in circulating fluidized-bed reactor using the Eulerian-Eulerian Approach. Ind Eng Chem Res 52 (2013) 18162-74.

[50] Oevermaan M, Gerber S, Behrendt F. Euler-lagrange/DEM simulation of wood gasification in a bubbling fluidized bed reactor. Particuology 7 (2009) 307-16.

[51] Couto N, Silva V, Monteiro E, Teixeira S, Chacartegui R, Bouziane K, Brito PSD, Rouboa A. Numerical and experimental analysis of municipal solid wastes gasification process. Appl Therm Eng 78 (2015) 185-95.

[52] Gang X, Bao-sheng J, Zhao-ping Z, Yong C, Ming-jiang M, Kefa C, Rui X, Ya-ji H, He H. Experimental study on MSW gasification and melting technology. Journal of Environmental Sciences 19 (2007) 1398-403.

[53] Campoy M, Gomez-Barea A, Vidal F, Ollero P. Air-steam gasification of biomass in a fluidised bed: Process optimisation by enriched air. Fuel Process Technol 90 (2009) 677-85.

[54] Wang Z, He T, Qin J, Wu J, Li J, Zi Z, Liu G, Wu G, Sun L. Gasification of biomass with oxygen enriched air in a pilot scale two-stage gasifier. Fuel 150 (2015) 386-93.

[55] Wang J, Cheng G, You Y, Xiao B, Liu S, He P, Guo D, Guo X, Zhang G. Hydrogen-rich gas production by steam gasification of municipal solid waste (MSW) using NiO supported on modified dolomite. Int J Hydrogen Energ 37 (2012) 6503-10.

[56] Kumar A, Jones D, Hanna M. Thermochemical Biomass Gasification: A Review of the Current Status of the Technology. Energies 2 (2009) 556-81.

[57] André RN, Pinto F, Franco C, Dias M, Gulyurtlu I, Matos M, Cabrita I. Fluidised bed co-gasification of coal and olive oil industry wastes fuel. Fuel 84 (2005) 1635–44.

[58] Pinto F, Lopes H, André RN, Dias M, Gulyurtlu I, Cabrita I. Effect of experimental conditions on gas quality and solids produced by sewage sludge cogasification. Sewage Sludge mixed with coal. Energy Fuel 21 (2007) 2737–45.

[59] Cheng Y, Thow Z, Wang C. Biomass gasification with CO_2 in a fluidized bed. Powder Technol 296 (2016) 87-101.

[60] Garcia L, Salvador ML, Arauzo J, Bilbao R. CO_2 as a gasifying agent for gas production from pine sawdust at low temperatures using a Ni/Al coprecipitated catalyst. Fuel Process Technol 69 (2001) 157-74.

[61] Renganathan T, Yadav M, Pushpavanam S, Voolapalli R, Cho Y. CO2 utilization for gasification of carbonaceous feedstocks: A thermodynamic analysis. Chem Eng Sci 83 (2012) 159-70.

[62] Corigliano O, Fragiacomo P. Technical analysis of hydrogen-rich stream generation through CO2 reforming of biogas by using numerical modeling. Fuel 158 (2015) 538–48.

[63] Hu M, Guo D, Ma C, Hu Z, Zhang Be, Xiao B, Luo S, Wang J. Hydrogen-rich gas production by the gasification of wet MSW (municipal solid waste) coupled with carbon dioxide capture. Energ 90 (2015) 857-863.

[64] Kwon EE, Yi H, Kwon HH. Urban energy mining from sewage sludge. Chemosphere 90 (2013) 1508–13.

[65] Gonzalez JF, Roman S, Bragado D, Calderon M. Investigation on the reactions influencing biomass air and air/steam gasification for hydrogen production. Fuel Process Technol 89 (2008) 764–72.

[66] Kumar A, Eskridge K, Jones D, Hanna MA. Steam-air fluidized bed gasification of distillers grains: effects of steam to biomass ratio, equivalence ratio and gasification temperature. Bioresour Technol 100 (2009) 2062–8.

[67] Hu G, Xu SP, Li SG, Xiao CG, Liu SQ. Steam gasification of apricot stones with olivine and dolomite as downstream catalysts. Fuel Process Technol 87 (2006) 375–82.

[68] Couto N, Silva V, Monteiro E, Brito P, Rouboa A. Using an Eulerian-granular 2-D multiphase CFD model to simulate oxygen air enriched gasification of agroindustrial residues. Renew Energ 77 (2015) 174-81.

[69] Silva V, Rouboa A. Optimizing the gasification operating conditions of forest residues by coupling a two-stage equilibrium model with a response surface methodology. Fuel Process Technol 122 (2014) 163–9.

[70] Louw J, Schwarz C, Knoetze J, Burger A. Thermodynamic modelling of supercritical water gasification: Investigating the effect of biomass composition to aid in the selection of appropriate feedstock material. Bioresource Technol 174 (2014) 11–23.

[71] Manyà JJ, Sánchez JL, Ábrego J, Gonzalo A, Arauzo J. Influence of gas residence time and air ratio on the air gasification of dried sewage sludge in a bubbling fluidised bed. Fuel 85 (2006) 2027–33.

[72] Yan F, Luo S, Hu Z, Xiao B, Cheng G. Hydrogen-rich gas production by steam gasification of char from biomass pyrolysis in a fixed-bed reactor: influence of temperature and steam on hydrogen yield and syngas composition. Bioresource Technol 101 (2010) 5633–7.

[73] Filippis P, Borgianni C, Paolucci M, Pochetti F. Prediction of syngas quality for two-stage gasification of selected waste feedstocks. Waste Manage 24 (2004) 633–9.

[74] Xiao J, Shen LH, Deng X, Wang ZM, Zhong XL. Study on characteristics of pressurized biomass gasification. Proc Chin Soc Electr Eng. 29 (5) (2009) 103−8.

[75] Niu M, Huang Y, Jin B, Wang X. Oxygen Gasification of Municipal Solid Waste in a Fixed-bed Gasifier. Chinese J Chem Eng 22 (2014) 1021–6.

[76] Miao Q, Zhu J, Barghi S, Wu C, Yin X, Zhou Z. Modeling Biomass Gasification in Circulating Fluidized beds: Model Sensitivity Analysis. International Journal of Energy and Power 2 (2013) 57-63.

[77] Arena U, Gregorio F. Gasification of a solid recovered fuel in a pilot scale fluidized bed reactor. Fuel 117 (2014) 528–36.

[78] Niu M, Huang Y, Jin B, Wang X. Simulation of Syngas Production from Municipal Solid Waste Gasification in a Bubbling Fluidized Bed Using Aspen Plus. Ind Eng Chem Res 52 (2013) 14768−75.

[79] Sun S, Tian H, Zhao Y, Sun R, Zhou H. Experimental and numerical study of biomass flash pyrolysis in an entrained flow reactor. Bioresour Technol 101 (2010) 3678-84.

[80] Zhang Y, Li B, Li H, Zhang B. Exergy analysis of biomass utilization via steam gasification and partial oxidation. Thermochim Acta 538 (2012) 21– 8.

[81] Wu Y, Yang W, Blasiak W. Energy and Exergy Analysis of High Temperature Agent Gasification of Biomass. Energies 7 (2014) 2107-22.

[82] Sreejith C, Muraleedharan C, Arun P. Energy and exergy analysis of steam gasification of biomass materials: a comparative study. Int J Amb Energ 34 (2013) 35-52.

[83] Prins M, Ptasinski K, Janssen F. Thermodynamics of gas-char reactions: first and second law analysis. Chem Eng Sci 58 (2003) 1003-11.

[84] Ionescu G, Rada E, Ragazzi M, Marculesc C, Badea A, Apostol T. Integrated municipal solid waste scenario model using advanced pretreatment and waste to energy processes. Energ Conv Manage 76 (2013) 1083–92.

[85] Ptasinski KJ, Prins MJ, Pierik A. Exergetic evaluation of biomass gasification. Energy 32 (2007) 568-74.

[86] Double JM, Bridgwater AV. Sensitivity of theoretical gasifier performance to system parameters. In W. Palz, J. Coombs, & D.O. Hall, Energy from biomass: 3rd E.C. conference London: Elsevier (1985) 915–9.

[87] Zhang Y, Kajitani S, Ashizawa M, Oki Y. Tar destruction and coke formation during rapid pyrolysis and gasification of biomass in a drop-tube furnace. Fuel 89 (2010) 302–9.

[88] Subramanyam V, Paramshivan D, Kumar A, Mondal M. Using Sankey diagrams to map energy flow from primary fuel to end use. Energ Conv Manage 91 (2015) 342–52.

[89] Montgomery D. Design and Analysis of Experiments. 5th Edition (2001), John Wiley & Sons.

[90] Rostami M, Farzaneh V, Boujmehrani A, Mohammadji M, Baskhsabadi H. Optimizing the extraction process of sesame seed´s oil using response surface method on the industrial scale. Ind Crop Prod 58 (2014) 160-5.

[91] Carpenter D, Bain R, Davis R, Dutta A, Feik C, Gaston K, Jablonski W, Phillips S, Nimlos M. Pilot-Scale Gasification of Corn Stover, Switchgrass, Wheat Straw, and Wood: 1. Parametric Study and Comparison with Literature. Ind Eng Chem Res 49 (2010) 1859-71.

[92] Karimipour S, Gerspacher R, Gupta R, Spiteri R. Study of factors affecting syngas quality and their interactions in fluidized bed gasification of lignite coal. Fuel 103 (2013) 308-20.

[93] Fermoso J, Gil M, Arias B, Plaza M, Pevida C, Pis J, Rubiera F. Application of response surface methodology to assess the combined effect of operating variables on high-pressure coal gasification for H2-rich gas production. Int J Hydrogen Energ 35 (2010) 1191-204.

[94] Silva VB, Rouboa A. Optimizing the gasification operating conditions of forest residues by coupling a two-stage equilibrium model with a response surface methodology. Fuel Process Technol 122 (2014) 163-9.

[95] Coetzer R, Keyser M. Experimental design and statistical evaluation of a full-scale gasification project, Fuel Process Technol 80 (2003) 263–78.

[96] Coetzer R, Keyser M. Robustness studies on coal gasification process variables. OriON 20 (2004) 89-108.

[97] Anderson M, Whitcomb P. DOE Simplified: Practical Tools for Effective Experimentation, 1st Edition (2005), Productivity Press.

[98] Myers R, Montgomery D. Response Surface Methodology. 2nd Edition (2002). New York: John Willey and Sons.

[99] Anderson M, Whitcomb P. RSM Simplified – Optimizing processes using Response Surface Methods for Design of Experiments. 1st Edition (2005), Productivity Press.

[100] Zhou H. Air and steam coal partial gasification in an atmospheric fluidized bed. Energ Fuel 19 (2005) 1619–23.

[101] Narvaez I, Orio A, Aznar MP, Corella, J. Biomass gasification with air in an atmospheric bubbling fluidized bed. Effect of six operational variables on the quality of the produced raw gas. Ind Eng Chem Res 35 (1996) 2110−20.

[102] Gomez-Barea A, Leckner B. Modeling of biomass gasification in fluidized bed. Prog Energy Combust Sci 36 (2010) 444−509.

[103] Arena U. Process and technological aspects of municipal solid waste gasification. A review. Waste Manage 32 (2012) 625-39.

[104] Wang J, Cheng G, You Y, Xiao B, Liu S, He P. Hydrogen-rich gas production by steam gasification of municipal solid waste (MSW) using NiO supported on modified dolomite. Int J Hydrogen Energy 37 (2012) 6503-10.

[105] Derringer G, Suich R. Simultaneous optimization of several variables. J Qual Technol 12 (1980) 214-9.

[106] Knowlton TM, Karri SBR, Issangya A. Scale-up of fluidized-bed hydrodynamics. Powder Technol 150 (2005) 72–7.

[107] Pinto F, André R, Carolino C, Miranda M, Abelha P, Direito D, Perdikaris N, Boukis I. Gasification improvement of a poor quality solid recovered fuel (SRF). Effect of using natural minerals and biomass wastes blends. Fuel 117 (2014) 1034-44.

[108] Brito P, Rodrigues F, Calado L, Oliveira A. Thermal Gasification Of Agro-industrial Residues. WIT Transactions on Ecology and The Environment, Vol 163, Waste Management and the Environment VI (2012) 95 – 102.

[109] Pinto F, André R, Franco C, Lopes H, Gulyurtlu I, Cabrita I. Co-gasification of coal and wastes in a pilot-scale installation 1: Effect of catalysts in syngas treatment to achieve tar abatement. Fuel 88 (2009) 2392-402.

[110] Pinto F, André R, Franco C, Carolino C, Costa R, Miranda M, Gulyurtlu I. Comparison of a pilot scale gasification installation performance when air or oxygen is used as gasification medium 1. Tars and gaseous hydrocarbons formation. Fuel 101 (2012) 102-14.

[111] Aljbour SH, Kawamoto K. Bench-scale gasification of cedar wood – Part II: effect of Operational conditions on contaminant release. Chemosphere 90 (2013) 1501–7.

[112] Kirubakaran V, Sivaramakrishnan V, Nalini R, Sekar T, Premalatha M, Subramanian P. A review on gasification of biomass. Renew Sust Energ Rev 13 (2009) 179–86.

[113] Rapagna S, Latif A. Steam gasification of almond shells in a fluidised bed reactor: The influence of temperature and particle size on product yield and distribution. Biomass Bioenerg 12 (1997) 281–8.

[114] Lv P, Chang J, Wang T, Fu Y, Chen Y. Hydrogen-rich gas production from biomass catalytic gasification. Energ Fuel 18 (2004) 228–33.

[115] Phanphanich M, Mani S. Drying characteristics of pine forest residues. Bioresources 5 (2009) 108-21.

[116] Hansson J, Leveau A, Hulteberg C. Biomass Gasifier Database for Computer Simulation Purposes. Nordlight AB, Rapport SGC 234, ©Svenskt Gastekniskt Center, August 2011.

[117] Bhavya B, Singh R, Bhaskar T. 3 - Preparation of feedstocks for gasification for synthetic liquid fuel production. In: Luque R, Speight J. (Ed.) Gasification for Synthetic Fuel Production, Woodhead Publishing, (2015) 57-71.

[118] Yang H, Chen H. 11 - Biomass gasification for synthetic liquid fuel production. In: Luque R, Speight J. (Ed.) Gasification for Synthetic Fuel Production, Woodhead Publishing, (2015) 241-75.

[119] Speight JG. 7 - Synthetic liquid fuel production from gasification. In: Luque R, Speight J. (Ed.) Gasification for Synthetic Fuel Production, Woodhead Publishing, (2015) 147-174.

[120] http://www.ottusa.com/synthetic_fuel/synthetic_fuel.htm, last access in September 26th 2017.

[121] Worley M, Yale J. Biomass Gasification Technology Assessment, NREL Consolidated Report. NREL/SR-5100-57085, November 2012.

[122] Raskin N, Palonen J, Nieminen J. Power boiler fuel augmentation with a biomass fired atmospheric circulating fluid-bed gasifier. Biomass Bioenerg 20 (2001) 471–81.

[123] Butterman H, Castaldi M. CO2 as a carbon neutral fuel source via enhanced Biomass Gasification. Environ Sci Technol 43 (2009) 9030-7.

[124] Mulas M, Murgia G, Pisani L, Russo R. A quasi-3D computer model of a planar solid-oxide fuel cell stack. In Proceedings of 3rd International Energy Conversion Engineering Conference, San Francisco, California, August 15-18, AIAA: CA, 2005.

[125] Peng XD, Toseland BA, Wang AW, Parris GE. Progress in development of LPDME process: kinetics and catalysts. In Proceedings of 1997 Coal Liquefaction & Solid Fuels Contractors Review Conference, Pittsburgh, Pennsylvania, September 3-4, NETL: Pittsburgh, 1997.

[126] Vassilev SV, Vassileva CG, Vassilev S. Advantages and disadvantages of composition and properties of biomass in comparison with coal: An overview. Fuel 158 (2015) 330–50.

[127] Nipattummakul N, Ahmed I, Gupta AK, Kerdsuwan S. Hydrogen and syngas yield from residual branches of oil palm tree using steam gasification. Int J Hydrogen Energ 36 (2011) 3835-43.

[128] Parthasarathy P, Narayanan K. Hydrogen production from steam gasification of biomass: Influence of process parameters on hydrogen yield - A review. Renew Energ 66 (2014) 570-9.

[129] Reza B, Soltani A, Ruparathna R, Sadiq R, Hewage K. Environmental and economic aspects of production and utilization of RDF as alternative fuel in cement plants:

A case study of Metro Vancouver Waste Management. Resour Conserv Recy 81 (2013) 105–14.

[130] Zhang XH, Deng SH, Wu J, Jiang W. A sustainability analysis of a municipal sewage treatment ecosystem based on emergy. Ecol Eng 36 (2010) 685–96.

[131] http://www.netresiduos.com/content.aspx?menuid=134&eid=992, last access in September 26th 2017.

[132] RTI International. Environmental and Economic Analysis of Emerging Plastics Conversion Technologies Final Project Report. RTI Project No. 0212876.000 (2012) https://plastics.americanchemistry.com/Sustainability-Recycling/Energy-Recovery/Environmental-and-Economic-Analysis-of-Emerging-Plastics-Conversion-Technologies.pdf, last access in September 26th 2017.

[133] Farver M, Frantz C. Garbage to Gasoline: Converting Municipal Solid Waste to Liquid Fuels Technologies, Commercialization, and Policy. Duke University Nicholas School of the Environment (2013).

[134] Couto N, Silva V, Monteiro E, Rouboa A. Assessment of Municipal Solid Wastes Gasification in a Semi-Industrial Gasifier Using Syngas Quality Indices. Energ 93 (2015) 964-73.

[135] http://www.energybc.ca/other/converter.html, last access in September 26th 2017.

[136] Caputo A, Pelagagge P. RDF production plants: I Design and costs. Appl Therm Eng 2002 (22) 423-37.

[137] Gilbert P, Alexander S, Thornley P, Brammer J. Assessing economically viable carbon reductions for the production of ammonia from biomass gasification. J Clean Prod 64 (2014) 581-9.

[138] Ahmad A, Zawawi N, Kasim F, Inayat A, Khasri A. Assessing the gasification performance of biomass: A review on biomass gasification process conditions, optimization and economic evaluation. Renew Sust Energ Rev 53 (2016) 1333-47.

[139] Gasafi E, Reinecke M, Kruse A, Schebek L. Economic analysis of sewage sludge gasification in supercritical water for hydrogen production. Biomass Bioenerg 32 (2008) 1085-96.

[140] Basye L, Swaminathan S. Hydrogen production costs—a survey. SENTECH, Inc. für das US Department of Energy, DOE/GO/10170-778, 1997.

[141] I.E.A. Experience curves for energy technology Policy. Paris: International Energy Agency (IEA); 2000.

Selected Papers

Paper I

2nd law analysis of Portuguese municipal solid waste gasification using CO2/air mixtures

N. Couto, V. Silva, J. Cardoso, A. Rouboa

Journal of CO2 Utilization 20 (2017) 347-356

Journal of CO_2 Utilization 20 (2017) 347–356

Contents lists available at ScienceDirect

Journal of CO_2 Utilization

journal homepage: www.elsevier.com/locate/jcou

2nd law analysis of Portuguese municipal solid waste gasification using CO_2/air mixtures

Nuno Couto[a], Valter Silva[b,*], J. Cardoso[b], Abel Rouboa[a,c]

[a] INEGI-FEUP, Faculty of Engineering, University of Porto, Porto, Porto, Portugal
[b] Polytechnic Institute of Portalegre, Portugal
[c] University of Trás-os-Montes and Alto Douro, Vila Real, Portugal

ARTICLE INFO

Keywords:
2nd law analysis
Municipal solid waste
Semi-industrial gasification plant
Carbon dioxide gasification
CFD
Tar content

ABSTRACT

Urbanization, mainly caused by population growth and industrialization, is causing serious environmental problems. Municipal solid waste (MSW) is one of the major challenges facing the world today. In Portugal the growing volume of MSW has become a central problem for municipalities, due to lack of space and the high costs to solve it. Gasification is starting to be considered as a possible alternative when dealing with municipal wastes. However, first is necessary to overcome some concerns related to the process, such as tar mitigation and carbon dioxide emissions.

The presented study focuses on a second law analysis conducted on Portuguese MSW gasification using carbon dioxide and air mixtures. To do so, a previously developed numerical model, validated using data from a semi-industrial plant, was used to assess carbon dioxide injection. First, influence of operational conditions on syngas exergy values was studied. Exergy values increased close to 6% when equivalent rate was increased from 0.15 to 0.25, steadily dropping with further increase. On the other hand, exergy values appear to steadily increase with carbon dioxide addition (14% when increased from 0 to 1) and reactor temperature (40% when increased from 700 to 900 °C).

Then, the influence of temperature and CO_2/MSW ratio on exergy efficiency, tar efficiency and carbon dioxide conversion was investigated. Results showed that both parameters have a positive effect on exergy efficiency. Conversely, CO_2/MSW ratio and gasification temperature lead to decreases in both tar exergy efficiency and in carbon dioxide.

1. Introduction

According to the World Urbanization Prospects by UN DESA's Population Division, 54% of the world's population currently lives in urban areas, a proportion that is expected to increase to 66% by 2050 [1]. Even more daunting is the fact that municipal solid wastes (MSW), one of the most important by-products of an urban lifestyle, is growing at an even faster rate.

At the beginning of this century there were 2900 million urban residents generating about 0.64 kg of MSW per person per day. Just 10 short years later, with an additional 100 million urban residents, urban waste generation increased to a staggering 1.2 kg per person per day representing 1300 million tons per year. According to current projections, by 2025 there will be 4300 million urban residents generating about 1.42 kg per person per day [2].

The treatment of these residues is quite expensive and often represents the single largest budgetary item of a city [2]. In fact, in Portugal the growing volume of MSW has become a major problem for municipalities, either due to lack of space or because of high costs to solve this problem.

Faced with this situation, and the further rationalization of development, the solutions identified as preferred to the problem of waste management are the prevention (avoiding or reducing waste production), recovery (recycling, energy recovery and others) and disposal in landfills (as a last resort).

Portugal is a country with scarce energy resources of fossil origin. In 2014, Portuguese energy dependence from outside stood at 71.5%, the lowest since 1995. However, the balance of trade (the difference between a country's imports and its exports) still shown a trade deficit of 5710 million euros [3]. In order to reduce energy dependency and secure the national supply, it is necessary to increase the relative weight of primary energy produced in the country.

* Corresponding author at: Campus Politécnico, 10, 7300-555 Portalegre, Portugal.
E-mail addresses: nunodiniscouto@hotmail.com (N. Couto), valter@fe.up.pt, valter.silva@ipportalegre.pt (V. Silva), jps.cardoso@ipportalegre.pt (J. Cardoso), rouboa@utad.pt (A. Rouboa).

http://dx.doi.org/10.1016/j.jcou.2017.06.001
Received 7 May 2016; Received in revised form 12 January 2017; Accepted 2 June 2017
Available online 26 June 2017

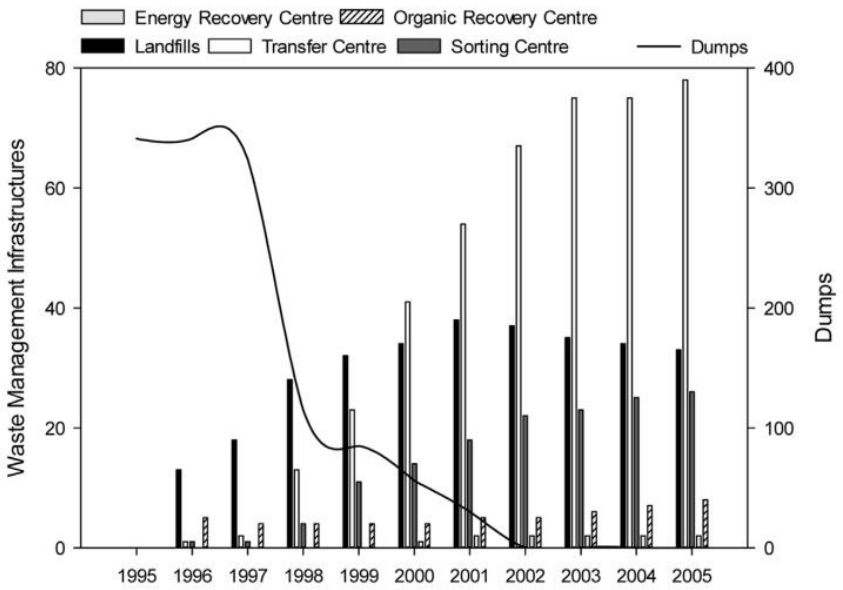

Fig. 1. Waste management infrastructures in Portugal from 1995 to 2005.

According to the Portuguese Environment Agency (APA) [3], in 2014, 4.72 million tons of municipal wastes were produced in Portugal, 2.44% more than in 2013, representing a reversal of the downward trend observed since the beginning of the decade. According to Teixeira et al. [4], most of the MSW in Portugal is still being sent to landfills and incineration continues to be the most common method of thermal treatment for waste-to-energy facilities (19% of MSW were incinerated in 2014).

Incineration allows the recovery of heat produced by combustion, but the recovered heat is usually consumed in the vicinity of the incineration plant. Furthermore, this type of technology entails high investment and operating costs while producing a wide variety of pollutants.

Given the above, gasification technology is becoming a viable alternative to the energetic recovery of MSW, due to its pollution minimization effects and capability in producing a synthesis gas that can be used in a wide variety of applications such as heat, electricity, chemicals and transport fuel [5].

Despite its many advantages, biomass and waste gasification have yet to represent more than 0.33% of the global gasification capacity worldwide [6]. In order to make the process more appealing to both private sector and government institutions, it is necessary to further develop the technology and increase research to find solutions for some of the most serious problems, such as CO_2 and tar production.

Recently, biomass gasification studies, using carbon dioxide as a gasifying agent, have been carried out with very exciting results. Chaiwatanodom et al. [7] performed a thermodynamic analysis using biomass gasification with recycled CO_2 and results show that recycling CO_2 increases syngas production. Butterman and Castaldi [8] demonstrated that CO_2 injection not only allows for the tailoring of the H_2/CO ratio but also leads to better char gasification. Renganathan et al. [9] presented a thermodynamic analysis using a Gibbs minimization approach and achieved complete carbon conversion by increasing CO_2 flow to the point that cold gas efficiencies higher than 100% were observed.

While literature regarding MSW gasification using CO_2 as a gasifying agent literature is still lacking, it has been reported that CO_2 addition can expedite the thermal cracking of volatiles and act like a catalyst [10]. Simultaneously, CO_2 injection during pyrolysis minimizes tar formation [11], which is crucial for MSW gasification to become the primary waste management and treatment process.

One way to expedite the mainstream of this technique is by optimizing the process with more efficient operating conditions. The method of exergy analysis is particularly appropriate in this regard usually being used to identify opportunities for process improvement and to evaluate different process alternatives.

However, to the best of our knowledge, work focused on thermodynamic analysis of MSW gasification are absence from the current literature.

To cover this significant void in current literature, gasification of Portuguese MSW using air and CO_2 mixtures was studied. A previous numerical model was used to collect further data on the MSW gasification process. Numerical results were validated against experimental results from a semi-industrial reactor. Influence of operational conditions on exergy values and exergy efficiency was investigated. Tar mitigation and carbon dioxide conversion were also examined.

2. Materials and methods

The first federal effort to improve waste disposal technology was made in 1965 when the Solid Waste Disposal Act (SWDA) was passed as an act of congress in the United States [12]. Prior to 1995, the overwhelming majority of wastes produced in Portugal were deposited in open dumps and the remaining going to controlled landfills.

The implementation of the first strategic plan for municipal solid waste (PERSU I) came to change the view of waste management in Portugal. The main goals of the national waste management plan were the total eradication of open dumps, the development of multi-municipal and intermunicipal MSW management systems, and the construction of news infrastructures.

Despite failing the initial timeframe, eradication of open dumps was achieved in 2002 and the uncontrolled disposal in dumps was replaced by the landfilling in sanitary sites. Fig. 1 displays the evolution of waste management infrastructures in Portugal from 1995 to 2005.

Above Figure shows that the number of dump sites in 1995 was close to 350; data regarding the remaining infrastructures is unavailable. Following the goals set by PERSU I (and PERSU II) the number of transfer centers, sorting centers, energy and organic recovery centers was increased over the years while dump sites were progressively decreased until its eradication [13].

Moving forward to present days, current situation is far better than the one found at the beginning of the century. According to APA [3], in 2014 from the 4.72 million tons of wastes produced, regarding direct disposal, only 42% were sent to landfills, 19% to incineration, 19% to mechanical and biological treatment, 9% to mechanical treatment, another 9% to material valorization and 2% to organic valorization.

Despite the hierarchy of waste management requiring landfills to be used as a last resort, Portugal is still far from achieving the goal of 29% set for landfilling proposed in the strategic plans. This goal seems even less attainable if we consider the total fraction of waste landfilled by both direct and indirect means, the latter representing dregs and rejects from process treatment, reaches an astounding 58%.

In Portugal, in 2012, total emissions of greenhouse gas (GHG), excluding forestry and land use, was estimated at about 69 million tons of CO_2 equivalent (CO_2e), representing an increase of 13.1% compared to 1990. CO_2 was the main gas responsible for the greenhouse gases, accounting for about 73.2% of total emissions, followed by CH_4 with 17.8 and N_2O with 6.5%. Regarding emissions by activity sector, the residues sector represented 11.9% [14].

2.1. Portuguese municipal solid waste characterization

Since model accuracy depends on using realistic data, the characterization and analysis of Portuguese MSW was carried out using data from the Oporto metropolitan area obtained from LIPOR, entity responsible for the management, treatment and recovery of solid waste municipal produced in the city.

Early estimates from 2016 indicate that 118.8 ktons of waste were produced on the first 3 months of the year alone. Although premature, this represents an increase in 5% when compared to the same period from last year.

During the management and treatment of collected MSW from 2014 samples were acquired for posterior physical characterization according to the categories in Table 1.

From the pre-treatment of MSW, usually via shredding and dehydration, a refuse derived fuel (RDF) containing just cellulosic and plastics is obtained [4]. Plastic residues are mainly comprised by polyethylene, polystyrene, and polyvinyl chloride while cellulosic materials are composed of cellulose, hemicelluloses, and lignin.

Since an ultimate analysis does not distinguish cellulosic materials, their composition was assumed to be similar to the one found by Onel et al. [15], whereas report informs of the relative quantities of each monomer in the MSW for plastics, as listed in Table 2.

This waste characterization was employed in the formulation of the MSW mixture in Fluent to model the gasification process. The proximate and ultimate analysis of this feedstock is shown in Table 3.

2.2. Experimental set-up

Even though conducted study focuses on numerical results it is imperative that numerical models are built upon realistic experimental data. In fact, one of the main strengths of our model is the fact that it was built using data collected in the gasification plant from the School of Technology and Management (ESTG) of the Polytechnic Institute of Portalegre (IPP).

Table 1
Physical characterization of the MSW in Oporto in 2014.

Category	% Weight
Putrefied residues	37.57
Paper	6.16
Cardboard	4.31
Composites	6.39
Textiles	7.74
Sanitary textiles	8.72
Plastics	12.10
Combustive non specified	0.93
Glass	5.53
Metals	2.45
Non-combustive non specified	0.50
Hazardous residues	0.01
Fine elements	7.59

Table 2
Chemical composition of MSW in Oporto in 2014.

Category	% Weight	Chemical formula
Cellulosic material	85.42	*
Polyethylene	10.99	$(C_2H_4)_n$
Polyethylene terephthalate	2.02	$(C_{10}H_8O)_n$
Polypropylene	0.81	$(C_3H_6)_n$
Polystyrene	0.76	$(C_8H_8)_n$

* It was considered the proportion of cellulose, hemicellulose and lignin found in Ref. [15].

Table 3
Ultimate and proximate analysis of Portuguese MSW.

Substrate Properties	MSW
Elementary analysis (%)	
N	1.4
C	48
H	6.3
O	43.6
Humidity (%)	17.6
Density (Kg/m^3)	247
Net Heat Value (MJ/kg biomass)	14.4
Proximal analysis (%)	
Ash	14.9
Volatile Matter	76.62
Fixed Carbon	8.46

The referred 200 kW pilot thermal plant, based on bubbling fluidized bed technology, has a processing capacity of approximately 100 kg/h. Biomass is introduced above the floating bed of inert material and usually operates between 750 and 850 °C, being regulated by changing the air/biomass ratio. Preheated air enters the gasifier via a series of (37) diffusers regulating the required flow rate while biomass enters the gasifier through a feeding system using an Archimedean screw variable and controllable speed. Syngas leaves the reactor at approximately 700 °C and passes through a gas cooling system cooling it to about 150 °C. While this is happening ash and other waste produced are first filtered out and then stored in a suitable tank. Finally, the syngas goes through a condenser where condensed liquids are removed by cooling the syngas to room temperature thus becoming ready to be used in other purposes.

The schematics as well as an extensive description of the gasification plant can be found elsewhere [16,17].

3. Mathematical model

The first necessary steps for the development of our model began early in the decade motivated by the lack of reliable numerical models capable of describing the gasification process in a pilot scale fluidized bed reactor.

Since our model is well documented in available literature we will just state the key points that define it. Both gas and dispersed phases were handled using a Eulerian − Eulerian approach. Constitutive properties of the dispersed phase were evaluated with the aid of the kinetic theory of granular flows while the gas-phase behavior was simulated employing the $k-\varepsilon$ turbulent model. Regarding the chemical model, when the developed model was upgraded to handle MSW, the devolatilization section had to be expanded to cope with the heterogeneity of said substrate. Tables 4 and 5 comprise the main equations regarding both hydrodynamic model and conservation equations for each phase and all the relevant reactions and their reaction rates, respectively.

Further details on the model can be found in Refs. [16,18].

In this study, our previously pyrolysis model with secondary tar generation was adopted [17]. The finite-rate/Eddy-dissipation model

Table 4
Hydrodynamic model and conservation equations for both gas and solid phases.

Hydrodynamic Model
Kinetic Energy:
$\frac{\partial}{\partial t}(\rho k) + \frac{\partial}{\partial x_i}(\rho k u_i) = \frac{\partial}{\partial x_j}\left[\left(\mu + \frac{\mu_t}{\sigma_k}\right)\right] + G_k + G_b - \rho\varepsilon - Y_M + S_k$
Dissipation Rate:
$\frac{\partial}{\partial t}(\rho\varepsilon) + \frac{\partial}{\partial x_i}(\rho\varepsilon u_i) = \frac{\partial}{\partial x_j}\left[\left(\mu + \frac{\mu_t}{\sigma_\varepsilon}\right)\frac{\partial \varepsilon}{\partial x_j}\right] + C_{1\varepsilon}\frac{\varepsilon}{k}(G_k + C_{3\varepsilon}G_b) - C_{2\varepsilon}\rho\frac{\varepsilon^2}{k} + S_\varepsilon$
Granular Eulerian Model:
$\frac{3}{2}\left[\left(\frac{\partial(\rho_S \alpha_S \Theta_S)}{\partial t} + \nabla.\,(\rho_s \alpha_s \vec{v_s} \Theta_s)\right)\right] = (-P_s\bar{I} + \bar{\bar{\tau}}_s)\colon \nabla(\vec{v_s}) + \nabla.\,(k_{\Theta a}\nabla(\Theta_s)) - \gamma_{\Theta a} + \phi_{ls}$

Conservation Equations

Gas Phase	Solid Phase
Energy:	
$\frac{\partial\left(\alpha_q\rho_q h_q\right)}{\partial t} + \nabla\cdot(\alpha_q\rho_q\vec{u}_q h_q) = -\alpha_q\frac{\partial\left(p_q\right)}{\partial t} + \bar{\bar{\tau}}_q\colon \nabla(\vec{u}_q) - \nabla\vec{q}_q + S_q + \sum_{p=1}^{n}(\vec{Q}_{pq} + \dot{m}_{pq}h_{pq})$	$\frac{\partial\left(\alpha_p\rho_p h_p\right)}{\partial t} + \nabla\cdot(\alpha_p\rho_p\vec{u}_p h_p) = -\alpha_p\frac{\partial\left(p_p\right)}{\partial t} + \bar{\bar{\tau}}_p\colon \nabla(\vec{u}_p) - \nabla\vec{q}_p + S_p + \sum_{q=1}^{n}(\vec{Q}_{pq} + \dot{m}_{pq}h_{pq})$
Mass:	
$\frac{\partial\left(\alpha_q\rho_q\right)}{\partial t} + \nabla\cdot(\alpha_q\rho_q\vec{u}_q) = -M_C\sum\gamma_C R_C$	$\frac{\partial\left(\alpha_p\rho_p\right)}{\partial t} + \nabla\cdot(\alpha_p\rho_p\vec{u}_p) = M_C\sum\gamma_C R_C$
Momentum:	
$\frac{\partial\left(\alpha_q\rho_q\vec{u}_q\right)}{\partial t} + \nabla\cdot(\alpha_q\rho_q\vec{u}_q\vec{u}_q) = -\alpha_q\nabla p_q + \alpha\rho_q g + \beta(u_q - u_p) + \nabla\cdot\alpha_q\bar{\bar{\tau}}_q + S_{pq}U_S$	$\frac{\partial\left(\alpha_p\rho_p\vec{u}_p\right)}{\partial t} + \nabla\cdot(\alpha_p\rho_p\vec{u}_p\vec{u}_p) = -\alpha_p\nabla p_p + \alpha\rho_p g + \beta(u_q - u_p) + \nabla\cdot\alpha_p\bar{\bar{\tau}}_p + S_{pq}U_S$

Table 5
Chemical reaction model.

Reactions	Reaction Rate
Pyrolysis:	
Cellulose → α_1*volatiles* + α_2*TAR* + α_3*char*	$r_1 = A_i exp\left(\frac{-E_i}{T_s}\right)(1-a_i)^n$
Hemicellulose → α_4*volatiles* + α_5*TAR* + α_6*char*	$r_2 = A_i exp\left(\frac{-E_i}{T_s}\right)(1-a_i)^n$
Lignin → α_7*volatiles* + α_8*TAR* + α_9*char*	$r_3 = A_i exp\left(\frac{-E_i}{T_s}\right)(1-a_i)^n$
Plastics → α_{10}*volatiles* + α_{11}*TAR* + α_{12}*char*	$r_4 = \left[\sum_{i=1}^{n} A_i exp\left(\frac{-E_i}{RT}\right)\right]\rho_v$
PrimaryTAR → *volatiles* + *SecondaryTAR*	$r_5 = 9.55 \times 10^4 exp\left(\frac{-1.12\times10^4}{T_g}\right)\rho_{TAR1}$
Homogeneous Reactions:	
$CO + 0.5O_2 \rightarrow CO_2$	$r_6 = 1.0 \times 10^{15} exp\left(\frac{-16000}{T}\right)C_{CO}C_{O_2}^{0.5}$
$CO + H_2O \rightarrow CO_2 + H_2$	$r_7 = 2780 exp\left(\frac{-1510}{T}\right)\left[C_{CO}C_{H_2O} - \frac{C_{CO_2}C_{H_2}}{0.0265 exp\left(\frac{3968}{T}\right)}\right]$
$CO + 3H_2 \leftrightarrow CH_4 + H_2O$	$r_8 = 3.0 \times 10^5 exp\left(\frac{-15042}{T}\right)C_{H_2O}C_{CH_4}$
$H_2 + 0.5O_2 \rightarrow H_2O$	$r_9 = 5.159 \times 10^{15} exp\left(\frac{-3430}{T}\right)T^{-1.5}C_{O_2}C_{H_2}^{1.5}$
$CH_4 + 2O_2 \rightarrow CO_2 + 2H_2O$	$r_{10} = 3.552 \times 10^{14} exp\left(\frac{-15700}{T}\right)T^{-1}C_{O_2}C_{CH_4}$
Heterogeneous Reactions:	
$C + 0.5O_2 \rightarrow CO$	$r_{11} = 596 T_P exp\left(\frac{-1800}{T}\right)$
$C + CO_2 \rightarrow 2CO$	$r_{12} = 2082.7 exp\left(\frac{-18036}{T}\right)$
$C + H_2O \rightarrow CO + H_2$	$r_{13} = 63.3 exp\left(\frac{-14051}{T}\right)$

was used to describe homogeneous reactions while the Kinetic/Diffusion Surface Reaction Model was employed for heterogeneous ones. The values for each one of the parameters shown in the pyrolysis reactions can be found in Ref. [19]. The Arrhenius rates and the kinetic parameters for these reactions as well as further explanation can be found in Ref. [17], and so can solver procedure details.

4. Exergy analysis

To further analyze the process of Portuguese MSW gasification using air/CO_2 mixtures and to optimize it with more efficient operating conditions an exergetic analysis was applied to the obtained data. Exergy analysis give a tremendous insight by considering the increase in entropy that is accompanied by any energy conversion process. In this work a similar methodology to calculate exergy used by Zhang et al. [20] and Parvez et al. [21] was employed.

In the described system, the exergy balance can be written as:

$$Ex_{MSW} + Ex_{CO_2} + Ex_{air} + Ex_{heat} \rightarrow Ex_{syngas} + Ex_{tar} \quad (1)$$

Where Ex_{MSW}, Ex_{CO_2}, Ex_{air}, Ex_{syngas} and Ex_{tar} represent the exergy rates of MSW, carbon dioxide, air, heat supplied to the gasifier, syngas and tar content, respectively.

Neglecting the kinetic and potential exergy, the total exergy of a flow can be defined by the sum of the chemical exergy rate and the physical exergy rate:

$$Ex = Ex_{ch} + Ex_{ph} \quad (2)$$

Where the chemical and physical exergy can be written, respectively as:

$$Ex_{ch} = \sum_i n_i\left(e_{0_i} + RT_0 ln\frac{n_i}{\sum n_i}\right) \quad (3)$$

$$Ex_{ph} = \sum_i n_i[(h-h_0) - T_0(s-s_0)] \quad (4)$$

Where n_i is the molar yield of gas component i (mol/kg), R is the ideal, or universal, gas constant and e_{0_i} is the standard chemical exergy of a pure chemical compound i. Also, s and h are entropy and enthalpy of a system at given temperature and pressure, and h_0 and s_0 are enthalpy and entropy of a system at the environmental temperature and pressure, respectively.

The differences $(h - h_0)$ and $(s - s_0)$ of ideal gases can be obtained using:

$$h - h_0 = \int_{T_0}^{T} c_p dT \quad (5)$$

$$s - s_0 = \int_{T_0}^{T} \frac{c_p}{T} dT - Rln\frac{P}{P_0} \quad (6)$$

Where c_p is the constant pressure specific heat capacity which can be calculated by:

$$c_p = a + bT + cT^2 + dT^3 \quad (7)$$

The coefficients a–d were taken from the literature [20].

To calculate the exergy of MSW with less complexity, Szargut and Styrylska [22] formed the following correlation:

$$Ex_{MSW} = \dot{m}\beta LHV_{MSW} \quad (8)$$

The formula of correlation factor β is given by:

$$\beta = \frac{1.0412 + 0.2160\left(\frac{H}{C}\right) - 0.2499\left(\frac{O}{C}\right)\left[1 + 0.7884\left(\frac{H}{C}\right)\right] + 0.0450\left(\frac{N}{C}\right)}{1 - 0.3035\left(\frac{O}{C}\right)} \quad (9)$$

Where O, C, H and N are the weight fractions of oxygen, carbon, hydrogen and nitrogen in the MSW, respectively.

Similarly, in this work the tar chemical exergy is simulated with help of another correlation for liquid fuels [23]:

$$Ex_{tar} = \dot{m}_{tar} LHV_{tar}\left(1.0401 + 0.1728\left(\frac{H}{C}\right) + 0.0432\left(\frac{O}{C}\right) + 0.2196\left(\frac{S}{C}\right)\left[1 - 2.0628\left(\frac{H}{C}\right)\right]\right) \quad (10)$$

Finally, to better understand the effects of substrate and operational parameters on reactor performance, exergy efficiency of syngas and tar were investigated. They can be calculated as being:

$$\varepsilon_{syngas} = \frac{Ex_{syngas}}{Ex_{MSW} + Ex_{CO_2} + Ex_{heat}} \quad (11)$$

$$\varepsilon_{tar} = \frac{Ex_{tar}}{Ex_{MSW} + Ex_{CO_2} + Ex_{heat}} \quad (12)$$

5. Results and discussion

Although an extremely powerful tool, numerical modelling alone should be use with relative caution. In fact, it is best to rely on extensive experimental work to both validate and upgrade developed models.

With this in mind, the first draft of our model was developed using a reliable set of experimental runs performed in the previously described plant. The ability to build a numerical model using data from a semi-industrial reactor allows us to be much closer to realistic commercial size conditions since the hydrodynamic phenomena in a laboratory scale fluidized bed are not the same as on large scales [24].

Gasification of Portuguese biomass substrates was first studied with exciting results that showed the potential for fossil fuel replacement [16,25,26]. During said studies continuous developments and expansions were performed in the model that allowed an increasingly detailed study of the gasification process.

To counter the improper disposal of municipal waste in landfills our

model had to undergo a restructuring on the devolatilization section in order to cope with the heterogeneity of MSW [17]. In those studies Portuguese MSW gasification was studied using air a gasifying agent [17,18]. Since, at that moment, the reactor couldn't handle said wastes, the model had to be validated using data collected from the literature. Still, the model proved to be able of predicting the behavior of all syngas species in a wide range of operating conditions with significant accuracy.

To further promote MSW treatment via carbon dioxide addition a similar approach would be ideal but unfortunately, for the time being, there isn't any experimental data available on the current literature on MSW gasification with CO_2.

One way around this problem is to assume the model will predict the gasification process using mixtures of air and CO_2 as it already successfully did for different conditions and substrates. This was precisely what we did in a preliminary study of CO_2/air mixtures [27]. The main findings of said study were:

- Study showed that increase in CO_2/biomass ratio promotes CO and CO_2 molar fractions while hindering H_2 and C_nH_m formation. This is expected since higher CO_2 content mainly promotes Boudouard reaction which leads to CO formation. Carbon dioxide also promotes reverse water-gas shift reaction and methane reforming (also known as dry reforming) leading to both H_2 and CH_4 depletion. CO_2 content is expected to increase since a considerable fraction of the gasifying agent leaves the reactor unreacted.
- Conversely, an increase in gasification temperature promotes both CO and H_2 content at the expense of CO_2 and C_nH_m. This is due to endothermic reactions being favored with higher temperature (according to Le Chatelier's principle).

While results for MSW gasification are extremely scarce those available corroborate with obtained results [27]. In any case, since the studied waste overwhelmingly consists of cellulosic material, the same techniques used to enhance the thermal treatment of biomass substrates will apply to MSW, which means that common biomass substrates and MSW will share the same overall tendencies [28,29].

5.1. Exergy values

Since gasification using carbon dioxide as a gasifying agent relies on highly endothermic reactions it requires an additional heat source, which can be direct, by introducing oxygen into the reactor and allowing oxidation reactions to provide the necessary heat, or indirect, by preforming combustion externally, using either biomass or syngas [30].

In this work it was decided to study air and CO_2 mixtures since the high costs of implementation of pure O_2 in large facilities is still uncertain.

As stated, analyzing exergy streams will allow us to find sources of inefficiencies, which are related to exergy destruction and exergy loss. First the exergy values of produced gas at various equivalent ratios and reactor temperatures will be investigated to find a good departure point. Using said point, CO_2-to-MSW ratio is slowly increased in order to investigate its influence on exergy values. Finally, the influence of the gasification temperature alone on exergy values in a CO_2 rich environment was studied.

Exergy values are based on 1 kg MSW.

5.1.1. Influence of ER on syngas exergy values

Equivalent ratio (ER) is one of the most significant parameters, which have effect on the gasification process including syngas composition. It is defined as the ratio between the actual air/fuel ratio and the stoichiometric air/fuel ratio:

$$ER = \frac{oxygen\ \ mass/dry\ \ MSW\ \ mass}{stoichiometric\ \ oxygen/MSW\ \ mass\ \ ratio} \quad (13)$$

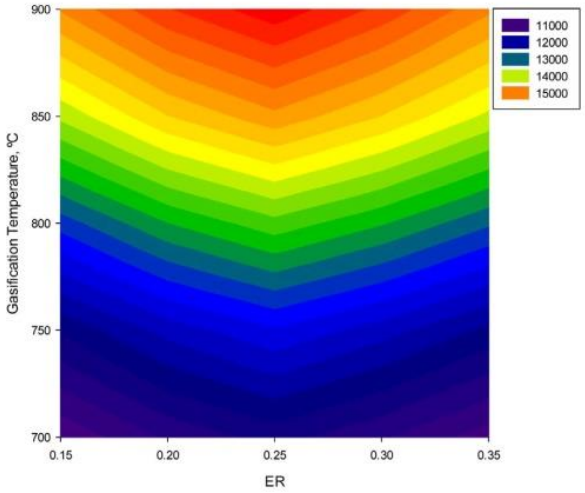

Fig. 2. Exergy values of syngas at various reactor temperatures and ER values (units: kJ).

ER was kept between 0.15 and 0.35 since all of the experiments previously conducted fell in this range and also because, according to Wang et al. [30], the ER values most suitable for gasification range between 0.2 and 0.4.

Fig. 2 presents the exergy values of syngas at various ER values and reactor temperatures. The presented filled contour graph greatly contributes in identifying where the hot spots (high exergy values) are thus quickly finding the optimal operational conditions.

Gasification temperature has a clear influence on exergy values (in depth explanation in chapter 5.1.3.), when temperature was increased from 700 °C to 900 °C (with an equivalent ratio of 0.25), exergy values went from 11,483 kJ to 15,737 kJ (increase over 37%).

ER however has a very distinct effect on exergy values, when it was first increased from 0.15 to 0.25 (with gasification temperature of 900 °C) exergy value increased from 14,818 kJ to 15,737 kJ, which represents an increase close to 6.2%. Further increase beyond 0.25 leads to a steady decrease in the exergy values. According to Prins et al. [31], past this maximum ER value, exergy values decrease due to a decrease in chemical exergy which is not fully compensated for by the increases in the physical exergy.

In summary, by increasing ER, one is mostly promoting combustion reactions (such as the partial combustion of char, CO and H_2) that will lead to higher levels of CO_2 and H_2O at the cost of CO and H_2 [32]. This variation leads to a substantially decrease in the calorific value of the produced gas. On the other hand, oxidation reactions promote carbon conversion which in turn will lead to an increase in gas yield. These two opposing influences are the main culprits for the obtained maximum.

Obtained results are consistent with current literature [31,33].

5.1.2. Influence of CO_2/MSW on syngas exergy values

After founding the optimal operational condition set for air gasification, one can use said set and increase the CO_2/MSW ratio to investigate the influence of carbon dioxide addition in the gasifying agent mixture. The ratio is defined as the ratio between the carbon dioxide mass flow rate and the MSW mass flow rate.

The exergy values for syngas composition as a function of CO_2/MSW ratio are shown in Fig. 3.

As stated, exergy values are determined by the sum of physical and chemical exergies of each individual syngas component. The former depends on enthalpy and entropy as well as individual gas yield of gas while the latter mainly depends on the yield of gas component.

According to the above Figure, overall exergy values appear to increase with carbon dioxide addition. CO_2/MSW ratio has two contradictory effects on the system; the first is the positive effect on syngas yield and carbon monoxide fraction which causes a sudden increase in the exergy values when carbon dioxide is first introduced. Past 0.4,

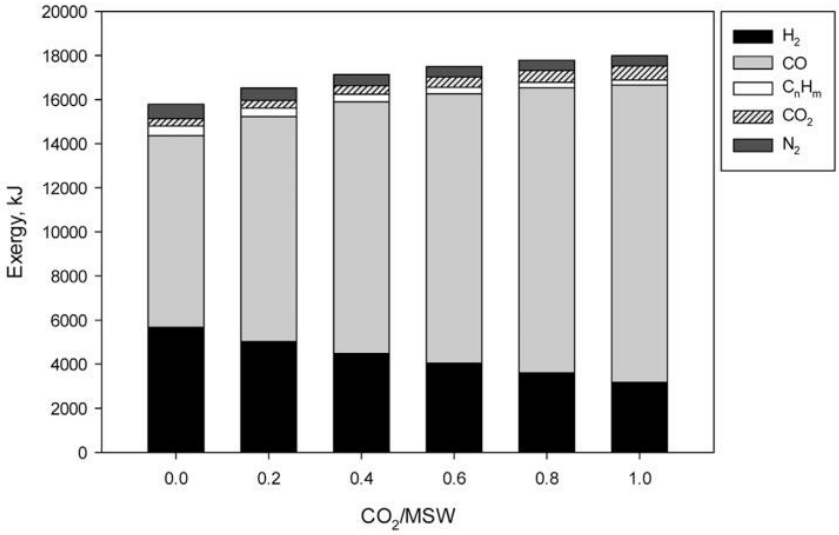

Fig. 3. Exergy values of syngas as a function of CO_2/MSW (Operating conditions: Temperature – 900 °C; ER – 0.25).

exergy values seem to slower its increasing rate due to the second effect which is the suppression of H_2 and C_nH_m, two main decisive elements in the calculation of syngas exergy.

Since both N_2 and CO_2 have such a low standard chemical exergy value and at this temperature hydrocarbon fraction is particularly low, hydrogen and carbon monoxide fraction vastly dictate the overall exergy value. Simultaneously, since CO_2 addition enhances both char gasification and pyrolysis, which leads to increase in carbon conversion, gas yield is expected to increase also promoting the overall exergy value.

As previously stated, gasification results using carbon dioxide as a gasifying agent are extremely scarce from the current literature, especially considering exergy values. In fact, the only available results, to the best of our knowledge, for CO_2-enhanced gasification that includes the concept of exergy is the work of Parvez et al. [21]. Although this particular study was conducted for rice straw, their results are in line with results presented in this chapter.

5.1.3. Influence of temperature on syngas exergy values

In the described plant, the reactor temperature is a dependent variable of the process, being controlled by adjusting ER or admission of biomass. However, by taking advantage of mathematical models, one may vary the gasification temperature to analyze its effect on the gasifier performance. This is crucial to better understand the gasification process since temperature has a predominant effect on reaction kinetics and the gasifier performance is very sensitive to the bed temperature change [30].

The exergy values for syngas composition as a function of gasification temperature are shown in Fig. 4.

Presented results show that gasification temperature has a strong influence on syngas exergy values since it leads to increases in enthalpy (and entropy) and gas yield, the two main responsible for exergy increase [33]. In fact, when the reactor temperature was increased from 700 °C to 900 °C the total energy of syngas increased from 12,824 to 17,986 kJ.

Comparing all three parameters, one can see that the effect of reactor temperature on the total syngas exergy (40%) was greater than that of CO_2/MSW ratio (14%) and obviously much greater than that of ER (6.2%). This is consistent with the current literature [21,33].

Conversely to carbon dioxide addition, increase in gasification temperature doesn't appear to slow its positively effect on exergy values within studied range. Current literature shows that positive impact of temperature on gasifier performance can go as why as 1200 °C [9].

5.2. Main contributions of CO_2 addition

According to the (limited) literature on biomass gasification with carbon dioxide as a gasifying agent, CO_2 addition can minimize some of the main setbacks of the process [34].

Fig. 5 displays influence of CO_2/MSW ratio and temperature on syngas exergy efficiency.

Results from Fig. 6 shows that CO_2/MSW ratio has a positive effect on syngas exergy efficiency, similarly to what was seen for exergy values, although with a less pronounced upsurge. This was expected since efficiency values are mostly determined by their energy/exergy values [20].

A more careful analysis shows that further increase in CO_2/MSW beyond 0.6 doesn't contribute to a substantial increase in exergy efficiency; in fact, over 0.8, efficiency appears to slightly decrease. This is caused by a considerable increase in biomass and carbon dioxide heating values [21].

Similarly to what occurred with exergy values, gasification temperature has a stronger influence on exergy efficiency all throughout the studied range. Overall, the highest exergy efficiency was found for a CO_2/MSW ratio of 0.8 and gasification temperature of 900 °C with 78.3%.

Although there are no results in the literature for municipal solid waste gasification to compare to, the few studies that investigate other biomass substrates appear to be in agreement with the obtained results [7,9,21].

Another major setback that researchers are still trying to avoid is related with tar formation. According to Devi et al. [35], tar can lead to serious problems during biomass gasification by blocking and fouling process equipments such as engines and turbines.

Recent studies have shown that CO_2 has the ability to act as a catalyst enhancing thermal cracking of volatiles leading to tar mitigation [36].

Fig. 6 displays influence of CO_2/MSW ratio and temperature on tar exergy efficiency.

Attentive analysis shows that Figs. 6 and 7 present opposite results. In fact, increase in both CO_2/MSW ratio and gasification temperature leads to a decrease in the tar exergy efficiency. Again, similarly to what was seen in previous studies, temperature has substantially stronger effect on efficiency values. Indeed, When CO_2/MSW ratio was increased to 1, tar efficiency decreased from 7.1% to 3.8% (keeping gasification temperature at 700 °C). Conversely, when temperature was increased from 700 °C to 900 °C tar efficiency decreased from 7.1% to 1.4% (keeping CO_2/MSW ratio at 0). This has to do with the fact that higher gasification temperatures dramatically reduce the yields of tar. This is

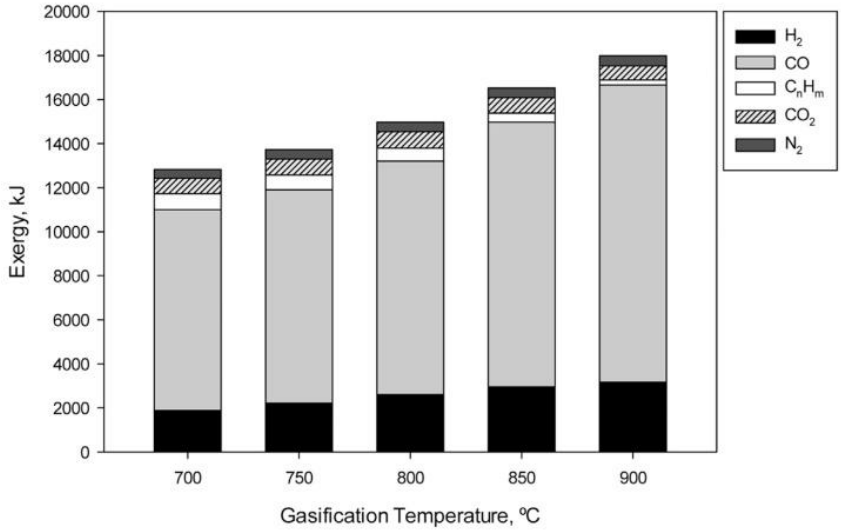

Fig. 4. Exergy values of syngas as a function of temperature (Operating conditions: CO_2/MSW – 1; ER – 0.25).

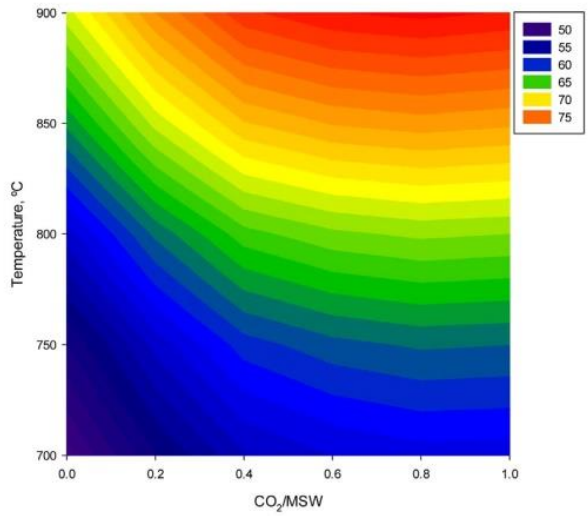

Fig. 5. Influence of CO_2/MSW ratio and Temperature on Syngas Exergy Efficiency (units: %).

consistent with the current literature [20,37].

Tar efficiencies obviously follow a very close trend to tar yield itself. Again, since substrate exergy value represents the dominant value on the exergy input, the exergy efficiency of tar is mainly dictated by the exergy value of tar.

One of the more exciting conclusions shared by recent studies is the positive contribution to the environment that carbon dioxide addition can have. One of the main contributions is the ability to reduce CO_2 pollution [8]. In fact, since CO_2 can be converted into CO, gasification using carbon dioxide as a gasifying agent can tremendously help in decreasing its emissions to the atmosphere. According to Butterman and Castaldi [8], it has the ability to process hundreds of millions of tons of CO_2 every year.

Carbon dioxide conversion can be given by:

$$X_{CO_2} = \frac{moles\ of\ CO_2\ in\ gasifying\ agent - moles\ of\ CO_2\ in\ produced\ gas}{moles\ of\ CO_2\ in\ gasifying\ agent} \quad (14)$$

Fig. 7 displays influence of CO_2/MSW ratio and temperature on carbon dioxide conversion.

Above Figure presents very interesting results regarding the impact of carbon dioxide on reactor performance from an environmental

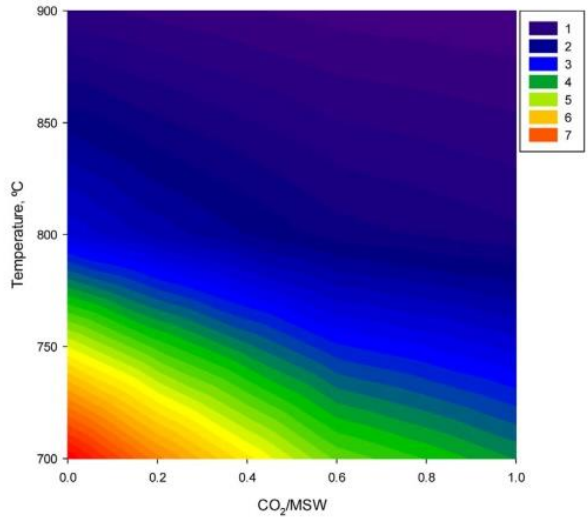

Fig. 6. Influence of CO_2/MSW and temperature on tar exergy efficiency (units: %).

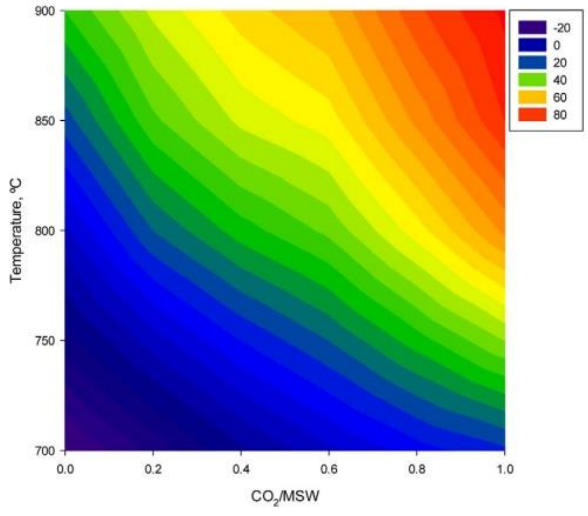

Fig. 7. Influence of CO_2/MSW and temperature no carbon dioxide conversion (units: %).

standpoint. Detailed examination shows that for lower temperature combined with low/absence CO_2 addition, carbon dioxide conversion appears to display negative values. The meaning behind this is that more CO_2 is leaving the reactor than the one being fed to [38]. Increasing both CO_2/MSW ratio and temperature results in a massive increase in carbon dioxide conversion. This can be explained with their positive influence on both Boudouard and reverse water-gas shift reactions that promote CO_2 conversion. Results are consistent with current literature [9,39].

Results presented in the chapter, as well as the previous ones, allows us to state that MSW gasification using CO_2 as a gasifying agent can indeed be a great alternative when dealing with municipal wastes. Due to the ability to tailor H_2/CO ratio, CO_2 gasification decreases substrate influence on the produced gas while ensuring the production of a syngas that can meet the requirements of a particular chosen industrial application [8]. Furthermore, as seen in Figs. Fig. 5 through Fig. 7, addition of carbon dioxide can reduce CO_2 production and tar formation while increasing the overall efficiency of the process.

Another crucial point is the already collection/transportation infrastructure that is available for MSW in Portugal that can tremendously help testing and expanding the process [40].

6. Conclusions

The goal of this study was to study Portuguese MSW gasification using air and carbon dioxide mixtures from a second law standpoint to assess the influence of carbon dioxide addition in reducing two major concerns related to municipal solid waste gasification, namely tar formation and CO_2 production.

A previously developed model was updated with new samples collected from the Oporto metropolitan area. Said model, validated multiple times using various types of substrate and operational conditions, was used to collect further data on the process.

The influence of ER, CO_2/MSW ratio and gasification temperature on syngas exergy values were studied separately for better analysis. Results showed that ER presented a maximum value of exergy at 0.25 due to a decrease in chemical exergy which was not fully compensated for by the physical exergy. Conversely, both CO_2/MSW ratio and gasification temperature appear to positively influence exergy values all throughout the studied range. From the 3 operational conditions gasification temperature had the strongest influence, followed by CO_2/MSW ratio.

Finally, influence of CO_2/MSW ratio and gasification temperature on exergy efficiency, tar exergy efficiency and carbon dioxide conversion was investigated. Results showed that both parameters have a positive effect on exergy efficiency, in a similar fashion to what was seen for exergy values. Conversely, CO_2/MSW ratio and gasification temperature lead to decreases in both tar exergy efficiency and in carbon dioxide.

Acknowledgements

We would like to express our gratitude to the Portuguese Foundation for Science and Technology (FCT) for the support to the grant SFRH/BD/86068/2012 and the project IF/01772/2014. We also would like to thank Dr. Paulo Brito for providing experimental data needed to complete this paper.

References

[1] U. Nations, World Urbanization Prospects: The 2014 Revision, Department of Economic and Social Affairs, Population Division, 2015.
[2] D. Hoornweg, P. Bhada-Tata, What a waste, A Global Review of Solid Waste Management, (2012).
[3] APA. Available from: http://www.apambiente.pt/index.php.
[4] S. Teixeira, et al., Prospective application of municipal solid wastes for energy production in Portugal, Energy Policy 71 (2014) 159–168.
[5] A.F. Kirkels, G.P.J. Verbong, Biomass gasification: still promising? a 30-year global overview, Renew. Sustain. Energy Rev. 15 (1) (2011) 471–481.
[6] H.A. Arafat, K. Jijakli, Modeling and comparative assessment of municipal solid waste gasification for energy production, Waste Manage. 33 (8) (2013) 1704–1713.
[7] P. Chaiwatanodom, S. Vivanpatarakij, S. Assabumrungrat, Thermodynamic analysis of biomass gasification with CO2 recycle for synthesis gas production, Appl. Energy 114 (2014) 10–17.
[8] H.C. Butterman, M.J. Castaldi, CO2 as a carbon neutral fuel source via enhanced biomass gasification, Environ. Sci. Technol. 43 (23) (2009) 9030–9037.
[9] T. Renganathan, et al., CO2 utilization for gasification of carbonaceous feedstocks: a thermodynamic analysis, Chem. Eng. Sci. 83 (2012) 159–170.
[10] E.E. Kwon, H. Yi, H.-H. Kwon, Thermo-chemical process with sewage sludge by using CO2, J. Environ. Manage. 128 (2013) 435–440.
[11] E.E. Kwon, M.J. Castaldi, Urban energy mining from municipal solid waste (MSW) via the enhanced thermo–chemical process by carbon dioxide (CO2) as a reaction medium, Bioresour. Technol. 125 (2012) 23–29.
[12] EPA, Solid Waste Management on Tribal Lands, (2015) Available from: http://www3.epa.gov/epawaste/inforesources/pubs/k02027.pdf.
[13] D. Pascoal, Analysis of the portuguese municipal solid waste management system, Mechanical Engineering, Universidade de Coimbra, 2012.
[14] REA, Relatório do Estado do Ambiente (In Portuguese), Departamento de Estratégias e Análise Económica, 2014.
[15] O. Onel, et al., Municipal solid waste to liquid transportation fuels −Part I: Mathematical modeling of a municipal solid waste gasifier, Comput. Chem. Eng. 71 (2014) 636–647.
[16] V. Silva, et al., Analysis of syngas quality from portuguese biomasses: an experimental and numerical study, Energy Fuels 28 (9) (2014) 5766–5777.
[17] N. Couto, et al., Numerical and experimental analysis of municipal solid wastes gasification process, Appl. Therm. Eng. 78 (2015) 185–195.
[18] N.D. Couto, et al., Assessment of municipal solid wastes gasification in a semi-industrial gasifier using syngas quality indices, Energy 93 (Part 1) (2015) 864–873.
[19] P. Grammelis, et al., Pyrolysis kinetics and combustion characteristics of waste recovered fuels, Fuel 88 (1) (2009) 195–205.
[20] Y. Zhang, et al., Exergy analysis of biomass utilization via steam gasification and partial oxidation, Thermochim. Acta 538 (2012) 21–28.
[21] A.M. Parvez, I.M. Mujtaba, T. Wu, Energy, exergy and environmental analyses of conventional, steam and CO2-enhanced rice straw gasification, Energy 94 (2016) 579–588.
[22] J. Szargut, T. Styrylska, Approximate evaluation of the exergy of fuels, Brennst Warm Kraft 16 (1964) 589–896.
[23] V.S. Stepanov, Chemical energies and exergies of fuels, Energy 20 (3) (1995) 235–242.
[24] N. Couto, et al., From laboratorial to pilot fluidized bed reactors: analysis of the scale-up phenomenon, Energy Convers. Manage. 119 (2016) 177–186.
[25] N. Couto, et al., Using an Eulerian-granular 2-D multiphase CFD model to simulate oxygen air enriched gasification of agroindustrial residues, Renew. Energy 77 (2015) 174–181.
[26] N. Couto, et al., Experimental and numerical analysis of coffee husks biomass gasification in a fluidized bed reactor, Energy Procedia 36 (2013) 591–595.
[27] N. Couto, V. Silva, A. Rouboa, Municipal solid waste gasification in semi-industrial conditions using air-CO2 mixtures, Energy 104 (2016) 42–52.
[28] H.C. Butterman, M.J. Castaldi, CO2 enhanced steam gasification of biomass fuels, 16th Annual North American Waste-to-Energy Conference, Philadelphia, Pennsylvania, USA, 2008.
[29] A.C.D. Freitas, R. Guirardello, Use of CO2 as a co-reactant to promote syngas production in supercritical water gasification of sugarcane bagasse, J. CO2 Utilization 9 (2015) 66–73.
[30] L. Wang, et al., Contemporary issues in thermal gasification of biomass and its application to electricity and fuel production, Biomass Bioenergy 32 (7) (2008) 573–581.
[31] M.J. Prins, K.J. Ptasinski, F.J.J.G. Janssen, Thermodynamics of gas-char reactions: first and second law analysis, Chem. Eng. Sci. 58 (3–6) (2003) 1003–1011.
[32] M. Niu, et al., Simulation of syngas production from municipal solid waste gasification in a bubbling fluidized bed using aspen plus, Ind. Eng. Chem. Res. 52 (42) (2013) 14768–14775.
[33] Y. Zhang, et al., Energy and exergy analyses of syngas produced from rice husk gasification in an entrained flow reactor, J. Clean. Prod. 95 (2015) 273–280.
[34] M. Hu, et al., Hydrogen-rich gas production by the gasification of wet MSW (municipal solid waste) coupled with carbon dioxide capture, Energy 90 (Part 1) (2015) 857–863.
[35] L. Devi, K.J. Ptasinski, F.J.J.G. Janssen, A review of the primary measures for tar elimination in biomass gasification processes, Biomass Bioenergy 24 (2) (2003) 125–140.
[36] E.E. Kwon, H. Yi, H.H. Kwon, Urban energy mining from sewage sludge, Chemosphere 90 (4) (2013) 1508–1513.
[37] L. Wei, et al., Steam gasification of biomass for hydrogen-rich gas in a free-fall reactor, Int. J. Hydrogen Energy 32 (1) (2007) 24–31.
[38] I. Ahmed, A.K. Gupta, Characteristics of cardboard and paper gasification with CO2, Appl. Energy 86 (12) (2009) 2626–2634.
[39] Y. Cheng, Z. Thow, C.-H. Wang, Biomass gasification with CO2 in a fluidized bed, Powder Technol. 296 (2016) 87–101.
[40] J. Hansson, A. Leveau, C. Hulteberg, Biomass Gasifier Database for Computer Simulation Purposes, in Rapport SGC 234, ©Svenskt Gastekniskt Center, 2011.

Nuno Couto After finishing his master's degree in Mechanical Engineering from University of Trás-os-Montes and Alto Douro in 2010, Nuno Couto moved to University of Porto where he currently attends his 4th year of PhD in Mechanical Engineering. Both his master's degree and PhD were funded by The Foundation for Science and Technology (FCT). In fact, his score in the PhD fellowship was within the top 10 highest in the country. In this short time frame N. Couto has published 19 articles in international journals and 14 international conferences becoming a lead researcher in gasification.

Valter Silva Dr. Valter Silva, is presently working as FCT Researcher in Polytechnic Institute of Portalegre. He did his PhD in Chemical Engineering from Porto University. Also, he obtained the expert degree in numerical simulation in Engineering by ANSYS and Polytechnic University of Madrid in 2015. V. Silva leads several energy and optimization projects funded by public and private institutions. Some Outcomes: 7 Book Chapters, papers 38 ISI papers (last 12 papers with ~4 Av. impact factor, H index: 14, funding (grants and projects as a leader): ~650 k€.

Abel Rouboa Professor at Engineering Department of University of Trás-os-Montes e Alto Douro. Teaching area: Fluid dynamics, Heat transfer and combustion. Lead of CFD research group (5 Ph.D., 3 Ph.D students and 5 Master students). P.I. of Biomechanics projects linked with Sport research groups of UTAD, UPorto and IST. Head of several RD projects on Applied and renewable energy financed by national and International funds. Outcomes: 12 Book Chapters, 64 ISI papers with 2.05 Av impact factor, H index: 11, G index: 17.

Paper II

Exergy analysis of Portuguese municipal solid waste treatment via steam gasification

N. Couto, V. Silva, E. Monteiro, A. Rouboa

Energy Conversion and Management 134 (2017) 235-246

Energy Conversion and Management 134 (2017) 235–246

Contents lists available at ScienceDirect

Energy Conversion and Management

journal homepage: www.elsevier.com/locate/enconman

Exergy analysis of Portuguese municipal solid waste treatment via steam gasification

Nuno Couto [a], Valter Silva [a], Eliseu Monteiro [a,b], Abel Rouboa [a,c,d,*]

[a] INEGI/Faculty of Engineering, University of Porto, Porto, Portugal
[b] C3i – Interdisciplinary Center for Research and Innovation, Polytechnic Institute of Portalegre, Portalegre, Portugal
[c] University of Trás-os-Montes and Alto Douro, Vila Real, Portugal
[d] MEAM Department, University of Pennsylvania, Philadelphia, PA, USA

ARTICLE INFO

Article history:
Received 16 October 2016
Received in revised form 16 December 2016
Accepted 17 December 2016
Available online 24 December 2016

Keywords:
Thermodynamic analysis
Municipal solid waste
Semi-industrial gasification plant
Steam Gasification
CFD
Tar content

ABSTRACT

The presented study focuses on a thermodynamic analysis conducted on steam gasification of Portuguese municipal solid wastes (MSW). Current literature addressing this issue is extremely scarce due to the complexity in handling MSW's heterogeneity. To fill this significant gap, a mathematical model built upon a reliable set of experimental runs from a semi-industrial gasifier was used to evaluate the effects of reactor temperature and steam-to-biomass ratio (SBR) on produced gas and tar content. Results from a previously studied biomass substrate were used as benchmark. Numerical results were validated with both experimental results and existing literature. Increase in gasification temperature led to a clear increase in both exergy values and exergy efficiency. On the other hand, increase in SBR led to a sharp increase in the exergy values when steam was first introduced, leading to relatively constant values when SBR was further increased. Regarding exergy efficiency, SBR led to a clear maximum value, which in the case of forest residues was found at SBR = 1, while for MSW at 1.5. In order to promote a more hydrogen-rich gas, data obtained from the numerical model was used to design an exergy efficiency optimization model based on the response surface method. Maximum hydrogen efficiency was found at 900 °C with a SBR of 1.5 for MSW and 1 for forest residues. Surprisingly, forest residues and MSW presented virtually the same maximum hydrogen efficiency.

1. Introduction

The potential threat created by climate change, due to high emission levels of greenhouse gases, has become a major motivation for renewable energy sources in general. Biomass is regarded as the renewable energy source with the highest potential to contribute to the energy needs of modern society. Its advantages compared to the fossil fuels are as follows: biomass is considered to be a carbon neutral fuel, making it possible to reduce carbon dioxide emissions [1]; its use may contribute to an increase in the energy security of the countries importing energy resources, decreasing their dependence on fossil and nuclear fuel supplies [2]; an increase in the energy use of biomass is an additional factor of economic support to the agriculture [2].

Another kind of biomass group is wastes being the municipal solid wastes (MSW) the largest waste stream around the world. The MSW management activities contribute to the generation of greenhouse gas and consequently to the climate change problem. Another environmental problem associated with MSW management systems is the potential generation of dioxins and furans associated to complete combustion [3].

Gasification is a waste-to-energy (WTE) conversion method that offers an attractive solution to both waste disposal and energy problems. However, gasification still has some economic and technical challenges, concerning the nature of the solid waste residues and its heterogeneity [4]. The greatest strength of gasification is the environmental performance, since emission tests indicate that gasification meets the existing limits and it can also have an important role in the reduction of landfill disposal [5].

As one of the most promising WTE technologies, gasification using preheated oxidizing agents such as air, oxygen, steam, or a mixture of these has been studied for decades and has been proven to produce a fuel gas with relatively high heating value [6], where additional heat provided into the gasification process improves the

* Corresponding author at: Rua Dr. Roberto Frias, Campus da FEUP, 400, 4200-465 Porto, Portugal.
E-mail addresses: nunodiniscouto@hotmail.com (N. Couto), vsilva@inegi.up.pt (V. Silva), elmmonteiro@portugalmail.pt (E. Monteiro), rouboa@seas.upenn.edu (A. Rouboa).

http://dx.doi.org/10.1016/j.enconman.2016.12.040
0196-8904/

decomposition of solid fuel and the cracking of volatiles. Among oxidizing agents, steam gasification provides fuel gas with lower heating values in the range of 12–18 MJ/N m^3 [7], which is higher than those from air gasification, while being less costly than oxygen gasification.

Nevertheless, further research must be conducted to allow biomass gasification, and in particular MSW gasification, to become the mainstream method of treatment for these substrates. Exergy analysis is a concept that combines energy, environment and sustainable development notions, and has been used to identify opportunities for process improvement and to evaluate different process alternatives [8]. The application of exergy destruction and efficiency analysis to process design can help identify and understand the high efficient energy production systems [9].

Therefore, it is not surprising that exergy analysis of biomass-gasification based process have engrossed attention due to the potential of biomass as a feedstock or as energy resource. Many researchers [10–12] performed exergy analysis to study gasification performance of different types of biomass and different degrees of sophistication regarding the use of steam as an oxidizer agent. Hosseini et al. [10] performed energy and exergy analysis of the steam and air fed sawdust gasification. The results show that the adiabatic temperature of biomass gasification significantly changes with the type of the gasifying medium. In addition, the exergy and energy efficiencies are observed to be higher when air is the gasifying medium rather than steam, while the system performance and exergy efficiencies are dependent on the moisture content of the feed biomass. Ptasinski et al. [11] evaluated the exergetic efficiencies in an idealized gasifier in which chemical equilibrium is reached, ashes are not considered and heat losses are neglected. The gasification efficiencies are evaluated at the carbon boundary point. They show that the exergy efficiencies of biofuels are lower than the corresponding energetic efficiencies. For liquid biofuels, gasification at the optimum point is not possible, and exergy efficiency can be improved by drying the biomass. Sreejith et al. [12] presents energy and exergy analyses of steam gasification of four biomass materials (coconut shell, coir pith, bamboo and eucalyptus). The exergy model is formulated based on a Redlich–Kwong real gas equilibrium model. Parametric variations with steam-to-biomass ratio and gasification temperature are presented for energy and exergy efficiencies of gasification. They found that the least irreversible gasification process is for coir pith, followed by coconut shell, bamboo and eucalyptus with the corresponding exergetic efficiencies of 79.2%, 77.5%, 74.4% and 68.3%, respectively.

All the available studies showed that exergy analysis can be an extremely useful tool for evaluating the effectiveness of the biomass gasification process. Unfortunately, due to the complexity of handle the heterogeneity of MSW, studies focusing on thermodynamic evaluations of these wastes are barely explored especially when it comes to analyzing steam as a gasifier agent.

In order to fill this significant gap on the current literature, the current study aims at analyzing MSW gasification from a second law analysis standpoint. To do so, a previously developed numerical model is used [13]. Results are validated with experimental data. Forest residues were used as benchmark for comparison with MSW. Influence of operational parameters on syngas composition and tar content is investigated. Their exergy values as well as process efficiency is analyzed. Finally, an optimization model is built to promote a more hydrogen-rich syngas.

2. Materials and methods

The developed mathematical model (presented in Section 4) was developed using experimental data collected in the gasification plant from the School of Technology and Management (ESTG) of the Polytechnic Institute of Portalegre (IPP). The plant has a semi-industrial fluidized bed gasifier with the capacity to process 100 kg/h and operates close to 850 °C. Having the ability to run tests in industrial-size conditions allows one to be much closer to realistic commercial size reactors since the hydrodynamic phenomena in a laboratory scale fluidized bed are not the same as on large scales [14]. Operation of the gasification plant is quite straightforward. First biomass substrate enters through the feeding system, which sends it to the gasifier. At the same time, preheated steam enters the gasifier via a series of diffusers regulating the flow rate. After the process is completed the syngas leaves the reactor at approximately 700 °C and passes through two heat exchangers – the first lowers syngas temperature to about 300 °C and the second to 150 °C. While this is happening ash and other produced wastes are first filtered out and then stored in a suitable tank. Finally, the syngas goes through a condenser which cools the gas to room temperature thus becoming ready to be used in another purpose. Extended detail on how the gasification plant is operated, including schematics of the reactor as well as the plant itself, can be found in [15].

2.1. Portuguese municipal solid waste and forest residues characterization

MSW was simulated according to the average proportion of organic components (dry basis) in actual MSW of Portugal [5] and used as feedstock for the simulations, as shown in Table 1. The characterization and analysis of Portuguese MSW (from now on we will be referring to as PMSW for simplicity) was carried out using data from the Oporto metropolitan area obtained from LIPOR (Intermunicipal Waste Management Service of Greater Porto), entity responsible for the management, treatment and recovery of solid waste municipal produced in the city.

It is assumed a MSW pre-treatment (in depth detail given in [16]) that gives rise to a refuse derived fuel which contains cellulosic and plastics only [5]. Cellulosic materials are mainly composed of cellulose, hemicelluloses, and lignin. Plastic residues are composed of polyethylene, polystyrene, and polyvinyl chloride.

A global chemical is obtained by dividing the values found in the ultimate analysis of each chemical element (C, H, O) by the value of the reference element carbon (C). This MSW global chemical formula was obtained based on its chemical characterization as shown in Table 1.

To properly assess the potential of PMSW a previously studied Portuguese biomass substrate will be used as benchmark. Forest residues [18] was selected for this purpose, since it reveled relevant energetic as well as economic benefits. In fact, previous studies have shown that both forest residues and MSW can be instrumental in replacing, or at least greatly diminish, fossil fuels [2,13]. According to Silva et al. [15], Portuguese territory is composed of about 35% of forest generating close to 113 thousand jobs (over 2% of active population) and 200 million euros per year in related economic activities. In addition, latest national reports

Table 1
MSW chemical composition.

Category	% Weight	Chemical formula
Cellulosic material	85.42	[a]
Polyethylene	10.99	$(C_2H_4)_n$
Polyethylene terephthalate	2.02	$(C_{10}H_8O)_n$
Polypropylene	0.81	$(C_3H_6)_n$
Polystyrene	0.76	$(C_8H_8)_n$

[a] It was considered the proportion of cellulose, hemicellulose and lignin found in Onel et al. [17].

indicate that the annual MSW production is just shy of 5 million tons. As stated, the majority of these wastes are still being deposited in landfills, leading not only to a serious environmental concern but, in many cases, to the single largest budgetary item of a city. The proximate and ultimate analysis of this feedstock is shown in Table 2.

3. Exergy model

In order to analyze the production of syngas and tar from the selected substrates and be able to make an assessment on the efficiency of the process an exergetic analysis was performed. In order to simplify the analysis a set of assumptions were followed [16]. In the described system, the exergy balance can be written as:

$$Ex_{biomass} + Ex_{steam} + Ex_{heat} = Ex_{syngas} + Ex_{tar} \quad (1)$$

where $Ex_{biomass}$, Ex_{steam}, Ex_{heat}, Ex_{syngas} and Ex_{tar} represent the exergy rates of forest rate or MSW, steam, heat supplied to the gasifier, syngas and tar content, respectively. Exergy rate can be defined by the sum of the chemical exergy rate and the physical exergy rate [19]:

$$Ex = Ex_{ch} + Ex_{ph} \quad (2)$$

where the chemical and physical exergy can be written [19], respectively as:

$$Ex_{ch} = \sum_i n_i \left(e_{0_i} + RT_0 \ln \frac{n_i}{\sum n_i} \right) \quad (3)$$

$$Ex_{ph} = \sum_i n_i [(h - h_0) - T_0 (s - s_0)] \quad (4)$$

where n_i is the molar yield of gas component i (mol/kg), R is the ideal, or universal, gas constant and e_{0_i} is the standard chemical exergy of a pure chemical compound i. Also, s and h are entropy and enthalpy of a system at given temperature and pressure, and h_0 and s_0 are enthalpy and entropy of a system at the environmental temperature and pressure, respectively. The values of the specific enthalpy and entropy as well as the standard chemical exergy of selected gases are shown in Table 3.

Similarly, the differences $(h - h_0)$ and $(s - s_0)$ of ideal gases can be calculated as:

$$h - h_0 = \int_{T_0}^{T} c_p dT \quad (5)$$

$$s - s_0 = \int_{T_0}^{T} \frac{c_p}{T} dT - R \ln \frac{P}{P_0} \quad (6)$$

where c_p is the constant pressure specific heat capacity which can be calculated by:

Table 2
Ultimate and proximate analyses of forest residues and PMSW.

Biomass properties	PMSW	Forest residues
Elementary analysis (%)		
N	1.4	2.4
C	48	43.0
H	6.3	5.0
O	43.6	49.6
Humidity (%)	17.6	11.3
Density (kg/m^3)	247	650
Net heat value (MJ/kg biomass)	14.4	21.2
Proximal analysis (%)		
Ash	14.9	0.2
Volatile matter	76.62	79.8
Fixed carbon	8.46	20.0

Table 3
Specific enthalpy, entropy and standard chemical exergy values of some materials at 25 °C, 1 atm.

Gas	h_0 (kJ/kmol)	s_0 (kJ/kmol K)	e_{0_i} (kJ/kmol)
H_2O (g)	9904	188.72	9500
H_2	8468	130.574	236,100
CO	8669	197.543	275,100
CO_2	9364	213.685	19,870
CH_4	–	–	831,650
C_2H_4	–	–	1,408,400
C_2H_6	–	–	1,495,000

$$c_p = a + bT + cT^2 + dT^3 \quad (7)$$

The coefficients a, b, c and d were taken from the literature [19].

To calculate the exergy of biomass (for both forest residues and MSW) with less complexity, the correlation developed by Szargut and Styrylska [20] was used:

$$Ex_{Biomass} = \dot{m} \beta LHV_{biomass} \quad (8)$$

The formula of correlation factor β is given by:

$$\beta = \frac{1.0412 + 0.2160\left(\frac{H}{C}\right) - 0.2499\left(\frac{O}{C}\right)\left[1 + 0.7884\left(\frac{H}{C}\right)\right] + 0.0450\left(\frac{N}{C}\right)}{1 - 0.3035\left(\frac{O}{C}\right)} \quad (9)$$

where O, C, H and N are the weight fractions of oxygen, carbon, hydrogen and nitrogen in the biomass, respectively.

The LHV of the biomass can be obtained by the relationship between HHV and LHV given by [21]:

$$LHV_{Biomass} = HHV_{Biomass} - h_g(0.09H - 0.01M) \quad (10)$$

where H, M and h_g are hydrogen percentage, moisture percentage and latent heat of steam, respectively.

Similarly, in this work the tar chemical exergy is simulated with help of another correlation for liquid fuels [22]:

$$Ex_{tar} = \dot{m}_{tar} LHV_{tar} \left(1.0401 + 0.1728\left(\frac{H}{C}\right) + 0.0432\left(\frac{O}{C}\right) + 0.2196\left(\frac{S}{C}\right)\left[1 - 2.0628\left(\frac{H}{C}\right)\right] \right) \quad (11)$$

Due to the difficulty in measuring transferred heat from external source to the reactor, one may assume that the exergy provided by external heat approaches the exergy increase in biomass and steam in respect to the environmental condition. In other words, one simply needs to calculate the difference from the values of specific enthalpy and entropy at different temperatures. This procedure was implemented in [19].

Finally, to better understand the effects of substrate and operational parameters on reactor performance, exergy efficiency of syngas and tar were investigated. They can be calculated as being [19]:

$$\varepsilon_{syngas} = \frac{Ex_{syngas}}{Ex_{biomass} + Ex_{steam} + Ex_{heat}} \quad (12)$$

$$\varepsilon_{tar} = \frac{Ex_{tar}}{Ex_{biomass} + Ex_{steam} + Ex_{heat}} \quad (13)$$

4. Mathematical model

A mathematical model built upon a reliable set of experimental runs can be extremely helpful in, not only extending these runs, saving considerable time and effort in the process. It was with this idea in mind that our numerical model was first developed in the study of biomass gasification [15].

The developed 2D model implemented an Eulerian-Eulerian approach to handle both gas and dispersed phases. The kinetic theory of granular flows was used to evaluate the constitutive properties of the dispersed phase, and the gas-phase behavior was simulated employing the $k-\varepsilon$ turbulent model.

Since our model is well documented in recent literature we will just state the key points that define it. Table 4 comprises main equations regarding both hydrodynamic model and conservation equations for each phase. Further details on the model can be found in [13,15]. Regarding the chemical model, there are two vital steps that need to be explained. First is related to the expansion of the devolatilization section. In fact, when the developed model was upgraded to handle MSW, the devolatilization section had to be expanded to cope with the heterogeneity of the substrate. Secondly, the chemical model had to be redesigned since steam gasification does not include exothermic reactions. All relevant reactions and their reaction rates are listed in Table 5 [23].

In this study, our previously pyrolysis model with secondary tar generation was adopted. The finite-rate/Eddy-dissipation model was used to describe homogeneous reactions while the Kinetic/Diffusion Surface Reaction Model was employed for heterogeneous ones.

5. Results and discussion

To properly investigate the described substrates, a numerical model able to describe the complex phenomena that occur during the process was developed. The model was first applied to coffee husks gasification with satisfactory results [18]. After several studies and continuous model expansions, a major upgrade on the devolatilization section was performed in order to deal with the heterogeneity of MSW [24]. Ideally one would like to validate the new upgraded model with the experimental set-up used earlier. However, due to unfortunate logistical and bureaucratic setbacks this was not possible. To work around the problem it was decided to validate the model using data collected from the literature [25]. Table 6 shows the operating conditions used to validate the numerical model for both studied substrates.

Fig. 1 compares the syngas composition using the operating conditions shown in Table 6, estimated by the model (shown in X-axis), with that measured in the experiments (shown in Y-axis) for both substrates.

From the above Figure one can see that, for both forest residues and MSW, the developed numerical model is capable of predicting syngas composition within a margin of error of 20%, very

Table 4
Hydrodynamic model and conservation equations for both gas and solid phases.

Hydrodynamic model	
Kinetic energy: $\frac{\partial}{\partial t}(\rho k)+\frac{\partial}{\partial x_i}(\rho k u_i)=\frac{\partial}{\partial x_j}\left[\left(\mu+\frac{\mu_t}{\sigma_k}\right)\right]+G_k+G_b-\rho\varepsilon-Y_M+S_k$	
Dissipation rate: $\frac{\partial}{\partial t}(\rho\varepsilon)+\frac{\partial}{\partial x_i}(\rho\varepsilon u_i)=\frac{\partial}{\partial x_j}\left[\left(\mu+\frac{\mu_t}{\sigma_\varepsilon}\right)\frac{\partial\varepsilon}{\partial x_j}\right]+C_{1\varepsilon}\frac{\varepsilon}{k}(G_k+C_{3\varepsilon}G_b)-C_{2\varepsilon}\rho\frac{\varepsilon^2}{k}+S_\varepsilon$	
Granular Eulerian model: $\frac{3}{2}\left[\left(\frac{\partial(\rho_s\alpha_s\Theta_s)}{\partial t}+\nabla.(\rho_s\alpha_s\vec{v}_s\Theta_s)\right)\right]=(-P_s\bar{I}+\bar{\tau}_s):\nabla(\vec{v}_s)+\nabla.(k_{\Theta a}\nabla(\Theta_s))-\gamma_{\Theta a}+\phi_{ls}$	
Conservation equations	
Gas phase	Solid phase
Energy: $\frac{\partial(\alpha_q\rho_q h_q)}{\partial t}+\nabla\cdot(\alpha_q\rho_q\vec{u}_q h_q)=-\alpha_q\frac{\partial(p_q)}{\partial t}+\bar{\bar{\tau}}_q:\nabla(\vec{u}_q)-\nabla\vec{q}_q+S_q+\sum_{p=1}^{n}(\vec{Q}_{pq}+\dot{m}_{pq}h_{pq})$	$\frac{\partial(\alpha_p\rho_p h_p)}{\partial t}+\nabla\cdot(\alpha_p\rho_p\vec{u}_p h_p)=-\alpha_p\frac{\partial(p_p)}{\partial t}+\bar{\bar{\tau}}_p:\nabla(\vec{u}_p)-\nabla\vec{q}_p+S_p+\sum_{q=1}^{n}(\vec{Q}_{pq}+\dot{m}_{pq}h_{pq})$
Mass: $\frac{\partial(\alpha_q\rho_q)}{\partial t}+\nabla\cdot(\alpha_q\rho_q\vec{u}_q)=-M_C\sum\gamma_C R_C$	$\frac{\partial(\alpha_p\rho_p)}{\partial t}+\nabla\cdot(\alpha_p\rho_p\vec{u}_p)=M_C\sum\gamma_C R_C$
Momentum: $\frac{\partial(\alpha_q\rho_q\vec{u}_q)}{\partial t}+\nabla\cdot(\alpha_q\rho_q\vec{u}_q\vec{u}_q)=-\alpha_q\nabla p_q+\alpha\rho_q g+\beta(u_q-u_p)+\nabla\cdot\alpha_q\bar{\bar{\tau}}_q+S_{pq}U_S$	$\frac{\partial(\alpha_p\rho_p\vec{u}_p)}{\partial t}+\nabla(\alpha_p\rho_p\vec{u}_p\vec{u}_p)=-\alpha_p\nabla p_p+\alpha\rho_p g+\beta(u_q-u_p)+\nabla\cdot\alpha_p\bar{\bar{\tau}}_p+S_{pq}U_S$

Table 5
Chemical reaction model.

Reactions	Reaction rate
Pyrolysis:	
Cellulose $\rightarrow \alpha_1$ *volatiles* $+\alpha_2$ *TAR* $+\alpha_3$ *char*	$r_1=A_i\exp\left(\frac{-E_i}{T_s}\right)(1-a_i)^n$
Hemicellulose $\rightarrow \alpha_4$ *volatiles* $+\alpha_5$ *TAR* $+\alpha_6$ *char*	$r_2=A_i\exp\left(\frac{-E_i}{T_s}\right)(1-a_i)^n$
Lignin $\rightarrow \alpha_7$ *volatiles* $+\alpha_8$ *TAR* $+\alpha_9$ *char*	$r_3=A_i\exp\left(\frac{-E_i}{T_s}\right)(1-a_i)^n$
Plastics $\rightarrow \alpha_{10}$ *volatiles* $+\alpha_{11}$ *TAR* $+\alpha_{12}$ *char*	$r_4=\left[\sum_{i=1}^{n}A_i\exp\left(\frac{-E_i}{RT}\right)\right]\rho_v$
Primary TAR $\rightarrow$ *volatiles* $+$ *Secondary TAR*	$r_5=9.55\times10^4\exp\left(\frac{-1.12\times10^4}{T_g}\right)\rho_{TAR1}$
Homogeneous reactions:	
$CO+H_2O\leftrightarrow CO_2+H_2$	$r_6=5.159\times10^{15}\exp\left(\frac{-3430}{T}\right)T^{-1.5}C_{O_2}C_{H_2}^{1.5}$
$C_2H_4+2H_2O\leftrightarrow 2CO+4H_2$	$r_7=3100.5\exp\left(\frac{-15{,}000}{T}\right)C_{C_2H_4}C_{H_2O}^2$
$CH_4+H_2O\leftrightarrow CO+3H_2$	$r_8=3.1005\exp\left(\frac{-15{,}000}{T}\right)\left[C_{H_2O}C_{CH_4}-\frac{C_{CO}C_{H_2}^2}{0.0265(32{,}900/T)}\right]$
Heterogeneous reactions:	
$C+CO_2\rightarrow 2CO$	$r_9=2082.7\exp\left(\frac{-18{,}036}{T}\right)$
$C+H_2O\rightarrow CO+H_2$	$r_{10}=63.3\exp\left(\frac{-14{,}051}{T}\right)$

Table 6
Operating conditions for the experimental gasification runs.

Experimental conditions	Forest residues			MSW		
Run	1	2	3	4	5	6
Temperature (°C)	815	815	790	620	493	705
Substrate admission (kg/h)	63	74	63	2.3	2.3	3
Air flow rate (N m^3/h)	94	98	98	6	6	6
Reactor type	Semi-industrial			Laboratorial		

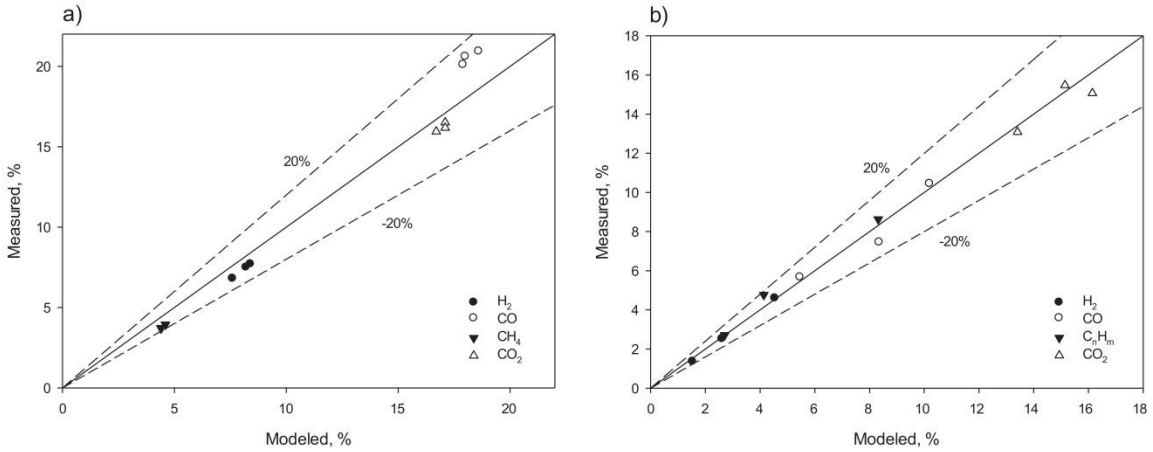

Fig. 1. Comparison between modeled and measured syngas composition for (a) forest residues and (b) MSW.

reasonable for an exceptionally complex system such as biomass gasification in a pilot scale reactor and MSW gasification in laboratorial scale. The biggest deviation was observed for CH_4 (and C_nH_m), which was expected since smaller fractions tend to produce higher relative errors. Furthermore, all light hydrocarbons and tar can lump into CH_4, which can explain the disagreement sometimes found. Besides, some degree of deviation may be attributed to the assumed simplifications followed by our model [15].

To better understand how operational parameters, which in this study are reactor temperature and SBR, influence exergy values it is wise to first study their influence on individual gas composition since they strongly dictate exergy values.

SBR can be defined as the steam mass flow rate divided by the fuel mass flow rate (dry basis). Fig. 2 depicts the influence of SBR on final syngas composition for both MSW and forest residues.

Increase in SBR promotes char and tar steam reforming as well as the water-gas shift reaction, leading to an increase in both CO_2 and H_2 molar fractions at the cost of CO and C_nH_m contents [23]. This is consistent with the obtained results.

Regarding hydrogen content, one can see that it reverses its trend when SBR is further increased beyond 1.5. This is related to excessive steam flow leading to a significant decrease in the reactor temperature. Since the main reactions responsible for hydrogen production are endothermic, a decrease in temperature will lead to a decrease in its content.

Despite presenting similar trends, substrates exhibit significant differences in their syngas molar fractions. Namely, forest residues display higher levels of C_nH_m and H_2 while MSW presents higher CO_2 and CO contents. One may explain this difference by using the fuel's chemical composition. In fact, according to Louw et al. [26], the maximum H_2 and CH_4 content are achieved when biomass with a low C:H ratio and low O_2 content is used while maximum CO and CO_2 content are reached when biomass with low O_2 content and high C:H ratio is used as feedstock. Since forest residues has higher C:H ratio (8.6 instead of 7.6), and a comparable oxygen content (49.6% instead of 43.6%), thus favoring H_2 and C_nH_m. Furthermore, higher biomass calorific values result in higher calorific syngas production. The relationship between biomass calorific content and syngas LHV can be explained considering the following points: (a) biomass calorific value is related to the amount of carbon and hydrogen present in the biomass; (b) a larger amount of these two elements allows production of larger quantities of hydrogen and carbon monoxide, the major contributors for the calorific value of the syngas. Nevertheless, since there are other biomass properties that can greatly influence the gasification process one must not take these conclusions as absolutes.

Increase in SBR also has a strong effect on both syngas yield and tar content. Since we are focusing on hydrogen-rich gas, Fig. 3 presents tar content and hydrogen yield for both substrates as a function of SBR.

Steam promotes volatile release and char conversion which are known to increase gas yield [27]. Moreover, promotion of steam reforming reactions leads to a drastically decrease in the tar content [28]. For a SBR higher than 1.5, one can see a considerable decrease in hydrogen yield. This can be explained by excessive amount of steam leading to a reduction in gas yield and hydrogen molar fraction, which is consistent with the current literature [29].

Although both substrates present very similar trends, forest residues exhibit a substantial higher hydrogen yield and slightly lower tar content. Despite having several reasons that might explain these differences, one can speculate that volatile content has a very significant influence [30]. In fact, higher volatile content is known for promoting higher residence time which in turn favors gasification reactions leading to a higher gas yield [31]. Furthermore, increase in residence time also leads to a considerable reduction in tar production [32]. Since forest residues has a higher volatile content, it comes with no surprise that it also presents lower tar content and higher hydrogen yield.

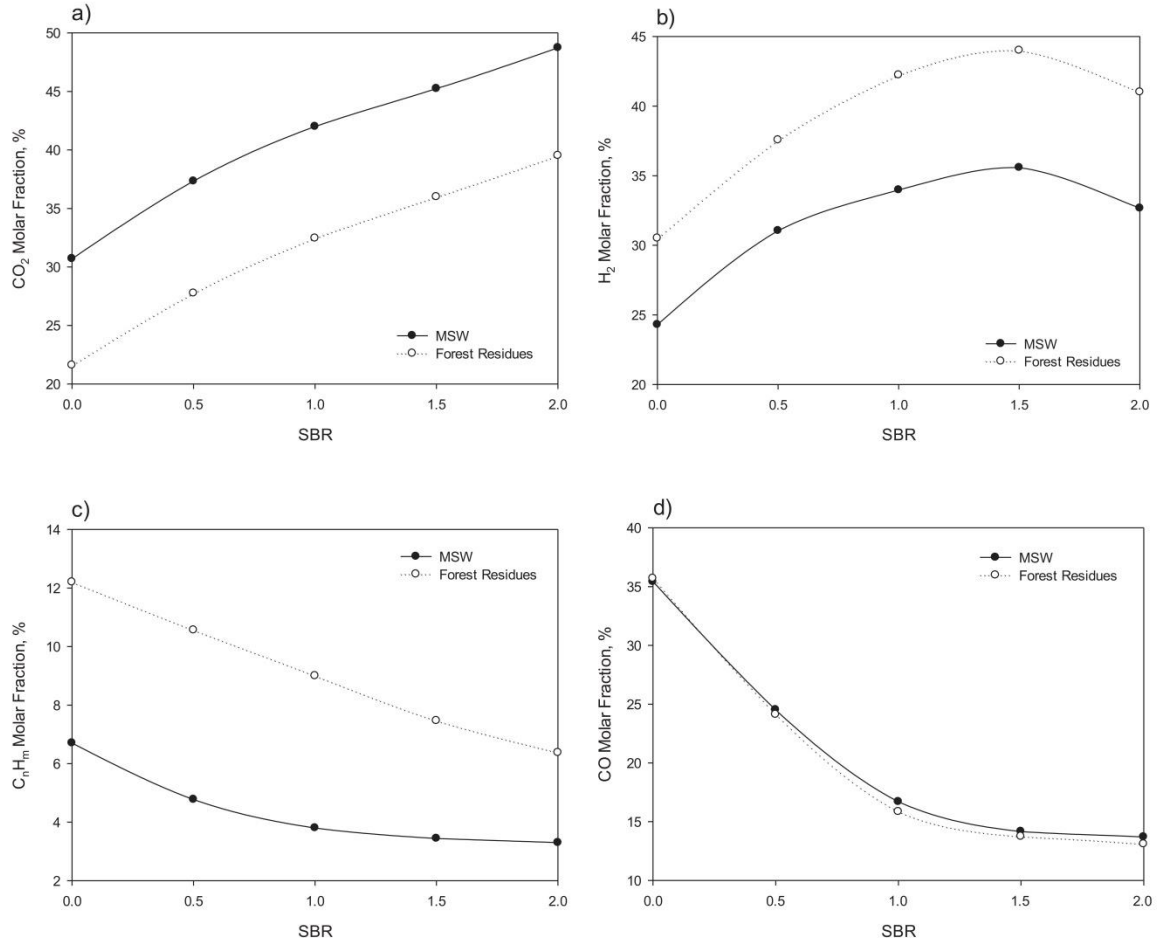

Fig. 2. Comparison between substrates as a function of SBR for (a) CO_2, (b) H_2, (c) C_nH_m and (d) CO. (Operating conditions: Fuel feed rate = 25 kg/h; Gasification temperature = 750 °C).

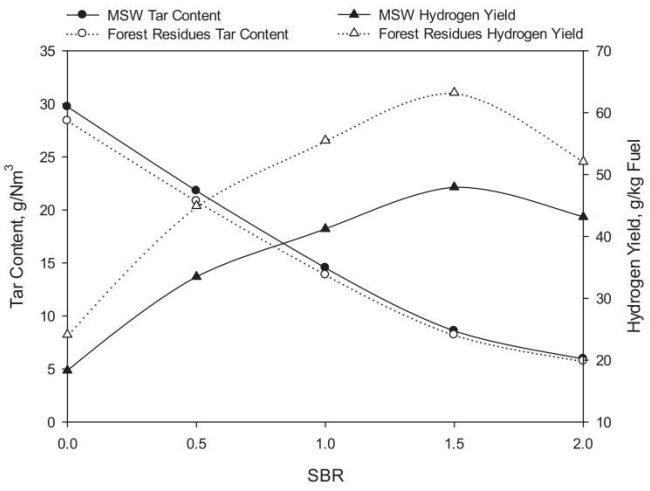

Fig. 3. Influence of SBR on tar content and hydrogen yield. (Operating conditions: Temperature – 750 °C; MSW admission – 25 kg/h).

Usually a dependent variable in the gasification process, reactor temperature has a predominant effect on reaction kinetics and on the gasifier performance. Fig. 4 describes the influence of reactor temperature on final syngas composition for both substrates.

According to the Le Chatelier's principal, increase in gasification temperature will favor products in endothermic reactions. Furthermore, promotion of endothermic reactions will lead to an increase in CO and H_2 content formation while decreasing CO_2 and C_nH_m [33]. This is consistent with obtained results.

Careful analysis shows that between 750 and 800 °C, hydrogen production becomes less pronounced while carbon monoxide further increases. In fact, in that range the standard Gibbs free energy of the Boudouard reaction (responsible for CO production) becomes less than that of the water-gas reaction (main responsible for hydrogen production at lower temperatures), meaning that the former dominates over the latter as temperature increases. This is consistent with the current literature [34].

Comparison between Figs. 3 and 5 show that gasification temperature has a stronger influence on both tar content (close to 90% decrease from initial value) and hydrogen yield (over 3.5 times increase from its initial value) when compared to SBR (tar decrease 80% and hydrogen yield increased around 2.4 times initial value). This can be explained with increase in reactor temperature enhancing steam reforming reactions, which in turn promotes both carbon conversion and gas yield [28]. Moreover, high temperature also favors destruction and reforming of tar leading to a decrease in tar content [35]. Having studied the influence of desired operational parameters it is now possible to calculate the corresponding exergy values.

5.1. Exergy values

The exergy values for both syngas composition and tar content as a function of SBR are shown in Fig. 6.

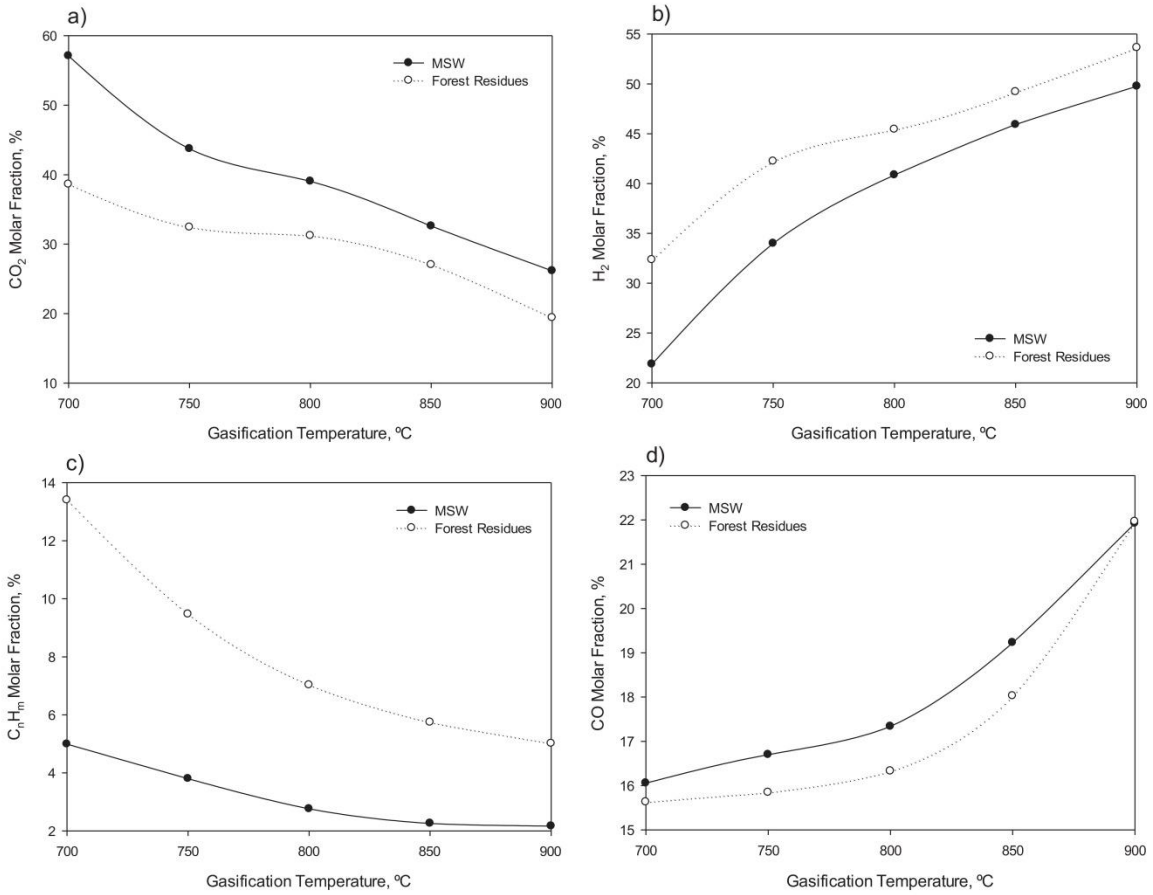

Fig. 4. Comparison between substrates as a function of gasification temperature for (a) CO_2, (b) H_2, (c) C_nH_m and (d) CO. (Operating conditions: Fuel feed rate = 25 kg/h; SBR = 1).

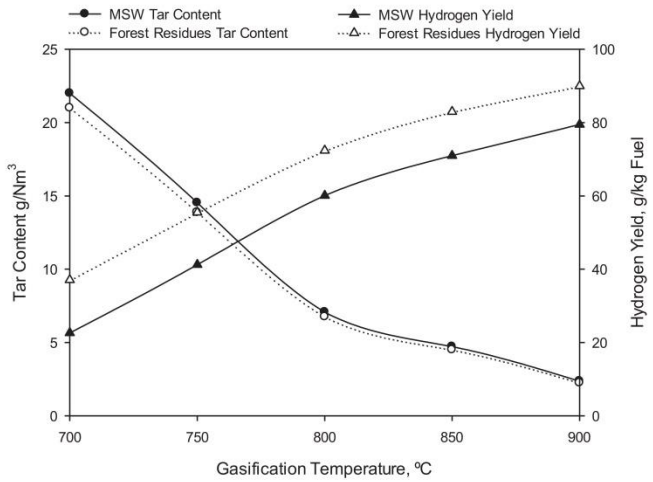

Fig. 5. Influence of gasification temperature on tar content and gas yield. Dry basis. (Operating conditions: Fuel feed rate = 25 kg/h; SBR = 1).

Exergy values are determined by the sum of physical and chemical exergies of each individual syngas component. The former depends on enthalpy and entropy as well as individual gas yield of gas while the latter mainly depends on the yield of gas composition.

SBR has two contradictory effects on the system; the first is the positive effect on syngas yield and hydrogen molar fraction which causes a sharp increase in the exergy values when steam is first introduced. Above 0.5 exergy values seem to remain somewhat constant which is caused by the second effect which is the suppression of CO and C_nH_m, two decisive elements in the calculation of syngas exergy [36].

Forest residues presents significantly higher exergy values in relation to MSW. This has to do with higher gas yield but mostly with C_nH_m content, since light hydrocarbons have a much higher standard chemical exergy when compared to hydrogen or even carbon monoxide. Conversely, MSW presents a very large CO_2 fraction, but since it has such low standard chemical exergy (i.e. ethylene has over 70 times its number) it can hardly contribute to the overall syngas exergy value.

Similarly to the effect of SBR in tar content, SBR leads to a considerable decrease in tar exergy value. As stated, the presence of steam favors tar steam reforming which obviously leads to tar consumption [37]. Both substrates presented very similar values but forest residues actually has the higher value. At first glance, this actually represents a reverse in results presented in Fig. 5. Then again, exergy results are presented per kg based, and since forest residues has the higher gas yield, more gas is formed per kilogram of substrate which means more tar content being released.

Fig. 7 illustrates the exergy values of gas components and tar content at various reactor temperatures. According to Zhang et al. [19], both syngas and tar exergy values are determined by their temperature and yield.

From Fig. 7 one can notice that gasification temperature has indeed a strong influence on syngas exergy values. This is certainly

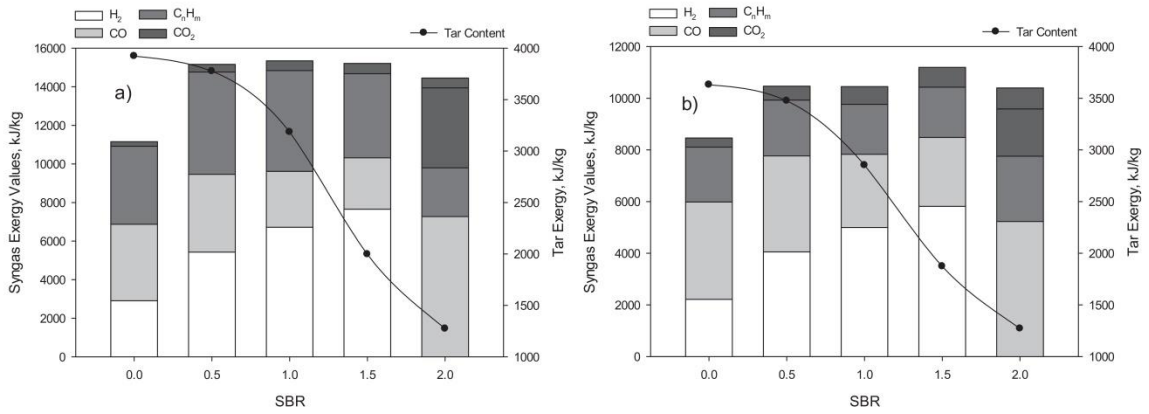

Fig. 6. Exergy values of gas components and tar content as a function of SBR for (a) forest residues and (b) MSW. (Operating conditions: Fuel feed rate = 25 kg/h; Gasification temperature = 750 °C).

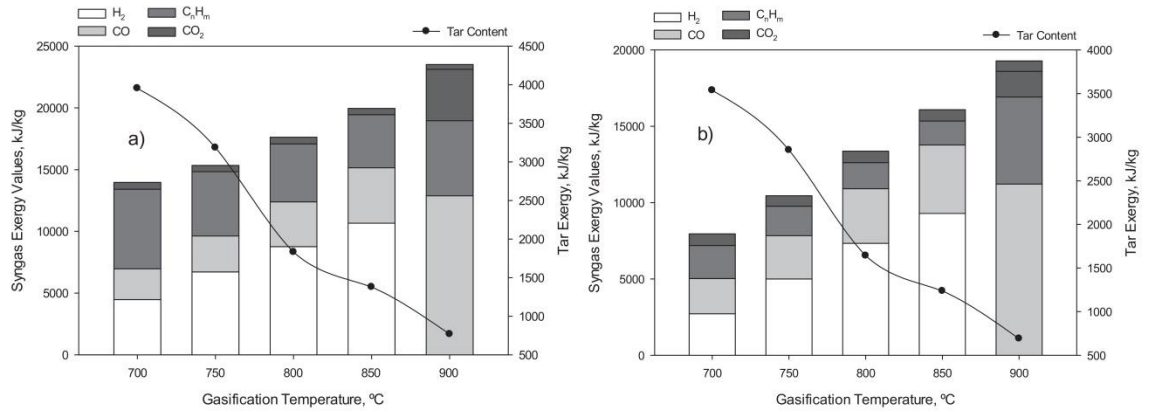

Fig. 7. Exergy values of gas components and tar content as a function of reactor temperature for (a) forest residues and (b) MSW. (Operating conditions: Fuel feed rate = 25 kg/h; SBR = 1).

expected since it leads to increases in enthalpy (and entropy) and gas yield, the two main responsible for exergy increase [38].

Comparing SBR to gasification temperature, one can see that the effect of reactor temperature on the total syngas exergy (68% increase from initial value) was much greater than that of SBR (37% increase from the initial value). This is consistent with the current literature [36].

Contrary to what happened with syngas, both gasification temperature and SBR present similar trend when it comes to tar exergy values. This is mainly due to both gasification temperature and SBR leading to tar decomposition though the enhancement of tar cracking reaction [19,36].

5.2. Process efficiencies

Presented results in the previous chapters are crucial to evaluate the potential efficiency of the gasification process. Theoretically, exergy analysis based on the second law of thermodynamics could better explain that the performance of engineering systems is degraded by the presence of irreversibility. Therefore, for industrial applications exergy consideration is an essential part of saving resources and efficient production.

Fig. 8 shows the exergy efficiency as a function of SBR for forest residues and MSW. Same operating conditions as the ones used throughout the paper were used so to give readers a better understanding of the process.

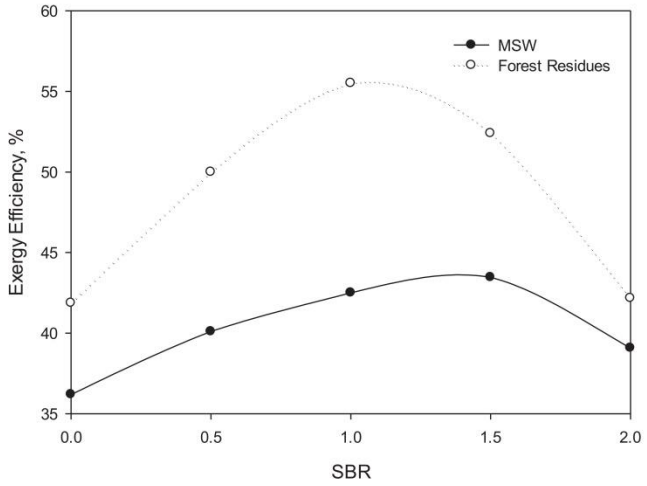

Fig. 8. Exergy efficiency as a function of SBR for forest residues and MSW.

For forest residues, results show that between 0 and 1, SBR leads to a drastic increase in exergy efficiency. Further increase in SBR leads to a sudden decrease in efficiency. This value is consistent with findings of other researchers [39]. Similarly, MSW also exhibits increasing trend with SBR although it appears to have a maximum value at 1.5. These reversing tendencies imply that further surplus

of steam is not reacting and that adding more steam is not efficient. The exergy efficiency calculated for MSW is significantly lower due to a combination of low gas yield and poor syngas LHV. Efficiency values for both forest residues and MSW are within range from what is commonly found in the current literature [11].

Comparison between Figs. 6 and 8 show that exergy efficiency and exergy values display similar trends. This was predictable since, according to Eq. (12), exergy efficiency is mainly determined by the exergy value of each individual gas component [40]. Still, exergy efficiency presents a more pronounced decrease after reaching a maximum value. This can be explained by the increase in the exergy values for heating biomass/MSW and steam. This is consistent with the current literature [19,36]. Fig. 9 depicts the exergy efficiency as a function of the gasification temperature for forest residues and MSW.

Conversely to SBR, gasification temperature has a positive influence on exergy efficiency all throughout the studied range. Both substrates present very similar trends, with forest residues having the higher efficiency. Again, exergy efficiency follows a close trend to the one found for exergy values although with a less pronounced upsurge. This is caused by a considerable increase in biomass and steam heating values. In fact, when temperature was increased from 700 °C to 900 °C exergy values for heating biomass and agents increased from 2193.7 to 2784.9 kJ per kg of substrate.

Similarly to what was seen with exergy values, gasification temperature has greater influence on efficiency when compared to SBR. This is due to increase in gasification temperature leading to increases in both endothermic reactions and gas yield. Results are in agreement with current literature [19,36]. Fig. 10 shows the tar exergy efficiency for both substrates as a function of SBR and gasification temperature, respectively.

Tar efficiencies follow a very close trend to the ones presented in Figs. 6 and 7. Since substrate exergy value represents the dominant value on the exergy input, the exergy efficiency of tar is mainly dictated by the exergy value of tar. Consequently, SBR and gasification temperature lead to a considerable decrease in

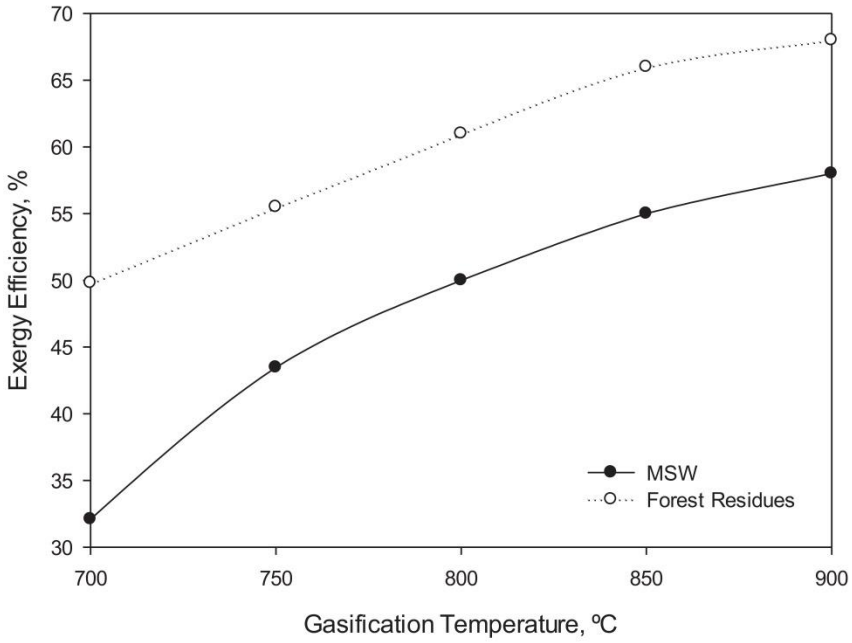

Fig. 9. Exergy efficiency as a function of temperature for forest residues and MSW.

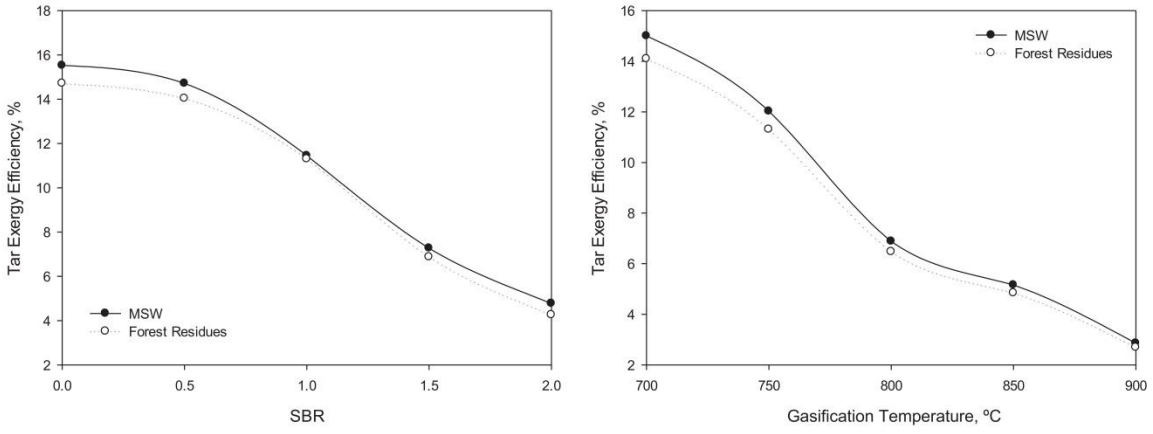

Fig. 10. Tar exergy efficiency for both substrates as a function of (a) SBR and (b) gasification temperature.

tar efficiency since they lead to a dramatically reduction of tar yield. This is consistent with the current literature [19,41].

According to Prins et al. [42], energy conversion processes, such as gasification, lead to entropy production caused by fluid flow, heat and mass transfer and chemical reactions. Increase in entropy causes exergy leaving any process to be always less than the exergy entering. This difference between exergy streams is usually called irreversibility. What this means is that in order to make a system more efficient, optimization of the operational conditions is a must. Therefore, an exergy efficiency optimization model was built using data obtained from the numerical model. The optimization model aims to establish where the maximum exergy efficiency is according to the substrate and operating conditions chosen. Particularly, in order to promote a more hydrogen-rich gas, the optimization model will focus on exergy flow rate of the produced hydrogen instead of syngas.

5.3. Exergy efficiency optimization - design of experiments

The empirical model was built minimizing the sum of the residues square to give the parameters of a second order response model.

$$Y = B_0 + \sum_{i=1}^{3} B_i \times X_i + \sum_{i=1}^{3} B_{i,i} \times X_i^2 + \sum_{j=2}^{3} \sum_{i<j}^{3} B_{i,j} \times X_i \times X_j \qquad (14)$$

where Y is the response, the X_i terms are the main factors ($-1 \leqslant X_i \leqslant 1$), temperature (1), steam-to-biomass ratio (2) and biomass type (3) and the B_i terms are the equation coefficients related to the main factors. The B_0 term is the interception coefficient, the $B_{i,i}$ terms are the quadratic effects (give the curvature to the response surface) and the $B_{i,j}$ terms symbolize the cross interactions between factors. The present design does not consider the use of replicates because the results are obtained by computer simulations. In this case, a test on lack of fit and analysis concerning pure error are not provided [43,44]. Despite these circumstances much of the standard statistical analyses remain relevant, including measurements of model-fit such as PRESS (predicted residual sum of squares). Fig. 11 shows that the empirical model accurately predicts the exergy model results. In fact there is no significant deviation between both models.

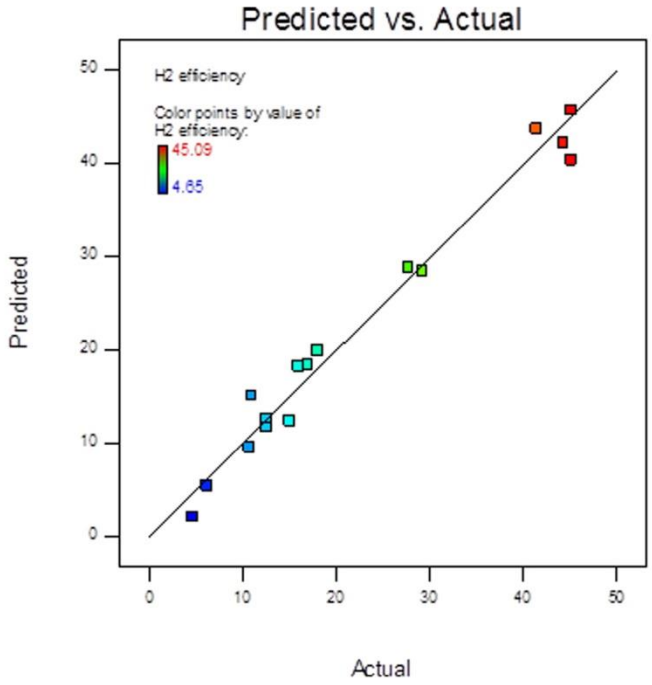

Fig. 11. Empirical model versus exergy model.

The Analysis of Variance (ANOVA) with high values for PRESS and "R-squared predicted" (not shown) also reinforced that the exergy efficiency response is well described by the empirical model in the design space [45]. Fig. 12 shows the hydrogen exergy efficiency as a function of the temperature and SBR for (a) forest residues and (b) MSW.

Unsurprisingly, both substrates presented very similar trends. In general, hydrogen efficiency increases with SBR since adding steam increases its chemical energy and exergy content. However, adding steam also demands additional energy (and therefore exergy).

For lower temperatures, especially lower than 800 °C, higher levels of SBR lead to a noticeable decrease in hydrogen efficiency. Without much literature to support this claim one can speculate that since excessive steam can lead to a decrease in gas yield and an increase in the denominator from Eq. (12) for introducing more steam, a decrease in hydrogen efficiency is a possibility. Regarding influence of gasification temperature one can clearly see that it has a positive effect on hydrogen efficiency all throughout the studied range. This can be explained by an increase in gas yield and enthalpy of gas component [19,46].

The interpolating polynomial indicated in Eq. (14) will provide the maximum values for hydrogen efficiency for both studied substrates. In Table 7, operating conditions to maximize the exergy efficiency through the optimization procedure are shown. Maximum hydrogen efficiency was found at 900 °C with a SBR of 1.5 for MSW and 1 for forest residues.

Surprisingly, forest residues and MSW present virtually the same maximum hydrogen efficiency. While forest residues has both the highest hydrogen molar composition as well as gas yield from the two it also has the higher substrate exergy value, leading to an overall lower hydrogen efficiency. Despite the effect of temperature and SBR not being fully addressed on the current literature, the available results support the conclusions made in this study [19,46].

Even though results from MSW were not on at same level with those from forest residues in regards to overall exergy efficiency, exciting results were seen in both tar and hydrogen efficiencies.

For Portugal, increase interest on MSW over forest residues goes even further since a pre-existing collection and transportation infrastructure currently available does not exist for the compared biomass resources. Furthermore, the undefined availability of sustainable forest residues, seasonal availability and local energy supply [47] that can lead to great uncertainty on the overall availability and sustainability of forest residues as a resource. All the above reasons combined with the fact that waste production is becoming one the main concerns of the 21st justifies the need for studying gasification for MSW treatment.

6. Conclusions

Influence of gasification temperature and steam to biomass ratio on exergy values of produced gas and tar content was studied. Results showed that when SBR was increased from 0 to 0.5, exergy values rose and then remained somewhat constant when SBR was further increased. Conversely, gasification temperature lead to a steady increase in exergy values all throughout the studied regime. Both SBR and reactor temperature lead to a drastically decrease in tar content. Forest residues present significantly higher syngas exergy values in relation to MSW.

Exergy efficiency as a function of SBR and temperature for forest residues and MSW was also studied. Results showed that maxi-

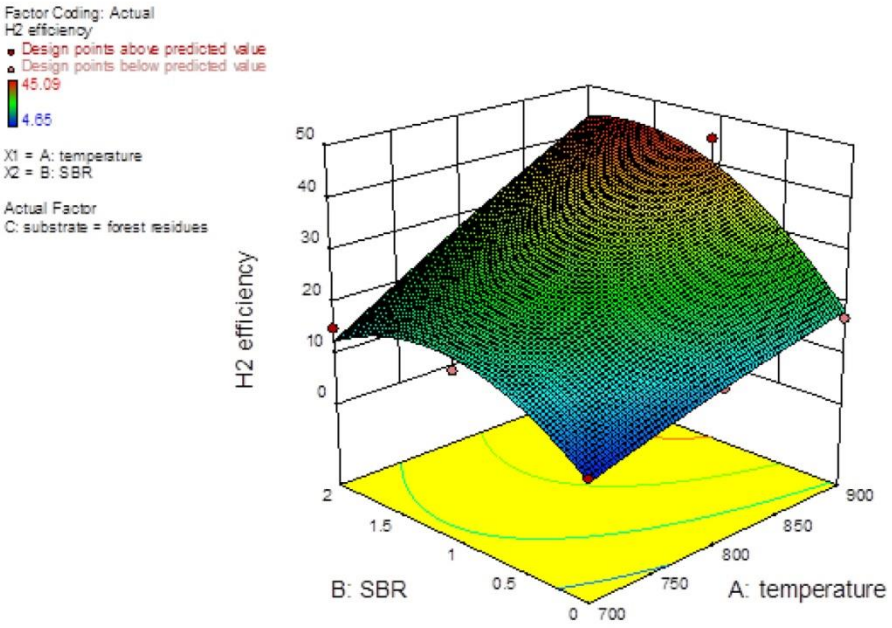

a

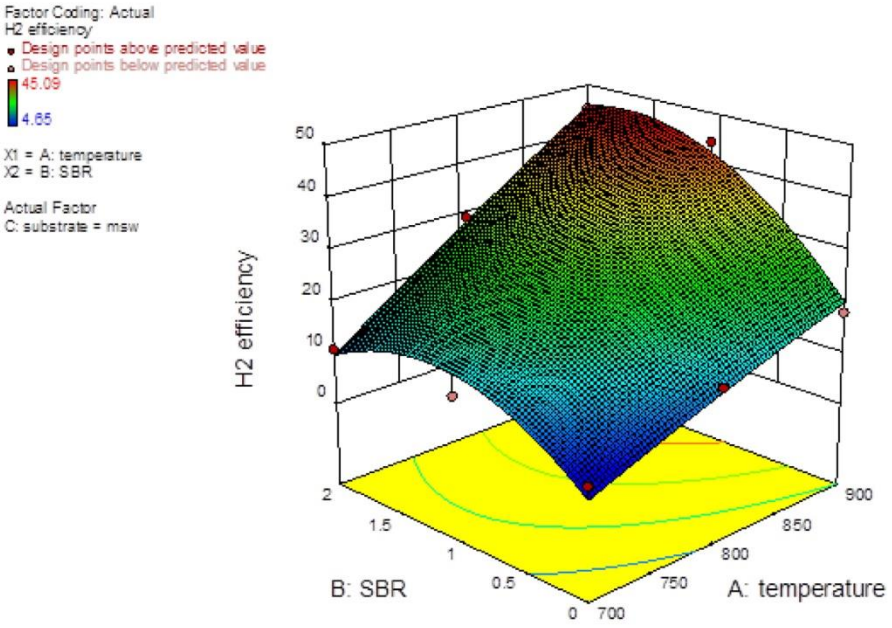

b

Fig. 12. (a) Hydrogen exergy efficiency as a function of temperature and SBR for forest residues. (b) Hydrogen exergy efficiency as a function of the temperature and SBR for MSW.

Table 7
Operation conditions and maximum exergy efficiency for forest residues and MSW.

Temperature (°C)	Forest residues 900	MSW 900
SBR	1	1.5
Maximum H_2 exergy efficiency (%)	50.6	50.2

mum efficiency is found at SBR = 1 from forest residues and SBR = 1.5 for MSW, gradually decreasing with further increase. Conversely to SBR, gasification temperature has a positive influence on exergy efficiency all throughout the studied range. Both substrates present very similar trends, with forest residues having the higher efficiency. SBR and gasification temperature lead to a considerable decrease in tar efficiency since they lead to a dramatically reduction of tar yield.

Finally an exergy efficiency model was designed to predict the optimal operation conditions for obtaining a more hydrogen-rich gas. Maximum hydrogen efficiency was found at 900 °C with a SBR of 1.5 for MSW and 1 for forest residues. Forest residues and MSW presented virtually the same maximum hydrogen efficiency.

Acknowledgements

We would like to express our gratitude to the Portuguese Foundation for Science and Technology (FCT) for the support to the grant SFRH/BD/86068/2012 and the project PTDC/EMS-ENE/6553/2014 as well as IF/01772/2014.

References

[1] Carpentieri M, Corti A, Lombardi L. Life cycle assessment (LCA) of an integrated biomass gasification combined cycle (IBGCC) with CO_2 removal. Energy Convers Manage 2005;46:1790–808.
[2] Ferreira S, Moreira NA, Monteiro E. Bioenergy overview for Portugal. Biomass Bioenergy 2009;33:1567–76.
[3] Shen B. Study on MSW catalytic combustion by TGA. Energy Convers Manage 2006;47:1429–37.
[4] Ng WPQ, Lam HL, Varbanov PS, Klemeš JJ. Waste-to-energy (WTE) network synthesis for municipal solid waste (MSW). Energy Convers Manage 2014;85:866–74.
[5] Teixeira S, Monteiro E, Silva V, Rouboa A. Prospective application of municipal solid wastes for energy production in Portugal. Energy Policy 2014;71:159–68.
[6] Lv P, Yuan Z, Ma L, Wu C, Chen Y, Zhu J. Hydrogen-rich gas production from biomass air and oxygen/steam gasification in a downdraft gasifier. Renew Energy 2007;32:2173–85.
[7] McKendry P. Energy production from biomass (part 3): gasification technologies. Bioresour Technol 2002;83:55–63.
[8] Sciubba E, Wall G. A brief commented history of exergy from the beginnings to 2004. Int J Thermodyn 2007;10:1–26.
[9] Dincer I. Environmental and sustainability aspects of hydrogen and fuel cell systems. Int J Energy Res 2007;31:29–55.
[10] Hosseini M, Dincer I, Rosen MA. Steam and air fed biomass gasification: comparisons based on energy and exergy. Int J Hydrogen Energy 2012;37:16446–52.
[11] Ptasinski KJ, Prins MJ, Pierik A. Exergetic evaluation of biomass gasification. Energy 2007;32:568–74.
[12] Sreejith CC, Muraleedharan C, Arun P. Energy and exergy analysis of steam gasification of biomass materials: a comparative study. Int J Ambient Energy 2013;34:35–52.
[13] Couto ND, Silva VB, Monteiro E, Rouboa A. Assessment of municipal solid wastes gasification in a semi-industrial gasifier using syngas quality indices. Energy 2015;93(Part 1):864–73.
[14] Couto N, Silva VB, Bispo C, Rouboa A. From laboratorial to pilot fluidized bed reactors: analysis of the scale-up phenomenon. Energy Convers Manage 2016;119:177–86.
[15] Silva V, Monteiro E, Couto N, Brito P, Rouboa A. Analysis of syngas quality from Portuguese biomasses: an experimental and numerical study. Energy Fuels 2014;28:5766–77.
[16] Couto ND, Silva VB, Rouboa A. Thermodynamic evaluation of Portuguese municipal solid waste gasification. J Clean Prod 2016;139:622–35.
[17] Onel O, Niziolek AM, Hasan MMF, Floudas CA. Municipal solid waste to liquid transportation fuels – Part I: Mathematical modeling of a municipal solid waste gasifier. Comput Chem Eng 2014;71:636–47.
[18] Couto N, Silva V, Monteiro E, Brito P, Rouboa A. Using an Eulerian-granular 2-D multiphase CFD model to simulate oxygen air enriched gasification of agroindustrial residues. Renew Energy 2015;77:174–81.
[19] Zhang Y, Li B, Li H, Zhang B. Exergy analysis of biomass utilization via steam gasification and partial oxidation. Thermochim Acta 2012;538:21–8.
[20] Szargut J, Styrylska T. Approximate evaluation of the exergy of fuels. Brennst Warm Kraft 1964;16:589–896.
[21] Basu P. Chapter 2 – Biomass characteristics. Biomass gasification and pyrolysis. Boston: Academic Press; 2010. p. 27–63.
[22] Stepanov VS. Chemical energies and exergies of fuels. Energy 1995;20:235–42.
[23] Couto ND, Silva VB, Rouboa A. Assessment on steam gasification of municipal solid waste against biomass substrates. Energy Convers Manage 2016;124:92–103.
[24] Couto N, Monteiro E, Silva V, Rouboa A. Hydrogen-rich gas from gasification of Portuguese municipal solid wastes. Int J Hydrogen Energy 2016;41:10619–30.
[25] Xiao G, Jin B-S, Zhong Z-P, Chi Y, Ni M-J, Cen K-F, et al. Experimental study on MSW gasification and melting technology. J Environ Sci 2007;19:1398–403.
[26] Louw J, Schwarz CE, Knoetze JH, Burger AJ. Thermodynamic modelling of supercritical water gasification: investigating the effect of biomass composition to aid in the selection of appropriate feedstock material. Bioresour Technol 2014;174:11–23.
[27] Campoy M, Gómez-Barea A, Ollero P, Nilsson S. Gasification of wastes in a pilot fluidized bed gasifier. Fuel Process Technol 2014;121:63–9.
[28] Wang J, Cheng G, You Y, Xiao B, Liu S, He P, et al. Hydrogen-rich gas production by steam gasification of municipal solid waste (MSW) using NiO supported on modified dolomite. Int J Hydrogen Energy 2012;37:6503–10.
[29] Yan F, Luo S-Y, Hu Z-Q, Xiao B, Cheng G. Hydrogen-rich gas production by steam gasification of char from biomass fast pyrolysis in a fixed-bed reactor: influence of temperature and steam on hydrogen yield and syngas composition. Bioresour Technol 2010;101:5633–7.
[30] Pinto F, André RN, Carolino C, Miranda M, Abelha P, Direito D, et al. Effect of using natural minerals and biomass wastes blends. Fuel 2014;117(Part B):1034–44.
[31] Manyà JJ, Sánchez JL, Ábrego J, Gonzalo A, Arauzo J. Influence of gas residence time and air ratio on the air gasification of dried sewage sludge in a bubbling fluidised bed. Fuel 2006;85:2027–33.
[32] Aljbour SH, Kawamoto K. Bench-scale gasification of cedar wood – Part II: Effect of operational conditions on contaminant release. Chemosphere 2013;90:1501–7.
[33] Loha C, Chatterjee PK, Chattopadhyay H. Performance of fluidized bed steam gasification of biomass – modeling and experiment. Energy Convers Manage 2011;52:1583–8.
[34] Song T, Wu J, Shen L, Xiao J. Experimental investigation on hydrogen production from biomass gasification in interconnected fluidized beds. Biomass Bioenergy 2012;36:258–67.
[35] Zhang X, Deng S, Wu J, Jiang W. A sustainability analysis of a municipal sewage treatment ecosystem based on energy. Ecol Eng 2010;36:685–96.
[36] Wu Y, Yang W, Blasiak W. Energy and exergy analysis of high temperature agent gasification of biomass. Energies 2014;7:2107.
[37] Pinto F, Lopes H, André RN, Dias M, Gulyurtlu I, Cabrita I. Effect of experimental conditions on gas quality and solids produced by sewage sludge cogasification. 1. Sewage sludge mixed with coal. Energy Fuels 2007;21:2737–45.
[38] Zhang Y, Zhao Y, Gao X, Li B, Huang J. Energy and exergy analyses of syngas produced from rice husk gasification in an entrained flow reactor. J Clean Prod 2015;95:273–80.
[39] Hernández JJ, Aranda G, Barba J, Mendoza JM. Effect of steam content in the air–steam flow on biomass entrained flow gasification. Fuel Process Technol 2012;99:43–55.
[40] Zhang Y, Li B, Li H, Liu H. Thermodynamic evaluation of biomass gasification with air in autothermal gasifiers. Thermochim Acta 2011;519:65–71.
[41] Wei L, Xu S, Zhang L, Liu C, Zhu H, Liu S. Steam gasification of biomass for hydrogen-rich gas in a free-fall reactor. Int J Hydrogen Energy 2007;32:24–31.
[42] Prins MJ, Ptasinski KJ, Janssen FJJG. Thermodynamics of gas-char reactions: first and second law analysis. Chem Eng Sci 2003;58:1003–11.
[43] Anderson MJ, Whitcomb PJ. RSM simplified: optimizing processes using response surface methods for design of experiments. Productivity Inc; 2005.
[44] Silva V, Rouboa A. Combining a 2-D multiphase CFD model with a response surface methodology to optimize the gasification of Portuguese biomasses. Energy Convers Manage 2015;99:28–40.
[45] Silva V, Rouboa A. Optimizing the gasification operating conditions of forest residues by coupling a two-stage equilibrium model with a response surface methodology. Fuel Process Technol 2014;122:163–9.
[46] Abuadala A, Dincer I. Efficiency evaluation of dry hydrogen production from biomass gasification. Thermochim Acta 2010;507–508:127–34.
[47] Vassilev SV, Vassileva CG, Vassilev VS. Advantages and disadvantages of composition and properties of biomass in comparison with coal: an overview. Fuel 2015;158:330–50.

Paper III

An experimental and numerical study on the Miscanthus gasification by using a pilot scale gasifier

N. Couto, V. Silva, E. Monteiro, A. Rouboa, P. Brito

Renewable Energy 109 (2017) 248-261

Renewable Energy 109 (2017) 248–261

Contents lists available at ScienceDirect

Renewable Energy

journal homepage: www.elsevier.com/locate/renene

An experimental and numerical study on the Miscanthus gasification by using a pilot scale gasifier

Nuno Dinis Couto [a], Valter Bruno Silva [a, d, *], Eliseu Monteiro [b, d], Abel Rouboa [a, c], Paulo Brito [d]

[a] INEGI-FEUP, Faculdade de Engenharia da Universidade do Porto, Porto, Portugal
[b] INEGI-FEUP, Polytechnic Institute of Portalegre, Portalegre, Portugal
[c] MEAM Department, University of Pennsylvania, Philadelphia, PA, USA
[d] C3i, Polytechnic Institute of Portalegre, Portalegre, Portugal

ARTICLE INFO

Article history:
Received 28 June 2016
Received in revised form
2 February 2017
Accepted 11 March 2017
Available online 15 March 2017

Keywords:
Gasifying agents
CO_2/ biomass ratio
CFD
Semi-industrial gasifier

ABSTRACT

This work comprises the study of several mixtures of air with O_2, CO_2 and steam in a pilot scale gasification plant. Out of eight substrates characteristic of south-central and southern Portugal, *Miscanthus* was chosen for revealing the highest potential for energy generation and for its friendliness from an ecological standpoint. Experiments with *Miscanthus* were performed in a pilot scale reactor and generated results were compared with ones from a numerical model, which consists of a Eulerian-Eulerian approach within the Fluent framework that is able to describe the transport of mass, momentum and energy for both solid and gas phases.

The numerical model was used to compare several gasifying agent mixtures and their impact on syngas composition and respective quality indices under similar operating conditions. The influence of equivalent, steam/biomass and CO_2/biomass ratios on syngas produced as well as temperature and cold gas efficiency were studied, and the most suitable application for each mixture was appraised based on the results.

1. Introduction

Since the industrial revolution, technological development has been in frank expansion and energy consumption has grown exponentially, particularly that produced from fossil fuels, leading the world to a major energy crisis [1]. In fact, environmental issues represent some of the most important challenges facing humanity today, which is why government institutions have taken matters into their own hands to reduce fossil fuel consumption and its environmental impact. The first international agreement which imposed reductions to greenhouse gas emissions was the Kyoto Protocol back in 2005, and although several countries have met the set targets, others have fallen well behind: the United States and China, for example, have emitted enough greenhouse gases to nullify the cutbacks made by other countries during the first Kyoto period (2008–2012). After the failure of COP (Conference of the Parties on Climate Change) in Copenhagen, the Paris meeting (COP21) later this year is the last chance to come to a consensus on a new protocol, which will mark a turning point in the fight against global warming [2]. It follows that now, more than ever, it is crucial to make a serious investment in an alternative energy source that, while able to meet the needs of an increasingly energy-dependent population, also does not worsen the current environmental problems.

Biomass has since long been considered as an alternative to fossil fuels for green production due to its zero net CO_2 emission [3]. In fact, in 2013, biomass and renewable waste accounted for more than 60% of the primary energy production from renewable sources of just under 125 million tons of oil equivalent, a number which represents slightly over 15% of primary energy production from all sources [4]. Despite these encouraging numbers there is still much work to be done and so it is crucial to keep investing in more efficient ways to convert biomass into energy.

In recent decades, from the wide range of methods available to convert biomass, thermochemical processes have received the

* Corresponding author. Campus Politécnico 10, 7300-555, Portalegre, Portugal.
E-mail addresses: nunodiniscouto@hotmail.com (N.D. Couto), valter.silva@ipportalegre.pt (V.B. Silva), ELMMonteiro@portugalmail.pt (E. Monteiro), rouboa@utad.pt (A. Rouboa), pbrito@estgp.pt (P. Brito).

http://dx.doi.org/10.1016/j.renene.2017.03.028
0960-1481/

most attention. Combustion remains to date the most widely used process, in which biomass is combusted to supply heat and power to industrial processes, albeit usually with very low net efficiency (20%–40%). Pyrolysis, in contrast, removes volatiles from biomass and produces char and tar, but due to limited end use applications and difficulty in downstream processing bio-oil, its employment is very restricted. As for gasification, it has been gaining preference over combustion due to its ability to use different feedstocks for different applications and meet high pollutant emission standards. Moreover, the fact that it achieves higher efficiencies shows promise, seeing that, according to Bridgwater et al. [5], the net system efficiency for gasification can exceed conventional combustion by 15%.

Despite the aforementioned advantages, some major challenges need to be addressed in order to replace or at least reduce the fossil fuel dependence, namely producing gas with high calorific value and low-price, but at the same time able to meet high environmental standards [6].

A way to do it is through the study of agents used to gasify the substrate, which can be air, pure O_2, steam, CO_2 or their mixtures, and are used to promote syngas characteristics and consequently obtain a gas suitable for a given application. Air, even though extremely cheap compared to other gasifier agents, allows for the production of a gas highly diluted in N_2 [7], whereas gasification with pure O_2 can achieve a much higher quality gas due to the absence of N_2, although with such high costs that its implementation in large facilities is still uncertain [8]. Gasification with steam can produce a gas rich in H_2, but due to relatively low reactivity, it is necessary to supply heat from an external source [9]. Lastly, CO_2 gasification can play a very important role in reducing CO_2 pollution but also requires indirect or external heat supply [10]. Table 1 presents a comparison between strengths and weaknesses for each gasifying agent.

Due to the high costs associated with biomass gasification experimental activities, more and more researchers turn to numerical simulation in their studies as an alternative and more efficient way to achieve the same results. Regarding numerical modeling on biomass gasification using different gasifying agent mixtures, Table 2 summarizes the most relevant studies and their respective findings.

The purpose of this paper is to analyze the gasification of a substrate characteristic of the Alqueva region, located in south-central Portugal, using O_2, steam, CO_2 and their respective mixtures with air. The added value of this work is a pioneer attempt to study these mixtures in semi-industrial conditions using the same operating parameters. To this end, a previously developed numerical model was used and its results were validated against experimental ones, obtained from a semi-industrial reactor. The influence of syngas composition and gasification temperature on process efficiency was studied. Finally, a comparison between mixtures was performed and their respective optimal application was determined.

2. Material and methods

2.1. Feedstock material

Given the growing concerns about climate change, namely heavy dependence on fossil fuels and rising energy costs, many countries, in particular Portugal, have been promoting renewable energy sources. The use of bio fuels comes forward as a contributing solution, since it leads to globally lower emissions when compared to using fossil fuels, and one of the breakthroughs of European Union legislation was the approval of so-called “energy crops” for bio fuel production [13].

The Alqueva (Alentejo, Portugal) irrigation perimeters, both built and projected, have a high potential to grow energy crops. The soil and ecological requirements of eight cultures (*Salix* spp, *Populus* spp, *Miscanthus x giganteus*, *Cynara cardunculus* L., *Arundo donax* L., *Panicum virgatum* L., *Hibiscus cannabinus* L., and *Jatropha curcas* L.) were previously studied. Although results showed that all crops analyzed grow in the Alqueva areas, *Miscanthus x giganteus* seems to be the most interesting from an ecological standpoint and its considerable potential for energy generation makes this substrate appealing for gasification, which is why it was chosen to feature the present study.

Prior to the actual gasification process, biomass analysis was carried out in the Laboratory of Chemistry of the High School of Technology and Management located in Portalegre, Portugal, since biomass characteristics can provide valuable information on how the gasification process will occur. This kind of analysis also provides crucial data to feed the implemented numerical model.

The instruments used in the performed analysis are as follow:

- Thermal Gravimetric Analysis – Data for proximal analysis;

The proximate analysis, for determination of moisture content, volatile matter, fixed carbon and ash in biomass, was performed using thermal gravimetric analysis (TGA, PerkinElmer, Thermal Analysis, STA 6000). Raw sample of crushed biomass is weighed

Table 1
Strengths and weakness for each gasifying agent.

Gasifying Mixture	Strengths	Weakness	Ref.
Air Gasification	No need for external energy Cheap Moderate char and tar content	Lower heating value (4–6 MJ/Nm^3) Highly diluted in N_2	[10]
O_2 Gasification	Higher heating value (10–15 MJ/Nm^3) Lower N_2 dilution Low char and tar content No need for external energy	Most expensive	[12]
Steam Gasification	Increases H_2/CO ratio Results in higher levels of H_2 Cost between air and O_2 Higher heating value (15–20 MJ/Nm^3)	Consumes H_2O Requires vaporization Requires external source of heat More corrosive environment High tar content	[10–12]
CO_2 Gasification	Utilizes CO_2 More efficient gasification Decreases H_2/CO ratio Results in higher levels of CO Converts CO_2 in CO	Highly endothermic Requires heat from external source	[10,11]

Table 2
Literature on relevant mathematical studies using different gasifying agents.

Ref.	Model considerations	Gasifying agent	Findings
[13]	Thermodynamic analysis using Aspen	CO_2	CO_2 recycle proved to increase syngas production.
[14]	Thermodynamic analysis using Aspen	CO_2, steam, O_2	Some operating parameters were able to produce CGE higher than 100%. Optimal temperature for complete carbon conversion was found at 850 °C.
[15]	Eulerian Method using FLUENT 14.0	CO_2-Air Mixture	CO_2-to-biomass ratio had tremendous influence on gasification performance.
[9]	Steady-state hybrid model of equilibrium and kinetics in FORTRAN	Steam	Steam-to-carbon ratio significantly affected gas composition. Tar concentration for steam gasification was much higher than that for O_2 gasification.
[16]	Eulerian-granular Model in FLUENT	O_2-enriched air	H_2 content decreased while CGE increased with O_2 one.
[17]	Equilibrium modeling approach	Steam	Steam lead to increases in H_2, CO_2 and CH_4 while CO decreased
[18]	Support vector machine algorithm	O_2-Steam Mixture	Optimal O_2 -steam ratios were studied for both heat release and required in coal gasification.
[19]	Thermodynamic model	O_2	With this particular system, 102 g of H_2 per kg of biomass were obtained, resulting in a CGE of 65.4%.
[20]	Aspen Plus coupled with FORTRAN subroutines.	Air-Steam mixture	Increase in air flow resulted in higher carbon conversion, tar reforming and gas yield while steam addition resulted in a more H_2 rich gas.

(10 mg) and placed in crucible of TGA and heated up to 900 °C. The fixed carbon is a solid combustible matter without the light and volatile compounds. It is a value obtained by subtracting the sum of ash, moisture and volatile matter from 100 where all values are on the same moisture reference base.

- Elemental Analysis - Determination of biomass composition with respect to the percentage of C, H, N and O;

Carbon (C), oxygen (O), hydrogen (H), nitrogen (N) and sulfur (S) content of the samples were determined by ultimate analysis conducted by Thermo Scientific Flash 2000 elemental analyzer. Samples were introduced to auto sampler of the analyzer and combusted at 950 °C, and then the content of compounds were measured simultaneously. Once the percentages of carbon, nitrogen, hydrogen, sulfur and ash were determined, the amount of oxygen was calculated by subtracting the total percentages of the mentioned elements from a hundred percent. All results were reported on dry basis.

- Calorific Value - Appraisal of energy contained in biomass.

Heating value was determined by ISO method using an IKA C200 oxygen bomb calorimeter. A 0.5 g sample was weighed in a quartz crucible and put in the calorimeter for combustion. Higher heating value was obtained after combustion by means of IKA C200 software. Heating value is reported in MJ/kg on dry basis. The Lower Heating Value (LHV) was determined by using the HHV obtained from the bomb calorimeter including the hydrogen content and moisture of the biomass components according to Basu [14].

Table 3
Biomass properties.

Biomass properties	*Mischantus*
Elementary analysis (wt. %)	
N	5.3
C	44.5
H	5.2
O	45.0
Humidity (%)	11.4
Bulk density (kg/m^3)	600
Net Heat Value (MJ/kg biomass)	18.6
Proximal analysis (wt. %)	
Ash	2.1
Volatile matter	64.4
Fixed carbon	22.1

From the tests carried out it was possible to compile the main biomass properties, available in Table 3.

Table 3 shows that the fixed carbon is 22.5 wt. % provided by the proximate analysis. The 44.5 wt. % is the elemental carbon provided by the ultimate analysis. These values are in agreement with other published data for Miscanthus [15,16].

2.2. Experimental setup

Gasification tests were performed in a semi-industrial gasification plant (Fig. 1), installed in the Industrial Park of Portalegre, Portugal. The plant is based on fluidized bed technology, with a processing capacity of approximately 100 kg/h, and operates between 750° and 850 °C.

Fig. 2 depicts a diagram of the biomass gasification unit used in the experiments.

The main components of the unit are as follow:

a) Biomass feed system with two storage silos to allow the loading of biomass into the reactor using an Archimedean screw variable and controllable speed;
b) Fluidized bed reactor as a tubular reactor of 0.5 m in diameter and 4.0 m in height; biomass enters the reactor at 0.5 m from its base, whereas preheated air is admitted from the base by means of a set of diffusers, providing a flow of about 70 m^3/h; three temperature sensors are installed inside in order to monitor and control the gasification temperature and ensure syngas leaves the reactor at 600 °C;
c) Gas cooling system comprising two heat exchangers; the first cools the synthesis gas to about 300 °C using a co-current air flow entering the unit and the second further cools the synthesis gas to about 150 °C by forced flow of air from the exterior;
d) Cellulosic bag filter which removes carbon particles and ash produced in the gasification;
e) The condenser, where condensed liquids are removed by cooling the syngas to room temperature, through a third heat exchanger.

The bottom bed of the reactor has a static height of 0.15 m and is composed by dolomite (calcium magnesium carbonate $CaMg(CO_3)_2$), with a solid density of about 2800 kg/m^3 and particle size 0.3–0.7 mm particles; 80 kg of dolomite composed the bottom bed. Preheated atmospheric air at 350 K was used as gasification agent, fed through a distributor plate. The biomass is fed at the bed surface, 0.50 m above the distributor plate, by means of a screw feeder.

Fig. 1. Photograph of the semi-industrial gasification plant in Portalegre, Portugal.

The fluidized bed was operated at atmospheric pressure and in bubbling regime according to Geldart classification, with superficial gas velocity of around 0.25 m/s (obtained by the Ergun equation [17]).

Geldart [18] identified particle size and gas particle density difference as the key characteristics influencing gas fluidization behavior. According to his classification that includes four types of particles, our fluidization regime can be classified in the group B that is called 'sandlike' particles or bubbly particles. For these particles, once the minimum fluidization velocity is exceeded, the excess gas appears in the form of bubbles.

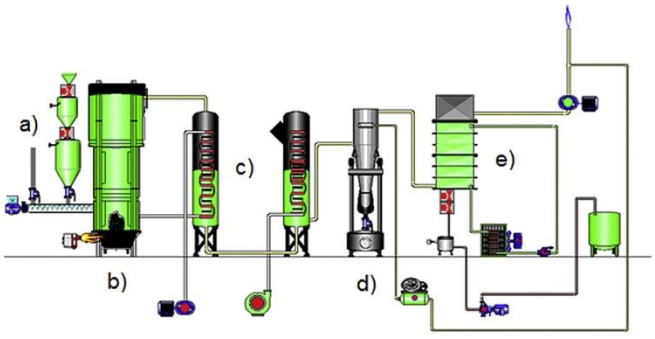

Fig. 2. Schematics of the gasification plant.

2.3. Analysis procedures

Syngas analysis was performed in a Varian 450-GC gas chromatograph with two TCD detectors that allow the detection of H_2, CO, CO_2, CH_4, O_2, N_2, C_2H_6, C_2H_4 (equipped respectively with CP81069, CP81071, CP81072, CP81073 and CP81025 Varian GC columns), using helium and nitrogen as carrier gases. Syngas samples were collected in appropriate collection and analysis Tedlar bags at the condenser exit every time gasification of a given feedstock composition has reached its stationary state. Collected syngas samples were injected directly from the sampling bags in the chromatograph (within one hour after sampling) using a peristaltic pump operating at its maximum rate through a Marpren tube. Chromatographic peaks for the different gases under analysis were identified based on their retention times, and by comparing them with the retention times of the same gases in the reference chromatogram of the custom solution, provided by Varian. Gas mass percentage composition was calculated on the basis of peak areas under the chromatographic signals.

3. Mathematical model

The two-dimensional mathematical model developed by Silva and Couto [16,24] for biomass gasification and extended by Couto et al. [25] for MSW gasification was used in this study. Gasification was modeled using the Fluent data base for a two-dimensional and a multi-phase (gas and solid) model. The solid phase was treated as a Eulerian granular model while the gas phase was deemed continuum. The main interaction between the phases was also modeled, namely heat exchange by convection, mass (the heterogeneous chemical reactions), and momentum (the drag in gas and solid phase). The numerical procedure can be perused in Ref. [25], and the next section describes the main governing equations.

3.1. Governing equations

Due to the high solid fraction inside the fluidized bed, the Eulerian method was used to simulate the biomass gasification process. In this model, stresses in the granular solid phase are obtained by the analogy between the random particle motion and the thermal motion of molecules within a gas accounting for the inelasticity of solid particles. As in a gas, the intensity of velocity fluctuation determines the stresses, viscosity, and pressure of the granular phase. The kinetic energy associated with velocity fluctuations is described by a pseudothermal temperature or granular temperature, which is proportional to the norm of particle velocity fluctuations. The conservation equation for the granular temperature, obtained from the kinetic theory of gases, takes the following form:

$$\frac{3}{2}\left[\left(\frac{\partial(\rho_s\alpha_s\Theta_s)}{\partial t}+\nabla\cdot(\rho_s\alpha_s\vec{v}_s\Theta_s)\right)\right]=\left(-P_s\bar{I}+\bar{\tau}_s\right):\nabla(\vec{v}_s)+\nabla\cdot(k_{\Theta a}\nabla(\Theta_s))-\gamma_{\Theta a}+\phi_{ls} \quad (1)$$

This expression is obtained from the kinetic theory of gases. The term $(-p_s\bar{I}+\bar{\tau}_s):\nabla(\vec{v}_s)$ describes the generation of energy by the solid stress tensor, φ_{ls} stands for the energy exchange between fluid and solid phase, γ_{Θ_a} for the collisional dissipation of energy and $k_{\Theta_a}\nabla(\Theta_s)$ for the diffusion energy, in which k_{Θ_a} is the diffusion coefficient. The diffusion coefficient for granular energy was computed by using the following equation due to Syamlal et al. [22]:

$$k_{\Theta_a} = \frac{15 d_s \rho_s \alpha_s \sqrt{\theta_s \pi}}{4(41-33\omega)}\left[1+\frac{12}{5}\omega^2(4\omega-3)\alpha_s g_{0,ss} + \frac{16}{15\pi}(41-33\omega)\omega\alpha_s g_{0,ss}\right] \quad (2)$$

where $\omega = (1+e_{ss})/2$; d is the biomass particle diameter; s is the solid phase.

The granular energy dissipation can be computed by using the expression derived by Lun et al. [23]. When the granular flow has a smaller volume fraction than the maximum possible value, a solid pressure is considered for the pressure gradient term in the momentum equation, which includes a kinetic term and a particle collision term:

$$p_s = \rho_s \alpha_s \theta_a + 2\rho_s(1+e_{ss})\alpha_s^2 g_{0,ss}\theta_a \quad (3)$$

The radial distribution function allows the different levels of compressibility. It works as a correction factor that gives the probability of collisions when the granular phase goes to denser states. Ansys Fluent provides empirical relations for the radial distribution function when there is one solid phase.

The standard k−ε model in ANSYS FLUENT has become the workhorse of practical engineering flow calculations in the time since it was proposed by Launder and Spalding [24]. It is a semi-empirical model, and the derivation of the model equations relies on phenomenological considerations and empiricism. The selection of this turbulence model is appropriate when the turbulence transfer between phases plays a predominant role as in the case of gasification in fluidized beds. The turbulence kinetic energy k and its rate of dissipation ε are obtained from the following transport equations:

$$\frac{\partial}{\partial t}(\rho k) + \frac{\partial}{\partial x_i}(\rho k u_i) = \frac{\partial}{\partial x_j}\left[\left(\mu + \frac{\mu_t}{\sigma_k}\right)\right] + G_k + G_b - \rho\varepsilon - Y_M + S_k \quad (4)$$

$$\frac{\partial}{\partial t}(\rho\varepsilon) + \frac{\partial}{\partial x_i}(\rho\varepsilon u_i) = \frac{\partial}{\partial x_j}\left[\left(\mu + \frac{\mu_t}{\sigma_\varepsilon}\right)\frac{\partial \varepsilon}{\partial x_j}\right] + C_{1\varepsilon}\frac{\varepsilon}{k}(G_k + C_{3\varepsilon}G_b) - C_{2\varepsilon}\rho\frac{\varepsilon^2}{k} + S_\varepsilon \quad (5)$$

G_k represents the generation of turbulence kinetic energy due to mean velocity gradients, G_b the generation of turbulence kinetic energy due to buoyancy, and Y_M the contribution of fluctuating dilatation in compressible turbulence to the overall dissipation rate.

To determine the turbulence kinetic energy as well as the dissipation rate, the following constants were assumed: $G_k = 1.0$ and $G_\varepsilon = 1.3$ stand for the turbulent Prandtl numbers for k and ε, respectively, and S_k and S_ε for user-defined source terms. $C_{1\varepsilon} = 1.44$, $C_{2\varepsilon} = 1.92$, and $C_{3\varepsilon} = 0$ are constants suggested by Launder and Spalding [24].

Seeing that they interact by means of energy, mass and momentum, the following table presents the relevant equations for both gas and solid phase.

In Table 4, $\vec{Q}_{pq}$ stands for the heat transfer intensity between fluid phase, pth, and solid phase, qth; h_q for the specific enthalpy of phase qth; and $\vec{q}_q$ for the heat flux. S_q is a source term due to chemical reactions, h_{pq} represents interface enthalpy, R_C the reaction rate, γ_c the stoichiometric coefficient and M_C the molecular weight. For solid phase, t_s is the particle phase stress tensor and P_s is particle phase pressure due to particle collisions. Finally, β stands for the gas-solid interphase drag coefficient, τ_g for the gas phase stress tensor and U_s for the mean solid velocity.

The above equations for fluid-fluid and for granular multiphase flows are solved by Fluent for both pth and qth phases. Further explanation on these equations can be found in Ref. [21].

3.2. Chemical reactions model

In the present study, three fundamental chemical processes were included [25]: devolatilization, homogeneous gas phase reactions and heterogeneous char reactions.

Table 5 presents the key reactions as well as reaction rates in the chemical model.

The chemical reaction rate coefficients are based on the Arrhenius law. During devolatilization and cracking, the water-shift reaction occurs and the gas species react with the supplied oxidizer and among themselves. The Arrhenius rates for these reactions as well as further explanation can be found in Ref. [21].

Homogeneous reactions are affected by both kinetic and turbulent mixing rates. The Finite-rate/Eddy-dissipation model was used seeing that it considers both Arrhenius and Eddy-dissipation reaction rates, and further considerations can be found in Ref. [21].

Regarding heterogeneous reactions, the Kinetic/Diffusion Surface Reaction Model [26] was applied. This model weights the effect of both the Arrhenius and the diffusion rate of the oxidant at the surface particle, which can be defined like so:

$$D_0 = C_1\frac{\left[(T_p + T_\infty)\div 2\right]^{0.75}}{d_p} \quad (6)$$

Whereas the Arrhenius rate can be expressed as follows:

$$r_{Arrehnius} = Ae^{-\left(\frac{E}{RT_p}\right)} \quad (7)$$

The final reaction rate weights both contributions and is defined as follows:

$$\frac{d_{m_p}}{d_t} = -A_p\frac{\rho R T_\infty Z_{ox}}{M_{w,ox}}\frac{D_0 r_{Arrehnius}}{D_0 + r_{Arrehnius}} \quad (8)$$

Table 4
Governing equations for gas and solid phases.

Gas Phase	Solid Phase
Energy:	
$\frac{\partial(\alpha_q\rho_q h_q)}{\partial t} + \nabla\cdot(\alpha_q\rho_q\vec{u}_q h_q) = -\alpha_q\frac{\partial(p_q)}{\partial t} + \bar{\bar{\tau}}_q : \nabla(\vec{u}_q) - \nabla\vec{q}_q + S_q + \sum_{p=1}^{n}(\vec{Q}_{pq} + \dot{m}_{pq}h_{pq})$	$\frac{\partial(\alpha_p\rho_p h_p)}{\partial t} + \nabla\cdot(\alpha_p\rho_p\vec{u}_p h_p) = -\alpha_p\frac{\partial(p_p)}{\partial t} + \bar{\bar{\tau}}_p : \nabla(\vec{u}_p) - \nabla\vec{q}_p + S_p + \sum_{q=1}^{n}(\vec{Q}_{pq} + \dot{m}_{pq}h_{pq})$
Mass:	
$\frac{\partial(\alpha_q\rho_q)}{\partial t} + \nabla\cdot(\alpha_q\rho_q\vec{u}_q) = -M_C\sum\gamma_C R_C$	$\frac{\partial(\alpha_p\rho_p)}{\partial t} + \nabla\cdot(\alpha_p\rho_p\vec{u}_p) = M_C\sum\gamma_C R_C$
Momentum:	
$\frac{\partial(\alpha_q\rho_q\vec{u}_q)}{\partial t} + \nabla\cdot(\alpha_q\rho_q\vec{u}_q\vec{u}_q) = -\alpha_q\nabla p_q + \alpha\rho_q g + \beta(u_q - u_p) + \nabla\cdot\alpha_q\bar{\bar{\tau}}_q + S_{pq}U_S$	$\frac{\partial(\alpha_p\rho_p\vec{u}_p)}{\partial t} + \nabla\cdot(\alpha_p\rho_p\vec{u}_p\vec{u}_p) = -\alpha_p\nabla p_p + \alpha\rho_p g + \beta(u_q - u_p) + \nabla\cdot\alpha_p\bar{\bar{\tau}}_p + S_{pq}U_S$

Table 5
Chemical reaction model.

Reactions	Reaction Rate
Pyrolysis:	
$Cellulose \rightarrow \alpha_1 volatiles + \alpha_2 TAR + \alpha_3 char$	$r_1 = A_i exp\left(\frac{-E_i}{T_s}\right)(1-a_i)^n$
$Hemicellulose \rightarrow \alpha_4 volatiles + \alpha_5 TAR + \alpha_6 char$	$r_2 = A_i exp\left(\frac{-E_i}{T_s}\right)(1-a_i)^n$
$Lignin \rightarrow \alpha_7 volatiles + \alpha_8 TAR + \alpha_9 char$	$r_3 = A_i exp\left(\frac{-E_i}{T_s}\right)(1-a_i)^n$
$Plastics \rightarrow \alpha_{10} volatiles + \alpha_{11} TAR + \alpha_{12} char$	$r_4 = \left[\sum_{i=1}^{n} A_i exp\left(\frac{-E_i}{RT}\right)\right]\rho_v$
$Primary\ TAR \rightarrow volatiles + SecondaryTAR$	$r_5 = 9.55 \times 10^4 exp\left(\frac{-1.12\times10^4}{T_g}\right)\rho_{TAR1}$
Homogeneous Reactions:	
$CO + 0.5O_2 \rightarrow CO_2$	$r_6 = 1.0 \times 10^{15} exp\left(\frac{-16000}{T}\right) C_{CO} C_{O_2}^{0.5}$
$CO + H_2O \rightarrow CO_2 + H_2$	$r_7 = 5.159 \times 10^{15} exp\left(\frac{-3430}{T}\right) T^{-1.5} C_{O_2} C_{H_2}^{1.5}$
$CO + 3H_2 \leftrightarrow CH_4 + H_2O$	$r_8 = 3.552 \times 10^{14} exp\left(\frac{-15700}{T}\right) T^{-1} C_{O_2} C_{CH_4}$
$H_2 + 0.5O_2 \rightarrow H_2O$	$r_9 = 2780 exp\left(\frac{-1510}{T}\right)\left[C_{CO} C_{H_2O} - \frac{C_{CO_2} C_{H_2}}{0.0265 exp\left(\frac{3968}{T}\right)}\right]$
$CH_4 + 2O_2 \rightarrow CO_2 + 2H_2O$	$r_{10} = 3.0 \times 10^5 exp\left(\frac{-15042}{T}\right) C_{H_2O} C_{CH_4}$
Heterogeneous Reactions:	
$C + 0.5O_2 \rightarrow CO$	$r_{11} = 596 T_P exp\left(\frac{-1800}{T}\right)$
$C + CO_2 \rightarrow 2CO$	$r_{12} = 2082.7 exp\left(\frac{-18036}{T}\right)$
$C + H_2O \rightarrow CO + H_2$	$r_{13} = 63.3 exp\left(\frac{-14051}{T}\right)$

This part was included in the CFD framework by using the User Defined Function tool.

The local mass fraction of each specie Y is computed by using a convection-diffusion equation as follows:

$$\frac{\partial}{\partial t}(\rho Y_i) + \nabla(\rho Y_i \vartheta) = -\nabla \cdot J_i + R_i + S_i \quad (9)$$

where J_i is the diffusion flux of species i due to concentration gradients, R_i is the net generation rate of species i due to homogeneous reaction, and S_i is a source term related to the species i production from the solid heterogeneous reaction. The diffusion flux was computed as a function of the turbulent Schmidt number.

3.3. Numerical procedure

Fluent, a finite volume method based CFD solver, was employed in this work to solve the stated problem. Mesh was built using GAMBIT software and the size of the cell in both the x- and y-directions was specified with a 1:1 ratio. The time step was decreased with decreasing cell size to help maintain numerical stability. To select the optimum number of cells, grid independence studies were performed.

The simulations are carried out on 4 different grids with increasing grid density in order to ensure a grid-independent solution. Table 6 displays the main characteristics of each mesh.

Table 6
Mesh characteristics.

Mesh	$x \times y$	Number of Elements
1	80 × 664	53,120
2	90 × 747	67,230
3	100 × 830	83,000
4	110 × 913	100,430

Molar fraction compositions for CH_4, CO, CO_2 and H_2 at gasifier outlet are compared for the described grids. The grid-independent solution is illustrated in Fig. 3.

The simulation results for the various meshes are found to be in good agreement with each other. As can be seen, the grids with number of cells exceeding than 83,000 cells reveal a small variation in parameter convergence less than 1%. Consequently, the grid with 83,000 cells is recommended to use for accurate calculations.

In order to avoid poor convergence, an unsteady model was used with a time step size of 1.0^{-4}s and the gasification time of the biomass was resolved by 400,000 time steps.

Boundary conditions used are presented in Table 7.

3.4. Selection of optimal range for gasifying agent-to-biomass ratio for numerical simulations

In order to properly investigate the influence of every gasifying agent on each air mixture, not only the fraction of the agent but also the agent-to-biomass fed ratio were studied. These ratios can help tremendously in characterizing and understanding the effects of each agent under study. The selected ratios are listed in Table 8.

Equivalent ratio (ER) was kept between 0.15 and 0.35 since all of the experiments conducted to validate the model fell in this range and also because, according to Wang et al. [10], the ER values most suitable for gasification range between 0.2 and 0.4.

The steam/biomass ratio (SBR) range was selected based on previous findings from our research team using the same facilities but for a different biomass substrate [20]. In the referred work, H_2 production was favored by increasing SBR, however with a less pronounced increase for SBR higher than 1 and achieving an asymptotic value after 1.5.

Selecting CO_2/biomass ratio (CDBR) can be quite challenging due to the lack of available literature, which only features a CDBR

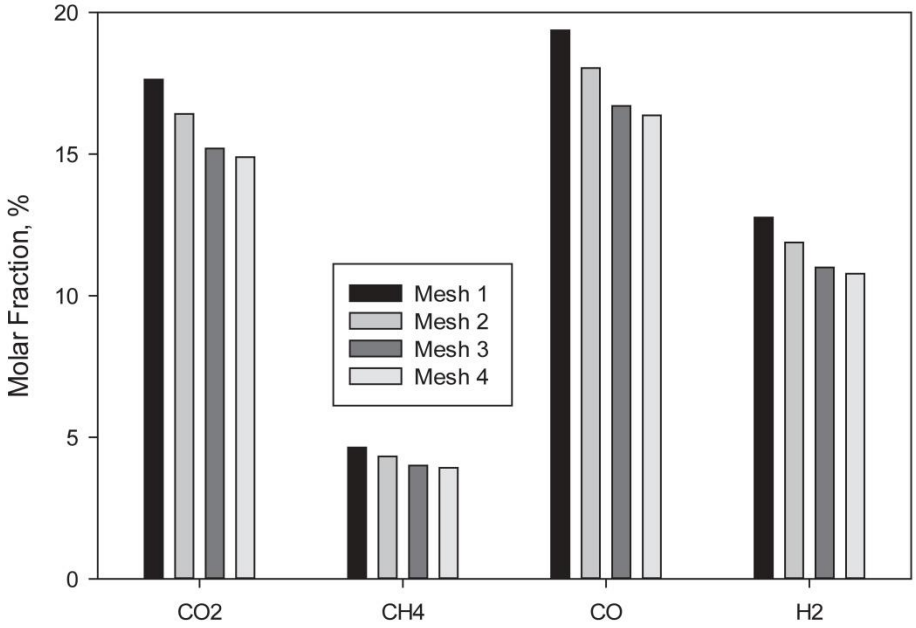

Fig. 3. Grid independence study for the described meshes.

Table 7
Boundary conditions used in the simulation.

Boundaries	Velocity	Pressure	Temperature
Walls	No slip	Zero gradient	Fixed value
Syngas outlet	No slip	Fixed value	Zero gradient
Biomass and Air Inlet	Fixed flow rate	Zero gradient	Fixed value

Table 8
Selected Ratios for gasifying agent comparison.

Gasifying agent	Nomenclature	Formula	Range
O_2	ER	$\frac{\text{Actual air/Biomass ratio}}{\text{Stoichiometric air/Biomass ratio}}$	0.15–0.35
Steam	SBR	$\frac{\text{Steam mass flow rate}}{\text{Biomass mass flowrate}}$	0–2
CO_2	CDBR	$\frac{CO_2 \text{ mass flow rate}}{\text{Biomass mass flow rate}}$	0–2.5

studies for low (0.57–1.39) [27] and high values (2–2.5) [28]. In the present study, the CDBR was studied from a low to high range in a first attempt to analyze this ratio in depth in semi-industrial conditions using a fluidized-bed reactor.

4. Results and discussion

The numerical model presented in section 3 has already been validated for coffee husks [20], forest residues [29] and vines pruning residues [19] using a pilot scale thermal gasification plant, and for municipal solid wastes in laboratory scale facilities [30,31]. It has also undergone changes over time to deal with various characteristics of the different biomasses studied.

Regarding *miscanthus* gasification, a large set of experimental runs were performed in the previously described facilities, and every run was performed twice in order to avoid off measurements. When deviation was higher than 5%, extra runs were performed to assure reproducibility below 5%, which is the typical average number for this kind of system [32]. Operating conditions from a chosen set of 5 experiments are presented in Table 9.

Fig. 4 illustrates the syngas composition obtained, both experimentally and numerically, as a function of ER.

In this work, ER was adjusted by varying the air flow rate into the reactor. Both numerical and experimental results show very similar trends seeing that, by increasing ER, all combustible gases (CO, CH_4 and H_2) decreased while CO_2 increased. With more O_2 inside the reactor, combustion reactions are promoted (in particular char, CO and H_2), leading to formation of CO_2 and H_2O at the expense of CO and H_2, a behavior consistent with that described in current literature [33,34]. As expected, the biggest deviation was observed for CH_4, since smaller fractions tend to produce higher relative errors [19].

The remaining operating conditions are consistent with the available literature and follow trends observed in other experimental runs for different biomass substrates.

In order to further validate the numerical model, the temperature distribution inside the reactor was studied using the three thermocouples previously mentioned. A comparison between the numerical model and experimental results is displayed in Table 10.

T1, T2 and T3 are located at 1.70, 2.50 and 3.85 m from the bottom. From the view point of the oxidizer, several stages can be differentiated: drying, devolatilization, volatile matter combustion and char gasification. Since there are only 3 thermocouples, it is impossible to determine where each reaction zone can be found, but since the first thermocouple is located 1.70 m above the air inlet, it is safe to assume that most stages are completed at that point and that gasification is the only process remaining. Therefore, it comes with no surprise that the temperature inside the reactor appears to drop almost linearly until it reaches syngas outlet, which can be attributed to exothermic reactions (namely combustion) occurring near the biomass inlet and producing heat, and then through the reactor length the heat is being consumed by the

Table 9
Operating conditions for the experimental gasification runs.

Operating Conditions	*Miscanthus* Pellets				
Runs	**1**	**2**	**3**	**4**	**5**
Temperature (°C)	800	800	800	750	850
Biomass Admission (Kg/h)	30	45	56	56	56
Air Flow Rate (Nm^3/h)	38	50	85	85	88

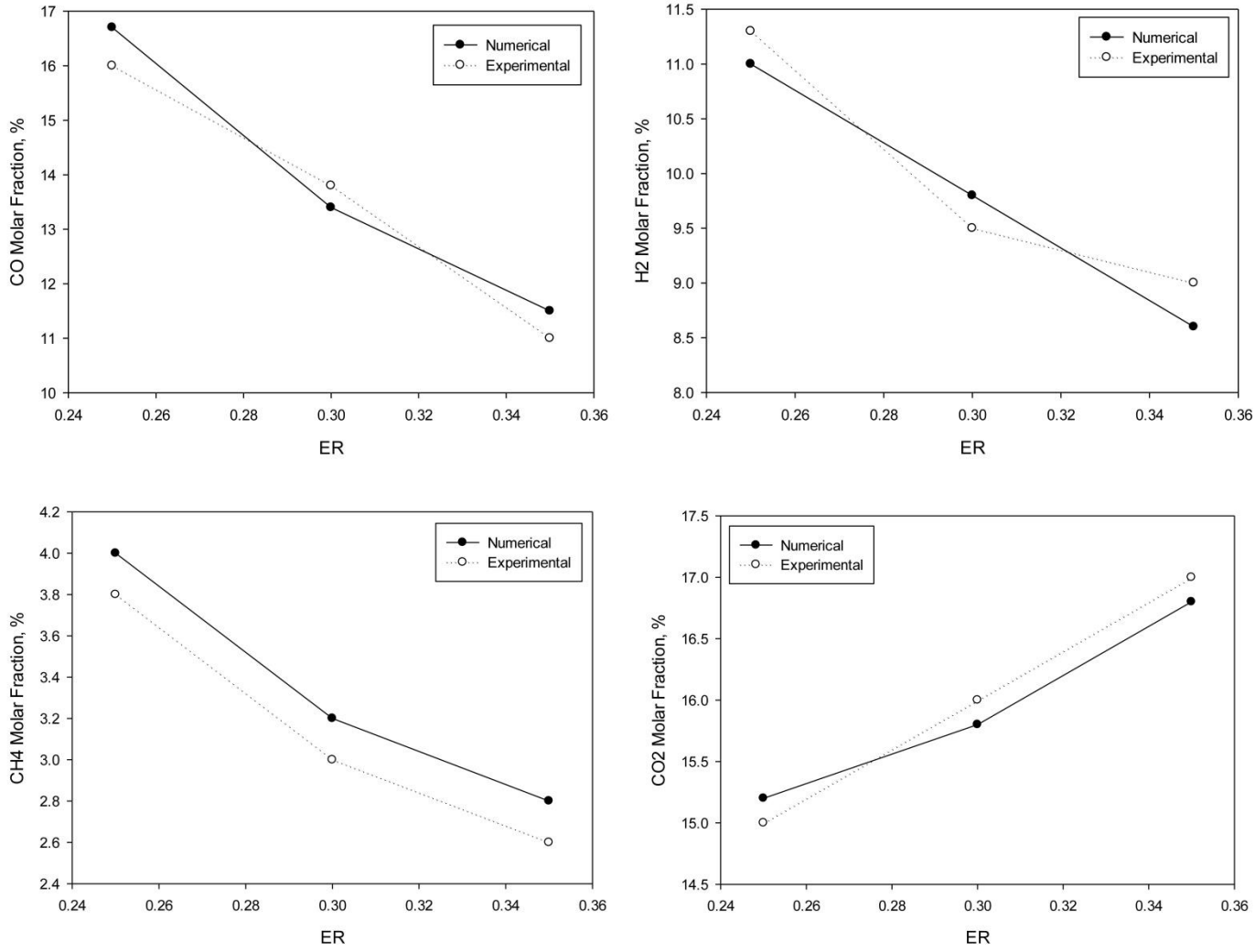

Fig. 4. Influence of ER on syngas composition revealed by both experimental and numerical results. (Runs 1, 2 and 3 from Table 9).

Table 10
Temperature distribution for experimental and numerical results (Runs 3, 4 and 5 from Table 9).

Runs	Type	T1	T2	T3
3	Numerical	755	570	430
	Experimental	749	548	414
4	Numerical	827	590	455
	Experimental	798	569	431
5	Numerical	886	654	490
	Experimental	851	612	455

gasification reactions. Even though no results for temperature distribution in a pilot scale up-flow atmospheric fluidized bed gasifier can be found in the literature, the findings from the very scarce sources available on the subject show consistency [35,36].

Overprediction in the temperature profile can be caused by considering the particle phase as continuum, leading to calculation errors for mass and energy transfers between phases, which was also found in the literature [37].

4.1. Air-O_2 mixture

Using air and O_2 mixtures (also known as O_2-enriched air) can be of great economic benefit over pure O_2 due to the fact that commercial air separators are much cheaper compared to distillation units [7].

Most of the research on O_2 influence on the gasification process, including some of the previous studies conducted by our team [20,29,38], focuses on O_2-enriched air [7,39–41]. While a very important parameter to study, the O_2 content in an air mixture can sometimes be misleading due to N_2 dilution and the effects of small variations on biomass admission in the syngas composition going unnoticed, hence our decision to study both O_2 content and ER for the same conditions and in greater depth. O_2 content was studied from 21% up to 40% in enriched air, and this range end value was chosen according to what is currently being used in commercial air separators based on membrane technologies.

Fig. 5 depicts the influence of O_2 content and ER on final syngas composition, respectively.

From observation of the above figures it is clear that increasing O_2 content promotes the formation of combustible gases, while increasing ER produces the opposite effect. Despite widely in accordance with the current literature [39–41], some studies contradict our results [42,43] which can be attributed to the way O_2 is introduced to the reactor. In fact, simply increasing the air flow also increases ER and O_2 content while using an air separator to increase O_2 content will cause the N_2 flow entering the reactor to

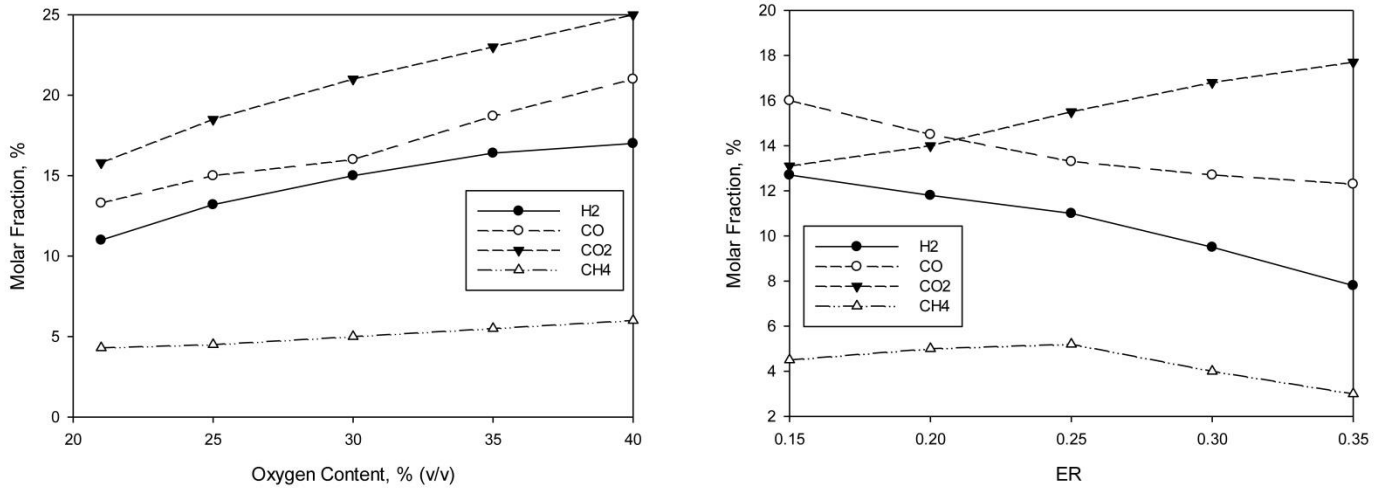

Fig. 5. Influence of a) oxygen content and b) ER on syngas composition (Operating conditions: Run 3 from Table 9).

decrease. However similar, both experiments lead to very different results and are behind the discrepancies found in the literature.

Rising O_2 content leads to an increase in all present species mainly due to the reduced dilution effect from N_2. Actually, increasing O_2 concentration in the air mixture decreases the N_2 entering the reactor, resulting in a syngas with less and less N_2. On the other hand, increasing ER by raising the air flow rate causes more N_2 to enter the reactor, causing the produced gas to be more diluted in N_2 and a poorer gas.

CH_4 content rises with that of O_2 mainly due to drop in N_2, even though a decrease would be expected due to CH_4 decomposition and to the enhancement of steam reactions at higher temperatures [40].

Regarding CO_2 content, it is obvious that increasing both O_2 content and ER will lead to a syngas richer in CO_2, which is due to the increase in O_2 in the reactor promoting combustion reactions that lead to CO_2 formation [39]. It is also clear that O_2 content has greater influence on CO_2 levels than ER, seeing that more CO and H_2 are available for oxidation and, therefore, more CO_2 is produced [39,40].

The fact that CO and H_2 content decrease with ER can be explained by a shorter residence time, seeing that, as air flow rate increases, it is no longer sufficient for CO and H_2 formation reactions to occur. In the same fashion, an increase in O_2 content will further promote combustion reactions (that also consume CO and H_2 to produce CO_2), since O_2 is more reactive to carbon than steam or CO_2 [39]. Higher levels of O_2 promote CO enrichment while lower ones favor H_2 content instead, which can be attributed to higher temperatures mainly promoting both Boudouard and reverse water-gas reactions, leading to higher levels of CO, while lower temperatures favor the primary water-gas and steam- CH_4 reforming reactions that, in turn, lead to higher H_2 levels.

As illustrated in Fig. 6, O_2 content and ER have great influence on gasification temperature.

Both O_2 content and ER lead to higher gasification temperatures, although O_2 has a greater impact. As they rise, oxidization reactions become more active, since more O_2 is available, causing more energy to be released. Compared to ER, more energy is released as O_2 content increases since there is less N_2 to absorb heat, a behavior consistent with [40].

In order to properly understand the influence of ER and O_2 content, cold gas efficiency (CGE) was investigated. CGE is defined by the following equation:

$$CGE = \frac{gas\ yield \times LHV\ of\ produced\ gas}{biomass\ yield \times LHV\ of\ Biomass}$$

Fig. 7 illustrates the influence of O_2 content and ER on cold gas efficiency, respectively.

A rise in O_2 content leads to an increase in CGE, whereas reducing the N_2 content in the gasifying agent mixture will inevitably encourage that of other syngas components, namely those responsible for determining gas quality through the low heating value (LHV), which directly influences CGE [44]. Moreover, increasing the O_2 content boosts residence time, which in turn promotes gasification reactions and carbon conversion, leading to higher gas yield [45].

Regarding the influence of ER in the CGE, 2 opposing phenomena are known to simultaneously occur: on one hand, LHV decreases due to the rising N_2 content in the syngas final composition and combustible gases (CO and H_2) being consumed through combustion; on the other hand, gas yield increases with ER due to an increase in temperature [44]. As depicted in Fig. 7b, a maximum CGE value was found for around ER = 0.25, which could be caused by tar cracking, known to cause a minor increase in the concentration of light hydrocarbons for ER of somewhere between 0.20 and 0.0–25 Even a slight increase in light hydrocarbon concentration can lead to a significant rise on syngas LHV, since they have much higher calorific values than either CO or H_2. This is consistent with other studies that found maximum efficiencies for ER near 0.25 [42,46] and means that too low of an equivalent ratio leads to poor gasification, despite high ER leading to a highly N_2-dilute syngas.

4.2. Air-steam mixture

Although gasification with O_2 -enriched air can produce a much higher quality gas, the high costs associated with its implementation still render the process viability in large facilities uncertain [8], and while steam gasification can produce a gas rich in H_2 at substantially lower cost than O_2 gasification, due to a lower reactivity, it is necessary to supply heat from an external source [9].

Several studies have therefore been conducted using air-steam gasification, since partial combustion of biomass using a hypostoichiometric amount of air releases the necessary energy for the steam reactions to occur [7,42].

Fig. 8 illustrates syngas composition for an air-steam mixture

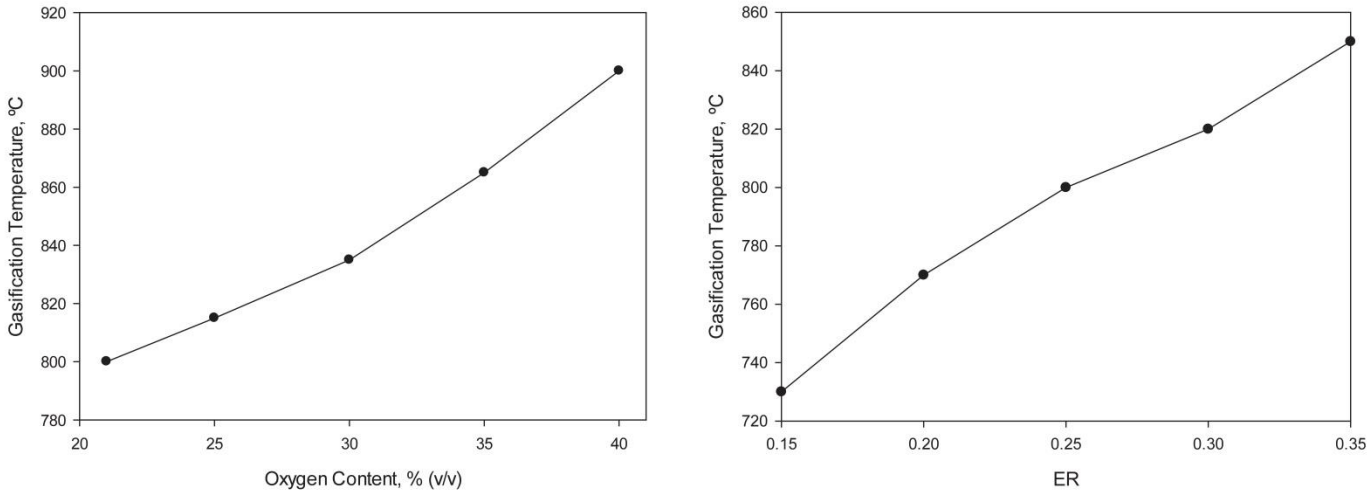

Fig. 6. Influence of a) oxygen content and b) ER on gasification temperature (Operating conditions: Run 3 from Table 9).

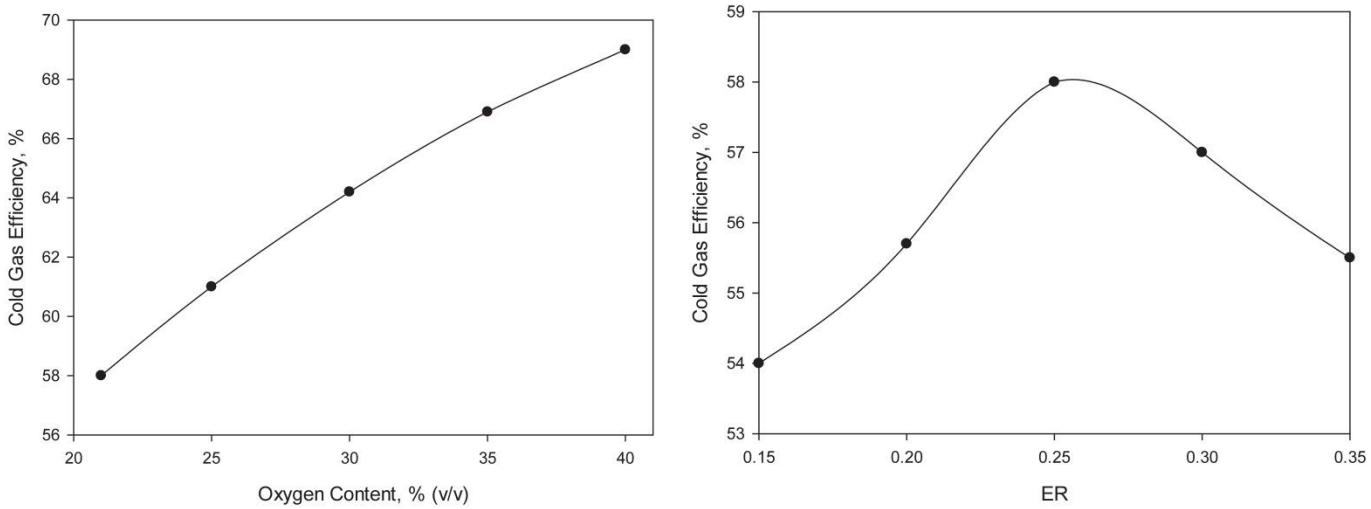

Fig. 7. Influence of a) O_2 content and b) ER on CGE (Operating conditions: Run 3 from Table 9).

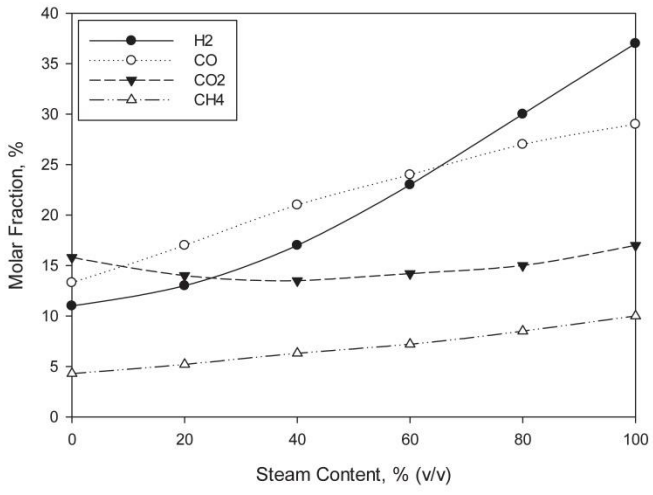

Fig. 8. Influence of steam content on syngas composition (dry base) (Operating conditions: Run 3 from Table 9).

with steam content ranging from 0% (air gasification) to 100% (pure steam gasification).

According to the results obtained, an increase in steam content has a positive effect on gas quality, partially due to the decrease of N_2. At the same time, with less air and a higher steam feeding rate, gasification reactions are favored over combustion ones [47].

H_2 and CO fractions rise, although CO to a lesser degree than H_2, especially for higher steam content, due to the promotion of the water-gas shift reaction over partial combustion and Boudouard reaction for higher steam flow rates [48]. An increase in CH_4 content relates to the decrease in oxidation of volatile matter, which is not balanced out by the consumption of CH_4 in the reforming reactions. These reactions have lower rates than oxidation ones but are most favored by low temperatures. CO_2 content displays a minimum fraction of near 40% mostly because combustion and water-shift reactions (which promote CO_2 production) and the Boudouard reaction (which promotes CO_2 consumption) cancel each other out. Results are consistent with current literature [47,49].

Nowadays, virtually all the available research presents results in dry base, meaning that the water conversion is not taken into account, and while studying results in dry base is crucial to better

predict the production of combustible gases, considering water conversion is just as important. Steam can be separated from syngas by condensation and recycled, although it requires re-heating, which entails considerable energy consumption and higher associated costs and causes the thermic efficiency of the process to be extremely low due to the low numbers in steam conversion. In fact, some authors [50] consider this to be the major downside of steam gasification and is yet to be answered.

It was thus decided to study the influence of SBR on syngas composition in wet base.

Fig. 9 shows the influence of SBR on syngas composition with regards to the steam content in the latter. In the range of 0–0.5, a considerable amount of the steam introduced into the reactor is consumed and for ratios lower than 0.1, there was actually not enough steam to react with biomass and so steam reactions did not reach equilibrium. Similar results were obtained by Hofbauer and Rauch [51]. Increasing SBR will mostly favor char and tar steam reforming and the water-gas shift reaction, which in turn will lead to an increase in CO_2 and H_2 content. In fact, according to Hernández et al. [47], for higher levels of steam, the water-gas shift reaction will dominate over the Boudouard one, and CO will be consumed to produce CO_2 and H_2.

Despite the increase in steam flow rate leading to a more calorific gas (due to the boost in H_2 and CH_4 content), a point is reached where a steam surplus no longer significantly increases the combustible gases content, but instead leads to a progressively higher steam fraction in the final syngas composition. Furthermore, the performed calculations for SBR = 2, found steam content to already be over 50%, and even though no results relating SBR to syngas composition in wet base were found in the literature, there is some relevant data that supports these findings. According to Barisano et al. [49], for ER = 0.21 and SBR = 0.4, steam content in syngas composition is around 40–50%, and Both Gil et al. [52] and Puchner et al. [53] found that, for SBR higher than 1, syngas composition has more than 60% steam that did not react. As expected, this phenomenon has a very significant impact on gasification efficiency, as illustrated in Fig. 10.

Fig. 10 shows a maximum for CGE at around SBR = 1, which is consistent with findings of other researchers [47]. There are two main opposing trends occurring: on one hand, LHV rises due to an increase in H_2 and CH_4 content; on the other, gas yield decreases due to a drop in temperature. In fact, SBR has a negative influence on gasification temperature, leading to less carbon conversion and therefore lower gas yield [54]. On top of that, for SBR higher than 1, additional steam will only increase its content on the final syngas composition without further reacting with biomass.

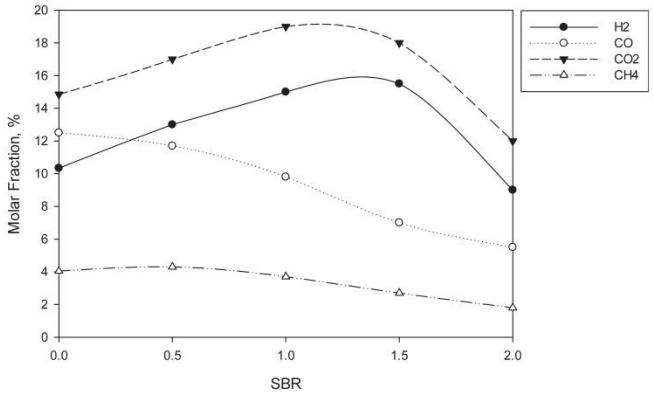

Fig. 9. Influence of SBR on syngas composition (wet base) (Operating conditions: Run 3 from Table 9).

Both air and steam flow rate need to be properly adjusted seeing that the former should be sufficient so that the temperature will significantly drop, thus contributing to endothermic reactions, and the latter should not exceed optimal flow so as not to shift the steam reforming and water-gas reactions backwards, consuming CO and H_2 to produce CO_2 and H_2O [55]. Overall, SBR higher than 1.5 is not recommended and the most promising range is between 0.5 and 1.

4.3. Air-carbon dioxide mixture

Even though steam gasification presents several advantages over air gasification, there are still some associated setbacks, such as the consumption of H_2O, which is an increasingly scarcer resource, whereas CO_2 gasification consumes an unwanted end product of various industrial processes. Moreover, this method can be used to process hundreds of millions of tons of CO_2 every year [11].

Since CO_2 gasification depends on highly endothermic reactions such as the Boudouard one, its application relies on the availability of an additional heat source, which can be direct, by introducing pure O_2 into the reactor and allowing oxidation reactions to provide the necessary heat, or indirect, by preforming combustion externally, using either biomass or syngas [56].

Fig. 11 depicts syngas composition for an air-CO_2 mixture with a CO_2 content ranging from 0% (air gasification) to 100% (pure CO_2 gasification).

From 0 to 40%, both CO_2 and CO molar fractions increase while that of H_2 decreases, seeing that a rise in CO_2 content and high temperature promote reverse water-gas shift and Boudouard reactions [11,28,56]. In fact, according to Butterman and Castaldi [11], the Boudouard is regarded as the main reaction in CO_2 gasification. Beyond 40% there is a clear change in behavior since that, by increasing CO_2 content in the gasifying agent mixture, one also decreases the air flow and therefore less exothermic reactions occur, causing the gasification temperature to considerably decrease. It is safe to assume that when CO_2 content is over 40%, the available oxygen is not enough to maintain the temperature necessary to promote said reactions. Also, according to the scarce literature on CO_2 gasification, in a very CO_2-rich environment, the water-gas shift reaction actually consumes CO and steam at the expense of H_2 and CO_2 [28]. Noticeable CO_2 content does not appear to have great influence on CH_4 content other than reducing O_2 availability and impairing complete and partial oxidation, which results in less CH_4 consumption. However, for very high CO_2 levels, very low temperatures actually decrease the pyrolysis rate, which is for the most part responsible for CH_4 formation. At the best of our knowledge and for the time being, literature concerning the influence of CO_2 on the gasifying mixture is very lacking, but in agreement with our findings [28].

Going from air to CO_2 gasification, the final gas composition will be almost absent of N_2 and mostly constituted by steam and CO_2, which can be captured and recycled in the process.

Direct gasification using air is thus a weaker choice as it produces very poor syngas due to the extremely high N_2 content, which dramatically decreases LHV and, in turn, CGE.

In order to study CO_2 addition in depth, the influence of CDBR on syngas composition, in N_2 free base and excluding H_2O and CO_2 content, was investigated.

Results illustrated in Fig. 12 are very different from the previously presented. To begin with, by increasing CDBR, one also increases the O_2 amount and, therefore temperature increases, contrary to previous study. With rising temperature both Boudouard and reverse watergas shift reactions are favored, leading to higher CO formation and H_2 consumption. CH_4 content decreases

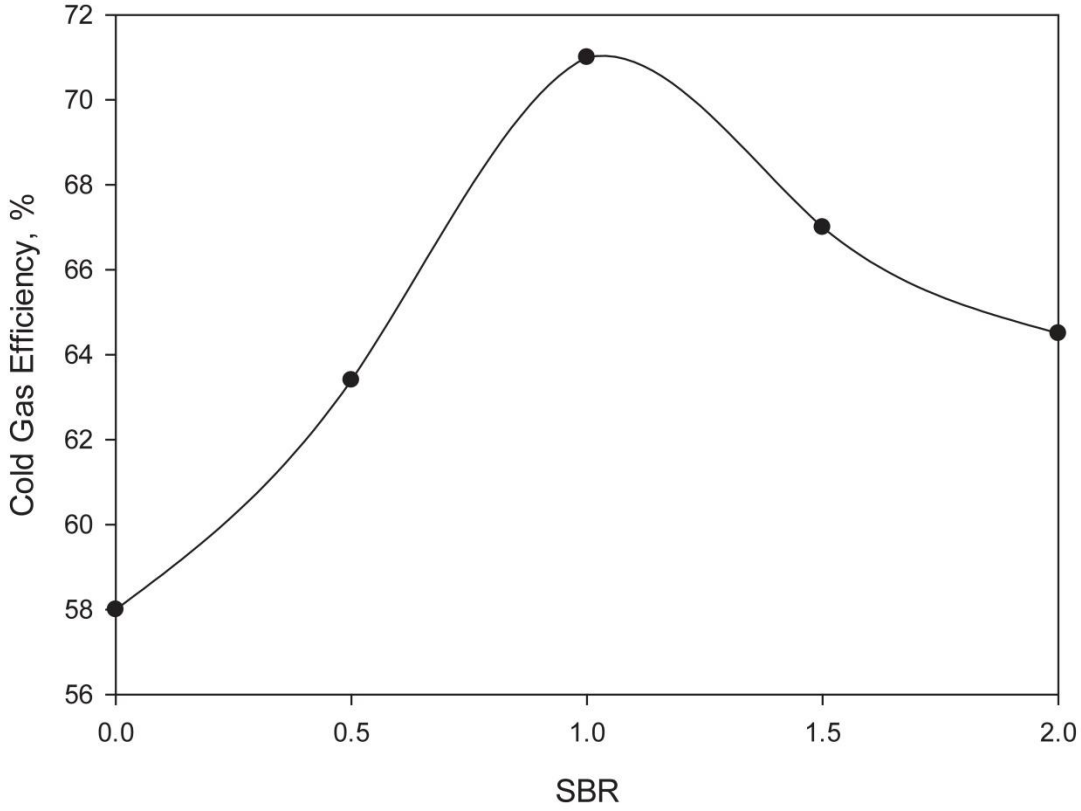

Fig. 10. Influence of SBR on CGE (Operating conditions: Run 3 from Table 9).

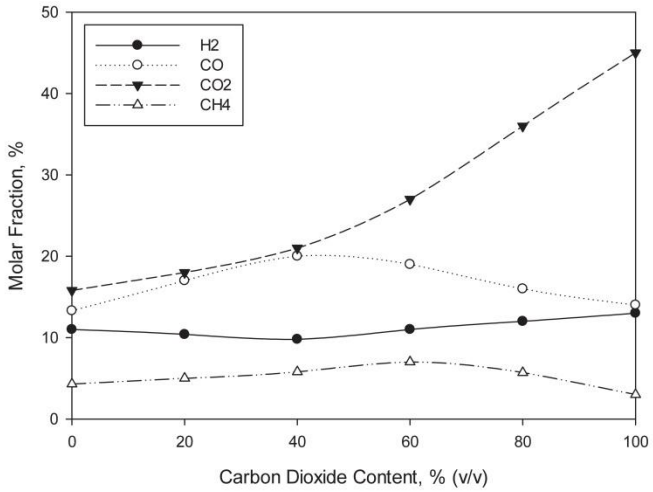

Fig. 11. Influence of carbon dioxide content on syngas composition (dry base) (Operating conditions: Run 3 from Table 9).

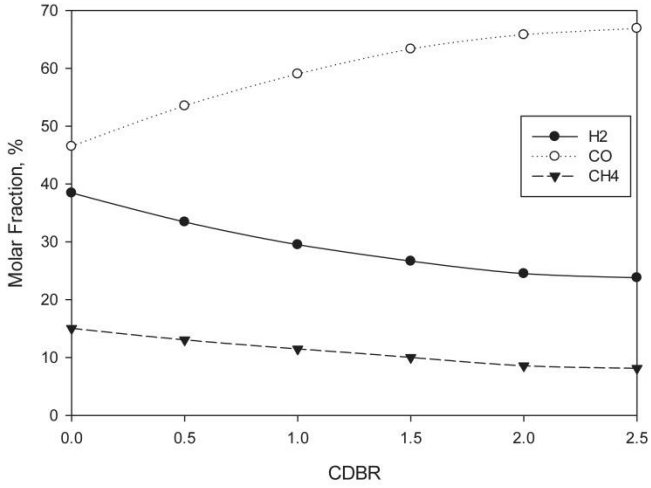

Fig. 12. Influence of CDBR on syngas composition (inert free base and excluding H_2O and CO_2) (Operating conditions: Run 3 from Table 9).

due to being consumed in the CH_4 reforming process to produce CO and H_2 and, on top of that, for high CO_2 concentrations, the Boudouard reaction is favored over the CH_4 formation one [56].

For CDBR over 2, results appear to reach an asymptotic value, which may be attributed to extremely high CO_2 atmospheres. A preliminary assumption can be made stating that high CO_2 atmospheres will reverse CO_2 consumption reactions, promoting the production of different components.

Although there are no results in the literature for such wide ranges of values to compare to, the few studies that present smaller ranges appear to be in agreement with the obtained results [11,28,29].

Finally, CGE was investigated in order to assess the influence of CO_2 addition on the efficiency of the gasification process.

Results from Fig. 13 show that CDBR has a positive influence over CGE and, contrary to what happens with ER and SBR, does not present a maximum efficiency value for the studied range, which is due to the increase of both syngas LHV and yield with rising CO_2 flow rate. Increasing CO_2 content (as well as air flow rate) leads to higher temperatures and promotes both Boudouard and reverse

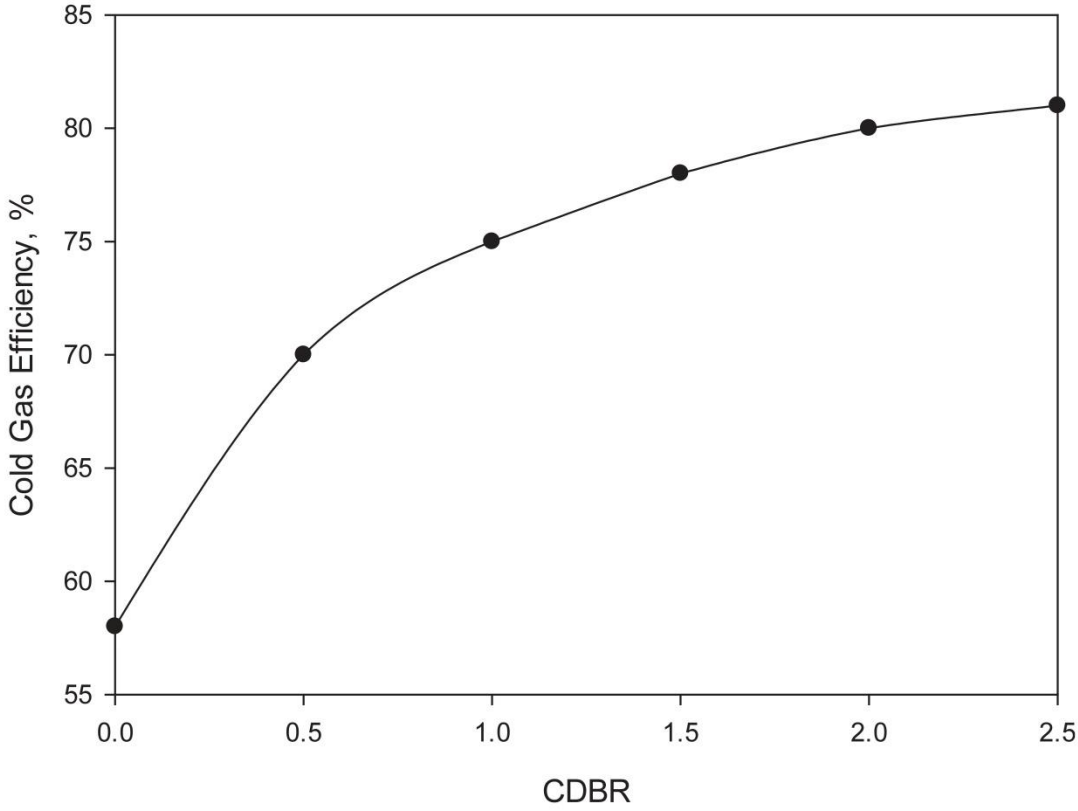

Fig. 13. Influence of CDBR on CGE (Operating conditions: Run 3 from Table 9).

water-gas shift reactions, which in turn increases LHV. The relationship between gas yield and CO_2 addition is yet to be addressed in the literature but it is safe to assume that an increase in temperature and carbon conversion are responsible for the increase in gas yield with CO_2.

Even though CGE can give a good indication on the gasification performance, it is crucial that other ratios and quality indices are also investigated, mainly because CGE does not take heat requirements or the sensible heat of the produced gas into consideration [57].

5. Conclusions

This study was motivated by the lack of data on mixtures of different gasifying agents in pilot scale conditions. In this work, mixtures of air with O_2, steam and CO_2 were studied with resort to a previously validated numerical model and the results were confirmed using a pilot scale plant.

For the mixture enriched with O_2, both ER and O_2 content were studied, showing a distinct behavior and; as for the air-steam mixture, results were presented in wet and dry basis and CGE presented a maximum for SBR = 1; last but not least, for the air-CO_2 mixture, the influence of CO_2 content as well as the CO_2/biomass ratio were investigated and results show promising trends.

A comparison between mixtures was also performed, and the air-steam mixture exhibited the highest H_2 content while the air-CO_2 one displayed the highest CO content, achieving the highest temperature within the reactor. All three mixtures led to an increase in LHV when compared to just air but the mixture enriched with O_2 displayed the lowest CGE while the air-CO_2 mixture exhibited the highest.

Ar-O_2 mixtures are recommended for power generation and can be used for catalyst-based FT synthesis and particularly for the production of specific chemicals such as urea, methanol and acetic acid, whereas air-steam can be used for numerous applications, such as H_2 production, synthetic fuels via the FT process and SOFC, among others.

Acknowledgements

We would like to express our gratitude to the Portuguese Foundation for Science and Technology (FCT) for the support to the grant SFRH/BD/86068/2012 and to project IF01772.

References

[1] K. Dutta, A. Daverey, J. Lin, Evolution retrospective for alternative fuels: first to fourth generation, Renew. Energy 69 (2014) 114–122.
[2] http://www.rtcc.org/2015/02/16/kyoto-protocol-10-years-of-the-worlds-first-climate-change-treaty/. Last access, 31 January 2017.
[3] E. Dogan, F. Seker, Determinants of CO_2 emissions in the European Union: the role of renewable and non-renewable energy, Renew. Energy 94 (2016) 429–439.
[4] http://ec.europa.eu/eurostat/statisticsexplained/index.php/Renewable_energy_statistics Last access, 31 January 2017.
[5] A.V. Bridgwater, A.J. Toft, J.G. Brammer, A techno-economic comparison of power production by biomass fast pyrolysis with gasification and combustion, Renew. Sust. Energ Rev. 6 (2002) 181–248.
[6] K. Jana, S. De, Biomass integrated gasification combined cogeneration with or without CO_2 capture – a comparative thermodynamic study, Renew. Energy 72 (2014) 243–252.
[7] V. Silva, A. Rouboa, Combining a 2-D multiphase CFD model with a response surface methodology to optimize the gasification of Portuguese biomasses,

Energ Convers. Manag. 99 (2015) 28–40.
[8] K. Maniatis, Progress in biomass gasification: an overview, in: A.V. Bridgwater (Ed.), Progress in Thermochemical Biomass Conversion, Blackwell Science, London, 2001, pp. 1–31.
[9] M. Hamad, A. Radwan, D. Heggo, T. Moustafa, Hydrogen rich gas production from catalytic gasification of biomass, Renew. Energy 85 (2016) 1290–1300.
[10] L. Wang, C. Weller, D. Jones, M. Hanna, Contemporary issues in thermal gasification of biomass and its application to electricity and fuel production, Biomass Bioenerg. 32 (2008) 573–581.
[11] H. Butterman, M. Castaldi, CO2 as a carbon neutral fuel source via enhanced Biomass Gasification, Environ. Sci. Technol. 43 (2009) 9030–9037.
[12] P. Parthasarathy, S. Narayanan, Hydrogen production from steam gasification of biomass: influence of process parameters on hydrogen yield – a review, Renew. Energ 66 (2014) 570–579.
[13] http://www.biofuelstp.eu/biofuels-legislation.html, Last access 31 January 2017.
[14] P. Basu, Biomass Gasification and Pyrolysis: Practical Design and Theory, Elsevier, 2010, p. 499.
[15] G. Xue, M. Kwapinska, A. Horvat, W. Kwapinski, Rabou, S. Dooley, K. Czajka, J. Leahy, Gasification of torrefied Miscanthus giganteus in an air-blown bubbling fluidized bed gasifier, Bioresour. Technol. 159 (2014) 397–403.
[16] Bilandzija N, Jurisic V, Voca N, Leto J, Matin A, Sito S, Krick T. Combustion properties of Miscanthus x giganteus biomass e Optimization of harvest time. J. Energy Inst.. (In Press).
[17] S. Ergun, Fluid flow through packed columns, Chem. Eng. Prog. 48 (1952) 89–94.
[18] D. Geldart, Types of gas fluidization, Powder Technol. 7 (1973) 285–292.
[19] V. Silva, E. Monteiro, N. Couto, P. Brito, A. Rouboa, Analysis of syngas quality from Portuguese biomasses: an experimental and numerical study, Energ Fuel 28 (2014) 5766–5777.
[20] N. Couto, V. Silva, A. Rouboa, Assessment on steam gasification of municipal solid waste against biomass substrates, Energ Convers. Manag. 124 (2016) 92–103.
[21] N. Couto, C. Silva Bispo, A. Rouboa, From laboratorial to pilot fluidized bed reactors: analysis of the scale-up phenomenon, Energ Convers. Manag. 119 (2016) 177–186.
[22] M. Syamlal, T.J. Rogers, MFIX Documentation, in: Theory Guide, vol. 1, National Technical Information Service, Springfield, VA, 1993. DOE/METC-9411004, NTIS/DE9400087.
[23] C. Lun, S.B. Savage, D. Jeffrey, N. Chepurniy, Kinetic theories for granular flow: inelastic particles in couette flow and slightly inelastic particles in a general flow field, J. Fluid Mech. 140 (1984) 223–256.
[24] B.E. Launder, D.B. Spalding, Lectures in Mathematical Models of Turbulence, Academic Press, London, England, 1972.
[25] J.A. Ruiz, M.C. Juárez, M.P. Morales, P. Muñoz, M.A. Mendívil, Biomass gasification for electricity generation: review of current technology barriers, Renew. Sust. Energ Rev. 18 (2013) 174–183.
[26] M.A. Field, Rate of combustion of size-graded fractions of char from a low rank coal between 1200K-2000K, Combust. Flame 13 (1969) 237–252.
[27] L. Garcia, M.L. Salvador, J. Arauzo, R. Bilbao, CO_2 as a gasifying agent for gas production from pine sawdust at low temperatures using a Ni/Al coprecipitated catalyst, Fuel Process Technol. 69 (2001) 157–174.
[28] Y. Cheng, Z. Thow, C. Wang, Biomass gasification with CO_2 in a fluidized bed, Powder Technol. 296 (2016) 87–101.
[29] V. Silva, A. Rouboa, Optimizing the gasification operating conditions of forest residues by coupling a two-stage equilibrium model with a response surface methodology, Fuel Process Technol. 122 (2014) 163–169.
[30] M. Dogru, A. Midilli, C. Howarth, Gasification of sewage sludge using a throated downdraft gasifier and uncertainty analysis, Fuel Process Technol. 75 (2002) 55–82.
[31] N. Couto, V. Silva, E. Monteiro, A. Rouboa, Assessment of municipal solid wastes gasification in a semi-industrial gasifier using syngas quality indices, Energy 93 (2015) 864–873.
[32] F. Pinto, R.N. André, C. Carolino, M. Miranda, P. Abelha, D. Direito, N. Perdikaris, I. Boukis, Effect of using natural minerals and biomass wastes blends, Fuel 117 (2014) 1034–1044.
[33] M. Niu, Y. Huang, B. Jin, X. Wang, Simulation of syngas production from municipal solid waste gasification in a bubbling fluidized bed using aspen plus, Ind. Eng. Chem. Res. 52 (2013) 14768–14775.
[34] I. Narváez, A. Orío, M.P. Aznar, J. Corella, Biomass gasification with air in an atmospheric bubbling fluidized bed. Effects of six operational variables on the quality of the produced raw gas, Ind. Eng. Chem. Res. 35 (1996) 2110–2120.
[35] Y. Kim, C. Yang, B. Kim, K. Kim, J. Lee, J. Moon, W. Yang, T. Yu, U. Lee, Air-blown gasification of woody biomass in a bubbling fluidized bed gasifier, Appl. Energ 112 (2013) 414–420.
[36] H. Liu, A. Elkamel, A. Lohi, M. Biglari, Computational fluid dynamics modeling of biomass gasification in circulating fluidized-bed reactor using the Eulerian-Eulerian Approach, Ind. Eng. Chem. Res. 52 (2013) 18162–18174.
[37] M. Oevermaan, S. Gerber, F. Behrendt, Euler-lagrange/DEM simulation of wood gasification in a bubbling fluidized bed reactor, Particuology 7 (2009) 307–316.
[38] V. Silva, A. Rouboa, Using a two-stage equilibrium model to simulate oxygen air enriched gasification of pine biomass residues, Fuel Process Technol. 109 (2013) 111–117.
[39] C. Huynh, S. Kong, Performance characteristics of a pilot-scale biomass gasifier using oxygen enriched air and steam, Fuel 103 (2013) 987–996.
[40] Z. Wang, T. He, J. Qin, J. Wu, J. Li, Z. Zi, G. Liu, G. Wu, L. Sun, Gasification of biomass with oxygen enriched air in a pilot scale two-stage gasifier, Fuel 150 (2015) 86–393.
[41] S. Thanapal, K. Annamalai, J. Sweeten, G. Gordillo, Fixed bed gasification of dairy biomass with enriched air mixture, Appl. Energ 97 (2012) 525–531.
[42] P.M. Lv, Z. Xiong, J. Chang, C.Z. Wu, Y. Chen, J.X. Zhu, An experimental study on biomass air-steam gasification in a fluidized bed, Bioresour. Technol. 95 (2004) 95–101.
[43] S. Turn, C. Kinoshita, Z. Zhang, D. Ishimura, J. Zhou, An experimental investigation of hydrogen production from biomass gasification, Int. J. Hydrogen Energ 23 (1998) 641–648.
[44] Q. Miao, J. Zhu, S. Barghi, C. Wu, X. Yin, Z. Zhou, Modeling biomass gasification in circulating fluidized beds: model sensitivity analysis, Int. J. Energy Power 2 (2013) 57–63.
[45] J.J. Manyà, J.L. Sánchez, J. Ábrego, A. Gonzalo, J. Arauzo, Influence of gas residence time and air ratio on the air gasification of dried sewage sludge in a bubbling fluidised bed, Fuel 85 (2006) 2027–2033.
[46] Y. Wang, K. Yoshikawa, T. Namioka, Y. Hashimoto, Performance optimization of two-staged gasification system for woody biomass, Fuel Process Technol. 88 (2007) 243–250.
[47] J.J. Hernández, G. Aranda, J. Barba, J.M. Mendoza, Effect of steam content in the air-steam flow on biomass entrained flow gasification, Fuel Process Technol. 99 (2012) 43–55.
[48] T. Song, J. Wu, L. Shen, J. Xiao, Experimental investigation on hydrogen production from biomass gasification in interconnected fluidized beds, Biomass Bioenerg. 36 (2012) 258–267.
[49] D. Barisano, G. Canneto, F. Nanna, E. Alvino, G. Pinto, A. Villone, M. Carnevale, V. Valerio, Steam/oxygen biomass gasification at pilot scale in an internally circulating bubbling fluidized bed reactor, Fuel Process Technol. 141 (1) (January 2016) 74–81.
[50] J. Corella, J. Toledo, G. Molina, Biomass gasification with pure steam in fluidized bed: 12 variables that affect the effectiveness of the biomass gasifier, Int. J. Oil Gas. Coal T 1 (2008) 194–207.
[51] H. Hofbauer, R. Rauch, Stoichiometric water consumption of steam gasification by the FICFB – gasification process, in: Progress in Thermochemical Biomass Conversion, Innsbruck, September 2000, pp. 199–208.
[52] J. Gil, M.P. Aznar, M.A. Caballero, E. Francés, J. Corella, Biomass gasification in fluidized bed at pilot scale with steam-oxygen mixtures. Product distribution for very different operating conditions, Energ Fuel 11 (1997) 1109–1118.
[53] B. Puchner, E. Höfberger, R. Rauch, H. Hofbauer, Biomass gasification with a CO2 absorptive bed material to produce a hydrogen rich gas, in: L. Sjunnesson, J.E. Carrasco, P. Helm, A. Grassi (Eds.), Proceedings of the 14th European Conference on Biomass for Energy Industry and Climate Protection, Paris, France, 17–21 October, ETA-Florence, Florence, Italy, 2005, ISBN 88-89407-07-7, pp. 631–634.
[54] B. Acharya, A. Dutta, P. Basu, An investigation into steam gasification of biomass for hydrogen enriched gas production in presence of CaO, Int. J. Hydrogen Energ 35 (2010) 1582–1589.
[55] C. Franco, F. Pinto, I. Gulyurtlu, I. Cabrita, The study of reactions influencing the biomass steam gasification process, Fuel 82 (2003) 835–842.
[56] P. Chaiwatanodom, S. Vivanpatarakij, S. Assabumrungrat, Thermodynamic analysis of biomass gasification with CO2 recycle for synthesis production, Appl. Energ 114 (2014) 10–17.
[57] T. Renganathan, M. Yadav, S. Pushpavanam, R. Voolapalli, Y. Cho, CO2 utilization for gasification of carbonaceous feedstocks: a thermodynamic analysis, Chem. Eng. Sci. 83 (2012) 159–170.

Paper IV

Multi-stage optimization in a pilot scale gasification plant

V. Silva, N. Couto, D. Eusébio, A. Rouboa, P. Brito, J. Cardoso, M. Trninic

International Journal of Hydrogen Energy 42 (2017) 23878-23890

INTERNATIONAL JOURNAL OF HYDROGEN ENERGY 42 (2017) 23878–23890

Available online at www.sciencedirect.com

ScienceDirect

journal homepage: www.elsevier.com/locate/he

Multi-stage optimization in a pilot scale gasification plant

Valter Silva [a,b,*], Nuno Couto [b], D. Eusébio [a], Abel Rouboa [b,c], P. Brito [a], J. Cardoso [a], M. Trninic [d]

[a] Polytechnic Institute of Portalegre, Portugal
[b] INEGI-FEUP, Faculty of Engineering, University of Porto, Porto, Portugal
[c] University of Trás-os-Montes and Alto Douro, Vila Real, Portugal
[d] Belgrad University, Department for Process Engineering and Environment, Serbia

ARTICLE INFO

Article history:
Received 20 November 2016
Received in revised form
22 April 2017
Accepted 27 April 2017
Available online 17 May 2017

Keywords:
Computer fluid dynamics
Pilot scale gasification plant
Design of experiments
Response surface method
Robust conditions
Six sigma

ABSTRACT

A 2-D multiphase CFD model was coupled with advanced statistical methods to find the best operating conditions to maximize a set of selected responses that characterize the normal operation of a pilot scale fluidized bed gasifier running Municipal Solid Waste. After using CFD simulations to compute 7 responses at 27 different operating conditions, a single response optimization based on the response surface method was carried out to identify the best operating conditions. Then, the desirability concept was advantageously used to proceed with a multiple optimization where all the responses were targeted under normal industrial conditions. The operating conditions that set the optimized responses not always coincide with the most stable process. To target both optimized and robust conditions a multiple optimization combining the response surface and the propagation of error methods were employed. Finally, the tolerance intervals were reduced to increase the process Cpk and six sigma standards about 20%. New measures to further increase the process performance were identified and the transmitted variation to the response from input factors was computed.

Introduction

According to Eurostat's latest reports, municipal waste (MW) generated in the EU-27 reached 239 million tons in 2014, representing a 5% decrease from the previous decade [1]. Portugal followed EU's trend with each Portuguese citizen producing 453 kg (almost 5% below the EU-27 average) [1]. Even with all the efforts led by government institutions to improve the Portuguese MSW management system, most of the produced wastes are still being sent to landfills [2]. Recent efforts are being carried out to fund research projects based on new approaches to convert waste to energy, such as gasification or anaerobic digestion. Main results have suggested that gasification could be a valuable option to mitigate the MSW environmental impact in Portugal [2].

Gasification can be defined as the conversion of a solid waste to synthetic gas by the partial oxidation of the feedstock

* *Corresponding author*. Campus Politécnico, 10, 7300-555 Portalegre, Portugal. Fax: +351 245 301 593.
E-mail addresses: valter@fe.up.pt, valter.silva@ipportalegre.pt (V. Silva), nunodiniscouto@hotmail.com (N. Couto), daniela.fle@ipportalegre.pt (D. Eusébio), rouboa@utad.pt (A. Rouboa), pbrito@estgp.pt (P. Brito), joao.pedro.sousa.cardoso@ipportalegre.pt (J. Cardoso), mtrninic@mas.bg.ac.rs (M. Trninic).
http://dx.doi.org/10.1016/j.ijhydene.2017.04.261

below stoichiometric combustion conditions. The synthetic gas is generally called "producer gas" or syngas and contains mainly carbon monoxide and hydrogen. However, some undesired products can be also found such as tar, alkali metals, chloride and sulphide, among others [3]. Gasification presents several advantages over waste combustion, namely and among others [3]: a) effective response to increasingly environmental restrictive regulations; b) syngas can be used both in highly efficient internally-fired cycles but also to produce valuable products as chemicals and fuels; and c) flexible use on different operating conditions and reactors.

Meanwhile, some drawbacks require further investigation. Besides high operating and capital costs, the syngas generated from MSW gasification is unstable due to changes in the feedstock properties. Indeed, the high heterogeneous nature of MSW implies significant variations in syngas yield and quality [4]. These variations can be reduced by implementing strategies such as MSW pre-processing, where undesired components are removed before introducing the wastes inside the gasifier. Further improvements can also be found by blending MSW with other feedstocks with more favorable characteristics, like forestry residues [5]. Portugal has a major potential considering biomass resources, merely forestry and pruning residues can potential produce 13,800 GWh, about 13% of the total primary energy demand in Portugal [6]. Also, running the gasifier under certain operating conditions will allow reliable operation with stable and improved syngas generation.

Optimized operation conditions for complex systems can be attained by using advanced combinations of numerical and statistical methodologies such as design of experiments (DoE) and response surface methods (RSM) [7,8]. DoE deals with several factors where all of them are varied altogether, instead of one at a time [7]. The great advantage of implementing this strategy is its success to consider multiple interactions between the factors. Furthermore, it also significantly reduces the number of runs necessary to extract meaningful information from data. Few works are found in the literature devoted to the use of DoE and RSM to analyze and optimize the operating conditions in gasification related processes [9–13]. Carpenter et al. [9] performed a total of 22 statistically designed experimental conditions to study the effects of fluidized bed temperature, the temperature of the secondary thermal cracker, and steam-to-biomass ratio on the gasification of four feedstocks. The authors concluded that there were significant differences between the feedstocks studied in terms of light gases formed. Karimipour et al. [10] applied RSM to the fluidized bed gasification of lignite coal considering as input factors coal feed rate, coal particle size and steam/O_2 ratio and as responses the quality of syngas evaluated based on five indices including carbon conversion, H_2/CO ratio, CH_4/H_2 ratio, gas yield, and gasification efficiency. They were able to find the best operating conditions to achieve syngas with a desired quality for different applications. To assess the combined effects of the operating variables on high-pressure coal gasification, Fermoso et al. [11] used a face centered central composite design based on RSM. Results revealed the effects of interaction between the tested variables, which would not have been possible by a traditional method. Silva and Rouboa [12] combined a thermodynamical dual stage model with RSM to optimize both hydrogen generation and cold gas efficiency by using forest residues for gasification. By using the operational conditions and desirability functions they were able to find the optimal conditions to achieve considerable economical energy savings without reducing the hydrogen generation. Coetzer and Keyser [13] used the method of factorial experimental design on the input factors of interest from a full-scale test gasifier concerning the Sasol-Lurgi coal gasification process. They developed empirical models (by using RSM) able to fit experimental data under different data sets. They concluded that the factorial experimental design combined with response surface analysis could be applied to a full-scale production process.

Because experimental runs conducted on industrial gasification plants or even on pilot scale gasification plants are very expensive, predictable models able to simulate the syngas composition and other responses of interest are required.

Mathematical models are being employed to work around this exact problem. By allowing for a simplified representation of reality they provide the ability to better understand the physical and chemical mechanisms inside the reactor without major investments nor time consuming experiments [14–16]. Different modeling approaches have been used by different researchers depending on the degree of complexity they are willing to endure. Equilibrium models are a popular method since they provide a quick way to calculate the maximum yield of a desired product [17]. However, since they don't take hydrodynamics, transport process or reaction kinetics into account results sometimes lack meaningful information. These setbacks led to the development of kinetic models, being much more accurate but also computationally expensive [16]. Increase in computational power is gradually replacing empirical or semi-empirical models with Computational Fluid Dynamics (CFD) to study biomass and waste gasification. These models can provide crucial insights into the flow field inside the reactor and can lead to a better understanding and improved performance of the operation while indicating solutions to potential problems [6,14,15].

There are few reports on the literature combining advanced statistical strategies with predictive models applied to gasification processes to find the most efficient combination of process variables that might be used during normal operation. Even fewer reports are found considering strategies to ensure a sustainable gasifier operability and throughput with minimal variations on the syngas generation (robust process) [18–20]. Silva and Rouboa [20] coupled the results obtained from a 2-D Eulerian–Eulerian biomass gasification model developed under the CFD framework with RSM to find the best operating conditions to generate syngas for different applications. Later, they proceed to do a multiple optimization coupling each one of the studied responses with the minimization of the error propagation. The authors were able to find the operation conditions that guaranteed both the best response and minimal variations caused by input factors.

This paper presents an advanced strategy coupling the response surface and propagation of error methods to go

towards six sigma standards concerning the operation of a bubbling fluidized bed gasifier fed by municipal solid wastes. Due to high costs inherent to pilot scale gasification runs, a 2-D multiphase Eulerian–Eulerian model developed within the framework of the commercial CFD code Fluent was used [6]. The model was previously validated under experimental runs performed at a pilot scale gasification plant by using 3 different biomasses [6] and under experimental data provided from municipal solid waste gasification [4]. Based on previous experiments and data obtained by the CFD model, a full factorial design was selected to determine the best operating conditions for several syngas quality indices. Later a multi-stage optimization including the error propagation as a response to identify the operating conditions less sensitive to variations was conducted. Finally, the system capability was improved and best options were determined to move results towards six sigma standards.

Methodology

Experimental set-up

To study the effect of different operating conditions in syngas composition and yield, several tests were performed in a pilot scale gasification plant. The gasification plant is comprised by an up-flow fluidized bed gasifier with a maximum pellet feeding of 75 kg/h; a feeding system allowing biomass discharges into the reactor at variable and controllable speed; a gas cooling system consisting of two heat exchangers; a filtering system to remove ash and carbon black particles; a condenser where liquid condensates are removed by cooling the syngas to room temperature; and a gas chromatograph allowing the detection of the generated gasification species. The schematic of the up-flow fluidized bed gasifier is depicted in Fig. 1. This gasifier is a tubular reactor of 0.5 m in diameter and 4.15 m in height, internally coated with ceramic refractory materials and with a bed made of 70 kg of dolomite. Further details concerning the pilot scale gasification plant can be found in Ref. [6].

Municipal solid waste characterization

Described system was first used to analyze the gasification process of Portuguese biomass substrates and their potential for fossil fuel replacement. Recently, to counter the improper disposal of municipal waste in landfills the focus shifted from biomass to MSW.

MSW is heterogeneous in nature, so wastes are pre-treated accordingly to the Portuguese management system. A detailed report considering the Portuguese management system can be found in Ref. [2]. These pre-treatment procedures generate which is known by refused derived fuel (RDF), and is mainly composed by cellulosic materials, paper, wood wastes, and plastic residues with a mean diameter of 10 mm. Cellulose, hemicellulose, and lignin are the main components from cellulosic materials [21] and plastics consist of polyethylene, polystyrene and poly-vinyl chloride [22]. The remaining products from MSW follow other routes for valorization or elimination. Table 1 shows the chemical composition from

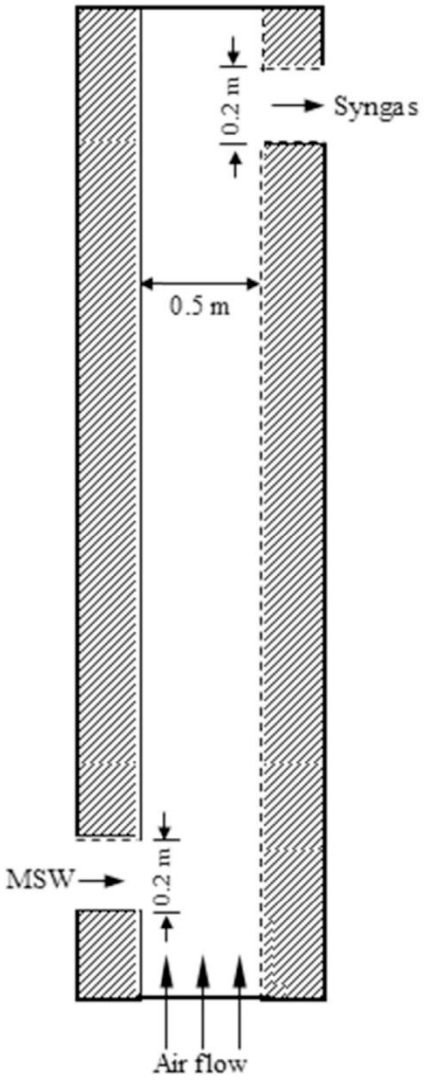

Fig. 1 – Gasifier schematics.

MSW treated in LIPOR. LIPOR is the entity responsible for the management, treatment and recovery of MSW in the Oporto metropolitan area. From Table 1, it can be observed that the ultimate analysis of LIPOR MSW considers cellulose, hemicelluloses, and lignin all in the same category. To compute their percentages for simulation purposes, data from cellulosic material composition was based on Onel's work [23]. Plastics composition is also depicted in Table 1. Data from Table 1 was used in the Fluent code.

Table 1 – Chemical composition of the MSW in Oporto in 2014.

Category	% weight	Chemical formula
Cellulosic material	85.42	*
Polyethylene	10.99	$(C_2H_4)_n$
Polyethylene terephthalate	2.02	$(C_{10}H_8O)_n$
Polypropylene	0.81	$(C_3H_6)_n$
Polystyrene	0.76	$(C_8H_8)_n$

Design of experiments applied to the MSW gasification process

In this study, temperature, air flowrate and MSW feeding rate will be used as numerical factors. These 3 factors will be combined at three levels providing a 3^k full factorial design with 27 runs. Experimental data gathered from a pilot scale gasification plant is expensive and time consuming, so the results for 27 runs were generated by a 2-D Eulerian–Eulerian multiphase CFD model [4]. The full factorial design takes all possible combinations of levels across the selected factors, as depicted in Table 2.

All the other remaining operating conditions were kept constant. The selected responses were H_2 generation, H_2/CO and CH_4/H_2 ratios, low heating value (LHV), carbon conversion, cold gas efficiency (CGE) and tar generation.

Mathematical model

The optimization procedure was carried out considering the results (steady-state condition) gathered by a two-dimensional numerical model previously developed by Couto et al. [4]. Major model guidelines are briefly discussed in the following lines.

Besides mass, energy and momentum balances for solid and gas phases, the model also describes the complex hydrodynamics phenomena by using the standard k–ε model implemented on the ANSYS FLUENT package. A fluidization velocity of 0.25 m/s was considered. An Eulerian–Eulerian approach was considered and equations for granular energy and granular energy dissipation were included following the work from Syamlal et al. [24].

The model also includes pyrolysis, homogeneous and heterogeneous reactions to account for the complex chemistry behind the MSW gasification process. Regarding pyrolysis, MSW is thermal decomposed into volatiles, char and tar. There are several approaches to describe this phenomenon and 3 main approaches are usually followed: a single step pyrolysis model, competing parallel pyrolysis and a pyrolysis model with generation of secondary tar. In this model we adopt a pyrolysis model with generation of secondary tar. MSW is mainly composed by cellulosic and plastic components, where the cellulosic material can be divided in cellulose, hemicellulose and lignin [4] and the plastics are mainly comprised by polyethylene, polystyrene, and polypropylene, among others. To distinguish the several components that comprise the MSW, the pyrolysis reactions of cellulosic and plastic groups are considered individually and following an Arrhenius kinetic expression.

Reactions for all the chemistry scheme are listed in Tables 3–5.

Mesh size was selected accordingly with hydrodynamic principles which suggest cells about 10–12 times larger than the particle size [27]. Also, a sensitivity analysis was performed considering minimal variations as a function of syngas composition, and velocity and turbulence profiles. Firstly, the convergence was obtained without implementing chemical reactions. Then, the chemical equations were included and the model was solved. Additional details can be found in Refs. [4,6].

Table 2 – 3^k full factorial design with corresponding factors and ranges.

Gasification run	MSW feeding rate (kg/h)	Air flowrate (m^3/h)	Gasification temperature (°C)
1	25	40	500
2			600
3			700
4		70	500
5			600
6			700
7		100	500
8			600
9			700
10	50	40	500
11			600
12			700
13		70	500
14			600
15			700
16		100	500
17			600
18			700
19	75	40	500
20			600
21			700
22		70	500
23			600
24			700
25		100	500
26			600
27			700

Discussion and results

CFD model validation

The developed model was effective to simulate the gasification behavior of different substrates under different sized

Table 3 – Kinetic data for the homogeneous reactions [25].

Reactions	A (ms^{-1} K^{-1})	E_a/R (K)
$CO + 0.5O_2 \rightarrow CO_2$	1.0×10^{15}	16000
$CO + H_2O \rightarrow CO_2 + H_2$	2780	1510
$CO + 3H_2 \leftrightarrow CH_4 + H_2O$	3.0×10^{5}	15042
$H_2 + 0.5O_2 \rightarrow H_2O$	5.159×10^{15}	3430
$CH_4 + 2O_2 \rightarrow CO_2 + 2H_2O$	3.552×10^{14}	15700

Table 4 – Kinetic data for the heterogeneous reactions [25].

Reactions	A (ms^{-1} K^{-1})	E_a/R (K)
$C + 0.5O_2 \rightarrow CO$	596	1800
$C + CO_2 \rightarrow 2CO$	2082.7	18036
$C + H_2O \rightarrow CO + H_2$	63.3	14051

Table 5 – Pyrolysis reactions and corresponding rates [26].

Reactions	Reaction rate
$Cellulose \rightarrow \alpha_1 volatiles + \alpha_2 TAR + \alpha_3 char$	$r_1 = A_i exp\left(\frac{-E_i}{T_s}\right)(1-a_i)^n$
$Hemicellulose \rightarrow \alpha_4 volatiles + \alpha_5 TAR + \alpha_6 char$	$r_2 = A_i exp\left(\frac{-E_i}{T_s}\right)(1-a_i)^n$
$Lignin \rightarrow \alpha_7 volatiles + \alpha_8 TAR + \alpha_9 char$	$r_3 = A_i exp\left(\frac{-E_i}{T_s}\right)(1-a_i)^n$
$Plastics \rightarrow \alpha_{10} volatiles + \alpha_{11} TAR + \alpha_{12} char$	$r_4 = \left[\sum_{i=1}^{n} A_i exp\left(\frac{-E_i}{RT}\right)\right]\rho_v$
$Primary\ TAR \rightarrow volatiles + Secondary\ TAR$	$r_5 = 9.55 \times 10^4 exp\left(\frac{-1.12\times10^4}{T_g}\right)\rho_{TAR1}$

reactors [4,6,28]. Indeed, minor deviations were found at a large set of operating conditions (error always lower than 20%). Firstly, the model was implemented to cope with several agro-industrial residues [6] and was then upgraded to deal with the peculiarities of municipal wastes [4]. Recently, the model was able to successfully predict the scale-up from a laboratorial reactor to the pilot scale plant [28]. Table 6 lists the relative errors between experimental and numerical results from several gas species at four experimental conditions gathered from a laboratorial reactor operating under MSW [4]. Further runs and corresponding validation can be found in the literature [4].

Results show that the model was able to effectively predict the syngas compositions trends in different operating conditions making it very useful to perform an optimizing study.

Empirical model validation

Guidelines from good statistical practices suggest that an empirical model should be kept as simple as possible. Additional terms should be only included if they would be able to explain variation beyond what's already accounted for [29]. A very expedite tool to select how far one should go on adding polynomial terms to the empirical model is the sequential model sum of squares (SMSS). SMSS provides the p-values for the model's term sources. Table 7 depicts the SMSS results for hydrogen generation. Similar analysis was carried out for all the other studied responses.

From Table 7, we can conclude that both linear (A, B and C) and quadratic (A^2, B^2 and C^2) terms can explain the process variation showing the smallest p-values. The table also depicts another statistical measure, the F value. Larger values of F imply more significant factors similarly to small p-values. When p-values are larger than 0.1 the terms are not by themselves considered as significant. The cubic terms are aliased so they should not be included. Quadratic model also includes linear and interaction terms (AB, BC, etc.), so this solution should be the one selected.

Table 6 – Experimental versus numerical data.

Run	1	2	3	4
Temperature (°C)	705	687	593	691
MSW admission (kg/h)	3	4	4	6
ER	0.4	0.3	0.3	0.2
Preheated air (°C)	352	352	307	352
Syngas fraction relative error (%)				
CO_2	3.95	8.97	4.04	4.17
H_2	7.86	6.90	9.63	7.41
N_2	6.88	2.51	2.07	4.18
CH_4	11.84	16.52	14.67	1.75
CO	3.60	6.92	5.33	2.94
C_2H_4	9.25	8.12	0.92	8.89

Table 7 – Sequential model sum of squares (hydrogen generation).

Source	Sum of squares	F value	p-value Prob > F
Mean vs total	1539.22		
Linear vs mean	586.25	466.92	<0.0001
2FI vs linear	3.72	4.2	0.0185
Quadratic vs 2FI	5.81	348.42	<0.0001
Cubic vs quadratic	0.073	4.85	0.0127
Residual	0.021		
Total	2135.09		

The development of the empirical model is based on Eulerian–Eulerian simulations under the CFD framework. Computer based simulations will always provide the same solution at certain operating conditions implying that the concept of replicates becomes meaningless. At these circumstances, the use of some statistical measures such as lack of fit do not bring any data of interest for analysis purpose.

However, measures such as R^2, R^2_{adj} and R^2_{pred} are still useful. The R^2 measures how well the model is able to fit correctly the experimental data or the computed based simulations as in the present case. The R^2 value can sometimes be misleading causing overfitting the data. The R^2_{adj} counteracts this overfitting giving a more reliable tool to evaluate the data fitting quality.

The R^2_{pred} measures how well the model is able to re-fit the data when one point is missing. When these measures are close enough a high quality fit is expected. Table 8 shows the result of these additional measures. From Table 8 R^2 presents the high value for the cubic model as expected. Indeed, adding additional terms will inflate the R^2 value. Also, the cubic model is aliased so it cannot be considered as a feasible option. Once again, the quadratic model stands out as the most valuable option with considerable high values for all the R^2 measures.

After selecting the empirical model and before applying it to generate the response surface, it is important to proceed to the analysis of variance (ANOVA) and confirm if all terms should be or not included. Myers and Montgomery [30] suggest that in response surface work it is customary to fit the full model. Anderson and Whitcomb [31] state that insignificant terms will not create much impact, so they could be excluded

Table 8 – Model summary statistics.

Source	R^2	R^2_{adj}	R^2_{pred}
Linear	0.9838	0.9817	0.9774
2FI	0.9901	0.9871	0.983
Quadratic	0.9998	0.9998	0.9996
Cubic	1	0.9999	0.9997

from the model. From Table 9, and following Anderson and Whitcomb suggestion, terms AB and A^2 were removed by using a backward reduction algorithm.

The final empirical model to predict the hydrogen generation and shown in coded form is as follows:

$$H_2 = 6.99 - 0.24A - 0.71B + 5.66C - 0.20AC - 0.52BC - 0.13B^2 + 0.97C^2 \quad (1)$$

The coded equation is useful for identifying the relative impact of the factors with their respective coefficients. Positive coefficients mean that increasing the factor leads to a response increase. By default, the high levels of the factors are coded as +1 and the low levels of the factors are coded as −1.

The last step to conclude about the model adequacy is to diagnose the residual for abnormalities. Basically, differences (residues) between experimental data and the computed model are analyzed to verify if the residuals are pure noise or if there are other reasons behind the residuals patterns. Fig. 2 depicts the normal probability as a function of internal studentized residuals. This kind of residuals means that none of the actual response data are deleted prior to calculating their deviation from the model prediction. The studentization is crucial for accurately estimating residuals because it adjusts for varying leverage in design points. When the residuals are normally distributed, they will fall in the red line. As it can be seen from Fig. 2, only minor deviations are found confirming the assumption of normality.

Also, a very helpful diagnostic can be found by plotting the residuals as a function of the predicted response. Fig. 3 displays a random scatter which again confirms the usefulness of the developed empirical model. Furthermore, this indicates that is not necessary to consider transforming the responses by using other mathematical functions such as log or square-root. The same procedure was followed considering the other responses. All of them presented minor deviations from normality and constancy of variance and can be accepted as suitable to describe the behavior of the corresponding responses in the experimental design space.

Single response optimization

When 3 factors (or more) are studied and it is impossible to depict all factors at once in a graph, it is always interesting to present the perturbation plot. Fig. 4 displays the effect of changing each one of the selected factors (MSW feeding rate (A), air flowrate (B), and gasification temperature (C)) on the hydrogen generation keeping all other operating conditions constant. The curvatures of each of the three factors from the center point dictate their significance. In this particular case,

Table 9 – ANOVA data.

Source	Sum of squares	F value	p-value Prob > F
Model	595.78	11911.5	<0.0001
A – MSW feeding rate	1	179.71	<0.0001
B – Air flowrate	8.95	1609.81	<0.0001
C – Temperature	576.3	103700	<0.0001
AB	0.016	2.9	0.1066
AC	0.47	84.94	<0.0001
BC	3.23	581.99	<0.0001
A^2	0.012	2.24	0.1528
B^2	0.11	19.03	0.0004
C^2	5.69	1023.98	<0.0001

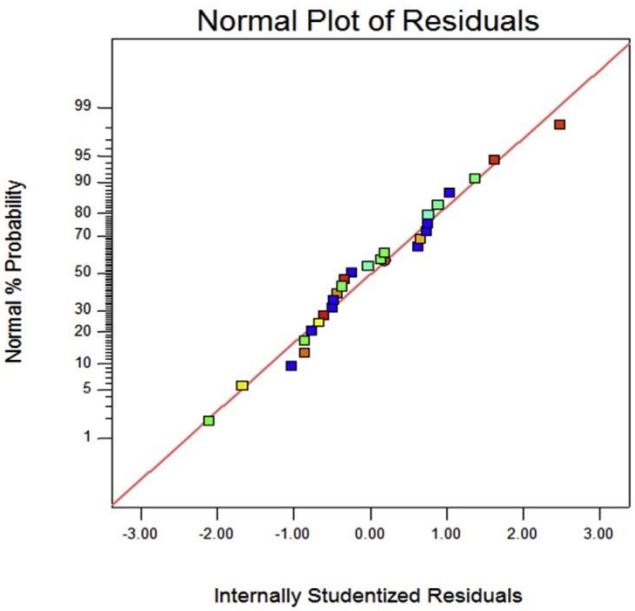

Fig. 2 – Normal plot of residuals. Dot colours are graded (from green to red) as the studied response value increases (green dots identify low values while red dots mean high values). (For interpretation of the references to colour in this figure legend, the reader is referred to the web version of this article.)

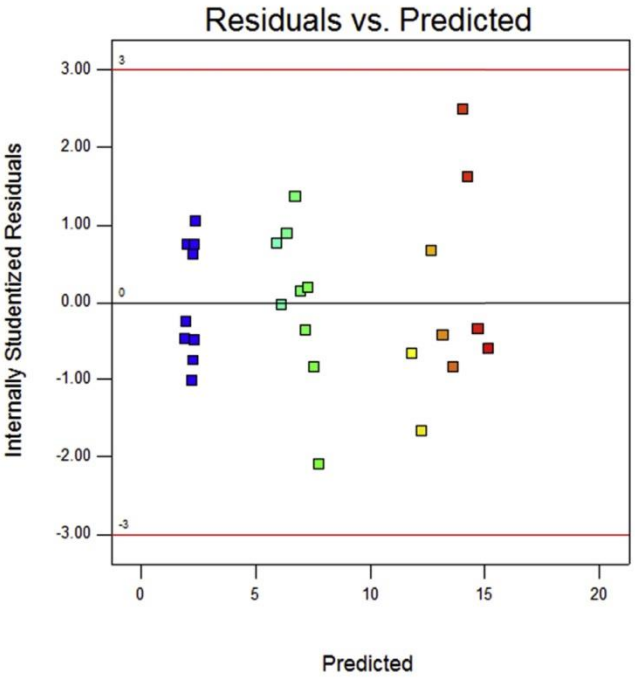

Fig. 3 – Residuals as a function of the predicted response.

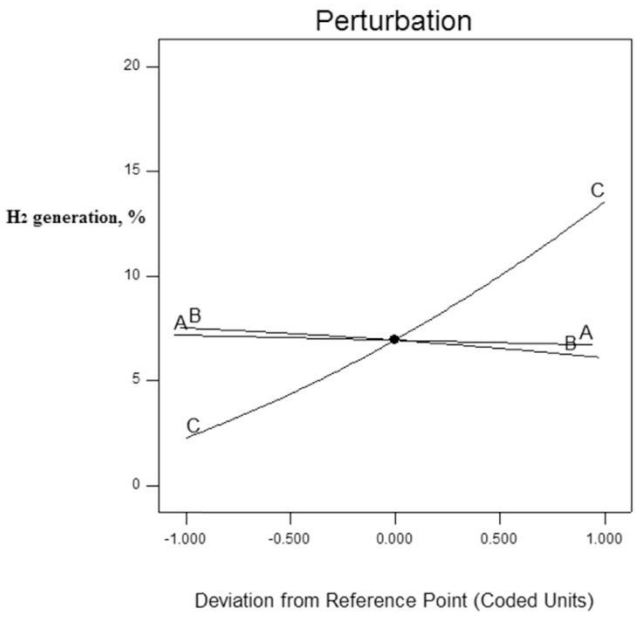

Fig. 4 – Perturbation plot for hydrogen generation. Coded units means that −1 is the response lower value, 0 the central value and +1 the higher value.

the sharp curvature of the gasification temperature (C) shows that the response "hydrogen molar fraction" is highly sensitive to this variable. On the other hand, the comparatively low curvatures from both MSW feeding rate (A) and air flowrate (B) shows less sensitivity of hydrogen production towards the change in these two factors. By using the perturbation plot as a departure point, the axis for contour or 3-D response surface plots can be easily defined keeping the analysis with the most interesting factors for the process.

Fig. 5 shows the response contour plots as a function of the most significant factors after running an optimization algorithm for a single response.

Fig. 5a shows how the studied factors affect hydrogen generation (MSW feeding rate was kept at a constant value of 25 kg/h). Once again, the selected factors to appear in the plot axis are in agreement with the perturbation plot, where large coefficients imply more significant factors. Investigated parameters appear to provoke opposite effects on hydrogen fraction; on one hand H_2 increased (over 6 times) when temperature was increased from 500 to 700 °C, while on the other hand H_2 decreased (around 16%) when air flowrate was increased from 40 to 100 m^3/h. Increase in air flowrate will mostly promote oxidizing reactions which explains why hydrogen fraction decreases since these reactions promote both CO_2 and H_2O at the expense of CO and H_2 [32]. Besides, since hydrogen generation reactions are mostly from endothermic nature, an increase in temperature will promote more hydrogen in the syngas mixture, in accordance with Le Chatelier's principle. The operating conditions able to maximize this particular response through the optimization procedure were about 700 °C and 40 m^3/h. Both the obtained maximum value as well as the overall trends are in agreement with available literature as well as previously attained experimental results [33–35].

In Fig. 5b H_2/CO ratio appears to be more sensible with air flowrate variation. Although an increase in air flowrate decreases both CO and H_2, the increase of steam inside the reactor strengthens the water-gas shift reaction encouraging CO consumption and H_2 generation. Furthermore, this steam surplus decreases bed temperature thus preventing CO formation [36]. Regarding the influence of gasification temperature on the H_2/CO ratio, it has a positive effect when temperature is first increased but that trend reverses once temperature reaches about 620 °C. Since hydrogen production reactions are mainly promoted at lower temperatures the ratio first presents a strong increase. However, since carbon monoxide is mainly promoted at higher temperatures the trend quickly reverses. This is consistent with available literature [37]. Optimal operating conditions to maximize this ratio were found at: MSW feeding rate = 75 kg/h; Air flowrate = 100 m^3/h; and temperature = 621 °C. Absolute values are extremely hard to validate since there are many parameters that greatly impact these ratios (reactor dimensions and feedstock properties, just to name a few) one cannot pinpoint experimental data from the current literature but the overall trends follow the obtained results [33,38].

Methane-to-hydrogen ratio appears to be highly dependent on the temperature variation, Fig. 5c. As temperature rises, endothermic reactions (mainly steam reforming and water-gas reactions) will be promoted leading to an increase in H_2 content at the expense of CH_4. Air flow rate has a much smaller effect on CH_4/H_2 ratio since it decreases both species similarly. These results are consistent with the current literature [39]. Near unity ratios were found in the 500 °C range (at a MSW feeding rate of 75 kg/h and an air flowrate of 40 m^3/h). While MSW isn't particularly known for high CH_4/H_2 ratios, at low temperatures pyrolysis has a predominant role in gasification leading to an overall higher ratio [40].

Fig. 5d highlights that gasification temperature has a positive influence on LHV while air flowrate has the exactly opposite effect. This is expected since the former promotes the formation of combustible gases (responsible for the syngas calorific value) while the latter prevents it. Overall calorific values for this particular waste are on the lower-hand (2–6 MJ/Nm^3) but within what is commonly found on the literature for MSW gasification using air as a gasifying agent (4–7 MJ/Nm^3) [3].

From Fig. 5e, it can be seen that both gasification temperature and air flowrate have a strong (positive) effect on carbon conversion (a value of MSW feeding rate = 27.5 kg/h was obtained at the maximum carbon conversion point). This can be explained with temperature favoring tar reforming leading to overall higher conversion [34]. Similarly, since oxidation reactions are exothermic (meaning they release energy into the reactor) leads to steam reforming reactions being promoted which in turn promotes carbon conversion [41]. The obtained values are also within the typical ranges for this kind of wastes [3].

Cold gas efficiency is mostly dictated by gas yield and syngas calorific value. While both gasification temperature and air flowrate promote gas yield (by enhancing reforming reactions) only temperature has a positive impact on the calorific value, thus explaining why parameters display opposed trends.

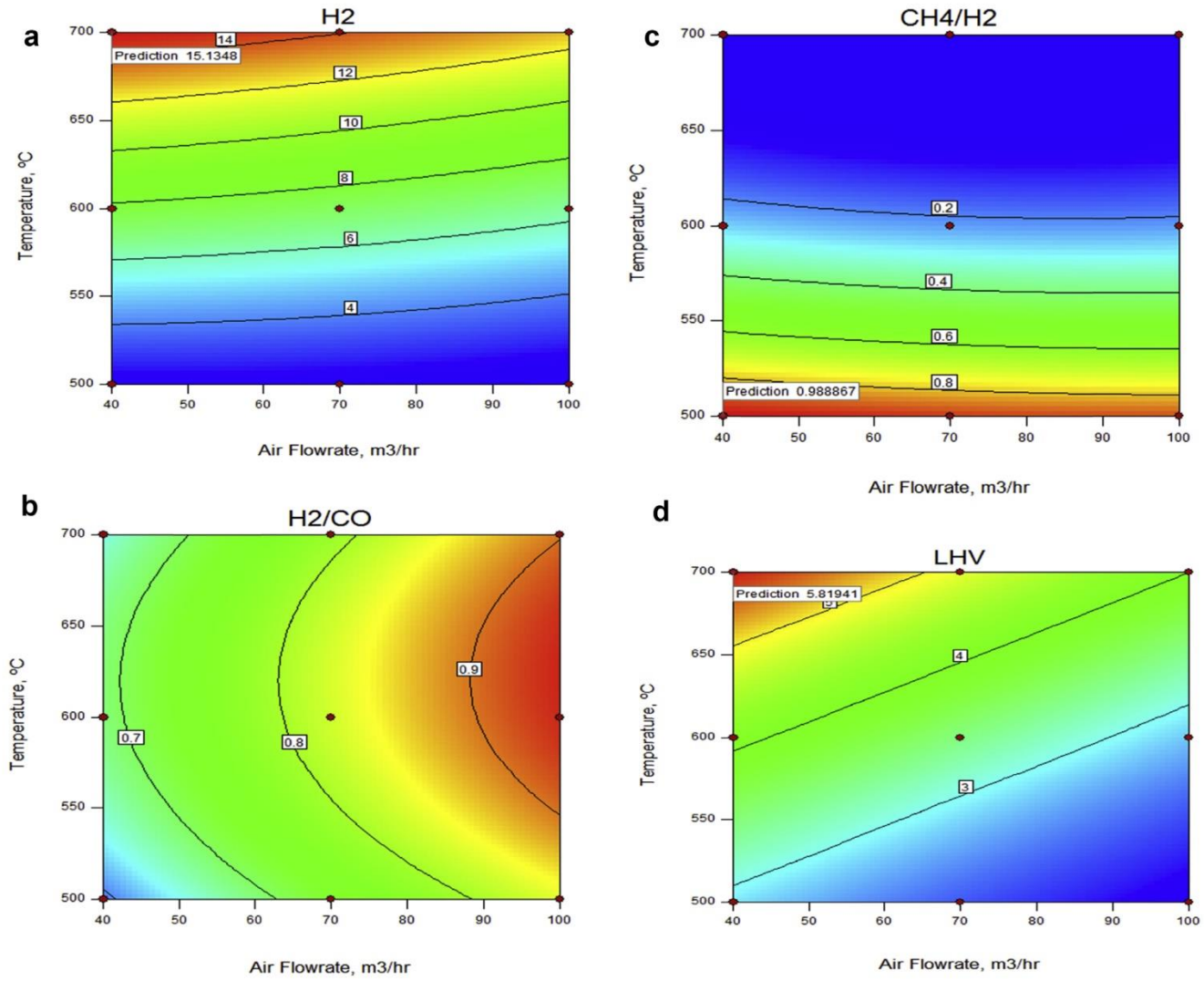

Fig. 5 – Contour response plots for a) H_2 generation; b) H_2/CO ratio; c) CH_4/H_2 ratio; d) LHV; e) Carbon conversion; f) Cold gas efficiency and g) tar generation.

Most commercial-size reactors found in the literature operating with MSW and using air or oxygen-enriched air as gasifying agent have a CGE of at least 50% and in some cases slightly exceeding 80% [3], which is consistent with the obtained results.

If one pays close attention to contour plots for carbon conversion and tar content (Fig. 5g) one will surely notice that they are the reverse of one another. This is to be expected since an increase in temperature (which both parameters lead to) enhances reforming reactions which in turn promotes carbon conversion which is known for improving tar decomposition. This is consistent with the available literature [33,34]. A minimal value of 8.1 g/Nm^3 was found at the highest values of temperature and air flowrate (MSW feeding rate = 25 kg/h).

Desirability function

So far, the previous analysis was performed considering a single response. However, an industrial environment requires the ability to lead with several restrictions and multiple goals. Sometimes, it is necessary to find a commitment between yields and energy savings or other responses of interest. To cope with several goals, one should combine all goals into a unique function, also known as an objective function. Derringer et al. [42] suggests the use of the desirability concept as a way to measure the success of combing multiple responses. Desirability can be computed as follows:

$$D = \left(\prod_{i=1}^{n} d_i \right)^{\frac{1}{n}} \quad (2)$$

where d_i is the desirability of each response and D is the overall desirability. D ranges from 0 to 1 (1 being the most desirable condition). Prior to computing desirability values, it is necessary to define the goals for each one of the selected responses (maximize, minimize, bounded between certain values or even equal to a fixed value) and also different weights in the case of some variables must be more important than others. Table 10 shows the goals for each one of the responses at different simulation scenarios. The imposed goals

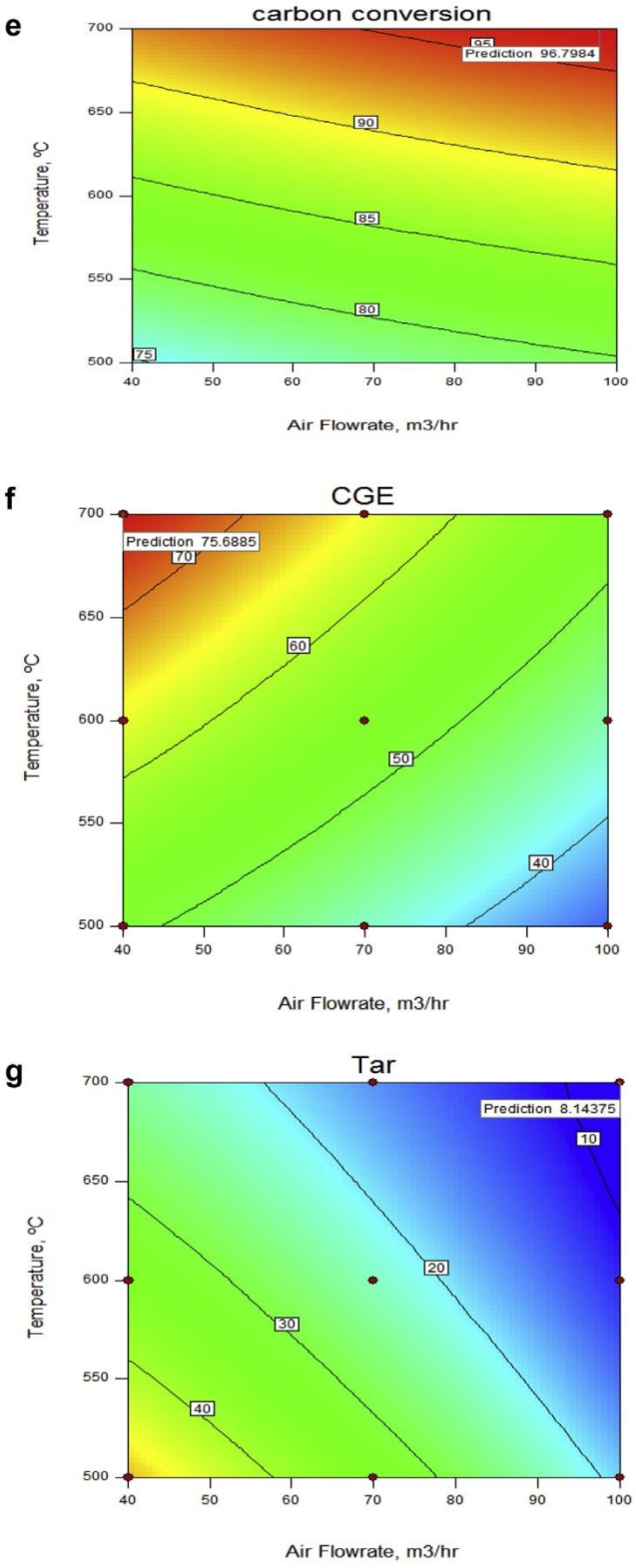

Fig. 5 – (*continued*).

are based in typical working responses at industrial conditions. Fig. 6 shows the optimal operating conditions and response values considering a complex study of 7 different responses. The purpose of this kind of methodology is quite obvious in an industrial environment. It is important to notice that the optimal operating conditions are now different from those found for single response optimization. Also, it is possible to tailor the required responses changing the input conditions.

Table 10 – Optimization scenarios based on different combined response targets.

Response	Optimization 1	Optimization 2
H_2, %	Maximize	Maximize
H_2/CO	Maximize	Maximize
CH_4/H_2	Minimize	Minimize
LHV, MJ/Nm^3	Maximize	4–7
Carbon conversion, %	Maximize	>90
Cold gas efficiency, %	Maximize	50–80
Tar, g/Nm^3	Minimize	<10

Robust operating conditions

When a single optimization is carried out it is possible to obtain the desired target (maximum, minimum or value within a range) at multiple points of operation. However, some of these points might set the process on a sharp peak of response. At these circumstances, one should select the operating conditions more robust to variation transmitted from input factors. These conditions can be found applying a mathematical tool named Propagation of error (POE). POE can be defined as the square root of the variance of the selected response. To proceed with POE, the standard deviation from each one of the studied input factors is needed. Data was obtained considering historical data from experiments gathered at the pilot scale gasification plant presented in "Section Experimental set-up". Standard deviations from the selected input factors can be found in Table 11.

Unfortunately, and in general, the setting of factors that meet the maximum of response are not at minimum POE. Once again, this problem (multi-optimization) can be overtaken taking advantage of using the desirability function where the response is maximized and POE is minimized. Fig. 7 shows the 3-D plot of hydrogen generation as a function of temperature and air flowrate a) at the optimal condition; b) combining the optimal and robust conditions.

From Fig. 7, it can be observed that combining the optimization procedure with robust conditions implies a decrease on hydrogen generation from 15% to about 9%. Also, the MSW feeding rate changes from 25 kg/h in Fig. 7a to 75 kg/h in Fig. 7b. Obviously, other results can be obtained considering different weights for each one of the studied responses. Also, considering that this approach is a numerical methodology it could be possible to attain similar results considering a different set of factors. This kind of information combined with acquired experience of operating a gasifier allows taking reliable and smart decisions considering a wide range of goals.

A similar approach was performed for the other responses of interest and is given in Table 12.

From Table 12, it can be observed that both carbon conversion and tar responses show the same set of operating conditions for single and combined optimization. This means that is possible to achieve the maximum performance of this response at the most stable operating conditions.

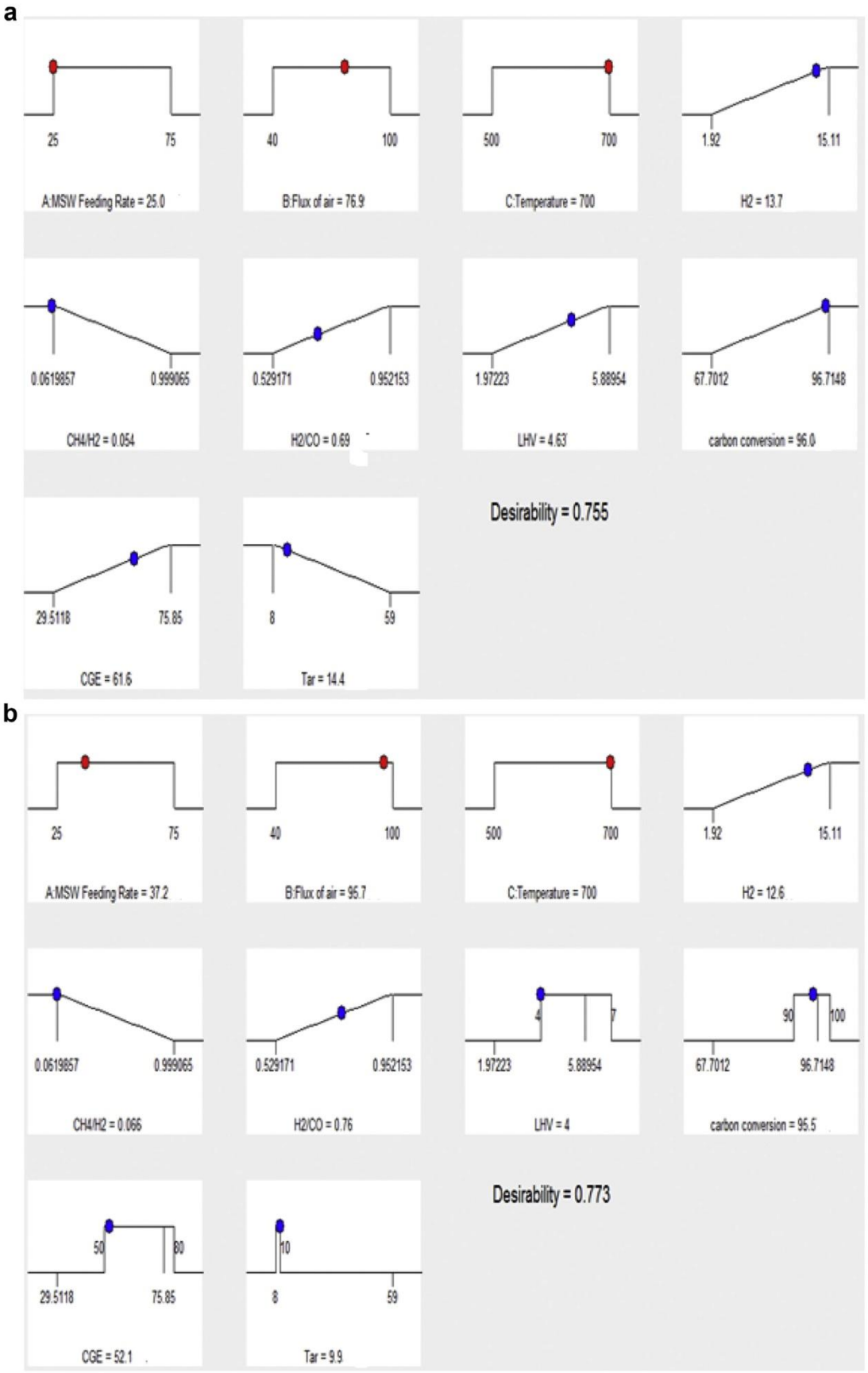

Fig. 6 – Optimal operating conditions and corresponding responses based on scenarios described in Table 9: a) optimization 1; and b) optimization 2.

Table 11 – Standard deviation for input factors.

Input factor	Standard deviation
MSW feeding rate, kg/h	8
Air flowrate, m^3/h	15
Temperature, C	5

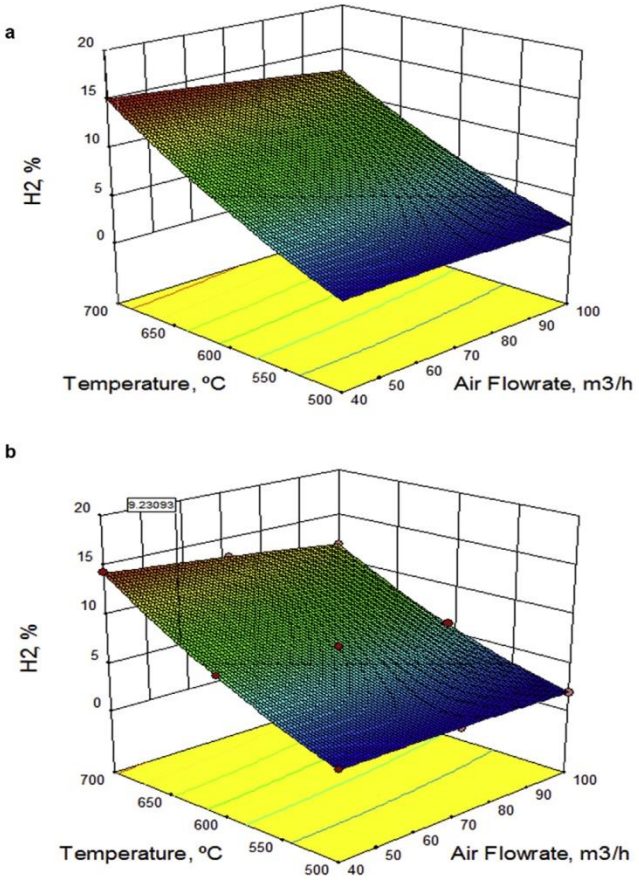

Fig. 7 – Hydrogen generation as a function of the temperature and air flowrate for a) single optimization; b) optimization combined with POE.

Improving the capability of the system towards six sigma standards

The tolerance intervals (95%) for hydrogen generation (combined optimization) are in the range 8.89–9.60. At industrial level, it is sometimes necessary to shorten these intervals and guarantee narrower boundaries and consequently less variation on the final syngas responses. We can assess and establish targets and tolerances for the selected responses by using a mathematical approach. To improve the system capability, Cpk, a mathematical model of the process is needed which can be obtained by the developed empirical model of the response surface method. Also, additional data from the design of experiments is needed: input factors, corresponding ranges and standard deviation and responses data. To end the process it is necessary to provide the response specifications. In this particular case, the new range will be 9–9.5. These new specifications narrow the former confidence/tolerance intervals obtained by coupling the selected response and corresponding POE. In such manner, the Cpk and 6 sigma level are increased about 20%. The new operating conditions are: MSW Feeding Rate = 72 kg/h; Air Flowrate = 40 m^3/h; Temperature = 622 °C.

At this level, the response interval can be accepted and assume that the response is satisfactory or decisions have to be taken to improve the process. Improvements can be attained: by reducing the standard deviation of the input factors with improved control devices and methods; by changing the intervals of the selected inputs or changing for different inputs; by changing the process design; by accepting the occurrence of some deviations; or then by refusing the opportunity to produce the syngas for certain applications that require minimal variation at this kind of response.

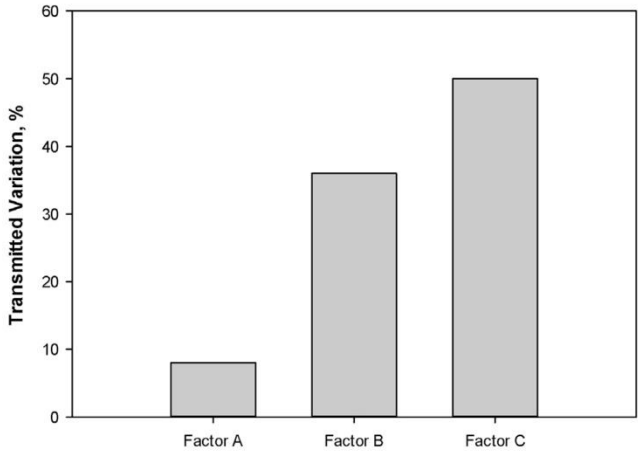

Fig. 8 – Transmitted variation to the response from input factors.

Table 12 – Combined optimization for single responses.

Response	Factors SO/SO + POE			Single optimization (SO)	SO + POE
	MSW feeding rate, kg/h	Air flowrate, m^3/h	Temperature, °C		
H_2/CO	75/25	100/100	621/610	0.94	0.80
CH_4/H_2	75/75	40/100	500/545	0.99	0.55
LHV, MJ/Nm^3	25/75	40/40	700/682	5.81	4.92
Carbon conversion, %	27.5/27.5	100/100	700/700	96.8	96.8
CGE, %	25/30	40/40	700/600	75.7	62.8
Tar, g/Nm^3	25/25	100/100	700/700	8.1	8.1

One possible solution is to control the inputs more effectively. Fig. 8 shows that the most variation transmitted to the response comes from the input factors B and C. Improving input factor A do not bring any advantage to the process, so our focus should be in input factors B and C. Some of the transmitted variation is also due to model development.

A similar approach can be followed for each single response or considering a combined optimization including all the responses.

Conclusions

A 3^k full factorial design with 27 runs generated by a 2-D Eulerian–Eulerian multiphase CFD model was used to proceed a single optimization based on the response surface method to target the best operating conditions for 7 different responses that quantitatively determine the gasifier performance. Using such approach, the best conditions for MSW Feeding Rate, Air Flowrate and Temperature were found. Also, it was possible to define the full behavior of these factors under the design space considering all the responses in a single and combined ways. A similar study was performed considering the normal response values in industrial environment and making use of the desirability function it was possible to get the best conditions that respect those targets. A procedure to combine both optimized and robust conditions was followed by combining response surface and propagation of error methods. In such manner, each response was obtained ensuring a stable syngas generation. Finally, and by using empirical equations from the response surface method combined with narrower specifications for each response was possible to improve the process Cpk and six sigma standards. One feasible solution to get further improvements suggests the standard deviation reduction by more restrictive control procedures on the input factors.

Acknowledgements

We would like to express our gratitude to the Portuguese Foundation for Science and Technology (FCT) for the support to the grant SFRH/BD/86068/2012 and the project IF01772.

REFERENCES

[1] http://ec.europa.eu/eurostat/statistics-explained/index.php/Municipal_waste_statistics, [Last accessed 13th October, 2016].
[2] Teixeira S, Monteiro E, Silva V, Rouboa A. Prospective application of municipal solid wastes for energy production in Portugal. Energ Policy 2014;71:159–68.
[3] Arena U. Process and technological aspects of municipal solid waste gasification. A review. Waste Manage 2012;32:625–39.
[4] Couto N, Silva V, Monteiro E, Rouboa A. Assessment of municipal solid wastes gasification in a semi-industrial gasifier using syngas quality indices. Energy 2015;93:864–73.
[5] Pinto F, André R, Carolino C, Miranda M, Abelha P, Direito D, et al. Gasification improvement of a poor quality solid recovered fuel (SRF). Effect of using natural minerals and biomass wastes blends. Fuel 2014:1034–44.
[6] Silva V, Couto N, Monteiro E, Brito P, Rouboa A. Analysis of syngas quality from Portuguese biomasses: an experimental and numerical study. Energ Fuel 2014;28:5766–77.
[7] Montgomery D. Design and analysis of experiments. 5th ed. John Wiley & Sons; 2001.
[8] Rostami M, Farzaneh V, Boujmehrani A, Mohammadji M, Baskhsabadi H. Optimizing the extraction process of sesame seed's oil using response surface method on the industrial scale. Ind Crop Prod 2014;58:160–5.
[9] Carpenter D, Bain R, Davis R, Dutta A, Feik C, Gaston K, et al. Pilot-scale gasification of Corn stover, switchgrass, wheat straw, and wood: 1. Parametric study and Comparison with literature. Ind Eng Chem Res 2010;49:1859–71.
[10] Karimipour S, Gerspacher R, Gupta R, Spiteri R. Study of factors affecting syngas quality and their interactions in fluidized bed gasification of lignite coal. Fuel 2013;103:308–20.
[11] Fermoso J, Gil M, Arias B, Plaza M, Pevida C, Pis J, et al. Application of response surface methodology to assess the combined effect of operating variables on high-pressure coal gasification for H_2-rich gas production. Int J Hydrogen Energy 2010;35:1191–204.
[12] Silva VB, Rouboa A. Optimizing the gasification operating conditions of forest residues by coupling a two-stage equilibrium model with a response surface methodology. Fuel Process Technol 2014;122:163–9.
[13] Coetzer R, Keyser M. Experimental design and statistical evaluation of a full-scale gasification project. Fuel Process Technol 2003;80:263–78.
[14] Liu H, Cattolica R, Seiser R. CFD studies on biomass gasification in a pilot-scale dual fluidized-bed system. Int J Hydrogen Energy 2016;41:11974–89.
[15] Xuan W, Guan Q, Zhang J. Kinetic model and CFD simulation for an entrained flow coal hydrogasifier and influence of structural parameters. Int J Hydrogen Energy 2016;41:20023–35.
[16] Manchasing C, Kuchonthara P, Chalermsinsuwan B, Piumsomboon P. Experiment and computational fluid dynamics simulation of in-depth system hydrodynamics in dual-bed gasifier. Int J Hydrogen Energy 2013;38:10417–30.
[17] Silva V, Rouboa A. Predicting the syngas hydrogen composition by using a dual stage equilibrium model. Int J Hydrogen Energy 2014;39:331–8.
[18] Hou J, Zhang J. Robust optimization of the efficient syngas fractions in entrained flow coal gasification using Taguchi method and response surface methodology. Int J Hydrogen Energy 2017;42:4908–21.
[19] Coetzer R, Keyser M. Robustness studies on coal gasification process variables. OriON 2004;20:89–108.
[20] Silva V, Rouboa A. Combining a 2-D multiphase CFD model with a Response Surface Methodology to optimize the gasification of Portuguese biomasses. Energ Convers Manage 2015;99:28–40.
[21] Xie J, Zhong W, Jin B, Shao Y, Liu H. Simulation on gasification of forestry residues in fluidized beds by Eulerian-Lagrangian approach. Bioresour Technol 2012;12:36–46.
[22] Scott D, Czernik S, Piskorz J, Radlein DSA. Fast pyrolysis of plastic wastes. Energ Fuel 1990;4:407–11.
[23] Onel O, Niziolek AM, Hasan MMF, Floudas CA. Municipal solid waste to liquid transportation fuels - part I:

mathematical modeling of a municipal solid waste gasifier. Comput Chem Eng 2014;71:636–47.
[24] Syamlal M, Rogers TJ. MFIX documentation. In: Theory guide, vol. 1. Springfield, VA: National Technical Information Service; 1993. DOE/METC-9411004, NTIS/DE9400087.
[25] Couto N, Monteiro E, Silva V, Rouboa A. Hydrogen-rich gas from gasification of Portuguese municipal solid wastes. Int J Hydrogen Energy 2016;41:10619–30.
[26] Couto N, Silva V, Rouboa A. Thermodynamic Evaluation of Portuguese municipal solid waste gasification. J Clean Prod 2016;139:622–35.
[27] Gelderbloom SJ, Gidaspow D, Lyczkowski RW. CFD simulations of bubbling/collapsing fluidized beds for three geldart groups. AIChE J 2003;49:844–58.
[28] Couto N, Silva V, Bispo C, Rouboa A. From laboratorial to pilot fluidized bed reactors: analysis of the scale-up phenomenon. Energ Convers Manage 2016;119:177–86.
[29] Anderson M, Whitcomb P. DOE simplified: practical tools for effective experimentation. 1st ed. Productivity Press; 2005.
[30] Myers R, Montgomery D. Response surface methodology. 2nd ed. New York: John Willey and Sons; 2002.
[31] Anderson M, Whitcomb P. RSM simplified – optimizing processes using response surface methods for design of experiments. 1st ed. Productivity Press; 2005.
[32] Niu M, Huang Y, Jin B, Wang X. Simulation of syngas production from municipal solid waste gasification in a bubbling fluidized bed using Aspen plus. Ind Eng Chem Res 2013;52:14768–75.
[33] Gonzalez JF, Roman S, Bragado D, Calderon M. Investigation on the reactions influencing biomass air and air/steam gasification for hydrogen production. Fuel Process Technol 2008;89:764–72.
[34] Kumar A, Eskridge K, Jones D, Hanna MA. Steam-air fluidized bed gasification of distillers grains: effects of steam to biomass ratio, equivalence ratio and gasification temperature. Bioresour Technol 2009;100:2062–8.
[35] Couto N, Silva V, Rouboa A. Municipal solid waste gasification in semi-industrial conditions using air-CO_2 mixtures. Energy 2016;104:42–52.
[36] Zhou H. Air and steam coal partial gasification in an atmospheric fluidized bed. Energy Fuel 2005;19:1619–23.
[37] Xiao J, Shen LH, Deng X, Wang ZM, Zhong XL. Study on characteristics of pressurized biomass gasification. Proc Chin Soc Electr Eng 2009;29:103–8.
[38] Gang X, Bao-sheng J, Zhao-ping Z, Yong C, Ming-jiang NI, Ke-fa C, et al. Experimental study on MSW gasification and melting technology. J Environ Sci 2007;19:1398–403.
[39] Narvaez I, Orio A, Aznar MP, Corella J. Biomass gasification with air in an atmospheric bubbling fluidized bed. Effect of six operational variables on the quality of the produced raw gas. Ind Eng Chem Res 1996;35:2110–20.
[40] Gomez-Barea A, Leckner B. Modeling of biomass gasification in fluidized bed. Prog Energy Combust Sci 2010;36:444–509.
[41] Wang J, Cheng G, You Y, Xiao B, Liu S, He P. Hydrogen-rich gas production by steam gasification of municipal solid waste (MSW) using NiO supported on modified dolomite. Int J Hydrogen Energy 2012;37:6503–10.
[42] Derringer G, Suich R. Simultaneous optimization of several variables. J Qual Technol 1980;12:214–9.

Paper V

Thermodynamic evaluation of Portuguese municipal solid waste gasification

N. Couto, V. Silva, A. Rouboa

Journal of Cleaner Production 139 (2016) 622-635

Journal of Cleaner Production 139 (2016) 622–635

Contents lists available at ScienceDirect

Journal of Cleaner Production

journal homepage: www.elsevier.com/locate/jclepro

Thermodynamic Evaluation of Portuguese municipal solid waste gasification

Nuno Dinis Couto [a], Valter Bruno Silva [a, *], Abel Rouboa [a, b, c]

[a] INEGI-FEUP, Faculty of Engineering, University of Porto, Porto, Portugal
[b] University of Trás-os-Montes and Alto Douro, Vila Real, Portugal
[c] MEAM Department, University of Pennsylvania, PA, 19020, Philadelphia, USA

ARTICLE INFO

Article history:
Received 24 February 2016
Received in revised form
3 August 2016
Accepted 18 August 2016
Available online 20 August 2016

Keywords:
Thermodynamic analysis
Portuguese municipal solid waste
Semi-industrial gasification plant
Cleaner syngas
CFD
Tar content

ABSTRACT

Through a massive population growth, waste management has become one of the main concerns of our time. In Portugal the growing volume of municipal solid waste has become a central problem for municipalities, due to lack of space and the high costs to solve it. Gasification has received a renewed interest in the municipal solid waste treatment since it limits dioxins formation, presents higher efficiency and requires less expensive gas cleaning equipment when compared to available methods gas. However, to make to process more appealing to both private sector and government institutions is necessary to overcome some concerns related to the process. To expedite the mainstream of this technology a first and second law analysis conducted on Portuguese municipal solid waste was carried out. The thermodynamic method was coupled with a previously developed numerical model. Said model was validated using data from a pilot scale plant. Both energy and exergy values were investigated in order to evaluate Portuguese municipal solid waste as an energy source. Optimal operating point was found at 900 °C for an equivalent ratio of 0.25. Tar content energy values decreased as high as 80% when temperature was increased to 900 °C. A comparison between several gasification efficiencies was investigated.

1. Introduction

According to the latest estimates provided by the United Nations Department of Economic and Social Affairs, Population Division, world population was 7.4 billion as of June 2016. The same report stated that world population is projected to reach the 8.5 billion mark by 2030 and 9.7 billion in 2050. At this rate, world population is likely to reach 11.2 billion in 2100, representing a 53% increase from today (United Nations et al., 2015).

In the past decade, due to this accelerated growth combined with high socio-economic development and rapid urbanization, municipal solid waste (MSW), one of the most important by-products of an urban lifestyle, has doubled, and is expected to triple in the next decade (Soltani et al., 2016). The treatment of these residues is quite expensive and often represents the single largest budgetary item of a city. Furthermore, incorrect management also entails large land use. According to Zhang et al. (2010a), approximately 28,500 tons of MSW can occupy 1 ha of land. This is becoming a major problem for municipalities in Portugal, particularly for Azores and Madeira (islands that are part of the national territory) with limited landfill space.

Although MSW is regarded as a green energetic source, its incorrect management may also produce greenhouse gases. In fact, from the available methods of treatment, landfill is still the most widely used (Soltani et al., 2016) despite posing an environmental risk to human health. Incineration has gained ground over landfills (Shareefdeen et al., 2015) since it can dramatically reduce the initial MSW volume while producing electricity and heat that can be used to power and heat nearby buildings. However, this type of technology entails high investment and operating costs while producing a wide variety of pollutants.

Gasification is becoming an increasingly attractive alternative to incineration due to its pollution minimization effects, higher overall efficiency and ability to produce a clean and portable gas (Ionescu et al., 2013). However, despite its many advantages, biomass and waste gasification have yet to represent more than 0.33% of the global gasification capacity worldwide (Arafat and

* Corresponding author. Rua Dr. Roberto Frias, Campus da FEUP, 400, 4200-465, Porto, Portugal.
E-mail addresses: nunodiniscouto@hotmail.com (N.D. Couto), vsilva@inegi.up.pt (V.B. Silva), rouboa@seas.upenn.edu (A. Rouboa).

http://dx.doi.org/10.1016/j.jclepro.2016.08.082
0959-6526/

Jijakli, 2013). To make the process more appealing to both private sector and government institutions, it is necessary to further develop the technology and increase research to find solutions for some of the most serious problems, such as CO_2 and tar production (Hu et al., 2015).

One way to expedite the mainstream of this technology is by optimizing the process with more efficient operating conditions. A more efficient process will be more cost effective (thus increasing the interest to commercialize it) while improving its environmental performance (which could lead governmental institutions to subsidize it or at least promote it).

Energetic and exergetic analysis are two common (and important) tools researchers use to improve system's efficiency. Energy analysis is usually used for establish the short-term feasibility of a system, while an exergetic analysis gives more realistic data due to the fact that thermodynamic processes have internal irreversibilities resulting in a loss of exergy even though there is no external energy loss to the system (Pellegrini and Oliveira, 2007).

There is an extensive literature on thermodynamic analysis of biomass gasification ranging from simple sensitivity analysis (Pérez et al., 2015) to integrated systems (Jia et al., 2015). Since experimental runs conducted on industrial gasification plants or even on pilot scale gasification plants can be extremely expensive, a large segment of studies uses mathematical models. In fact, these models, with the ability to theoretically simulate any physical condition, allow studying the gasification process without resorting to major investments and/or the need for long waiting periods (with all the bureaucratic and logistical problems associated).

According to Gómez-Barea and Leckner (2010), there are two major approaches to model gasification in fluidized beds: equilibrium modeling and kinetic. Regarding energy and exergy analyses coupled with gasification modeling, the research bulk is focused on equilibrium analysis. The work of Prins et al. (2003) and Abuadala et al. (2010) are perhaps the most recognized. The former carried out an extensive analysis on availability and irreversibility for the biomass gasification process using both air and steam as gasifying agents while the latter focused on maximizing hydrogen production by optimizing operating conditions.

However, work focused exclusively on thermodynamic analysis of MSW gasification is extremely scarce in the current literature. The few available papers center on two main segments: plasma gasification (Zhang et al., 2013) and specific wastes derived from MSW (Rao et al., 2004). Plasma gasification technology in the United States is developing fast, and could be an optimal root to divert MSW from landfill and produce valuable by-products; however the technology is still young requiring extremely large initial investments and the operational costs are considerable higher relative to incineration. Researching specific wastes derived from MSW (such as plastic and food wastes, etc.) has an important role in determining the influence of individual components but lacks the carryover to complex systems.

In order to fill this significant gap data from Portuguese MSW collected from the Oporto metropolitan area was used to study the feasibility of MSW gasification in the country. A first and second law thermodynamic analysis was carried out in order to improve MSW conversion from an efficiency and ecofriendly standpoint. A previously developed numerical model was used to collect further data on the MSW gasification process. Simulated data was compared with experimental results.

2. Materials and methods

The numerical model (presented in chapter 3) was developed using experimental data collected in the gasification plant from the School of Technology and Management (ESTG) of the Polytechnic Institute of Portalegre (IPP). The plant, in addition to its didactic functions, is aimed at the study of biomass as an energy source, taking into account not only energetic aspects but also environmental perspectives related to the quality of the emissions caused by the burning of obtained gases.

The pilot thermal plant, shown in Fig. 1, has a processing capacity of approximately 100 kg/h and is based on bubbling fluidized bed technology. Biomass is introduced above the floating bed of inert material and usually operates between 750 and 850 °C, being regulated by changing the air/biomass ratio. The unit has the following components:

a) Biomass feed system: consisting of two storage silos and speed-controllable auger to discharge the material inside the reactor at a chosen rate; to ensure that no air enters the biomass feed system, the storage silos are provided with two electropneumatic valves installed which open and close alternately;
b) Fluidized bed reactor: tubular reactor with 0.5 m diameter and 4.15 m in height and coated with refractory material; the biomass is admitted at 0.5 m from the base; air, preheated, enters the reactor at its base through a set of nozzles at a selected flow rate; the fluidized bed is provided with 70 kg of dolomite ($CaCO_3$); 3 temperature sensors are installed inside the reactor to monitor and control the gasification process; the reactor operates with a negative pressure gradient produced with the aid of a vacuum pump installed on the end of the process; reactor temperature is controlled by the amount of air admitted to the reactor;
c) Gas cooling system: comprised by two heat exchangers; the first cools the syngas, using a co-current system with air entering the unit, to a temperature close to 300 °C and the second one cools the syngas down to 150 °C with forced convection;
d) Gas cleaning system: carbon particles produced in the gasification process are removed to a cellulosic bag filter; filter cleaning is done by the injection of syngas at high pressure; coal is collected in a tank;
e) Condenser: the removal of liquid condensate is made by cooling the gas to room temperature in a coil heat exchanger.

The schematics as well as an extensive description of the gasification plant can be found elsewhere (Silva et al., 2014; Couto et al., 2015a).

2.1. Portuguese municipal solid waste evolution

Before the late nineteens Portugal's situation regarding solid waste management was dramatic with 76% going to open landfills and 14% going to controlled landfills. Due to an overwhelming change in public opinion, caused by landscape and soil degradation as well as disease spreading in local populations, national governments were forced to implement the first National Waste Management Plan (PERSU) (Magrinho et al., 2006). Since then, Portugal has been slowly reversing the previously stablish trend. Fig. 2 presents the development of MSW generation and respective final destination in Portugal from 2001 to 2010.

Despite decreasing landfills from over 75% to 60% the strategy aimed at the total eradication of open dumps failed. In February 2007 PERSU II was ratified to target the period between 2007 and 2016. The new national plan tried to carry on the previous waste management policy, taking into account new requirements formulated at national and EU level, in particular by ensuring compliance with Community targets for diverting biodegradable municipal waste from landfill, while trying to remedy the

Fig. 1. Photograph of the semi-industrial gasification plant in Portalegre, Portugal.

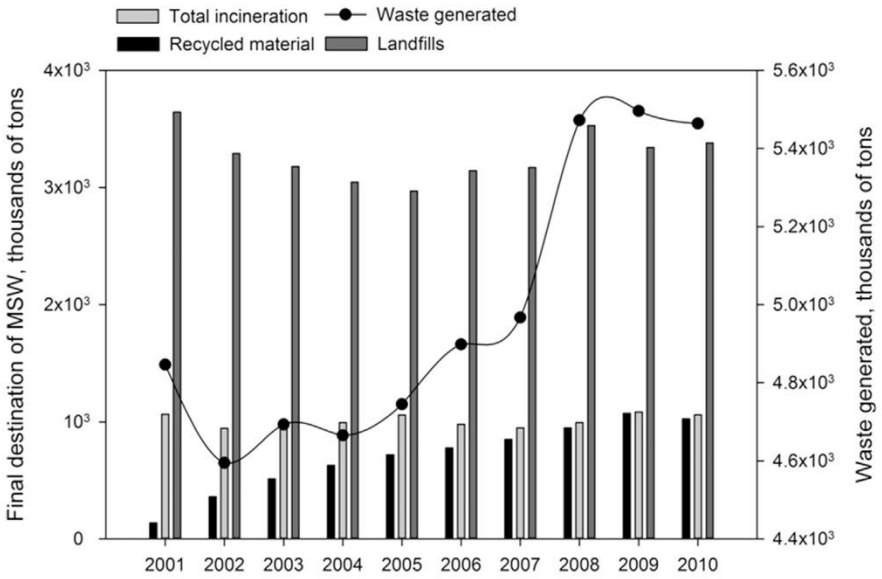

Fig. 2. MSW generation and final destination in Portugal from 2001 to 2010.

limitations mentioned on the implementation of PERSU I.

Still, according to the European Environment Agent (EEA, 2013), Portugal needs to intensify the implementation of the plan while adding considerable efforts to fulfil the EU targets. Gasification is becoming an increasingly attractive technology to treat MSW, through clean gas production, and thus becoming a valuable root to achieve those targets.

2.1.1. MSW characterization and LIPOR's sorting plant

Since model accuracy depends on using realistic data, the characterization and analysis of Portuguese MSW was carried out using data from the Oporto metropolitan area obtained from LIPOR, the entity responsible for the management, treatment and recovery of solid waste municipal produced in the city. Based on modern municipal waste management concepts that stand for the implementation of integrated systems and reduction of waste disposal in landfills, LIPOR has developed an integrated strategy for the recovery, treatment and confinement of municipal waste, based on three main areas: multi-material recovery, organic recovery and energy recovery, which are complemented by a landfill where rejected and previously prepared waste is sent to.

Every year, LIPOR treats about 500,000 tons of municipal waste that are produced by roughly 1 million inhabitants. Early estimates from 2016 indicate that 240,648 tons of wastes were produced in the first half of the year. Although premature, this represents an increase in 2.7% when compared to the same period from last year. After years of undefined trends, these figures seem to indicate a return to the increasing trend in municipal waste production that occurred during the period between 2002 and 2010 (up to 18%), which can be explained by the improvement of the macroeconomic situation of the country, which increased the level of consumption and, consequently, the production of waste. During the management and treatment of collected MSW samples were acquired for posterior physical characterization. Table 1 describes the obtained samples.

To better understand how the physical characterization was obtained as well as the steps necessary to formulate the chemical composition used in the simulations it is best to understand how the sorting process works. The following is a summarized step-by-step process of LIPOR's sorting plant (full process description can be viewed at (LIPOR, 2016)):

The materials from the Ecocontainer, the door-to-door

Table 1
Physical characterization of the MSW in Oporto in 2014.

Category	% Weight
Putrefied residues	37.57
Paper	6.16
Cardboard	4.31
Composites	6.39
Textiles	7.74
Sanitary textiles	8.72
Plastics	12.10
Combustive non specified	0.93
Glass	5.53
Metals	2.45
Non-combustive non specified	0.50
Hazardous residues	0.01
Fine elements	7.59

packaging collection, the Ecofone and other special circuits are discharged in the Sorting Plant reception area. These discharges are subject to an inspection, to record its quality. The materials are placed in the pre-sorting cabin, where pre-sorting is done, resulting in 3 streams: large film, large rejected and other materials of large dimension. After passing the pre-sorting cabin, the materials are forwarded to a "bag-opener", to homogenize the material.

The materials, after passing through the "bag-openers" (so the material homogenate), are forwarded to the ballistic sorter. Ballistic sorting equipment is a device that allows the sorting of material in 3 fractions: thin, rolling and flat. The equipment is assembled with a pre-defined inclination, and consists of a set of perforated bars, which in a continuous movement, sorts the materials.

The materials, which in the ballistic section followed the rolling's path, are forwarded to the respective hopper. Before they get to the rolling hopper, the materials go through two automatic sorting systems: an automatic vacuum system that sucks all the light and flexible materials; and an electromagnet, which sorts all ferrous metals and forward them through a hopper, to a metal baler, where they are pressed and sent to recycling industries.

The escalators sent to the respective hopper, are transported to the rolling sorting cabin. The sorting cabin consists of two rows of parallel sorting, where is sorted sequentially 4 materials (PET, PEHD, Mixed Plastics and CPLF). The materials follows to Foucault currents, where aluminum is sorted by a magnetic flux process that allows automatic sorting of the material. The remaining material is considered process rejected.

From the described pre-treatment of MSW done by LIPOR, a refuse derived fuel (RDF) simply containing cellulosic materials and plastics is obtained (comprised of putrefied wastes, paper, wood wastes, and plastic residues). The remaining MSW components follow another route for valorization or elimination, as described above. It has been shown that the plastic residues are mainly composed of polyethylene, polystyrene, and polyvinyl chloride (Scott et al., 1990) while cellulosic materials are composed of cellulose, hemicelluloses, and lignin (Baliban et al., 2010).

Since the ultimate analysis from LIPOR does not distinguish between cellulosic materials, their composition was presupposed to be similar to the one found by Onel et al. (2014), where the cellulosic material comprises cellulose, hemicellulose and lignin. Regarding the plastics group, LIPOR report shows the relative quantities of each monomer in the MSW. Therefore, it was possible to take into account different monomers for the plastics group as shown in Table 2.

Table 2
Chemical composition of the MSW in Oporto in 2014.

Category	% Weight	Chemical formula
Cellulosic material	85.42	[a]
Polyethylene	10.99	$(C_2H_4)_n$
Polyethylene terephthalate	2.02	$(C_{10}H_8O)_n$
Polypropylene	0.81	$(C_3H_6)_n$
Polystyrene	0.76	$(C_8H_8)_n$

[a] It was considered the proportion of cellulose, hemicellulose and lignin found in Onel et al. (2014).

3. Thermodynamic methodology

Thermodynamic analyses are used to evaluate how energy streams affect the overall performance of a given system. Through mathematical models, these analyses can help determining the effects of parameters on the optimal system's operating point. In this particular study the goal is to use first and second law analysis to improve MSW conversion from an efficiency and ecofriendly standpoint. In order to simplify the analysis the following assumptions were made (Pellegrini and Oliveira, 2007):

- Steady State;
- Kinetic and potential energy ignored;
- Ideal gas principles apply for the gases;
- Syngas is only formed with H_2, CO, CO_2, N_2, C_nH_m and it is at chemical equilibrium;
- Heat losses from the components are neglected;
- T_0 is 25 °C and P_0 101.325 kPa;
- Ash residues are negligible;
- Gasifier is isothermal and at equilibrium condition.

3.1. Energy analysis

The overall energy balance can be expressed as the total energy input rate equal to total energy output rate ($E_{in} = E_{out}$), with all energy terms being:

$$\dot{Q} + \sum \dot{m}_{in} h_{in} = \dot{W} + \sum \dot{m}_{out} h_{out} \quad (1)$$

Where $\dot{Q}$ is the heat rate, $\dot{W}$ is the work rate and h is the specific enthalpy. Applying this concept to the current study, energy transferred as heat can be written as:

$$\dot{Q}_{MSW} + \dot{Q}_{heatedair} = \dot{Q}_{syngas} + \dot{Q}_{tar} + \dot{Q}_{system} \quad (2)$$

The fuel's energy input can be calculated as:

$$\dot{Q}_{MSW} = \dot{m}_{MSW} \times LHV_{MSW} \quad (3)$$

Where LHV is the lower heating value and $\dot{m}_{MSW}$ is the mass flow rate for MSW. As long as there is no condensation occurring, the power of supplied air can be given by:

$$\dot{Q}_{air} = \dot{m}_{air} \sum_{1}^{j} w_j c_{p,j} (T - T_0) \quad (4)$$

Where w_j is the mass fraction and c_{pj} the specific heat of a component, T and T_0 represent preheat gas temperature and ambient temperature, respectively. To calculate the energy associated with the produced syngas one can use:

$$\dot{Q}_{syngas} = \dot{m}_{syngas} \times LHV_{syngas} \quad (5)$$

Similarly, tar content energy can be obtained by simply:

$$\dot{Q}_{tar} = \dot{m}_{tar} \times LHV_{tar} \quad (6)$$

So, in order to calculate the cold gas energy efficiency one can simply put it:

$$\eta_{coldgas} = \frac{\dot{Q}_{syngas}}{\dot{Q}_{MSW} + \dot{Q}_{air}} \tag{7}$$

3.2. Exergy analysis

As stated, exergy analyses are far superior to energetic ones, since energetic analyses do not take into consideration irreversibilities that occur in every thermodynamic process. In this work the same methodology to calculate exergy used by Zhang et al. (2015) was employed. Exergy rate can be defined by the sum of the chemical exergy rate and the physical exergy rate:

$$Ex = Ex_{ch} + Ex_{ph} \tag{8}$$

Where the chemical and physical exergy can be written, respectively as:

$$Ex_{ch} = \sum_i n_i \left(e_{0_i} + RT_0 ln \frac{n_i}{\sum n_i} \right) \tag{9}$$

$$Ex_{ph} = \sum_i n_i [(h - h_0) - T_0(s - s_0)] \tag{10}$$

Where n_i is the molar yield of gas component i (mol/kg), R is the ideal, or universal, gas constant and e_{0_i} is the standard chemical exergy of a pure chemical compound i and it can be found in Zhang et al. (2015). Also, s and h are entropy and enthalpy of a system at given temperature and pressure, and h_0 and s_0 are enthalpy and entropy of a system at the environmental temperature and pressure, respectively.

In order to calculate the exergy of MSW with less complexity, taking into account its heterogeneous, the introduced correlation by Szargut and Styrylska (1964) was used:

$$Ex_{MSW} = \dot{m}_{MSW} \beta LHV_{MSW} \tag{11}$$

The formula of correlation factor β is given by:

$$\beta = \frac{1.0412 + 0.2160\left(\frac{H}{C}\right) - 0.2499\left(\frac{O}{C}\right)\left[1 + 0.7884\left(\frac{H}{C}\right)\right] + 0.0450\left(\frac{N}{C}\right)}{1 - 0.3035\left(\frac{O}{C}\right)} \tag{12}$$

Where O, C, H and N are the weight fractions of oxygen, carbon, hydrogen and nitrogen in the MSW, respectively.

Similarly, in this work the tar chemical exergy is simulated with help of another correlation for liquid fuels (Stepanov, 1995):

$$Ex_{tar} = \dot{m}_{tar} LHV_{tar} \left(1.0401 + 0.1728\left(\frac{H}{C}\right) + 0.0432\left(\frac{O}{C}\right) + 0.2196\left(\frac{S}{C}\right)\left[1 - 2.0628\left(\frac{H}{C}\right)\right] \right) \tag{13}$$

Using the previous equations the exergy balance simply becomes:

$$\sum_{in} Ex_{in} = \sum_{out} Ex_{out} + \dot{I} \tag{14}$$

$\dot{I}$ Represents the internal exergy destruction rate due to irreversibility (unlike energy, exergy can actually be destroyed). The *in* and *out* subscripts stand for inlet and outlet, respectively.

Using the same principal as in the energy analysis, syngas exergy efficiency can be calculated as being:

$$\varepsilon_{syngas} = \frac{Ex_{syngas}}{Ex_{MSW} + Ex_{air}} \tag{15}$$

Similarly, tar content exergy efficiency can be written as:

$$\varepsilon_{tar} = \frac{Ex_{tar}}{Ex_{MSW} + Ex_{air}} \tag{16}$$

4. Mathematical model

Experimental studies conducted in pilot scale or industrial reactors like the one presented in chapter 2 are fairly absent from the available literature. The reason why is due to the difficulty in regulating operating parameters but mostly due to the high cost of a gasification plant, which can reach tens of millions of euros depending on the generated power (Alauddin et al., 2010). Having a model capable of predicting gasification process in industrial-size conditions allows one to be much closer to realistic commercial size reactors since the hydrodynamic phenomena in a laboratory scale fluidized bed are not the same as on large scales (Couto et al., 2016). However, due to the extreme complexity of the gasification process, largely due to the chemical and physical interactions that occur throughout, the ability of numerical models to correctly predict experimental data collected from pilot scale or industrial reactors is usually very limited. In fact, the lack of reliable models was the main motivation for the first draft of the developed model early in the decade (Couto et al., 2015b). Both the key points that define the model as well as the main upgrades done in recent years are explained in the next subchapters.

4.1. Governing equations

Due to the high solid fraction inside the fluidized bed, the Eulerian method was used to simulate the MSW gasification process, and described using the kinetic theory of gases. Since turbulence transfer has a predominant role in the gasification process in fluidized beds, the standard $k-\varepsilon$ model was used, and the dissipation rate constants suggested by Launder and Spalding (1972) were employed to determine turbulence kinetic energy. The MSW gasification model includes fluid flow, heat and mass transfer, and the gas and solid phases are governed by the equations below.

4.1.1. Gas phase

The energy conservation equation for gas phase is as follows:

$$\frac{\partial\left(\alpha_q\rho_q h_q\right)}{\partial t}+\nabla\cdot\left(\alpha_q\rho_q\vec{u}_q h_q\right)=-\alpha_q\frac{\partial\left(p_q\right)}{\partial t}+\bar{\bar{\tau}}_q:\nabla\left(\vec{u}_q\right)-\nabla\vec{q}_q+S_q+\sum_{p=1}^{n}\left(\vec{Q}_{pq}+\dot{m}_{pq}h_{pq}\right) \tag{17}$$

The momentum equation for gas phase can be expressed like so:

$$\frac{\partial\left(\alpha_q\rho_q\vec{u}_q\right)}{\partial t}+\nabla\cdot\left(\alpha_q\rho_q\vec{u}_q\vec{u}_q\right)=-\alpha_q\nabla p_q+\alpha\rho_q g+\beta(u_q-u_p)+\nabla\cdot\alpha_q\bar{\bar{\tau}}_q+S_{pq}U_S \tag{18}$$

The continuity equation for gas phase is given by:

$$\frac{\partial\left(\alpha_q\rho_q\right)}{\partial t}+\nabla\cdot\left(\alpha_q\rho_q\vec{u}_q\right)=-M_C\sum\gamma_C R_C \tag{19}$$

4.1.2. Solid phase

The energy conservation equation for solid phase is as follows:

$$\frac{\partial\left(\alpha_p\rho_p h_p\right)}{\partial t}+\nabla\cdot\left(\alpha_p\rho_p\vec{u}_p h_p\right)=-\alpha_p\frac{\partial\left(p_p\right)}{\partial t}+\bar{\bar{\tau}}_p:\nabla\left(\vec{u}_p\right)-\nabla\vec{q}_p+S_p+\sum_{q=1}^{n}\left(\vec{Q}_{pq}+\dot{m}_{pq}h_{pq}\right) \tag{20}$$

The momentum equation for solid phase can be expressed like so:

$$\frac{\partial\left(\alpha_p\rho_p\right)}{\partial t}+\nabla\cdot\left(\alpha_p\rho_p\vec{u}_p\right)=M_C\sum\gamma_C R_C \tag{21}$$

The continuity equation for solid phase is given by:

$$\frac{\partial\left(\alpha_p\rho_p\vec{u}_p\right)}{\partial t}+\nabla\cdot\left(\alpha_p\rho_p\vec{u}_p\vec{u}_p\right)=-\alpha_p\nabla p_p+\alpha\rho_p g+\beta(u_q-u_p)+\nabla\cdot\alpha_p\bar{\bar{\tau}}_p+S_{pq}U_S \tag{22}$$

Where $\vec{Q}_{pq}$ stands for the heat transfer intensity between fluid phase, pth, and solid phase, qth, h_q for the specific enthalpy of phase qth and $\vec{q}_q$ for heat flux; S_q is a source term due to chemical reactions and h_{pq} the enthalpy of the interface. R_C represents the reaction rate, γ_c the stoichiometric coefficient and M_C the molecular weight. Regarding the solid phase, t_s is the particle phase stress tensor and P_s the particle phase pressure due to particle collisions. Finally, β stands for the gas-solid interphase drag coefficient, τ_g for the gas phase stress tensor and U_s for the mean velocity solid. The above equations for fluid-fluid and granular multiphase flows are solved by Fluent. Further explanation on these equations can be found in Couto et al. (2015a).

4.2. Chemical reactions model

During MSW gasification, residues are first dried and heated up to 160 °C and then, during the devolatilization process which occurs at temperatures up to 700 °C, residues go through thermal cracking to produce light gases, tar and char.

A pyrolysis model with secondary tar generation was adopted. MSW is mainly composed by cellulosic and plastic components, and while cellulosic material can be divided in cellulose, hemicellulose and lignin (Onel et al., 2014), plastics comprise polyethylene, polystyrene, and polypropylene, among others. The reactions of cellulosic and plastics are considered individually. The primary pyrolysis equations can be defined as:

$$Cellulose\xrightarrow{r_1}\alpha_1 Volatiles+\alpha_2 Tar+\alpha_3 Char \tag{23}$$

$$Hemicellulose\xrightarrow{r_2}\alpha_4 Volatiles+\alpha_5 Tar+\alpha_6 Char \tag{24}$$

$$Lignin\xrightarrow{r_3}\alpha_7 Volatiles+\alpha_8 Tar+\alpha_9 Char \tag{25}$$

$$Plastics\xrightarrow{r_4}\alpha_{10} Volatiles+\alpha_{11} Tar+\alpha_{12} Char \tag{26}$$

Secondary tar generation reaction can be written as:

$$PrimaryTar\xrightarrow{r_5}Volatiles+SecundaryTar \tag{27}$$

The kinetics for cellulosic material and plastics as well as the global reaction for secondary pyrolysis can also be found in Couto et al. (2015a). While pyrolysis involves thermal cracking of molecular structures, gasification involves the conversion to volatile products. In fact, char and volatiles gasify using CO_2, H_2 or steam. In an auto-thermal gasification process, partial oxidation of combustible gas, vapors and char provide the necessary heat to the thermal cracking of tars and hydrocarbons and to the gasification of char:

$$CO+0.5O_2\rightarrow CO_2 \tag{28}$$

$$H_2+0.5O_2\rightarrow H_2O \tag{29}$$

$$C+0.5O_2\rightarrow CO \tag{30}$$

The Kinetic/Diffusion Surface Reaction Model (Field, 1969) was employed to deal with these reactions. From the wide spectrum of gasification reactions the main endothermic reactions considered in this work were the following:

- Water-gas shift (WGS):

$$CO+H_2O\leftrightarrow CO_2+H_2 \tag{31}$$

- Methanation:

$$CO+3H_2\leftrightarrow CH_4+H_2O \tag{32}$$

- Primary water-gas reaction:

$$C+H_2O\leftrightarrow CO+H_2 \tag{33}$$

- Boudouard reaction:

$$C+CO_2\leftrightarrow 2CO \tag{34}$$

- Dry reforming:

$$CH_4+CO_2\leftrightarrow 2H_2+2CO \tag{35}$$

Seeing that homogeneous reactions are affected by both kinetic and turbulent mixing rates, a finite-rate/Eddy-dissipation model was used which considers both Arrhenius and Eddy-dissipation reaction rates. The Arrhenius rates and the kinetic parameters for all reactions as well as further explanation can be found in Couto et al. (2015a), and so can solver procedure details (Couto et al., 2015a).

5. Results and discussion

5.1. Model validation

The numerical model presented in Chapter 4 is the result of continuous improvement on the described set of phenomena that includes fluid flow, heat transfer, and chemical reactions models necessary for modeling the gasification process. At the same time, the software related parameters have been optimized to mimic similar conditions to those found in experimental activities and thus obtaining more realistic results.

The model was first applied to the study of Portuguese biomass gasification (Silva et al., 2014). To validate the numerical model a wide range of operational conditions were tested in the described plant for several Portuguese biomass substrates. Table 3 shows 9 operating conditions for 3 distinct substrates (representing just a fraction of the overall conducted runs used to validate the numerical model).

Fig. 3 compares modeled and measured gas composition for the described operating conditions. Presented results show that the developed numerical model has the ability to predict the obtained synthetic gas composition within a satisfactory margin of error of 20%, commonly found in similar studies (Silva and Rouboa, 2015). The biggest deviation was observed for CH_4, which was expected since smaller fractions tend to produce higher relative errors. Furthermore, all light hydrocarbons and tar can lump into CH_4, which can explain the disagreement sometimes found (Silva et al., 2014).

To counter the improper disposal of municipal waste in landfills the model had to undergo a restructuring on the devolatilization section in order to cope with the heterogeneity of MSW (Couto et al., 2015a). Ideally one would like to validate the new upgraded model with the experimental set-up used earlier. However, due to unfortunate logistical and bureaucratic setbacks this was not possible. To work around the problem it was decided to validate the upgraded model using data collected from the literature (Gang et al., 2007). Table 4 shows the operating conditions for 9 experimental runs used to validate the numerical model.

Fig. 4 matches the composition of obtained gas that is estimated by the model with that measured in the experiments. Comparison between Figs. 3 and 4 shows that the upgrade done to the model allowed a more complex system to perform in a similar fashion and in some cases to predict syngas composition slightly better. This was due to a more realistic devolatilization model and the inclusion of light hydrocarbons. Nevertheless, some differences can be observed due to some simplifying assumptions followed by the model, which are explained in detail in Silva et al. (2014).

Having a model not only able to correctly predict trends but also the overall compositions, gives the user the ability to forecast scenarios while minimizing costs. This can become extremely time-efficient since it can eliminate or at least greatly diminish the necessary experimental runs with all the bureaucratic and logistical problems associated with it.

5.2. Assessment of operational conditions

Before exploring the effects of gasification temperature and equivalence ratio (ER) on the system's energy and exergy values it is desirable to study their influence on the process main products. To do so, it is only necessary to resort to the above validated model. Equivalence ratio is defined as the ratio between the actual air/fuel ratio and the stoichiometric air/fuel ratio:

$$ER = \frac{oxygen\ mass/dry\ MSW\ mass}{stoichiometric\ oxygen/MSW\ ratio} \tag{36}$$

In this study ER was kept in the 0.15–0.35 range since it's well documented that the most suitable values for gasification are found between 0.2 and 0.4 (Wang et al., 2008). In addition to studying the impact on syngas composition is also important to study the impact on one of the major concerns related to municipal solid waste gasification, tar formation (Hu et al., 2015). The model predictions about the influence of ER on syngas molar fraction and tar content are shown in Fig. 5.

From the above Figure one can see that ER has a positive effect on both CO_2 and N_2 while having a negative hold on the rest. This can be easily explained by the increase in oxygen content in the reactor promoting oxidation reactions that consume CO and H_2 to produce CO_2, since O_2 is more reactive to carbon than steam or CO_2. Although to a smaller degree ER negatively affects C_nH_m content by enhancing steam reactions at higher temperatures leading to methane decomposition (Wang et al., 2015).

The way O_2 is introduced to the reactor is crucial to the produced gas outcome. In fact, by simply increasing air flow one is also increasing ER and O_2 content leading to produced gas more diluted in N_2 (which also leads to a poorer gas) while using an air separator to increase O_2 content will cause the N_2 flow entering the reactor to decrease. Also, as air flow rate increases, a shorter residence time is expected. If the residence time is not sufficient to allow CO and H_2 to occur their molar fraction is also expected to decrease.

Tar formation is one of the major concerns regarding syngas quality. Tar condenses at lower temperatures, leading to blocking and fouling process equipment such as engines and turbines (Devi et al., 2003). It is than necessary to eliminate this by-product or at least greatly diminish to make way for large-scale commercialization.

A decrease in tar content around 70% with the rise of ER to 0.35 is observed in Fig. 5. This can be related to more energy being released as oxidization reactions become more active since more O_2

Table 3
Operating conditions for validation purposes.

Experimental conditions	Forest residues			Coffee husk			Vines pruning		
Run	1	2	3	4	5	6	7	8	9
Temperature (°C)	815	815	790	815	790	790	790	790	815
Admission Biomass (Kg/h)	63	74	63	28	28	41	25	55	55
Air Flow Rate (Nm^3/h)	94	98	98	75	72	80	52	40	40
Test results									
Syngas NHV (MJ/Nm^3)	5.16	5.02	4.93	3.34	3.20	3.07	1.99	3.46	4.02
Cold Gasification Efficiency	0.41	0.30	0.37	0.60	0.47	0.42	0.55	0.45	0.49

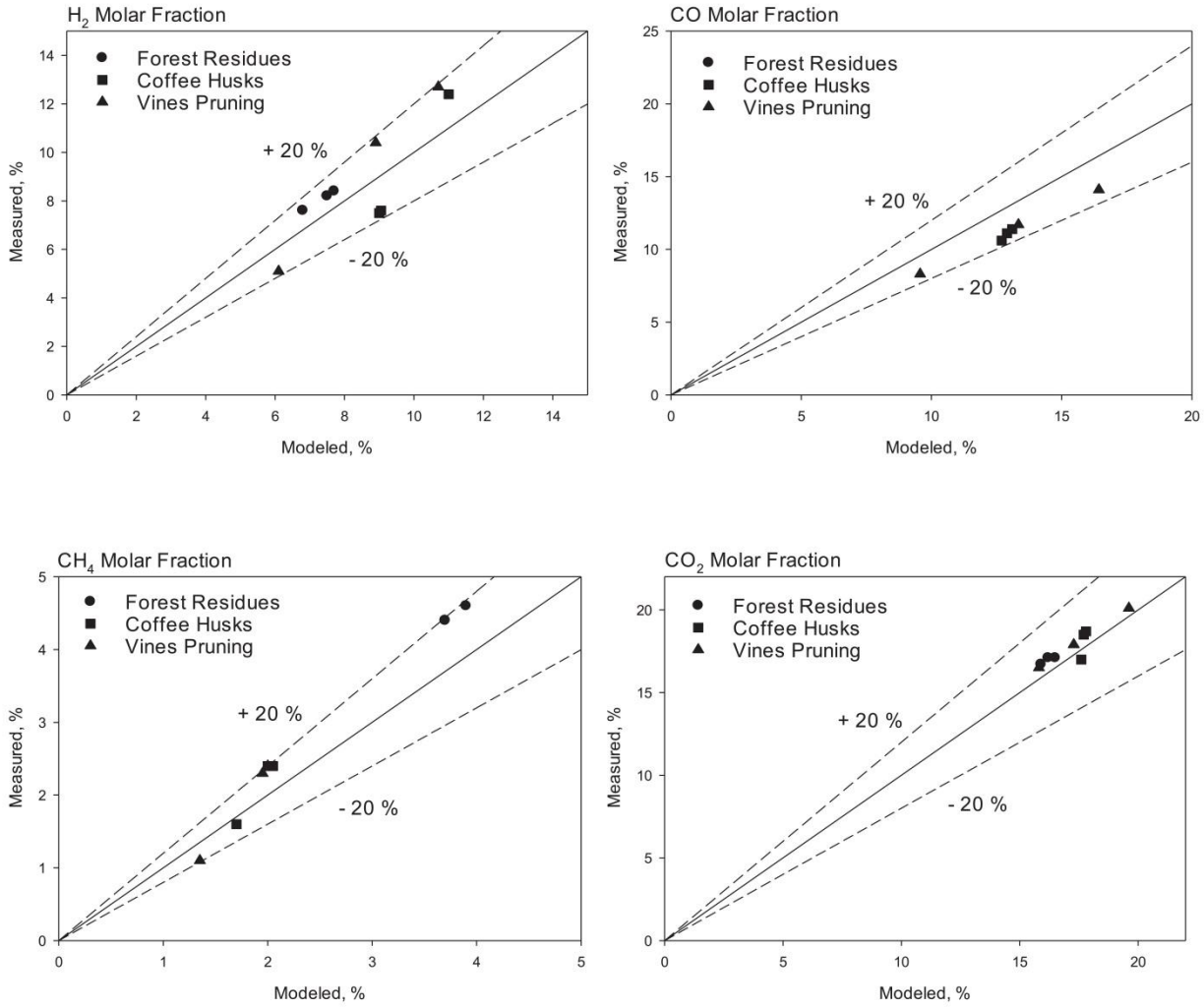

Fig. 3. Comparison between modeled and measured syngas composition for biomass substrates.

Table 4
Operating conditions for the experimental gasification runs.

Run	1	2	3	4	5	6	7	8	9
Temperature (°C)	493	705	602	507	687	593	516	691	507
MSW Admission (Kg/h)	2.3	3	3	3	4	4	4	6	6
ER	0.5	0.4	0.4	0.4	0.3	0.3	0.3	0.2	0.2
Preheated Air (°C)	290	352	296	281	352	307	282	352	279

is available. This increase in available energy leads to higher temperatures inside the reactor which, in turn, enhances steam reforming reactions, thus promoting carbon conversion (Wang et al., 2012). This leads to increase in gas yield, which is known for improving tar decomposition.

In a self-heated gasifier, gasification temperature will most likely be controlled by adjusting ER or admission of MSW, which means that it tends to be treated as a dependent variable in the process (Couto et al., 2015c). However, due to its predominant effect on reaction kinetics and on the gasifier performance it is wise to analyze its effects on the gasifier performance independently. The model predictions about the influence of gasification temperature on syngas molar fraction and tar content are shown in Fig. 6.

The effect on gasifier performance can be simply explained with the Le Chatelier's principle, which states that higher temperatures favor products in endothermic reactions. In fact, for low temperatures (usually bellow 800 °C), the endothermic nature of the H_2 production reactions (steam reforming and water-gas reactions) results in an increase in H_2 content and a decrease in C_nH_m content. For higher temperatures, usually above 750 °C, reverse water-gas (rWGS), primary water-gas and Boudouard reactions play a crucial role increasing CO content at the expense of CO_2. Additionally, high temperature also favors destruction and reforming of tar leading to a decrease in tar content as it can be observed in Fig. 6. The results are consistent with the current literature (Gonzalez et al., 2008; Kumar et al., 2009).

5.3. Energy values

Based on 1 kg MSW, the energy values of syngas and tar from air gasification at different gasification temperatures and ER values are calculated and analyzed.

5.3.1. Syngas energy values

The energy values of syngas components at various ER values are shown in Fig. 7. As stated, by increasing ER, more active combustion reactions, such as the partial combustion of char, CO and H_2 will occur leading to higher levels of CO_2 and H_2O at the cost of CO and H_2 (Niu et al., 2013). C_nH_m presents a very low molar fraction level and it decreases slightly with increase of ER due to

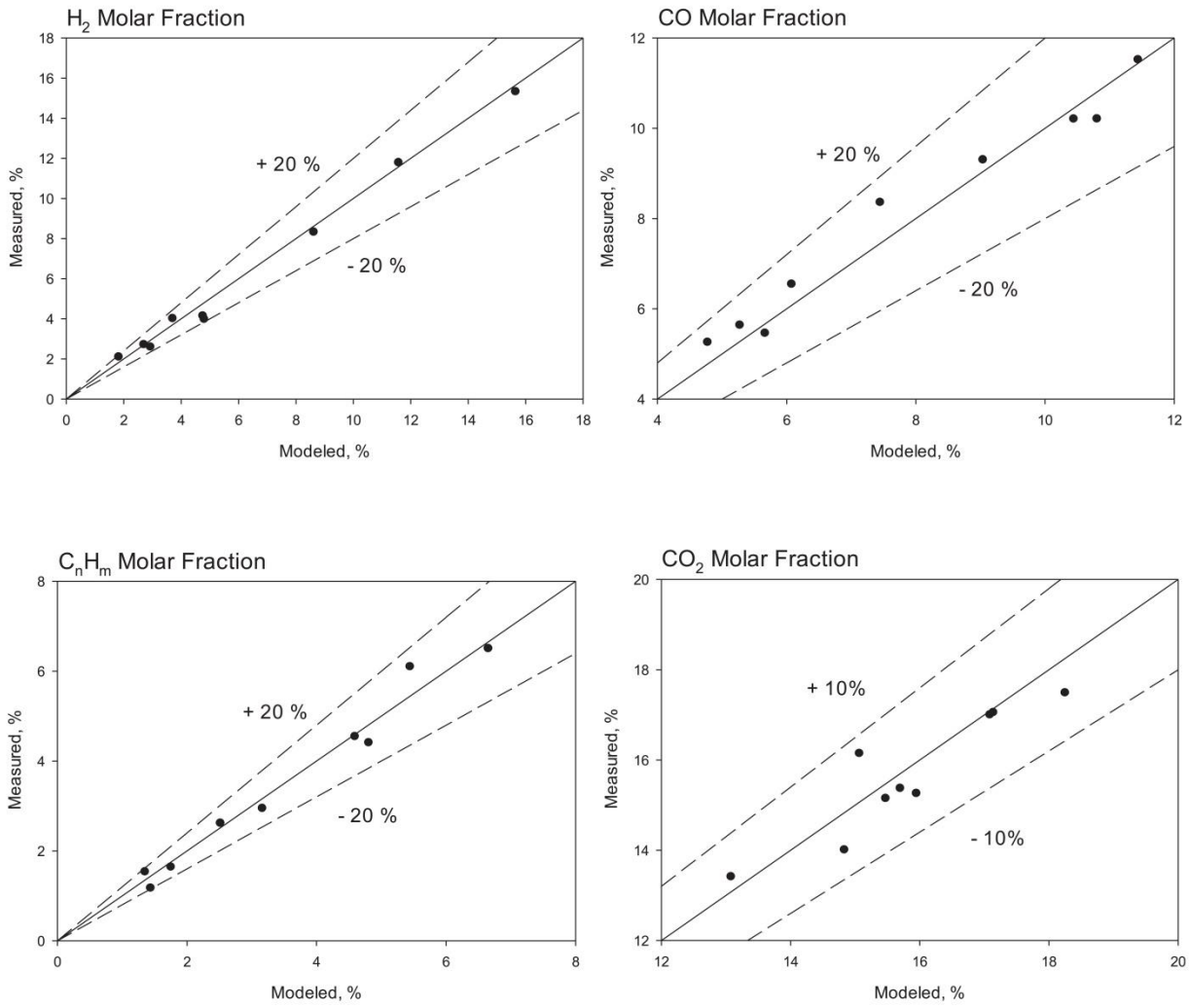

Fig. 4. Comparison between modeled and measured syngas composition for MSW.

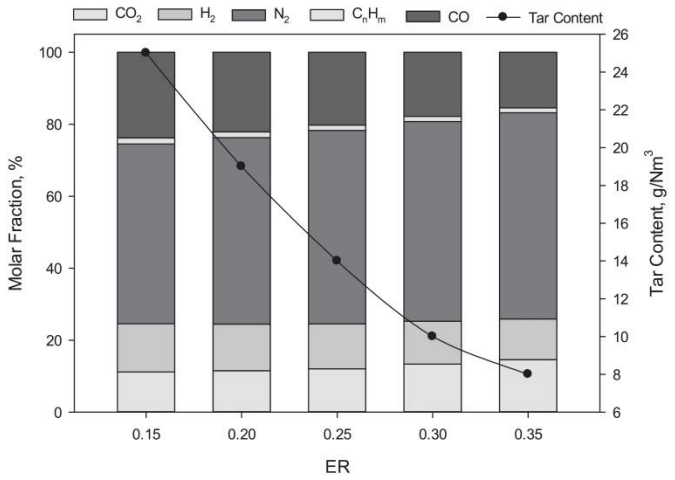

Fig. 5. Influence of ER on syngas molar fraction and tar content. Dry basis. (Operating conditions: Temperature - 700 °C; MSW admission – 25 kg/h).

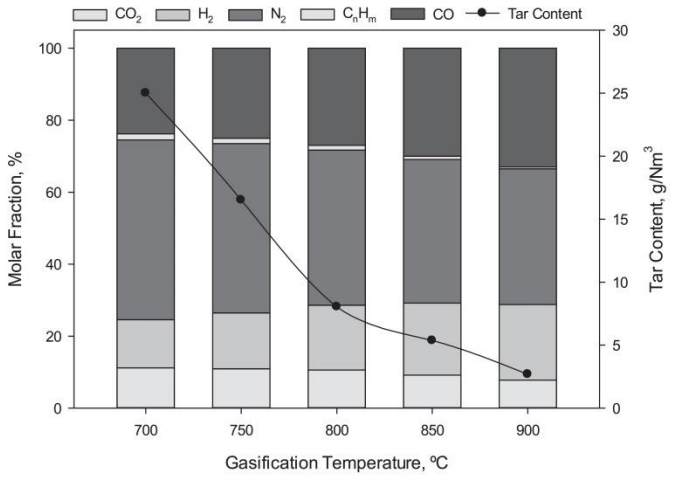

Fig. 6. Influence of temperature on syngas molar fraction and tar content. Dry basis. (Operating conditions: ER – 0.15; MSW admission – 25 kg/h).

strengthening of steam reforming reaction. N_2 is expected to increase simply because additional air is entering the gasifier.

From Fig. 7 one can see that when ER was increased from 0.15 to 0.25 syngas total energy value increased from 13,507 kJ to 14,642 kJ and then decreased to 14,169 kJ when ER was further increased to 0.35. This can be explained by the initially increase in the gross heat

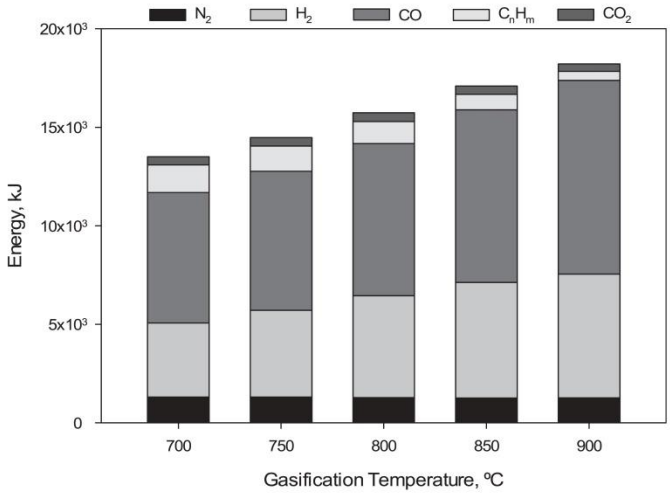

Fig. 7. Energy values of gas components at various ER values.

of combustion contained in syngas when air is added due to conversion of solid carbon. At the solid carbon boundary, addition of further air leads to a decrease in the combustion energy and an increase in sensible energy of the gas. This is consistent with the current literature (Hu et al., 2015; Zhang et al., 2015).

Current literature agrees that reactor temperature is one of the most influential factors affecting the product gas composition and related properties (Sun et al., 2010). It is thus imperative to analyze its influence on syngas energy values as well.

Fig. 8 shows the effects of reactor temperature on the total syngas energy. Since syngas energy values are determined by its enthalpy and molar yield (as shown in chapter 3) they are expected to increase with increasing temperature. In fact, when the reactor temperature was increased from 700 °C to 900 °C the total energy of syngas increased from 13,507 to 18,219 kJ.

Comparing both parameters, one can see that the effect of reactor temperature on the total syngas energy (34.9%) was much greater than that of ER (8.4%). This is consistent with the current literature (Zhang et al., 2015). One can notice that energy values follow a similar pattern to that found for syngas composition. This has to do with energy values being determined by the temperature and yield of each individual gas component.

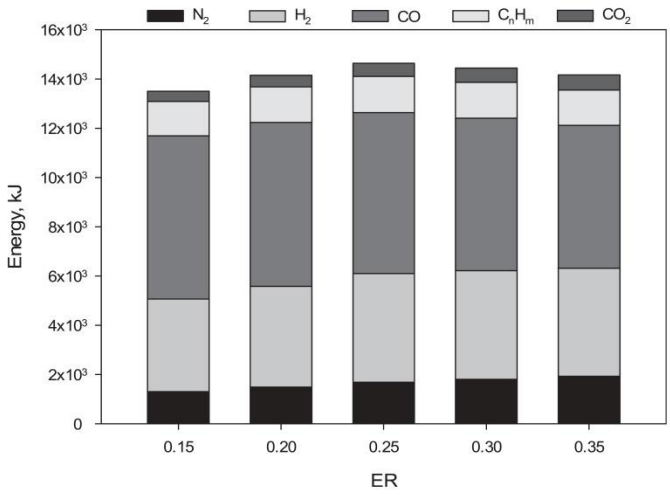

Fig. 8. Energy values of gas components at various reactor temperatures.

5.3.2. Tar energy values

Although attempts have been made to suppress tar production from the gasification process it is still one of the main concerns keeping the technology from being widely use and commercially successful. Because of this, it is a necessity to increase the efforts on studying this undesired by-product and ways to suppress or at least greatly diminished it. A main absence can be found on the current literature for thermodynamic analysis of tar production, especially for industrial conditions. Fig. 9 exhibits tar energy values at different reactor temperatures and ER values.

Contrary to syngas, both gasification temperature and ER present the same trend when it comes to tar energy values. This is mainly due to increases in gasification temperature and ER leading to lower tar yields. Although higher gasification temperatures are known for increasing physical energy, a dramatically reduction in tar yield will lead to a decrease in the total physical energy of tar content. This decrease in tar yield was already explained and it is due to the enhancement of tar cracking reaction at elevated temperatures. This is consistent with the current literature (Zhang et al., 2012; Wu et al., 2014).

5.4. Exergy values

Based on 1 kg MSW, the exergy values of syngas and tar from air gasification at different gasification temperatures and ER values are calculated and analyzed.

5.4.1. Syngas exergy values

Following the sequence establish in the previous chapter, Fig. 10 presents the exergy values of gas components at various ER values and temperatures. Regarding calculations, exergy values primarily differ from the energy values due to the inclusion of entropy.

After careful examination, one can see that Fig. 10 shares great similarities with Figs. 7 and 8. In fact, exergy values are lower than energy values while sharing the same trends. This can be easily understood since both physical and chemical exergy values tend to be lower than the corresponding energy values. This is consistent with the current literature (Niu et al., 2013; Sreejith et al., 2013). Similarly to Figs. 7 and 10a also presents a maximum value for ER = 0.25. According to Prins et al. (2003), and clearly witness in the presented results, past this maximum ER value, both energy and exergy values decrease due to a decrease in both chemical energy (and exergy) which is not fully compensated for by the increases in the physical energy (and exergy).

Regarding influence of reactor temperature, when temperature was increased from 700 °C to 900 °C, exergy values went from 10,727 kJ to 14,632 kJ (increase over 36%). This is a clear statement on the effect gasification temperature has over ER, which only gained 6.3% (from 10,727 kJ to 11,407 kJ) when ER was increased from 0.15 to 0.25.

5.4.2. Tar exergy values

Fig. 11 exhibits tar exergy values at various ER values and temperatures. When ER is increased from 0.15 to 0.35, exergy values decline from 1611.75 kJ to 663.61 kJ. Similarly, increase in gasification temperature leads to a drastic reduction in exergy values from 1611.75 kJ to 307.40 kJ. These trends can be explained by the promotion of gas yield by both ER and gasification temperature leading to tar decomposition (Ionescu et al., 2013). This is consistent with the current literature (Zhang et al., 2012).

5.5. Process efficiency

Most of the scientific community defines the efficiency of given process as the ratio of desired output over input. Regarding

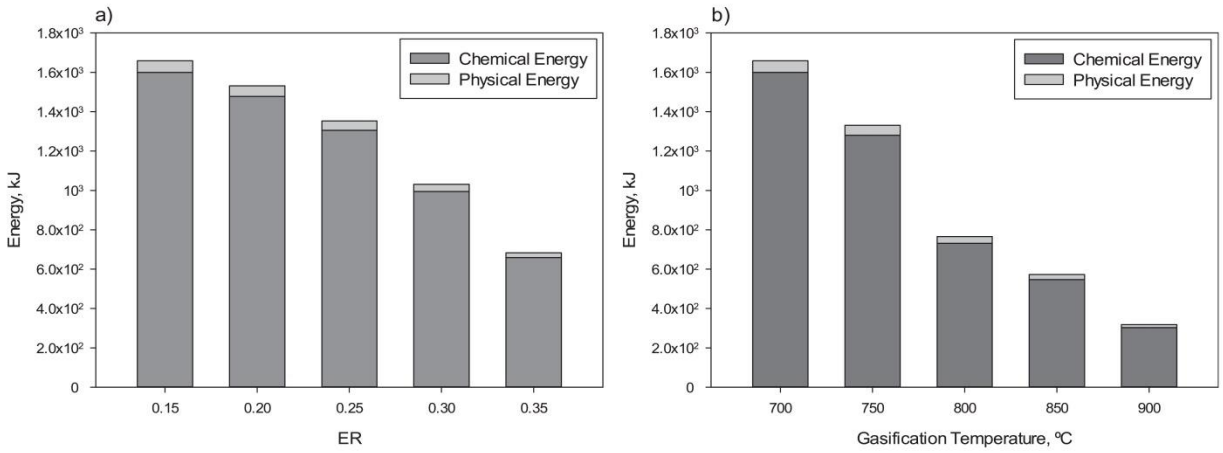

Fig. 9. Energy values of tar content at various a) ER values and b) reactor temperatures.

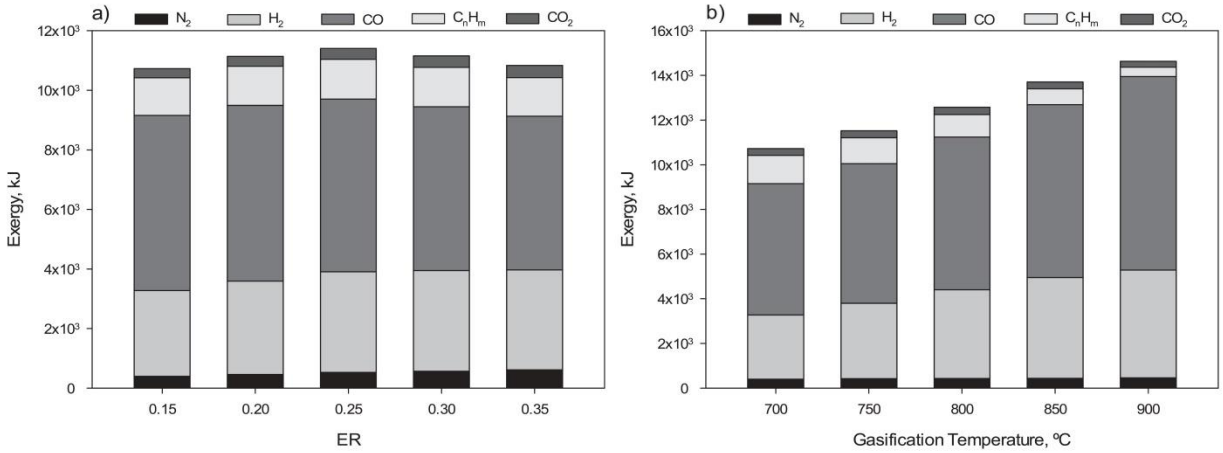

Fig. 10. Exergy values of gas components at various a) ER values and b) reactor temperatures.

gasification process, its efficiency is usually defined by the cold gas efficiency. Despite being an important parameter it has some shortcomings, especially neglecting the energy in the unconverted char as well as the sensible heat of the produced gas and in particular, as well as the increase in entropy due to conversion of a solid fuel into gaseous compounds (Prins et al., 2003). Because of this it is imperative to also study exergy efficiencies since they avoid said drawbacks. Fig. 12 shows the energetic and exergetic efficiencies of gas components and tar content at various ER values and reactor temperatures.

After careful analysis one can see that both energy and exergy efficiencies follow the same trend presented by their respective

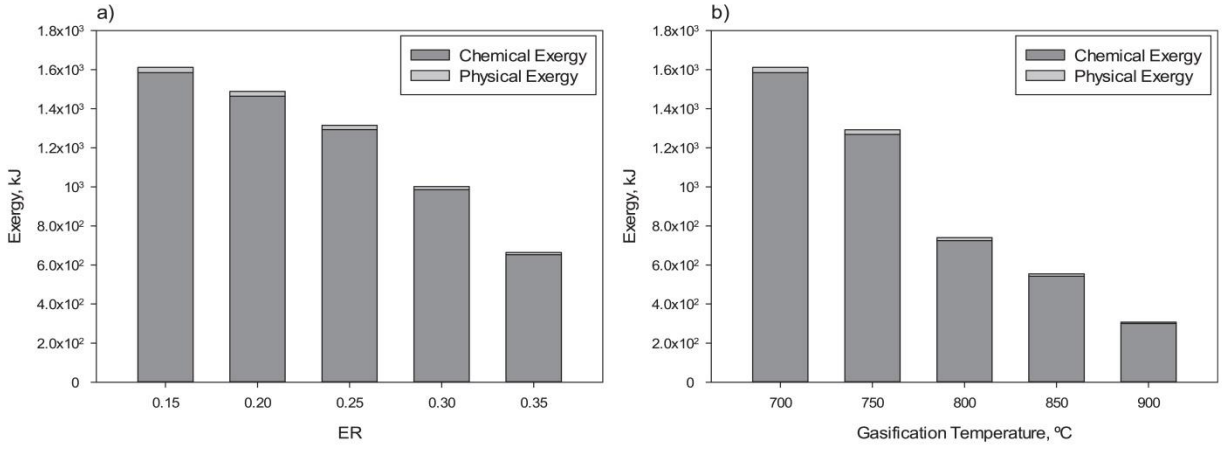

Fig. 11. Energy values of tar content at various a) ER values and b) reactor temperatures.

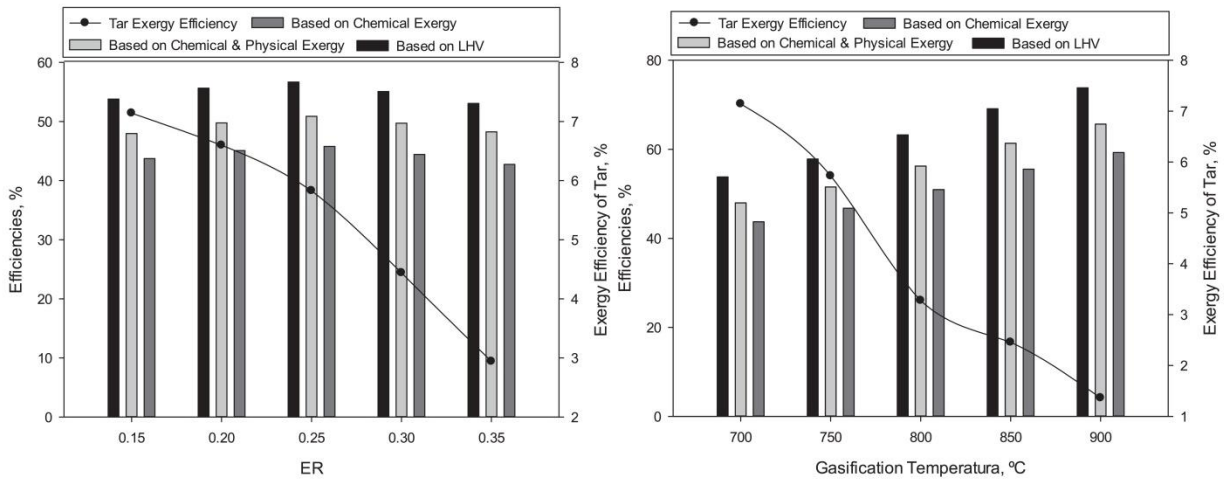

Fig. 12. Comparison between gasification efficiencies at various a) ER values and b) reactor temperatures.

values. This is expected since efficiency values are mostly determined by their energy/exergy values (Zhang et al., 2012). Efficiency based on LHV is higher than both exergy efficiencies. This was already addressed and is due to increase in entropy being disregarded in the energy efficiency. Obviously chemical and physical exergy based efficiency is higher than just chemical exergy based efficiency since physical exergy presents a positive value (Ptasinski et al., 2007).

Regarding ER influence on gasification efficiencies, when ER was increased from 0.15 to 0.25 LHV based efficiency increased from 53.8% to 56.7%, chemical exergy based efficiency rose from 43.7% to 45.8% and chemical and physical exergy based efficiency increased from 48% to 50.9%. After 0.25 all efficiencies decreased almost linearly. According to Double and Bridgwater (1985), this point represents the optimum point of operation for an air-blown biomass gasifier, giving an excellent indication where the gasifier should operate to be at the highest efficiency level possible. This is consistent with the current literature (Prins et al., 2003; Alauddin et al., 2010).

Reactor temperature influence on the other hand presents a very different tendency. In fact, when temperature was increased from 700 °C to 900 °C LHV based efficiency increased from 53.8% to 73.8%, Chemical exergy based efficiency rose from 43.7% to 59.3% and chemical and physical exergy based efficiency increased from 48% to 65.7%. Indeed all studied efficiencies steadily rose within the studied range at a much higher rate when compared to ER. This is due to increase in gasification temperature promoting both endothermic reactions and gas yield. This is consistent with the current literature (Alauddin et al., 2010; Wu et al., 2014).

Tar exergy efficiencies follow a very close trend to tar exergy values presented in Fig. 11. Both ER and reactor temperature led to a drastically decrease in tar efficiency. When ER was increased from 0.15 to 0.35 tar efficiency decreased from 7.2% to 2.9%. Conversely, when temperature was increased from 700 to 900 °C tar efficiency decreased from 7.2% to 1.4%. This was already explained and has to do with the fact that higher gasification temperatures dramatically reduce tar yields. This is consistent with the current literature (Zhang et al., 2010b, 2012).

To better understand the gasifier's overall energy flow a Sankey diagram was created. These diagrams are great visualization process tools and in this particular case were used to map energy consumption and corresponding transformation from source (MSW and air) to end use (syngas and tar). Fig. 13 displays the created Sankey diagram for the optimal set of operational

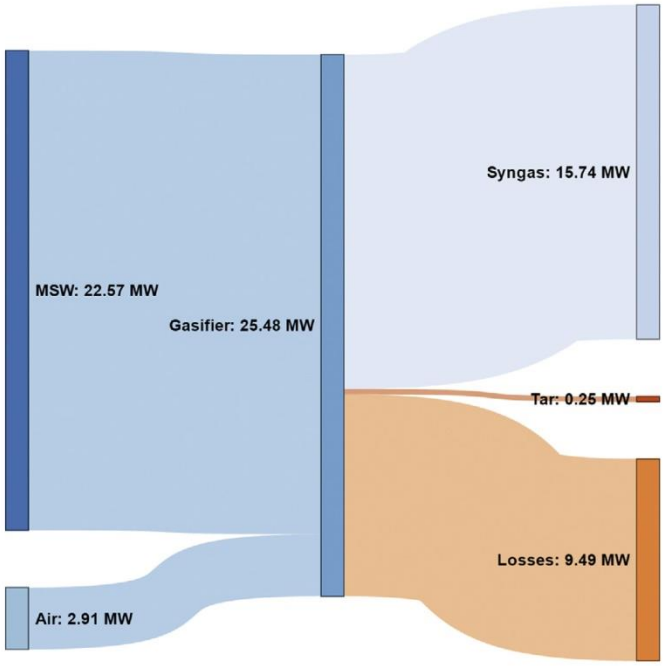

Fig. 13. Sankey diagram (Operational conditions: ER – 0.25; Gasification temperature – 900 °C).

conditions found in the thermodynamic analysis.

Even with a simplified diagram one can clearly see the overall energy flow thus quickly identifying system's efficiency (instead of power one could display the same diagram in terms of efficiency) and the overall losses. Ideally one would apply these diagrams to the entire plant to identify the sectors with the highest potential for improvement as well as identifying measures to reduce GHG emissions (Subramanyam et al., 2015).

6. Conclusions

Accelerated population growth combined with high socio-economic development and rapid urbanization has led to one of the greatest challenges facing modern society, the management of municipal solid waste. Not only does its incorrect management negatively impact public health and the environment but its

treatment usually represents the single largest budgetary item of a city. As a possible solution to this problem, gasification of MSW from Portugal, in particular from the Oporto metropolitan area, was investigated.

A previously developed numerical model was employed and its results validated using data collected from the literature, and then expanded to predict process results using a pilot scale gasifier. Influence of reactor temperature and equivalent ratio on both energy and exergy values of produced gas and tar content was studied. Regarding syngas values, one could see that the effect of reactor temperature on the total syngas energy was much greater than that of ER (over 30% increase versus less than 10%). Tar values on the other hand decreased as high as 80% when temperature was increased from 700 to 900 °C.

Energetic and exergetic efficiencies of gas components and tar content at various ER values and reactor temperatures were also studied. The set of operational conditions that promoted the highest overall efficiency were found at 0.25 and 900 °C. In this particular point a Sankey diagram was created for visualization purposes.

By applying a robust and proven numerical model to the thermodynamic analysis of MSW gasification the work presents a set of interesting results on the optimal operating point of an industrial size system. The pre-existing collection and transportation infrastructure that is currently available for municipal waste combined a safe residue disposal via an optimal route for waste-to-energy with the possibility for efficiency optimization as shown in this paper makes the gasification of MSW in Portugal a very attractive process.

Acknowledgements

We would like to express our gratitude to the Portuguese Foundation for Science and Technology (FCT) for the support to the grant SFRH/BD/86068/2012 and the projects PTDC/EMS-ENE/6553/2014 and IF 01772.

References

Abuadala, A., Dincer, I., Naterer, G., 2010. Exergy analysis of hydrogen production from biomass gasification. Int. J. Hydrogen Energy 35, 4981–4990.
Alauddin, Z., Lahijani, P., Mohammadi, M., Mohamed, A., 2010. Gasification of lignocellulosic biomass in fluidized beds for renewable energy development: a review. Renew. Sust. Energy Rev. 14, 2852–2862.
Arafat, H., Jijakli, K., 2013. Modeling and comparative assessment of municipal solid waste gasification for energy production. Waste Manag. 33, 1704–1713.
Baliban, R., Elia, J., Floudas, C., 2010. Toward novel biomass, coal, and natural gas processes for satisfying current transportation fuel demands, 1: process alternatives, gasification modeling, process simulation, and economic analysis. Ind. Eng. Chem. Res. 49, 7343–7370.
Couto, N., Silva, V., Monteiro, E., Teixeira, S., Chacartegui, R., Bouziane, K., Brito, P.S.D., Rouboa, A., 2015. Numerical and experimental analysis of municipal solid wastes gasification process. Appl. Therm. Eng. 78, 185–195.
Couto, N., Silva, V., Monteiro, E., Brito, P., Rouboa, A., 2015. Using an Eulerian-granular 2-D multiphase CFD model to simulate oxygen air enriched gasification of agroindustrial residues. Renew. Energy 77, 174–181.
Couto, N., Silva, V., Monteiro, E., Rouboa, A., 2015. Assessment of municipal solid wastes gasification in a semi-industrial gasifier using syngas quality indices. Energy 93, 864–873.
Couto, N., Silva, V., Bispo, C., Rouboa, A., 2016. From laboratorial to pilot fluidized bed reactors: analysis of the scale-up phenomenon. Energy Conv. Manag. 119, 177–186.
Devi, L., Ptasinski, K., Janssen, F., 2003. A review of the primary measures for tar elimination in biomass gasification processes. Biomass Bioenergy. 24, 125–140.
Double, J.M., Bridgwater, A.V., 1985. Sensitivity of theoretical gasifier performance to system parameters. In: Palz, W., Coombs, J., Hall, D.O. (Eds.), Energy from Biomass: 3rd E.C. Conference. Elsevier, London, pp. 915–919.
EEA Report No 2/2013. Portugal – Municipal Waste Management. Available online: http://www.eea.europa.eu/publications/managing-municipal-solid-waste, (accessed 03.08.16.).
Field, M.A., 1969. Rate of combustion of size-graded fractions of char from a low rank coal between 1200K–2000K. Combust. Flame 13, 237–252.
Gang, X., Bao-sheng, J., Zhao-ping, Z., Yong, C., Ming-jiang, M., Kefa, C., Rui, X., Ya-ji, H., He, H., 2007. Experimental study on MSW gasification and melting technology. J. Environ. Sci. 19, 1398–1403.
Gómez-Barea, A., Leckner, B., 2010. Modeling of biomass gasification in fluidized bed. Prog. Energy Combust. 36, 444–509.
Gonzalez, J.F., Roman, S., Bragado, D., Calderon, M., 2008. Investigation on the reactions influencing biomass air and air/steam gasification for hydrogen production. Fuel Process. Technol. 89, 764–772.
Hu, M., Guo, D., Ma, C., Hu, Z., Zhang, Be, Xiao, B., Luo, S., Wang, J., 2015. Hydrogen-rich gas production by the gasification of wet MSW (municipal solid waste) coupled with carbon dioxide capture. Energy 90, 857–863.
Ionescu, G., Rada, E., Ragazzi, M., Marculesc, C., Badea, A., Apostol, T., 2013. Integrated municipal solid waste scenario model using advanced pretreatment and waste to energy processes. Energy Conv. Manag. 76, 1083–1092.
Jia, J., Abudula, A., Wei, L., Sun, B., Shi, Y., 2015. Thermodynamic modeling of an integrated biomass gasification and solid oxide fuel cell system. Renew. Energy 81, 400–410.
Kumar, A., Eskridge, K., Jones, D., Hanna, M.A., 2009. Steam-air fluidized bed gasification of distillers grains: effects of steam to biomass ratio, equivalence ratio and gasification temperature. Bioresour. Technol. 100, 2062–2068.
Launder, B.E., Spalding, D.B., 1972. Lectures in Mathematical Models of Turbulence. Academic Press, London, England.
LIPOR, 2016. Sorting Plant Description. Available online: http://www.lipor.pt/pt/residuos-urbanos/valorizacao-multimaterial/descricao-do-processo/ (accessed 03.08.16.).
Magrinho, A., Ddilet, F., Semiao, V., 2006. Municipal solid waste disposal in Portugal. Waste Manag. 26, 1477–1489.
Niu, M., Huang, Y., Jin, B., Wang, X., 2013. Simulation of syngas production from municipal solid waste gasification in a bubbling fluidized bed using aspen plus. Ind. Eng. Chem. Res. 52, 14768–14775.
Onel, O., Niziolek, A.M., Hasan, M., Floudas, C.A., 2014. Municipal solid waste to liquid transportation fuels - part I: mathematical modeling of a municipal solid waste gasifier. Comput. Chem. Eng. 71, 636–647.
Pellegrini, L., Oliveira, S., 2007. Exergy analysis of sugarcane bagasse gasification. Energy 32, 314–327.
Pérez, J., Benjumea, P., Melgar, A., 2015. Sensitivity analysis of a biomass gasification model in fixed bed downdraft reactors: effect of model and process parameters on reaction front. Biomass Bioenergy 83, 403–421.
Prins, M., Ptasinski, K., Janssen, F., 2003. Thermodynamics of gas-char reactions: first and second law analysis. Chem. Eng. Sci. 58, 1003–1011.
Ptasinski, K.J., Prins, M.J., Pierik, A., 2007. Exergetic evaluation of biomass gasification. Energy 32, 568–574.
Rao, M., Singh, S., Sodha, M., Dubey, A., Shyam, M., 2004. Stoichiometric, mass, energy and exergy balance analysis of countercurrent fixed-bed gasification of post-consumer residues. Biomass Bioenergy 27, 155–171.
Scott, D., Czernik, S., Piskorz, J., Radlein, D., 1990. Fast pyrolysis of plastic wastes. Energy Fuel 4, 407–411.
Shareefdeen, Z., Elkamel, A., Tse, S., 2015. Review of current technologies used in municipal solid waste-to-energy facilities in Canada. Clean. Technol. Environ. 17, 1837–1846.
Silva, V., Rouboa, A., 2015. Combining a 2-D multiphase CFD model with a response surface methodology to optimize the gasification of Portuguese biomasses. Energy Conv. Manag. 99, 28–40.
Silva, V., Monteiro, E., Couto, N., Brito, P., Rouboa, A., 2014. Analysis of syngas quality from Portuguese biomasses: an experimental and numerical study. Energy Fuel 28, 5766–5777.
Soltani, A., Sadiq, R., Hewage, K., 2016. Selecting sustainable waste-to-energy technologies for municipal solid waste treatment: a game theory approach for group decision-making. J. Clean. Prod. 113, 388–399.
Sreejith, C., Muraleedharan, C., Arun, P., 2013. Energy and exergy analysis of steam

gasification of biomass materials: a comparative study. Int. J. Amb. Energy 34, 35–52.
Stepanov, V.S., 1995. Chemical energy and exergy of fuels. Energy 20, 235–242.
Subramanyam, V., Paramshivan, D., Kumar, A., Mondal, M., 2015. Using Sankey diagrams to map energy flow from primary fuel to end use. Energy Conv. Manag. 91, 342–352.
Sun, S., Tian, H., Zhao, Y., Sun, R., Zhou, H., 2010. Experimental and numerical study of biomass flash pyrolysis in an entrained flow reactor. Bioresour. Technol. 101, 3678–3684.
Szargut, J., Styrylska, T., 1964. Approximate evaluation of the exergy of fuels. Brennst Warme Kraft 16, 589–596.
United Nations, Department of Economic and Social Affairs, Population Division, 2015. World Population Prospects: the 2015 Revision, Key Findings and Advance Tables. Working Paper No. ESA/P/WP.241.
Wang, L., Weller, C., Jones, D., Hanna, M., 2008. Contemporary issues in thermal gasification of biomass and its application to electricity and fuel production. Biomass Bioenergy 32, 573–581.
Wang, J., Cheng, G., You, Y., Xiao, B., Liu, S., He, P., Guo, D., Guo, X., Zhang, G., 2012. Hydrogen-rich gas production by steam gasification of municipal solid waste (MSW) using NiO supported on modified dolomite. Int. J. Hydrogen Energy 37, 6503–6510.
Wang, Z., He, T., Qin, J., Wu, J., Li, J., Zi, Z., Liu, G., Wu, G., Sun, L., 2015. Gasification of biomass with oxygen enriched air in a pilot scale two-stage gasifier. Fuel 150, 386–393.
Wu, Y., Yang, W., Blasiak, W., 2014. Energy and exergy analysis of high temperature agent gasification of biomass. Energies 7, 2107–2122.
Zhang, X.H., Deng, S.H., Wu, J., Jiang, W., 2010. A sustainability analysis of a municipal sewage treatment ecosystem based on emergy. Ecol. Eng. 36, 685–696.
Zhang, Y., Kajitani, S., Ashizawa, M., Oki, Y., 2010. Tar destruction and coke formation during rapid pyrolysis and gasification of biomass in a drop-tube furnace. Fuel 89, 302–309.
Zhang, Y., Li, B., Li, H., Zhang, B., 2012. Exergy analysis of biomass utilization via steam gasification and partial oxidation. Thermochim. Acta 538, 21–28.
Zhang, Q., Wu, Y., Dor, L., Yang, W., Blasiak, W., 2013. A thermodynamic analysis of solid waste gasification in the plasma gasification melting process. Appl. Energy 112, 405–413.
Zhang, Y., Zhao, Y., Gao, X., Li, B., Huang, J., 2015. Energy and exergy analyses of syngas produced from rice husk gasification in an entrained flow reactor. J. Clean Prod. 95, 273–280.

Paper VI

Assessment on steam gasification of municipal solid waste against biomass substrates

N. Couto, V. Silva, A. Rouboa

Energy Conversion Management 124 (2016) 92-103

Energy Conversion and Management 124 (2016) 92–103

Contents lists available at ScienceDirect

Energy Conversion and Management

journal homepage: www.elsevier.com/locate/enconman

Assessment on steam gasification of municipal solid waste against biomass substrates

Nuno Dinis Couto [a], Valter Bruno Silva [a,*], Abel Rouboa [a,b,c]

[a] INEGI-FEUP, Faculdade de Engenharia da Universidade do Porto, Porto, Portugal
[b] MEAM Department, University of Pennsylvania, Philadelphia, PA 19020, USA
[c] UTAD, University of Trás-os-Montes and Alto Douro, Portugal

ARTICLE INFO

Article history:
Received 12 April 2016
Received in revised form 29 June 2016
Accepted 30 June 2016
Available online 9 July 2016

Keywords:
Steam gasification
Municipal solid waste
Biomass
CFD
Semi-industrial gasifier

ABSTRACT

Waste management is becoming one of the main concerns of our time. Not only does it takes up one of the largest portions of municipal budgets but it also entails extensive land use and pollution to the environment using current treatment methods. Steam gasification of Portuguese municipal solid wastes was studied using a previously developed computational fluid dynamics (CFD) model, and experimental and numerical results were found to be in agreement. To assess the potential of Portuguese wastes, these results were compared to those obtained from previously investigated Portuguese biomass substrates and steam-to-biomass ratio was used to characterize and understand the effects of steam in the gasification process. The properties of syngas produced from municipal solid waste and from biomass substrates were compared and results demonstrated that wastes present the lowest carbon conversion, gas yield and cold gas efficiency with the highest tar content. Nevertheless, the pre-existing collection and transportation infrastructure that is currently available for municipal waste does not exist for the compared biomass resources which makes it an interesting process. In addition a detailed economic study was carried out to estimate the environmental and economic benefits of installing the described system. The hydrogen production cost was also estimated and compared with alternative methods.

1. Introduction

The world is going through an intense process of urbanization and municipal solid waste (MSW), one of the most important by-products of an urban lifestyle, is growing at higher rate. According to the latest reports [1], in just 10 years the production of MSW increased from 680 to 1300 million tons per year, which represents an average increase of 0.64–1.2 kg of MSW per person per day. Current projections estimate an increase to 1.42 kg of MSW per person per day by 2025, which would translate into an annual generation of 2.2 thousand million tons.

The treatment of these residues is quite expensive and often represents the single largest budgetary item of a city. Worldwide MSW management costs from 2012 exceeded 190 thousand millio n euros and are expected to reach 350 thousand million by 2025 [1]. Of all methods of waste disposal, landfill is still the most used today, although it is becoming less and less popular due to the lack of available land and due to the emission of CH_4 and other landfill gases, which can cause numerous contamination problems. Incineration has gained ground over landfills [2] since it can reduce the solids volume in waste, decreasing the space it takes up and reducing the stress on already overflowing landfills. However, waste incineration is expensive and poses challenges of air pollution and ash disposal.

Gasification is becoming an increasingly attractive technology to treat MSW with fewer emissions than other methods of treatment [3]. It has been mostly used in waste-to-energy (WTE) plants, and one of its most promising results was achieved for the production of H_2-rich gas [4].

Research has shown that steam gasification of MSW provides one of the most cost-competitive means of obtaining H_2-rich gas while meeting environmental requirements set by international committees [5]. He et al. [6,7] are responsible for a considerable body of work on this matter, studying from the influence of various operating conditions to the use of catalysts developed for the production of H_2-rich gas. Later, that same group also developed a modified dolomite catalyst able to significantly eliminate tar produced in the gasification process while increasing H_2 production [8]. Moreover, steam gasification can help minimize tar formation

* Corresponding author at: Rua Dr. Roberto Frias, Campus da FEUP, 400, 4200-465 Porto, Portugal.
E-mail addresses: nunodiniscouto@hotmail.com (N.D. Couto), vsilva@inegi.up.pt (V.B. Silva), rouboa@seas.upenn.edu (A. Rouboa).

http://dx.doi.org/10.1016/j.enconman.2016.06.077
0196-8904/

[9], which is a major concern regarding MSW gasification that needs to be addressed so as to render it the main waste management and treatment process.

So far presented studies were mainly conducted in laboratory-scale facilities but it is imperative to devote efforts to study the process in semi-industrial or industrial conditions in order to convey this technology to commercial stage. In fact, data collected from laboratory studies can rarely be used to design commercial reactors, which can be tens or even hundreds of times larger, since it is necessary to gather information from reactors with similar dimensions to avoid errors and reduce high level risks and uncertainty [10].

Numerical models can be used to facilitate this process without major investments and/or the need for long waiting periods as they provide the ability to simulate any physical condition relatively quickly and inexpensively. However, due to their extreme complexity, realistic models on MSW gasification are still very scarce.

Our research team was able to use our previously published numerical model for biomass air gasification by upgrading it to handle the heterogeneity of MSW [11]. After validating the new model for semi-industrial conditions, an assessment of the potential of syngas produced from Portuguese MSW (PMSW for abbreviation) [12] was carried out.

The aim of this study is to investigate the potential of steam gasification in the treatment of PMSW. A new validation was performed to demonstrate the potential of the previously developed numerical model and semi-industrial conditions were used. To gain better understanding of the potential of the studied residues, a comparison to characteristic Portuguese biomasses was performed and steam-to-biomass ratio (SBR) was used to characterize and understand the effects of steam in the gasification of different substrates. Finally, the reduction of landfills as well as annual savings in imported fuels by using the described process was investigated. The overall hydrogen production cost was predicted and subsequently compared to alternative conversion methods.

2. Materials and methods

2.1. Portuguese municipal solid waste characterization

Until 1996 the management of municipal solid waste in Portugal was carried out by governmental institutions and, due to lack of appropriate legislation, the deposition in open dumps was the dominant method of treatment. Since then the management of MSW has undergone substantial change due to the approval of the National Waste Management Plans (PERSU). Despite the plan's success in eradicating open dumps, most of the targets set were not achieved [13]. Therefore, taking into account the need to modernize the MSW system, PERSU II was ratified in 2006 to target the period of 2007–2016.

In the decade from 2001 to 2010, landfilling remained the dominant option (60% and over) but with a decreasing trend, mainly due to recycling, which steadily increased to 12% in 2010. In 2012, 4.53 million tons of waste were produced in Portugal, 12.5% less than the recorded amount of 5.18 million tons in 2010 and also below the 4.88 million documented in 2011, according to data from the Environment Ministry. These figures show a reversal in the increasing production of municipal waste trend that occurred during the period between 2002 and 2010 (up to 18%) [14], which can be explained by the deterioration of the macroeconomic situation of the country, which reduced the level of consumption and, consequently, the production of waste.

The characterization and analysis of PMSW was carried out using data from the Oporto metropolitan area. LIPOR (Intermunicipal Waste Management Service of Greater Porto) is an association of Municipalities, established in 1982, whose main objective is the management, treatment and recovery of solid waste municipal produced in eight municipalities in the Oporto metropolitan area. Wastes are pre-treated accordingly to the Portuguese management system described by Teixeira et al. [2].

Early reports from 2015 indicate a production of about 361,000 tons of MSW from January to September at an average of 1.363 kg/hab.day [15]. Analyzing previous years and assuming similar tendencies, it is expected a total production of 480,000 tons at an average of 1.357 kg/hab.day by the end of the year. During the management and treatment of MSW collected in 2014, samples were collected to characterize the waste and results are presented in Fig. 1.

Refuse Derived Fuel (RDF) containing cellulosic materials and plastics is obtained from the pre-treatment of MSW via shredding and dehydration. During the pre-treatment process components such as metals, glass, combustive and non-combustive non specified materials as well as hazardous residues and fine elements are removed. After removing said components, cellulosic materials are represented by all the remaining constituents (obviously excluding plastics). Plastic residues are mainly comprised by polyethylene, polystyrene, and polyvinyl chloride [16] while cellulosic materials are composed of cellulose, hemicelluloses, and lignin [17].

Since an ultimate analysis does not distinguish between cellulosic materials, their composition was presupposed to be similar to the one found by Onel et al. [18], whereas report informs of the relative quantities of each monomer in the MSW for plastics, as listed in Table 1. This waste characterization was employed in the formulation of the MSW mixture in Fluent to model the gasification process.

2.2. Biomass substrates characteristics

Biomass utilization represents a crucial component in Portugal's strategic plan in reducing its foreign energy dependence. Portuguese biomass resources are diverse but an important contribution can be found from agricultural-related residues. Coffee husks, forest and vineyard pruning residues are largely available and have attractive low costs.

Portuguese forest covers 3.2 million ha, which corresponds to 35.4% of the national territory and is the basis of an economic sector that generates about 113,000 direct jobs (2% of the workforce).

The wine sector is one of the most important in the Portuguese economy, contributing very significantly to the final value of agricultural production and exportation, with a remarkably high contribution to the balance of trade; it is one of the few agri-food sectors with a positive trade balance. There is a great interest by Portuguese entities to study the best ways to valorize the residues and sub-products generated by this industry.

When processed, coffee generates a significant amount of agricultural wastes. Coffee husks, comprised of dry outer skin, pulp and parchment, are probably the major residues from the handling and processing of coffee. One of the major problems facing industries nowadays is how to dispose of these residues (there are more than two millions tons yearly [19]), since they contain some amount of caffeine, polyphenols and tannins, which makes them toxic in nature.

The total primary energy demand in Portugal amounted to 243,311 GW h in 2014 [20]. According to Ferreira et al. [21], forest and pruning residues alone can potentially produce 13,768 GW h per year (about 5.7% of the total primary energy demand in the country). Additionally, the energy production from bioresources (biomass, solid urban waste, and biogas) was 29,400 GW h in 2014. Previous data showed that both forest and pruning residues can play an important role in the Portuguese energy scenario.

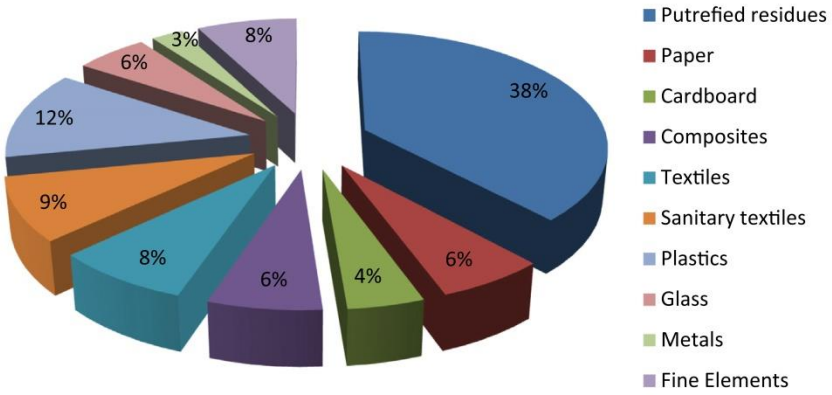

Fig. 1. Physical characterization of the MSW from Oporto in 2014.

Table 1
Chemical composition of the MSW.

Category	% weight	Chemical formula
Cellulosic material	85.42	–[a]
Polyethylene	10.99	$(C_2H_4)_n$
Polyethylene terephthalate	2.02	$(C_{10}H_8O)_n$
Polypropylene	0.81	$(C_3H_6)_n$
Polystyrene	0.76	$(C_8H_8)_n$

[a] It was considered the proportion of cellulose, hemicellulose and lignin found in Onel et al. [18].

These residues, especially coffee husks, require proper treatment or recovery to minimize environmental impact and increase their corresponding economic value. A large variety of technologies has been developed in recent decades to deal with this problem. Among the proposed technologies, those oriented toward energy recovery, including combustion and gasification of biomasses has attracted much interest.

2.3. Experimental set-up

Studies using semi- or industrial reactors are necessary to address one of the major concerns regarding gasification, which is the scale-up phenomenon. It is not an exact science and, since hydrodynamic phenomena are quite different for larger scale reactors, results from pilot- rather than laboratory-scale are crucial in avoiding errors and reducing risks and uncertainty when designing industrial reactors.

Our research team has therefore been testing a semi-industrial gasification plant, installed in the Industrial Park of Portalegre, Portugal. The design and operating parameters of the pilot scale bubbling fluidized bed gasifier are reported in Table 2. The plant is based on fluidized bed technology, with a processing capacity of approximately 100 kg/h, usually operating between 750 °C and 850 °C. Fig. 2 portrays the biomass gasification unit used in the experiments.

Table 2
Main design and operating parameters of the pilot scale gasifier.

Geometrical parameters	Internal diameter: 0.5 m Total height: 4.15 m Wall thickness: 0.01 m
Feedstock capacity	Up to 100 kg/h
Thermal output	About 300 kW
Typical bed amount	70 kg
Bed material	Dolomite
Oxidizing agent	Air (but also allows different agents)
Feeding system	Archimedes screw feeder
Range of bed temperatures	500–1000 °C
Oxidizing agent temperature	300 °C
Range of fluidizing velocities	0.2–1 m/s
Syngas treatments	Cyclone, scrubber, flare

The main components of the unit are the following (all components that make up the gasification plant are fully explained in [22]): (a) Biomass feeding system; (b) Fluidized bed reactor (tubular of 0.5 m in diameter and 4.15 m in height); (c) Gas cooling system; (d) Cellulosic bag filter; (e) Condenser.

To properly assess the potential of PMSW, previously studied Portuguese biomass substrates will be use as benchmarks. Coffee husks [22], forest residues [23] and vines pruning residues [24] were studied using the described pilot-scale thermal gasification plant, for which relevant energetic as well as economic benefits were found. Data regarding proximate and ultimate analysis for the referred substrates is presented in Table 3.

3. Mathematical model

The gasification process comprises a set of phenomena that includes fluid flow, heat transfer, and chemical reactions. Due to its complexity it can only be solved by applying several governing mathematical expressions, mostly based on conservation equations.

Our model was first developed to describe the gasification of Portuguese biomasses in a pilot-scale fluidized bed gasifier [22]. A Eulerian–Eulerian approach was implemented to handle both gas and dispersed phases, the kinetic theory of granular flows was used to evaluate the constitutive properties of the dispersed phase, and the gas-phase behavior was simulated employing the k–ε turbulent model.

The standard k–ε model in ANSYS FLUENT has become the workhorse of practical engineering flow calculations in the time since it was proposed by Launder and Spalding [25]. It is a semi-empirical model, and the derivation of the model equations relies on phenomenological considerations and empiricism. The selection of this turbulence model is appropriate when the turbulence transfer between phases plays a predominant role as in the case of gasification in fluidized beds.

In the granular Eulerian model, stresses in the granular solid phase are obtained by the analogy between the random particle motion and the thermal motion of molecules within a gas accounting for the inelasticity of solid particles. As in a gas, the intensity of velocity fluctuation determines the stresses, viscosity, and pressure of the granular phase. The kinetic energy associated with velocity fluctuations is described by a pseudothermal temperature or granular temperature, which is proportional to the norm of particle velocity fluctuations.

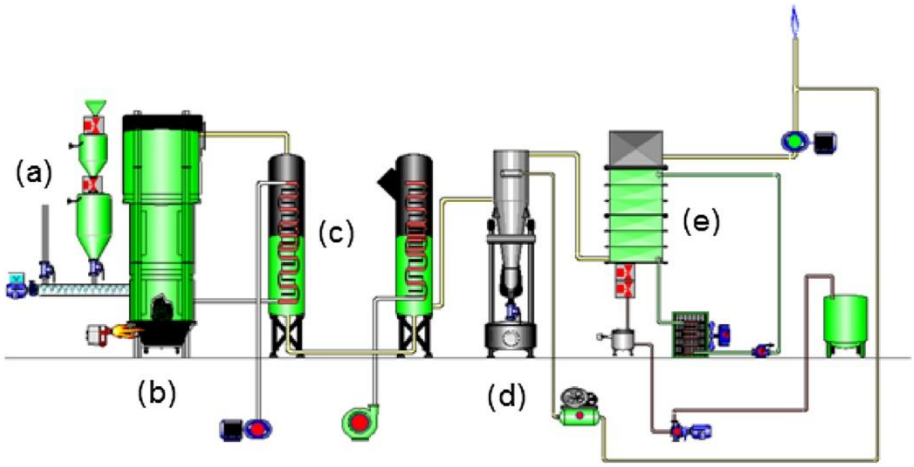

Fig. 2. Schematics of the gasification plant.

Table 3
Ultimate and proximate analyses of coffee husks, forest, vine-pruning residues, PMSW and Wang's MSW.

Substrate properties	Forest residues	Coffee husk	Vines pruning	PMSW	Wang's MSW
Elementary analysis (dry ash free)					
N (%)	2.4	5.2	2.6	1.39	0.78
C (%)	43	40.1	41.3	47.99	49.51
H (%)	5	5.6	5.5	6.3	6.42
O (%)	49.6	49.1	50.6	43.58	35.69
Humidity (%)	11.3	25.3	13.3	17.55	NA
Density (kg/m^3)	650	500	265	247	235.5
Lower heating value (MJ/kg biomass)	21.2	20.9	15.1	14.4	19.99
Proximal analysis (%)					
Ash	0.2	2.5	3.1	14.92	7.12
Volatile matter	79.8	83.2	83.6	76.62	77.52
Fixed carbon	20	14.3	13.3	8.46	15.36

The two-dimensional mathematical model was then extended for MSW gasification [12]. The solid phase was regarded as an Eulerian granular model while the gas phase was considered as a continuum. The main interaction between phases was also modeled, as well as heat exchange, mass, and momentum. To cope with the heterogeneity of MSW, the devolatilization section had to be modified.

It goes without saying that the current study is heavily based on the previous models and both hydrodynamic model and conservation equations for each phase were taken from [12,22]. Table 4 summarizes the key points (Further details on the model can be found in [12,22]).

On the other hand, the chemical model had to be redesigned since steam gasification does not include exothermic reactions. All relevant reactions and their reaction rates are listed in Table 5. According to Arena [26], the following is the sequence of steps that occur during the gasification of a solid waste:

- Heating and drying (MSW is dried and heated up to 160 °C).
- Devolatilization (MSW goes through thermal cracking to produce light gases, tar and char).
- Chemical reactions (between CO, CO_2, H_2 and steam with the hydrocarbon gases and carbon from MSW producing gaseous products).

In this study, our previously pyrolysis model with secondary tar generation was adopted [11]. The finite-rate/Eddy-dissipation model was used to describe homogeneous reactions while the Kinetic/Diffusion Surface Reaction Model was employed for heterogeneous ones. The Arrhenius rates and the kinetic parameters for these reactions as well as further explanation can be found in [11], and so can solver procedure details.

3.1. Numerical procedure

Fluent, a finite volume method based CFD solver, was employed in this work to solve the stated problem. Mesh was built using GAMBIT software and quadrilateral cells of uniform grid spacing were used. So as to simplify the presented problem, the up-flow atmospheric fluidized bed gasifier was regarded as a two-dimensional geometry, which in turn was discretized with up to 83,000 cells with average mesh intervals of 0.005 m.

In order to avoid poor convergence, an unsteady model was used with a time step size of 10^{-4} s and the gasification time of the biomass was resolved by 400,000 time steps. The convective terms in the momentum and energy equations were discretized using the second order upwind scheme and SIMPLE scheme was used to solve the pressure-velocity coupling. In this work, a relative convergence criterion of 10^{-6} for residuals of the continuity and momentum equations and of 10^{-8} for residual energy equation were prescribed. Gas-solid flow was previously solved excluding chemical reactions but, after finding the established flow pattern, chemical reactions were included and the full system was solved.

4. Results and discussion

4.1. Model validation

The described numerical model is the result of systemic changes that allowed an increasingly detailed study of the gasification process. Early in the decade, when the model was first developed, the aim was to study gasification of biomass substrates using a reliable set of experimental runs performed in the previously described plant [22,23]. The work was motivated by the lack of reliable numerical models capable of describing the gasification process in a pilot scale fluidized bed reactor.

Having a model capable of predicting gasification process in industrial conditions allows us to be much closer to realistic commercial size reactors since the hydrodynamic phenomena in a laboratory scale fluidized bed are not the same as on large scales [10].

Regarding MSW gasification, the model was first applied to the study of PMSW gasification using air as a gasifying agent [11,12]. To do so, the model had to be restructured to cope with the heterogeneity of solid wastes.

Table 4
Hydrodynamic model and conservation equations for both gas and solid phases.

Hydrodynamic model
Kinetic Energy:
$\frac{\partial}{\partial t}(\rho k)+\frac{\partial}{\partial x_i}(\rho k u_i)=\frac{\partial}{\partial x_j}\left[\left(\mu+\frac{\mu_t}{\sigma_k}\right)\right]+G_k+G_b-\rho\varepsilon-Y_M+S_k$
Dissipation rate:
$\frac{\partial}{\partial t}(\rho\varepsilon)+\frac{\partial}{\partial x_i}(\rho\varepsilon u_i)=\frac{\partial}{\partial x_j}\left[\left(\mu+\frac{\mu_t}{\sigma_\varepsilon}\right)\frac{\partial\varepsilon}{\partial x_j}\right]+C_{1\varepsilon}\frac{\varepsilon}{k}(G_k+C_{3\varepsilon}G_b)-C_{2\varepsilon}\rho\frac{\varepsilon^2}{k}+S_\varepsilon$
Granular Eulerian model:
$\frac{3}{2}\left[\left(\frac{\partial(\rho_s\alpha_s\Theta_s)}{\partial t}+\nabla\cdot(\rho_s\alpha_s\vec{v}_s\Theta_s)\right)\right]=(-P_s\bar{I}+\bar{\tau}_s):\nabla(\vec{v}_s)+\nabla\cdot(k_{\Theta a}\nabla(\Theta_s))-\gamma_{\Theta a}+\varphi_{ls}$

Conservation equations	
Gas phase	Solid phase
Energy:	
$\frac{\partial(\alpha_q\rho_q h_q)}{\partial t}+\nabla\cdot(\alpha_q\rho_q\vec{u}_q h_q)=-\alpha_q\frac{\partial(p_q)}{\partial t}+\bar{\bar{\tau}}_q:\nabla(\vec{u}_q)-\nabla\vec{q}_q+S_q+\sum_{p=1}^{n}(\vec{Q}_{pq}+\dot{m}_{pq}h_{pq})$	$\frac{\partial(\alpha_p\rho_p h_p)}{\partial t}+\nabla\cdot(\alpha_p\rho_p\vec{u}_p h_p)=-\alpha_p\frac{\partial(p_p)}{\partial t}+\bar{\bar{\tau}}_p:\nabla(\vec{u}_p)-\nabla\vec{q}_p+S_p+\sum_{q=1}^{n}\left(\vec{Q}_{pq}+\dot{m}_{pq}h_{pq}\right)$
Mass:	
$\frac{\partial(\alpha_q\rho_q)}{\partial t}+\nabla\cdot(\alpha_q\rho_q\vec{u}_q)=-M_C\sum\gamma_C R_C$	$\frac{\partial(\alpha_p\rho_p)}{\partial t}+\nabla\cdot(\alpha_p\rho_p\vec{u}_p)=M_C\sum\gamma_C R_C$
Momentum:	
$\frac{\partial(\alpha_q\rho_q\vec{u}_q)}{\partial t}+\nabla\cdot(\alpha_q\rho_q\vec{u}_q\vec{u}_q)=-\alpha_q\nabla p_q+\alpha\rho_q g+\beta(u_q-u_p)+\nabla\cdot\alpha_q\bar{\bar{\tau}}_q+S_{pq}U_S$	$\frac{\partial(\alpha_p\rho_p\vec{u}_p)}{\partial t}+\nabla\cdot(\alpha_p\rho_p\vec{u}_p\vec{u}_p)=-\alpha_p\nabla p_p+\alpha\rho_p g+\beta(u_q-u_p)+\nabla\cdot\alpha_p\bar{\bar{\tau}}_p+S_{pq}U_S$

Table 5
Chemical reaction model.

Reactions	Reaction rate
Pyrolysis:	
Cellulose $\rightarrow \alpha_1$ *volatiles* $+\alpha_2$ *TAR* $+\alpha_3$*char*	$r_1=A_i\,exp\left(\frac{-E_i}{T_s}\right)(1-a_i)^n$
Hemicellulose $\rightarrow \alpha_4$ *volatiles* $+\alpha_5$ *TAR* $+\alpha_6$ *char*	$r_2=A_i\,exp\left(\frac{-E_i}{T_s}\right)(1-a_i)^n$
Lignin $\rightarrow \alpha_7$ *volatiles* $+\alpha_8$ *TAR* $+\alpha_9$ *char*	$r_3=A_i\,exp\left(\frac{-E_i}{T_s}\right)(1-a_i)^n$
Plastics $\rightarrow \alpha_{10}$ *volatiles* $+\alpha_{11}$ *TAR* $+\alpha_{12}$ *char*	$r_4=\left[\sum_{i=1}^{n}A_i\,exp\left(\frac{-E_i}{RT}\right)\right]\rho_v$
Primary TAR $\rightarrow$ *volatiles* $+$ *Secondary TAR*	$r_5=9.55\times10^4 exp\left(\frac{-1.12\times10^4}{T_g}\right)\rho_{TAR1}$
Homogeneous reactions:	
$CO+H_2O\leftrightarrow CO_2+H_2$	$r_6=5.159\times10^{15}exp(\frac{-3430}{T})T^{-1.5}C_{O_2}C_{H_2}^{1.5}$
$C_2H_4+2H_2O\leftrightarrow 2CO+4H_2$	$r_7=3100.5\,exp\left(\frac{-15.000}{T}\right)C_{C_2H_4}C_{H_2O}^2$
$CH_4+H_2O\leftrightarrow CO+3H_2$	$r_8=3.1005\,exp\left(\frac{-15.000}{T}\right)\left[C_{H_2O}C_{CH_4}-\frac{C_{CO}C_{H_2}^2}{0.0265(32.900/T)}\right]$
Heterogeneous reactions:	
$C+CO_2\rightarrow 2CO$	$r_9=2082.7\,exp(\frac{-18036}{T})$
$C+H_2O\rightarrow CO+H_2$	$r_{10}=63.3\,exp(\frac{-14051}{T})$

Since, at that moment, the reactor couldn't handle said wastes, the model had to be validated using data collected from the literature. Still, the model proved to be able of predicting the behavior of all syngas species in a wide range of operating conditions with significant accuracy.

To validate the model for MSW gasification using steam, a similar approach was adopted and the work of Wang et al. [8] was chosen as a reference due to the extensive data available on MSW gasification with steam. Based on the characteristics of MSW from China, raw materials were prepared according to the average proportion of organic components (dry basis) for gasification, as displayed in Table 6.

In order to perform simulations with the Wang's MSW composition [8] using Fluent code, a global chemical formula is needed. In this case since the ultimate and proximate analysis is available (Table 3) one can simply use to get the necessary formula. Comparison between Wang's experimental results and those produced with our numerical model are available in Tables 7 and 8. Relative errors between numerical and experimental can be computed as:

$$Relative\ error\ (\%)=\frac{(numerical\ value-experimental\ value)}{experimental\ value}\times 100\% \quad (1)$$

The numerical model predicts the experimental data reasonably well being robust enough to predict the syngas composition at different operating conditions. Relative errors lower than 20% were found for all the presented fractions. This range of errors is very promising considering such complex systems and is in agreement with other works found in the literature [24]. Furthermore, the range of errors between experimental results gathered from the literature and the ones found for the described plant was quite similar. Nevertheless, some differences can be observed due to some simplifying assumptions followed by our model, which are explained in detail in [22].

Table 6
Wang et al. [8] MSW characteristics.

Organic compounds (%)					Low heating value (MJ/kg)
Kitchen garbage	Plastic	Wood and yard waste	Paper	Textile	
42.37	9.57	11.4	16.71	19.95	19.99

Table 7
Influence of temperature on syngas molar composition for both experimental and numerical runs.

Temperature (°C)	SBR	Experimental				Model			
		H_2	CO	CO_2	C_nH_m	H_2	CO	CO_2	C_nH_m
700	1.23	32.70	30.10	19.00	18.20	35.68	28.64	21.57	16.44
750	1.23	47.20	23.80	19.70	9.30	49.58	21.73	22.28	10.50
800	1.23	56.70	16.40	21.20	5.70	54.17	14.17	24.50	6.68
850	1.23	59.30	15.00	22.10	3.60	63.13	12.69	24.81	4.23

Table 8
Influence of SBR on syngas molar composition for both experimental and numerical runs.

Temperature (°C)	SBR	Experimental				Model			
		H_2	CO	CO_2	C_nH_m	H_2	CO	CO_2	C_nH_m
800	0	28.40	35.60	13.20	22.80	27.04	33.61	15.36	25.87
800	0.73	48.70	22.80	15.70	12.80	43.34	24.99	17.71	15.02
800	1.23	55.90	17.60	20.80	5.70	52.51	19.66	23.35	6.50
800	2.08	53.50	16.90	24.00	5.60	50.86	15.03	27.21	6.48

4.2. Influence of steam in the gasification of different substrates

Steam-to-biomass ratio (SBR) is used throughout this work in order to emphasize the effects of small variations on biomass admission, which often go unnoticed [27]. Moreover, SBR can help tremendously in characterizing and understanding the effects of steam in the gasification of different substrates. The SBR can be defined as the steam mass flow rate divided by the fuel mass flow rate (dry basis).

$$SBR = \frac{Steam\ mass\ flow\ rate}{Biomass\ substrate\ mass\ flow\ rate} \quad (2)$$

The SBR was varied over a range of values from 0 to 2 by holding the other variables constant. SBR can be caused to vary either by changing the fuel rate or by adjusting the steam flow. However, in order to ensure a more uniform residence time, steam flow rate was kept constant. Fig. 3 depicts the influence of SBR on syngas molar fraction for all the studied fuels.

Although slight variations can be observed, a rising SBR leads to an increase in H_2 and CO_2 and a decrease in CO and C_nH_m for all studied fuels. Increasing SBR will mostly favor char and tar steam reforming as well as the water-gas shift reaction, which in turn will lead to an increase in CO_2 and H_2 content at the expense of CO and C_nH_m. In fact, according to Hernández et al. [28], for steam gasification, the water-gas shift reaction will dominate over the Boudouard one and CO will be consumed to produce CO_2 and H_2. These results are consistent with the current literature [8]. An increase in CH_4 content relates to the decrease in oxidation of volatile matter, which is not balanced out by the consumption of CH_4 in the reforming reactions. These reactions have lower rates than oxidation ones but are most favored by low temperatures. However at higher steam levels the steam reforming can in fact shift CH_4 consumption will also be affected.

Excessive steam intake will lead to a significant drop in gasification temperature (solid line in Fig. 3), which in turn will have a negative effect on endothermic reactions, impairing product generation, which explains the decrease in H_2 after SBR = 1.5, and producing insufficient heat to promote steam reforming and primary water-gas reactions. Furthermore, excessive steam could shift the steam reforming and water gas reactions backwards, consuming CO and H_2 to produce CO_2 and H_2O [29]. In fact, the gasification temperature has a predominant effect on syngas composition, as illustrated in Fig. 4.

A boost in gasification temperature leads to an increase in both CO and H_2 molar fractions and a decrease in CO_2 and C_nH_m content for all studied substrates. Variations can be explained by the Le Chatelier's principle, which states that higher temperatures favor products in endothermic reactions. In fact, endothermic reactions like the Boudouard and the reverse water-gas shift ones will promote CO formation while primary water-gas and steam reforming reactions will favor H_2 production. According to Song et al. [30], the Boudouard reaction replaces water-gas reaction as the predominant reaction as temperature increases, which causes more carbon to react with CO_2 and form CO but react less with steam to produce H_2, which accounts for the increase in CO growth rate while that of H_2 decreases. These results are consistent with the current literature [31].

Figs. 3 and 4 allow for the conclusion that all presented fuels share similar trends regardless of the studied conditions. Regardless, there are substantial differences in syngas molar fraction depending on the chosen substrate. According to [10], the chemical composition of biomass and produced gas are intimately related. Louw et al. [32] found that maximum H_2 and CH_4 yields are attained when biomass with a low C:H ratio and low O_2 content is used while maximum CO and CO_2 yields are attained when biomass with low O_2 content and high C:H ratio is used as feedstock (Table 3). This may explain why coffee husks present the highest H_2 and C_nH_m content while forest residues present the display levels of CO and CO_2.

However, there are other biomass properties that can greatly influence the gasification process. For instance, it can be observed that biomass substrate and syngas calorific values are intimately related. Effectively, as illustrated in Fig. 5, the syngas with highest caloric value is obtained from forest residues, which is the most energetic fuel. This relationship can be explained considering that the calorific value of a fuel depends on the amount of C and H_2 within and that higher contents enable the production of larger quantities of H_2 and CO, the major contributors to the calorific value of the syngas. In fact, in this study, the syngas low heating value (LHV) is calculated like so:

$$LHV = \frac{(CO \times 12.63 + H_2 \times 10.79 + CH_4 \times 35.81 + C_2H_2 \times 56.09 + C_2H_4 \times 59.03 + C_2H_6 \times 63.74)}{100} \quad (3)$$

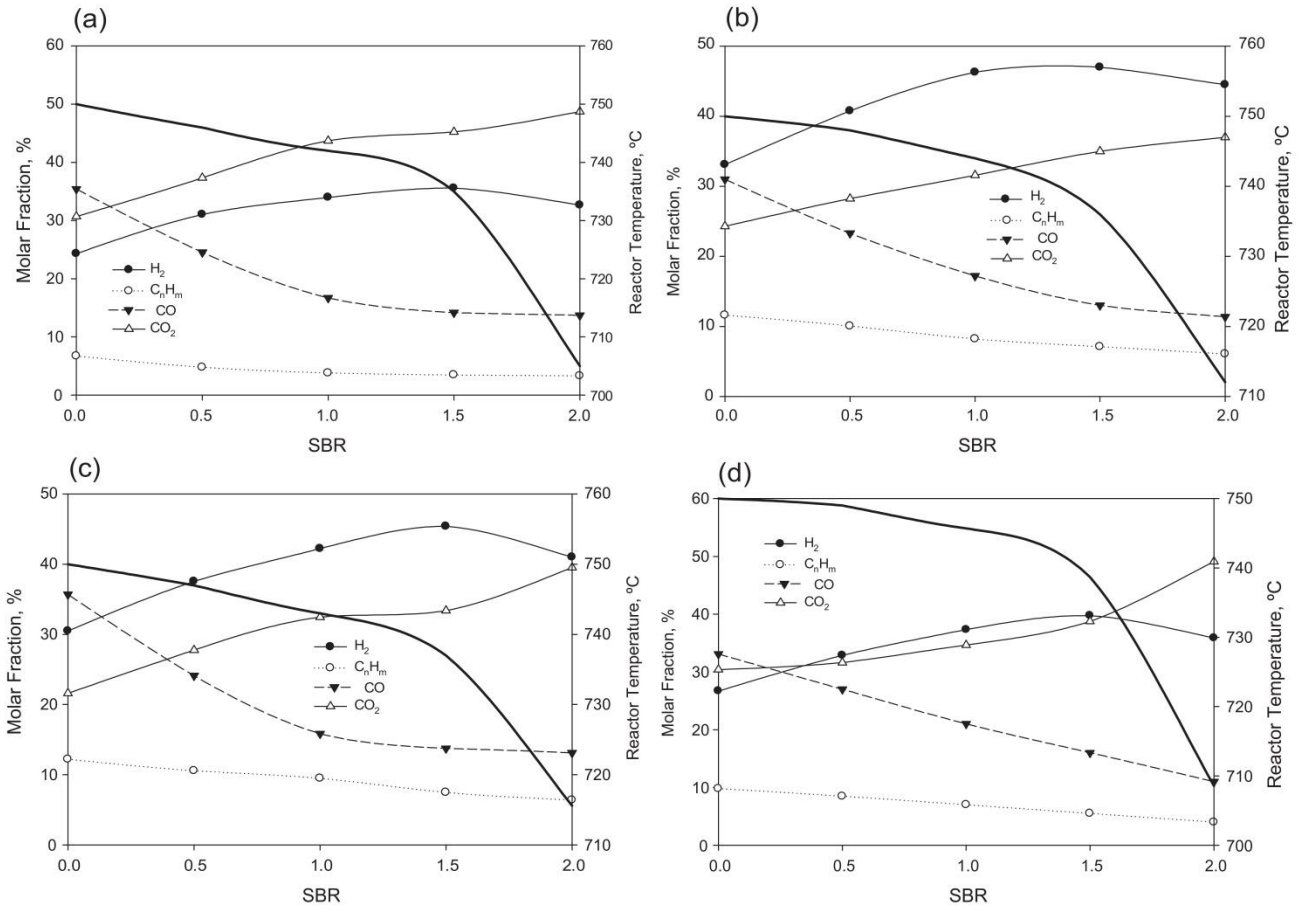

Fig. 3. Influence of SBR on syngas molar fraction for (a) MSW, (b) coffee husks, (c) forest residues and (d) vines pruning. Results shown exclude steam content. (Operating conditions: fuel feed rate = 25 kg/h; gasification temperature = 750 °C.)

Although MSW has a greater LHV than vines pruning (Table 3), its resulting syngas is actually poorer due to its low content in light hydrocarbons, leading to a significant drop on syngas LHV, since they have much higher calorific values than either CO or H_2.

SBR negatively influences LHV seeing that it leads to a CO and C_nH_m content decrease, two major contributors to the syngas calorific value, which is consistent with the current literature [33].

Fig. 6 depicts the effect of SBR on gas yield. Contrary to LHV, gas yield is positively influenced by SBR for all tested fuels, which is to be expected since the steam introduced during the gasification process is responsible for the release of volatiles and char conversion [34]. Vines pruning presents the highest gas yield (over 1.8 N m^3/kg) while MSW presents the lowest (slightly over 1.4 N m^3/kg). This will be addressed later in the chapter.

Gas yield appears to drop for higher steam levels (above SBR = 1.5), possibly because the excessive steam reduces the temperature inside the reactor. These results are in agreement with previous studies [35].

The opposing trends observed for LHV and gas yield (Figs. 5 and 6, respectively) lead to a maximum value for cold gas efficiency (CGE) as shown in Fig. 7. CGE can be defined as follows:

$$CGE = \frac{Gas\ yield \times LHV_{syngas}}{Fuel\ flow\ rate \times LHV_{fuel} + Heat\ addition} \quad (4)$$

As can be observed, coffee husks, forest residues and vines pruning present very similar values and a maximum efficiency at around SBR = 1. This value is consistent with findings of other researchers [28]. This limit is accounted for by the combined decrease in syngas calorific value (Fig. 5) and increase in gas yield (Fig. 6) with SBR.

On the other hand, a maximum value of CGE was found at SBR = 1.5 for MSW. The gasification efficiency calculated for MSW is much lower than for the other 3 substrates (in some cases over 20%) due to a combination of low gas yield and poor syngas LHV. It is worth mentioning that since only a handful of SBR values was studied (0, 0.5, 1, 1.5 and 2) it is impossible to determine the exact optimal ratio for each fuel.

Carbon conversion (CC) is defined as the ratio between mass flow rate of carbon in the syngas composition and the mass flow rate of carbon fed with the fuel. CC indicates the amount of unconverted material, providing a measure of chemical efficiency of the process, and can be expressed as follows:

$$Carbon\ Conversion = \frac{12 \times M}{X_C \times m} \quad (5)$$

where M represents the total molar flow rate of carbon in syngas composition; X_C the carbon fraction in the fuel; and m the fuel flow rate into the gasifier. The carbon conversion for the various fuels as a function of SBR is illustrated in Fig. 8.

Similarly to what happens with gas yield, vines pruning presents the highest carbon conversion while MSW displays the lowest. The presence of steam leads to more tar participating in steam gasification [36], which is conductive to rapid growth in gas yield (Fig. 6) and carbon conversion [33]. Furthermore, an increase in steam content enhances steam reforming reactions,

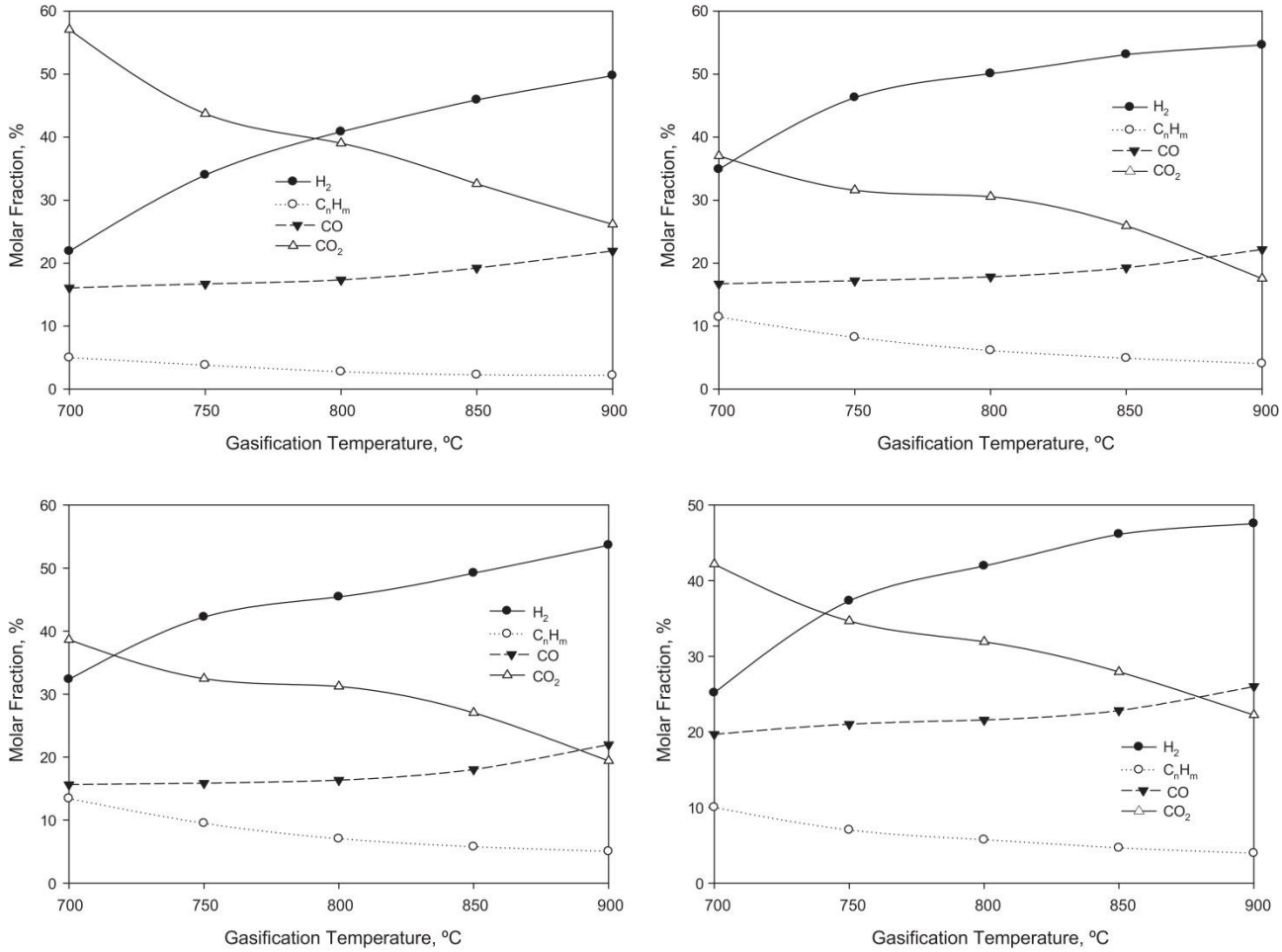

Fig. 4. Influence of gasification temperature on syngas molar fraction for (a) MSW, (b) coffee husks, (c) forest residues and (d) vines pruning. Results shown exclude steam content. (Operating conditions: fuel feed rate = 25 kg/h; SBR = 1.)

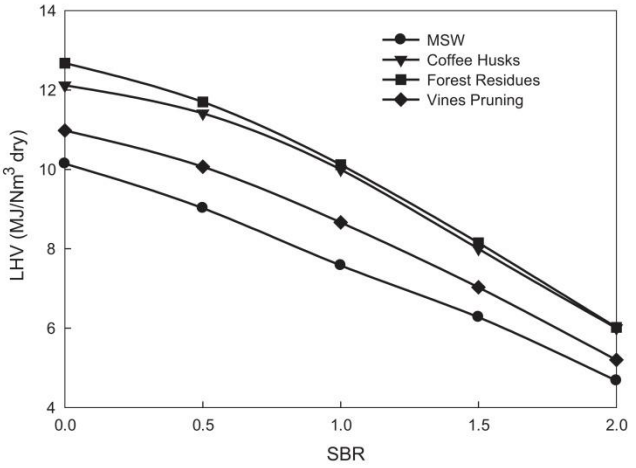

Fig. 5. Influence of SBR on syngas LHV for all studied substrates. Results shown exclude steam content. (Operating conditions: fuel feed rate = 25 kg/h; gasification temperature = 750 °C.)

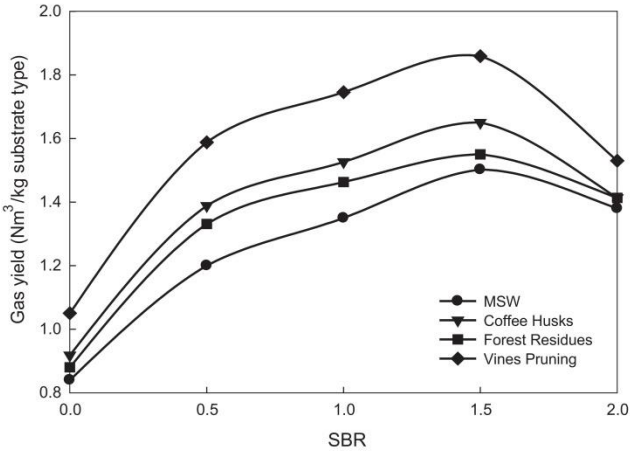

Fig. 6. Influence of SBR on gas yield for all studied substrates. Results shown exclude steam content. (Operating conditions: fuel feed rate = 25 kg/h; gasification temperature = 750 °C.)

which in turn promote carbon conversion [8]. However, similarly to gas yield and CGE, carbon conversion exhibits a decreasing trend which becomes sharper beyond 1.5. This is consistent with the work of Yan et al. [37], which states that an excessive amount of steam can lead to a reduction in gas yield and carbon conversion.

Although steam flow was kept constant to assure uniform residence time, substrates with different size particles lead to different residence times [33,38]. Moreover, increasing residence time promotes gasification and carbon conversion reactions, leading to a higher gas yield [39]. This may account for the discrepancies between results for the studied fuels.

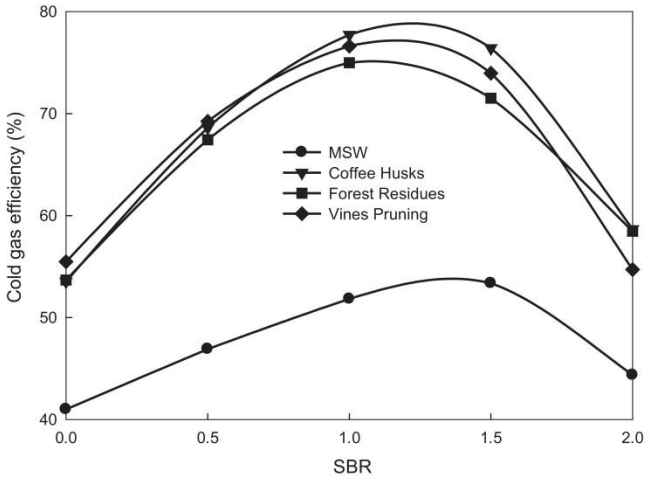

Fig. 7. Influence of SBR on cold gas efficiency for all studied substrates. Results shown exclude steam content. (Operating conditions: fuel feed rate = 25 kg/h; gasification temperature = 750 °C.)

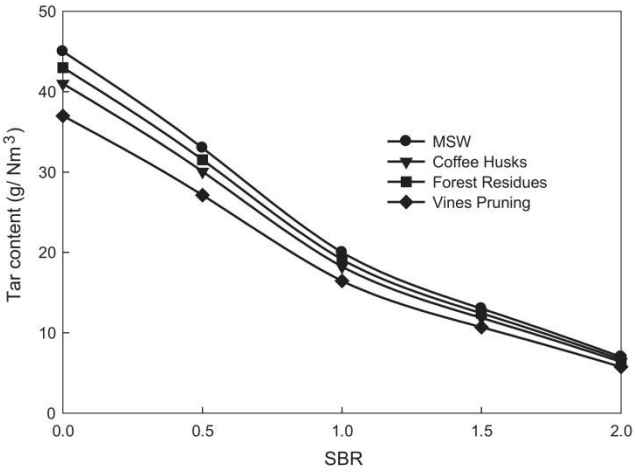

Fig. 9. Influence of SBR on carbon conversion for all studied substrates. Results shown exclude steam content. (Operating conditions: Fuel feed rate = 25 kg/h; gasification temperature = 750 °C.)

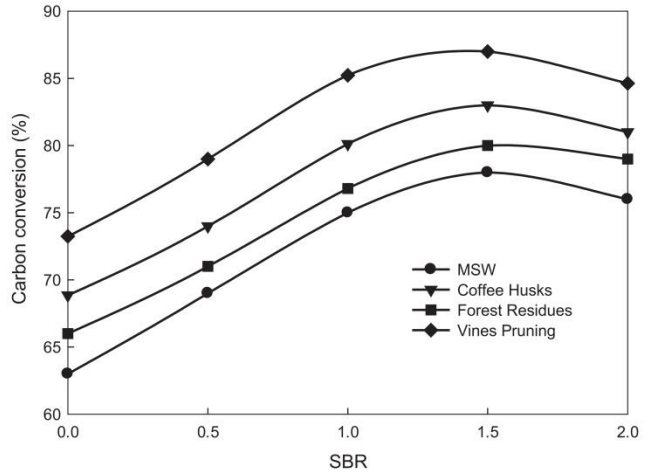

Fig. 8. Influence of SBR on carbon conversion for all studied substrates. Results shown exclude steam content. (Operating conditions: Fuel feed rate = 25 kg/h; gasification temperature = 750 °C.)

Although tar production is a major concern regarding the gasification process (especially for MSW) [9], steam gasification can aid in tar mitigation by promoting gas yield, which is known for improving tar decomposition. Following the work of Yan et al. [37], Aljbour and Kawamoto [40] observed a reduction in tar production due to an increase in residence time. On the other hand, higher volatile content leads to an increase in residence time that in turn will favor gasification reactions [41]. Since vines pruning has the highest volatile content from the studied fuels [22], it comes with no surprise that it also presents the lowest tar content. Results are presented in Fig. 9. Increasing SBR leads to tar steam reforming, which in turn leads to a reduction in tar content, a behavior consistent with that reported in the current literature [8].

4.3. Assessment of steam gasification in the treatment of PMSW

Even though the results from PMSW are not on par with those from other studied fuels, gasification can still be an advantageous alternative when handling municipal wastes. By allowing a safe residue disposal via an optimal route for waste-to-energy, steam gasification of MSW becomes a very attractive process and the pre-existing collection and transportation infrastructure that is currently available does not exist for the compared biomass resources, rendering it an even more interesting process [42].

There are two other relevant concerns that further increase the interest on MSW gasification in relation to biomass substrates, namely the undefined availability of sustainable biomass resources, seasonal availability and local energy supply [43] that can lead to great uncertainty on the overall availability and sustainability of biomass as a resource; and the fact that waste production is becoming one the main concerns of the 21st century seeing that, according to the latest report regarding MSW production [1], approximately 1.3 billion tons of MSW were produced in 2012, a value which is projected to double by 2025. Overcoming these issues justifies the need for studying gasification for MSW treatment.

Steam gasification is an effective process of renewable H_2 generation, capable of producing the highest yield of H_2 from biomass while simultaneously offering a cleaner product with minimal environmental impact. In fact, according to Nipattummakul et al. [44], it is an effective mode of producing renewable H_2 without leaving any carbon footprint in the environment.

H_2 can play a key role in the replacement of fossil fuels [45]. It exhibits excellent properties both as fuel and as an energy carrier, and when generated via the combustion of renewable resources, it significantly reduces pollutant emissions. However, the majority of H_2 is produced from fossil fuels, while only 4% is produced from renewable sources [45]. Due to the negative effect that fossil fuels have on the environment as well as their negative economic impact on importing countries, it is crucial to look for an alternative source of H_2 generation. It follows that if MSW were to be used for H_2 production, not only would it protect the environment, but it would also provide a sustainable source of H_2.

In this section, previously obtained results are analyzed in an economic perspective in a framework of hydrogen production through RDF gasification. To assess the potential of this system it is necessary to compare it with conventional management practices such as landfills.

Some of the considerable costs and benefits associated with RDF production and utilization are summarized in Table 9 (detailed explanation on these considerations can be found in the work of Reza et al. [46]).

Processing and converting MSW to RDF has both costs and benefits. On one hand, it consumes energy and produces emissions. On

Table 9
Considerable costs and benefits associated with RDF production and utilization.

Associated costs	Associated benefits
Operational costs	Fuel savings
Plant construction and land cost	Reduction of landfilling expenses
Additional costs for hydrogen production	Recovered material
Transportation costs	Employment impact

the other hand, recovered materials, such as ferrous metals, can be sent to a secondary market for sale thus decreasing the cost for processing and converting. On top of that, by choosing this technology over landfills, only a small percentage of waste ends up being deposited resulting in at least 60% landfill reduction.

According to Zhang et al. [47], approximately 28,500 tons of MSW can occupy 1 ha of land. Therefore, by applying this technology to 2.72 million tons of MSW (Portuguese production of MSW sent to landfills in 2012 [14]), over 57 ha of land can be saved from landfilling each year. This reduction can be extremely beneficial not only in financial savings but most important in a substantial decrease in air emissions.

A 2012 EPA study commissioned by the American Chemistry Council's Plastics Division and conducted by RTI International [48], estimated that gasification results in a net carbon emission savings of 0.3–0.6 tons of carbon equivalent (TCE) per dry ton of MSW when compared to landfill disposal. This net savings is due mainly to the energy produced through gasification because even in the scenario with the landfill recovering energy, the gasification facility produces energy in a much more efficient way [49].

The following analysis is based on the results from Section 4.2 for MSW applied to the gasification plant described in Section 2. Chosen operational conditions are: SBR of 1.5; gasification temperature of 750 °C and MSW feed rate of 50 kg/h. The higher feed rate (half of full capacity) since, from experimental analysis, this feed corresponds to the optimal operating condition (more stable gasification results). Also, from previous studies [12] we know that hydrogen production isn't seriously affected by operating at higher MSW feed. Considering a syngas composition comprising 36.2% of H_2 and a 1.51 m^3 of syngas produced per kg of RDF, which in turns, gives 0.55 m^3 of H_2 per kg of RDF. Considering that 1 m^3 of H_2 can translate to roughly 0.002 barrels of oil (boe) [50], one can estimate both the number of barrels of crude oil saved and the annual savings from the collected data.

With the Oil Brent Price currently around 45 euros, Portugal spends on average 4.971 thousand million euros a year on international transactions, importing close to 110 million crude oil Brent Barrels, although the yearly budget used to be much higher when the price per barrel was over 100 euros. By resorting to MSW gasification with steam, and considering the conditions described above, an estimated expense of about 81.5 million euros could be avoided, which represents a global decrease of 1.8 million crude oil Brent Barrels imported.

Table 10 shows several parameters taken into account to perform this economic evaluation. The capital cost of a gasification plant of 50 kg/h identical to the one previously described is around 450,000 € that are linear amortized in its life time of 20 years with residual value of zero. Assuming a cost of 20 €/ton of RDF (commonly found in similar situations [51]) the minimum cost for hydrogen production is close to 2.66 €/kg.

Considering an annual hydrogen production of 216,342 cubic - meters from 660 tons of MSW (which are converted to 396 tons of RDF) one can expect to save 432 barrels of crude and avoid almost 232 cubic meters of landfill a year. On top of that one can expect to recover at last 66 kg (10% of the total MSW) which, as stated, can be sent to a secondary market for sale. Estimating a net carbon emission savings of 0.45 TCE per dry ton of MSW one can estimate reduction of 297 TCE per year.

Table 10
Economic and environmental impact from the conducted simulations.

Operational costs		
RDF feed	396	ton/year
RDF costs	20	€/ton
Total RDF costs	7920	€/year
Dolomite feed	3.3	ton/year
Dolomite costs	55	€/ton
Total dolomite costs	181.5	€/year
Electricity costs	2059	€/year
Personnel costs	41,328	€/year
Maintenance costs	10,890	€/year
Plant construction and additional costs		
Fluidized bed gasification plant 50 kg/h	450,000	€
Associated benefits		
Fuel savings	432.68	boe/year
Landfill reduction	231.58	m^2/year
Emission reduction	297	TCE/year
Recovered material	66	kg/year
Hydrogen production		
Syngas production (1.51 m^3/kg RDF)	597,960	m^3/year
Hydrogen production	216,342	m^3/year
Operational result		
Total production costs	62,379	€/year
Linear amortization (20 years)	22,500	€/year
Total production benefits	33,108	€/year
Total hydrogen production costs	2.66	€/kg

Considered benefits and costs have been calculated based on actual data from Portalegre's plant, expert judgments, and construction and operation costs of analogous waste treatment plants in Europe. Although at different scales and applications, existing economic studies corroborate the obtained data [46,48,52–54].

There are several sources that are currently being used for H_2 production. Fig. 10 depicts energy efficiency and H_2 production cost for the main processes and compares it with obtained results for MSW gasification.

Out of all presented methods, MSW gasification appears to be very well balanced, displaying an average efficiency and a low production cost, and is the only process with a renewable source, since all other relevant methods depend on fossil fuels.

Although hydrogen production cost for this particular study was slightly higher than expected it is crucial to mention that the comparison was made with large facilities, some having an annual H_2 production which exceeds the production of the studied process by a factor of more than 100. While this makes the comparison between the data difficult, they certainly allow for an optimistic prediction.

In fact, one can only assume that with a bigger installation the average hydrogen production costs would only decrease. According to Farver and Frantz [49], larger facilities of over 100 metric tons of MSW per day are predicted to be more profitable but as yet do not exist. This also brings us to a very important aspect, which is the learning effect. The economic analysis is presented based on current or recent costs. However, learning effects reduce these costs as more units are built and experience is accumulated [55]. The impact on total plant costs can be significant. According to the International Energy Agency [56], for emerging technologies, a 50% reduction of total plant costs may be achieved after the installation of 10 plant units.

This data is of utmost importance considering the Portuguese economic overview. Portugal is a country poor in energy resources of fossil origin and with a recorded energy dependence on imports

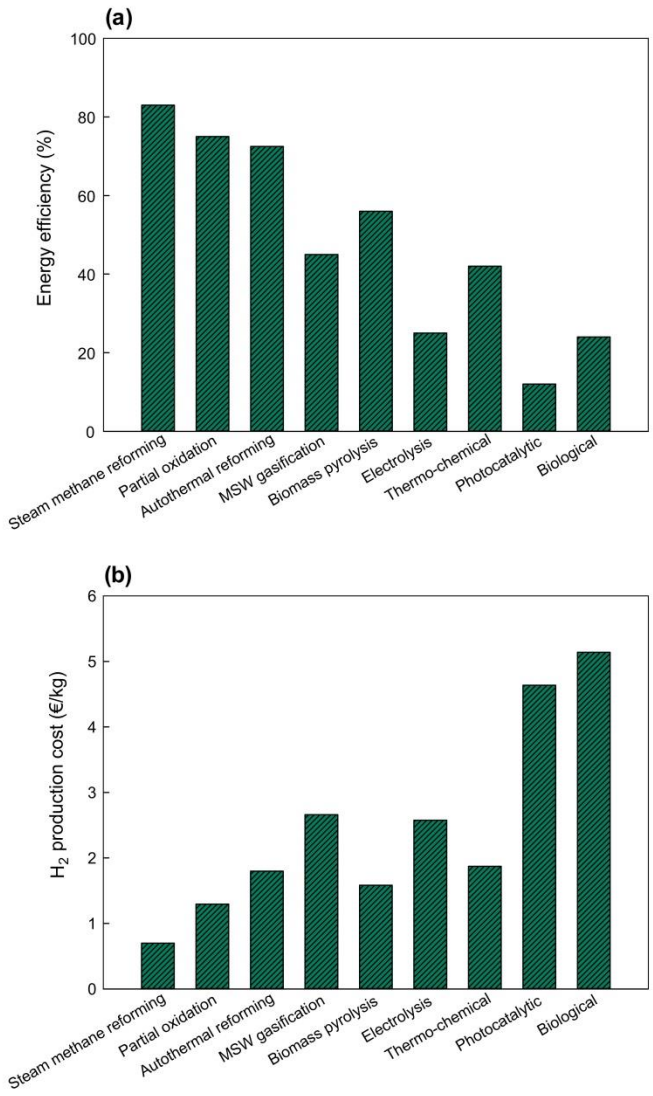

Fig. 10. Comparison between H_2 production methods for (a) energy production and (b) H_2 production cost [26].

of energy products of 79.4% in 2012, which translates into an expense of over 7 thousand million euros to meet power requirements. In order to reduce energy dependency and secure the national supply, it is necessary to increase the relative weight of primary energy produced in Portugal.

Considering the latest national report, in 2012, 4.53 million tons of MSW were produced in Portugal [14]. According to Teixeira et al. [2], most of the MSW in Portugal is sent to landfill and incineration continues to be the most common method of thermal treatment for waste-to-energy facilities. The state of development of gasification technology and its increasing adoption rate, along with environmental restrictions and laws, show that gasification is a viable and cleaner alternative for MSW conversion to energy.

Although quantifying the global volume of harmful emissions saved from reducing the total amount of municipal solid waste going to landfill is extremely difficult it is unquestionably that reducing methane, volatile organic compounds, and hazardous air pollutants (such as benzene, toluene, and ethylbenzene) will have a positive effect on environmental and human health.

In fact, reduction of MSW sent to landfills in one of the greatest benefits of hydrogen production from MSW gasification. Transportation costs and tipping fees are growing increasingly expensive as more landfills are closed while few are opened. This type of relief to a constrained landfill system holds enormous promise, particularly for Azores and Madeira (islands that are part of the national territory) with limited landfill space and regions of the country with high tipping fees for waste disposal.

These results show the potential benefits of MSW gasification, not only at an environmental level, but also on an economic one. However, these figures should be regarded only as indicative and an economic viability study must be carried out with the valuable assistance of numerical simulation.

5. Conclusions

One of the greatest challenges facing modern society is the excessive waste generation and its incorrect management. The treatment of these residues is quite expensive and, out of the available methods of treatment, landfill is still the most widely used despite posing an environmental risk to human health. In this work, the steam gasification of municipal solid residues from Portugal, in particular from the Oporto metropolitan area, was investigated as a possible solution to this problem. Our previously developed numerical model was employed and its results validated using data collected from the literature, and then expanded to predict process results using a semi-industrial gasifier. To properly assess the capabilities of the Portuguese municipal solid waste, the numerical results were compared with those obtained from previously investigated Portuguese biomass substrates. Syngas resulting from PMSW proved rich in both CO and CO_2, which lead to a gas with low calorific value. Results demonstrated that, compared to the studied biomass substrates, Portuguese wastes present the lowest carbon conversion, gas yield and CGE while displaying the highest tar content. The influence of steam gasification on both harmful emissions avoided and annual savings was studied. By resorting to MSW gasification with steam, an estimated annual savings of about 81.5 million euros could be attained, which represents a global budget decrease of 1.63%, and an average of over 57 ha land can be saved from landfilling each year. Although purely indicative, these figures present very promising estimates for the future.

Acknowledgements

We would like to express our gratitude to the Portuguese Foundation for Science and Technology (FCT) for the support to the Grant SFRH/BD/86068/2012 and the project PTDC/EMS-ENE/6553/2014 as well as IF/01772/2014.

References

[1] Hoornweg D, Bhada-Tata P. What a waste a global review of solid waste management. Urban development series knowledge papers, vol. 15; 2012. <http://siteresources.worldbank.org/INTURBANDEVELOPMENT/Resources/336387-1334852610766/What_a_Waste2012_Final.pdf> [last access in June 7th].

[2] Teixeira S, Monteiro E, Silva V, Rouboa A. Prospective application of municipal solid wastes for energy production in Portugal. Energy Policy 2014;71:159–68.

[3] Al-Hamamre Z, Al-Mater A, Sweis F, Rawajfeh K. Assessment of the status and outlook of biomass energy in Jordan. Energy Convers Manage 2014;77:183–92.

[4] Zheng X, Chen C, Ying Z, Wang B. Experimental study on gasification performance of bamboo and PE from municipal solid waste in a bench-scale fixed bed reactor. Energy Convers Manage 2016;117:393–9.

[5] Weil S, Hamel S, Krumm W. Hydrogen energy from coupled waste gasification and cement production – a thermochemical concept study. Int J Hydrogen Energy 2006;31:1674–89.

[6] He M, Hu Z, Xiao B, Li J, Guo X, Luo S, et al. Hydrogen-rich gas from catalytic steam gasification of municipal solid waste (MSW): influence of catalyst and temperature on yield and product composition. Int J Hydrogen Energy 2009;34:195–203.

[7] He M, Xiao B, Liu S, Guo X, Luo S, Xu Z, et al. Hydrogen-rich gas from catalytic steam gasification of municipal solid waste (MSW): influence of steam to MSW ratios and weight hourly space velocity on gas production and composition. Int J Hydrogen Energy 2009;34:2174–83.

[8] Wang J, Cheng G, You Y, Xiao B, Liu S, He P, et al. Hydrogen-rich gas production by steam gasification of municipal solid waste (MSW) using NiO supported on modified dolomite. Int J Hydrogen Energy 2012;37:6503–10.

[9] Moghadam R, Yusup S, Azlina W, Nehzati S, Tavasoli A. Investigation on syngas production via biomass conversion through the integration of pyrolysis and air–steam gasification processes. Energy Convers Manage 2014;87:670–5.

[10] Couto N, Silva V, Monteiro E, Bispo C, Rouboa A. From laboratorial to pilot fluidized bed reactors: analysis of the scale-up phenomenon. Energy Convers Manage 2016;119(2016):177–86.

[11] Couto N, Silva V, Monteiro E, Teixeira S, Chacartegui R, Bouziane K, et al. Numerical and experimental analysis of municipal solid wastes gasification process. Appl Therm Eng 2015;78:185–95.

[12] Couto N, Silva V, Monteiro E, Rouboa A. Assessment of municipal solid wastes gasification in a semi-industrial gasifier using syngas quality indices. Energy 2015;93:964–73.

[13] Ribeiro A, Castro F, Macedo M, Carvalho J. Waste management in Portugal and Europe – an overview of the past, present and future. In: "WASTES: Solutions, Treatments and Opportunities" 1st International Conference, September 12th – 14th.

[14] <http://www.netresiduos.com/content.aspx?menuid=134&eid=992> [last access in June 7th].

[15] <http://portal.lipor.pt:7777/pls/apex/f?p=2020:21:0> [last access June 7th].

[16] Scott D, Czernik S, Piskorz J, Radlein DSA. Fast pyrolysis of plastic wastes. Energy Fuel 1990;4:407–11.

[17] Xie J, Zhong W, Jin B, Shao Y, Liu H. Simulation on gasification of forestry residues in fluidized beds by Eulerian-Lagrangian approach. Bioresource Technol 2012;12:36–46.

[18] Onel O, Niziolek AM, Hasan MMF, Floudas CA. Municipal solid waste to liquid transportation fuels – Part I: Mathematical modeling of a municipal solid waste gasifier. Comput Chem Eng 2014;71:636–47.

[19] Fan L, Pandey A, Mohan R, Soccol CR. Acta Biotechnol 2000;20:41–52.

[20] <http://www.pordata.pt> [last access June 7th].

[21] Ferreira S, Moreira N, Monteiro E. Biomass Bioenergy 2009;33:1567–76.

[22] Silva V, Monteiro E, Couto N, Brito P, Rouboa A. Analysis of syngas quality from Portuguese biomasses: an experimental and numerical study. Energy Fuel 2014;28:5766–77.

[23] Couto N, Silva V, Monteiro E, Brito P, Rouboa A. Using an Eulerian-granular 2-D multiphase CFD model to simulate oxygen air enriched gasification of agroindustrial residues. Renew Energy 2015;77:174–81.

[24] Silva V, Rouboa A. Combining a 2-D multiphase CFD model with a Response Surface Methodology to optimize the gasification of Portuguese biomasses. Energy Convers Manage 2015;99:28–40.

[25] Launder B, Spalding B. Lectures in mathematical models of turbulence. London, England: Academic Press; 1972.

[26] Arena U. Process and technological aspects of municipal solid waste gasification: a review. Waste Manage 2012;32:625–39.

[27] Miao Q, Zhu J, Barghi S, Wu C, Yin X, Zhou Z. Modeling biomass gasification in circulating fluidized beds: model sensitivity analysis. Int J Energy Power 2013;2(3):57–63.

[28] Hernández JJ, Aranda G, Barba J, Mendoza JM. Effect of steam content in the air-steam flow on biomass entrained flow gasification. Fuel Process Technol 2012;99:43–55.

[29] Franco C, Pinto F, Gulyurtlu I, Cabrita I. The study of reactions influencing the biomass steam gasification process. Fuel 2003;82:835–42.

[30] Song T, Wu J, Shen L, Xiao J. Experimental investigation on hydrogen production from biomass gasification in interconnected fluidized beds. Biomass Bioenergy 2012;36:258–67.

[31] Loha C, Chatterjee P, Chattopadhyay H. Performance of fluidized bed steam gasification of biomass – modeling and experiment. Energy Convers Manage 2011;52:1583–8.

[32] Louw J, Schwarz C, Knoetze J, Burger A. Thermodynamic modelling of supercritical water gasification: investigating the effect of biomass composition to aid in the selection of appropriate feedstock material. Bioresource Technol 2014;174:11–23.

[33] Luo S, Xiao B, Hu Z, Liu S, Guo X, He M. Hydrogen-rich gas from catalytic steam gasification of biomass in a fixed bed reactor: Influence of temperature and steam on gasification performance. Int J Hydrogen Energ 2009;34:2191–4.

[34] Campoy M, Gómez-Barea A, Ollero P, Nilsson S. Gasification of wastes in a pilot fluidized bed gasifier. Fuel Process Technol 2014;121:63–9.

[35] Lv PM, Xiong ZH, Chang J, Wu CZ, Chen Y, Zhu JX. An experimental study on biomass air-steam gasification in a fluidized bed. Bioresour Technol 2004;95:95–101.

[36] Reed TB. Biomass gasification principle and technology. Park Ridge, NJ: Noyes Data Corporation; 1981.

[37] Yan F, Luo S, Hu Z, Xiao B, Cheng G. Hydrogen-rich gas production by steam gasification of char from biomass pyrolysis in a fixed-bed reactor: influence of temperature and steam on hydrogen yield and syngas composition. Bioresource Technol 2010;101:5633–7.

[38] Rapagna S, Latif A. Steam gasification of almond shells in a fluidised bed reactor: the influence of temperature and particle size on product yield and distribution. Biomass Bioenergy 1997;12:281–8.

[39] Nanda S, Isen J, Dalai A, Kozinski J. Gasification of fruit wastes and agro-food residues in supercritical water. Energy Convers Manage 2016;110:296–306.

[40] Aljbour SH, Kawamoto K. Bench-scale gasification of cedar wood – Part II: Effect of operational conditions on contaminant release. Chemosphere 2013;90:1501–7.

[41] Pinto F, André R, Carolino C, Miranda M, Abelha P, Direito D, et al. Gasification improvement of a poor quality solid recovered fuel (SRF). Effect of using natural minerals and biomass wastes blends. Fuel 2014;117:1034–44.

[42] Hansson J, Leveau A, Hulteberg C. Biomass gasifier database for computer simulation purposes. Nordlight AB, Rapport SGC 234, ©Svenskt Gastekniskt Center; August 2011.

[43] Vassilev SV, Vassileva CG, Vassilev S. Advantages and disadvantages of composition and properties of biomass in comparison with coal: an overview. Fuel 2015;158:330–50.

[44] Nipattummakul N, Ahmed I, Gupta AK, Kerdsuwan S. Hydrogen and syngas yield from residual branches of oil palm tree using steam gasification. Int J Hydrogen Energy 2011;36:3835–43.

[45] Parthasarathy P, Narayanan K. Hydrogen production from steam gasification of biomass: Influence of process parameters on hydrogen yield – a review. Renew Energy 2014;66:570–9.

[46] Reza B, Soltani A, Ruparathna R, Sadiq R, Hewage K. Environmental and economic aspects of production and utilization of RDF as alternative fuel in cement plants: a case study of Metro Vancouver Waste Management. Resour Conserv Recy 2013;81:105–14.

[47] Zhang XH, Deng SH, Wu J, Jiang W. A sustainability analysis of a municipal sewage treatment ecosystem based on emergy. Ecol Eng 2010;36:685–96.

[48] RTI International. Environmental and economic analysis of emerging plastics conversion technologies final project report. RTI Project No. 0212876.000; 2012. <https://plastics.americanchemistry.com/Sustainability-Recycling/Energy-Recovery/Environmental-and-Economic-Analysis-of-Emerging-Plastics-Conversion-Technologies.pdf> [last access in June 7th].

[49] Farver M, Frantz C. Garbage to gasoline: converting municipal solid waste to liquid fuels technologies, commercialization, and policy. Duke University Nicholas School of the Environment; 2013.

[50] <http://www.energybc.ca/other/converter.html> [last access in June 7th]

[51] Caputo A, Pelagagge P. RDF production plants: I Design and costs. Appl Therm Eng 2002;22:423–37.

[52] Gilbert P, Alexander S, Thornley P, Brammer J. Assessing economically viable carbon reductions for the production of ammonia from biomass gasification. J Clean Prod 2014;64:581–9.

[53] Ahmad A, Zawawi N, Kasim F, Inayat A, Khasri A. Assessing the gasification performance of biomass: a review on biomass gasification process conditions, optimization and economic evaluation. Renew Sustain Energy Rev 2016;53:1333–47.

[54] Gasafi E, Reinecke M, Kruse A, Schebek L. Economic analysis of sewage sludge gasification in supercritical water for hydrogen production. Biomass Bioenergy 2008;32:1085–96.

[55] Basye L, Swaminathan S. Hydrogen production costs—a survey. SENTECH, Inc. für das US Department of Energy; 1997 [DOE/GO/10170-778].

[56] I.E.A. Experience curves for energy technology policy. Paris: International Energy Agency (IEA); 2000.

Paper VII

Hydrogen-rich gas from gasification of Portuguese municipal solid wastes

N. Couto, E. Monteiro, V. Silva, A. Rouboa

International Journal of Hydrogen Energy 41 (2016) 10619-10630

Available online at www.sciencedirect.com

ScienceDirect

journal homepage: www.elsevier.com/locate/he

Hydrogen-rich gas from gasification of Portuguese municipal solid wastes

Nuno Couto [a], Eliseu Monteiro [b], Valter Silva [a], Abel Rouboa [a,c,d,*]

[a] INEGI-CIENER, Faculty of Engineering, University of Porto, Porto, Portugal
[b] INEGI-CIENER, Polytechnic Institute of Portalegre, Portalegre, Portugal
[c] Engineering Department of University of Trás-os-Montes e Alto Douro, Vila Real, Portugal
[d] MEAM Department, University of Pennsylvania, Philadelphia, PA, 19020, USA

ARTICLE INFO

Article history:
Received 12 January 2016
Received in revised form
7 April 2016
Accepted 13 April 2016
Available online 27 May 2016

Keywords:
Gasification
Hydrogen-rich gas
Municipal solid wastes
CFD
Semi-industrial gasifier

ABSTRACT

Gasification has been identified as a promising method of municipal solid waste (MSW) conversion to energy due to its pollution minimization effects and high overall efficiency. Recent studies have been carried out to produce hydrogen through MSW gasification with promising results. Despite this, it is still necessary to develop mathematical models able to assist the advance of this technology and to make way for large-scale commercialization.

A previously developed and validated numerical model was used to predict and analyze the viability of hydrogen-rich gas generation from MSW gasification in a semi-industrial fluidized bed gasifier. Influence of equivalence ratio, carbon-dioxide-to-MSW ratio, steam-to-MSW ratio, reactor temperature and catalyst used was investigated. The content of hydrogen in the generated gas increased up to 40% with the presence of NiO/MD catalysts, while reducing the tar content and increasing the gas yield. Finally, to assess the capabilities of the Portuguese wastes results were compared with previously studied Portuguese biomass substrates.

Introduction

The depletion of fossil fuels reserves, geopolitical fears associated with fossil fuel scarcity, and issues of environmental pollution and climate change as well as the need to ensure independence of energy supply make the low-carbon economy with a crucial hydrogen vector inevitable in the coming years.

Hydrogen as a clean energy carrier is expected to satisfy a considerable portion of the world's future energy needs [1,2]. It can be used in internal combustion engines as well as in fuel cells with less pollution on the environment, since the combustion with oxygen produces water as its only by-product [3]. Moreover, it has the highest energy content in comparison to other common fuels.

A rising concern is that fossil fuels make up by far the largest contemporary source of hydrogen (approximately 97% [4]). Taking into account fossil fuels scarcity concerns along with high carbon footprint [5] research on renewable alternative source of hydrogen is needed [6]. Biagini et al. [7] conducted an experimental study to evaluate the performance of the different thermo-chemical technologies (i.e. combustion,

* *Corresponding author*. Quinta de Prados, Apartado 1013, 5001-801, Vila Real, Portugal. Tel.: +351 259350317; fax: +351 259 350 356.
E-mail addresses: nunodiniscouto@hotmail.com (N. Couto), ELMMonteiro@portugalmail.pt (E. Monteiro), vsilva@inegi.up.pt (V. Silva), rouboa@utad.pt, rouboa@seas.upenn.edu (A. Rouboa).
http://dx.doi.org/10.1016/j.ijhydene.2016.04.091
0360-3199/

Nomenclature

A, B	calibration constants
A_i	pre-exponential factor
$C_{1\varepsilon}$, $C_{2\varepsilon}$, $C_{3\varepsilon}$	Constants
C_p	Specific heat capacity
D_0	Diffusion rate coefficient
E_i	activation energy
G_k	Generation of turbulence kinetic energy due to the mean velocity gradients
G_b	Generation of turbulence kinetic energy due to buoyancy
h_q	Specific enthalpy of phase
h_{pq}	Heat transfer coefficient between the fluid phase and the solid phase
k	Thermal conductivity
Nu	Nusselt Number
$\dot{m}$	Biomass flow entering into the gasifier
M	Total mole flow of carbon in the syngas components
M_i	Molecular weight of each the species
M_c	Molecular weight
$M_{w,i}$	Molecular weight of i component
p	Gas pressure
Pr	Prandtl Number
p_s	Particle phase pressure due to particle collisions
$\overrightarrow{Q}_{pq}$	Heat transfer between pth and qth phases
$\overrightarrow{q}_q$	Heat flux
q^{th}	Specific enthalpy
R	Universal gas constant
$\mathbf{R_i}$	Net generation rate of specie i due to homogeneous reaction
Re	Reynolds Number
R_c	Reaction rate
$\mathbf{S_i}$	Source term of the species i production from the solid heterogeneous reaction
S_k	User-defined source terms
S_q	Source term due to chemical reactions
S_ε	User-defined source terms
T	Temperature
t_s	Particle phase stress tensor
U	Mean velocity
v	Instantaneous velocity
$\mathbf{X_C}$	Carbon fraction in the biomass (obtained from the ultimate analysis)
Y	Mass Fraction
Y_M	Contribution of the fluctuating dilatation in compressible turbulence to the overall dissipation rate

Other symbols

α	Volume fraction
β	gas–solid interphase drag coefficient
γ_c	Stoichiometric coefficient
γ_{Θ_2}	Collisional dissipation of energy
ε	dissipation rate
ρ	Density
φ_{ls}	Energy exchange between gas and solid phases
k_{Θ_2}	Diffusion coefficient
$k_{\Theta_2}\nabla(\Theta_s)$	Diffusion energy
$(-p_s\bar{\bar{I}}+\bar{\bar{\tau}}_s):\nabla(\vec{v}_s)$	Generation of energy by the solid stress tensor.
τ	Tensor stress
μ	Viscosity

Subscripts

g	gas phase
s	solid phase
i	component

gasification, electrolysis and syngas separation) for hydrogen production from biomass. They reported that the hydrogen production was maximized for the gasification/separation process followed by gasification/electrolysis and the least being combustion/electrolysis. Therefore, among the aforementioned technology options, gasification of biomass is identified as the most efficient and economical route for hydrogen production.

Among biomass sources, municipal solid wastes (MSW) are the largest volume of residues produced worldwide; at the same time, the citizens' demands for an environmentally sound management of MSW have significantly increased during the last decades [8].

The Integrated Solid Waste Management includes several solutions to achieve lower environmental and social impacts. These solutions combine different alternatives such as waste generation reduction, material recovery, recycling, and energy recovery and as least desirable option, landfills. This practice is incorporated to any modern strategy involving MSW management [9]. The disposal of MSW has become a critical and costly problem. The traditional landfilling method requires large amounts of land and contaminates air, water and soil [10]. Furthermore, incineration has drawbacks as well particularly harmful emissions of acidic gases (SOx, HCl, NOx, etc.), dioxin and leachable toxic heavy metals [9].

The application of MSW gasification has enormous prospects in energy security, mitigation of climate change and sustainable settlement development. A number of thermochemical processes can convert the carbonaceous materials of biomass to a combustible syngas where gasification plays lead role [9].

Gasification is a high-temperature partial oxidation process in which a solid carbonaceous feedstock such as MSW is converted into a gaseous mixture (H_2, CO, CO_2, CH_4, light hydrocarbons, tar, char, ash and minor contaminates) using an oxidizing agent [11]. Several studies have been performed to increase the hydrogen production yield from biomass gasification [12]. Due to the large range of investigations, experimental [13–15], mathematical and computational [16–19] approaches have been applied to conduct these studies. Regarding MSW gasification, available studies are still very scarce especially considering semi-industrial or industrial conditions.

He et al. [13,14] studied the influence of steam to MSW ratios and weight hourly space velocity [13] and the influence of catalyst and temperature on yield and product composition

[14] of the steam gasification of municipal solid waste in a bench-scale downstream fixed bed reactor. They found that calcined dolomite has a good catalytic performance for steam gasification of MSW, and that higher steam to MSW ratios results in higher conversion of MSW into hydrogen-rich gas.

Wang et al. [15] further increased the study of the catalyst using NiO supported on modified dolomite for hydrogen-rich gas production from steam gasification of MSW in a lab-scale fixed bed. They conclude that the catalysts could significantly eliminate the tar in the gas production and increase the hydrogen yield. In addition, higher temperature contributed to higher hydrogen production and gas yield.

Onel et al. [16] presents a generic gasifier model using MSW towards the production of liquid fuels. Using a nonlinear parameter estimation approach, the unknown gasification parameters are obtained to match the experimental gasification results. The results suggest that a generic MSW gasifier model can be obtained with an average uncertainty of 8.75%.

Couto et al. [17,18] developed a two-dimensional CFD model for MSW gasification and an Eulerian–Eulerian approach was used to describe the transport of mass, momentum and energy for the solid and gas phases. After validating the model with experimental data available in the literature, an evaluation on the potential of syngas produced from Portuguese MSW was made.

The aim of this paper is to deepen the study on hydrogen production from Portuguese MSW gasification. A validation was performed to prove the potential of the previously developed numerical model in predicting H_2 production. The numerical model was then used to study the influence of several gasifying agents as well as reactor temperature on syngas composition (including hydrogen yield) as well as tar content and gas yield. Regarding the influence of the catalyst three different scenarios were studied: no catalyst, dolomite and modified dolomite (NiO/MD). Finally, to get a better understanding of the capabilities of the studied residues, a comparison with characteristic Portuguese biomasses was performed.

Materials and methods

MSW was modeled according to the average proportion of organic components (dry basis) in actual MSW of Portugal [9] and used as feedstock for the simulations, as shown in Table 1.

Table 1 – Chemical composition of the MSW.

Category	% Weight Portugal Adapted from Teixeira et al. [9]	Chemical formula
Cellulose	49.34%	$C_6H_{10}O_5$
Hemicelluloses	13.72%	$C_5H_8O_4$
Lignin	22.16%	$C_{20}H_{22}O_{10}$
Polyethylene	11.14%	$(C_2H_4)_n$
Polyethylene terephthalate	2.05%	$(C_{10}H_8O)_n$
Polypropylene	0.82%	$(C_3H_6)_n$
Polystyrene	0.77%	$(C_8H_8)_n$

It is assumed a MSW pre-treatment that gives rise to a refuse derived fuel which contains cellulosic and plastics only [9]. Cellulosic materials are mainly composed of cellulose, hemicelluloses, and lignin. Plastic residues are composed of polyethylene, polystyrene, and poly-vinyl chloride.

A global chemical is obtained by dividing the values found in the ultimate analysis of each chemical element (C, H, O) by the value of the reference element carbon (C). The MSW global chemical formula was obtained based on its chemical characterization as shown in Table 1.

The simulations of the MSW gasification were performed in a fluidized bed gasifier with 0.5 m in diameter and 4.15 m of height, internally coated with ceramic refractory materials.

The MSW enters the reactor at the height of 0.5 m, from its base, and preheated air or steam enters the reactor coming from the base through a set of 37 diffusers, ensuring an adjustable flow. The bed material is made of 70 kg of calcium magnesium carbonate $CaMg(CO_3)$, also known as dolomite.

The schematics as well as an extensive description of the gasification plant can be found elsewhere [20].

Mathematical model

Computational fluid dynamics (CFD) is the science of predicting fluid flow, heat transfer, chemical reaction and other related phenomena by solving numerical set of the governing mathematical equations which are mostly based on conservation equations.

Bubbling fluidized-bed models are generally based on the two-phase flow theory of fluidization for the description of the process hydrodynamics. The two-phase (gas and solid) fluid dynamics is of great importance for the design and operation of the bubbling fluidized bed gasifiers. MSW gasification involves several fundamental processes. Firstly, volatile components in the MSW such as light gases and tar are released by pyrolysis. These species undergo homogeneous gas phase reactions forming CO, CO_2, H_2, H_2O which then combust and gasify the char. Each process must be understood and modeled when modeling MSW gasifiers.

The fluid dynamics of such gas–solid two-phase flow is very complex and strongly dominated by particle-to-particle interactions. Modeling pyrolysis is crucial for MSW gasification purposes. The chemical reaction rate coefficients are based on the Arrhenius law. During the devolatilization and cracking water shift reaction will occur, the gas species react with the supplied oxidizer and among them. All homogeneous and heterogeneous reactions and their reaction rates using in the model are given in Table 2.

Both homogeneous and heterogeneous reactions are preceded from pyrolysis reactions. The finite-rate/Eddy-dissipation model was used to treat the homogeneous while the Kinetic/Diffusion Surface Reaction Model was employed on the heterogeneous ones. The Arrhenius rates and the kinetic parameters for these reactions as well as further explanation can be found in Ref. [17], and so can solver procedure details [17].

MSW is thermally decomposed into volatiles, char and tar. There are several approaches to describe this phenomenon which the main approaches are: a single step pyrolysis model,

Table 2 – Homogeneous and heterogeneous reactions.

Chemical reactions	Reaction rate	Ref.
Homogeneous reactions [21]:		
$CO + 0.5O_2 \rightarrow CO_2$	$r_1 = 1.0 \times 10^{15} \exp\left(\frac{-16000}{T}\right) C_{CO} C_{O_2}^{0.5}$	[22]
$CO + H_2O \rightarrow CO_2 + H_2$	$r_2 = 2780 \exp\left(\frac{-1510}{T}\right)\left[C_{CO} C_{H_2O} - \frac{C_{CO_2} C_{H_2}}{0.0265 \exp\left(\frac{3968}{T}\right)}\right]$	[22]
$CO + 3H_2 \leftrightarrow CH_4 + H_2O$	$r_3 = 3.0 \times 10^{5} \exp\left(\frac{-15042}{T}\right) C_{H_2O} C_{CH_4}$	[22]
$H_2 + 0.5O_2 \rightarrow H_2O$	$r_4 = 5.159 \times 10^{15} \exp\left(\frac{-3430}{T}\right) T^{-1.5} C_{O_2} C_{H_2}^{1.5}$	[22]
$CH_4 + 2O_2 \rightarrow CO_2 + 2H_2O$	$r_5 = 3.552 \times 10^{14} \exp\left(\frac{-15700}{T}\right) T^{-1} C_{O_2} C_{CH_4}$	[22]
Heterogeneous reactions [21]:		
$C + 0.5O_2 \rightarrow CO$	$r_6 = 596 T_P \exp\left(\frac{-1800}{T}\right)$	[22]
$C + CO_2 \rightarrow 2CO$	$r_7 = 2082.7 \exp\left(\frac{-18036}{T}\right)$	[22]
$C + H_2O \rightarrow CO + H_2$	$r_8 = 63.3 \exp\left(\frac{-14051}{T}\right)$	[22]

competing parallel pyrolysis and a pyrolysis model with generation of secondary tar. In this model we adopt a pyrolysis model with generation of secondary tar expressed in Table 3. The MSW is mainly composed by cellulosic and plastic components, where the cellulosic material can be divided in cellulose, hemicellulose and lignin and the plastics are mainly comprised by polyethylene, polystyrene, and polypropylene, among others.

To distinguish the several components that comprise the MSW, the pyrolysis reactions of cellulosic and plastic groups are considered individually and following an Arrhenius kinetic expression.

The momentum equations are solved for the gas and the solids phases. The model follows an Eulerian–Eulerian approach, which means that both gas and solid phases are described by a continuum approach, and modeled similar to single phase flow with an additional term, accounting for the interaction with the solid phase.

In order to describe particle collisions and to predict the frequency of pressure fluctuations, bubble formation, and particle segregation, the so-called two-fluid model based on the assumption that the gas and particulate phases form two interpenetrating continua are solved. The conservation of mass and momentum equations and constitutive relations are given in Table 4. Further details on the model are given in Couto et al. [17].

The choice of turbulence model in the gas phase is a key issue. The kinetic theory of granular flow is used in the two-fluid model to simulate particle collision for closure (Table 5). A Fluent standard k–ε model was chosen for the turbulence model, as this is the most appropriate model when turbulence transfer between phases plays an important role in gasification in fluidized beds. k is the turbulence kinetic energy and ε is the dissipation rate.

Numerical procedure

Quadrilateral cells with a size roughly 12 times larger than the particle size [28] were selected after performing some simulation runs and insignificant differences were found considering syngas composition, temperature, velocity and turbulence profiles. Also, the selection of cells with this size is in agreement with the literature [32] based on hydrodynamic issues. Convergence criteria for residuals were 10^{-8} for continuity and momentum equations and 10^{-14} for energy equation. The model was first solved considering the absence

Table 3 – Pyrolysis model.

Chemical reactions	Reaction rate	Ref.
Primary pyrolysis		
$Cellulose \rightarrow \alpha_1 volatiles + \alpha_2 TAR + \alpha_3 char$	$r_9 = A_i \exp\left(\frac{-E_i}{T_s}\right)(1 - a_i)^n$	[24]
$Hemicellulose \rightarrow \alpha_4 volatiles + \alpha_5 TAR + \alpha_6 char$	$r_{10} = A_i \exp\left(\frac{-E_i}{T_s}\right)(1 - a_i)^n$	[24]
$Lignin \rightarrow \alpha_7 volatiles + \alpha_8 TAR + \alpha_9 char$	$r_{11} = A_i \exp\left(\frac{-E_i}{T_s}\right)(1 - a_i)^n$	[24]
$Plastics \rightarrow \alpha_{10} volatiles + \alpha_{11} TAR + \alpha_{12} char$	$r_{12} = \left[\sum_{i=1}^{n} A_i \exp\left(\frac{-E_i}{RT}\right)\right]\rho_v$	[25]
Secondary pyrolysis		
$Primary\ \ TAR \rightarrow volatiles + Secondary\ \ TAR$	$r_{13} = 9.55 \times 10^{4} \exp\left(\frac{-1.12 \times 10^{4}}{T_g}\right)\rho_{TAR1}$	[26]

Table 4 – Conservation equations for each phase and the constitutive relations.

Mass Conservation	Ref.
Solid phase	
$\frac{\partial}{\partial t}(\alpha_s\rho_s)+\nabla.(\alpha_s\rho_s v_s)=S_{sg}$	[27]
Gas phase	
$\frac{\partial}{\partial t}(\alpha_g\rho_g)+\nabla.(\alpha_g\rho_g v_g)=S_{gs}$	[27]
$S_{sg}=-S_{gs}=M_c\sum\gamma_c R_c$	
Ideal gas equation	
$\frac{1}{\rho_g}=\frac{RT}{p}\sum_{i=1}^{n}\frac{Y_i}{M_i}$	
Momentum conservation	
Solid phase	
$\frac{\partial}{\partial t}(\alpha_s\rho_s v_s)+\nabla.(\alpha_s\rho_s v_s v_s)=-\alpha_s\nabla p_s+\alpha\rho_s g+\beta(v_g-v_s)+\nabla.\alpha_s\tau_s+S_{sg}U_s$	[27]
Gas phase	
$\frac{\partial}{\partial t}(\alpha_g\rho_g v_g)+\nabla.(\alpha_g\rho_g v_g v_g)=-\alpha_g\nabla p_g+\alpha\rho_g g+\beta(v_g-v_s)+\nabla.\alpha_g\tau_g+S_{gs}U_s$	[27]
Energy conservation	
$\frac{\partial(\alpha_q\rho_q h_q)}{\partial t}+\nabla.(\alpha_q\rho_q\vec{u}_q h_q)=-\alpha_q\frac{\partial(p_q)}{\partial t}+\bar{\tau}_q:\nabla(\vec{u}_q)-\nabla.\vec{q}_q+S_q+\sum_{p=1}^{n}(\vec{Q}_{pq}+\dot{m}_{pq}h_{pq}-\dot{m}_{pq}h_{pq})$	[27]
$Q_{pq}=h_{pq}(T_p-T_q)$	[28]
$h_{pq}=\frac{6k_p\alpha_q\alpha_p Nu_q}{d_p^2}$	[29]
$Nu_q=(7-10\alpha_g+5\alpha_g^2)(1+0.7Re_s^{0.2}Pr_g^{0.33})+(1.33-2.4\alpha_g+1.2\alpha_g^2)Re_s^{0.7}Pr_g^{0.33}$	[28]

Table 5 – Hydrodynamic model.

Hydrodynamic model	Ref.
Kinetic energy	
$\frac{\partial}{\partial t}(\rho k)+\frac{\partial}{\partial x_i}(\rho k u_i)=\frac{\partial}{\partial x_j}\left[\left(\mu+\frac{\mu_t}{\sigma_k}\right)\right]+G_k+G_b-\rho\varepsilon-Y_M+S_k$	[30]
Dissipation rate	
$\frac{\partial}{\partial t}(\rho\varepsilon)+\frac{\partial}{\partial x_i}(\rho\varepsilon u_i)=\frac{\partial}{\partial x_j}\left[\left(\mu+\frac{\mu_t}{\sigma_\varepsilon}\right)\frac{\partial\varepsilon}{\partial x_j}\right]+C_{1\varepsilon}\frac{\varepsilon}{k}(G_k+C_{3\varepsilon}G_b)-C_{2\varepsilon}\rho\frac{\varepsilon^2}{k}+S_\varepsilon$	[30]
$Gk=1.0;\ G\varepsilon=1.3;\ C1\varepsilon=1.44;\ C2\varepsilon=1.92;\ C3\varepsilon=0$	[28]
Granular Eulerian Model	
$\frac{3}{2}\left[\left(\frac{\partial(\rho_s\alpha_s\Theta_s)}{\partial t}+\nabla.(\rho_s\alpha_s\vec{v}_s\Theta_s)\right]=(-P_s\bar{I}+\bar{\tau}_s):\nabla(\vec{v}_s)+\nabla.(k_{\Theta a}\nabla(\Theta_s))-\gamma_{\Theta a}+\varphi_{ls}$	[31]

of chemical reactions. Then, and with a consolidated flow pattern, the chemical reactions were included and the model was solved.

Results and discussion

The presented model was first developed for the study of Portuguese biomass gasification [20]. To validate the model, experimental results obtained in the plant described in chapter 2 were used. Table 6 shows the operating conditions of the runs chosen to validate the model.

Fig. 1 shows a comparison between experimental results and those obtained by the numerical model for hydrogen molar fraction found in the performed runs.

Despite variations the model is able to predict reasonably well the gasification process in a semi-industrial reactor with relative errors less than 20%. This range is as expected for such a complex system. Sources of deviation are intimately related to some simplifications [20].

Table 6 – Operating conditions for the experimental gasification runs.

Gasification run	Biomass type	Admission biomass (Kg/h)	Air flow rate (Nm^3/h)	Gasification temperature (°C)
1	Forest Residues	63	94	815
2		74	98	815
3		63	98	790
4	Coffee Husks	28	75	815
5		28	72	790
6		41	80	790
7	Vines Pruning	25	52	790
8		55	40	790
9		55	40	815

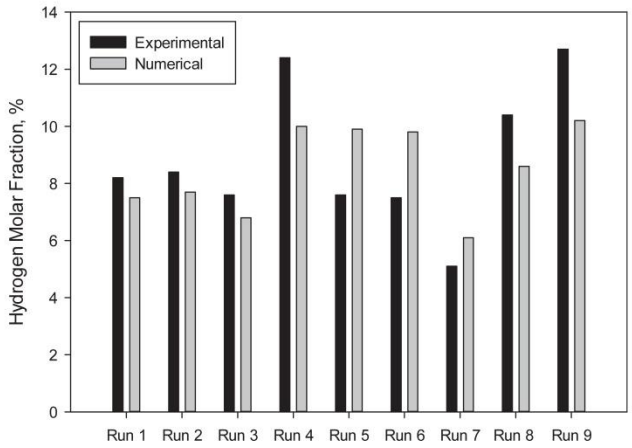

Fig. 1 – Numerical and experimental hydrogen molar fraction for the 9 gasification runs defined in Table 6.

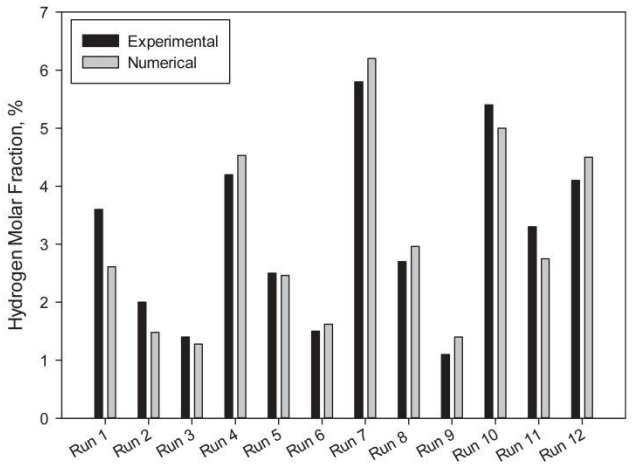

Fig. 2 – Numerical and experimental hydrogen molar fractions for the 12 gasification runs defined in Table 7.

After performing several studies with Portuguese biomass substrates, model was upgraded to predict MSW gasification. Due to the inability of performing experiments in the same reactor, results available in the literature were used. Table 7 shows the operating conditions for 12 experimental runs used to validate the numerical model with MSW.

Fig. 2 shows a comparison between experimental results from the literature [33] and those obtained by the numerical model for hydrogen molar fraction.

Again, despite the increase in the system's complexity, the model was able to predict the gasification process reasonably well for a large spectrum of operating conditions.

Note that in Figs. 1 and 2 only presents hydrogen mole fraction as the core of the article is its production, but the model predicted equally well for all the remaining species.

Effect of equivalence ratio

Equivalence ratio (ER) is one of the most significant parameters, which have effect on the gasification process including syngas composition. ER is the ratio of the actual air/fuel ratio to the stoichiometric air/fuel ratio. The ratio was kept between 0.15 and 0.35 since all of the experiments conducted to validate the model fell in this range and also because the ER values most suitable for gasification range between 0.2 and 0.4.

The model predictions about the influence of ER on syngas molar fraction and hydrogen yield are shown in Fig. 3.

It can be observed that when ER rose, the CO_2 content increased, while CO and H_2 content decreased. With an increase in O_2 content combustion reactions (that consume CO and H_2 to produce CO_2) will be promoted, since O_2 is more reactive to carbon than steam or CO_2.

Although to a smaller degree ER negatively affects C_nH_m content by enhancing steam reactions at higher temperatures leading to methane decomposition [34].

Increasing ER by raising the air flow rate also causes more N_2 to enter the reactor, causing the produced gas to be more diluted in N_2 and a poorer gas. The fact that CO and H_2 content decrease with ER can also be explained by a shorter residence time, seeing that, as air flow rate increases, it is no longer sufficient for CO and H_2 formation reactions to occur. The influence of ER on tar content and gas yield is shown in Fig. 4. A decrease in tar release around 68% with the rise of ER to 0.35 is observed. Gas yield on the other hand increased with the rise of ER. Oxidation reactions are exothermic and therefore lead to an increase in temperature inside the reactor. This increase in temperature enhances steam reforming reactions, which in turn promote carbon conversion [15]. This leads to increase in gas yield, which is known for improving tar decomposition.

Effect of steam to biomass ratio

As the gasification medium is a very important parameter in governing the gas yield and composition, the effect of using steam instead of air was also studied. The steam to biomass ratio (SBR) is defined as the steam mass flow rate divided by the biomass mass flow rate in dry basis. The use of steam as a gasifying agent increases the partial pressure of H_2O inside the gasification reactor which favors the water gas, water gas shift and steam reforming reactions, leading to increased H_2

Table 7 – Operating conditions for the experimental gasification runs.

Run	1	2	3	4	5	6	7	8	9	19	11	12
Temperature (°C)	720	620	493	705	602	507	687	593	516	691	593	507
MSW Admission (Kg/h)	2.3	2.3	2.3	3	3	3	4	4	4	6	6	6
Air Flow Rate (Nm^3/h)	6	6	6	6	6	6	6	6	6	6	6	6
ER	0.5	0.5	0.5	0.4	0.4	0.4	0.3	0.3	0.3	0.2	0.2	0.2
Preheated Air (°C)	352	283	290	352	296	281	352	307	282	352	308	279

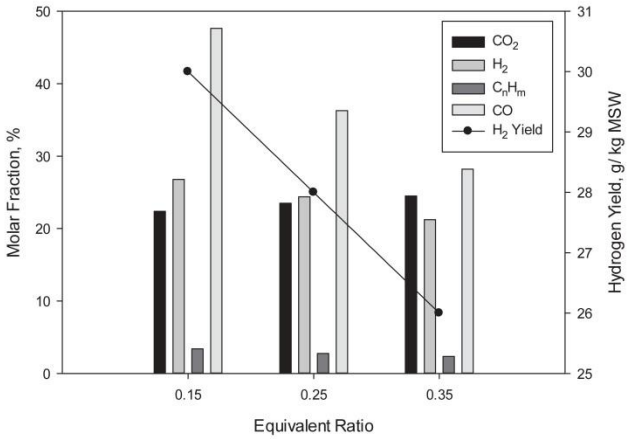

Fig. 3 – Influence of ER on syngas molar fraction and hydrogen yield. Dry and N_2-free basis. (Operating conditions: Temperature – 700 °C; MSW admission – 25 kg/h).

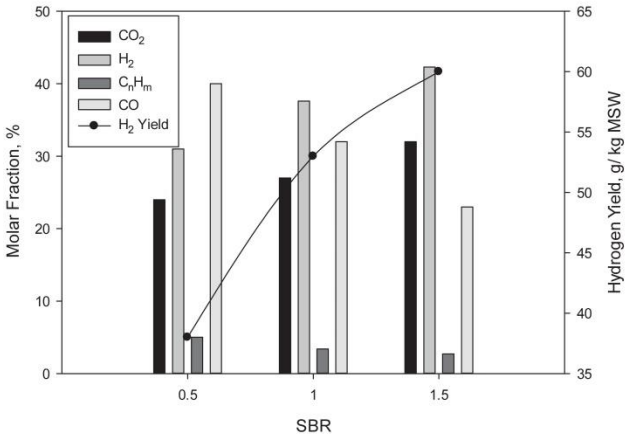

Fig. 5 – Influence of SBR on syngas molar fraction and hydrogen yield. Dry and N_2-free basis. (Operating conditions: Temperature – 700 °C; MSW admission – 25 kg/h).

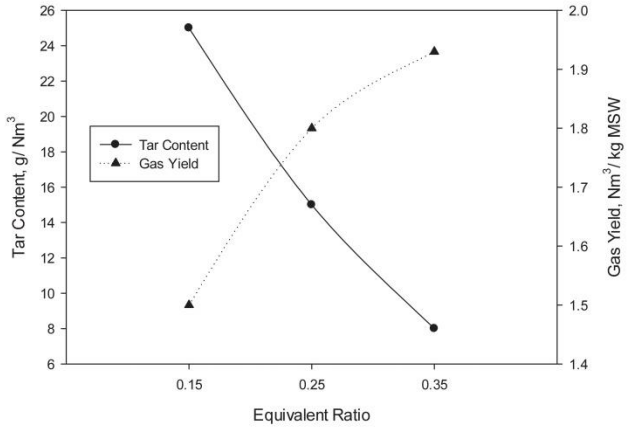

Fig. 4 – Influence of ER on tar content and gas yield. Dry and N_2-free basis. (Operating conditions: Temperature – 700 °C; MSW admission – 25 kg/h).

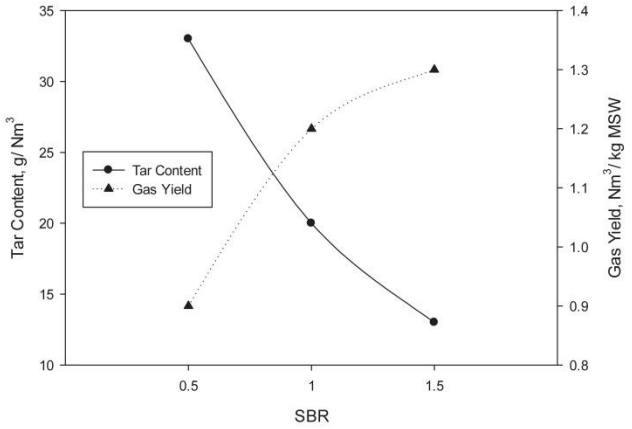

Fig. 6 – Influence of SBR on tar content and gas yield. Dry and N_2-free basis. (Operating conditions: Temperature – 700 °C; MSW admission – 25 kg/h).

production [35]. The SBR was varied over a range of values from 0 to 1.5 by holding the other variables constant. This range was selected based on previous findings from our research team using the same facilities but for a different biomass substrate. Fig. 5 shows the syngas molar fractions as a function of the SBR.

The presence of steam in gas-phase reactions will mostly favor char and tar steam reforming as well as water–gas shift reaction, which in turn will lead to an increase in CO_2 and H_2 content at the expense of CO and C_nH_m. In fact water–gas shift reaction will be the dominant reaction and CO will be consumed to produce CO_2 and H_2. These results are consistent with the current literature [15].

Moreover, it can be found from Fig. 6 that with the introduction of steam, tar content remarkably decreases, which is attributed to steam reforming of the tar with an increased partial pressure of steam. This promotion of the steam reforming reactions led to a rapid increase of dry gas yield as shown in Fig. 6, which agrees with the reduction of tar. The results obtained agree with those found in literature [36,37].

Effect of carbon dioxide to MSW ratio

Although poorly studied the addition of carbon dioxide as a gasifier agent has been showing promising results. Not only uses an unwanted end product of various industrial processes instead of steam (which is becoming an increasingly rarer resource) but also enhances both char gasification and pyrolysis and has the ability to act as a catalyst enhancing thermal cracking of volatiles leading to tar mitigation.

The effect of carbon dioxide as a gasifying agent was studied using CO_2-to-MSW ratio (which we will refer from now on "CDMR" for simplicity). The CDMR was varied over a range of values from 0 to 1 by holding the other variables constant. To the best of our knowledge this ratio is yet to be addressed in the current literature, although some work has been made using CO_2-to-biomass [38–40].

Fig. 7 shows the syngas molar fractions as a function of CDMR.

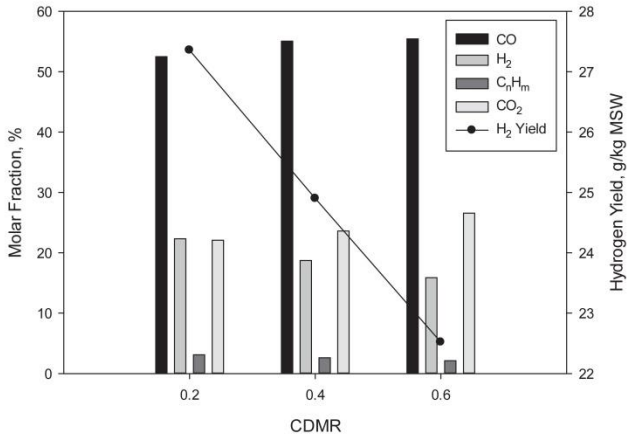

Fig. 7 – Influence of CDMR on syngas molar fraction and hydrogen yield. Dry and N_2-free basis. (Operating conditions: Temperature – 700 °C; MSW admission – 25 kg/h).

Results show that increase in CDMR leads to higher levels of CO and CO_2 and lower levels of H_2 and C_nH_m. This is explained by higher CO_2 content mainly promoting Boudouard and reverse water–gas shift reactions which leads to CO content increasing while H_2 decreases. C_nH_m molar fraction slightly decreases due to being consumed via CH_4 reforming to produce CO and H_2 [41]. CO_2 content increases since a considerable fraction of the gasifying agent leaves the reactor unreacted.

CO_2 addition is also responsible for decreasing one of the major concerns related to MSW gasification, tar formation [42]. Fig. 8 shows CDMR influence on tar content and gas yield.

Results show that increasing CDMR positively influences the gas yield and negatively influences the tar content. Since CO_2 addition enhances both char gasification and pyrolysis, which leads to increase in carbon conversion, gas yield is expected to increase. The catalyst effect of CO_2 enhances thermal cracking of volatiles leading to a substantial decrease in tar content. In fact, some authors found tar mitigation up to 50% when CO_2 was added [43].

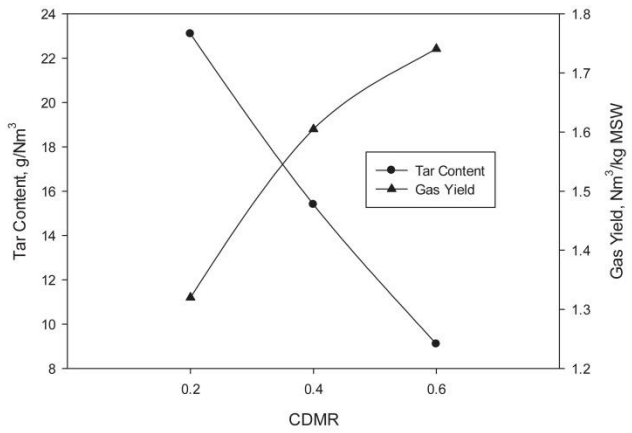

Fig. 8 – Influence of CDMR on tar content and gas yield. Dry and N_2-free basis. (Operating conditions: Temperature – 700 °C; MSW admission – 25 kg/h).

Despite no results in the literature were found for MSW, those available for biomass are in agreement with the obtained results [38–40]. Since the municipal wastes considered consist of over 85% of cellulosic material is safe to say that the trends for MSW will be similar to the biomass.

Effect of the reactor temperature

Gasification temperature is one of the most influential factors affecting the product gas composition and properties. The main reactions of the gasification are endothermic and thus strengthened by increasing temperature. Since the water gas, water gas shift, steam reforming and Boudouard reactions occur simultaneously, the contents and ratios of H_2, CO, CO_2 and C_nH_m in the product gas are affected by temperature and partial pressures of reactants. Therefore, the reactor temperature had a significant influence on the syngas compositions. As shown in Fig. 9, higher temperatures considerably resulted in higher H_2 contents.

At temperatures above 750 °C, the endothermic nature of the H_2 production reactions (steam reforming and water–gas reactions) results in an increase in H_2 content and a decrease in C_nH_m content with an increase in temperature. At temperatures above 850 °C, both steam reforming and the Boudouard reactions dominate, resulting in increases in CO content. It can be concluded that Boudouard reactions, carbon gasification reaction, together with the secondary cracking reactions of tar, were the main factors responsible for the increase in H_2 and CO contents.

Moreover, high temperature also favors destruction and reforming of tar leading to a decrease in tar content and an increase in gas yield because of higher conversion efficiency as it can be observed in Fig. 10. The results obtained are also confirmed in the literature [44,45].

Effect of the catalysts for MSW gasification

The use of catalysts in biomass gasification may not be essential, but it can help under certain conditions being the tar

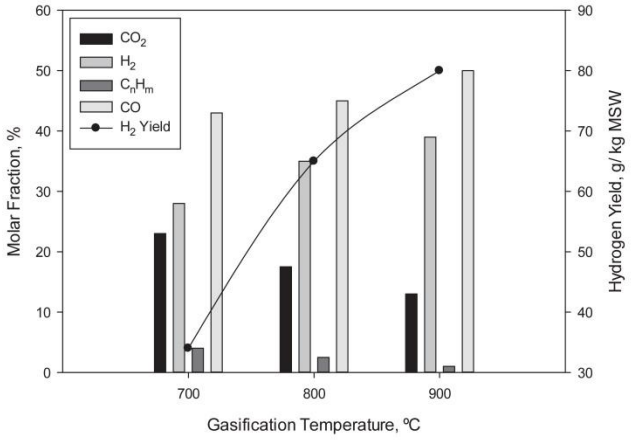

Fig. 9 – Influence of temperature on syngas molar fraction and hydrogen yield. Dry and N_2-free basis. (Operating conditions: ER – 0.25; SBR – 1; CDMR – 0.4; MSW admission – 25 kg/h).

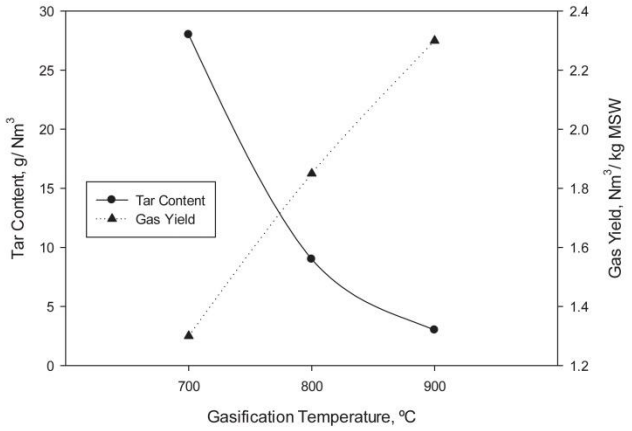

Fig. 10 – Influence of temperature on tar content and gas yield. Dry and N_2-free basis. (Operating conditions: ER – 0.25; SBR – 1; CDMR – 0.4; MSW admission – 25 kg/h).

formation one of the major issues. Similarly, during MSW gasification process tar is formed and some catalysts can be used to eliminate or at least greatly diminished the tar produced. The choice of a catalyst for reforming reactions is to be made keeping in mind their purpose and practical use. Earth metal catalysts such as dolomite had attracted much interest in this regard, because it is inexpensive and abundant and can notably reduce the tar content of the product gas from a gasifier [46]. Ni-based catalysts are highly effective as a reforming catalyst for reduction of tar as well as for correction of the CO/H_2 ratio through methane conversion. Nickel is relatively inexpensive and commercially available though not as cheap as dolomite. Simulations were performed considering 3 different scenarios: no catalyst, by using dolomite and by using NiO catalyst such as in Jingbo et al. [15]. Fig. 11 shows this comparison for ER equal to 0.25, SBR equal to one and CDMR equal to 0.4.

As far as the composition of the permanent gases is concerned, hydrogen remarkably increases (the production is more than twice and three times using dolomite or NiO/MD, respectively). NiO/MD led to the lowest hydrocarbons (C_nH_m), with reductions around 50%, and to the highest H_2 contents. Both of these factors indicate that dolomite and NiO/MD are active for tar destruction but not for methane reforming, as is to be expected. There is also an increase in the production of CO and the decrease of CO_2.

Dolomite usually shows some catalytic effect in promoting hydrocarbons destruction by cracking reactions, steam reforming reactions and CO_2 reforming reactions. Thus, CO and H_2 contents are expected to increase, as shown in Fig. 11.

Fig. 12 shows the results obtained under the same conditions save for the nature of the bed inventory material. A remarkable difference in the results is immediately apparent when some catalyst is introduced in the reactor bed: the production of gas increases by more than 20% using dolomite and by more than 30% using NiO/MD, with a consequential and also remarkable reduction in tar content by 2 fold (dolomite) and 4 fold (NiO/MD).

Effect of biomass substrate

To assess the potential of Portuguese municipal residues a comparison was made with 3 characteristic biomass substrates previously studied. Coffee husks [20], forest residues [47] and vines pruning residues [48] were studied using the described pilot-scale thermal gasification plant, for which relevant energetic as well as economic benefits were found. Fig. 13 shows the syngas molar fractions for all four fuels.

For this particular set of operating conditions coffee husks presents both the highest H_2 and C_nH_m molar fractions, while forest residues presents both the highest CO and CO_2 molar fractions. This can be explained by the chemical composition of each fuel. In fact, biomasses with a low C:H ratio and low O_2 content are responsible for maximum H_2 and CH_4 yields while biomasses with low O_2 content and high C:H ratio are responsible for maximum CO and CO_2 yields. This is consistent with the work of Louw et al. [49].

Fig. 14 shows the influence of substrate type on tar content and gas yield. Vines pruning presents both the highest gas yield and the lowest tar content while MSW presents both the lowest gas yield and the highest tar content. This can be explained by higher volatile content leading to an increase in residence time

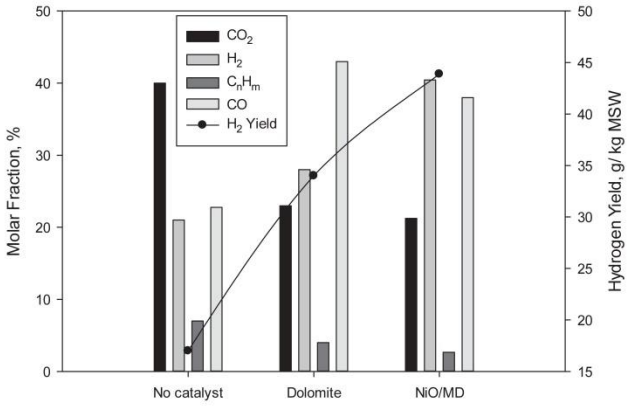

Fig. 11 – Influence of catalyst type on syngas molar fraction and hydrogen yield. Dry and N_2-free basis. (Operating conditions: ER – 0.25; SBR – 1; Temperature – 700 °C; CDMR – 0.4; MSW admission – 25 kg/h).

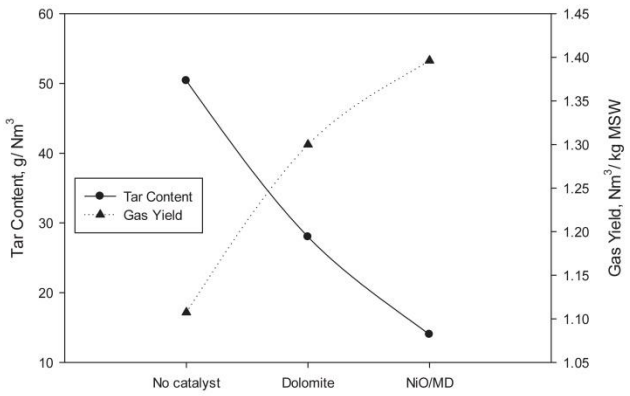

Fig. 12 – Influence of temperature on tar content and gas yield. Dry and N_2-free basis. (Operating conditions: ER – 0.25; SBR – 1; Temperature – 700 °C; CDMR – 0.4; MSW admission – 25 kg/h).

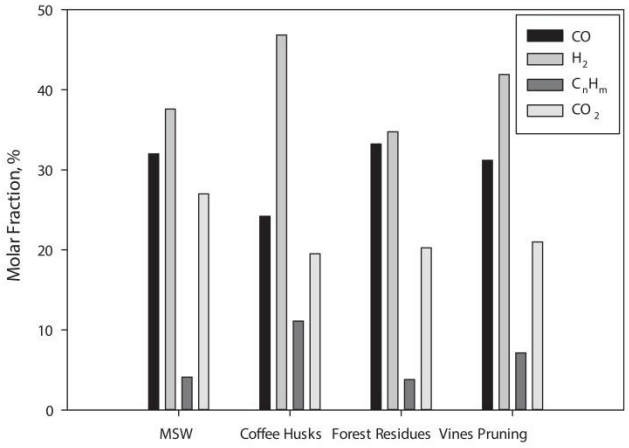

Fig. 13 – Influence of substrate type on syngas molar fraction and hydrogen yield. Dry and N_2-free basis. (Operating conditions: ER – 0.25; SBR – 1; Temperature – 700 °C; CDMR – 0.4; MSW admission – 25 kg/h).

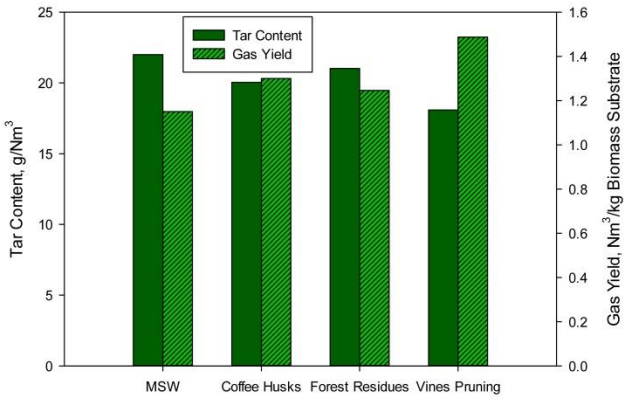

Fig. 14 – Influence of substrate type on tar content and gas yield. Dry and N_2-free basis. (Operating conditions: ER – 0.25; SBR – 1; Temperature – 700 °C; CDMR – 0.4; MSW admission – 25 kg/h).

that in turn will favor gasification reactions which leads to a higher gas yield [50]. Moreover, promoting gas yield is known for improving tar decomposition. This is consistent with the literature on the subject [51]. Since MSW has the lowest volatile content from the studied fuels [20], it comes with no surprise that it also presents the highest tar content.

Conclusion

A previously developed and validated two dimensional CFD model for MSW gasification has been used to predict and analyze the viability of the hydrogen generation from MSW gasification. Chosen limits for the several studied parameters were selected based on previous studies and available literature. The following conclusions can be drawn from the simulated results:

- The increase of ER has a negative effect on H_2 production because the oxidation reactions are favored when the reaction medium had higher contents of oxygen. On the other hand, the increase of ER has a positive effect on the reduction of tar content with increased gas yield.
- The use of steam as a gasifying agent in gas-phase reactions results in the decomposition of hydrocarbons and increasing contents of H_2. The introduction of steam also leads to more tar participating in steam reforming, which led to a rapid increase of gas yield and tar reduction because of higher conversion efficiency.
- The reactor temperature had a significant influence on the syngas compositions, since the main reactions of the gasification are endothermic. Higher temperature contributes to higher hydrogen content. Moreover, high temperature also favors destruction and reforming of tar leading to a decrease in tar content and an increase in gas yield because of higher conversion efficiency.
- CO_2 as a gasifying agent has a strong influence on syngas composition. With higher CO_2 Boudouard and reverse water–gas shift reactions are promoted leading to higher CO content while H_2 presented lower content. Results show that increasing CO_2-to-MSW ratio positively influences gas yield while negatively influences the tar content. This is related to enhancement in char gasification and pyrolysis as well as enhancement in thermal cracking of volatiles.
- Catalysts can significantly increase the content of hydrogen and decrease the yield of tar in the gasification of MSW. With the presence of NiO/MD catalysts, the tar was almost eliminated, the gas yield remarkably increased. Particularly, the content of hydrogen in the generated gas increased to 40%. Therefore, the NiO/MD is a promising catalyst for the application of hydrogen production from MSW steam gasification.
- MSW was also compared with previously studied Portuguese biomass substrates. Results shown that MSW produced lower H_2 and C_nH_m due to low C:H ratio and low O_2 content. On the other hand due to low volatile content it also presented high tar content and lower gas yield than the other studied fuels.

Acknowledgments

We would like to express our gratitude to the Portuguese Foundation for Science and Technology (FCT) for the support to the grant SFRH/BD/86068/2012 and the project PTDC/EMS-ENE/6553/2014.

REFERENCES

[1] Winter C-J. Hydrogen energy – abundant, efficient, clean: a debate over the energy-system-of-change. Int J Hydrogen Energy 2009;34:S1–52.
[2] Balat H, Kirtay E. Hydrogen from biomass – present scenario and future prospects. Int J Hydrogen Energy 2010;35:7416–26.
[3] Tanksale A, Beltramini JN, Lu GQM. A review of catalytic hydrogen production processes from biomass. Renew Sustain Energy Rev 2010;14:166–82.
[4] Koroneos C, Dompros A, Roumbas G. Hydrogen production via biomass gasification – a life cycle assessment approach. Chem Eng Process 2008;47:1261–8.
[5] Caputo AC, Palumbo M, Pelagagge PM, Scacchia F. Economics of biomass energy utilization in combustion and gasification plants: effects of logistic variables. Biomass Bioenergy 2005;28:35–51.
[6] Muradov NZ, Veziroglu TN. Green path from fossil-based to hydrogen economy: an overview of carbon-neutral technologies. Int J Hydrogen Energy 2008;33:6804–39.
[7] Biagini E, Masoni L, Tognotti L. Comparative study of thermochemical processes for hydrogen production from biomass fuels. Bioresour Technol 2010;101:6381–8.
[8] Achillas Ch, Vlachokostas Ch, Moussiopoulos N, Banias G, Kafetzopoulos G, Kara-Giannidis A. Social acceptance for the development of a waste-to-energy plant in an urban area. Resour Conserv Recycl 2011;55:857–63.
[9] Teixeira S, Monteiro E, Silva V, Rouboa A. Prospective application of municipal solid wastes for energy production in Portugal. Energy Policy 2014;71:159–68.
[10] Porteous A. Energy from waste incineration – a state of the art emissions review with emphasis on public acceptability. Appl Energy 2001;70:157–67.
[11] Couto N, Rouboa A, Silva V, Monteiro E, Bouziane K. Influence of the biomass gasification processes on the final composition of syngas. Energy Procedia 2013;36:596–606.
[12] Ahmed Tigabwa Y, Ahmad Murni M, Yusup Suzana, Inayat Abrar, Khan Zakir. Mathematical and computational approaches for design of biomass gasification for hydrogen production: a review. Renew Sustain Energy Rev 2012;16:2304–15.
[13] He Maoyun, Xiao Bo, Liu Shiming, Guo Xianjun, Luo Siyi, Xu Zhuanli, et al. Hydrogen-rich gas from catalytic steam gasification of municipal solid waste (MSW): influence of steam to MSW ratios and weight hourly space velocity on gas production and composition. Int J Hydrogen Energy 2009;34:2174–83.
[14] He Maoyun, Hu Zhiquan, Xiao Bo, Li Jianfen, Guo Xianjun, Luo Siyi, et al. Hydrogen-rich gas from catalytic steam gasification of municipal solid waste (MSW): influence of catalyst and temperature on yield and product composition. Int J Hydrogen Energy 2009;34:195–203.
[15] Wang Jingbo, Cheng Gong, You Yanli, Xiao Bo, Liu Shiming, He Piwen, et al. Hydrogen-rich gas production by steam gasification of municipal solid waste (MSW) using NiO supported on modified dolomite. Int J Hydrogen Energy 2012;37:6503–10.
[16] Onel O, Niziolek AM, Hasan MMF, Floudas CA. Municipal solid waste to liquid transportation fuels e part I: mathematical modeling of a municipal solid waste gasifier. Comput Chem Eng 2014;71:636–47.
[17] Couto N, Silva V, Monteiro E, Teixeira S, Chacartegui R, Bouziane K, et al. Numerical and experimental analysis of municipal solid wastes gasification process. Appl Therm Eng 2015;78:185–95.
[18] Couto N, Silva V, Eliseu E, Rouboa A. Assessment of municipal solid wastes gasification in a semi-industrial gasifier using syngas quality indices. Energy (93) 864–873.
[19] Silva V, Rouboa A. Predicting the syngas hydrogen composition by using a dual stage equilibrium model. Int J Hydrogen Energy 2014;39:331–8.
[20] Silva V, Monteiro E, Couto N, Brito P, Rouboa A. Analysis of syngas quality from portuguese biomasses: an experimental and numerical study. Energy Fuel 2014;28:5766–77.
[21] Zhou H, Meng H, Long Y, Li Q, Zhang Y. An overview of characteristics of municipal solid waste fuel in China: physical, chemical composition and heating value. Renew Sustain Energy Rev 2014;36:107–22.
[22] Eaton M, Smoot D, Hill C, Eatough N. Components, formulations, solutions, evaluation, and application of comprehensive combustion models. Prog Energy Combust 1999;25:387–436.
[24] Grammelis P, Basinas P, Malliopoulou A, Sakellaropoulos. Pyrolysis kinetics and combustion characteristics of waste recovered fuels. Fuel 2009;88:195–205.
[25] Wu C, Chang C, Hor J. On the thermal treatment of plastic mixtures of MSW: pyrolysis kinetics. Waste Manage 1993;13:221–35.
[26] Broson ML, Howard JB, Longwell JP, Peter WA. Products yields and kinetics from the vapor phase cracking of wood pyrolysis tars. AICHE J 1989;35:120–8.
[27] Zhang Q, Dor L, Yang W, Blasiak W. Eulerian model for municipal solid waste gasification in a fixed-bed plasma gasification melting reactor. Energy Fuel 2011;25:4129–37.
[28] Gunn DJ. Transfer of heat or mass to particles in fixed and fluidized beds. Int J Heat Mass Transf 1978;21:467–76.
[29] Arnavat M, Bruno J, Coronas A. Review and analysis of biomass gasification models. Renew Sust Energy Rev 2010;14:2841–51.
[30] Launder B, Spalding B. Lectures in mathematical models of turbulence. London, England: Academic Press; 1972.
[31] Cowin SC. A theory for the flow of granular materials. Powder Technol 1974;9:61–9.
[32] Gelderbloom SJ, Gidaspow D, Lyczkowski RW. CFD simulations of bubbling/collapsing fluidized beds for three geldart groups. AIChE J 2003;49:844–58.
[33] Gang X, Bao-sheng J, Zhao-ping Z, Yong C, Ming-jiang NI, Ke-fa C, et al. Experimental study on MSW gasification and melting technology. J Environ Sci 2007;19:1398–403.
[34] Wang Z, He T, Qin J, Wu J, Li J, Zi Z, et al. Gasification of biomass with oxygen enriched air in a pilot scale two-stage gasifier. Fuel 2015;150:386–93.
[35] Kumar A, Jones D, Hanna M. Thermochemical biomass gasification: a review of the current status of the technology. Energies 2009;2:556–81.
[36] André RN, Pinto F, Franco C, Dias M, Gulyurtlu I, Matos MAA, et al. Fluidised bed co-gasification of coal and olive oil industry wastes fuel. Fuel 2005;84:1635–44.
[37] Pinto F, Lopes H, André RN, Dias M, Gulyurtlu I, Cabrita I. Effect of experimental conditions on gas quality and solids produced by sewage sludge cogasification. Sewage Sludge mixed with coal. Energy Fuel 2007;21:2737–45.
[38] Cheng Y, Thow Z, Wang C. Biomass gasification with CO_2 in a fluidized bed. Powder Technol 2016. In Press, Corrected Proof, Available online 27 December 2014.
[39] Garcia L, Salvador ML, Arauzo J, Bilbao R. CO_2 as a gasifying agent for gas production from pine sawdust at low temperatures using a Ni/Al coprecipitated catalyst. Fuel Process Technol 2001;69:157–74.
[40] Renganathan T, Yadav M, Pushpavanam S, Voolapalli R, Cho Y. CO_2 utilization for gasification of carbonaceous feedstocks: a thermodynamic analysis. Chem Eng Sci 2012;83:159–70.

[41] Corigliano O, Fragiacomo P. Technical analysis of hydrogen-rich stream generation through CO_2 reforming of biogas by using numerical modeling. Fuel 2015;158:538–48.
[42] Hu M, Guo D, Ma C, Hu Z, Zhang Be, Xiao B, et al. Hydrogen-rich gas production by the gasification of wet MSW (municipal solid waste) coupled with carbon dioxide capture. Energy 2015;90:857–63 (http://www.sciencedirect.com/science/article/pii/S0360544215010178).
[43] Kwon EE, Yi H, Kwon HH. Urban energy mining from sewage sludge. Chemosphere 2013;90:1508–13.
[44] Gonzalez JF, Roman S, Bragado D, Calderon M. Investigation on the reactions influencing biomass air and air/steam gasification for hydrogen production. Fuel Process Technol 2008;89:764–72.
[45] Kumar A, Eskridge K, Jones D, Hanna MA. Steam-air fluidized bed gasification of distillers grains: effects of steam to biomass ratio, equivalence ratio and gasification temperature. Bioresour Technol 2009;100:2062–8.
[46] Hu G, Xu SP, Li SG, Xiao CG, Liu SQ. Steam gasification of apricot stones with olivine and dolomite as downstream catalysts. Fuel Process Technol 2006;87:375–82.
[47] Couto N, Silva V, Monteiro E, Brito P, Rouboa A. Using an Eulerian-granular 2-D multiphase CFD model to simulate oxygen air enriched gasification of agroindustrial residues. Renew Energy 2015;77:174–81.
[48] Silva V, Rouboa A. Optimizing the gasification operating conditions of forest residues by coupling a two-stage equilibrium model with a response surface methodology. Fuel Process Technol 2014;122:163–9.
[49] Louw J, Schwarz C, Knoetze J, Burger A. Thermodynamic modelling of supercritical water gasification: investigating the effect of biomass composition to aid in the selection of appropriate feedstock material. Bioresour Technol 2014;174:11–23.
[50] Manyà JJ, Sánchez JL, Ábrego J, Gonzalo A, Arauzo J. Influence of gas residence time and air ratio on the air gasification of dried sewage sludge in a bubbling fluidised bed. Fuel 2006;85:2027–33.
[51] Yan F, Luo S, Hu Z, Xiao B, Cheng G. Hydrogen-rich gas production by steam gasification of char from biomass pyrolysis in a fixed-bed reactor: influence of temperature and steam on hydrogen yield and syngas composition. Bioresour Technol 2010;101:5633–7.

Paper VIII

From laboratorial to industrial gasification: Analysis of the scale-up phenomenon

N. Couto, V. Silva, C. Bispo, A. Rouboa

Energy Conversion Management 119 (2016) 177-186

Energy Conversion and Management 119 (2016) 177–186

Contents lists available at ScienceDirect

Energy Conversion and Management

journal homepage: www.elsevier.com/locate/enconman

From laboratorial to pilot fluidized bed reactors: Analysis of the scale-up phenomenon

N. Couto [a], V.B. Silva [a], C. Bispo [a], A. Rouboa [a,b,c,*]

[a] INEGI-FEUP/ECT, Institute of Science and Innovation in Mechanical and Industrial Engineering, University of Porto, Portugal
[b] Engineering Department of University of Trás-os-Montes e Alto Douro, Vila Real, Portugal
[c] MEAM Department, University of Pennsylvania, Philadelphia, PA 19104-6391, USA

ARTICLE INFO

Article history:
Received 21 October 2015
Received in revised form 26 March 2016
Accepted 28 March 2016
Available online 19 April 2016

Keywords:
Scale-up
CFD
Pilot scale reactor
Uncertainty analysis
Laboratory-scale reactor

ABSTRACT

One of the major setbacks regarding commercial size reactors is the scale-up phenomenon. Studies linking laboratory-scale to industrial-scale experiments are extremely scarce due to hard logistic and associated costs that are significant high. The use of numerical models can help to fill this gap thus minimizing the risk and uncertainty associated with this phenomenon.

To assess the potential of numerical models to correctly predict the scale-up of a laboratory-scale reactor to a pilot scale one, a previously published numerical model was used. The two-dimensional model was built using data from a pilot scale gasification plant. After validating the model with pilot scale results, model was extended to predict biomass gasification in a laboratory-scale reactor. Numerical results in laboratory-scale were validated using experimental data available from the literature. Experimental errors were collected to perform uncertainty analysis. Height/cross section ratio between both reactors was chosen according to previously relevant studies. Influence of operation parameters in produced gas was investigated for both reactors. Residence time, temperature, syngas calorific and both carbon monoxide and hydrogen contents were higher for the large scale reactor. Still, the ability to predict correct trends was present in most cases for both reactors. Residence time proved to be one of the main factors for different results for different sizes. Also, the substrate characteristics such as the volatile content and size showed a considerable influence on the obtained results.

1. Introduction

According to recent reports [1], even with all the efforts led by government institutions to reduce the consumption of fossil fuels and its resulting damage to the environment, fossil fuels now provide over 87% of the world's primary energy supply. Even more disturbing is the ever increasing energy demand that increasingly requires investment in new structures.

However, it is possible to use these new and necessary investments in opportunities to build more efficient, less polluting and more flexible energy systems that are also less vulnerable to rising and volatile fossil fuel prices [1].

In order to meet these serious issues, recent decades were characterized by an increased interest on gasification-based technologies due to its significant environmental benefits over conventional ones [2]. Gasification also presents several environmental benefits when compared with other competitive technologies such as incineration, namely, with reduced char addition to soils, NOx emissions and landfill disposal option being able to respond to the increasingly environmental restrictive regulations applied around the world [3]. Biomass can be an important source in reducing fossil fuels dependence and, therefore, should be part of a national strategy considering energy generation [3]. Due to a high content in agricultural residues [4], Portugal may become a leading example in the efficient use of biomass. Several studies [4,5] were made considering the use of substrates such as forest residues and vines pruning for energy generation purposes. Ferreira et al. [4] analyzed the potential of different substrates to be used under different energy conversion technologies and discussed their implementation and legal framework. Silva et al. [5] developed a 2-D multiphase model to simulate the gasification of large available biomasses in Portugal by using a semi-industrial fluidized bed reactor. However, a great effort is still necessary to develop and implement simple actions to value these residues and related by-products. An important first step would be conducting experi-

* Corresponding author at: Mechanical Engineering and Applied Mechanics Department, University of Pennsylvania, 33rd Walnut Street, Main Building, Philadelphia, PA 19104-6391, USA.
E-mail address: rouboa@seas.upenn.edu (A. Rouboa).

http://dx.doi.org/10.1016/j.enconman.2016.03.085
0196-8904/

ments able to characterize the substrate behavior and predict the gasification process for commercial reactors.

Most experimental studies found in the literature use laboratory scale reactors, mainly due to lower operating costs and being more accessible when it comes to controlling the various operational parameters and boundary conditions [6]. Studies conducted in industrial reactors are limited due to the difficulty of regulating the operating parameters but mainly due to the high cost of a gasification plant, which can reach tens of millions of euros depending on the generated power [7].

From the studies concerning laboratory scale reactors the following are highlights of some recent ones. Xiao et al. [8] used low-temperature gasification to study energy recovery from waste tire. Influence of equivalent ratio and temperature on carbon black yield was analyzed. Results showed that carbon balance reached 95% when temperature was over 600 °C. Sarker et al. [9] used a lab-scale fluidized bed reactor to gasify alfalfa and wheat straw pellets. Impact of semi-continuous solid feeding and equivalent ratio on several gasification variables such as gas lower heating value, specific gas yield, cold gas efficiency and carbon conversion efficiency was studied. Optimal operational point for alfalfa and wheat straw was found for equivalent ratios of 0.35 and 0.3, respectively. Moghadam et al. [10] integrated pyrolysis and steam gasification processes in order to obtain the optimum condition of syngas production. The impact of reaction temperature, equivalence ratio and steam-to-biomass ratio was investigated. The effect of using different biomasses in a steam environment was studied by Loha et al. [11]. They also developed an equilibrium model and the corresponding validation was performed using experimental data collected by the author in a laboratory scale fluidized bed gasifier.

Although these studies, among others, are very important for increasing fundamental knowledge of the gasification process, it is imperative to devote time to studies that utilize pilot scale or industrial reactors. Indeed, a major concern regarding coal and biomass gasification is the scale-up. The scale-up has brought problems for engineers since the beginnings of fluidization history, culminating in its best-known failure example of the first bubbling-bed, Fischer–Tropsch in 1950 [12]. Scale-up is not an exact science, it is too complicated to use information collected from laboratory studies and use it to design a commercial reactor that can be tens or even hundreds of times larger. There are key factors that rule this transition and whose prediction is still not well known. When changing from a small reactor to a larger one, the hydrodynamics changes significantly which means that substrate particles behave differently. Also, the residence time is different causing a great influence on the chemical reactions. Both contributions lead to final syngas compositions which can differ substantially, at least, in their absolute value. For this reason, it is necessary to gather data from reactors with similar dimensions to avoid errors and reduce high level risks and uncertainty [13]. One way around this issue without resorting to major investments and/or the need for long waiting periods (with all the bureaucratic and logistical problems associated) is the use of numerical models. These models provide the ability to theoretically simulate any physical condition while being relatively inexpensive and quickly executed. Different modeling approaches have being attempted by several research groups [14–16]. One of the most traditional and simple approaches considers the gasification process in thermodynamic equilibrium [14]. The equilibrium models are especially advantageous considering their quick and easy convergence and its importance as a design tool. However, they are unable to predict any hydrodynamics aspects of the gasification process as well as important profile distributions inside the reactor. Hameed et al. [15] used kinetic models for describing the rate equations for the different reactions that occur in the reduction zone of a biomass gasifier. More complex approaches involve gas–solid flow, chemical reactions and interaction between phases [16]. Meaningful information can be extracted from powerful simulation models and used to predict experimental results in laboratorial and industrial scales.

In the present study a previously developed numerical model was used to study the scale-up effects between a laboratory-scale and a pilot scale reactor using two Portuguese agro-industrial residues. Model was first validated against results from a pilot scale reactor. Model was then expended to predict the results in laboratory scale reactor. Literature was used to validate the model in lab-scale conditions. Influence of gasification temperature and oxygen content in both reactors was also studied. Finally, influence of biomass type on scale-up effect was analyzed.

2. Materials and experimental set-up

Experimental runs were performed in a pilot scale bubbling fluidized bed gasifier. The schematics of the pilot scale gasification plant are depicted in Fig. 1.

All components that comprise the gasification plant are fully detailed in electronic supplementary material. The upcoming analysis is considered for forest and vine pruning residues. Data regarding proximate and ultimate analysis are found in Table 1. Also, data regarding these substrate availability in Portugal can be found in [5] and in electronic supplementary material.

3. Mathematical model

Even though scale-up phenomenon is one of the major problems concerning biomass gasification there is still a clear lack of work done on the problem mainly due to the costs associated with industrial size gasifiers. In order to properly study the scale-up, a numerical study using different size reactors ranging from laboratory to pilot scale was performed. The two-dimensional mathematical model developed and detailed by Couto and Silva [17] was applied in this study. A brief description of the mathematical model is highlighted in the next lines.

Mass and momentum balances are considered for both phases (solid and gas). Due to the characteristics of fluidized bed gasifiers [18], turbulence between phases can be modeled by using the standard k–ε model in ANSYS FLUENT. Detailed equations can be found in [5]. The multi-phase approach considers the gas phase as continuous and the solid phase follows the granular Eulerian model. Equations for granular temperature were based on the Syamlal et al. [19] and Lun et al. [20] works. Detailed equations can also be found in [5].

The main equations governing the chemistry behind the developed model are depicted in Table 2. Devolatilization is the thermal decomposition of solid fuels. Biomass is assumed to be comprised of cellulose, hemicellulose and lignin [21] and with each component contributing proportionally to the biomass [22]. Devolatilization representative equations and kinetics are depicted in Table 2.

Homogeneous gas-phase reactions are modeled considering the finite-rate/Eddy-dissipation model which considers both the Arrhenius and Eddy-dissipation reaction rates. The minimum value of the Arrhenius and Eddy dissipation rates can be defined as the net reaction rate. Heterogeneous reactions follow the Kinetic/Diffusion Surface Reaction Model [25,26]. Baum et al. [25] applied this model to simulate the behavior of coal particles. Field [26] used this approach to describe the heterogeneous reactions that occur in the char gasification of a low rank coal at high temperatures. This model weights the effect of the Arrhenius rate and the diffusion rate of the oxidant at the surface particle.

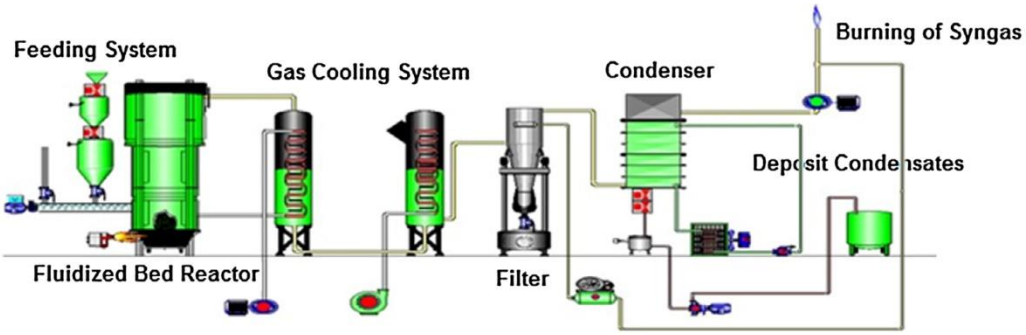

Fig. 1. Schematics of the biomass gasification semi-industrial plant.

Table 1
Ultimate and Proximate Analyses of Forest and Vine Pruning Residues.

Biomass proprieties	Forest residues	Vines pruning
Elementary analysis (%)		
N	2.4	2.6
C	43	41.3
H	5	5.5
O	49.6	50.6
Humidity (%)	11.3	13.3
Density (kg m^{-3})	650	265
Net heat value (MJ kg^{-1} biomass)	21.2	15.1
Proximal analysis (%)		
Ash	0.2	3.1
Volatile matter	79.8	83.6
Fixed carbon	20	13.3

Energy conservation is also considered for both phases. Correlations for heat transfer coefficients are detailed in [5].

Quadrilateral cells with a size roughly 12 times larger than the particle size [27] were selected after performing some simulation runs and insignificant differences were found considering syngas composition, temperature, velocity and turbulence profiles. Also, the selection of cells with this size is in agreement with the literature [28] based on hydrodynamic issues. Convergence criteria for residuals were 10^{-8} for continuity and momentum equations and 10^{-14} for energy equation. The model was first solved considering the absence of chemical reactions. Then, and with a consolidated flow pattern, the chemical reactions were included and the model was solved.

4. Results and discussion

In order to successfully study the scale-up phenomenon it is first necessary to validate the numerical model for both laboratorial and pilot scale conditions. To validate the model under pilot scale conditions data from the already described reactor was used. For laboratorial conditions, validation was made using data available in the literature.

4.1. Validation for semi-industrial conditions

Using data collected from a pilot scale up-flow gasifier it was possible to build a model able to predict the biomass gasification. In Table 3 are shown some of the operating conditions selected from the performed experimental runs. Additional data regarding

Table 2
Chemistry model reactions [5,23,24].

Reactions	Reaction rate
Devolatilization	
Biomass → Char + Volatiles + Steam + Ash	$r_1 = A_i \exp\left(\frac{-E_i}{T_s}\right)(1-a_i)^n$
Volatiles → $\alpha_1 CO + \alpha_2 CO_2 + \alpha_3 CH_4 + \alpha_4 H_2$	$r_2 = A_i \exp\left(\frac{-E_i}{T_s}\right)(1-a_i)^n$
Homogeneous reactions	
$CO + 0.5O_2 \rightarrow CO_2$	$r_3 = 1.0 \times 10^{15} \exp\left(\frac{-16.000}{T}\right) C_{CO} C_{O_2}^{0.5}$
$CO + H_2O \rightarrow CO_2 + H_2$	$r_4 = 2780 \exp\left(\frac{-1510}{T}\right)\left[C_{CO} C_{H_2O} - \frac{C_{CO_2} C_{H_2}}{0.0265 \exp\left(\frac{3968}{T}\right)}\right]$
$CO + 3H_2 \leftrightarrow CH_4 + H_2O$	$r_5 = 3.0 \times 10^{5} \exp\left(\frac{-15.042}{T}\right) C_{H_2O} C_{CH_4}$
$H_2 + 0.5O_2 \rightarrow H_2O$	$r_6 = 5.159 \times 10^{15} \exp\left(\frac{-3430}{T}\right) T^{-1.5} C_{O_2} C_{H_2}^{1.5}$
$CH_4 + 2O_2 \rightarrow CO_2 + 2H_2O$	$r_7 = 3.552 \times 10^{14} \exp\left(\frac{-15.700}{T}\right) T^{-1} C_{O_2} C_{CH_4}$
Eddy dissipation rate	
$r_{Eddy\text{-}dissipation} = \alpha_{i,r} M_{w,i} A \rho \frac{\varepsilon}{k} \min\left(\min_R\left(\frac{Y_R}{\alpha_{R,r} M_{w,R}}\right), B \frac{\sum_P y_P}{\sum_i^N \alpha_{i,r} M_{w,i}}\right)$	
Heterogeneous reactions	
$C + 0.5O_2 \rightarrow CO$	$r_8 = 596 T_P \exp\left(\frac{-1800}{T}\right)$
$C + CO_2 \rightarrow 2CO$	$r_9 = 2082.7 \exp\left(\frac{-18.036}{T}\right)$
$C + H_2O \rightarrow CO + H_2$	$r_{10} = 63.3 \exp\left(\frac{-14.051}{T}\right)$
Kinetic/diffusion surface reaction model	
$\frac{d m_p}{d t} = -A_p \frac{\rho R T_\infty Z_{ox}}{M_{w,ox}} \frac{D_0 r_{Arrhenius}}{D_0 + r_{Arrhenius}}$	

Table 3
Operating conditions for the experimental gasification runs.

Gasification run	Biomass type	Admission biomass (kg h^{-1})	Air flow rate (N m^3 h^{-1})	Gasification temperature (°C)
1	Forest residues	63	94	815
2		74	98	815
3		63	98	790
4	Vines pruning	25	52	790
5		55	40	790
6		55	40	815

the performed runs in the pilot scale gasifier can be seen in [17]. 2 biomasses (forest and vine pruning residues) largely available in Portugal but also with considerable energetic potential were investigated.

Syngas composition obtained in the experimental runs as well as in the numerical model can be seen in Fig. 2. Variation of any of the operating condition has a great influence on the produced gas. In depth analysis on these parameters will be made in the next sections.

The numerical model predicts the experimental data reasonably well being robust enough to predict the syngas composition at different operating conditions. Relative errors lower than 20% were found for all the presented fractions. This range of errors is very promising considering such complex systems and is in agreement with other works found in the literature [29]. Sources of deviation are intimately related to some simplifications [17].

Forest residues are richer in carbon while vine pruning residues are richer in hydrogen. When a biomass is richer in such elements, the corresponding syngas is also richer in CO and H_2, respectively [30]. Moreover, a direct link can be made between biomass and syngas calorific value. Effectively, it was with no surprise, that a syngas with higher caloric value was obtained from the forest residues since it is the most energetic biomass (Table 1). Once again, the developed model is able to predict such behavior.

From Runs 1 and 2, it can be observed that the increase in biomass intake caused a slight decrease in the calorific values. This trend is consistent with other studies [31] and has to do with the fact that an increase in biomass flow rate reduces the extent of reaction, and equilibrium of the steam methane reforming reaction and primary water–gas reaction are not attained.

4.2. Validation for laboratory conditions

To validate the use of the developed model in the study of the scale-up phenomenon, it is necessary to evaluate its performance under laboratorial and pilot scale experimental conditions. Accordingly, the numerical model was first validated using experimental results (Fig. 2) collected from the performed runs. Since no results were gathered in laboratorial scale reactor data available in the literature was needed. The work from Campoy et al. [32] was used to validate the model in laboratorial scale conditions since extensive information not only on the gasification process and biomass substrate used but also regarding reactor geometry, necessary to build the numerical model, was available. Table 4 shows the gasification conditions selected for the model validation.

Syngas molar fractions for both experimental and numerical results are depicted in Fig. 3.

Results from the numerical model show a very reasonable agreement with the experimental data at laboratory scale reactor. Similar errors were found for additional runs. Again, variation can be explained due to the complexity of a gasification system.

In depth analysis on the presented results can be seen in [32].

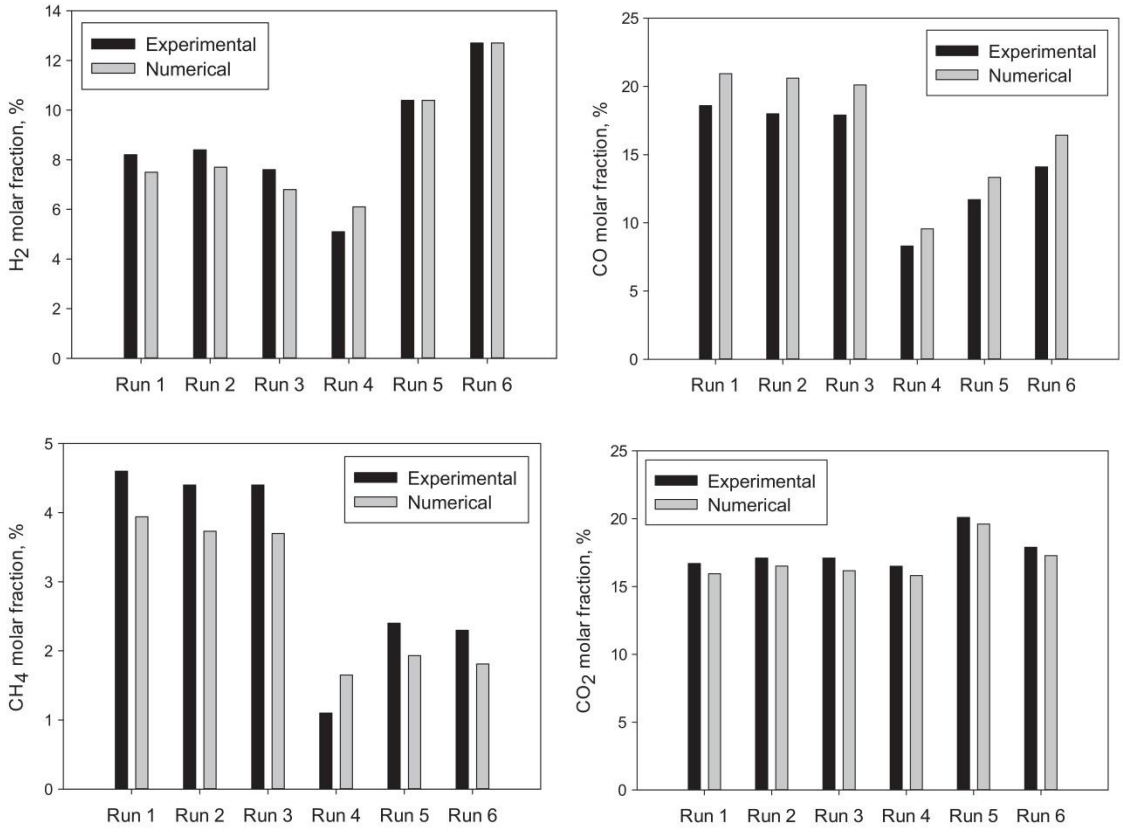

Fig. 2. CFD and experimental molar fractions for the 6 gasification runs defined in Table 3.

Table 4
Experimental gasification conditions used for the model validation.

Gasification run	Biomass feeding rate (kg h^{-1})	Flux of air (N m^3 h^{-1})	Oxygen flow rate (N m^3 h^{-1})	Steam flow rate (kg h^{-1})	Gasification temperature (°C)
1	12.2	17.0	0.0	2.5	804
2	12.2	17.0	0.0	5.1	789
3	15.0	17.0	0.0	3.2	786
4	10.0	9.1	1.2	5.6	790
5	16.2	10.6	1.4	4.7	781
6	12.0	7.7	1.0	6.5	765

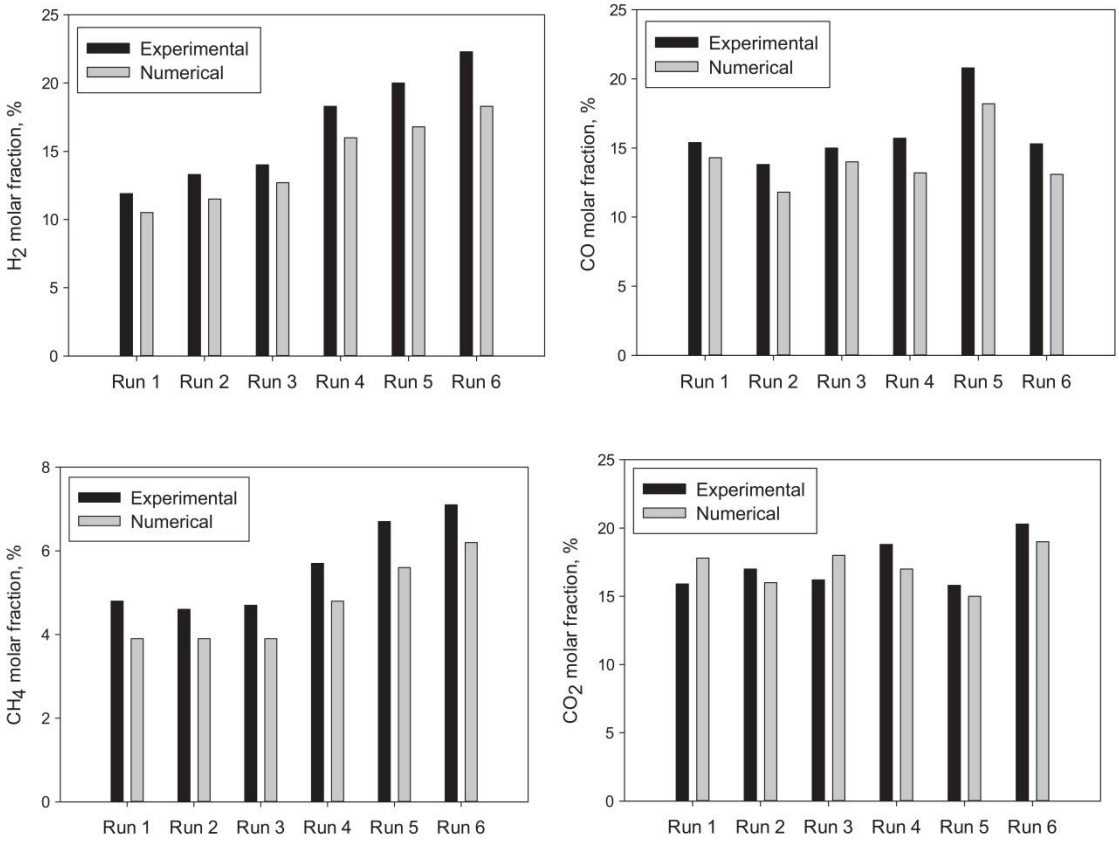

Fig. 3. CFD and experimental molar fractions for the 6 gasification runs defined in Table 4.

Range of errors between laboratory-scale and industrial was quite similar.

4.3. Uncertainty analysis

The validity of numerical models requires a reliable and accurate measurement capability of the instruments used in collecting the experimental data.

All measurements and instruments have certain characteristics. An understanding of these ordinary qualities is the first step toward accurate measurement. Errors and uncertainties are inherent in both the instrument and the process of making the measurement, and too much confidence should not be placed on any single reading.

Errors and uncertainties in the experiments can appear from various factors like instrument selection, instrument condition, instrument calibration, observation and reading, surroundings, and test planning [33]. In the experiments of forest residues and vine pruning's gasification, temperatures, flow rates and pressure drops were measured with appropriate instruments.

4.3.1. Total uncertainties in reactor temperatures

During the gasification process of forest residues and vines pruning, the average uncertainties arisen from the measurement of temperatures are classified as follows:

- The average uncertainty arisen from the fabrication of thermocouples ±0.3%.
- The average uncertainty arisen from the connecting devices and settling of thermocouples ±0.5%.
- The average uncertainty arisen from the interaction of thermocouples with the SCADA system ±0.02%.

Individual uncertainties like the ones mentioned above can be put together into a combined uncertainty by simply root the sum of the squares of each uncertainty:

$$\text{Combined Uncertainty} = \sqrt{a^2 + b^2 + c^2 + \dots} \quad (1)$$

4.3.2. Total uncertainties in pressure drops

During the gasification process of forest residues and vines pruning, the average uncertainties arisen from the measurement

Table 5
Combined uncertainties for the main parameters.

Total uncertainties in reactor temperatures	±0.58%
Total uncertainties in pressure drops	±0.75%
Total uncertainties in biomass flow rates	±1.44%
Total uncertainties in air flow rate	±1.2%
Total uncertainties in syngas outflow rate	±1.75%

of pressure drops are classified as the average uncertainty arisen from fabrication and connecting devices of pressure transducers ±0.75%.

4.3.3. Total uncertainties in biomass flow rates

The average uncertainties arisen from the measurement of flow rates were systematically presented below:

- The average uncertainty arisen from time recorder ±1%.
- The average uncertainty arisen from the vibration of balance instrument ±0.015%.
- The average uncertainty arisen from weighing of biomass ±1%.
- The average uncertainty arisen from the determination of wet feed rate of biomass ±0.25%.

4.3.4. Total uncertainties in air flow rate

The average uncertainty arisen from the calculation of the air flow rate ± 1.2%.

4.3.5. Total uncertainties in syngas outflow rate

Gasification gas analysis was performed in a Varian 450-GC gas chromatograph with two TCD detectors that allow the detection of H_2, CO, CO_2, CH_4, O_2, N_2, C_2H_6, C_2H_4 (equipped respectively with CP81069, CP81071, CP81072, CP81073 and CP81025 Varian GC columns), using helium and nitrogen as carrier gases. Gasification gas samples for the above referred analysis were collected in appropriate collection and analysis Tedlar bags at the condenser exit every time gasification of a given feedstock composition has reached its stationary state. Collected gasification gas samples were injected directly from the sampling bags in the chromatograph (within 1 h after sampling) using a peristaltic pump operating at its maximum rate through a Marpren tube. Chromatographic peaks for the different gases under analysis were identified based on their retention times, and by comparing them with the retention times of the same gases in the reference chromatogram of the custom solution, provided by Varian.

Gas molar percentage composition was calculated on the basis of peak areas under the chromatographic signals.

With all this in mind the average uncertainty obtained from the calculation of the gas volumetric flow rate is ±1.75%.

Table 5 presents the combined uncertainties for the all the main parameters measured in the gasification process. Results are in agreement with the limited literature available on the subject [34].

Also, it should be noted that regarding the experimental gasification runs, every run was performed twice in order to avoid off measurements. When deviation was higher than 5%, extra runs were performed to assure reproducibility below 5%, which is typical for this kind of system [32].

4.4. Results from pilot-scale reactor

After validating the numerical model and reaffirming the reliance on experimental results, it is now possible to study the influence of several operating parameters on the final composition of the gas produced in pilot scale conditions.

Fig. 4 shows the influence of oxygen content on syngas molar fractions for different biomass substrates. Gasification temperature was chosen to be around 800 °C. Biomass and air inlet flow rate were selected to be at 50 kg/h and 75 N m^3/h, respectively.

With the increase of oxygen content in the reactor, either by adding oxygen into air mixture or simply by increasing the air flow rate, one is promoting the oxidization reactions such as particle combustion of char, CO and H_2, that in turn will lead to higher CO_2 and H_2O contents to the detriment of CO and H_2 [35].

However, increase in oxygen content leads to an increase in all of the presented species mainly due to the decrease in the dilution effect from nitrogen. In fact, by increasing the oxygen concentration in the air mixture one is decreasing the nitrogen entering the reactor, leading to a syngas with less and less nitrogen.

Methane fraction rises with oxygen content mainly due to the reduction in N_2 content, since oxygen content has a direct influence in the gasification temperature, increase in oxygen content leads to a slight decrease in CH_4 content due to methane formation reaction being exothermic and therefore not being promoted at higher temperatures [36].

According to [37] chemical composition from both biomass and produced gas have a directed link. As previously stated, a biomass with higher content of carbon and hydrogen will generally produce a syngas with higher content of CO and H_2, leading to a syngas with higher calorific value. This is noticeable in the obtained results. Still, there are other biomass properties that can greatly influence not only syngas composition but the efficiency of the process.

For instance, the gasification efficiency decreases with increasing biomass moisture content since high moisture content influences the chemical reactions inside the gasifier [38]. Instead of

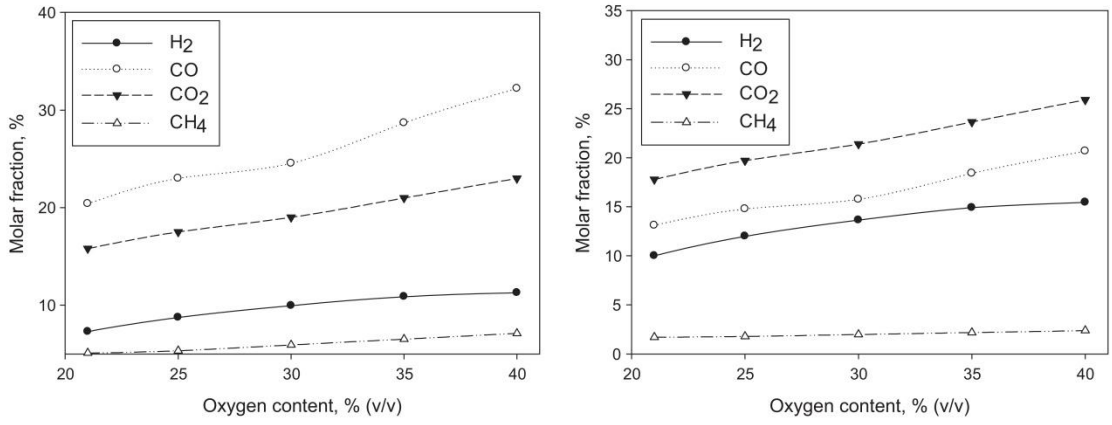

Fig. 4. Syngas molar fractions as a function of oxygen content for (a) forest residues and (b) vines pruning.

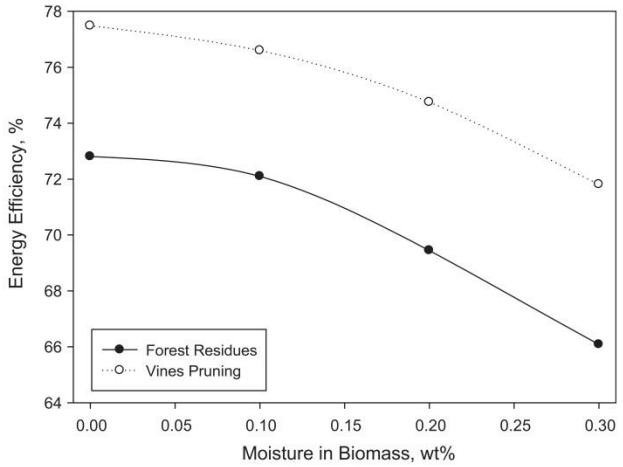

Fig. 5. Energy efficiency as a function of the moisture content in both biomasses.

being consumed by the endothermic reactions (responsible of producing CO and H_2), liberated heat is consumed by water evaporation. Therefore, higher efficiencies are obtained for biomass with less moisture content because higher amounts of CO and H_2 are produced. Fig. 5 shows the influence of biomass moisture content on energy efficiency of the gasification process.

Results clearly show that biomass moisture has a very relevant effect on energy efficiency. Again, these results are consistent with the current literature [38]. However, the process with the highest efficiency was obtained by biomass with higher moisture level. In this particular case, since the moisture levels from both substrates are quite similar (only 2% difference) other biomass properties can have a greater influence on efficiency results. Because of this, results comparing both biomass type and other operating parameters such as oxygen content are very scarce [39]. In those studies no clear relationship between them was found. In the current study both biomasses presented very similar trends, only varying in the molar concentration of some species. Namely, forest residues presented higher levels of CO and CH_4 while vines pruning presented higher levels of H_2 and CO_2. Properties like chemical composition and moisture already discussed can be used as an explanation for this variation but also particle size and density can have a direct influence on gasification process. Because of this it's not possible to make any direct relation between biomass type and oxygen content of gasifying medium.

Fig. 6 shows the influence of gasification temperature for different biomass substrates on syngas molar fractions.

It is clear that increasing gasification temperature, syngas with higher CO and H_2 will be produced [5]. In fact, according to Le Chatelier's principle, higher temperatures will favor endothermic reactions which in turn will promote the production of H_2 (through primary water–gas reaction and steam-methane reforming) and CO (through Boudouard reaction as well as reverse water–gas shift reaction) [35]. In contrast, the CH_4 and CO_2 contents follow the opposite trend. As stated, CH_4 content decreases with the increase of gasification temperature because the methane reaction formation is exothermic. This is consistent with the literature [36]. This was seen in both biomass substrates as the phenomenon is independent of the type of biomass and only depends on the gasification temperature. Again forest residues showed a higher CO and CH_4 content while vines pruning presented higher levels of H_2 and CO_2. Similarly to the oxygen content effect it's not possible to identify any relevant effect of temperature as a function of the employed biomass.

4.5. Results from laboratory-scale reactor

The same studies performed in Section 4.4 were remade using a new mesh. Reactor dimensions were chosen accordingly to the work of Pinto et al. [40] on the gasification improvement of poor quality solid recovered fuel and later on the co-gasification of coal and wastes [41]. Lab-scale gasifier had a total height of 2.75 m and internal diameter of 17.5 cm.

In order to compare the obtained compositions, the same operating conditions were used. Nonetheless, input flow rates of semi-industrial installation were close to 20 times higher than those of laboratory scale, as for similar numerical values flow rates of laboratory scale reactor were in g/min, while those of semi-industrial were in kg/h. Therefore, the residence time in semi-industrial reactor gasifier was around 20% higher.

Figs. 7 and 8 recreate studies performed in Figs. 4 and 6 this time for laboratory scale. At this point only forest residues will be considered as the biomass substrate. Influence of biomass type in scale-up will be addressed later in the chapter.

Comparison from the above Figures with results from Section 4.4 shows us that both reactors present the very similar trends. In short, increasing oxygen content oxidization reactions are favorable leading to higher CO_2 and H_2O contents to the detriment of CO and H_2 [35]. However, increase in oxygen content leads to an increase in all of the presented species mainly due to the decrease in the dilution effect from nitrogen.

On the other hand, increase in gasification temperature will lead to higher CO and H_2 while CH_4 and CO_2 contents decreases due to favoring of endothermic reactions [36].

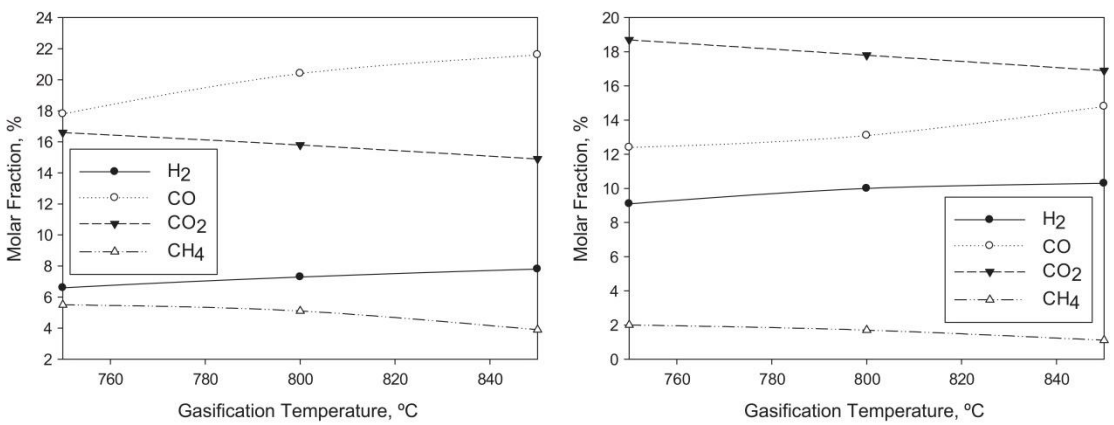

Fig. 6. Syngas molar fractions as a function of the gasification temperature for (a) forest residues and (b) vines pruning.

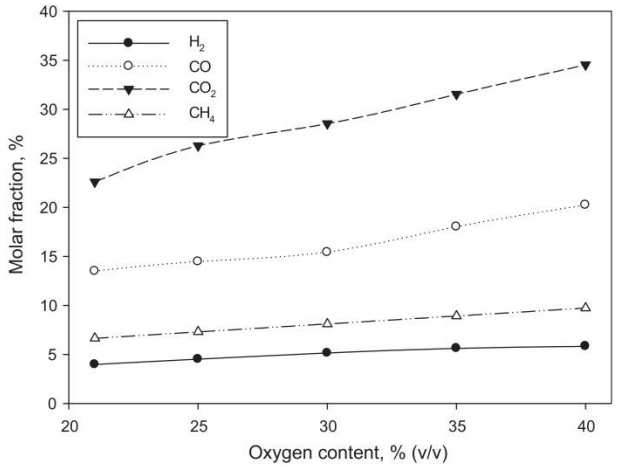

Fig. 7. Syngas molar fractions as a function of oxygen content for lab-scale reactor.

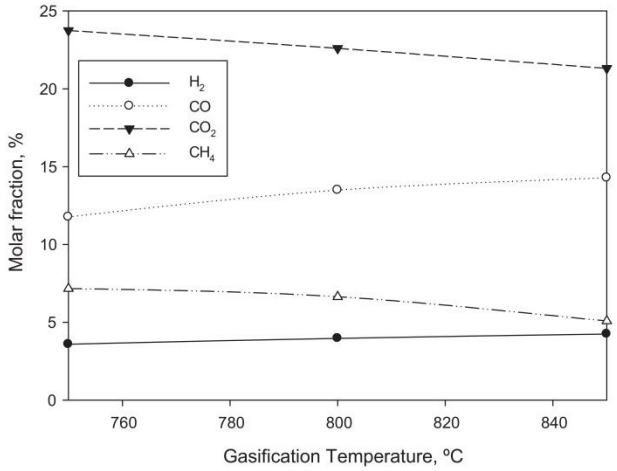

Fig. 8. Syngas molar fractions as a function of gasification temperature for lab-scale reactor.

4.6. Scale-up analysis

At this time the model has been validated for both pilot and laboratorial scale conditions and presented similar relative error and capability in correctly predict trends for different operating conditions. Meaning that it is now possible to compare both reactors using the same biomass type as well as operating conditions without the influence of the model being responsible for the variation in results.

According to Knowlton et al. [13] one of the major concerns regarding biomass gasification is the scale-up effect. The nonlinear hydrodynamic behavior combined with complex chemistry schemes can greatly impact the gas–solid flow [6]. Because of this, larger particles are more difficult to scale-up than smaller ones.

Although trends were similar between reactors there were significant differences regarding gasification products. Table 6 summarizes some of most relevant findings.

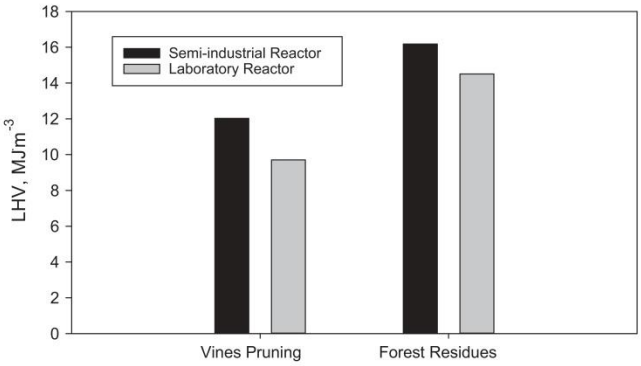

Fig. 9. Effect of scale-up on syngas low heating value for all studied biomass types. (Operating conditions were 800 °C gasification temperature and 21% oxygen content.)

In fact, laboratory scale reactor led to a syngas with higher levels in CO_2 and CH_4 and lower CO and H_2 ones. This has to do with higher residence time in semi-industrial reactor will favor gasification reactions thus leading to a syngas with higher calorific value [40].

Moreover, the increase in residence time promotes gasification reactions and carbon conversion leading to higher gas yield [42].

Scale-up effects can also be seen in other gasification parameters such as syngas calorific value and biomass type. Fig. 9 shows the scale-up effects in syngas calorific value for the two studied biomass substrates.

Generally, biomass with higher heating value will produce syngas with higher heating value as well [30]. So, it comes with little surprise that syngas with higher heating value was produced by forest residues, a more energetic substrate.

Effects of scale-up on syngas composition were already studied but in a summarized manner due to shorter residence time, laboratory scale reactor led to a produced gas with higher CO_2 and CH_4 and lower CO and H_2 content [41]. Being the later 2 the ones with the most influence in the syngas calorific content.

So far the influence of biomass type on scale-up effects in biomass gasification hasn't been properly explained in literature. There are several biomass properties that can influence scale-up, namely chemical structure, volatile content, size particle, just to name a few.

Some studies on co-gasification showed that coal mixed with pine presented an increase in gas yield due to the higher volatile content of pine [43]. Increase in gas yield is related to tar decomposition into smaller and gaseous molecules. According to Aljbour and Kawamoto [44] a reduction in tar production by increasing the residence time was observed. So, it is possible to say that higher volatile content will lead to an increase in the residence time that in turn will favor gasification reactions [40]. Well, since vines pruning has the highest volatile content of the two [5] it comes with no surprise that it also presents the biggest difference between both reactors as seen in Fig. 9.

Particle size can play a very important role in the scale-up effects. As previously stated, different size particles scale-up differently. In fact, larger particles are more difficult to scale-up than

Table 6
Most relevant findings regarding gasification products for different reactors.

Gasification product	Findings
Residence time	Residence time was shorter for laboratory-scale reactor
Gas composition	Syngas obtained in laboratorial runs presented higher levels of CH_4 and CO_2 and lower levels of CO and H_2
Gas yield	Gas yield was higher in semi-industrial reactor
Temperature	Temperature was higher in semi-industrial reactor

smaller ones. Also, according to [13], scale-up becomes more complex by needing to know how the particle density in the fluidized bed reactor changes with diameter. So a larger particle or denser biomass type will be harder to scale-up and it will also be harder to correctly predict the biomass gasification process than in a smaller one with less density. This can be explained by smaller particles, due to their larger surface areas per mass unit, can facilitate faster gasification rates [45]. Regarding produced gas composition from smaller biomass particles, Rapagna et al. [46] found that smaller particles led to a syngas with higher CO and H_2 contents. Because of this smaller particles can result in higher gas energy content [47]. So, again, it comes with no surprise that forest residues, which has a smaller particle than vines pruning [48], has a syngas with higher gas calorific content.

Numerical modeling has great potential in predicting scale-up effects on the gasification process. However, at this point in the development of numerical models the use of CFD alone to scale-up a new process must be used with caution. Extensive experimental work is still required for successful scale-up.

5. Conclusion

The scale-up of a new fluidized bed process is the most difficult type of scale-up. However, the use of techniques based on experience and design models can minimize risk and uncertainty. Computation Fluid Dynamics has potential in predicting the effect of scale on biomass gasification. In order to test the true potential of numerical models to predict the effects of scale-up, a two-dimensional model was build using data from a semi-industrial gasification plant. Height/cross section ratio between both reactors was chosen according to previously relevant studies.

Influence of gasification temperature, oxygen content and biomass type on different reactors size was studied. Bigger reactors led to syngas with higher contents in CO and H_2 due to residence time in those reactors being longer. In fact, residence time showed to be a major influence on the scale-up effects.

Influence of biomass type in different reactors was yet to be properly addressed on the current literature. An attempt on answering was made. Volatile content as well as particle size showed a considerable influence on the obtained results.

Acknowledgements

We would like to express our gratitude to the Portuguese Foundation for Science and Technology (FCT) for the support given to the grant SFRH/BD/86068/2012 and to project PTDC/EMS-ENE/6553/2014 and IF01772/2014. We also would like to thank Dr. Paulo Brito and Dr. Eliseu Monteiro for providing experimental data needed to complete this paper.

Appendix A. Supplementary material

Supplementary data associated with this article can be found, in the online version, at http://dx.doi.org/10.1016/j.enconman.2016.03.085.

References

[1] <http://2014.newclimateeconomy.report/energy/> [last accessed 08th October, 2015].
[2] Jayaraman K, Gökalp I. Pyrolysis, combustion and gasification characteristics of miscanthus and sewage sludge. Energy Convers Manage 2015;89:83–91.
[3] Al-Hamamre Z, Al-Mater A, Sweis F, Rawajfeh K. Assessment of the status and outlook of biomass energy in Jordan. Energy Convers Manage 2014;77:183–92.
[4] Ferreira S, Moreira N, Monteiro E. Bioenergy overview for Portugal. Biomass Bioenerg 2009;33:1567–76.
[5] Silva V, Monteiro E, Couto N, Brito P, Rouboa A. Analysis of syngas quality from Portuguese biomasses: an experimental and numerical study. Energy Fuel 2014;28:5766–77.
[6] Eaton AM, Smoot LD, Hill SC, Eatough CN. Components, formulations, solutions, evaluation, and application of comprehensive combustion models. Prog Energy Combust 1999;25:387–436.
[7] Alauddin Z, Lahijani P, Mohammadi M, Mohamed R. Gasification of lignocellulosic biomass in fluidized beds for renewable energy development: a review. Renew Sust Energy Rev 2010;14:2852–62.
[8] Xiao G, Ni M, Chi y, Cen K. Low-temperature gasification of waste tire in a fluidized bed. Energy Convers Manage 2008;49:2078–82.
[9] Sarker S, Arauzo J, Nielsen H. Semi-continuous feeding and gasification of alfalfa and wheat straw pellets in a lab-scale fluidized bed reactor. Energy Convers Manage 2015;99:50–61.
[10] Moghadam R, Yusup S, Azlina W, Nehzati S, Tavasoli A. Investigation on syngas production via biomass conversion through the integration of pyrolysis and air–steam gasification processes. Energy Convers Manage 2014;87:670–5.
[11] Loha C, Chatterjee P, Chattopadhyay H. Performance of fluidized bed steam gasification of biomass – modeling and experiment. Energy Convers Manage 2011;52:1583–8.
[12] Squires AM. Contribution toward a history of fluidization. In: Proceedings of the joint meeting of Chemical Engineering Society of China and AIChE. Chemical Industry Press; 1982. p. 322–53.
[13] Knowlton TM, Karri SBR, Issangya A. Scale-up of fluidized-bed hydrodynamics. Powder Technol 2005;150:72–7.
[14] Silva V, Rouboa A. Optimizing the gasification operating conditions of forest residues by coupling a two-stage equilibrium model with a response surface methodology. Fuel Process Technol 2014;122:163–9.
[15] Hameed S, Ramzan N, Rahman Z, Zafar M, Riaz S. Kinetic modeling of reduction zone in biomass gasification. Energy Convers Manage 2014;78:367–73.
[16] Gao X, Zhang Y, Li B, Yu X. Model development for biomass gasification in an entrained flow gasifier using intrinsic reaction rate submodel. Energy Convers Manage 2016;108:120–31.
[17] Couto N, Silva V, Monteiro E, Brito P, Rouboa A. Using an Eulerian-granular 2-D multiphase CFD model to simulate oxygen air enriched gasification of agroindustrial residues. Renew Energy 2015;77:174–81.
[18] Launder BE, Spalding DB. Lectures in mathematical models of turbulence. London (England): Academic Press; 1972.
[19] Syamlal M, Rogers TJ, MFIX documentation: Volume 1. Theory guide, National Technical Information Service, Springfield, VA; 1993. DOE/METC-9411004, NTIS/DE9400087.
[20] Lun C, Savage SB, Jeffrey D, Chepurniy N. Kinetic theories for granular flow: inelastic particles in Couette flow and slightly inelastic particles in a general flow field. J Fluid Mech 1984;140:223–56.
[21] Xue Q, Heindel TJ, Fox RO. A CFD model for biomass fast pyrolysis in fluidized-bed reactors. Chem Eng Sci 2011;66:2440–52.
[22] Couto N, Silva VB, Monteiro E, Teixeira S, Chacartegui R, Bouziane K, et al. Numerical and experimental analysis of municipal solid wastes gasification process. Appl Therm Eng 2015;78:185–95.
[23] Badzioch S, Hawsley PGW. Kinetics of thermal decomposition of pulverized coal particles. Ind Eng Chem Des Dev 1970;4:521–30.
[24] Grammelis P, Basinas P, Malliopoulou A, Sakellaropoulos G. Pyrolysis kinetics and combustion characteristics of waste recovered fuels. Fuel 2009;88:195–205.
[25] Baum M, Street P. Predicting the behavior of coal particles. Combust Sci Technol 1971;3:231–43.
[26] Field MA. Rate of combustion of size-graded fractions of char from a low rank coal between 1200 K–2000 K. Combust Flame 1969;13:237–52.
[27] Gunn DJ. Transfer of heat or mass to particles in fixed and fluidized beds. Int J Heat Mass Trans 1978;21:467–76.
[28] Gelderbloom SJ, Gidaspow D, Lyczkowski RW. CFD simulations of bubbling/collapsing fluidized beds for three Geldart groups. AIChE J 2003;49:844–58.
[29] Silva V, Rouboa A. Combining a 2-D multiphase CFD model with a Response Surface Methodology to optimize the gasification of Portuguese biomasses. Energy Convers Manage 2015;99:28–40.
[30] Brito P, Rodrigues F, Calado L, Oliveira A. Thermal gasification of agro-industrial residues. WIT transactions on ecology and the environment. Waste Manage Environ VI 2012;163:95–102.
[31] Turn S, Kinoshita C, Zhang Z, Ishimura D, Zhou J. An experimental investigation of hydrogen production from biomass gasification. Int J Hydrogen Energy 1998;23:641–8.
[32] Campoy M, Gomez-Barea A, Vidal F, Ollero P. Air-steam gasification of biomass in a fluidised bed: process optimisation by enriched air. Fuel Process Technol 2009;90:677–85.
[33] Holman JP. Experimental methods for engineers. 4th ed. New York (USA): McGraw-Hill; 1984.
[34] Dogru M, Midilli A, Howarth C. Gasification of sewage sludge using a throated downdraft gasifier and uncertainty analysis. Fuel Process Technol 2002;75:55–82.
[35] Beheshti SM, Ghassemi H, Shahsavan-Markadeh R. Process simulation of biomass gasification in a bubbling fluidized bed reactor. Energy Convers Manage 2015;94:345–52.
[36] Silva V, Rouba A. Using a two-stage equilibrium model to simulate oxygen air enriched gasification of pine biomass residues. Fuel Process Technol 2013;109:111–7.

[37] Couto N, Rouboa A, Silva V, Monteiro E, Bouziane Khalid. Influence of the biomass gasification processes on the final composition of syngas. Energy Procedia 2013;36:596–606.
[38] Karamarkovic R, Karamarkovic V. Energy and exergy analysis of biomass gasification at different temperatures. Energy 2010;35:537–49.
[39] Qian K, Kumar A, Patil K, Bellme D, Wang D, Yuan W, et al. Effects of biomass feedstocks and gasification conditions on the physiochemical properties of char. Energies 2013;6:3972–86.
[40] Pinto F, André R, Carolino C, Miranda M, Abelha P, Direito D, et al. Gasification improvement of a poor quality solid revovered fuel (SRF). Effect of using natural minerals and biomass wastes blends. Fuel 2014;117:1034–44.
[41] Pinto F, André R, Franco C, Lopes H, Gulyurtlu I, Cabrita I. Co-gasification of coal and wastes in a pilot-scale installation 1: Effect of catalysts in syngas treatment to achieve tar abatement. Fuel 2009;88:2392–402.
[42] Manyà JJ, Sánchez JL, Ábrego J, Gonzalo A, Arauzo J. Influence of gas residence time and air ratio on the air gasification of dried sewage sludge in a bubbling fluidised bed. Fuel 2006;85:2027–33.
[43] Pinto F, André R, Franco C, Carolino C, Costa R, Miranda M, et al. Comparison of a pilot scale gasification installation performance when air or oxygen is used as gasification medium 1. Tars and gaseous hydrocarbons formation. Fuel 2012;101:102–14.
[44] Aljbour SH, Kawamoto K. Bench-scale gasification of cedar wood – Part II: Effect of operational conditions on contaminant release. Chemosphere 2013;90:1501–7.
[45] Kirubakaran V, Sivaramakrishnan V, Nalini R, Sekar T, Premalatha M, Subramanian P. A review on gasification of biomass. Renew Sust Energy Rev 2009;13:179–86.
[46] Rapagna S, Latif A. Steam gasification of almond shells in a fluidised bed reactor: the influence of temperature and particle size on product yield and distribution. Biomass Bioenerg 1997;12:281–8.
[47] Lv P, Chang J, Wang T, Fu Y, Chen Y. Hydrogen-rich gas production from biomass catalytic gasification. Energy Fuel 2004;18:228–33.
[48] Phanphanich M, Mani S. Drying characteristics of pine forest residues. BioResources 2009;5:108–21.

Paper IX

Municipal solid waste gasification in semi-industrial conditions using air-CO2 mixtures

N. Couto, V. Silva, A. Rouboa

Energy 104 (2016) 42–52

Energy 104 (2016) 42–52

Contents lists available at ScienceDirect

Energy

journal homepage: www.elsevier.com/locate/energy

Municipal solid waste gasification in semi-industrial conditions using air-CO_2 mixtures

Nuno Couto [a], Valter Silva [a, *], Abel Rouboa [a, b]

[a] INEGI-FEUP, Faculdade de Engenharia da Universidade do Porto, Porto, Portugal
[b] MEAM Department, University of Pennsylvania, Philadelphia, PA 19020, USA

ARTICLE INFO

Article history:
Received 20 October 2015
Received in revised form
19 February 2016
Accepted 18 March 2016
Available online 16 April 2016

Keywords:
Syngas quality indices
Gasification
Municipal solid wastes
Carbon dioxide
CFD
Semi-industrial gasifier

ABSTRACT

The gasification of MSW (municipal solid wastes) using CO_2 as a gasifying agent has been object of growing interest in recent years. Although quite limited, studies have shown that CO_2 can behave as a catalyst and accelerate the thermal cracking of volatiles as well as minimize tar formation, and even give a positive contribute to environment. Despite these promising features, it is still necessary to develop mathematical models able to assist the advance of this technology.

A previously published numerical model validated for numerous substrates (including MSW) and operating conditions in a pilot scale plant was used as a baseline to study MSW gasification with air-CO_2 mixtures. Real MSW data from Oporto metropolitan area were used as model inputs and numerical results were validated against experimental ones.

Results demonstrate that increasing CO_2 content boosts carbon conversion, CO_2 conversion, and cold gas efficiency while mitigating tar production. Also, due to the ability to tailor H_2/CO ratio, air-CO_2 mixtures can be used for catalyst-based Fischer–Tropsch synthesis and particularly for the production of specific chemicals such as urea, methanol and acetic acid.

1. Introduction

Industrial and economic development coupled with rampant energy consumption have resulted in serious environmental problems, and seeing that population growth and waste production go hand in hand, the latter has become a major 21st century concern. According to the latest report from the World Bank's Urban Development Department regarding MSW (municipal solid waste) production, approximately 1.3 billion tons of MSW were produced in 2012 [1], and even more frightening is the estimate that this figure could double by 2025.

Gasification has been mentioned as a promising alternative to the available methods of treatment due to its pollution minimization effects and higher overall efficiency. Furthermore, it has been a readily available technology with a worldwide capacity of 122,106 thermal MW since 2010 [2]. Despite its many advantages, biomass and waste gasification still only represent 0.33% of the global gasification capacity [2].

One way to make it more appealing to both private sector and government institutions is by optimizing syngas characteristics and consequently obtaining a gas suitable for a given application. This can be accomplished through the study of the different agents used to gasify the substrate. The most common is air and although extremely cheap compared to other gasifying agents, allows for the production of a gas highly diluted in N_2, whereas gasification with pure O_2 can achieve a much higher quality gas due to the absence of N_2, although with such high costs that its implementation in large facilities is still uncertain. Gasification with steam has seen a growing interest in recent years since it can produce a gas rich in H_2, with higher calorific value (by reducing diluting effect of N_2 from air) and less expensive than oxygen. However, due to relatively low reactivity, it is necessary to supply heat from an external source [3].

Although poorly studied the addition of carbon dioxide as a gasifying agent has recently been carried out with very exciting results. Although an even more endothermic process than steam gasification, it uses an unwanted end product of various industrial processes instead of steam (which is becoming an increasingly

* Corresponding author. Campus da FEUP, Rua Dr. Roberto Frias, 400. Zip code: 4200-465, Porto, Portugal. Tel.: +351 229 578 710; fax: +351 229 537 352.
E-mail addresses: nunodiniscouto@hotmail.com (N. Couto), vsilva@inegi.up.pt (V. Silva), rouboa@utad.pt (A. Rouboa).

http://dx.doi.org/10.1016/j.energy.2016.03.088
0360-5442/

rarer resource) but also enhances both char gasification and pyrolysis and has the ability to act as a catalyst enhancing thermal cracking of volatiles leading to tar mitigation. Furthermore, unlike steam gasification, CO_2 gasification doesn't require additional heat for phase change, it permits easier access to both micropores and macropores to create a more porous char structure and it is a far less corrosive gasification medium. By allowing a more reactive char to enhance thermochemical conversion it results in a more efficient gasification. Additionally, CO_2 gasification can play a very important role in reducing CO_2 pollution having the ability to process hundreds of millions of tons of CO_2 every year [4]. One of the key aspects of CO_2 gasification is the ability to tailor H_2/CO ratio to supply syngas as feedstock for an extremely wide variety of applications [4]. Lastly, gasification with CO_2 decreases the effect of biomass on the produced gas, allowing for the controlled production of syngas thus meeting the requirements of a particular industrial application [4]. To the best of our knowledge there is very limited data regarding MSW gasification with CO_2 as a gasifying agent. Modeling studies predicting CO_2 gasification of municipal solid wastes are required for its successful implementation and may allow gasification to be a realistic solution to the MSW disposal and fossil fuel overuse problems.

The aim of this paper is to study MSW gasification using air-CO_2 mixtures using a model previously validated for various substrates, including MSW. Firstly, the influence of CO_2 addition in the gasifying agent mixture was studied and, in order to gain better understanding of CO_2 influence, both content and gasifying agent-to-waste ratio were studied and syngas quality indices with CO_2/biomass ratio were investigated. The influence of CO_2 content on CO_2 conversion as well as on gasification product formation was studied and, finally, applications for MSW gasification using CO_2 and air mixtures were analyzed.

2. Materials and methods

Gasification was carried out in a pilot thermal gasification plant, installed in Portalegre's Industrial Park (Fig. 1). Its reactor is about 4.15 m high and 0.5 m wide and has 70 kg of dolomite in the bed and a processing capacity of 70 kg/h. The process was operated at atmospheric pressure in the range of 750 °C to 850 °C. The substrate flow rate ranged from 25 kg/h to 75 kg/h, and the volumetric flow rate of air (at starting conditions), was set to around 75 m^3/h to 100 m^3/h before being reduced to ca. 40 m^3/h to 60 m^3/h upon stabilization of the gasification process.

Since the fluid dynamic phenomena in laboratory scale reactors are quite different for larger scales, results from a semi-industrial plant like the one described, whose 200 kW reactor produces an average syngas flow rate close to 100 Nm^3/h, are crucial in avoiding errors and reducing risks and uncertainty when designing industrial reactors.

The schematics as well as an extensive description of the gasification plant can be found elsewhere [5,6].

2.1. Municipal solid waste characterization

Seeing that model accuracy comes from realistic data, both characterization and analysis of MSW in the Oporto metropolitan area were carried out.

LIPOR is an association of Municipalities of greater Porto, established in 1982, whose main objective is the management, treatment and recovery of solid waste municipal produced in eight municipalities in the Oporto metropolitan area. Wastes are pre-treated accordingly to the Portuguese management system described by Teixeira et al. [7] and reports from 2014 indicate a production of about 479 kton of MSW/year at an average of

Fig. 1. Photograph of the semi-industrial gasification plant in Portalegre, Portugal.

1.355 kg/hab.day. Fig. 2 depicts the monthly average of produced wastes throughout 2014.

As presented in Fig. 3, almost 80% of the total waste produced was channeled to energy recovery and just 5% ended up in landfills.

Samples were acquired during the management and treatment of collected MSW for posterior physical characterization according to the categories in Fig. 4.

RDF (Refuse Derived Fuel) containing cellulosic materials and plastics is obtained from the pre-treatment of MSW via shredding and dehydration. Plastic residues are mainly comprised by polyethylene, polystyrene, and polyvinyl chloride while cellulosic materials are composed of cellulose, hemicelluloses, and lignin.

Since an ultimate analysis does not distinguish cellulosic materials, their composition was presupposed to be similar to the one found by Onel et al. [8], whereas report informs of the relative quantities of each monomer in the MSW for plastics, as listed in Table 1.

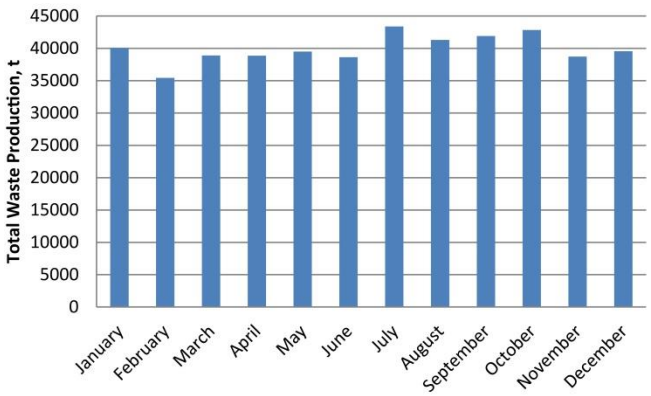

Fig. 2. Monthly average of MSW produced in Oporto in 2014.

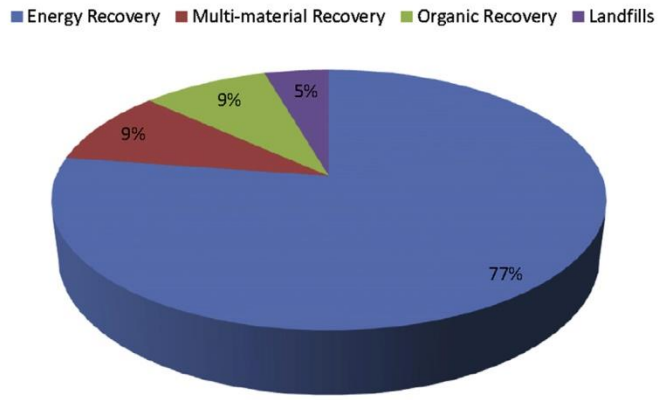

Fig. 3. Average final destination of MSW in Oporto in 2014.

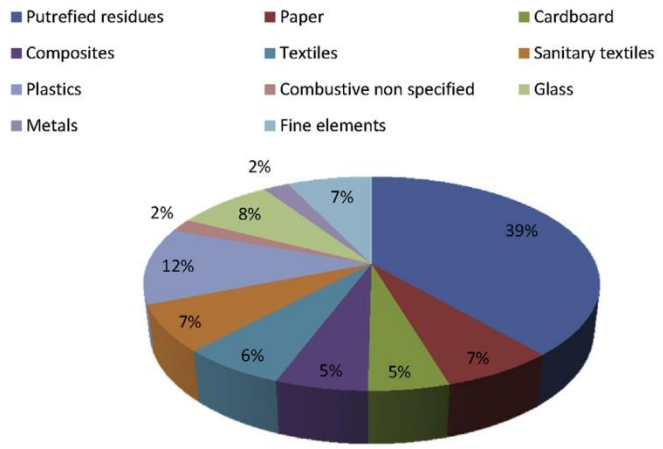

Fig. 4. Physical characterization of the MSW in Oporto in 2014.

This waste characterization was employed in the formulation of the MSW mixture in Fluent to model the gasification process.

3. Mathematical model

The gasification of MSW is an extremely complex process due to the physical and chemical interactions that occur throughout. Bubbling fluidized-bed models are generally based on the two-phase flow theory of fluidization for the description of the process hydrodynamics. The two-phase (gas and solid) fluid dynamics is of great importance for the design and operation of the bubbling fluidized bed gasifiers.

In fact, correctly modeling the interaction between phases is crucial since they exchange heat by convection, mass over the heterogeneous chemical reactions, and momentum due to the drag between gas and solid phase. The model follows an Eulerian–Eulerian approach, which means that both gas and solid phases are described by a continuum approach, and modeled similar to single phase flow with an additional term, accounting for the interaction with the solid phase. The following table presents the relevant equations for both gas and solid phase.

Table 1
Chemical composition of the MSW.

Category	% weight	Chemical formula
Cellulosic material	85.22%	[a]
Polyethylene	11.14%	$(C_2H_4)_n$
Polyethylene terephthalate	2.05%	$(C_{10}H_8O)_n$
Polypropylene	0.82%	$(C_3H_6)_n$
Polystyrene	0.77%	$(C_8H_8)_n$

[a] It was considered the proportion of cellulose, hemicellulose and lignin found in Onel et al. [8].

In Table 2, $\overrightarrow{Q}_{sg}$ stands for the heat transfer intensity between fluid phase, subscript 'g', and solid phase, subscript 's'; h_g for the specific enthalpy of phase g; and $\overrightarrow{q}_g$ for the heat flux. S_g is a source term due to chemical reactions, h_{sg} represents interface enthalpy, R_C the reaction rate, γ_C the stoichiometric coefficient and M_C the molecular weight. For solid phase, α_s is the particle phase stress tensor and p_s is particle phase pressure due to particle collisions. Finally, β stands for the gas–solid interphase drag coefficient, $\overline{\overline{\tau}}_g$ for the gas phase stress tensor and U_S for the mean solid velocity.

Further explanation on these equations can be found in Ref. [6].

3.1. Hydrodynamic model

Due to the high solid fraction inside the fluidized bed, the Eulerian method was used to simulate the MSW gasification process, and described using the kinetic theory of gases.

Granular Eulerian model is described by the following conservation equation for granular temperature:

$$\frac{3}{2}\left[\left(\frac{\partial(\rho_s\alpha_s\Theta_s)}{\partial t}\right)+\nabla\cdot(\rho_s\alpha_s\overrightarrow{v}_s\Theta_s)\right]=(-p_s\bar{I}+\bar{\tau}_s):\nabla(\overrightarrow{v}_s)+\nabla\cdot\left(k_{\Theta_a}\nabla(\Theta_s)\right)-\gamma_{\Theta a}+\phi_{ls} \quad (1)$$

This expression is obtained from the kinetic theory of gases. The term $(-p_s\bar{I}+\bar{\tau}_s):\nabla(\overrightarrow{v}_s)$ describes the generation of energy by the solid stress tensor, ϕ_{ls} stands for the energy exchange between fluid and solid phase, γ_{Θ_a} for the collisional dissipation of energy and $k_{\Theta_a}\nabla(\Theta_s)$ for the diffusion energy, in which k_{Θ_a} is the diffusion coefficient.

Since turbulence transfer has a predominant role in the gasification process in fluidized beds, the standard $k-\varepsilon$ model was used. Turbulence kinetic energy (k) and dissipation rate (ε) are respectively given by:

$$\frac{\partial}{\partial t}(\rho k)+\frac{\partial}{\partial x_i}(\rho k u_i)=\frac{\partial}{\partial x_j}\left[\left(\mu+\frac{\mu_t}{\sigma_k}\right)\right]G_k+G_b-\rho\varepsilon-Y_M+S_k \quad (2)$$

$$\frac{\partial}{\partial t}(\rho\varepsilon)+\frac{\partial}{\partial x_i}(\rho\varepsilon u_i)=\frac{\partial}{\partial x_j}\left[\left(\mu+\frac{\mu_t}{\sigma_\varepsilon}\right)\right]+C_{1\varepsilon}\frac{\varepsilon}{k}(G_\varepsilon+C_{3\varepsilon}G_b)-C_{2\varepsilon}\rho\frac{\varepsilon^2}{k}+S_\varepsilon \quad (3)$$

G_k represents the generation of turbulence kinetic energy due to mean velocity gradients, G_b the generation of turbulence kinetic energy due to buoyancy, and Y_M the contribution of fluctuating dilatation in compressible turbulence to the overall dissipation rate. To determine the turbulence kinetic energy as well as the dissipation rate, the following constants were assumed: $G_k = 1.0$ and $G_\varepsilon = 1.3$ stand for the turbulent Prandtl numbers for k and ε, respectively, $C_{1\varepsilon} = 1.44$, $C_{2\varepsilon} = 1.92$, and $C_{3\varepsilon} = 0$ are default constants commonly used in Fluent and S_k and S_ε for user-defined source terms.

3.2. Chemical reactions model

MSW gasification involves several fundamental processes. Firstly, volatile components in the MSW such as light gases and tar are released by pyrolysis. These species undergo homogeneous gas

Table 2
Governing equations for gas and solid phases.

Gas phase	Solid phase
Energy:	
$\frac{\partial(\alpha_g\rho_g h_g)}{\partial t}+\nabla\cdot(\alpha_g\rho_g\vec{u}_g h_g)=-\alpha_g\frac{\partial(p_g)}{\partial t}+\bar{\bar{\tau}}_g:\nabla(\vec{u}_g)-\nabla\vec{q}_g+S_g+\sum_{g=1}^{n}(\vec{Q}_{sg}+\dot{m}_{sg}h_{sg})$	$\frac{\partial(\alpha_s\rho_s h_s)}{\partial t}+\nabla\cdot(\alpha_s\rho_s\vec{u}_s h_s)=-\alpha_s\frac{\partial(p_s)}{\partial t}+\bar{\bar{\tau}}_s:\nabla(\vec{u}_s)-\nabla\vec{q}_s+S_{ps}+\sum_{s=1}^{n}(\vec{Q}_{sg}+\dot{m}_{sg}h_{sg})$
Mass:	
$\frac{\partial(\alpha_g\rho_g)}{\partial t}+\nabla\cdot(\alpha_g\rho_g\vec{u}_g)=-M_C\sum\gamma_C R_C$	$\frac{\partial(\alpha_s\rho_s)}{\partial t}+\nabla\cdot(\alpha_s\rho_s\vec{u}_s)=M_C\sum\gamma_C R_C$
Momentum:	
$\frac{\partial(\alpha_g\rho_g\vec{u}_g)}{\partial t}+\nabla\cdot(\alpha_g\rho_g\vec{u}_g\vec{u}_g)=-\alpha_g\nabla p_g+\alpha\rho_g g+\beta(u_g-u_g)+\nabla\cdot\alpha_g\bar{\bar{\tau}}_g+S_{sg}U_S$	$\frac{\partial(\alpha_s\rho_s\vec{u}_s)}{\partial t}+\nabla\cdot(\alpha_s\rho_s\vec{u}_s\vec{u}_s)=-\alpha_s\nabla p_s+\alpha\rho_s g+\beta(u_s-u_s)+\nabla\cdot\alpha_s\bar{\bar{\tau}}_s+S_{sg}U_S$

phase reactions forming CO, CO_2, H_2, H_2O which then combust and gasify the char. Each process must be understood and modeled when modeling MSW gasifiers.

For low temperatures, in the range between 500 and 650 °C, the WGS (water-gas shift) reaction is predominant and results in the production of H_2:

$$CO + H_2O \leftrightarrow CO_2 + H_2 - 41.1\ \text{MJ/kmol} \quad (4)$$

During pyrolysis, steam produced from heating and drying processes combines with CO to produce H_2, which, in turn, can produce CH_4 through direct hydrogenation reactions.

$$CO + 3H_2 \leftrightarrow CH_4 + H_2O\ - 227\ \text{MJ/kmol} \quad (5)$$

For higher temperatures, in the range of 700–1200 °C, rWGS (reverse water-gas), primary water-gas and Boudouard reactions play a crucial role:

$$C + H_2O \leftrightarrow CO + H_2 + 131\ \text{MJ/kmol} \quad (6)$$

$$C + CO_2 \leftrightarrow 2CO + 172\ \text{MJ/kmol} \quad (7)$$

Above 800 °C, CH_4 can be reformed using CO_2 (also known as dry reforming) to produce H_2 and CO.

$$CH_4 + CO_2 \leftrightarrow 2H_2 + 2CO + 247\ \text{MJ/kmol} \quad (8)$$

However, since these reactions are endothermic, it is necessary to supply heat from an external source, which can be direct, via the introduction of pure O_2 into the reactor so that oxidation reactions can provide the necessary heat:

$$CO + 0.5O_2 \rightarrow CO_2 - 283\ \text{MJ/kmol} \quad (9)$$

$$H_2 + 0.5O_2 \rightarrow H_2O - 242\ \text{MJ/kmol} \quad (10)$$

$$C + 0.5O_2 \rightarrow CO - 111\ \text{MJ/kmol} \quad (11)$$

Seeing that homogeneous reactions (reactions 4–5, 8–10) are affected by both kinetic and turbulent mixing rates, a finite-rate/Eddy-dissipation model was used which considers both Arrhenius and Eddy-dissipation reaction rates. Regarding heterogeneous reactions (reactions 6, 7 and 11), the Kinetic/Diffusion Surface Reaction Model was employed. The Arrhenius rates and the kinetic parameters for these reactions as well as further explanation can be found in Ref. [6], and so can solver procedure details [6].

3.2.1. Pyrolysis

Modeling pyrolysis is crucial for MSW gasification purposes. The chemical reaction rate coefficients are based on the Arrhenius law. During the devolatilization and cracking water shift reaction will occur, the gas species react with the supplied oxidizer and among them.

MSW is thermally decomposed into volatiles, char and tar. There are several approaches to describe this phenomenon which the main approaches are: a single step pyrolysis model, competing parallel pyrolysis and a pyrolysis model with generation of secondary tar. In this model we adopt a pyrolysis model with generation of secondary tar. The MSW is mainly composed by cellulosic and plastic components, where the cellulosic material can be divided in cellulose, hemicellulose and lignin and the plastics are mainly comprised by polyethylene, polystyrene, and polypropylene, among others.

To distinguish the several components that comprise the MSW, the pyrolysis reactions of cellulosic and plastic groups are considered individually and following an Arrhenius kinetic expression.

The primary pyrolysis equations can be defined as:

$$Cellulose \xrightarrow{r_1} \alpha_1 Volatiles + \alpha_2 Tar + \alpha_3 Char \quad (12)$$

$$Hemicellulose \xrightarrow{r_2} \alpha_4 Volatiles + \alpha_5 Tar + \alpha_6 Char \quad (13)$$

$$Lignin \xrightarrow{r_3} \alpha_7 Volatiles + \alpha_8 Tar + \alpha_9 Char \quad (14)$$

$$Plastics \xrightarrow{r_4} \alpha_{10} Volatiles + \alpha_{11} Tar + \alpha_{12} Char \quad (15)$$

Moreover, a secondary pyrolysis was considered where volatiles and secondary tar are generated:

$$Primary\ Tar \xrightarrow{r_5} Volatiles + Secundary\ Tar$$

The devolatilization rate of MSW is assumed to be the sum of the rates of its components: cellulose, hemicellulose and lignin. Each component contributes proportionally to MSW. This fact implies that interactions between the biomass components have no effect on the pyrolysis. This assumption is in agreement with [9] and a previous paper from the authors [5].

The kinetics for the cellulosic material can be given as follows:

$$r_i = \frac{da_i}{dt} = A_i exp\left(\frac{-E_i}{T_s}\right)(1-a_i)^n \quad (17)$$

where i stands for cellulose, hemicellulose and lignin (r_{1-3}).

Regarding the kinetic reactions for plastics, the following reactions were used:

$$r_4 = \left[\sum_{i=1}^{n} A_i exp\left(\frac{-E_i}{RT}\right)\right]\rho_v$$

Also a secondary pyrolysis was considered where volatiles and secondary tar are generated, as follows:

$$Primary\ Tar \xrightarrow{r_5} Volatiles + Secondary\ Tar$$

Due to the difficulty to treat this secondary pyrolysis a simplified global reaction is used:

$$r_5 = 9.55 \times 10^4 exp\left(\frac{-1.12 \times 10^4}{T_g}\right)\rho_{Tar1} \quad (20)$$

The kinetics for both cellulosic material and as plastics, as well as can the global reaction for secondary pyrolysis can also be found in Ref. [6].

4. Results and discussion

The presented numerical model was validated using various substrates as well as different reactors and underwent several upgrades in order to handle the various characteristics of biomass and cope with the heterogeneity of municipal wastes. Table 3 compiles the most relevant findings.

Substrate composition has a clear effect on syngas composition. While operating parameters were carefully selected to be the closest possible for all substrates, Xiao's MSW was investigated for slightly different parameters [10]. The influence of biomass substrates on gasification products has already been studied in depth so no further comments will be made on the subject.

Regarding the ability of the numerical model to correctly predict the experimental data collected from semi-industrial reactors for different substrates, Fig. 5 presents some comparisons.

Operating conditions for each comparison in Fig. 5 can be seen in Table 4.

The numerical model is capable of predicting substrate content reasonably well even for MSW, a substantially more complex system, with a maximum error of 19.6%, found for CH_4. Sometimes, all light hydrocarbons and tar are lumped into CH_4, which can explain the disagreement sometimes found. Still, this margin of error is very reasonable for system such as biomass gasification in a pilot scale reactor. After validating the model for MSW gasification in a laboratorial scale reactor, MSW gasification was then investigated using the semi-industrial reactor [10]. A detailed explanation regarding the simplifying assumptions followed by our model can be found in Refs. [5,6].

Since the numerical model is able to reasonably predict the gasification process for different conditions and substrates, it is safe to assume that it is also able to simulate the same conditions using mixtures of air and CO_2.

4.1. Influence of gasifying mixture

CO_2 addition can minimize some of the main setbacks of MSW gasification. However, CO_2 gasification relies on highly endothermic reactions being necessary the use of external energy sources.

In this work it was decided to study air and CO_2 mixtures since the high costs of implementation of pure O_2 in large facilities is still uncertain.

The influence of CO_2 addition in the gasifying agent mixture was studied in three separate ways:

Table 3
Key findings for different substrates.

Substrate	H_2/CO	CH_4/H_2	LHV	CGE	Ref.
Coffee husks	0.69–0.76	0.10–0.22	3.20–3.36	51.0–68.0	6
Forest residues	0.36–0.37	0.50–0.83	4.92–5.2	58.3–78.9	6
Vines pruning	0.71–0.78	0.12–0.27	3.70–3.85	62.6–83.1	6
Xiao's MSW	0.67–0.72	0.06–0.22	3.38–4.93	53.8–64.3	10

a) Keeping MSW/gasifying agent ratio constant, so that both CO_2 and air flow rates have to be simultaneously varied in order to modify the CO_2 content.
b) Allowing the MSW/gasifying agent ratio to vary by investigating three different equivalent ratios while the CO_2-to-MSW ratio is allowed to vary.
c) Finally, the influence of the gasification temperature on gas produced in a CO_2 rich environment was studied.

In all 3 cases, influence of operational parameter on tar content was investigated.

4.1.1. Influence of CO_2 content

Fig. 6 illustrates syngas composition and tar content for air-CO_2 mixtures with CO_2 content ranging from 0% (air gasification) to 100% (pure CO_2 gasification).

CO_2 has a strong influence on syngas composition. At lower percentages (0–40%) CO increases while H_2 decreases, boosting temperature, and promoting both Boudouard and water-gas shift reactions and encouraging CO and steam content at the expense of CO_2 and H_2 [4].

Increasing CO_2 content beyond 40% causes a significant variation in the syngas composition. H_2 appears to increase slightly while CO decreases substantially, and CO_2 increases at an even higher rate. This sudden change is due to a severe temperature drop with rising CO_2 content, seeing that more CO_2 in the mixture reduces air flow and impairs exothermic reactions. It is thus assumed that beyond 40% the available O_2 is not sufficient to maintain the desired gasification temperature, even though the very rich CO_2 environment promotes the water gas shift reaction, producing H_2 at the expense of CO [11].

The influence of CO_2 in C_nH_m appears to be insignificant. Since components are promoted mainly by pyrolysis, the most significant effect CO_2 can have is temperature reduction, which inevitably decreases its rate. On the other hand, with less O_2 available, both complete and partial oxidation occur less and therefore CH_4 is less consumed [11].

Results for both biomass and MSW gasification concerning CO_2 influence are very scarce at this point but the available literature is in agreement with the results presented [4,11].

CO_2 content in the gasifying agent mixture also has a strong influence on tar content. In fact, since CO_2 addition enhances both char gasification and pyrolysis, which leads to increase in carbon conversion, tar content is expected to decrease, as can be seen from 0 to 60%. Beyond this point, the available O_2 is not sufficient to maintain the desired gasification temperature leading to a decrease in carbon conversion which, in turn, leads to an increase in tar content. This is consistent with [12].

4.1.2. Influence of CO_2-to-MSW ratio

Studying the influence of the CO_2-to-MSW ratio can help understand the role of CO_2 in the gasification process, particularly in the production of syngas. To the best of our knowledge, the CO_2-to-MSW ratio (which we will refer from now on “CDMR” for simplicity) is yet to be addressed in the current literature, and the CO_2-to-biomass one has barely been discussed [4,11]. However, studying CDMR offers several advantages, namely that the influence of N_2 dilution is not as high and that possible small variations in MSW admission in the syngas composition will not go unnoticed to such a high degree.

While a very important parameter to study, the O_2 content in an air mixture can sometimes be misleading due to N_2 dilution and the effects of small variations on biomass admission in the syngas composition going unnoticed, hence our decision to study both O_2 content and ER (equivalent ratio) for the same

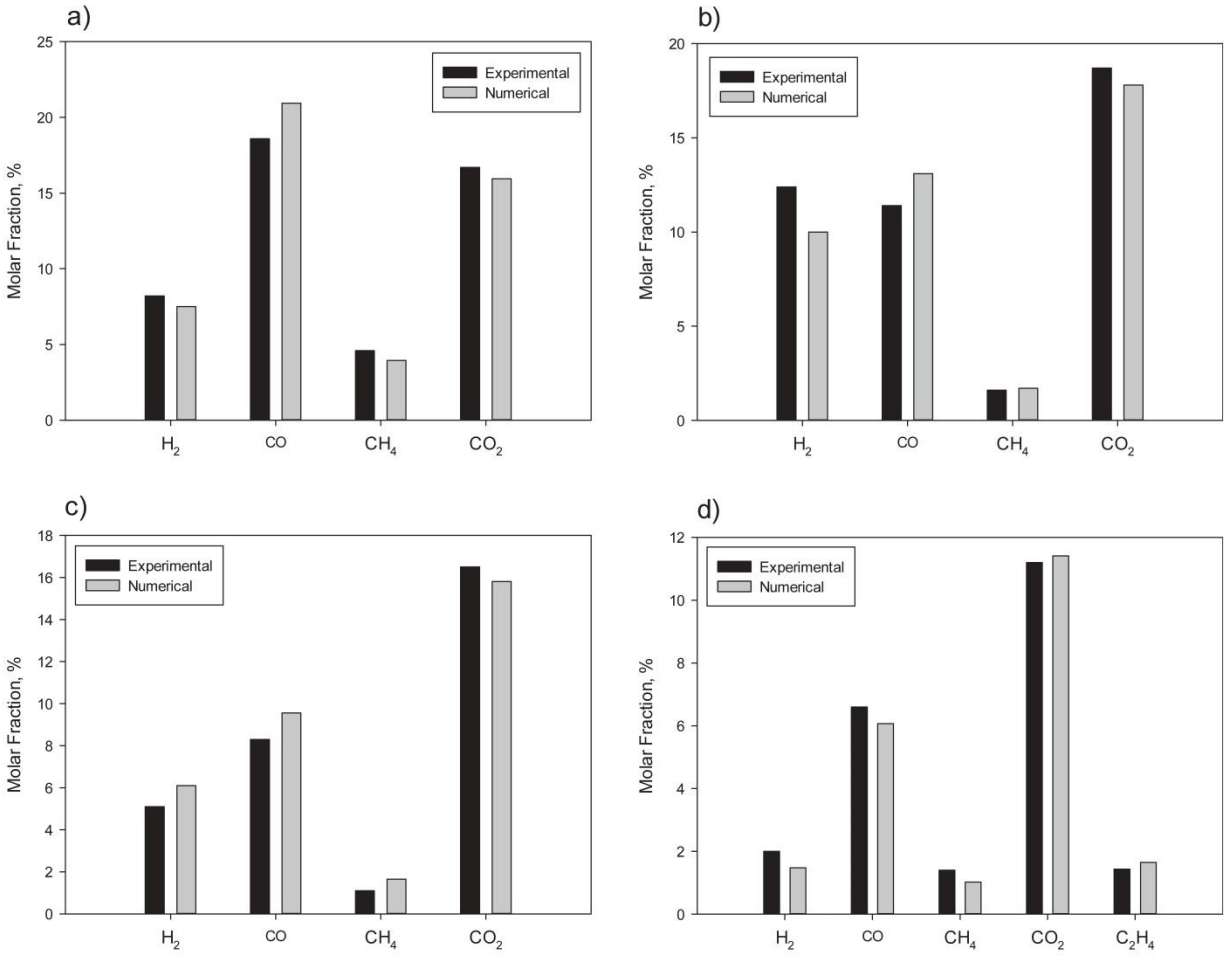

Fig. 5. Syngas molar fractions obtained both experimentally and numerically for a) forest residues, b) coffee husks, c) vines pruning and d) Xiao's MSW.

Table 4
Operating conditions for Fig. 5 (total pressure bellow 1 bar was assumed).

Experimental conditions	Forest residues	Coffee husk	Vines pruning	Xiao's MSW
Temperature (°C)	815	815	790	620
Substrate admission (Kg/h)	63	28	25	2.3
Air flow rate (Nm^3/h)	94	75	52	6
Reactor type	Semi-industrial	Semi-industrial	Semi-industrial	Laboratorial

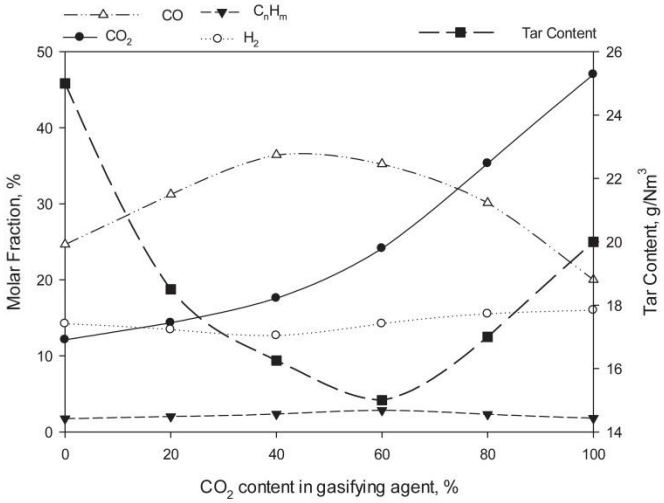

Fig. 6. Influence of CO_2 content on syngas composition and tar content (excluding steam).

conditions and in greater depth. ER was kept between 0.15 and 0.35 since all of the experiments conducted to validate the model fell in this range and also because, according to Wang et al. [13], the ER values most suitable for gasification range between 0.2 and 0.4.

In accordance with previous gasification studies [10], the equivalence ratio can be defined as:

$$ER = \frac{oxygen\ mass/dry\ MSW\ mass}{stoichiometric\ oxygen/MSW\ ratio} \quad (21)$$

In this work ER is varied by changing the air flow rate and maintaining other conditions constant.

In order to study both CO_2 and air addition in depth, the influence of both CDMR and ER on syngas composition and tar content was investigated. Results are illustrated in Fig. 7.

Contrary to what happened with CO_2 content in a gasifying mixture, increasing ER leads to a temperature boost due to an increase in O_2 rate. Since higher temperatures and higher CO_2 content

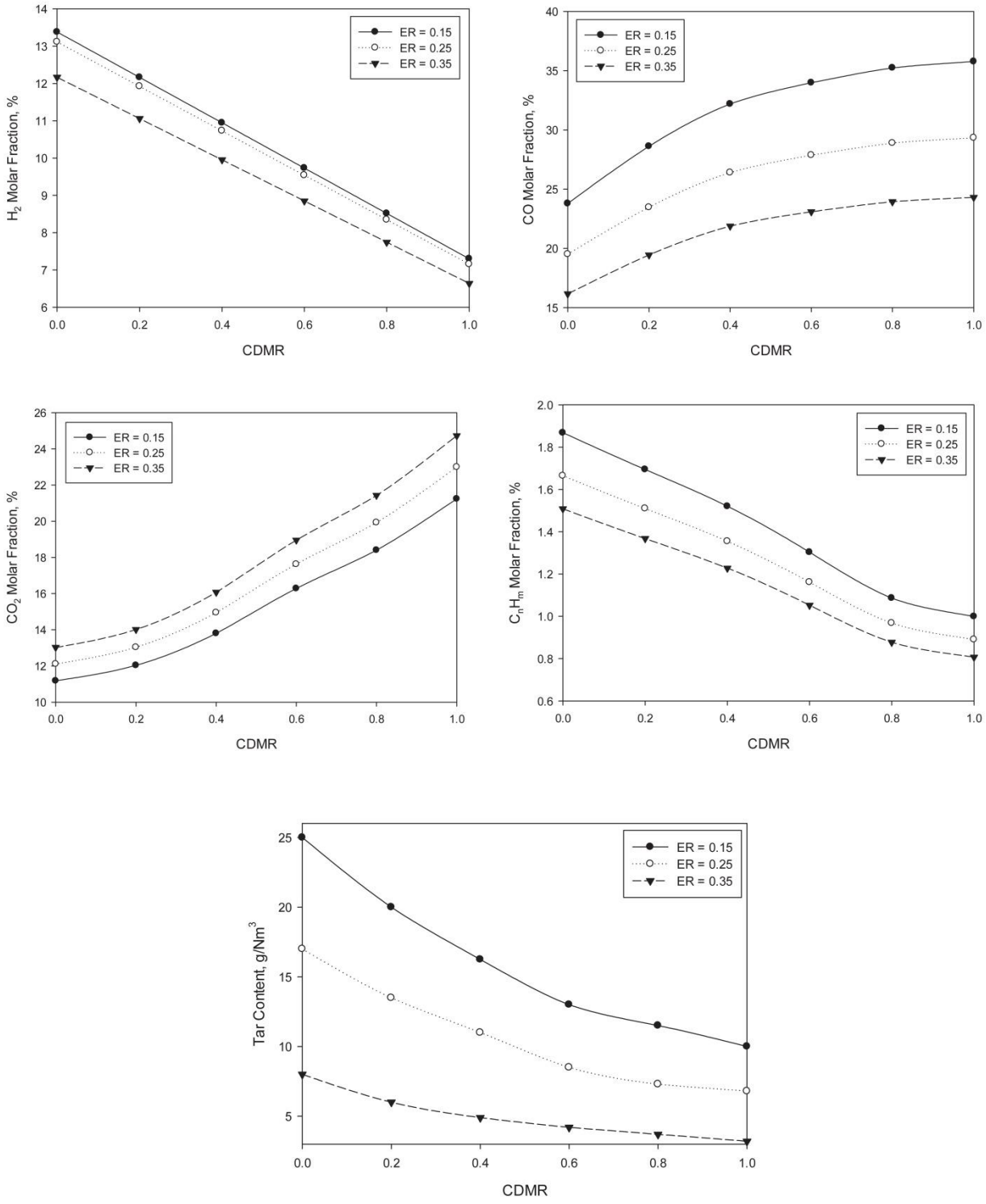

Fig. 7. Influence of CDMR and ER on syngas composition and tar content.

mainly promote Boudouard and reverse water-gas shift reactions, CO content increases while that of H_2 decreases. The amount of CH_4 and C_2H_4 also decreases slightly due to being consumed via CH_4 reforming to produce CO and H_2 [14]. On top of that, for high CO_2 concentrations, the Boudouard reaction is favored over that of CH_4 formation, and CO_2 content is expected to increase since a considerable fraction of the gasifying agent leaves the reactor unreacted.

Even though no results in the literature were found for MSW, those available for different biomass substrates appear to be in agreement with the obtained results [4,11]. It is important to refer that, although the heterogenic nature of MSW can lead to unexpected results, the fact that MSW from LIPOR consists of over 85% of cellulosic material means that techniques to enhance the thermal treatment of biomass substrates will also aid the processing of MSW [15].

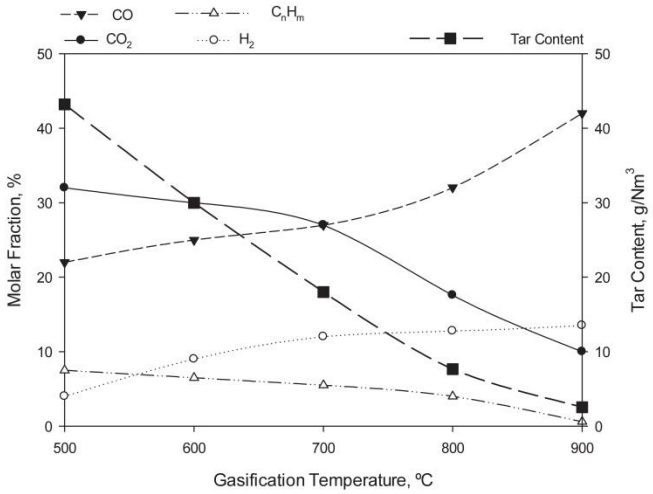

Fig. 8. Influence of gasification temperature on syngas composition and tar content.

Increases in both ER and CDMR promote tar decomposition. Oxidation reactions, which are promoted by ER, are exothermic and therefore lead to an increase in temperature inside the reactor. This increase in temperature enhances steam reforming reactions, which in turn promote carbon conversion [12]. This leads to an increase in gas yield, which is known for improving tar decomposition. On the other hand, the catalyst effect of CO_2 enhances thermal cracking of volatiles leading to a substantial decrease in tar content.

4.1.3. Influence of gasification temperature

From observation of both Figs. 6 and 7 it is clear that temperature plays a very important role and that the gasifier performance is very sensitive to bed temperature variation. In fact, Wang et al. [13] found that reactor temperature was the most important operating variable for MSW gasification and similar results were found in previous work from our research team [10].

The effect of temperature on syngas composition and tar content for MSW gasification with CO_2 and air mixtures is depicted in Fig. 8. According to Fig. 6, the most promising results were obtained when CO_2 content was 40%, since for higher percentages the available O_2 is not sufficient to maintain the desired temperature, leading to a decline in endothermic reactions, which is why CO_2 content was set to 40%.

An increase in gasification temperature has a positive influence on both CO and H_2 content [6] seeing that, according to Le Chatelier's principle, higher temperatures favor products in endothermic reactions. Since the primary water-gas reaction is endothermic, increasing gasification temperature leads to a higher fraction of H_2. At the same time, both endothermic Boudouard and reverse water-gas shift reactions will promote CO formation.

The thermodynamic feasibility of the water-gas shift reaction decreases with rising reaction temperature while the reverse reaction displays the exact opposite trend [16], which leads to CO formation and H_2 consumption. Around 700 °C, the standard Gibbs free energy of the Boudouard reaction becomes less than that of the water-gas reaction, meaning that the former dominates over the latter as temperature increases. In other words, more carbon reacts

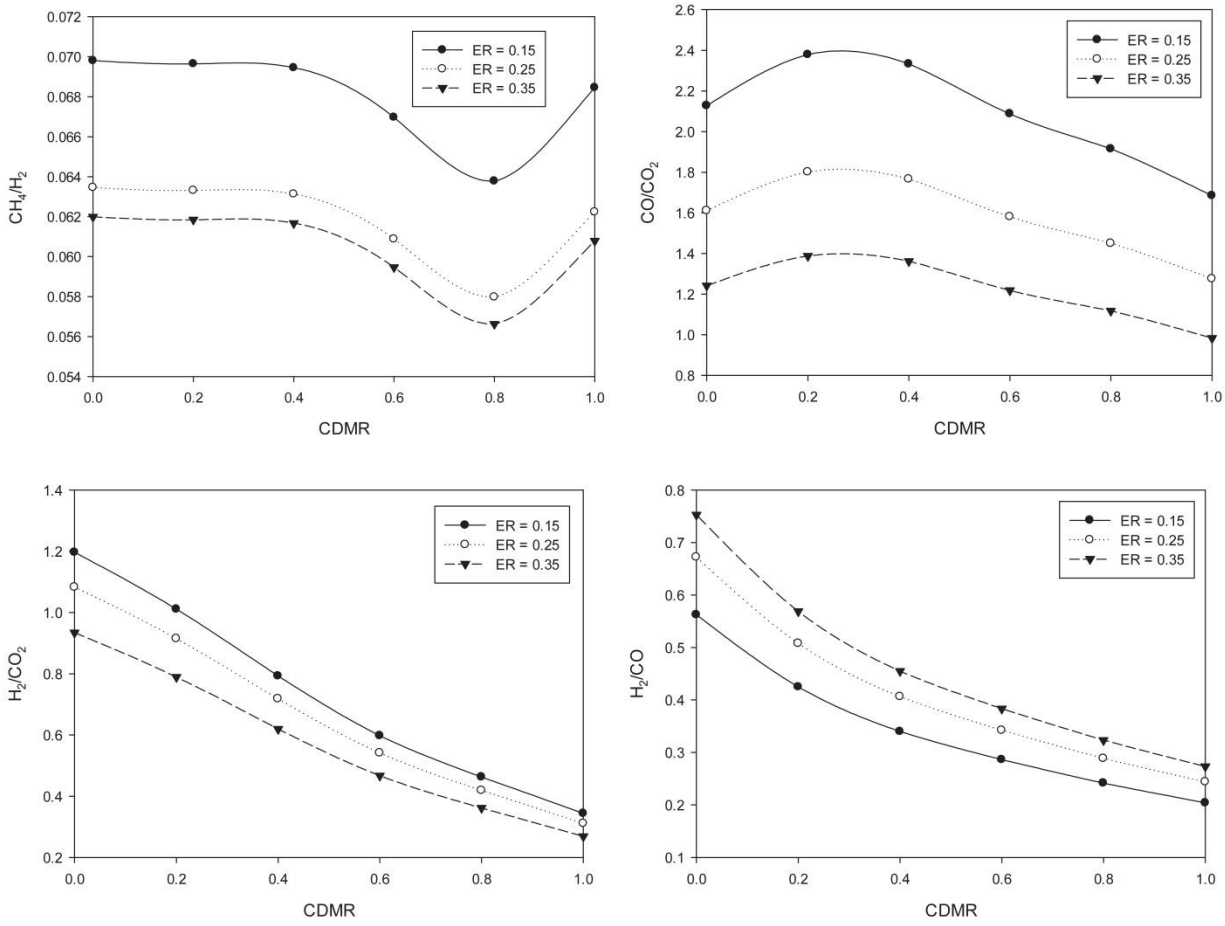

Fig. 9. Influence of CDMR and ER on syngas quality indices.

with CO_2 to form CO, and less reacts with steam to produce H_2, which explains why CO content increases while that of H_2 decreases [17]. H_2 content does not drop significantly due to H_2 production reactions (primary water-gas and CH_4 reforming) almost canceling out consumption ones (reverse water-gas) [17].

Moreover, encouraging CO_2–CH_4 reactions results in a decrease in CH_4 fraction, seeing that, CH_4 reforming using CO_2 (also known as dry reforming) is a highly endothermic reaction (even more so than the Boudouard one) and is mainly promoted at temperatures over 800 °C [18].

As expected gasification temperature has a strong influence on tar decomposition. As stated, increase in temperature leads to increases in both carbon conversion and gas yield which are known for improving tar decomposition. Moreover, since CO_2 addition enhances both char gasification and pyrolysis, which leads to increase in carbon conversion, gas yield is also expected to increase. This again, promotes tar decomposition.

4.2. Syngas quality indices derived from CO_2 addition

Gasification product quality not only gives a good indication of process efficiency, but also what its most suitable application is. This can be particularly important for applications that require specific gas characteristics but not particularly high efficiencies.

H_2/CO and CH_4/H_2 ratios are very important when choosing the right application for each syngas, since a higher CH_4/H_2 ratio is preferable for domestic purposes whereas both H_2/CO ratio and the sum of H_2 and CO gas percentages are important measures of syngas quality for the chemical industry [19]. Additionally, H_2/CO can give a good indication of the extent of the water-gas shift reaction since higher temperatures will promote CO formation while lower ones will instead promote that of H_2.

Usually CO/CO_2 and H_2/CO_2 ratios indicate the promotion of gasification reactions at the expense of combustion ones. However, since CO_2 is also being added as a gasifying agent, such considerations are harder to make, although the CO/CO_2 ratio can still give insight into the Boudouard reaction, namely that a decrease in that ratio implies a reduced extent of the reaction [20].

Fig. 9 shows the effect of CDMR as well as ER on the syngas quality indices (expressed in mol/mol), which provides crucial information on the evolution of the reactions governing the process. The exact same operating conditions as in previous chapters were chosen.

With rising air flow rate, more active oxidization reactions will occur leading to higher CO_2 and H_2O levels at the expense of CO and H_2 [21], which causes both H_2/CO_2 and CO/CO_2 ratios to decrease. On the other hand, as the amount of steam inside the reactor increases, the water-gas shift reaction encourages CO consumption and H_2 production. Moreover, the extra steam available decreases bed temperature, preventing CO formation and thus increasing the H_2/CO ratio [22]. The influence of ER on CH_4/H_2 ratio is limited as it affects both species, but since the H_2 fraction is much larger than that of CH_4, it is easier to detect slight variations. These results are consistent with the current literature [23].

Regarding CDMR, there is some variation within ratios that appears to be caused by a drop in temperature as CO_2 content increases. For instance, increasing the CO_2 flow rate impairs the dry reforming reaction, meaning that both CH_4 and C_2H_4 are less consumed to produce H_2 and CO. On the other hand, the water-gas shift reaction is much less endothermic and therefore does not require such high temperatures to keep consuming H_2, so that consuming less C_nH_m improves the CH_4/H_2 ratio.

On the same note, for lower CO_2 flow rates, most of its content is used to produce CO via the Boudouard reaction, improving the CO/CO_2 ratio, but for higher rates, not only the decrease in temperature will no longer promote the reaction but also there will not be sufficient MSW to react with CO_2. In other words, most of the CO_2 injected will leave the reactor unreacted, reducing the CO/CO_2 ratio. Both H_2/CO and H_2/CO_2 ratios are expected to decrease since H_2 is consumed to form CO (rWGS), and unreacted CO_2 from the gasifying mixture obviously contributes to its increase in syngas composition. To the best of our knowledge, no data other than on H_2/CO was found on syngas quality indices, but since the individual molar fractions of the mixture are in agreement with the literature, it is safe to assume that the indices themselves are also correct [4].

Besides syngas quality indices, there are other gasification products that can help determine process quality, namely CC (Carbon Conversion) and CGE (Cold Gas Efficiency).

Carbon conversion is defined as the fraction of carbon from MSW converted to carbon in syngas composition, and it gives an indication of the amount of unconverted material to provide a measure of chemical efficiency of the process. It can be expressed as follows:

$$Carbon\ Conversion = \frac{12 \times M}{X_c \times m} \tag{22}$$

where M stands for the total molar flow rate of carbon in syngas composition, X_c for the carbon fraction in the MSW and m for the MSW flow rate into the gasifier.

CGE can be defined as follows:

$$CGE = \frac{Gas\ yield \times HHV\ of\ product\ gas}{HHV\ of\ fuel + Heat\ addition} \tag{23}$$

Since CO_2 can be converted into CO, decreasing its emissions to the atmosphere, it was also decided to study its conversion, which is given by:

$$X_{CO_2} = \frac{moles\ of\ CO_2\ in\ gasifying\ agent - moles\ of\ CO_2\ in\ produced\ gas}{moles\ of\ CO_2\ in\ gasifying\ agent} \tag{24}$$

Figs. 10–12 depict the influence of CDMR as well as ER on CC, X_{CO_2} and CGE.

An increase in ER has negative effects on all of the studied variables since it entails the production of higher levels of CO_2 and, as expected, CGE also decreases due to the reduction of combustible gases, a behavior consistent with that reported in Ref. [10].

On the other hand, CDMR promotes all of the studied products. Both Boudouard and reverse water-gas shift reactions promote carbon and CO_2 conversion, and due to oxidation reactions promoting the formation of CO_2 over combustible gases, CO_2 conversion shows negative values for low CDMR, which means that more CO_2 is leaving the reactor than that being fed [24]. CGE is also improved since both LHV (low heating value) and gas yield increase with CO_2 content, which is consistent with the scarce literature on the subject [11,16].

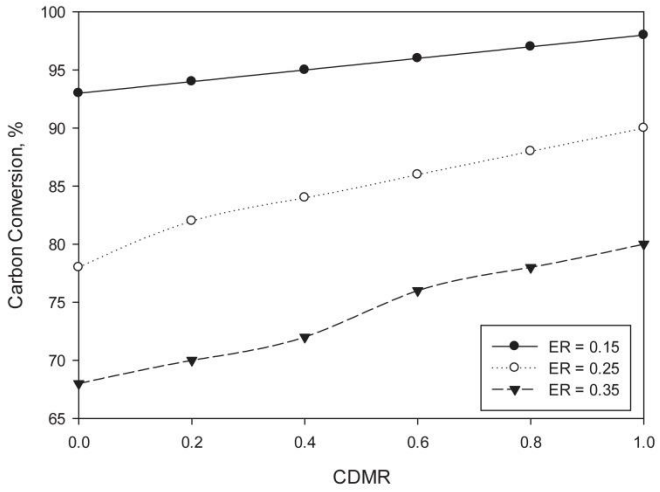

Fig. 10. Carbon Conversion as a function of CDMR and ER.

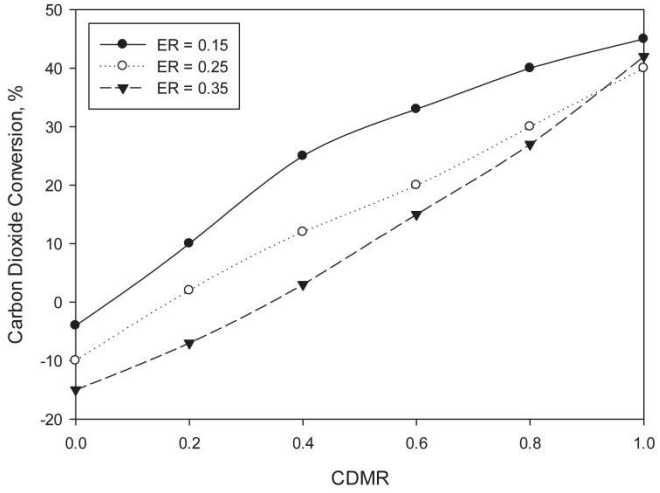

Fig. 11. CO_2 Conversion as a function of CDMR and ER.

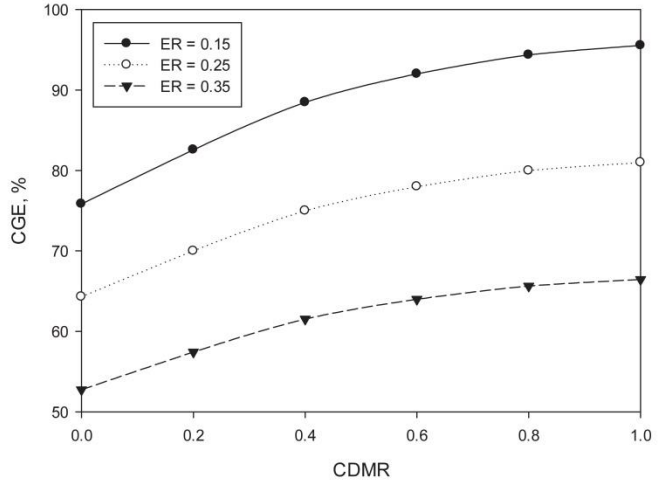

Fig. 12. CGE as a function of CDMR and ER.

4.3. Applications for MSW gasification with CO_2

MSW Gasification can be a great alternative when dealing with municipal wastes, as not only does it allow for safe residue disposal but can also be an optimal route for waste-to-energy processes. Moreover, the fact that it displays identical LHV when compared to conventional biomass substrates and that a pre-existing collection/transportation infrastructure that does not exist for conventional biomass resources makes it an even more interesting process [25].

Due to its characteristics, syngas from MSW has been used both for fuel gas and synthetic fuel application, although mainly for the latter than the former in recent years [26]. Syngas composition for fuel gas applications does not require very strict specifications as long as a high enough heating value is supplied through combustible gases, whereas chemical and fuel production require not only high H_2 content but also low CO_2 and CH_4 content Synthetic fuels can be produced from syngas via the Fischer-Tropsch (FT) process.

On the other hand, biomass gasification with CO_2 as its gasifying agent can be used for an extremely wide variety of applications [4,16] due to the ability to tailor H_2/CO ratio via of CO_2 injection. As observed by Butterman and Castaldi [4], the H_2/CO ratio has a clear impact on the optimal application for a given substrate. Higher H_2/CO ratios allow for the operation of SOFC (solid oxide fuel cells) [27] while mid H_2/CO ratios are more appropriate for FT synthesis of liquid fuels. Mid-to-lower ratios are mainly suitable for catalyst-based FT synthesis whereas very low ratios are particularly suitable for the production of a specific biomass-derived liquid chemical [28] which can be obtained by CO_2 injection during thermal processing.

This means that CO_2 gasification decreases substrate influence on the produced gas and, at the same time, is able to ensure the production of a syngas that can meet the requirements of a particular chosen industrial application [4].

In addition to improving the gas obtained, adding CO_2 to the gasification process can reduce two major concerns related to municipal solid waste gasification, namely tar formation and CO_2 production.

5. Conclusions

In this study, the gasification of municipal solid residues from Oporto was investigated using a previously developed numerical model and its results were validated against experimental ones using a semi-industrial reactor.

The influence of CO_2 addition in the gasifying agent mixture with air was studied in three separate ways: keeping the biomass/gasifying agent ratio constant; allowing biomass/gasifying agent ratio to vary; and increasing gasification temperature in a CO_2 rich environment.

To gain better understanding on the influence of the addition of CO_2 in the process, its impact on syngas quality indices was also studied and results demonstrated that both H_2/CO and H_2/CO_2 ratios decrease with rising CO_2 flow rate while the CO/CO_2 and CH_4/H_2 ratios increased. Opposite trends were observed for lower rates.

Furthermore, results established that increasing CO_2 content boosts carbon and, CO_2 conversion, process efficiency, and even mitigates the tar produced. In fact, when CDMR was increased from 0 to 1 tar content mitigation exceeded 50%. Since tar and CO_2 production are two of the main concerns regarding MSW gasification, the results presented in this study are promising.

Finally, the influence of CO_2 content on optimal process application was investigated and results revealed that CO_2 injection has the ability to tailor H_2/CO ratio, meaning that CO_2 gasification can decrease substrate influence and thus control syngas production to meet the requirements of a particular chosen industrial application.

Acknowledgments

We would like to express our gratitude to the Portuguese Foundation for Science and Technology (FCT) for the support to the grant SFRH/BD/86068/2012 and the project PTDC/EMS-ENE/6553/2014 as well as IF/01772/2014.

References

[1] Hoornweg D, Bhada-Tata P. What a waste a global review of solid waste management. Urban Development Series Knowledge Papers 15. 2012. http://siteresources.worldbank.org/INTURBANDEVELOPMENT/Resources/336387-1334852610766/What_a_Waste2012_Final.pdf. last access in February 12th.
[2] Arafat H, Jijakli K. Modeling and comparative assessment of municipal solid waste gasification for energy production. Waste Manag 2013;33:1704–13.
[3] Umeki K, Yamamoto K, Namioka T, Yoshikawa K. High temperature steam-only gasification of woody biomass. Appl Energy 2010;87:791–8.
[4] Butterman H, Castaldi M. CO2 as a carbon neutral fuel source via enhanced Biomass Gasification. Environ Sci Technol 2009;43:9030–7.
[5] Couto N, Silva V, Monteiro E, Teixeira S, Chacartegui R, Bouziane K, et al. Numerical and experimental analysis of municipal solid wastes gasification process. Appl Therm Eng 2015;78:185–95.
[6] Silva V, Monteiro E, Couto N, Brito P, Rouboa A. Analysis of syngas quality from portuguese biomasses: an experimental and numerical study. Energy Fuel 2014;28:5766–77.
[7] Teixeira S, Monteiro E, Silva V, Rouboa A. Prospective application of municipal solid wastes for energy production in Portugal. Energy Policy 2014;71:159–68.
[8] Onel O, Niziolek AM, Hasan MMF, Floudas CA. Municipal solid waste to liquid transportation fuels - part I: mathematical modeling of a municipal solid waste gasifier. Comput Chem Eng 2014;71:636–47.
[9] Xue Q, Heindel T, Fox R. A CFD model for biomass fast pyrolysis in fluidized-bed reactors. Chem Eng Sci 2011;66:2440–52.
[10] Couto N, Silva V, Monteiro E, Rouboa A. Assessment of municipal solid wastes gasification in a semi-industrial gasifier using syngas quality indices. Energy 2015;93:864–73.
[11] Cheng Y, Thow Z, Wang C. Biomass gasification with CO_2 in a fluidized bed. Powder Technol 2014 [in press], Corrected Proof, Available online 27 December 2014.
[12] Wang J, Cheng G, You Y, Xiao B, Liu S, He P, et al. Hydrogen-rich gas production by steam gasification of municipal solid waste (MSW) using NiO supported on modified dolomite. Int J Hydrogen Energy 2012;37:6503–10.
[13] Wang L, Weller C, Jones D, Hanna M. Contemporary issues in thermal gasification of biomass and its application to electricity and fuel production. Biomass Bioenergy 2008;32:573–81.
[14] Corigliano O, Fragiacomo P. Technical analysis of hydrogen-rich stream generation through CO2 reforming of biogas by using numerical modeling. Fuel 2015;158:538–48.
[15] Butterman H, Castaldi M. CO2 enhanced steam gasification of biomass fuels. In: Proceedings of the 16th annual north American waste-to-energy conference, May 19-21, Philadelphia, PA; 2008.
[16] Renganathan T, Yadav M, Pushpavanam S, Voolapalli R, Cho Y. CO2 utilization for gasification of carbonaceous feedstocks: a thermodynamic analysis. Chem Eng Sci 2012;83:159–70.
[17] Song T, Wu J, Shen L, Xiao J. Experimental investigation on hydrogen production from biomass gasification in interconnected fluidized beds. Biomass Bioenergy 2012;36:258–67.
[18] Fidalgo B, Menéndez JA. Syngas production by CO2 reforming of CH4 under microwave heating – challenges and opportunities. In: Indarto A, Palgunadi J, editors. Syngas: production, applications and environmental impact. Hauppauge, NY,: Nova Science Publishers, Inc.; 2011. p. 121–49.
[19] Bhavya B, Singh R, Bhaskar T. Gasification for synthetic fuel production, fundamentals. Process Appl 2015;3:57–71.
[20] Hernández JJ, Aranda G, Barba J, Mendoza JM. Effect of steam content in the air-steam flow on biomass entrained flow gasification. Fuel Process Technol 2012;99:43–55.
[21] Gomez-Barea A, Leckner B. Modeling of biomass gasification in fluidized bed. Prog Energy Combust Sci 2010;36:444–509.
[22] Zhou H. Air and steam coal partial gasification in an atmospheric fluidized bed. Energy Fuel 2005;19:1619–23.
[23] Narvaez I, Orio A, Aznar MP, Corella J. Biomass gasification with air in an atmospheric bubbling fluidized bed. Effect of six operational variables on the quality of the produced raw gas. Ind Eng Chem Res 1996;35:2110–20.
[24] Ahmed I, Gupta AK. Characteristics of cardboard and paper gasification with CO_2. Appl Energy 2009;86:2626–34.
[25] Hansson J, Leveau A, Hulteberg C. Biomass gasifier database for computer simulation purposes. Nordlight AB, Rapport SGC 234, ©Svenskt Gastekniskt Center. August 2011.
[26] Raskin N, Palonen J, Nieminen J. Power boiler fuel augmentation with a biomass fired atmospheric circulating fluid-bed gasifier. Biomass Bioenergy 2001;20:471–81.
[27] Mulas M, Murgia G, Pisani L, Russo R. A quasi-3D computer model of a planar solid-oxide fuel cell stack. In: Proceedings of 3rd international energy conversion engineering conference, San Francisco, California, August 15–18, AIAA: CA; 2005.
[28] Peng XD, Toseland BA, Wang AW, Parris GE. Progress in development of LPDME process: kinetics and catalysts. In: Proceedings of 1997 coal liquefaction & solid fuels contractors review conference, Pittsburgh, Pennsylvania, September 3-4, NETL: Pittsburgh; 1997.

Paper X

Assessment of Municipal Solid Wastes Gasification in a Semi-industrial Gasifier using Syngas Quality Indices

N. Couto, V. Silva, E. Monteiro, A. Rouboa

Energy 93 (2015) 864-873

Energy 93 (2015) 864–873

Contents lists available at ScienceDirect

Energy

journal homepage: www.elsevier.com/locate/energy

Assessment of municipal solid wastes gasification in a semi-industrial gasifier using syngas quality indices

Nuno Dinis Couto [a], Valter Bruno Silva [a], Eliseu Monteiro [b], Abel Rouboa [a, c, *]

[a] INEGI-FEUP, Faculdade de Engenharia da Universidade do Porto, Porto, Portugal
[b] INEGI-FEUP, Polytechnic Institute of Portalegre, Portalegre, Portugal
[c] MEAM Department, University of Pennsylvania, Philadelphia, PA 19020, USA

ARTICLE INFO

Article history:
Received 13 May 2015
Received in revised form
4 September 2015
Accepted 14 September 2015
Available online 22 October 2015

Keywords:
Syngas quality indices
Gasification
Municipal solid wastes
CFD
Semi-industrial gasifier

ABSTRACT

In this work a comprehensive two-dimensional CFD model was used in order to assess the potential of syngas produced from gasification of Portuguese MSW (municipal solid waste) by using a semi-industrial gasification plant. An Eulerian–Eulerian approach within the computational fluid dynamics Fluent framework was used to describe the transport of mass, momentum and energy for both solid and gas phases. Pyrolysis was also modeled. Numerical results were validated against experimental ones. Results were in good agreement with each other. Influence of temperature, MSW admission and equivalent ratio on products of gasification and their concentrations were studied. Considering operating conditions influence on the combustible gases, it was concluded that gasification temperature had the greatest influence on syngas heating value. After analyzing syngas composition and other gasification products the best use for a particular produced syngas was investigated. For the MSW used in this work one of the most promising uses for the obtained syngas was for chemical fuel application.

1. Introduction

MSW (municipal solid waste) collection and disposal is a major urban environment issue in the world today. MSW to energy generates a renewable energy source and has attracted the attention of both national and local governments with various preferential policies.

There are emergent support schemes worldwide to promote power generation from renewable energy sources [1] because of the retreating conventional sources of energy, frequent energy security issues, and increasing public environmental awareness.

According to the concept of sustainable waste disposal, a successful treatment of MSW should be safe, effective, and environmentally friendly [2]. However, the current waste-disposal methods do not meet these goals. Landfills occupy large amounts of land and lead to serious environment problems [3]. Incineration technology was developed to reduce the total volume of waste and make use of the chemical energy of MSW for energy production. However, MSW incineration is a highly complex technology, which involves large investments and high operating costs. On top of that, these types of systems produce a wide variety of pollutants that can be harmful to human health. Meaning that it is necessary to find a new way to not only eliminate or control the toxic emissions from chemically complex MSW but also minimize investment and operating costs.

During gasification of MSW, the chemical energy content in the carbonaceous fractions of the waste is converted, under sub-stoichiometric conditions, to a gaseous product or syngas [4]. As a waste-to-energy technology, gasification offers remarkable opportunities for increasing overall plant efficiencies by utilization of the syngas in higher efficiency electricity-production system, such as gas turbines, reciprocating engines [5] and fuels cells [6]. The syngas specific composition depends upon the fuel source and the processing technique. The substantial variations in syngas composition and heating value are among the largest barriers toward their usage [7].

Therefore, measurements of the gas-species composition of the syngas produced from gasification of MSW under different operating condition of gas temperature and residence time showed that carbon monoxide, hydrogen, methane, ethane and acetylene are

* Corresponding author. Quinta de Prados, Apartado 1013, 5001-801 Vila Real, Portugal. Tel.: +351 259350317; fax: +351 259 350 356.
E-mail addresses: nunodiniscouto@hotmail.com (N.D. Couto), vbrsilva@utad.pt (V.B. Silva), ELMMonteiro@portugalmail.pt (E. Monteiro), rouboa@seas.upenn.edu (A. Rouboa).

http://dx.doi.org/10.1016/j.energy.2015.09.064
0360-5442/

the main gas-phase species present in the syngas under gas temperature conditions in the range between 750 and 900 °C, typical in commercial gasification technologies [8].

Measurements of tars composition in the syngas produced from MSW [8] showed that benzene and benzene derivatives are the main tar components under typical gasification conditions, which are also the main tar components obtained from biomass gasification [9]. Since tar formation can cause severe problems in the gasification process it is necessary to maximize its removal. Devi et al. [10] provided an overview of the primary methods used for tar removal. According to the authors all tars should be prevented or eliminated in the gasifier by manipulating factors like operating conditions, addition of active bed materials and possible reactor design modifications.

The production of syngas from the gasification of MSW is a recent subject and, hence, shortly reported in the scientific literature [6,11,12].

Syngas application greatly depends not only on MSW composition but also on operating conditions. In fact, optimization of the operating conditions can improve syngas characteristics from a certain application like, fuels and chemical synthesis applications or for hydrogen and fuel gas applications, among others [13].

The traditional approach indispensable to establish commercial plant technology is based on full experimental investigations, progressing from a laboratory scale test unit to a pilot scale plant, before building a full-scale commercial demonstration plant. Results from semi-industrial plants present far more importance for commercial ones due to the fact that results are much more close to reality than laboratory ones. For process optimization, an extensive investigation of the plant behavior depending on various operating parameters is required for each scale up step. To support this optimization procedure, mathematical models are helpful to reduce the temporal and financial efforts.

Numerical models can also be very useful for predicting the gasification process including syngas composition and in particular syngas quality indices. There are several papers in the literature trying to successfully describe the gasification process using different substrates [14–16].

The aim of this paper is to assess the syngas production from MSW gasification using a numerical method. For this propose, a two-dimensional mathematical model developed and validated in an earlier work [17] based on an Eulerian–Eulerian approach and capable to simulate fluidized-bed MSW gasification within Fluent is used. The model was validated using data collected from the literature and then expended to predict the process on a semi-industrial gasifier. Applications of syngas obtained from MSW gasification in the Lipor (North of Portugal) is taken as a case study. An assessment of the potential of gasification can only be made after modeling the products of gasification and their concentrations at different operating conditions. In this study, we attempted to do so for MSW by predicting the relative concentrations of process products using the computer package Fluent. Using a wide set of experiments the obtained concentrations, as well as other gasification products, the best use for the syngas produced will be investigated.

2. Materials and methods

The simulations were performed in an up-flow atmospheric fluidized bed gasifier. This fluidized bed reactor is a tubular reactor of 0.5 m in diameter and 4.15 m of height, internally coated with ceramic refractory materials; MSW enters the reactor at the height of 0.5 m, from its base, and preheated air at 600 K enters the reactor coming from the base through a set of diffusers, ensuring an adjustable flow. The schematics of the fluidized reactor as well as in depth analysis on the gasification plant can be seen in [15,17].

2.1. Municipal solid waste characterization

MSW increases significantly in industrialized and developing countries, raising questions about sustainable municipal solid waste management. This results from the collection of waste in large urban areas, and comprises materials such as household waste, plastic, paper, glass, metals, and garden waste [18]. The composition of municipal solid waste depends on both the season and geographic location. The heterogeneous nature of the wastes affects the physical properties in terms of size, elemental composition, moisture content, heating value, ash content, volatile content and other contaminants. Therefore, the wastes are pre-treated accordingly to the Portuguese management system described by Teixeira et al. [3].

Lipor is the entity responsible for the management, treatment and recovery of MSW in the Oporto metropolitan area. This includes eight municipalities in the Oporto metropolitan area and a production of about 500 Ktons/year of MSW [19]. During the year 2012 a sampling campaign was carried out. A criteria analysis of the waste collected was held, and the physical characterization by categories is shown in Table 1.

From the pre-treatment results a RDF which contains cellulosic materials and plastics due to putrefied wastes, paper, wood wastes, and plastic residues. The remaining MSW components follow another route for valorization or elimination. Plastic residues are mainly composed of polyethylene, polystyrene, and poly-vinyl chloride [20] and the cellulosic materials are composed of cellulose, hemicelluloses, and lignin [21].

Given that the ultimate analyses does not distinguish the cellulosic materials, it was postulated that their composition was similar to the one found in Onel et al. [16], where the cellulosic material comprises cellulose, hemicellulose and lignin. Regarding the plastics group, report shows the relative quantities of each monomer in the MSW. Therefore, it was possible to take into account different monomers for the plastics group as shown in Table 2.

In order to model the gasification process it is necessary to formulate the MSW mixture in Fluent. Waste characterization shown in Table 2 can be used to this end. Ultimate analysis of the mixture is used to found fractions of carbon (C), hydrogen (H) and oxygen (O).

3. Mathematical model

The two-dimensional mathematical model developed by Silva and Couto [15,22] for biomass gasification and extended by Couto

Table 1
Physical characterization of the MSW [19].

Category	Winter (% weight)	Summer (% weight)
Putrefied residues	44.34%	44.29%
Paper	4.74%	5.30%
Cardboard	2.61%	4.21%
Composites	4.68%	5.40%
Textiles	5.73%	6.76%
Sanitary textiles	11.20%	6.28%
Plastics	10.98%	13.44%
Combustive non specified	0.09%	0.97%
Glass	4.29%	4.80%
Metals	2.15%	1.97%
Non-combustive non specified	0.41%	0.46%
Hazardous residues	0.06%	0.01%
Fine elements	8.72%	8.10%

Table 2
Chemical composition of the MSW.

Category	% Weight	Chemical formula
Cellulosic material	85.22%	[a]
Polyethylene	11.14%	$(C_2H_4)_n$
Polyethylene terephthalate	2.05%	$(C_{10}H_8O)_n$
Polypropylene	0.82%	$(C_3H_6)_n$
Polystyrene	0.77%	$(C_8H_8)_n$

[a] It was considered the proportion of cellulose, hemicellulose and lignin found in Onel et al. [16].

et al. [17] for MSW gasification was applied in this study. The gasification was modeled using Fluent data base for a two-dimensional model and multi-phase (gas and solid) model. The solid phase was treated as an Eulerian granular model while the gas phase is considered as continuum. The main interaction between the phases is also modeled, heat exchange by convection, mass (the heterogeneous chemical reactions), and momentum (the drag in gas and solid phase). Numerical procedure can be seen in Ref. [17].

4. Results and discussion

In order to validate the numerical model presented in Ref. [17] results from a semi-industrial gasification plant were used. First the model was developed for biomass gasification. 3 biomasses largely available in Portugal but also with potential to substitute fossil fuels were selected. Validation with Portuguese biomass was already shown in several other works [15,22].

After study the biomass gasification the model had to be upgraded to cope with the heterogeneity of MSW, which means that the devolatilization section was modified [17].

Due to the lack of data regarding experimental municipal waste gasification in semi-industrial (or industrial) facilities, data was collected from the literature [23]. In Table 3 are shown the operating conditions for 12 experimental runs used to validate the numerical model.

Table 4 shows the syngas composition from the gasification process obtained experimentally and numerically by using a CFD model.

The model can predict syngas composition for all the species in a large spectrum of operating conditions reasonably well. The largest errors are found for species at minor molar fractions. Deviations can be explained mainly due to:

- The lack of data on the characteristics of waste has led to the use of constants of other biomasses which may differ from the actual one.
- The kinetic constants were taken from the literature and can differ greatly from source to source.

Further experimental comparison was made using the calorific value of the produced gas. The capability in predicting the influence of several operating conditions on the syngas calorific value is shown in Figs. 1 and 2.

Above Figures show that not only the developed model can predict syngas composition for all the combustible species but can successfully predict the trends for the key operating conditions and their influence on the syngas quality. In fact, gasification temperature has a positive influence on LHV (low heating value) while ER (equivalent ratio) presents the exactly opposite trend. Both these trends are consistent with the available literature and will be explained later in the chapter. Maximum LHV error was around 16%.

Another crucial key of the numerical models is their ability to predict profile gas composition inside the reactor during gasification process. Fig. 3 shows profile gas composition for the main combustible gases produced in the process.

It can be seen that methane, hydrogen and carbon monoxide present their highest values at the biomass inlet, right above biomass inlet and higher in the reactor, respectively. For methane this is due to where the reduction phase is located and these gases are formed which is consistent with [24]. For the case of both CO and H_2 while they present similar profiles it is noticeable that in the lower regions of the reactor CO is more pronounce than H_2. In fact, at greater heights H_2 is favorable simply due to lower temperature enhance H_2 production by primary water–gas reaction and steam-methane reforming reactions while at higher temperatures (lower in the reactor) primary water–gas as well as Boudouard reaction will favor more CO production [25]. This is consistent with the available literature [15,17,22,26].

A wide set of numerical experiments were selected to gather the most data regarding the gasification process. 5 runs for each of the 3 operating conditions were performed. In order not to make Table 5 too long only initial, middle and final conditions are presented.

In order to avoid over oxidation of metals in MSW gasification temperature should be lower than 700 °C [27,28]. At the same time, gasification temperature should be higher than 500 °C or reactants will jam the gasifier [29,30]. MSW and air flow rate were chosen according to the gasifiers maximum feeding rate conditions.

Figs. 4–6 show the influence of gasification temperature, ER (equivalent ratio) and MSW admission rate on syngas molar fractions, respectively. Operating conditions were taken from Table 5.

In accordance with previous gasification studies [31], the equivalence ratio can be defined as:

$$\mathrm{ER} = \frac{\text{oxygen mass/dry } MSW \text{ mass}}{\text{stoichiometric oxygen /MSW ratio}} \quad (1)$$

In this work ER is varied by changing the air flow rate and maintaining other conditions constant.

As stated, by increasing air flow into the gasifier one is increasing the ER. With a surplus of air (or oxygen) more active oxidization reactions (such as particle combustion of char, CO and H_2) will occur leading to higher levels of CO_2 and H_2O at the cost of CO and H_2 [32]. Both CH_4 and C_2H_4 present very low molar fraction levels and both decrease slightly with increase of ER. N_2 is expected to increase with the ER since more air is entering the gasifier. This exact trend can be seen in Fig. 4.

Table 3
Operating conditions for the experimental gasification runs.

Run	1	2	3	4	5	6	7	8	9	19	11	12
Temperature (°C)	720	620	493	705	602	507	687	593	516	691	593	507
MSW admission (Kg/h)	2.3	2.3	2.3	3	3	3	4	4	4	6	6	6
Air flow rate (Nm^3/h)	6	6	6	6	6	6	6	6	6	6	6	6
ER	0.5	0.5	0.5	0.4	0.4	0.4	0.3	0.3	0.3	0.2	0.2	0.2
Preheated air (°C)	352	283	290	352	296	281	352	307	282	352	308	279

Table 4
Syngas composition (numerical and experimental) for the experimental gasification runs.

Runs	CO_2		H_2		N_2		CH_4		CO		C_2H_4	
	Exp	Num	Exp	Num	Exp	Num	Exp	Num	Exp	Num	Exp	Num
1	8.90	7.71	3.60	2.61	68.40	70.82	2.60	2.65	6.50	6.39	3.24	3.12
2	11.20	11.41	2.00	1.48	69.80	74.81	1.40	1.02	6.60	6.07	1.43	1.65
3	12.80	14.00	1.40	1.28	70.50	72.84	0.80	0.50	4.80	4.51	1.11	1.23
4	12.40	12.89	4.20	4.53	59.60	63.70	3.80	4.25	8.60	8.91	3.89	4.25
5	14.50	15.10	2.50	2.46	66.80	68.10	1.80	1.54	8.00	7.27	2.16	3.11
6	14.80	13.90	1.50	1.62	67.90	69.00	0.90	0.72	5.00	5.23	1.58	1.78
7	15.60	17.00	5.80	6.20	48.20	49.41	4.60	5.36	9.10	9.73	5.91	5.43
8	14.10	14.67	2.70	2.96	65.30	66.65	1.50	1.28	6.00	5.68	2.17	2.19
9	16.00	16.58	1.10	1.40	69.30	71.06	0.80	0.51	5.30	5.12	1.63	2.34
10	15.10	15.73	5.40	5.00	44.30	46.15	5.70	5.80	10.20	10.50	7.87	8.57
11	15.50	15.30	3.30	2.75	60.30	63.10	2.20	2.42	8.10	8.60	3.20	3.48
12	14.20	14.92	4.10	4.50	61.60	59.50	1.80	2.05	9.50	10.11	1.89	2.45

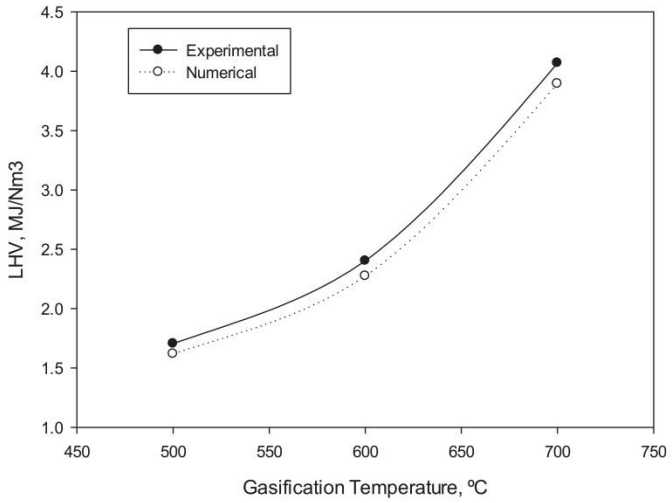

Fig. 1. Influence of gasification temperature on syngas LHV for both experimental and numerical results (operating conditions: ER = 0.5; MSW feed rate = 2.3 kg/h; Air flux = 6 m^3/h).

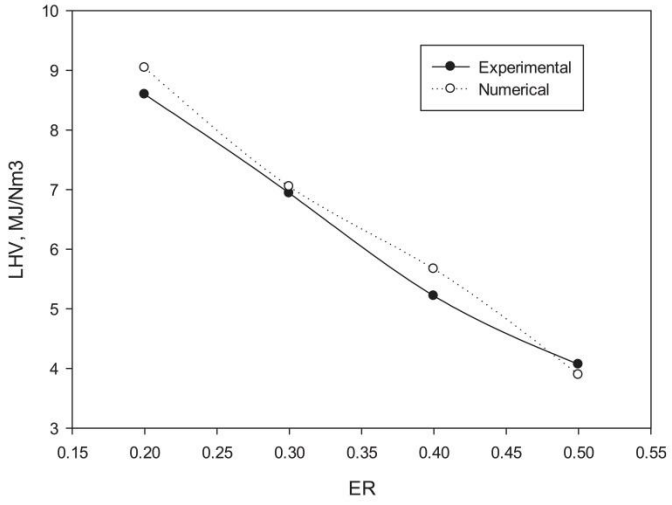

Fig. 2. Influence of ER on syngas LHV for both experimental and numerical results (operating conditions: Gasification temperature = 700 °C; MSW feed rate = 2.3 kg/h; Air flux = 6 m^3/h).

According to the literature [33] for all the studied MSW there was a clear decrease in syngas calorific value with the increase of MSW flow. With faster admission by the gasifier, reduces the extent of reaction from steam-methane reforming reaction and primary water–gas reaction and equilibria is not attained. Also Beaumont and Schwob [34] reported that because of the shorter residence time for the char in the gasifier a loss of some energy content was found. What this leads in terms of syngas composition is an obvious decrease in CO mole fraction and small but visible effect in H_2 and CH_4 fraction. This is visible in Fig. 5.

In a self-heated gasifier, gasification temperature will most likely be controlled by adjusting ER or admission of MSW. For this reason gasification temperature tends to be a dependent variable in the MSW gasification process. On the other hand, temperature has a predominant effect on reaction kinetics and the gasifier performance is very sensitive to the bed temperature change. Therefore, the bed temperature was selected to analyze its effect on the gasifier performance. Increasing on gasification temperature has a positive influence on the combustible gases such as CO and H_2 [15]. Since primary water–gas reaction is endoenergetic, increase of gasification temperature leads to higher fraction of H_2, in accordance with Le Chatelier's principle. Because of this, pyrolysis has a predominant role in MSW gasification at low temperatures such as the ones being studied because the low energy limits the endothermic reactions such as char gasification and steam reforming [35]. Also, strengthening the endothermic steam-methane reactions results in a decrease in CH_4 fraction. Again this is noticeable in Fig. 6.

A combustible gas such as CO, H_2, CH_4 and C_2H_4 in the syngas composition determines its quality through the LHV (low heating value) and the gasification efficiency. Next on Fig. 7 influence of MSW and air flow as well as gasification on syngas LHV is presented. Operating conditions are still relative to Table 5.

It is clear that increasing gasification temperature from 500 °C to 700 °C LHV greatly increases while increasing MSW and air flow actually has a negative influence on LHV. This phenomenon was previously explained but in summary increase in gasification temperature leads to an increase of H_2 and CO content, which in turn increases LHV of syngas produced. According to the literature [36] decrease of LHV with increase of ER can be explained by the enlarging dilution effect of N_2. Other than this the decrease of LHV levels with increase of both MSW and air flow could be easily explained by analyzing syngas composition in Figs. 4–6, i.e. if an operating condition has negative effects on the combustible syngas gases, the respective LHV will decrease as well. It is important to refer that levels of LHV appear to be smaller than the papers used as reference mainly due to small temperature range being studied (specially 500–600 °C).

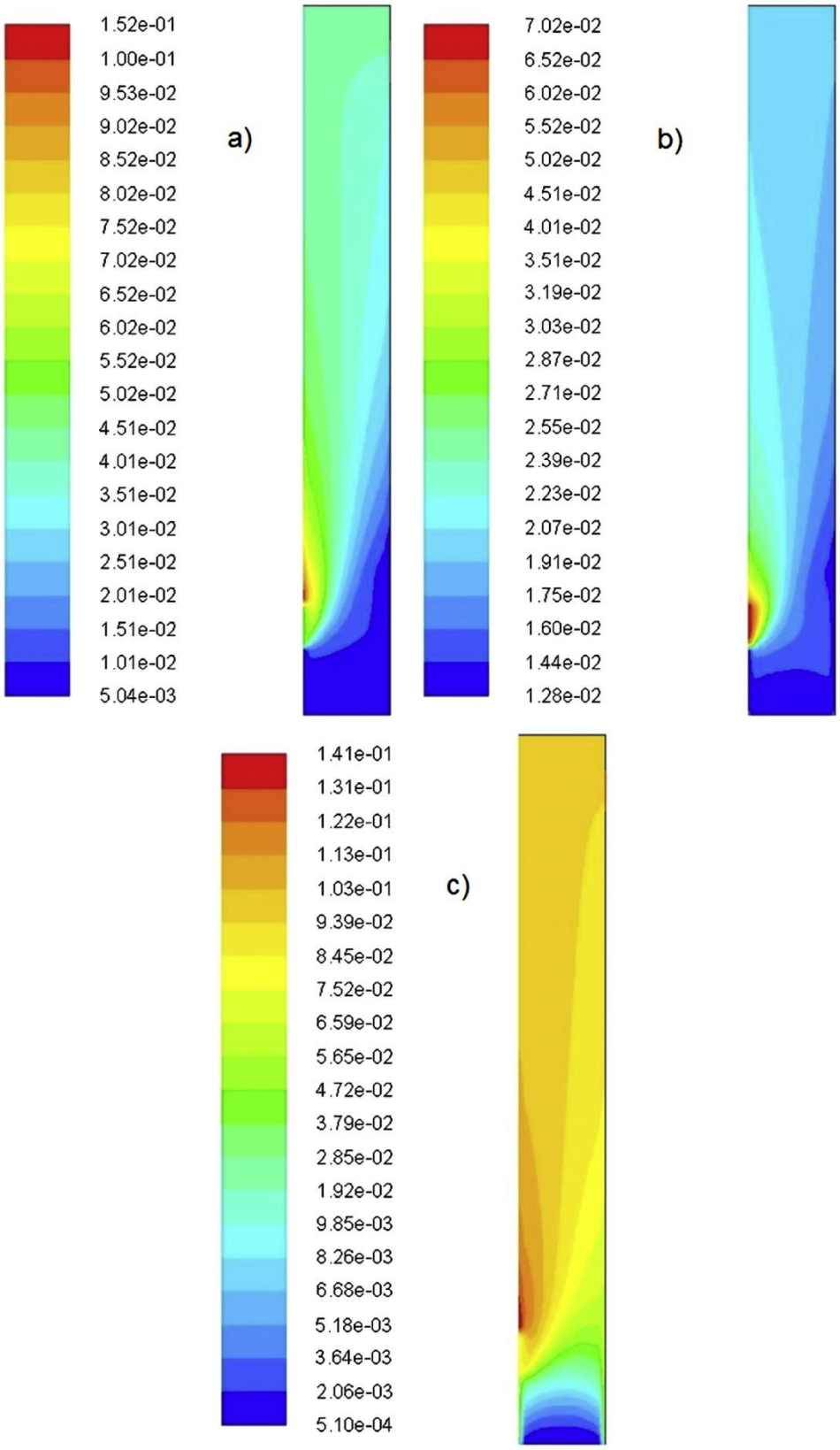

Fig. 3. Contours of the (a) H_2, (b) CH_4 and (c) CO molar fractions in the gas mixture (run 12).

Table 5
Gasification operating conditions.

Gasification run	Feeding rate of MSW (kg/h)	Flux of air (m^3/h)	Gasification Temperature (°C)
1	25	40	500
2			600
3			700
4		70	500
5			600
6			700
7		100	500
8			600
9			700
10	50	40	500
11			600
12			700
13		70	500
14			600
15			700
16		100	500
17			600
18			700
19	75	40	500
20			600
21			700
22		70	500
23			600
24			700
25		100	500
26			600
27			700

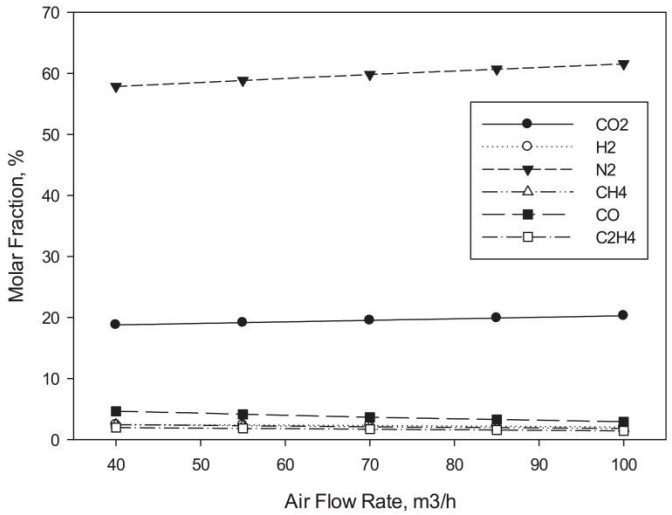

Fig. 4. Influence of air flow rate on syngas molar fraction (operating conditions: MSW feed rate = 25 kg/h; Gasification temperature: 500–700 °C).

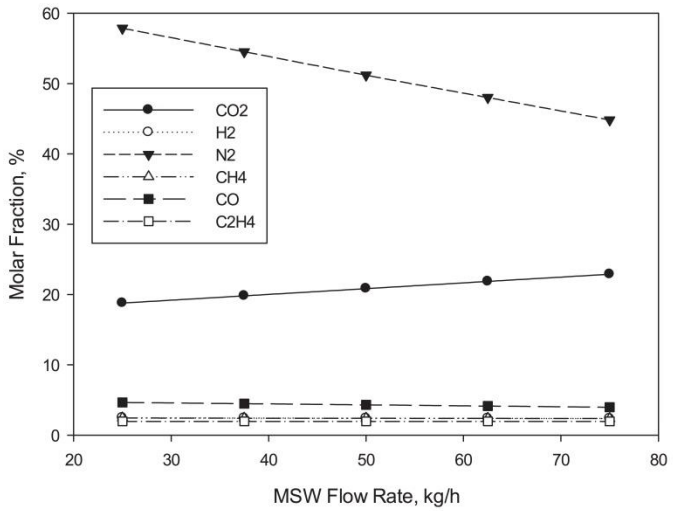

Fig. 5. Influence of biomass flow rate on syngas molar fraction (operating conditions: Air flow rate = 40 kg/h; Gasification temperature: 500–700 °C).

4.1. Syngas quality indices and hydrogen production

Hydrogen is one of the key energy sources due to its potential to provide energy for industry, residences, transportation and mobile applications. Therefore, one of the focuses in gasification research is to find a way to improve its production [37]. The hydrogen molar ratio rises with an increase in temperature but decreases with the increase of ER. The reason why H_2 decreases with ER has to do with more active oxidization reactions will occur leading to higher levels of CO_2 and H_2O at the cost of CO and H_2. Regarding the increase with temperature it is known that, according to Le Chatelier's principle, higher temperatures favor products in endothermic reactions. Therefore, the endothermic reaction was strengthened, leading to an increase in the hydrogen content.

Syngas quality indices such as H_2/CO and CH_4/H_2 ratios are very important for choosing the correct application for each syngas. For domestic purposes a higher CH_4/H_2 ratio is preferable. For the chemical industry H_2/CO ratio as well as the sum of H_2 and CO gas percentages are two important measures of syngas quality [38]. A syngas with a high percentage of CO + H_2 has strong reducing power, while a high value of the ratio H_2/CO indicates a syngas useful for chemical syntheses [38]. H_2/CO ratio higher than 1.70 should be presented in syngas to make it useful for the chemical industry to syntheses products such as methanol and virgin naphtha. Whereas such a ratio is easily obtained by gasifying methane, it is not possible by gasifying other wastes. Increase in H_2/CO ratio can only be accomplished by an injection of water [38].

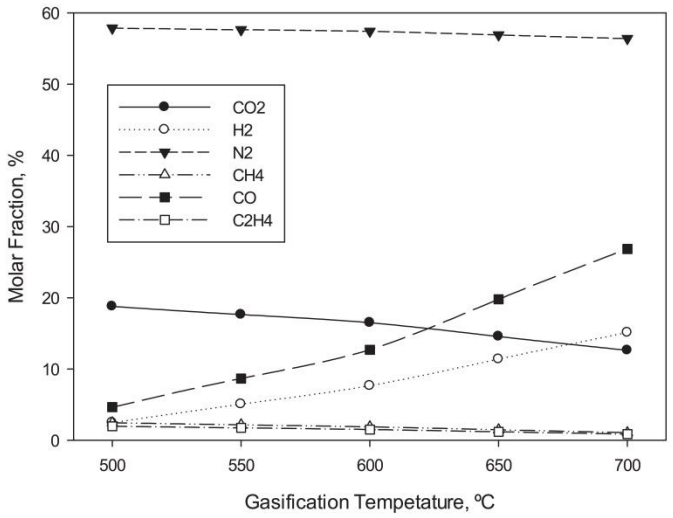

Fig. 6. Influence of gasification temperature on syngas molar fraction (operating conditions: MSW feed rate = 25 kg/h; Air flow rate = 40 kg/h).

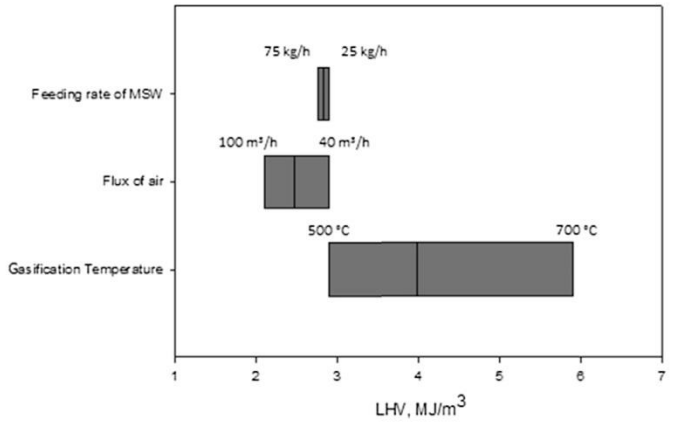

Fig. 7. Influence of operating conditions on syngas LHV (conditions from Table 5).

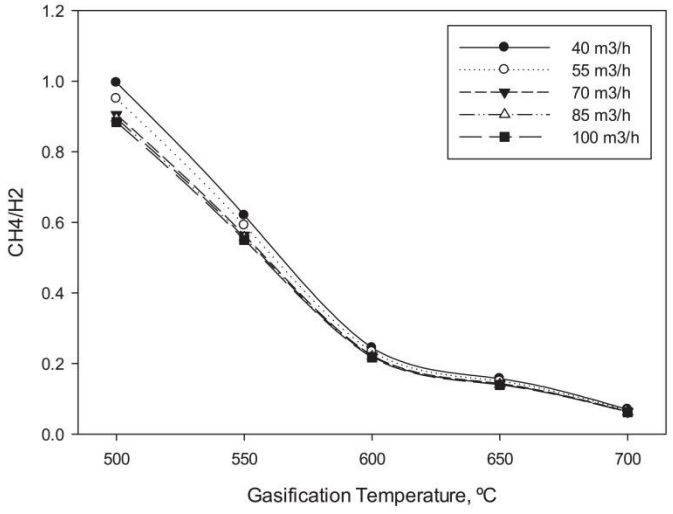

Fig. 8. Syngas CH_4/H_2 molar ratio as a function of the temperature and air flow rate (Runs 1 through 9).

Fig. 8 shows the influence of gasification temperature and ER on syngas CH_4/H_2 molar ratio using operating conditions from runs 1 through 9 in Table 5.

From Fig. 8 is clear that CH_4/H_2 ratio sharply decreases with gasification temperature. This can be easily explained referring that, according to Le Chatelier's principle, increasing temperature will promote higher levels of H_2. And on the other hand, due to the strengthening of the endothermic steam-methane reactions a decrease in CH_4 fraction is also expected. It is also clear that influence of gasification temperature diminishes with higher temperature simply because within the temperature range studied, decrease in CH_4 is somewhat constant while at higher temperature endoenergetic reactions will favor CO formation instead of H_2. This phenomenon will be further explained later in this section. Influence of ER on CH_4/H_2 ratio is very small since it decreases both species in the same way, although since H_2 fraction is much larger is easy to detect smaller changes than CH_4. Since MSW intake virtually has no impact on CH_4/H_2 ratio no graph is presented on the subject.

Fig. 9 shows the influence of gasification temperature, ER and MSW admission on syngas H_2/CO molar ratio. Fig. 9a uses operating conditions from runs 1 through 9 while Fig. 9b uses constant air flow (40 m^3/h) to study gasification temperature and MSW admission.

From analyses of Fig. 9 it can be seen that at low temperatures, gasification temperature has a positive influence on H_2/CO ratio but at higher temperatures the opposite trend occurs. This is due to the fact that at low temperatures H_2 production is enhanced by primary water–gas reaction as well as steam-methane reforming reactions while at higher temperatures primary water–gas as well as Boudouard reaction will favor more CO production. At the same

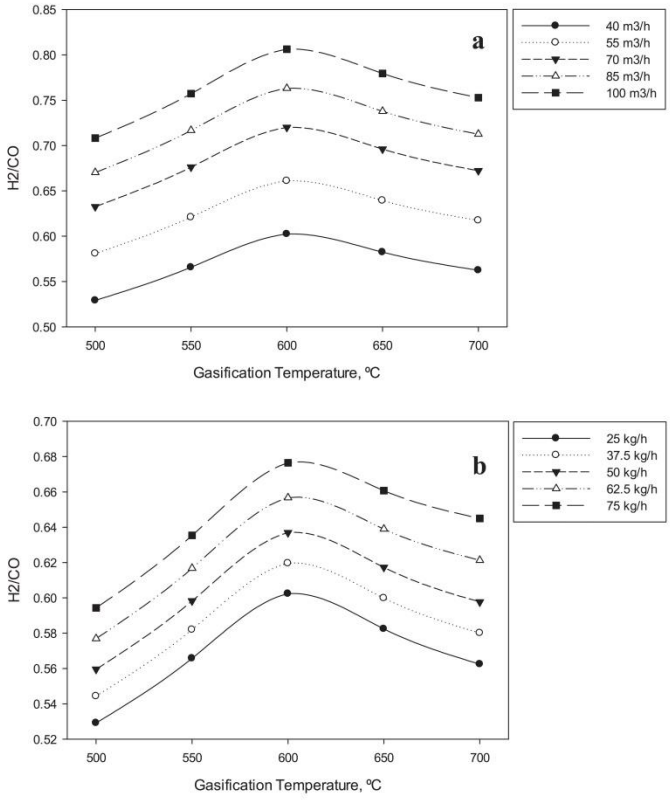

Fig. 9. a. Syngas H_2/CO molar ratio as a function of the temperature and air flow rate (Runs 1 through 9). b Syngas H_2/CO molar ratio as a function of the temperature and MSW admission (operating conditions: Air flow rate = 40 kg/h).

time, by reverse water–gas shift reaction, H_2 is actually converted to CO and a faster growth rate is observed in CO than H_2. This is consistent with [25].

A low ER ensures high syngas quality due to higher values of the combustible gases. Nevertheless, when the ER is too low, the gasification agent cannot supply enough oxygen to convert char into CO or CO_2. Like was previous mentioned, increase in ER favors the partial combustion of char, CO and H_2.

As was to be expected MSW admission has a positive effect on H_2/CO ratio simply because MSW admission barely has any effect on H_2 fraction while having a negative effect on CO, and therefore affecting positively the H_2/CO ratio.

Even though data regarding similar operating conditions as well as reactor dimensions are very limited in the literature results from both CH_4/H_2 and H_2/CO indices appear to follow the common trend among them [23,31,33].

Obviously results will always slightly diverge not only due to different gasifier geometries and operating conditions but, equally important, different MSW material properties.

To complete the study on syngas quality and the gasification performance it is necessary to study both CC (carbon conversion) as well as CGE (cold gas efficiency).

The carbon conversion defines the fraction of carbon from MSW converted to carbon in syngas composition. It gives an indication of the amount of unconverted material and provides a measure of chemical efficiency of the process. It can be given by:

$$Carbon\ Conversion = \frac{12 \times M}{X_c \times m} \tag{2}$$

where M is the total mole flow of carbon in the syngas components X_C is the carbon fraction in the MSW and m is the MSW flow into the gasifier.

CGE can be defined as the percentage of the heating value of MSW converted into the heating value of the product gas. It can be computed as follows:

$$CGE = \frac{Gas\ Yield \times HHV\ of\ product\ gas}{HHV\ of\ fuel + Heat\ addition} \tag{3}$$

Figs. 10 and 11 describe the influence of gasification temperature as well as ER on CC and CGE, respectively.

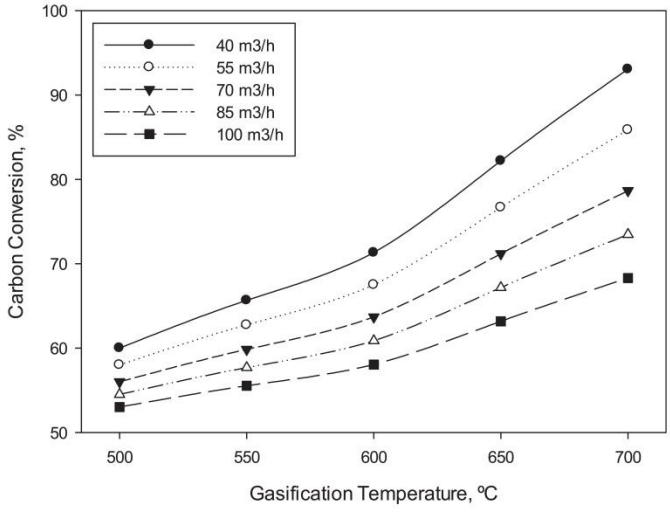

Fig. 10. Carbon conversion as a function of the temperature and air flow rate (operating conditions: Air flow rate = 40 kg/h).

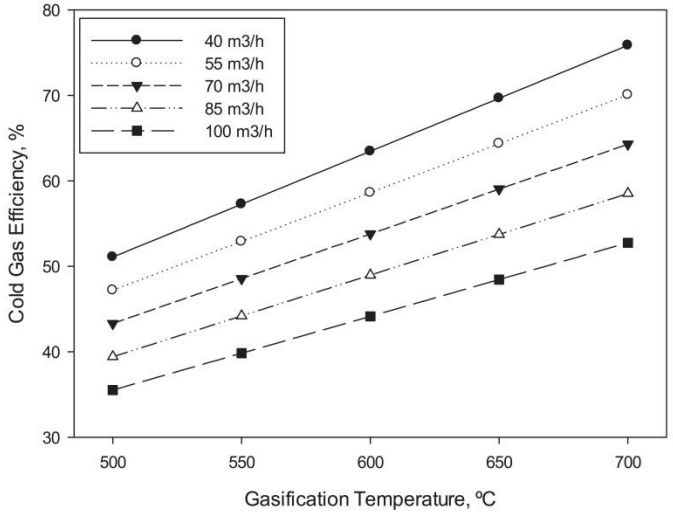

Fig. 11. Cold gas efficiency as a function of the temperature and air flow rate (operating conditions: Air flow rate = 40 kg/h).

According to Figs. 10 and 11, gasification temperature appears to have a positive effect on both carbon conversion and cold gas efficiency. Increase of CO and H_2 content with temperature can explain this trend. At lower temperatures the system efficiency as well as carbon conversion showed a relatively small growth with rising temperature, because of the sustained decrease in CH_4 molar fraction. This is consistent with [32,33].

Increase on ER has negative effects in both carbon conversion and cold gas efficiency. This has to do with higher levels of CO_2 being produced with ER. Also it is expected that CGE should decrease with ER since the combustible gases decrease with ER.

According to Arena U [39] the typical ranges of variation on process performance parameters in air or oxygen-enriched air gasification of municipal solid waste are: 90%–99% carbon conversion efficiency; 50–80% cold gas efficiency; 4–7 MJ/Nm^3 syngas low heating value. It can be noted that all the results presented so far fall within the range. Again, some minor discrepancies may be found but the errors can be assumed as very reasonable for such a complex system.

4.2. MSW gasification: possible applications

MSW as well as other biomass substrates can help to replace or at least diminish the use of fossil fuels. Not only does it have a LHV nearly as high as most of the conventional biomass feedstock but also has a pre-existing collection/transportation infrastructure that does not exist for conventional biomass resources [40].

Alongside LHV there are other gasification products that dictate the best use for a particular produced syngas. In Table 6 desirable syngas characteristics for the various options are summarized.

According to Table 6, as well as the results from sections 4 and 4.1, it can be seen that the optimal application for the syngas obtained from Lipor's MSW and the operating conditions chosen is synthetic fuels. In fact there is substantial work on the subject [41–43]. According to [44], a metric ton of USA MSW can produce up to 145 L of ultra clean diesel fuel or up to 165 L of ultra clean gasoline.

Materials of biological nature can help to replace natural gas and fuels made from fossil. This can be of great help to the reduction of greenhouse gas. By converting MSW (along with all the other organic matter) it is possible to eliminate the increase of carbon dioxide which would otherwise occur by burning fossil fuels.

Table 6
Desirable syngas characteristics for different applications [13].

Product		H_2/CO	Hydrocarbons	LHV	Temperature, °C
Synthetic Fuels		0.6	Low	Not important	300–400
Methanol		2	Low	Not important	100–200
Hydrogen		High	Low	Not important	100–200
Fuel Gas	Boiler	Not important	High	High	250
	Turbine	Not important	High	High	500–600

Generally, requirements for syngas characteristics for fuels and chemical synthesis applications are far more critical than for hydrogen and fuel gas applications. Syngas high low quantities of inerts such as N_2 can in fact be extremely beneficial for fuels and chemicals synthesis since it considerably reduces the size and cost of downstream equipment. Also higher temperatures can benefit production of fuels, chemical synthesis and hydrogen. In fact, at temperatures over 1200 °C little or no tar, methane, or higher hydrocarbons are formed, while syngas (H_2 and CO) production is maximized. If higher temperatures cannot be achieved inside the BFB gasifier, tar cracking might be required. Typically, though, this is not the case and therefore gas cleanup is somewhat minimal for synthesis applications [13].

Other operating parameters like gasification pressure as well the oxidant use can have a great degree of influence on the optimal syngas output. High pressures, over 20 bar, can be advantageous for fuel and chemical synthesis. On the other hand, air can have a detrimental effect to synthesis processes due to nitrogen diluting the product gas. Changing steam to oxygen ratio input can be used to adjust the H_2/CO ratio in order to match desirable syngas characteristics [13].

Even though guidelines from Table 6 can give a good indication on optimal syngas use, it should not be interpreted as strict requirements. Supporting process equipment such as scrubbers, compressors, coolers, etc. can be used to adjust the condition of the product syngas to match those optimal for the desired end-use [13].

To the best of our knowledge there are limited data regarding syngas quality indices for MSW. Also, data regarding syngas obtained from MSW using a pilot scale thermal gasification plant is very limited. The majority of the literature shows syngas compositions obtained in a laboratory or small-scale gasifier. These two factors combine make the results presented in this work very significant to MSW gasification in semi-industrial conditions.

5. Conclusions

In order to study MSW gasification a comprehensive two-dimensional model was developed in Fluent framework. An Eulerian–Eulerian approach was used to describe the transport of mass, momentum and energy for the solid and gas phases. CFD model included with a chemical model including homogeneous, heterogeneous and devolatilization reactions. Due to its importance in the MSW gasification a pyrolysis model was also incorporated. The model was validated using data collected from the literature and then expended to predict the process on a semi-industrial gasifier. Municipal solid waste from the North of Portugal was used in this study. First influence of gasification temperature, ER and MSW admission on syngas composition was studied. Variation of LHV within the range of the studied operating conditions was than investigated. It was seen that gasification temperature had the most influence on LHV levels. Influence of the same parameters on, not only hydrogen production as well as, syngas quality indices such as CH_4/H_2, H_2/CO, Carbon conversion and cold gas efficiency were studied. Obtained results were in agreement with what was found in the literature. Some minor discrepancies may be found but the errors can be assumed as very reasonable for such a complex system. According to syngas quality indices, optimal application for the syngas obtained from Lipor's MSW and the operating conditions chosen is fuels and chemical synthesis applications.

Acknowledgments

We would like to express our gratitude to the Portuguese Foundation for Science and Technology (FCT) for the support to the grant SFRH/BD/86068/2012.

References

[1] Commission of the European Community. The support of electricity from renewable energy sources. Brussels: Commission of the European Community; 2008.
[2] Sakai S, Sawell SE, Chandler AJ, Eighmy TT. World trends in municipal solid waste management. Waste Manage 1996;16(5–6):341–50.
[3] Teixeira S, Monteiro E, Silva V, Rouboa A. Prospective application of municipal solid wastes for energy production in Portugal. Energ Policy 2014;71:159–68.
[4] Belgiorno V, De Feo G, Della Rocca C, Napoli RMA. Energy from gasification of solid wastes. Waste Manage 2003;23:1–15.
[5] Bridgwater AV. The technical and economic feasibility of biomass gasification for power generation. Fuel 1995;14(5):631–53.
[6] Doyle TS, Dehouche Aravind PV, Liu M, Stankovic S. Investigating the impact and reaction pathway of toluene on a SOFC running on syngas. Int J Hydrogen Energy 2014;39(23):12083–91.
[7] Monteiro E, Sotton J, Bellenoue M, Moreira N, Malheiro S. Experimental study of syngas combustion at engine-like conditions in a rapid compression machine. Exp Therm Fluid Sci 2011;35:1473–9.
[8] Kwon E, Westby KJ, Castaldi MJ. An investigation into the syngas production from municipal solid waste (MSW) gasification under various pressures and CO_2-concentration atmospheres. In: Proceedings of the 17th Annual North American waste-to-energy conference; 2009. NAWTEC17.
[9] Palma C. Modelling of tar formation and evolution for biomass gasification: a review. Appl Energ 2013;111:129–41.
[10] Devi L, Ptasinski K, Janssen F. A review of the primary measures for tar elimination in biomass gasification processes. Biomass Bioenergy 2003;24:125–40.
[11] Alamo G, Hart A, Grimshaw A, Lundstrøm P. Characterization of syngas produced from MSW gasification at commercial-scale ENERGOS plants. Waste Manage 2012;32(10):1835–42.
[12] Pressley P, Aziz T, Carolis J, Barlaz M, He F, Li F, et al. Municipal solid waste conversion to transportation fuels: a life-cycle estimation of global warming potential and energy consumption. J Clean Prod 2014;70(1):145–53.
[13] Worley M, Yale J. Biomass gasification technology assessment, NREL consolidated report. NREL/SR-5100-57085. November 2012.
[14] Cornejo P, Farías O. Mathematical modeling of coal gasification in a fluidized bed reactor using an Eulerian granular description. Int J Chem React Eng 2011;9:1515–42.
[15] Silva V, Monteiro E, Couto N, Brito P, Rouboa A. Analysis of syngas quality from Portuguese biomasses: an experimental and numerical study. Energy Fuel 2014;28:5766–77.
[16] Onel O, Niziolek AM, Hasan MMF, Floudas CA. Municipal solid waste to liquid transportation fuels – part I: mathematical modeling of a municipal solid waste gasifier. Comput Chem Eng 2014;71:636–47.
[17] Couto N, Silva V, Monteiro E, Teixeira S, Chacartegui R, Bouziane K, et al. Numerical and experimental analysis of municipal solid wastes gasification process. Appl Therm Eng 2015;78:185–95.
[18] Magrinho A, Didelet F, Semião V. Municipal solid waste disposal in Portugal. Waste Manage 2006;26:1477–89.
[19] SUMA e Serviços Urbanos e Meio Ambiente, S.A, Caracterização dos RSU da Fracção Indiferenciada da LIPOR, 2012. Matosinhos.
[20] Scott D, Czernik S, Piskorz J, Radlein DSA. Fast pyrolysis of plastic wastes. Energy Fuel 1990;4:407–11.

[21] Xie J, Zhong W, Jin B, Shao Y, Liu H. Simulation on gasification of forestry residues in fluidized beds by Eulerian–Lagrangian approach. Bioresour Technol 2012;12:36–46.
[22] Couto N, Silva V, Monteiro E, Brito P, Rouboa A. Using an Eulerian-granular 2-D multiphase CFD model to simulate oxygen air enriched gasification of agroindustrial residues. Renew Energy 2015;77:174–81.
[23] Gang X, Bao-sheng J, Zhao-ping Z, Yong C, Ming-jiang NI, Ke-fa C, et al. Experimental study on MSW gasification and melting technology. J Environ Sci 2007;19:1398–403.
[24] Xue Q, Fox R. An Euler–Euler CFD model for biomass gasification in fluidized bed. In: NETL, conference on multiphase flow science. Morgantown, WV; May 22–24, 2012.
[25] Xiao J, Shen LH, Deng X, Wang ZM, Zhong XL. Study on characteristics of pressurized biomass gasification. Proc Chin Soc Electr Eng 2009;29(5):103–8.
[26] Turn S, Kinoshita C, Zhang Z, Ishimura D, Zhou J. An experimental investigation of hydrogen production from biomass gasification. Int J Hydrogen Energy 1998;23:641–8.
[27] Suzuki T, Takahashi M. Development of fluidized bed gasification and swirl-flow melting process for municipal solid waste. In: 2nd International conference on combustion, incineration/pyrolysis and emission control, Seoul, Korea, June 8–10; 2002. p. 1–10.
[28] Shohichi O, Morihiro O. Study on behavior of heavy metals in MSW direct melting process and utilization of melt solidified products. In: 2nd International conference on combustion, incineration/pyrolysis and emission control, Seoul, Korea, June 8–10; 2002. p. 134–42.
[29] Ming-jiang NI, Gang X, Yong C, Jian-hua Y, Qi M, Wen-li Z, et al. Study on pyrolysis and gasification of wood in MSW. J Environ Sci 2006;18(2):407–15.
[30] Gang X, Yong C, Ming-jiang NI, Qi M, Wen-li Z, Ke-fa C. Fluidized bed gasification of PE plastic in municipal solid waste. J Chem Ind Eng 2006;57(1):146–50.
[31] Niu M, Huang Y, Jin B, Wang X. Oxygen gasification of municipal solid waste in a Fixed-bed gasifier. Chin J Chem Eng 2014;22(9):1021–6.
[32] Niu M, Huang Y, Jin B, Wang X. Simulation of syngas production from municipal solid waste gasification in a bubbling fluidized bed using Aspen plus. Ind Eng Chem Res 2013;52:14768–75.
[33] Miao Q, Zhu J, Barghi S, Wu C, Yin X, Zhou Z. Modeling biomass gasification in circulating fluidized beds: model sensitivity analysis. Int J Energy Power 2013;2(3):57–63.
[34] Beaumont O, Schwob Y. Influence of physical and chemical parameters on wood pyrolysis. Ind Eng Chem Process Des Dev 1984;23:637–41.
[35] Gomez-Barea A, Leckner B. Modeling of biomass gasification in fluidized bed. Prog Energy Combust Sci 2010;36(4):444–509.
[36] Narvaez I, Orio A, Aznar MP, Corella J. Biomass gasification with air in an atmospheric bubbling fluidized bed. Effect of six operational variables on the quality of the produced raw gas. Ind Eng Chem Res 1996;35(7):2110–20.
[37] Abuadala A, Dincer I, Naterer GF. Exergy analysis of hydrogen production from biomass gasification. Int J Hydrogen Energy 2010;35:4981–90.
[38] Filippis P, Borgianni C, Paolucci M, Pochetti F. Prediction of syngas quality for two-stage gasification of selected waste feedstocks. Waste Manage 2004;24:633–9.
[39] Arena U, Gregorio F. Gasification of a solid recovered fuel in a pilot scale fluidized bed reactor. Fuel 2014;117:528–36.
[40] Hansson J, Leveau A, Hulteberg C. Biomass gasifier database for computer simulation purposes. Nordlight AB, Rapport SGC 234, ©Svenskt Gastekniskt Center. August 2011. http://www.sgc.se/ckfinder/userfiles/files/SGC234.pdf.
[41] Bhavya B, Singh R, Bhaskar T. Gasification for synthetic fuel production, fundamentals, processes applications, vol. 3; 2015. p. 57–71.
[42] Yang H, Chen H. Gasification for synthetic fuel production, fundamentals, processes and applications, vol. 11; 2015. p. 241–75.
[43] Speight JG. Gasification for synthetic fuel production, fundamentals, processes and applications, vol. 7; 2015. p. 277–301.
[44] http://www.ottusa.com/synthetic_fuel/synthetic_fuel.htm, last access, 15th April, 2015.

Paper XI

Numerical and Experimental Analysis of Municipal Solid Wastes Gasification Process

N. Couto, V. Silva, E. Monteiro, S. Teixeira, R. Chacartegui, K. Bouziane, P. Brito, A. Rouboa

Applied Thermal Engineering 78 (2015) 185-195

Applied Thermal Engineering 78 (2015) 185–195

Contents lists available at ScienceDirect

Applied Thermal Engineering

journal homepage: www.elsevier.com/locate/apthermeng

Research paper

Numerical and experimental analysis of municipal solid wastes gasification process

Nuno Couto [a, b], Valter Silva [a, b], Eliseu Monteiro [b, c], Sandra Teixeira [a], Ricardo Chacartegui [d], K. Bouziane [e], P.S.D. Brito [c], Abel Rouboa [a, b, f, *]

[a] University of Trás-os-Montes and Alto Douro, Vila Real, Portugal
[b] INEGI, Faculty of Engineering, University of Porto, Porto, Portugal
[c] C3i – Interdisciplinary Center for Research and Innovation, Polytechnic Institute of Portalegre, Lugar da Abadessa, Apartado 148, 7301-901 Portalegre, Portugal
[d] Energy Engineering Department, University of Seville, Seville, Spain
[e] Pôle EREP, Université Internationale de Rabat, 11000 Salé el Jadida, Technopolis, Morocco
[f] MEAM Department, University of Pennsylvania, Philadelphia, PA, USA

HIGHLIGHTS

- A multiphase 2-D model coupled with chemical reaction for MSW gasification.
- The numerical model is developed under the CFD Fluent framework.
- SYNGAS generation from biomass residues gasification is studied.
- Numerical and experimental (semi-industrial BFB gasifier) data are compared.

ARTICLE INFO

Article history:
Received 2 May 2014
Accepted 18 December 2014
Available online 27 December 2014

Keywords:
Gasification
Municipal solid wastes
CFD
Eulerian–Eulerian approach

ABSTRACT

As the quantity of municipal solid waste (MSW) increases with economic growth, problems arise in regard to sustainable management solutions. Thermal treatment presents a valid option for reducing the amounts of post-recycling waste to be landfilled. Incineration technology, besides reducing the total volume of waste and making use of the chemical energy in MSW for power generation, has negative environmental impact from high emission of pollutants. Recent policy to tackle climate change and resources conservation stimulated the development of renewable energy and landfill diversion technology, thereby giving gasification technology development renewed importance. In this work a two-dimensional CFD model for MSW gasification was developed and an Eulerian–Eulerian approach was used to describe the transport of mass, momentum and energy for the solid and gas phases. This model is validated using experimental data from the literature. The numerical results obtained are in good agreement with the reported experimental results.

1. Introduction

The amounts of municipal solid waste (MSW) produced increase with economic growth in both industrialised and developed countries, raising the issue of sustainable management solutions [1].

MSW management activities contribute to the generation of greenhouse gas and consequently to the climate change problem. Landfill waste decomposition contributes greatly to the formation of these gases [2–5]. Another environmental problem associated with MSW management systems is the potential generation of dioxins and furans associated to complete combustion of wastes [2].

Thermal treatments are a valid option for reducing the amounts of post-recycling waste to be landfilled, which is considered to be one of the most sanitary disposal methods [3].

It should be noted that biogas production is not an alternative to thermal treatments like incineration or gasification because biogas

* Corresponding author. MEAM Department, University of Pennsylvania, Philadelphia, PA, USA.
E-mail addresses: rouboa@seas.upenn.edu, rouboa@hotmail.com (A. Rouboa).

http://dx.doi.org/10.1016/j.applthermaleng.2014.12.036
1359-4311/

is produced from the organic fraction of MSW and thermal treatment is applied to the non-organic, non-recyclable fraction [4].

In theory, gasification is a more suitable technology even where the market for thermal product is difficult, however the constraint with gasification of MSW is the technology which is not yet proven at commercial scale [4].

Raw MSW contains a large amount of non-combustible material, and therefore requires pre-processing before sending it to a gasifier. The pre-processing must be able to meet the requirements of the gasifier and be flexible enough to handle MSW variability. This flexibility must be in terms of the type of material handled and its frequency of delivery. The pre-processing area is assumed to be similar to a Refuse Derived Fuel (RDF) facility. Some recyclables and non-combustibles are removed from the MSW to make a higher heating value product that is sized appropriately for gasification [5]. Therefore, incineration continues to be the most common method of thermal treatment for waste-to-energy facilities. However, with the enhancement of environmental restrictions and the development of gasification technology, gasification presents an increasingly efficient and viable alternative to incineration. Gasification is a waste-to-energy conversion scheme that offers a most attractive solution to both waste disposal and energy problems. However, gasification still has some economic and technical challenges, concerning the nature of the solid waste residues and its heterogeneity [4–6]. The greatest strength of gasification is the environmental performance, since emission tests indicate that gasification meets the existing limits and it can also have an important role in the reduction of landfill disposal [3].

Incineration reduces the initial volume of the waste by as much as 85% and offers solutions for problems such as waste odour and leachate. The incineration process creates a large amount of solid residues which are divided into bottom ash and fly ash. Bottom ash represents 85–90% of the total ash produced and is collected at the base of the combustion chamber. This type of ash consists primarily of coarse non-combustible material, unburned organic matter and grate siftings [7]. These are disposed of in sanitary landfills. Fly ash are finely divided particles of ash which are normally entrained in the combustion gases. Fly ash is recovered from the gas stream by a combination of precipitators and cyclones. Incineration technology was developed to reduce the total volume of waste and make use of the chemical energy of MSW for energy generation. However, the incineration process also creates high emissions of pollutant species such as NOx, SOx, HCl, as well as harmful organic compounds and heavy metals. Another problem with MSW incineration is corrosion of the incineration system by alkali metals in solid residues and fly ash [8].

Recent policies to tackle climate change and resource conservation such as the Kyoto Protocol, the deliberations at Copenhagen in 2009 and the Landfill Directive of the European Union have stimulated the development of renewable energy and landfill diversion technology, thereby giving the development gasification technology renewed importance [9].

Gasification is a thermochemical process that involves the oxidation of matter using a fraction of oxidizing agent in low quantities, inferior to the stoichiometric need. Gasification is considered an efficient and environmentally friendly way of extracting energy from different sources of organic materials [10]. Various studies [4,5,11–13] pointed out that gasification is an emerging but promising technology, especially when compared with commercially-available technologies, such as direct combustion. For instance, Murphy and McKeogh [4], Jones et al. [5] and Lymberopoulos [11], suggested that gasification has better performance, e.g. higher electrical and overall efficiency, lower emissions and lower investment costs than direct combustion. Boustouler and Reynolds [12] corroborates with Lymberopoulos [11] in this regard but also claimed that reduced slagging problems is another advantage of gasification. Roos [13] discussed in more details environmental benefits of biomass gasification, including (i) reduced carbon emissions as a result of improvement in energy efficiency and char addition to soils, (ii) reduced use of fertilizers and runoff of nutrients from soils amended with char-containing ash, and (iii) reduced NOx emissions due to better control of the combustion process.

The environmental performance is one of the greatest strengths of gasification technology, which is often considered a comprehensive response to the increasingly restrictive regulations applied around the world [4,9]. Independently-verified emissions tests indicate that gasification is able to meet existing emissions limits and can have a great effect on the reduction of landfill disposal option. Economic aspects are probably the crucial factor for a relevant market penetration, since gasification-based plants tends to have ranges of operating and capital costs about 10% higher than those of conventional combustion-based plants [9]. This is mainly a consequence of the ash melting system and the added complexity of the technology.

The technical challenges to overcome for a wider market penetration of commercial advanced gasification technologies can be investigated with the development of numerical simulation methods validated with experimental results of MSW gasification.

Gasification involves a set of fairly complex phenomena such as heat and mass transfer, fluid dynamics, and different chemical reactions. Numerous approaches to modelling gasification in CFD [14–19] and non-CFD [20–24] have been made. Currently there are three numerical techniques used for the studying gasification in fluidized beds in literature and these are Eulerian–Lagrangian with single particle or a particle parcel and a group of particles, Eulerian–Eulerian Two Fluid Model and Discrete Element Method within Eulerian–Lagrangian concept [14]. Literature concerning the numerical modelling of fluidized bed gasifier could be divided into three parts based on the geometric regions of fluidized bed furnace. It is dense bed, splash zone and freeboard/riser of fluidized bed units. Regarding dense bed most of studies are done with Eulerian–Eulerian Two Fluid Model approach [19]. Most of the literature in fluidized bed gasification is overlooking three-dimensional behaviours [14].

Cornejo and Farías [15] developed three-dimensional numerical model that describes the process of coal gasification in fluidized-bed reactors using an Eulerian–Eulerian approach. The main contribution of this work was implementing some sub-models within the FLUENT code in order to handle reactive fluidized-beds in complex geometries.

Xie et al. [16] developed a three-dimensional numerical model to simulate forestry residues gasification in a fluidized bed reactor using an Eulerian–Lagrangian approach. The model predicts product gas composition and carbon conversion efficiency in good agreement with experimental data.

Baliban et al. [17] proposed an approach for modelling of a biomass gasifier which is validated for lignocellulosic type of biomass with experimental data.

Onel et al. [18] presents a generic gasifier model towards the production of liquid fuels using municipal solid wastes. Using a nonlinear parameter estimation approach, the unknown gasification parameters are obtained to match the experimental gasification results. The results suggest that a generic MSW gasifier mathematical model can be obtained in which the average error is 8.75%.

Silva et al. [19] developed a two-dimensional Fluent based model to simulate the gasification of agro-industrial residues. The numerical simulation results were compared and validated versus a set of runs using three kind of biomass residues that were gasified

in a bubbling fluidized pilot scale unit. Their results are in good agreement with the experimental data obtained at three different operating conditions.

Thermodynamic equilibrium models are very useful tools to study the influence of most parameters for any biomass system because of their gasifier design independence. In general, the thermodynamic equilibrium models consider two approaches both giving the same results: the stoichiometric approach, which requires a clearly defined reaction mechanism that incorporates all chemical reactions and species involved, and the non-stoichiometric approach which is based on the system minimization of the Gibbs free energy [20]. Several equilibrium models have been used to predict syngas composition from different biomass substrates [20–24].

The aim of this paper is to analyse MSW gasification using a numerical method. A two-dimensional mathematical model was developed using an Eulerian–Eulerian approach to model the MSW gasification in a fluidized-bed reactor within Fluent [25]. The model takes detailed chemistry into account as homogeneous reactions for the gaseous phase and heterogeneous reactions to the solid phase, and also the modelling of heat and mass transfer and momentum. Pyrolysis is included considering a model with generation of secondary tar. The choice of a fluidized bed reactor is due to the fact that is widely used in industry for converting coal and there is a good understanding of pyrolysis and gasification in this kind of reactor. Fluidized beds are also capable of being scaled up to medium and large scale, overcoming limitations found in smaller scale, fixed-bed designs [26]. In order to validate the numerical results obtained in this work we refer to an experimental study on MSW gasification and melting technology conducted by Xiao et al. [27].

2. Materials and methods

2.1. Description of Portuguese waste management

The Portuguese MSW management system involves collection, storage, treatment and disposal as shown in Fig. 1.

There are two possible routes for wastes collection – the selected and unselected wastes collection. The selected collection includes ecopoints and door-to-door collection with ecocentres and biodegradable municipal waste collection. Ecopoints are devoted to separate collection based on the use of different containers for glass, paper/cardboard, and plastic/metal, placed together at ecopoints preferably located on public thoroughfares and strategic points. Ecocentres are sorting centres, where the selected wastes from the ecopoints are delivered for recovery. In addition to the materials referred to above as part of mechanical recycling, there are other specific fluxes of wastes (used oils, batteries, electrical and electronic wastes, construction and demolition residues, end-of-life vehicles and used cooking oil).

The unselected collection is devoted to the collection of raw MSW. Raw MSW contains a large amount of non-combustible material, and therefore requires pre-processing before sending it to a gasifier. This pre-processing is made in the so-called mechanical and biologic treatment (MBT) station, where the biodegradable waste and the recyclable wastes are separated reducing the amount of waste to landfill.

They must be able to meet the requirements of the gasifier and be flexible enough to handle MSW variability. This flexibility must be in terms of the type of material handled and its frequency of delivery.

This pre-processing area is assumed to be similar to a Refuse Derived Fuel (RDF) facility. Some recyclables and non-combustibles are removed from the MSW to make a higher heating value product.

Transfer stations provide the facilities required for unselected wastes when landfills or the mechanical biological treatment (MBT) station are far away. Therefore, unselected collection can be understood as the sum of landfill wastes with energetic and organic refuse.

MBT plants are designed to process mixed household wastes as well as commercial and industrial wastes. The MBT tolerates recycling paper, metal, plastic and glass. It can produce RDF or stabilize the biodegradable materials by composting or anaerobic digestion.

Biodegradable wastes can be converted into compost, carbon dioxide and water under an aerobic process. Composting is the common process for organic recovery of the wastes into soil conditioner. The remaining non-biodegradable wastes are recycled to recover materials for new products [28].

The RDF can be further used as alternative fuel in cement kilns or incinerated to produce energy. The ash formed during incineration contains mostly inorganic constituents of the wastes and is often landfilled [28].

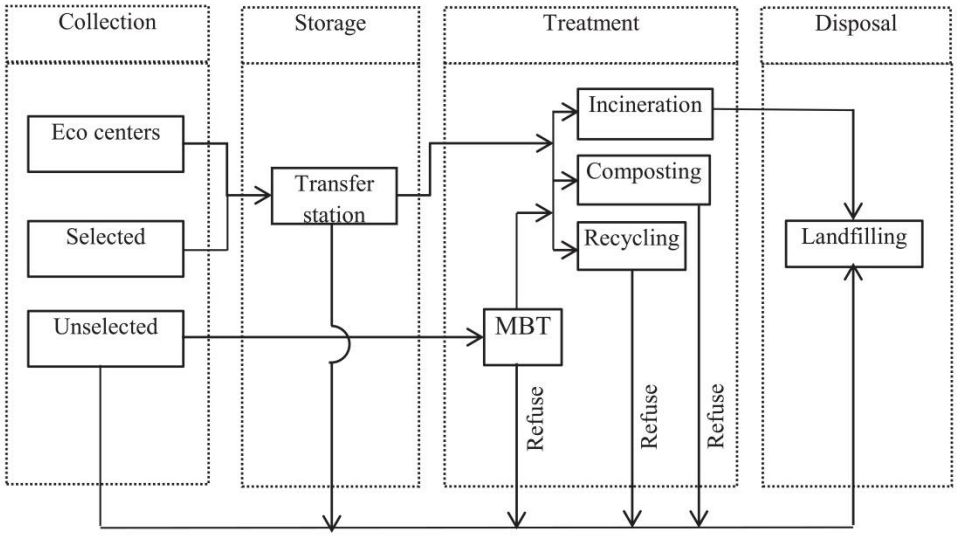

Fig. 1. Schematic overview of the Portuguese waste management system [3].

Wastes from unselected collection as well as waste coming from MBT, incineration plants, composting and recycling refuse are disposed of in landfills. Landfilling is the last treatment to be adopted because it causes severe environmental impact from greenhouse gases released into the atmosphere and also from leachate percolating into ground water. To help minimize the environmental impact, the biogas generated by anaerobic reactions can be used as fuel to produce heat and power [29].

2.2. Standard municipal solid waste characterization

MSW increases significantly in industrialized and developing countries, raising questions about sustainable municipal solid waste management. This results from the collection of waste in large urban areas, and comprises materials such as household waste, plastic, paper, glass, metals, and garden waste [30]. The composition of municipal solid waste depends on both the season and geographic location. The heterogeneous nature of the wastes affects the physical properties in terms of size, elemental composition, moisture content, heating value, ash content, volatile content and other contaminants. Therefore, the wastes are pre-treated accordingly to the Portuguese management system described previously.

Lipor is the entity responsible for the management, treatment and recovery of MSW in the Oporto metropolitan area. This includes eight municipalities in the Oporto metropolitan area and a production of about 500,000 tons/year of MSW by 984,047 inhabitants [31]. During the year 2012 Lipor carried out two sampling campaigns in the winter and in the summer. A criteria analysis of the waste collected was held, and the physical characterization by categories is shown in Table 1.

As an outcome of the pre-treatment defined previously results an RDF which contains cellulosic materials and plastics due to putrefied wastes, paper, wood wastes, and plastic residues. The remaining MSW components follow another route for valorization or elimination. It has been shown that the plastic residues are mainly composed of polyethylene, polystyrene, and poly-vinyl chloride [32] and the cellulosic materials are composed of cellulose, hemicelluloses, and lignin [17].

Given that the ultimate analyses of the Lipor does not distinguish the cellulosic materials, it was postulated that their composition was similar to the one found in Ref. [18], where the cellulosic material comprises cellulose, hemicellulose and lignin. Regarding the plastics group, Lipor report shows the relative quantities of each monomer in the MSW. Therefore, it was possible to take into account different monomers for the plastics group as shown in Table 2.

To enable the use of Fluent code to perform the numerical simulations a global chemical formula of the MSW is necessary.

Table 1
Physical characterization of the MSW [31].

Category	% Weight
Putrefied residues	44.34%
Paper	4.74%
Cardboard	2.61%
Composites	4.68%
Textiles	5.73%
Sanitary textiles	1.20%
Plastics	10.98%
Combustive non specified	0.09%
Glass	4.29%
Metals	2.15%
Non-combustive non specified	0.41%
Hazardous residues	0.06%
Fine elements	8.72%

Table 2
Chemical composition of the MSW.

Category	% Weight	Chemical formula
Cellulosic material	85.22%	[a]
Polyethylene	11.14%	$(C_2H_4)_n$
Polyethylene terephthalate	2.05%	$(C_{10}H_8O)_n$
Polypropylene	0.82%	$(C_3H_6)_n$
Polystyrene	0.77%	$(C_8H_8)_n$

[a] It was considered the proportion of cellulose, hemicellulose and lignin found in Ref. [18].

This calculation was performed based on the chemical characterization of waste shown in Table 2. The fractions of carbon (C), hydrogen (H) and oxygen (O) are found by ultimate analysis of the mixture. The total carbon was the sum of the carbon in all the hydrocarbons. The same procedure is made for the calculation of the total hydrogen and total oxygen. This calculation is performed by dividing the values found in the ultimate analysis of each chemical element by the value of the reference element carbon (C).

3. Mathematical model

The purpose of this section is to develop a modelling approach able to predict the final composition of the syngas resulting from gasification using numerical simulation. The improved state-of-the art CFD models enable the design and optimization of the gasification processes [33]. The numerical simulation was performed using the CFD solver Fluent based on finite volume method. The gasification was modelled using Fluent data base for a two-dimensional model and multi-phase (gas and solid) model. The solid phase was treated as an Eulerian granular model while the gas phase is considered as continua. The main interaction between the phases is also modelled, heat exchange by convection, mass (the heterogeneous chemical reactions), and momentum (the drag in gas and solid phase). In the next section the governing equations will be described.

3.1. Energy conservation

The energy conservation equation for both phases (gas and solid) is as follows [34]:

$$\frac{\partial(\alpha_q\rho_q h_q)}{\partial t}+\nabla\cdot(\alpha_q\rho_q\vec{u}_q h_q)=-\alpha_q\frac{\partial(p_q)}{\partial t}+\bar{\tau}_q:\nabla(\vec{u}_q)-\nabla\cdot\vec{q}_q+S_q+\sum_{p=1}^{n}\left(\vec{Q}_{pq}+\dot{m}_{pq}h_{pq}-\dot{m}_{pq}h_{pq}\right) \quad (1)$$

where $\vec{Q}_{pq}$ is the heat transfer intensity between fluid phase pth and solid phase qth, h_q the specific enthalpy of phase qth, $\vec{q}_q$ the heat flux, S_q is a source term due to chemical reactions and h_{pq} the enthalpy of the interface.

Equation (2) [35] describes the rate of energy transfer as a function of the temperature difference between the phases; where the heat transfer coefficient between the phases

$$Q_{pq}=h_{pq}(T_p-T_q) \quad (2)$$

pth and qth is given by h_{pq}.

The heat transfer coefficient is associated to the Nusselt number of solid phase qth, and k_p is the thermal conductivity for phase pth [33]:

$$h_{pq} = \frac{6k_p\alpha_q\alpha_p Nu_q}{d_p^2} \tag{3}$$

Nusselt number is correlated by [35]:

$$Nu_q = \left(7 - 10\alpha_g + 5\alpha_g^2\right)\left(1 + 0.7\mathrm{Re}_s^{0.2}\mathrm{Pr}_g^{0.33}\right) + \left(1.33 - 2.4\alpha_g + 1.2\alpha_g^2\right)\mathrm{Re}_s^{0.7}\mathrm{Pr}_g^{0.33} \tag{4}$$

where Re_s is the Reynolds number based on the diameter of the solid phase and the relative velocity, Pr_g is the Prandtl number of the gas phase.

3.2. Momentum model

The gas and solid phase momentum equations are as follow: Equation (5) refers to solid phase momentum equation, t_s are the particle phase stress tensor and P_s is the particle phase pressure due to particle collisions. The equation (6) represents the gas phase momentum equation, were β is the gas–solid interphase drag coefficient, τ_g the gas phase stress tensor and U_s the mean velocity of solid [34].

$$\frac{\partial}{\partial t}(\alpha_s\rho_s v_s) + \nabla\cdot(\alpha_s\rho_s v_s v_s) = -\alpha_s\nabla p_s + \alpha\rho_s g + \beta(v_g - v_s) + \nabla\cdot\alpha_s\tau_s + S_{sg}U_s \tag{5}$$

$$\frac{\partial}{\partial t}(\alpha_g\rho_g v_g) + \nabla\cdot(\alpha_g\rho_g v_g v_g) = -\alpha_g\nabla p_g + \alpha\rho_g g + \beta(v_g - v_s) + \nabla\cdot\alpha_g\tau_g + S_{gs}U_s \tag{6}$$

3.3. Mass balance model

The biomass feed changes from solid phase into gas phase by reacting with oxygen, steam and carbon dioxide. The continuity equations for solid and gas phases are given by the equations (7) and (8), respectively [34].

$$\frac{\partial}{\partial t}(\alpha_s\rho_s) + \nabla\cdot(\alpha_s\rho_s v_s) = S_{sg} \tag{7}$$

$$\frac{\partial}{\partial t}(\alpha_g\rho_g) + \nabla\cdot(\alpha_g\rho_g v_g) = S_{gs} \tag{8}$$

where v is the instantaneous velocity of gas/solid phase, ρ the density and α the volume fraction, the subscripts s denotes the solid phase and subscripts g the gas phase. The mass source term due to heterogeneous reaction, S is expressed by the following equation:

$$S_{sg} = -S_{gs} = M_c\sum\gamma_c R_c \tag{9}$$

In which R_c is the reaction rate, γ_c the stoichiometric coefficient and M_c the molecular weight. The solid phase density was assumed to be constant. The gas phase density was calculated on the basis of ideal gas equation:

$$\frac{1}{\rho_g} = \frac{RT}{p}\sum_{i=1}^{n}\frac{Y_i}{M_i} \tag{10}$$

where R is the universal gas constant, T the temperature of the gas mixture, p the gas pressure, Y_i the mass fraction and M_i the molecular weight of each the species.

3.4. Turbulence model

A Fluent standard k-ε model was chosen for the turbulence model, as this is the most appropriate model when turbulence transfer between phases plays an important role in gasification in fluidized beds. k is the turbulence kinetic energy and ε is the dissipation rate. They are determined by the next transport equations [36]:

$$\frac{\partial}{\partial t}(\rho k) + \frac{\partial}{\partial x_i}(\rho k u_i) = \frac{\partial}{\partial x_j}\left[\left(\mu + \frac{\mu_t}{\sigma_k}\right)\right] + G_k + G_b - \rho\varepsilon - Y_M + S_k \tag{11}$$

$$\frac{\partial}{\partial t}(\rho\varepsilon) + \frac{\partial}{\partial x_i}(\rho\varepsilon u_i) = \frac{\partial}{\partial x_j}\left[\left(\mu + \frac{\mu_t}{\sigma_\varepsilon}\right)\frac{\partial\varepsilon}{\partial x_j}\right] + C_{1\varepsilon}\frac{\varepsilon}{k}(G_k + C_{3\varepsilon}G_b) - C_{2\varepsilon}\rho\frac{\varepsilon^2}{k} + S_\varepsilon \tag{12}$$

From Eq. (11) G_k is the generation of turbulence kinetic energy due to the mean velocity gradients, G_b the generation of turbulence kinetic energy due to buoyancy, and Y_M the contribution of the fluctuating dilatation in compressible turbulence to the overall dissipation rate. In the Eq. (12) $G_k = 1.0$ and $G_\varepsilon = 1.3$ are the turbulent Prandtl numbers for k and ε, respectively, S_k and S_ε are user-defined source terms. $C_{1\varepsilon} = 1.44$, $C_{2\varepsilon} = 1.92$, and $C_{3\varepsilon} = 0$ are constants suggested by Launder and Spalding [35].

3.5. Granular Eulerian model

Granular Eulerian model is described by the following conservation equation for the granular temperature [37]:

$$\frac{3}{2}\left[\left(\frac{\partial(\rho_s\alpha_s\Theta_s)}{\partial t} + \nabla\cdot(\rho_s\alpha_s\vec{v}_s\Theta_s)\right)\right] = \left(-P_s\bar{\bar{I}} + \bar{\bar{\tau}}_s\right):\nabla(\vec{v}_s) + \nabla\cdot(k_{\Theta a}\nabla(\Theta_s)) - \gamma_{\Theta a} + \phi_{ls} \tag{13}$$

This equation is obtained from the kinetic theory of gases. The term $(-P_s\bar{\bar{I}} + \bar{\bar{\tau}}_s):\nabla(\vec{v}_s)$ describes the generation of energy by the solid stress tensor, ϕ_{ls} is the energy exchange between the fluid phase and the solid phase, $\gamma_{\Theta a}$ the collisional dissipation of energy and $k_{\Theta a}\nabla(\Theta_s)$ the diffusion energy ($k_{\Theta a}$ is the diffusion coefficient).

The stress in the granular solid phase is achieved by relating the random particle motion and the thermal motion of molecules within a gas accounting for the inelasticity of solid particles. In a gas the intensity of velocity fluctuation determines the stresses, viscosity and pressure of granular phase.

3.6. Chemical reactions model

The chemical reaction rate coefficients are based on the Arrhenius law. Actually, they are empirical and determined by fitting the experimental data. During the devolatilization and cracking water shift reaction will occur, the gas species react with the supplied oxidizer and among them. The most common homogenous gas-phase reactions are [38]:

$$CO + 0.5\,O_2 \rightarrow CO_2 + 283\ \mathrm{kJ/mol} \tag{14}$$

$$CO + H_2O \rightarrow CO_2 + H_2 + 41.1\ \mathrm{kJ/mol} \tag{15}$$

$$CO + 3H_2 \leftrightarrow CH_4 + H_2O + 206.1\ \mathrm{kJ/mol} \tag{16}$$

$$H_2 + 0.5\,O_2 \rightarrow H_2O + 242\ \text{kJ/mol} \quad (17)$$

$$CH_4 + 2O_2 \rightarrow CO_2 + 2H_2O + 35.7\ \text{kJ/mol} \quad (18)$$

The Arrhenius rates for each one of these reactions can be expressed as follows, respectively [39,40]:

$$r_{CO\_Combustion} = 1.0 \times 10^{15} \exp\left(\frac{-16000}{T}\right) C_{CO} C_{O_2}^{0.5} \quad (19)$$

$$r_{H_2\ Combustion} = 5.159 \times 10^{15} \exp\left(\frac{-3430}{T}\right) T^{-1.5} C_{O_2} C_{H_2}^{1.5} \quad (20)$$

$$r_{CH_4\ Combustion} = 3.552 \times 10^{14} \exp\left(\frac{-15700}{T}\right) T^{-1} C_{O_2} C_{CH_4} \quad (21)$$

$$r_{water.gas.shift} = 2780 \exp\left(\frac{-1510}{T}\right)\left[C_{CO} C_{H_2O} - \frac{C_{CO_2} C_{H_2}}{0.0265 \exp\left(\frac{3968}{T}\right)}\right] \quad (22)$$

The Eddy dissipation reaction rate can be expressed using the following equation [25]:

$$r_{Eddy-dissipation} = \alpha_{i,r} M_{w,i} A \rho \frac{\varepsilon}{k} min\left(min_R\left(\frac{Y_R}{\alpha_{R,r} M_{w,R}}\right), B \frac{\sum_p y_p}{\sum_i^N \alpha_{i,R} M_{w,i}}\right) \quad (23)$$

The minimum value of these two contributions can be defined as the net reaction rate.

The heterogeneous reactions of char (the solid devolatilization residue) with the species O_2 and H_2O are very complex processes. They demand a mass diffusion balance of the oxidizing species at the surface of the biomass particle with the surface reactions of those species with the char. The composition and the temperature of the gases, as well as the temperature, size and porosity of the particle are important to determining the overall rate of the char.

The most used overall simplified heterogeneous reactions are [38]:

$$C + 0.5O_2 \rightarrow CO + 110.5\ \text{kJ/mol} \quad (24)$$

$$C + CO_2 \rightarrow 2CO - 172.4\ \text{kJ/mol} \quad (25)$$

$$C + H_2O \rightarrow CO + H_2 - 131.3\ \text{kJ/mol} \quad (26)$$

The heterogeneous reactions are influenced by many factors, namely, reactant diffusion, breaking up of char, interaction of reactions and turbulence flow. In order to include both diffusion and kinetic effects the Kinetic/Diffusion Surface Reaction Model [41] was applied. This model weights the effect of the Arrhenius rate and the diffusion rate of the oxidant at the surface particle. The diffusion rate coefficient can be defined as [25]:

$$D_0 = C_1 \frac{\left[(T_p + T_\infty) \div 2\right]^{0.75}}{d_p} \quad (27)$$

The Arrhenius rate can be defined as follows:

$$r_{Arrehnius} = A_e - \left(\frac{E}{RT_p}\right) \quad (28)$$

The final reaction rate weights both contributions and is defined as follows [25]:

$$\frac{d_{m_p}}{d_t} = -A_p \frac{\rho R T_\infty Z_{ox}}{M_{w,ox}} \frac{D_0 r_{Arrehnius}}{D_0 + r_{Arrehnius}} \quad (29)$$

This model was included in the CFD framework by using the User Defined Function tool.

3.6.1. Pyrolysis

Both homogeneous and heterogeneous reactions are preceded from pyrolysis reactions. Modelling pyrolysis is crucial for MSW gasification purposes.

MSW is thermal decomposed into volatiles, char and tar. There are several approaches to describe this phenomenon and 3 main approaches are usually followed: a single step pyrolysis model, competing parallel pyrolysis and a pyrolysis model with generation of secondary tar.

In this model we adopt a pyrolysis model with generation of secondary tar. The MSW is mainly composed by cellulosic and plastic components, where the cellulosic material can be divided in cellulose, hemicellulose and lignin [17,18] and the plastics are mainly comprised by polyethylene, polystyrene, and polypropylene, among others.

To distinguish the several components that comprise the MSW, the pyrolysis reactions of cellulosic and plastic groups are considered individually and following an Arrhenius kinetic expression.

The primary pyrolysis equations can be defined as follows:

$$Cellulose \xrightarrow{r1} \alpha_1\ volatiles + \alpha_2\ Tar + \alpha_3\ Char \quad (30)$$

$$Hemicellulose \xrightarrow{r2} \alpha_4\ volatiles + \alpha_5\ Tar + \alpha_6\ Char \quad (31)$$

$$Lignin \xrightarrow{r3} \alpha_7\ volatiles + \alpha_8\ Tar + \alpha_9\ Char \quad (32)$$

$$Plastics \xrightarrow{r4} \alpha_{10}\ volatiles + \alpha_{11}\ Tar + \alpha_{12}\ Char \quad (33)$$

The kinetics for the cellulosic material can be given as follows:

$$r_i = \frac{da_i}{dt} = A_i \exp\left(\frac{-E_i}{T_s}\right)(1 - a_i)^n \quad (34)$$

Where i stands for cellulose, hemicellulose and lignin (r_{1-3}), A_i is the pre-exponential factor, E_i is the activation energy and n is the order reaction. The values for each one of these parameters can be found in Ref. [42]. Average values were considered.

Regarding the kinetic reactions for plastics, data was obtained from Ref. [43] by using the following reactions:

$$r_4 = \left[\sum_{i=1}^{n} A_i \exp\left(\frac{-E_i}{RT}\right)\right] \rho_v \quad (35)$$

where A_i, E_i and ρ_v are the pre-exponential factor, the activation energy and the volatiles density, respectively, and can be found in Ref. [43]. i stands for each one of the plastics that comprise the analysed MSW along this paper.

In this model, it is considered a secondary pyrolysis where is generated volatiles and secondary tar, as follows:

$$Primary\ Tar \xrightarrow{r5} volatiles + Secondary\ Tar$$

Because, this secondary pyrolysis is also very difficult to treat, a simplified global reaction is used [44]:

$$r_5 = 9.55 \times 10^4 \exp\left(\frac{-1.12 \times 10^4}{T_g}\right) \rho_{Tar1} \quad (36)$$

3.7. Numerical procedure

The simulations were performed in an up-flow atmospheric fluidized bed gasifier. This fluidized bed reactor is a tubular reactor of 0.5 m in diameter and 4.15 m of height, internally coated with ceramic refractory materials; MSW enters the reactor at the height of 0.5 m, from its base, and preheated air at 600 K enters the reactor coming from the base through a set of diffusers, warranting a flow of about 70 m^3/h. The schematics of the fluidized reactor are depicted in Fig. 2 and the bed is made of 70 kg of dolomite.

The problem under consideration is solved by using a finite volume method based CFD solver FLUENT. The unstructured quadrilateral cells of non-uniform grid spacing are generated using GAMBIT. The grid is chosen to be sufficiently fine to capture the steep gradients in the vicinity of the cylinder. The second order upwind scheme is used to discretize the convective terms in the momentum and energy equations. The SIMPLE scheme is used for solving the pressure–velocity coupling. The system of algebraic equations is solved using the Gauss–Siedel point-by-point iterative method in conjunction with the algebraic multi-grid method solver. Relative convergence criterion for residuals of 10^{-8} was prescribed in this work.

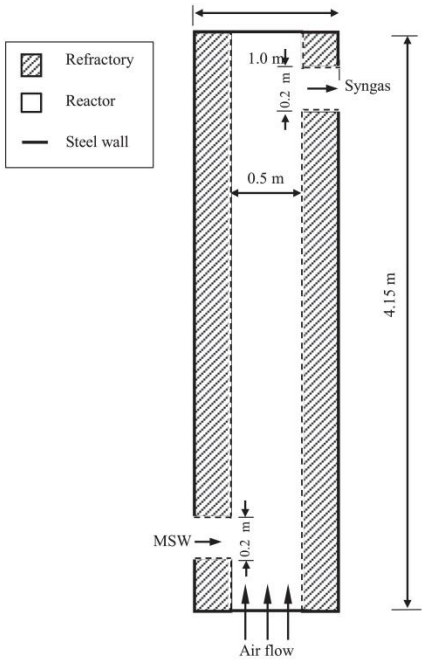

Fig. 2. Gasifier geometry.

Table 3
Xiao et al. [27] MSW characteristics.

Organic compounds (%)					Low heating value (kJ/kg)
Kitchen garbage	Plastic	Wood and yard waste	Paper	Textile	
61	20	10	8	1	17,960

4. Results and discussion

Despite having sparse data about municipal solid waste gasification in semi-industrial or industrial facilities, experimental data about MSW gasification in China was gathered from the literature [27]. Based on the characteristics of MSW from China, raw materials were prepared according to the average proportion of organic components (dry basis) for gasification, as displayed in Table 3.

In order to perform simulations with the Xiao MSW composition [27] using Fluent code, a global chemical formula is needed. Using the same procedure that was used and described for Lipor MSW and assuming that kitchen garbage, wood and yard waste, paper and textile, are assumed to be cellulosic materials, and the plastics materials with the same relative composition of the Lipor MSW, the global chemical formula is obtained.

4.1. Model validation

In order to validate the mathematical model proposed previously, numerical simulations were carried out using the Xiao MSW. The results obtained numerically were compared with the experimental results of Xiao et al. [27]. The results of run 1 are shown in Fig. 3 for the gasification conditions defined in Table 4. Relative errors between numerical and experimental results are depicted in Table 5. The relative error is computed as follows:

$$Relative\ error\,(\%) = \frac{(numerical\ value - experimental\ value)}{experimental\ value} \times 100\% \quad (37)$$

The model estimates reasonably all the species in a large spectrum of operating conditions. The largest errors are found for species at minor molar fractions. Despite these numerical results being within the range of values of the experimental results, there

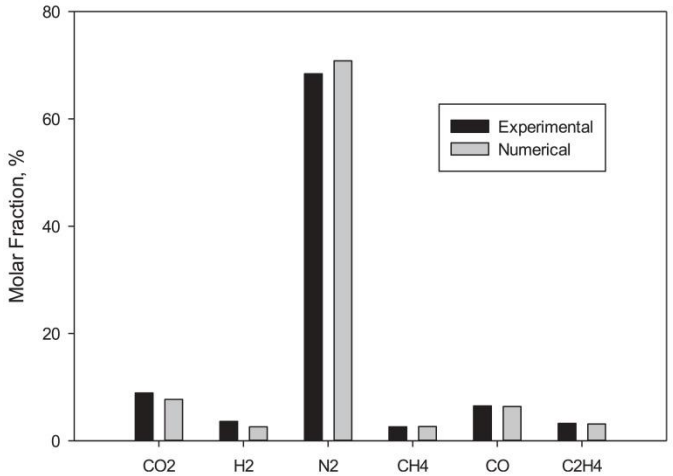

Fig. 3. Comparison of the CFD and experimental results for run 1 as defined in Table 4.

Table 4
Experimental gasification conditions used for the model validation.

Gasification run	Feeding rate of MSW (kg/h)	Flux of air (m^3/h)	Temperature of gasification (°C)	Temperature of preheated air (°C)
1	2.3	6	720	352
2			620	283
3			493	290
4	3	6	705	352
5			602	296
6			507	281
7	4	6	687	352
8			593	307
9			516	282
10	6	6	691	352
11			593	308
12			507	279

Table 5
Relative error of the several syngas species along the 12 gasification runs.

Gasification run	Relative error according to equation (37) (%)					
	CO_2	H_2	N_2	CH_4	CO	C_2H_4
1	−13.37	−27.50	3.54	1.92	−1.69	−3.70
2	1.88	−26.00	7.18	−27.14	−8.03	15.38
3	9.37	−8.57	3.32	−37.50	−6.04	10.81
4	3.95	7.86	6.88	11.84	3.60	9.25
5	4.14	−1.60	1.95	−14.44	−9.13	43.98
6	−6.08	8.00	1.62	−20.00	4.60	12.66
7	8.97	6.90	2.51	16.52	6.92	−8.12
8	4.04	9.63	2.07	−14.67	−5.33	0.92
9	3.62	27.27	2.54	−36.25	−3.40	43.56
10	4.17	−7.41	4.18	1.75	2.94	8.89
11	−1.29	−16.67	4.64	10.00	6.17	8.75
12	5.07	9.76	−3.41	13.89	6.42	29.63

are still a few deviations which are justified by some simplifications performed, such as: i) The lack of data on the characteristics of waste has led to the use of constants of other biomasses which may differ from the actual one, ii) The kinetic constants were taken from the literature and can differ greatly from source to source.

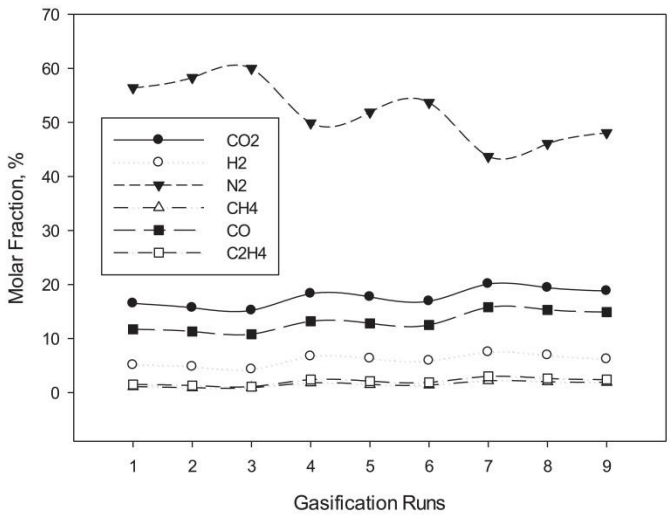

Fig. 4. CFD molar fractions of the Lipor MSW for 9 gasification conditions defined in Table 6.

Table 6
Gasification conditions for the Lipor MSW.

Gasification run	Feeding rate of MSW (kg/h)	Flux of air (m^3/h)
1	25	40
2		70
3		100
4	50	40
5		70
6		100
7	75	40
8		70
9		100

4.2. Results of Lipor MSW gasification

After validating the numerical model, numerical simulations were carried out and the results obtained for syngas gasification of Lipor's MSW are shown in Fig. 4 for the gasification conditions defined in Table 6.

These results are within the range of literature results [45,46].

Fig. 5 shows the contours of the H_2, CH_4, CO_2, and CO mole fractions in the gas mixture.

The highest values for CO_2 are located at the syngas outlet, which is consistent with the results of Qingluan and Rodney [45] and Oevermann et al. [46]. CO shows the opposite trend.

For CH_4 its higher value is found immediately above the biomass inlet, where the reduction phase takes place and these gases are formed, which is consistent with the results of Qingluan and Rodney [45].

The values of N_2 are not shown because are closely constant throughout the gasifier due to the unreacted characteristics of this gas, besides its possible combination with oxygen at high temperatures. This behaviour is also consistent with the results of Qingluan and Rodney [45].

The MSW collected by Lipor is representative of a population of 984,047 inhabitants, for a total of 500,000 tonnes of urban solid waste per year. Based on the numerical results of the gasification, it is possible to compute the production of 7.8×10^8 m^3 of syngas during a year based on 500,000 tons of MSW.

This is a very interesting factor for Lipor incineration of waste. Lipor consumes about 20,000 m^3 of natural gas per year to spray the waste before entry into the combustion chamber. Therefore, it could be advantageous for Lipor to consider replacing this natural gas with syngas resulting from municipal solid waste gasification.

5. Conclusion

In this work, we have modelled gasification as an alternative incineration process for energy recovery from MSW. A two-dimensional mathematical model was developed using the fluent code. An Eulerian–Eulerian approach was used to describe the transport of mass, momentum and energy for the solid and gas phases. The model was tested using gasification experimental data from the literature. The model reproduces the key features of municipal solid waste gasification. The numerical results achieved show reasonable agreement with the experimental results, with some deviations. Numerical simulations were made for the study of gasification of municipal solid waste from the North of Portugal, carried out particularly by Lipor, the entity responsible for the MSW management system in the Porto metropolitan area. These results agree partially well with the experimental data. The very heterogeneous nature of the MSW and the consequent variance of the properties such as elemental composition, density, water content, and structure leads to uncertainties in the modelling of MSW

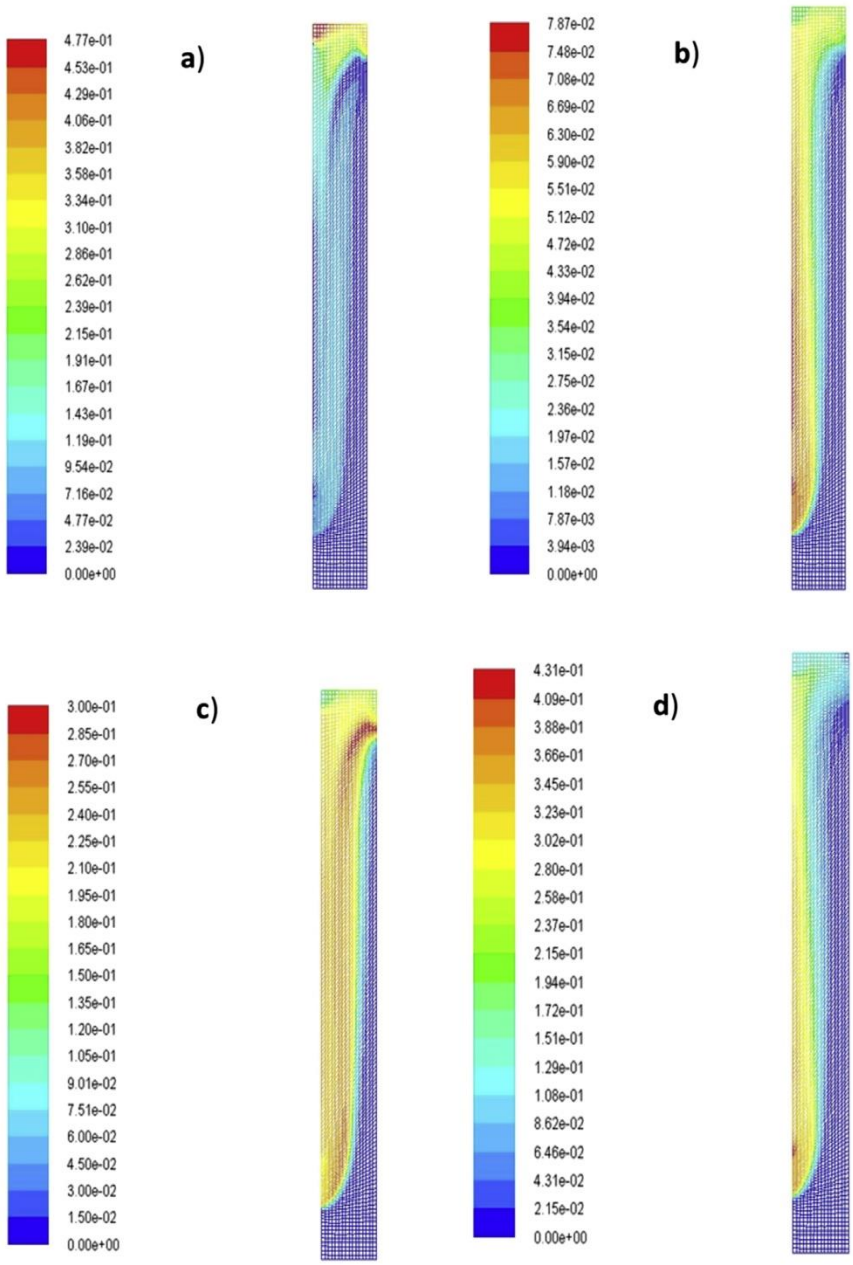

Fig. 5. Mole fraction contours for: (a) H_2, (b) CH_4, (c) CO_2, (d) CO.

gasification, and should be kept in mind when comparing the numerical results whit the experimental results.

For Lipor it would be interesting to consider using a gasification unit instead of the incineration. The associated production of syngas was estimated to be around 7.8×10^8 m^3/year. However, a study of economic viability must be carried out, as well as optimization of the gasification process where the numerical simulation can give a valuable assistance.

Acknowledgements

We would like to express our gratitude to LIPOR (Serviço Intermunicipalizado de Gestão de Resíduos do Grande Porto) for their financial support and to the Portuguese Foundation for Science and Technology (FCT) for the given support to the grant SFRH/BPD/71686 and to the project PTDC/AAC-AMB/103119/2008.

References

[1] I.S. Antonopoulos, A. Karagiannidis, L. Elefsiniotis, G. Perkoulidis, A. Gkouletsos, Development of an innovative 3-stage steady-bed gasifier for municipal solid waste and biomass, Fuel Proc. Technol. 92 (2011) 2389–2396.

[2] A. Smith, K. Brown, S. Ogilvie, K. Rushton, J. Bales, Waste Management Option and Climate Change, European Communities, Final report to the European Commission, DG Environment, Luxembourg, 2001.

[3] P. Sousa, A. Soares, E. Monteiro, A. Rouboa, Prospective application of municipal solid wastes for energy production in Portugal, Energy Policy 71 (2014) 159–168.

[4] J.D. Murphy, E. McKeogh, Technical, economic and environmental analysis of energy production from municipal solid waste, Renew. Energy 29 (2004) 1043–1057.

[5] S.B. Jones, Y. Zhu, C. Valkenburg, Municipal Solid Waste (MSW) to Liquid Fuels Synthesis, in: A Techno-economic Evaluation of the Production of Mixed Alcohols, vol. 2, Pacific Northwest National Laboratory, Richland, WA, 2009.

[6] Mohammad Asadullah, Barriers of commercial power generation using biomass gasification gas: a review, Renew. Sust. Energy Rev. 29 (2014) 201–215.

[7] A. Karagiannidis, St Kontogianni, D. Logothetis, Classification and categorization of treatment methods for ash generated by municipal solid waste incineration: a case for the 2 greater metropolitan regions of Greece, Waste Manage. 33 (2013) 363–372.

[8] Qinglin Zhang, Liran Dor, Dikla Fenigshtein, Weihong Yang, Wlodzmierz Blasiak, Gasification of municipal solid waste in the plasma gasification melting process, Appl. Energy 90 (2012) 106–112.

[9] Umberto Arena, Process and technological aspects of municipal solid waste gasification: a review, Waste Manage. 32 (2012) 625–639.

[10] Thu Lan T. Nguyen, John E. Hermansen, Rasmus Glar Nielsen, Environmental assessment of gasification technology for biomass conversion to energy in comparison with other alternatives: the case of wheat straw, J. Clean. Prod. 53 (2013) 138–148.

[11] N. Lymberopoulos, Microturbines and their Application in Bio-energy, European Commission, 2004. DG-TREN Contract Report No. NNE5-PTA-2002-003/1.

[12] M. Boustouler, A. Reynolds, Guidebook Supports Small-scale Biomass Project Development in NY Biomass Magazine, 2009. Available from: biomassmagazine.com/articles/3748/guidebook-supports-small-scale–biomass-projectdevelopment-in-ny.

[13] C.J. Roos, Clean Heat and Power Using Biomass Gasification for Industrial and Agricultural Projects, Northwest Clean Energy Application Center, U.S. Department of Energy, 2010. Available from: www.energy.wsu.edu/Documents/BiomassGasification_2010.

[14] A. Gómez-Barea, B. Leckner, Modeling of biomass gasification in fluidized bed, Prog. Energy Combust. 36 (2010) 444–509.

[15] P. Cornejo, O. Farías, Mathematical modeling of coal gasification in a fluidized bed reactor using an Eulerian granular description, Int. J. Chem. React. Eng 9 (2011) 1515–1542.

[16] J. Xie, W. Zhong, B. Jin, Y. Shao, H. Liu, Simulation on gasification of forestry residues in fluidized beds by Eulerian–Lagrangian approach, Bioresour. Technol. 12 (2012) 36–46.

[17] R.C. Baliban, J.A. Elia, C.A. Floudas, Toward novel biomass, coal, and natural gas processes for satisfying current transportation fuel demands, 1: process alternatives, gasification modeling, process simulation, and economic analysis, Ind. Eng. Chem. Res. 49 (2010) 7343–7370.

[18] O. Onel, A.M. Niziolek, M.M.F. Hasan, C.A. Floudas, Municipal solid waste to liquid transportation fuels – part I: mathematical modeling of a municipal solid waste gasifier, Comput. Chem. Eng (2014), http://dx.doi.org/10.1016/j.compchemeng.2014.03.008.

[19] V. Silva, E. Monteiro, N. Couto, P.S.D. Brito, A. Rouboa, Analysis of syngas quality from Portuguese biomasses: an experimental and numerical study, Energy Fuels (2014), http://dx.doi.org/10.1021/ef500570t.

[20] V. Silva, A. Rouboa, Using a two-stage equilibrium model to simulate oxygen air enriched gasification of pine biomass residues, Fuel Proc. Technol. 109 (2013) 111–117.

[21] V. Silva, A. Rouboa, Predicting the syngas hydrogen composition by using a dual stage equilibrium model, Int. J. Hydrog. Energy 39 (2014) 331–338.

[22] Z.A. Zainal, R. Ali, C.H. Lean, K.N. Seetharamu, Prediction of performance of a downdraft gasifier using equilibrium modeling for different biomass materials, Energy Convers. Manage. 42 (2001) 1499–1515.

[23] S. Jarungthammachote, A. Dutta, Thermodynamic equilibrium model and second law analysis of a downdraft waste gasifier, Energy 32 (2007) 1660–1669.

[24] M. Ruggiero, G. Manfrida, An equilibrium model for biomass gasification processes, Renew. Energy 16 (1999) 1106–1109.

[25] FLUENT Inc, FLUNENT 6.2 User's Guide, Fluent Inc, Centerra Resource Park, 10 Cavendish Court, Lebanon, NH 03766, 2005.

[26] E. Kurkela, M. Nieminen, P. Simell, Development and commercialisation of biomass and waste gasification technologies from reliable and robust cofiring plants towards synthesis gas production and advanced cycles, in: 2nd World Conference on Biomass for Energy, Industry and Climate Protection, Rome, 2004.

[27] Xiao Gang, Jin Bao-sheng, Zhong Zhao-ping, Chi Yong, N.I. Ming-jiang, Cen Kefa, Xiao Rui, Huang Ya-ji, Huang He, Experimental study on MSW gasification and melting technology, J. Environ. Sci. 19 (2007) 1398–1403.

[28] Stantec, Waste to Energy: a Technical Review of Municipal Solid Waste Thermal Treatment Practices, Stantec Consulting Ltd, Canada, 2011.

[29] Eliseu Monteiro, Vishveshwar Mantha, Abel Rouboa, Prospective application of farm cattle manure for bioenergy production in Portugal, Renew. Energy 36 (2011) 627–631.

[30] Alexandre Magrinho, Filipe Didelet, Viriato Semião, Municipal solid waste disposal in Portugal, Waste Manage 26 (2006) 1477–1489.

[31] SUMA – Serviços Urbanos e Meio Ambiente, S.A, Caracterização dos RSU da Fracção Indiferenciada da LIPOR, 2012. Matosinhos.

[32] D. Scott, S. Czernik, J. Piskorz, D.S.A. Radlein, Fast pyrolysis of plastic wastes, Energy Fuel 4 (1990) 407–411.

[33] M. Arnavat, J. Bruno, A. Coronas, Review and analysis of biomass gasification models, Renew. Sust. Energy Rev. 14 (2010) 2841–2851.

[34] Qinglin Zhang, Liran Dor, Weihong Yang, Wlodzimierz Blasiak, Eulerian model for municipal solid waste gasification in a fixed-bed plasma gasification melting reactor, Energy Fuel 25 (9) (2011) 4129–4137.

[35] D.J. Gunn, Transfer of heat or mass to particles in fixed and fluidized beds, Int. J. Heat Mass Transf. 21 (1978) 467–476.

[36] B. Launder, B. Spalding, Lectures in Mathematical Models of Turbulence, Academic Press, London, England, 1972.

[37] S.C. Cowin, A theory for the flow of granular materials, Powder Technol. 9 (2–3) (1974) 61–69.

[38] A. Demirbas, Hydrogen production from biomass by the gasification process, J. Energy Sources 24 (2002) 59–68.

[39] M. Eaton, D. Smoot, C. Hill, N. Eatough, Components, formulations, solutions, evaluation, and application of comprehensive combustion models, Prog. Energy Combust. 25 (1999) 387–436.

[40] J.A. Rouboa, A. Silva, A.J. Freire, A. Borges, J. Ribeiro, P. Silva, J.L. Alexandre, Numerical analysis of convective heat transfer in nanofluid, Numer. Anal. Appl. Math. Int. Conf. Numer. Anal. Appl. Math. 1048 (1) (2008) 819–822.

[41] M.A. Field, Rate of combustion of size-graded fractions of char from a low rank coal between 1200K–2000K, Combust. Flame 13 (1969) 237–252.

[42] P. Grammelis, P. Basinas, A. Malliopoulou, Sakellaropoulos, Pyrolysis kinetics and combustion characteristics of waste recovered fuels, Fuel 88 (2009) 195–205.

[43] C. Wu, C. Chang, J. Hor, On the thermal treatment of plastic mixtures of MSW: pyrolysis kinetics, Waste Manage. 13 (1993) 221–235.

[44] M.L. Broson, J.B. Howard, J.P. Longwell, W.A. Peter, Products yields and kinetics from the vapor phase cracking of wood pyrolysis tars, AICHE J. 35 (1989) 120–128.

[45] Qingluan Xue, Rodney Fox, An Euler-Euler CFD model for biomass gasification in fluidized bed, in: NETL Conference on Multiphase Flow Science. Morgantown, WV, May 22–24, 2012.

[46] M. Oevermann, S. Gerber, F. Behrendt, Numerical simulation of wood gasification in a fluidized bed reactor using Euler–Euler modeling, in: Proceedings of the European Combustion Meeting, 2009.

Glossary

$C_{1\varepsilon}$, $C_{2\varepsilon}$, $C_{3\varepsilon}$: constants
C_p: specific heat capacity
G_k: generation of turbulence kinetic energy due to the mean velocity gradients
G_b: generation of turbulence kinetic energy due to buoyancy
d: hydraulic diameter
g: gravity acceleration
h_{pq}: heat transfer coefficient between the fluid phase and the solid phase
k: thermal conductivity
M_c: molecular weight
$M_{w,i}$: molecular weight of i component
Nu: Nusselt number
$\dot{m}_{pq}$: mass flow between the fluid phase and the solid phase
P_s: is the particle phase pressure due to particle collisions
p: gas pressure
$\overrightarrow{q}_q$: heat flux
qth: specific enthalpy
Q_{pq}: heat transfer intensity between phases
R: universal gas constant
R_c: reaction rate
S: mass source term due to heterogeneous reactions
S_k: user-defined source terms
S_q: source term due to chemical reactions
S_ε: user-defined source terms
T: temperature
U: mean velocity
v: instantaneous velocity
Y: mass fraction

Y_M: contribution of the fluctuating dilatation in compressible turbulence to the overall dissipation rate

Other symbols

α: volume fraction
β: gas–solid interphase drag coefficient
ρ: density
ϕ_{ls}: energy exchange between the fluid phase and the solid phase.
k_{Θ_a}: diffusion coefficient
$k_{\Theta_a}\nabla(\Theta_s)$: diffusion energy
$(-p_s\bar{I}+\bar{\tau}_s):\nabla(\vec{v}_s)$: generation of energy by the solid stress tensor.
γ_{Θ_a}: collisional dissipation of energy
τ: tensor stress
μ: viscosity
γ_c: stoichiometric coefficient

Subscripts

g: gas phase
s: solid phase
i: component

Paper XII

Using an eulerian-granular 2-D multiphase CFD model to simulate oxygen air enriched gasification of agroindustrial residues

N. Couto, V. Silva, E. Monteiro, P. Brito, A. Rouboa

Renewable Energy 77 (2015) 174-181

Renewable Energy 77 (2015) 174–181

Contents lists available at ScienceDirect

Renewable Energy

journal homepage: www.elsevier.com/locate/renene

Using an Eulerian-granular 2-D multiphase CFD model to simulate oxygen air enriched gasification of agroindustrial residues

Nuno Couto [a], Valter Silva [a, *], Eliseu Monteiro [b], Paulo Brito [b], Abel Rouboa [a, c]

[a] INEGI-FEUP/ECT, Faculdade de Engenharia da Universidade do Porto, Universidade de Trás-os-Montes e Alto Douro, Vila Real, Porto, Portugal
[b] C3i – Centro Interdisciplinar de Investigação e Inovação, Instituto Politécnico Portalegre, IPP-ESTG, Lugar da Abadessa, Apartado 148, 7301-901, Portalegre, Portugal
[c] MEAM Department, University of Pennsylvania, PA 19020, Philadelphia, USA

ARTICLE INFO

Article history:
Received 22 January 2014
Accepted 29 November 2014
Available online 23 December 2014

Keywords:
Pilot scale gasification plant
CFD
Fluidized bed gasifier
Oxygen air enriched

ABSTRACT

A 2-D numerical model based on the Computational Fluid Dynamic (CFD) framework was developed to investigate the influence of oxygen-enriched air on a biomass gasification process. Both gas and solid phases were described using and Eulerian–Eulerian approach exchanging mass, energy and momentum. The kinetic theory of granular flow was used to evaluate the constitutive properties of the dispersed phase and the gas phase behavior was simulated employing the k–ε turbulent model. Three experimental runs were performed in order to validate the model. Good agreement was shown between experimental and numerical results. The numerical model also predicted the influence of the oxygen content on the gasification temperature, steam to biomass ratio and on the final syngas composition. It can be observed that the hydrogen and nitrogen molar fractions decrease as a function of the oxygen content and that the carbon dioxide shows the opposite trend. On the other hand, there is only a slight increase of the methane molar fraction. Finally, the effects of both oxygen content and steam to biomass ratio on the cold gas efficiency were studied. It was verified that the cold gas efficiency increases with the oxygen content and decreases slightly with the steam to biomass ratio.

1. Introduction

Nowadays, the major concern regarding power generation supply is to decrease dependence on fossil fuels and develop a new set of renewable alternatives capable of minimizing pollutant emissions and global warming effects while being able to ensure a global energy future [1]. The use of biomass has been regarded as a potential energy source solution with the great benefit of being environmental friendly [2]. Portugal has recently adopted new policies regarding energy production and renewable energy sources. Currently, Portugal's biomass conversion technologies are virtually limited to combustion, making it essential to invest in other technologies, such as gasification, that have already successfully been used in other countries. Portugal's biomass residues are related to forestry, the wood processing industry, agricultural wastes and coffee husks, among others [3].

The success of biomass gasification in other countries is essentially the result of being one of the most economical routes for the production of renewable hydrogen [4], the downside being that it involves high levels of complexity in areas such as fluid flow, heat transfer and elaborate chemistry just to name a few. Because of this and because realistic experiments are expensive to assemble, numerical studies are usually required. Due to the complex non-linear hydrodynamic behavior [5], scale-up is still one of the major problems to be handled considering the biomass and coal gasification [6]. In the literature there are several papers concerning the use of CFD approaches to model the gasification process [7–9].

Snider et al. [7] developed a three-dimensional computational model in order to describe the coal gasification process considering an Eulerian–Lagrangian approach coupled with energy transport and homogeneous and heterogeneous chemistry described by reduced-chemistry. Reactor design improvements were attained by using the developed model, namely, identifying regions of stagnant particles.

Gerber et al. [8] developed an Eulerian multiphase model to investigate a fluidized bed composed by wood and char particles. The authors validated their model under experimental data gathered in a lab-scale bubbling fluidized bed gasifier. Several operating

* Corresponding author. Quinta de Prados, Apartado 1013, 5001-801 Vila Real. Tel.: +351 259350317.
E-mail addresses: nunodiniscouto@hotmail.com (N. Couto), vbrsilva@utad.pt (V. Silva), ELMMonteiro@portugalmail.pt (E. Monteiro), pbrito@estgp.pt (P. Brito), rouboa@utad.pt (A. Rouboa).

http://dx.doi.org/10.1016/j.renene.2014.11.089
0960-1481/

Nomenclature

A, B	calibration constants
$C_{1\varepsilon}$, $C_{2\varepsilon}$, $C_{3\varepsilon}$	constants
C_p	specific heat capacity
D_0	diffusion rate coefficient
G_k	generation of turbulence kinetic energy due to the mean velocity gradients
G_b	generation of turbulence kinetic energy due to buoyancy
h_{pq}	heat transfer coefficient between the fluid phase and the solid phase
k	thermal conductivity
M_c	molecular weight
$M_{w,i}$	molecular weight of i component
p	gas pressure
$\vec{q}_q$	heat flux
qth	specific enthalpy
R	universal gas constant
R_c	reaction rate
S_k	user-defined source terms
S_q	source term due to chemical reactions
S_ε	user-defined source terms
T	temperature
U	mean velocity
v	instantaneous velocity
Y	mass fraction
Y_M	contribution of the fluctuating dilatation in compressible turbulence to the overall dissipation rate

Other symbols

α	volume fraction
ρ	density
ϕ_{ls}	energy exchange between the fluid phase and the solid phase
$k_{\Theta a}$	diffusion coefficient
$k_{\Theta a}\nabla(\Theta_s)$	diffusion energy
$(-P_s\bar{I}+\bar{\tau}_s):\nabla(\vec{v}_s)$	generation of energy by the solid stress tensor
$\gamma_{\Theta a}$	collisional dissipation of energy
τ	tensor stress
μ	viscosity
γ_c	stoichiometric coefficient

Subscripts

g	gas phase
s	solid phase
i	component

conditions such as wood feeding admission, initial bed height or reactor throughput were studied. They concluded a low influence of the studied operating conditions on the syngas composition but a very strong influence on the tar content.

Muilenburg [9] developed a Fluent based model in order to model the combustion and gasification of biomass fuels in a downdraft gasifier. The biomass particles were modeled as coal particles by using an empirical formula derived from off-site proximate and ultimate analysis. It was verified that different fuels showed similar temperature and mixture fraction patterns.

In the recent years oxygen streams with up to 40% (v/v) purity have been obtained using commercial air separators based on membrane technologies [10]. The investment and operational costs of this technology are considerably lower when compared to distillation units [11]. The major drawback for commercial implementation of this technology based on distillation units is the high cost of the oxygen production process [12].

Some researchers [13–15] studied the use of different gasification mediums such as air/steam, oxygen/steam and oxygen enriched air. It was verified that using pure oxygen allows higher carbon conversion efficiencies and gas heating values. However, the production of oxygen from air separation is still expensive. Huynh and Kong [13] investigated the effect of using oxygen enriched-air and steam mixtures as gasifying agents on syngas composition, heating values and NO_X emissions during gasification and combustion. The oxygen content in the enriched air varied from 21% (v/v) to 45% and 80% (v/v) on dry basis. The authors concluded that using oxygen-enriched air and steam gasification increases the lower heating value of syngas as well as the yield of gases such as H_2 or CO. Liu et al. [14] studied oxygen-enriched two-stage underground coal gasification to improve the caloric value of the syngas and to extend gas production times. The composition of the gas produced and the role of the temperature field were analyzed. It was shown that the caloric value of the syngas improves with increased oxygen concentration in the first stage. Silva and Rouboa [15] developed an equilibrium model to simulate the downdraft gasifier and to predict the gasification of pine biomass residues. The model allowed determining the temperature at the carbon boundary point, which is the optimum gasification point. It was observed that the hydrogen and carbon monoxide molar fractions decrease as function of the oxygen content and that carbon dioxide shows the opposite trend. The increase of the oxygen content led to increased energy and exergy efficiencies.

This paper aims at presenting a numerical methodology within the framework of the commercial CFD code Fluent applied to gasification of Portuguese agro-industrial residues to produce syngas. It also aims to study the influence of oxygen concentration as a gasifier agent on several gasification parameters such as temperature, steam to biomass ratio and cold gas efficiency. The numerical simulation results were compared and validated versus a set of runs using coffee husks which were gasified in a bubbling fluidized semi-industrial unit.

2. Materials and experimental set-up

Fig. 1 shows a diagram of the biomass gasification plant used in the experiments. The experiments were performed in a gasification pilot scale plant based on an up-flow fluidized bed gasifier, Fig. 2. An extended description of the semi-industrial plant can be found in Ref. [16]. The proximate and ultimate analyses of coffee husks are shown in Table 1. These data will be integrated in the development model. Table 2 shows the experimental conditions and the syngas analysis. Data will be validated under experimental data.

3. Mathematical model

A 2-D multi-phase model was developed under the Fluent framework to describe the gasification phenomenon for a pilot-scale bubbling fluidized bed reactor. An Eulerian–Eulerian approach was followed considering that a semi-industrial gasifier encloses a system with millions of particles and consequently high solid phase volume fractions. At these circumstances, the use of the

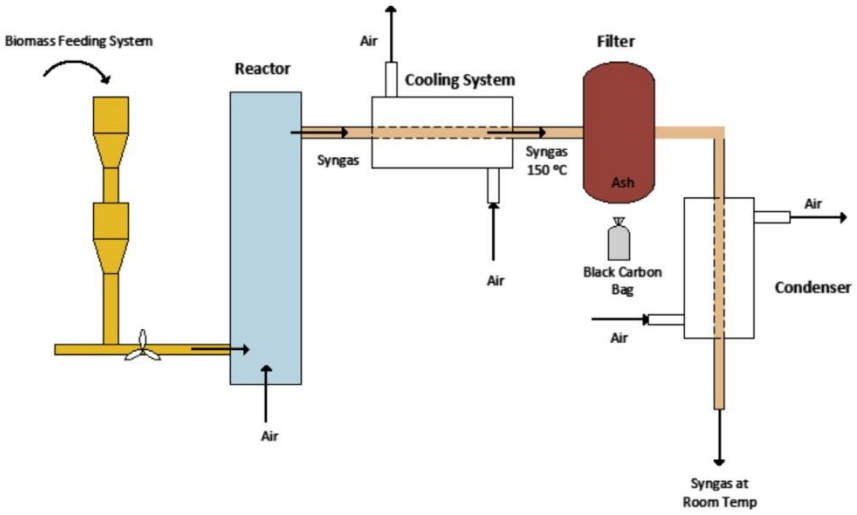

Fig. 1. Schematics of the biomass gasification semi-industrial plant at Portalegre, Portugal. The main components of the unit are described in the text.

kinetic theory of granular flows is especially appropriated. Both phases are allowed to exchange mass, momentum and heat. The model also includes homogeneous and heterogeneous chemical reactions. The software does not include the mathematical treatment for the devolatilization phenomenon. To solve this issue some pseudo-heterogeneous reactions were considered. Mass and momentum balances for both phases were included. The gas phase was considered as ruled by the ideal gas behavior and density of the solid phase as constant.

3.1. Turbulence model

The k–ε model [18] provided in ANSYS FLUENT is appropriate when the turbulence transfer between phases assumes the main role. This is true when we deal with the gasification phenomenon in a fluidized bed gasifier.

The transports equations can be defined as follows:

$$\frac{\partial}{\partial t}(\rho k)+\frac{\partial}{\partial x_i}(\rho k u_i)=\frac{\partial}{\partial x_j}\left[\left(\mu+\frac{\mu_t}{\sigma_k}\right)\right]+G_k+G_b-\rho\varepsilon-Y_M+S_k \tag{1}$$

$$\frac{\partial}{\partial t}(\rho\varepsilon)+\frac{\partial}{\partial x_i}(\rho\varepsilon u_i)=\frac{\partial}{\partial x_j}\left[\left(\mu+\frac{\mu_t}{\sigma_\varepsilon}\right)\frac{\partial\varepsilon}{\partial x_j}\right]+C_{1\varepsilon}\frac{\varepsilon}{k}(G_k+C_{3\varepsilon}G_b)-C_{2\varepsilon}\rho\frac{\varepsilon^2}{k}+S_\varepsilon \tag{2}$$

3.2. Granular Eulerian model

The conservation equation for the granular temperature obtained from kinetic theory of gasses can be expressed as follows:

$$\frac{3}{2}\left[\left(\frac{\partial(\rho_s\alpha_s\Theta_s)}{\partial t}+\nabla\cdot(\rho_s\alpha_s\vec{v}_s\Theta_s\right)\right]=(-P_s\bar{I}+\bar{\tau}_s):\nabla(\vec{v}_s)+\nabla\cdot(k_{\Theta a}\nabla(\Theta_s))-\gamma_{\Theta a}+\phi_{ls} \tag{3}$$

3.3. Chemical reactions model

3.3.1. Devolatilization

Biomass decompositions are in agreement with the following equation:

$$Biomass\rightarrow Char+Volatiles+Steam+Ash \tag{4}$$

It should be noticed that under this simulation the ash content is not taking into account.

The volatile matter is assumed to be composed by the following species:

$$Volatiles\rightarrow\alpha_1 CO+\alpha_2 CO_2+\alpha_3 CH_4+\alpha_4 H_2 \tag{5}$$

Data from Table 1 is used to determine the biomass mixture composition.

As far as we know there are no data concerning the exact distribution of the volatiles in biomass. So, it was assumed a single rate model developed by Badzioch and Hawsley [19] which computes reliable devolatilization rates in a simple way. The demoisturization phenomenon was also included. These two pseudo-heterogeneous reactions were modeled with a single reaction rate, in agreement with Arrhenius law.

3.3.2. Homogeneous gas-phase reactions

Both kinetic and turbulent mixing rate effects [20] were considered when modeling the homogeneous gas-phase reactions. Fluent provides the finite-rate/Eddy-dissipation model, which considers both the Arrhenius and Eddy-dissipation reaction rates. The water–gas shift reaction and the CO, H_2 and CH_4 combustion reactions were considered as being:

$$CO+H_2O\leftrightarrow CO_2+H_2 \tag{6}$$

$$CO+0.5\,O_2\rightarrow CO_2 \tag{7}$$

$$H_2+0.5\,O_2\rightarrow H_2O \tag{8}$$

$$CH_4+2O_2\rightarrow CO_2+2H_2O \tag{9}$$

The Arrhenius rates for each one of these reactions can be expressed as follows [21]:

$$r_{CO\_Combustion}=1.0\times10^{15}\exp\left(\frac{-16000}{T}\right)C_{CO}C_{O_2}^{0.5} \tag{10}$$

$$r_{H2Combustion}=5.159\times10^{15}\exp\left(\frac{-3430}{T}\right)T^{-1.5}C_{O_2}C_{H_2}^{1.5} \tag{11}$$

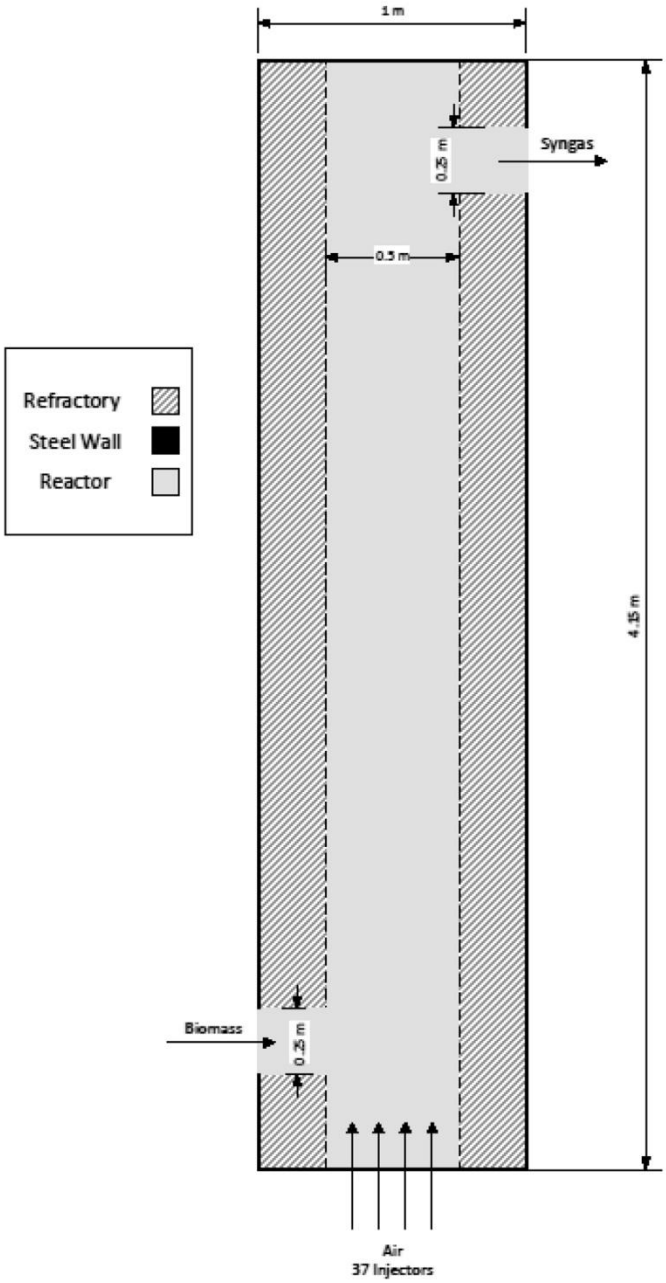

Fig. 2. Schematics of the bubbling fluidized bed gasifier.

$$r_{CH4Combustion} = 3.552 \times 10^{14} \exp\left(\frac{-15700}{T}\right) T^{-1} C_{O_2} C_{CH_4} \quad (12)$$

Table 1
Coffee husks properties.

Coffee husks properties			
Ultimate analysis (%)		**Proximate analysis (%)** [17]	
N	5.2	Ash	2.5
C	40.1	Volatile matter	83.2
H	5.6	Fixed carbon	14.3
O	49.1	**Empirical formula**	
Humidity (%)	25.3	$CH_{1.676}O_{0.918}N_{0.111}$	
Density (kg/m^3)	500		
Net heat value (MJ/kg biomass)	20.9		

Table 2
Experimental operating conditions and syngas analysis.

	Coffee husks		
	Run 1	Run 2	Run 3
Experimental conditions			
Temperature (°C)	815	790	790
Admission biomass (kg/h)	28	28	41
Air flow rate (Nm^3/h)	75	72	80
Ratio $O_2/O_{2\ Stoichiometric}$	2.63	2.52	1.96
Syngas flow rate (Nm^3/h)	106	88	116
Syngas fraction (dry basis)			
H_2	12.4	7.6	7.5
CO	11.4	11.1	10.6
CH_4	1.6	2.4	2.4
CO_2	18.7	17	18.5
N_2	52.3	54.2	55.2
Syngas NHV			
KWh/kg	0.73	0.65	0.63
Cold gasification efficiency	0.6	0.47	0.42

$$r_{water.gas.shift} = 2780 \exp\left(\frac{-1510}{T}\right)\left[C_{CO}C_{H_2O} - \frac{C_{CO_2}C_{H_2}}{0.0265\exp\left(\frac{3968}{T}\right)}\right] \quad (13)$$

The Eddy dissipation reaction rate can be expressed using the equation below:

$$r_{Eddy-dissipation} = \alpha_{i,r} M_{w,i} A \rho \frac{\varepsilon}{k} \min\left(\min_R\left(\frac{Y_R}{\alpha_{R,r} M_{w,R}}\right), B\frac{\sum_p y_p}{\sum_i^N \alpha_{i,R} M_{w,i}}\right) \quad (14)$$

The minimum value of these two contributions can be defined as the net reaction rate.

3.3.3. Heterogeneous reaction rate

Char combustion, H_2O and CO_2 char gasification were included as heterogeneous reactions.

$$C + O_2 \rightarrow CO_2 \quad (15)$$

$$C + H_2O \rightarrow CO + H_2 \quad (16)$$

$$C + CO_2 \rightarrow 2CO \quad (17)$$

With the aim of including both diffusion and kinetic effects the Kinetic/Diffusion Surface Reaction Model [22,23] was used. This model weights the effect of the Arrhenius rate and the diffusion rate of the oxidant at the surface particle. The diffusion rate coefficient can be defined as:

$$D_0 = C_1 \frac{\left[(T_p + T_\infty) \div 2\right]^{0.75}}{d_p} \quad (18)$$

The Arrhenius rate is as follows:

$$r_{Arrehnius} = A_e - \left(\frac{E}{RT_p}\right) \quad (19)$$

The final reaction rate weighs both contributions and is defined as being:

$$\frac{d_{m_p}}{d_t} = -A_p \frac{\rho R T_\infty Z_{ox}}{M_{w,ox}} \frac{D_0 r_{Arrehnius}}{D_0 + r_{Arrehnius}} \tag{20}$$

This model was applied by using a User Defined Function.

The system was simulated considering properties from the Fluent database and from standard thermodynamic tables.

3.4. Energy conservation

The energy conservation equation must be solved for each phase, using the following equation:

$$\frac{\partial(\alpha_q \rho_q h_q)}{\partial t} + \nabla \cdot (\alpha_q \rho_q \vec{u}_q h_q) = -\alpha_q \frac{\partial(p_q)}{\partial t} + \bar{\tau}_q : \nabla(\vec{u}_q) - \nabla \cdot \vec{q}_q + S_q + \sum_{p=1}^{n} \left(\vec{Q}_{pq} + \dot{m}_{pq} h_{pq} - \dot{m}_{pq} h_{pq}\right) \tag{21}$$

The rate of energy transfer is assumed as function of the temperature difference between phases and the heat transfer coefficient is given as a function of the Nusselt number.

3.5. Numerical procedure

A fine grid is selected to capture the steep gradients between neighbor areas. The non-uniform grid spacing was generated using GAMBIT.

The second order upwind scheme is used to discretize the convective terms in the momentum and energy equations. The SIMPLE scheme is used for solving the pressure–velocity coupling. The system of algebraic equations is solved using the Gauss-Siedel point-by-point iterative method in conjunction with the algebraic multi-grid method solver. Relative convergence criterion of 10^{-8} for residuals of the continuity and momentum equations and 10^{-14} for residual energy equation were assumed.

4. Results and discussion

As stated numerical results collected from the developed model were validated against experimental data gathered from a semi-industrial thermal gasification plant. Due to their expense these kind of experimental results are rarely gathered and used to validate a numerical model, laboratory or small-scale gasifiers are used instead. In Fig. 3 experimental and numerical results for the different gasification runs described in Table 2 are presented.

Good agreement between experimental and numerical data was found (the maximum error in all the simulated data was 20%). The

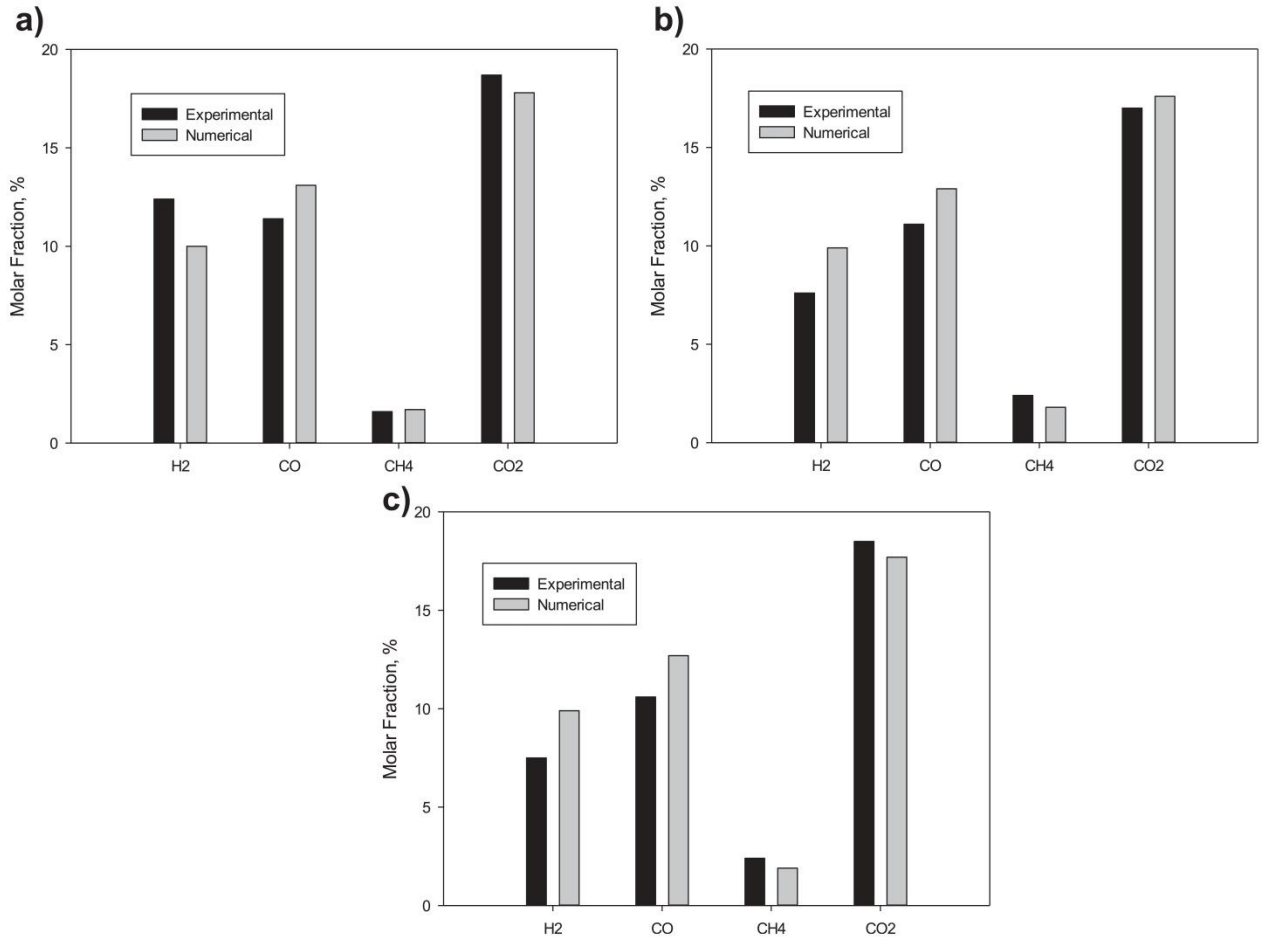

Fig. 3. Experimental and numerical molar syngas compositions from a) run 1 b) run 2 and c) run 3.

simulation can follow the changes of the syngas composition (experimental data) as a function of the different operating conditions. Despite being found some differences, the errors can be assumed as very reasonable for such a complex system and the results trends are in agreement with those found in the literature [20]. The model performance could be improved by getting more appropriated kinetic data, namely, concerning the distribution of the volatiles in biomass. Additionally, tar decomposition and chemical reactions for ash and some light hydrocarbons were not included. Fig. 4 shows the mole fraction distribution contours of H_2, CH_4 and CO_2 in the gas mixture. The highest values for both H_2 and CO_2 are located immediately above the air inlets (with CO_2 reaching its highest values more abruptly), CH_4 on the other hand reaches higher values much more smoothly and at greater heights. At the bottom of the gasifier there is a large amount of unconverted carbon which becomes reduced along the gasifier height. Volatile combustion also leads to increased amounts of CO_2 at higher positions in the gasifier. All of these results are in agreement with the literature [24].

Gas composition and hydrogen generation in biomass gasification are affected by several operation condition parameters. The influence of parameters such as gasification temperature and steam to biomass ratio as a function of different oxygen content in the enriched air gas were tested. Fig. 5 shows how oxygen content affects syngas composition. It can be observed that the hydrogen and nitrogen molar fractions decrease as a function of the oxygen content and that the carbon dioxide shows the opposite trend. On the other hand, there is only a slight increase of the methane molar fraction. These trends are in agreement with the results found by Turn et al. [24].

Fig. 6 shows the hydrogen molar fraction from syngas composition as a function of the steam to biomass ratio and the oxygen content. The steam to biomass ratio can be defined as the ratio between the steam mass flow rate and the fuel mass flow rate. The steam to biomass ratio was varied from 0 to 1.5 (by holding the other variables as constant) and the oxygen content from 21 to 40 % (v/v). Higher values of SBR leads to a product gas with more hydrogen [15,25]. At low values of SBR, the main phenomena behind the hydrogen production are carbon and methane reforming. The hydrogen generation increases slowly for SBRs higher than 1 and achieves an asymptotic value for SBRs higher than 1.5. This implies that the surplus steam is not reacting and that adding more

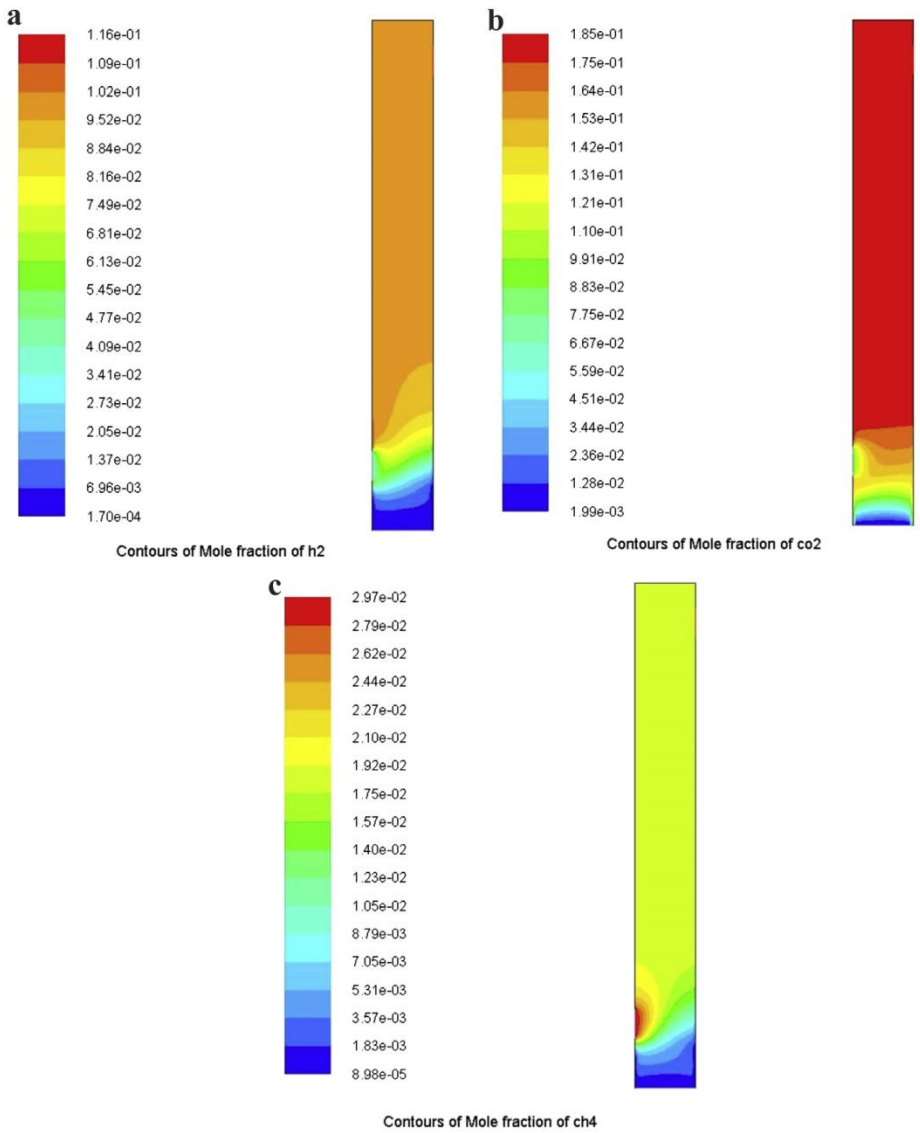

Fig. 4. Contours of a) H_2, b) CO_2 and c) CH_4 molar fractions in the gas mixture from run 1, respectively.

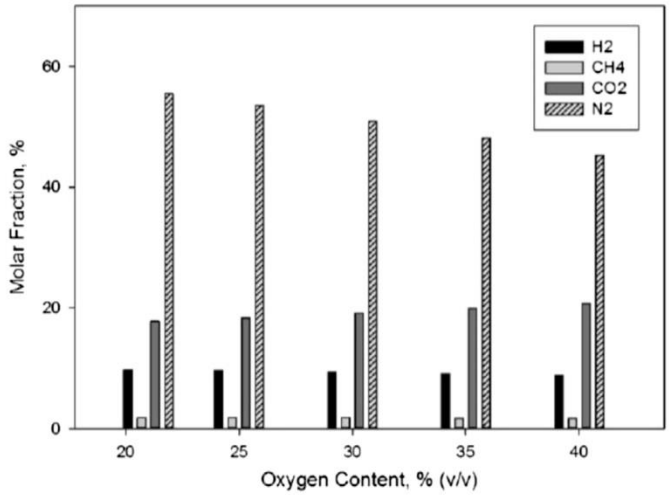

Fig. 5. Syngas molar fractions as a function of the oxygen content (operating conditions from run 1).

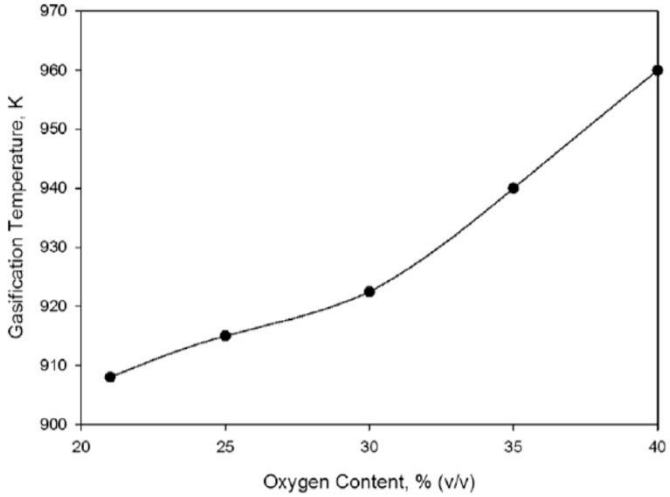

Fig. 7. Gasification temperature (range 900–960 K) as a function of oxygen content (SBR = 0).

steam is not efficient. Following the same trend from Fig. 5, the hydrogen fraction drops with the raising of the oxygen content [24,25].

Fig. 7 illustrates the gasification temperature as a function of different oxygen content in the enriched air gas from 21% (v/v) to 40% (v/v). The figure shows that the gasification temperature increases as a function of the oxygen content.

In order to properly understand the influence of parameters such as SBR and oxygen content the cold gas efficiency (CGE) should be investigated. CGE is defined as the percentage of the heating value of biomass converted into the heating value of the product gas.

In Fig. 8, CGE was studied as a function of SBR and oxygen content from 21 to 40% (v/v). It can be verified that the cold gas efficiency increases with the oxygen content and decreases slightly with the steam to biomass ratio. This is due to the addition of steam, resulting in more energy being used to vaporize it and the endothermic reactions are not favored. Also the gasification temperature increases with the oxygen content, explaining the improved efficiencies. In fact the higher the gasification

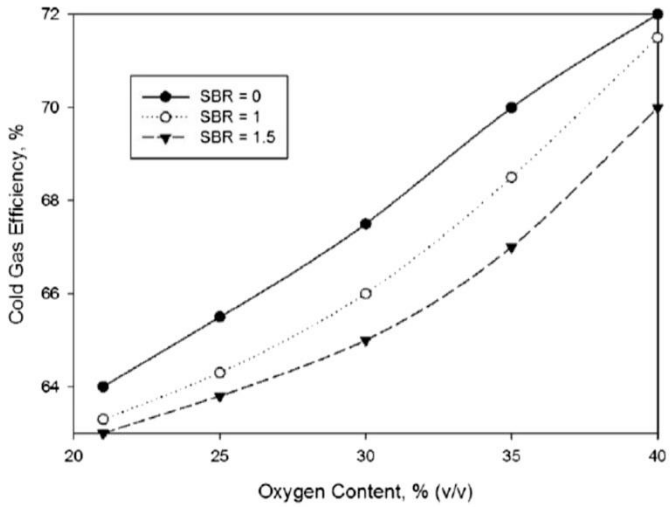

Fig. 8. Cold gas efficiency as a function of the oxygen content and the steam to biomass ratio (operating conditions based in run 1).

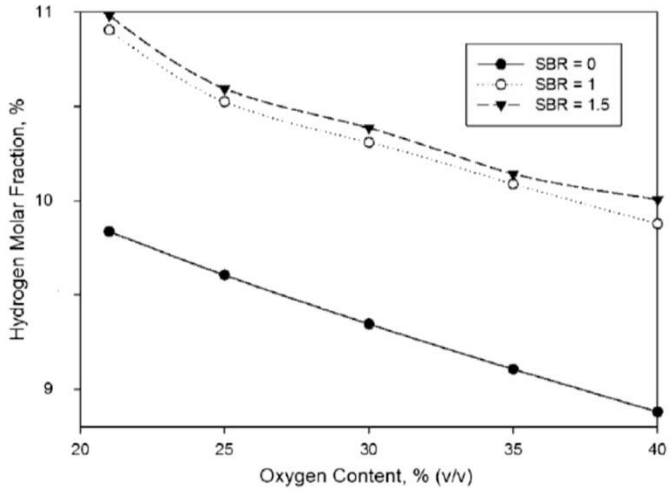

Fig. 6. Hydrogen molar fraction from syngas composition as a function of the steam to biomass ratio and oxygen content.

temperature the higher is the percentage of physical exergy in the syngas [15].

The developed model predicts the syngas composition and cold gas efficiency at different operating conditions in a semi-industrial scale with reasonable accuracy, showing the effective trend of each one of the light gases. This a power tool for designing large scale systems that may be dominant in the near future. The adopted simplifications are identified and will be the subject of analysis in future papers.

5. Conclusions

Using a commercial CFD code a multiphase 2-D model was developed in order to simulate the gasification process using biomass substrates available in Portugal. The model was calibrated and validated using experimental data and operating information from a semi-industrial fluidized bed gasifier using coffee husks as biomass substrate. Three experimental runs were made in order to validate the model. Good agreement was shown between experimental and numerical results. The numerical model also predicted

the influence of the oxygen content on the gasification temperature, steam to biomass ratio and on the final syngas composition. It can be observed that the hydrogen and nitrogen molar fractions decrease as a function of the oxygen content and that the carbon dioxide shows the opposite trend. On the other hand, there is only a slight increase of the methane molar fraction. The effects of both oxygen content and steam to biomass ratio on cold gas gasification were studied. It was verified that the cold gas efficiency increases with the oxygen content and decreases slightly with the steam to biomass ratio. Differences were observed mainly due to some simplifications that were included in the numerical simulation development, namely, proximal analysis and reaction kinetic data were taken from the literature, light hydrocarbons and ash were not treated and a 2-D geometry was adopted.

Acknowledgments

We would like to express our gratitude to the Portuguese Foundation for Science and Technology (FCT) for the support given to grants SFRH/BPD/71686 and SFRH/BD/86068/2012 and to project PTDC/AAC-AMB/103119/2008 and ALTERCEXA – POCTEC Program.

References

[1] Ciferno P, Marano J. Benchmarking biomass gasification technologies for fuels, chemicals and hydrogen production. U.S. Department of Energy, National Energy Technology Laboratory; 2002. Available from: http://www.netl.doe.gov/technologies/coalpower/gasification/pubs/pdf/BMassGasFinal.pdf [accessed 29.11.13].
[2] Kirkels A, Verbong G. Biomass gasification: still promising? A 30-year global overview. Renew Sustain Rev 2011;15:471–81.
[3] Ferreira S, Moreira N, Monteiro E. Bioenergy overview for Portugal. Biomass Bioenergy 2009;33:1567–76.
[4] Kirtay E. Recent advances in production of hydrogen from biomass. Energy Convers Manage 2011;52:1778–89.
[5] Eaton AM, Smoot LD, Hill SC, Eatough CN. Components, formulations, solutions, evaluation, and application of comprehensive combustion models. Prog Energy Combust 1999;25:387–436.
[6] Knowlton TM, Karri SBR, Issangya A. Scale-up of fluidized-bed hydrodynamics. Powder Technol 2005;150:72–7.
[7] Snider D, Clark S, ÓRourke J. Eulerian–Lagrangian method for three-dimensional thermal reacting flow with application to coal gasifiers. Chem Eng Sci 2011;66:1285–95.
[8] Gerber S, Behrendt F, Oevermann M. An Eulerian modeling approach of wood gasification in a bubbling fluidized bed reactor using char as bed material. Fuel 2010;89:2903–17.
[9] Muilenburg M. Computational modeling of the combustion and gasification zones in a downdraft gasifier. Master Thesis. Iowa University; 2011.
[10] Higman C, Burgt M. Gasification. Elsevier; 2008.
[11] Campoy M, Barea A, Vidal F, Ollero P. Air–steam gasification of biomass in a fluidised bed: process optimisation by enriched air. Fuel Process Technol 2009;90:677–85.
[12] Maniatis K. Progress in biomass gasification: an overview. In: Bridgwater AV, editor. Progress in thermochemical biomass conversion, London; 2001.
[13] Huynh CV, Kong SC. Performance characteristics of a pilot-scale biomass gasifier using oxygen-enriched air and steam. Fuel 2013;103:987–96.
[14] Hongtao L, Feng C, Xia P, Kai Y, Shuqin L. Method of oxygen-enriched two-stage underground coal gasification. Min Sci Technol (China) 2011;21:191–6.
[15] Silva V, Rouboa A. Using a two-stage equilibrium model to simulate oxygen air enriched gasification of pine biomass residues. Fuel Process Technol 2013;109:111–7.
[16] Couto N. Energetic and exergetic analysis of biomass gasification. Master Thesis, Vila Real. 2012.
[17] Wilson L, John G, Mhilu C, Yang W, Blasiak W. Coffee husks gasification using high temperature air/steam agent. Fuel Process Technol 2010;91:1330–7.
[18] Launder BE, Spalding DB. Lectures in mathematical models of turbulence. London, England: Academic Press; 1972.
[19] Badzioch S, Hawsley PGW. Kinetics of thermal decomposition of pulverized coal particles. Ind Eng Chem Des Dev 1970;4:521–30.
[20] Yu L, Lu J, Zhang X, Zhang S. Numerical simulation of the bubbling fluidized bed coal gasification by the kinetic theory of granular flow. Fuel 2007;86:722–34.
[21] Wang X, Jin B, Zhong W. Three dimensional of fluidized bed coal gasification. Chem Eng Process 2009;48:695–705.
[22] Baum M, Street P. Predicting the behavior of coal particles. Combust Sci Technol 1971;3:231–43.
[23] Field MA. Rate of combustion of size-graded fractions of char from a low rank coal between 1200k–2000k. Combust Flame 1969;13:237–52.
[24] Turn S, Kinoshita C, Zhang Z, Ishimura D, Zhou J. An experimental investigation of hydrogen production from biomass gasification. Int J Hydrogen Energy 1998;23:641–8.
[25] Basu P. Biomass gasification and pyrolysis: practical design and theory. Elsevier; 2010. 499.

Paper XIII

Analysis of syngas quality from Portuguese biomasses: An experimental and numerical study

V.B. Silva, N. Couto, E. Monteiro, P. Brito, A. Rouboa

Energy & Fuels 28 (2014) 5766-5777

---

energy&fuels

Article

pubs.acs.org/EF

Analysis of Syngas Quality from Portuguese Biomasses: An Experimental and Numerical Study

Valter Silva,[†] Eliseu Monteiro,[‡] Nuno Couto,[†] Paulo Brito,[§] and Abel Rouboa*[,†,∥]

[†]INEGI-FEUP/ECT, Universidade de Trás-os-Montes e Alto Douro, Vila Real, Portugal

[‡]IPP-ESTG, Portalegre, Portugal

[§]C3i—Centro Interdisciplinar de Investigação e Inovação, Instituto Politécnico Portalegre, Portalegre, Portugal

[∥]MEAM Department, University of Pennsylvania, Philadelphia 19020, Pennsylvania, United States

ABSTRACT: A comprehensive two-dimensional multiphase model was developed to describe the gasification of three large available Portuguese biomasses in a pilot scale fluidized bed gasifier within the computational fluid dynamics Fluent framework. An Eulerian−Eulerian approach was implemented to handle both the gas and the dispersed phases. The kinetic theory of granular flows was used to evaluate the constitutive properties of the dispersed phase, and the gas-phase behavior was simulated employing the $k-\varepsilon$ turbulent model. Devolatilization phenomenon was also modeled. Results from the numerical model were later compared with experimental data also gathered for the three Portuguese biomasses. The simulated syngas compositions are in good agreement with the experimental results with maximum deviations of 20% (considering all simulations and biomasses). The effect of the gasification temperature and steam-to-biomass ratio on the syngas composition was evaluated as well as the cold gas efficiency, H_2/CO ratio, CH_4/H_2 ratio, and carbon conversion. From this analysis, it was possible to define which biomass has the greater potential to be used concerning the selected application. Among the three biomasses, it was concluded that coffee husks and vine-pruning residues show better H_2/CO ratios, while the higher CH_4/H_2 ratios are obtained by using the forest residues. The highest cold gas efficiencies were obtained by using the vine-pruning residues. These data are crucial to describe scenarios concerning the potential use of biomass as a source of energy in Portugal.

1. INTRODUCTION

Biomass utilization for fuel, products, and power is recognized worldwide as a critical component for a nation's strategic plan when it faces continued and growing dependence on imported oil.[1] Portugal has a good potential for generating energy from biomass to partially replace coal or petroleum. The biomass resources that can be used for energy generation are diverse, but in Portugal, an important contribution can be found from agricultural-related residues. Coffee husks, forest and vines pruning residues are largely available and have attractive low costs. Coffee husks show an economical advantage, since they should not be pelletized. Additionally, the use of these residues avoids their dumping and the corresponding environmental consequences. Typical values for the coffee industry indicate that about 20% of coffee is converted into husks, solid waste, and parchment. It was verified that coffee husks generated in Portuguese industry have a calorific value of 15.100 MJ/kg. The coffee husk heating value and composition in terms of volatile matter and ultimate analysis shows that they have acceptable energy properties considering typical biomasses.[2] Portugal is one of the main wine producers in the world generating about 700 million dm^3 of wine per year. There is a great interest by Portuguese entities to study the best ways to valorize the residues and subproducts generated by this industry. The potential energy derived from pruning residues is depicted in Table 1. About 35% of Portuguese territory is composed of forest. It is estimated that economic activities related to the Portuguese forestry generates about 113 thousand jobs and about 200 million euros/year. Table 1 shows the amounts of forest residues produced in Portugal and the corresponding energy potential.

Table 1. Potential Energy from Pruning and Forest Residues in Portugal[3]

biomass	alcohol equivalent (millions of dm^3)	production (10^6 ton/year)	TWh/year
pruning residues	357.7		2.2
forest residues		6.5	11.6

The total primary energy demand in Portugal amounted to 104 000 GWh in 2005.[3] From Table 1, it can be noticed that only forest and pruning residues can potentially produce 13 800 GWh (about 13.3% of the total primary energy demand in Portugal). Additionally, the power production from bioresources was 9750 GWh in 2005 (including biomass, municipal solid waste, and biogas). Previous data show that both forest and pruning residues can play an important role in the Portuguese energy scenario.

These residues require adequate treatment or recovery to minimize environmental impact and increase their corresponding economic value. A large variety of technologies has been developed in recent decades to deal with this problem. Among the proposed technologies, those oriented toward energy recovery, including combustion and gasification of biomasses,

Received: February 5, 2014
Revised: July 28, 2014
Published: July 28, 2014

have attracted much interest.[4] There are several methods to convert the biomass feedstock to energy, but it is expected that biomass gasification will become the dominant technology.[5] Biomass gasification is very attractive because the obtained gases are intermediates in high-efficiency power production.[5] Additionally, the environmental performance is one of the greatest strengths of gasification technology, which often is considered a sound response to the increasingly restrictive regulations applied around the world. On the other hand, the use of gasifiers instead of combustors shows clear advantages, namely, the generation of a syngas with improved quality to be used in the production of Fischer-tropsch liquids, fuel cells, clean fuel combustion, and cheaper CO_2 underground sequestration. Biomass gasification also brings high expectations toward the generation of hydrogen.

Hydrogen is one of the key energy sources due to its potential to provide energy for industry, residences, transportation, and mobile applications. Indeed, hydrogen can replace petroleum-based fuels in the transportation sector and can even supply remote stations that cannot be fueled by conventional distribution grids.[6] Additionally, hydrogen production can be environmentally friendly when green technologies such as biomass gasification are employed. The worldwide commercial production of hydrogen is approximately 40 million tonnes.[7] However, most of the traditional technologies for hydrogen production are fossil-fuel based, 80−85% of the world's total production being derived from natural gas via steam−methane reforming,[8] which is a very energy-intensive process that releases large amounts of carbon dioxide and other greenhouse gases.

Hydrogen can be obtained by other processes than steam reformation of methane, namely, water electrolysis, biological processes using microorganisms, or by thermocatalytic reformation of hydrogen-enriched organic compounds.[9] Among the aforementioned technology options, biomass gasification is identified as the most efficient and economic route for hydrogen production.[10]

A gasification system includes a set of phenomena such as fluid flow, heat transfer, and complex chemistry that can only be solved by applying several governing mathematical equations, mostly based on conservation equations, that is, mass, heat, and momentum. This level of complexity can be achieved using computer fluid dynamic (CFD) tools. However, only a few studies regarding the use of CFD tools have been reported to simulate the fluidized bed biomass gasification. Two main approaches are considered to describe the solid phases: the Eulerian−Eulerian approach (a continuum approach for both phases) and the Eulerian−Lagrangian approach (a continuum approach for the fluid phase and a discrete particle method for the solid phase). Xie et al.[11] developed a three-dimensional numerical model to compute the syngas composition by using forestry residues as feedstock and using the Eulerian−Lagrangian approach as numerical method. The experimental gasification experiments were carried out in a lab-scale pine gasifier. The Eulerian−Lagrangian approach implies a huge computational effort, and more versatile computing solutions can be found using an Eulerian−Eulerian approach. Xue and Fox[12] developed an Eulerian−Eulerian computational fluid dynamics model to simulate wood gasification using air as a fluidization agent in a lab-scale fluidized bed gasifier (FBG). Simulations provided detailed information on several processes such as the dynamic particle processes, char elutriation, and gas composition at the reactor outlet. The same authors[13] used an Euler−Euler-based CFD model to describe the trend of biomass decomposition versus temperature with a kinetic model based on superimposed hemicellulose, cellulose, and lignin reactions. It was concluded that biomass particle size and superficial gas velocity influenced tar yield and residence time considerably with a fixed bed height. Gungor and Yildirim[14] computed the axial and radial distribution of syngas mole fraction and temperature across an atmospheric CFB biomass gasifier by using a two-dimensional (2-D) model that uses the particle-based approach and integrates and simultaneously predicts the hydrodynamic and gasification aspects. The authors claimed that the developed model computes successfully the radial and axial profiles of the bed temperature and H_2, CO, CO_2, and CH_4 volumetric fractions and tar concentration versus gasifier temperature with errors lower than 25%. These works compare the numerical results versus experimental results gathered in laboratory setups. Indeed, there is a lack of experimental data where the numerical results can be confirmed with pilot scale or industrial setups, namely, using fluidized bed technology. The scaleup is still one of the major problems to be handled considering the biomass and coal gasification.[15] This is related to the complex nonlinear hydrodynamic behavior, chaotic nature, and complicated reactions that strongly impact the gas−solid flow behavior.[16] Additionally, the lack of data is also related to the expense of experiments for obtaining valuable information on fluidized bed gasifiers in pilot scale or industrial dimensions. This implies an urgent need for both theoretical as well as experimental approaches to obtain more helpful data and information.

The use of fluidized bed technology in biomass gasification units makes it possible to use relatively smaller gasifiers and larger capacities than with a fixed bed. The higher efficiency of a fluidized bed comes from its higher specific reaction area when compared to a fixed bed. Fluidized beds have also proven to permit more versatile units in terms of feed materials of different characteristics and origins.[17]

This paper aims to present a numerical methodology within the framework of the commercial CFD code (Fluent) applied to the gasification of Portuguese agro-industrial residues. The use of coffee husks, forest and vine-pruning residues is studied concerning the generation of hydrogen and the quality of syngas based on different indices including carbon conversion, H_2/CO ratio, CH_4/H_2 ratio, and cold gas efficiency (CGE). The numerical simulation results were compared and validated versus a set of runs using these residues that were gasified in a bubbling fluidized pilot scale unit.

2. MATERIALS AND EXPERIMENTAL SETUP

The gasification runs were performed using the three biomass feedstocks. The proximate and ultimate analyses of these feedstocks are shown in Table 2.

The experiments were performed in a pilot-scale gasification plant, which is based on an up-flow fluidized bed gasifier operating at up to 850 °C, under a total pressure below 1 bar, and at a maximum pellet feeding rate of 70 kg/h. Figure 1 displays a diagram of the biomass gasification plant used in the experiments.

The main components of the unit are the following: (a) a biomass feed system with two inline storage tanks that allow discharging the biomass into the reactor using an Archimedes' screw at a variable and controllable speeds—the two storage tanks act as buffers to avoid air entering through the feeding system; (b) a tubular fluidized bed reactor, 0.5 m in diameter and 2.5 m in height, internally coated with ceramic refractory materials; biomass enters the reactor at a height of 0.4 m from the base, and preheated air enters the reactor from the base

dx.doi.org/10.1021/ef500570t | Energy Fuels 2014, 28, 5766−5777

Table 2. Humidity, Density, Net Heat Value, and Ultimate and Proximate Analyses of Coffee Husks, Forest and Vine-Pruning Residues

biomass properties	forest residues	coffee husks	vine-pruning residues
elementary analysis (%)			
N	2.4	5.2	2.6
C	43.0	40.1	41.3
H	5.0	5.6	5.5
O	49.6	49.1	50.6
humidity (%)	11.3	25.3	13.3
density (kg/m^3)	650	500	265
net heat value (MJ/kg biomass)	21.2	20.9	15.1
proximal analysis (%)[18]			
ash	0.2	2.5	3.1
volatile matter	79.8	83.2	83.6
fixed carbon	20.0	14.3	13.3

through a set of diffusers, with a flow of about 70 m^3/h (the schematic of the fluidized reactor are depicted in Figure 2); (c) a gas-cooling system consisting of two heat exchangers; the first exchanger cools the syngas to about 570 K using a cocurrent air flow that enters the unit, and the second heat exchanger cools the syngas to 420 K by a forced flow of air coming from the exterior; (d) a cellulosic bag filter that allows the removal of carbon black and ash particles produced during the gasification process; filter cleaning is done with pressurized syngas injection; black carbon is collected at bottom of the bag filter and stored in a proper tank; (e) a condenser where liquid condensates are removed by cooling the syngas to room temperature on a third tube heat exchanger. Gasification runs were performed using coffee husks, forest and vine-pruning residues at 790 and 815 °C.

Syngas analysis was performed in a Varian 450-GC gas chromatograph with two thermal conductivity detectors that allow the detection of H_2, CO, CO_2, CH_4, O_2, N_2, C_2H_6, and C_2H_4 (equipped, respectively, with CP81069, CP81071, CP81072, CP81073, and CP81025 Varian GC columns), using helium as carrier gas.

3. MATHEMATICAL MODEL

A numerical model was built according to experimental data gathered from the Portalegre pilot-scale setup. To simulate the gasification process a multiphase (gas and solid phase) model from a Fluent database was used. In the comprehensive 2-D numerical model, the gas phase is treated as continuous, and the solid phase is described through an Eulerian granular model. Interactions between both phases were modeled as well, since both phases exchange heat by convection, momentum (given the drag between gas phase and solid phase), and mass (given the heterogeneous chemical reactions).

3.1. Mass Balance Model. The continuity equation for the gas and solid phases are given by

$$\frac{\partial}{\partial t}(\alpha_g \rho_g) + \nabla\cdot(\alpha_g \rho_g v_g) = S_{gs} \tag{1}$$

$$\frac{\partial}{\partial t}(\alpha_s \rho_s) + \nabla\cdot(\alpha_s \rho_s v_s) = S_{sg} \tag{2}$$

The biomass feed reacts with the oxygen steam and carbon dioxide to change solid phase into gas phase, so S, which is defined as the mass source term due to heterogeneous reactions, can be expressed as follows:

$$S_{sg} = -S_{gs} = M_c \sum \gamma_c R_c \tag{3}$$

The ideal gas behavior was considered for computing the gas-phase density:

$$\frac{1}{\rho_g} = \frac{RT}{p}\sum_{i=1}^{n}\frac{Y_i}{M_i} \tag{4}$$

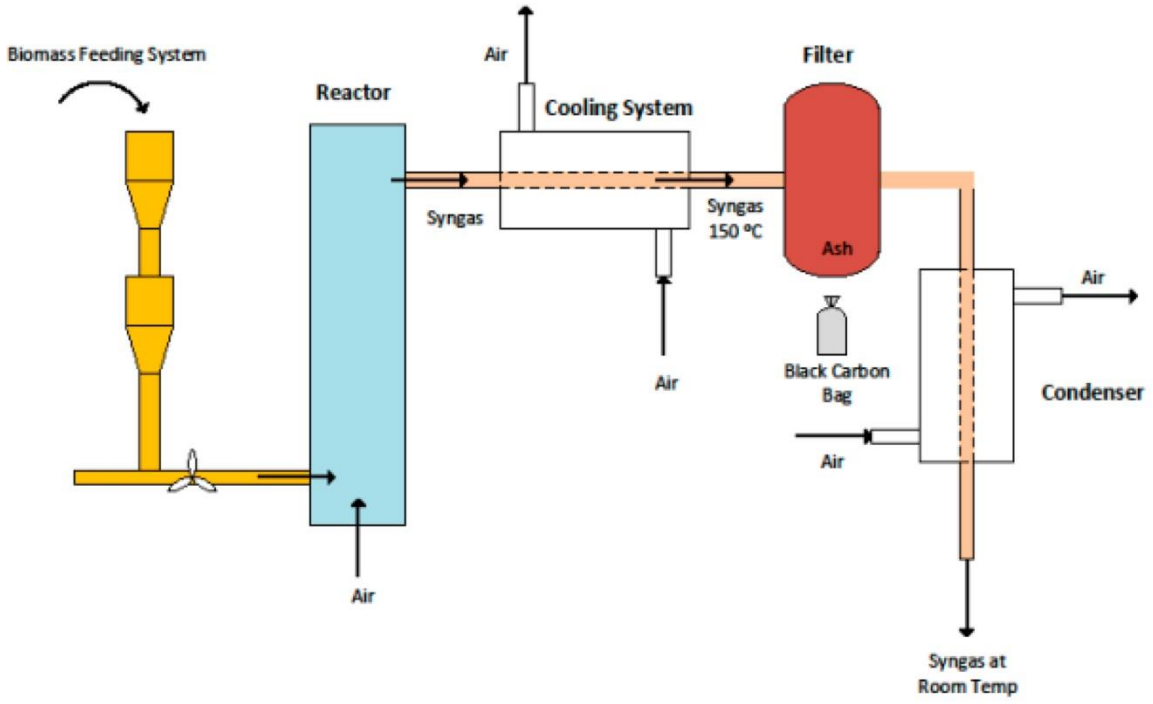

Figure 1. Biomass gasification semi-industrial plant at Polytechnic Institute of Portalegre, Portugal. The main components of the unit are described in the text.

dx.doi.org/10.1021/ef500570t | Energy Fuels 2014, 28, 5766−5777

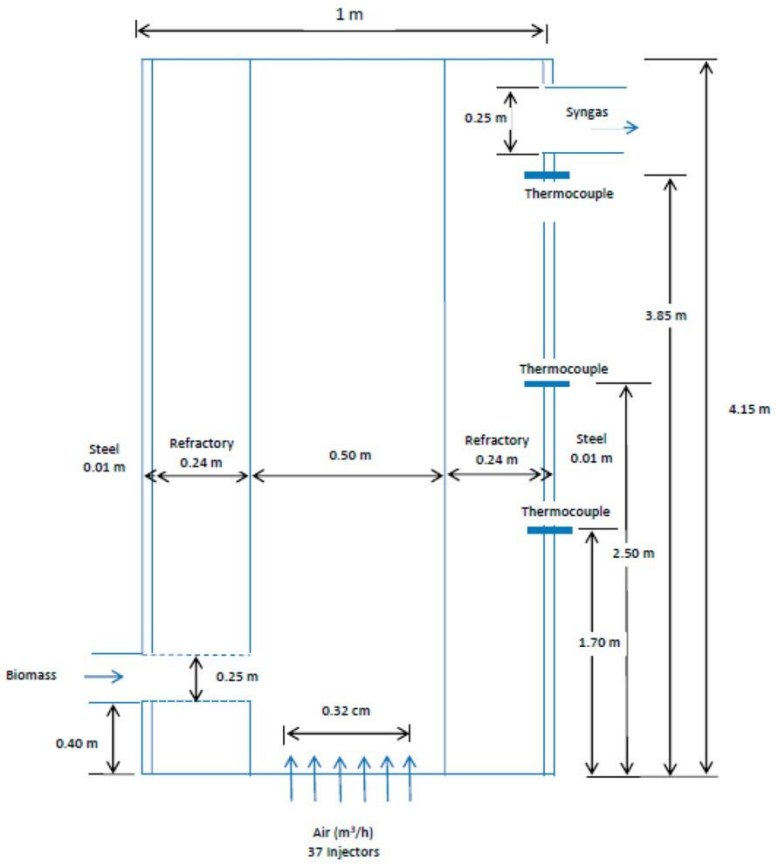

Figure 2. Schematic of the bubbling fluidized bed gasifier.

The solid-phase density was assumed as constant.

3.2. Momentum Equations. The momentum equation of the gas phase is

$$\frac{\partial}{\partial t}(\alpha_g \rho_g v_g) + \nabla\cdot(\alpha_g \rho_g v_g v_g) = -\alpha_g \nabla p_g + \alpha \rho_g g + \beta(v_g - v_s) + \nabla\cdot\alpha_g \tau_g + S_{gs} U_s \quad (5)$$

The momentum equations of solid phase can be written as

$$\frac{\partial}{\partial t}(\alpha_s \rho_s v_s) + \nabla\cdot(\alpha_s \rho_s v_s v_s) = -\alpha_s \nabla p_s + \alpha \rho_s g - \beta(v_g - v_s) + \nabla\cdot\alpha_s \tau_s + S_{sg} U_s \quad (6)$$

3.3. Turbulence Model. The standard $k-\varepsilon$ model in ANSYS FLUENT has become the workhorse of practical engineering flow calculations in the time since it was proposed by Launder and Spalding.[19] It is a semiempirical model, and the derivation of the model equations relies on phenomenological considerations and empiricism. The selection of this turbulence model is appropriate when the turbulence transfer between phases plays a predominant role as in the case of gasification in fluidized beds.

The turbulence kinetic energy k and its rate of dissipation ε are obtained from the following transport equations:

$$\frac{\partial}{\partial t}(\rho k) + \frac{\partial}{\partial x_i}(\rho k u_i) = \frac{\partial}{\partial x_j}\left[\left(\mu + \frac{\mu_t}{\sigma_k}\right)\right] + G_k + G_b - \rho\varepsilon - Y_M + S_k \quad (7)$$

$$\frac{\partial}{\partial t}(\rho \varepsilon) + \frac{\partial}{\partial x_i}(\rho \varepsilon u_i) = \frac{\partial}{\partial x_j}\left[\left(\mu + \frac{\mu_t}{\sigma_\varepsilon}\right)\frac{\partial \varepsilon}{\partial x_j}\right] + C_{1\varepsilon}\frac{\varepsilon}{k}(G_k + C_{3\varepsilon}G_b) - C_{2\varepsilon}\rho\frac{\varepsilon^2}{k} + S_\varepsilon \quad (8)$$

3.4. Granular Eulerian Model. In the granular Eulerian model, stresses in the granular solid phase are obtained by the analogy between the random particle motion and the thermal motion of molecules within a gas accounting for the inelasticity of solid particles. As in a gas, the intensity of velocity fluctuation determines the stresses, viscosity, and pressure of the granular phase. The kinetic energy associated with velocity fluctuations is described by a pseudothermal temperature or granular temperature, which is proportional to the norm of particle velocity fluctuations.

The conservation equation for the granular temperature, obtained from the kinetic theory of gases, takes the following form:

dx.doi.org/10.1021/ef500570t | Energy Fuels 2014, 28, 5766−5777

$$\frac{3}{2}\left[\left(\frac{\partial(\rho_s\alpha_s\Theta_s)}{\partial t} + \nabla\cdot(\rho_s\alpha_s\vec{v}_s\Theta_s)\right)\right] = (-P_s\bar{I} + \bar{\tau}_s)\colon \nabla(\vec{v}_s) + \nabla\cdot(k_{\Theta a}\nabla(\Theta_s)) - \gamma_{\Theta a} + \varphi_{ls} \quad (9)$$

The diffusion coefficient for granular energy was computed by using the following equation due to Syamlal et al.[20]

$$k\theta_{s=15d_s/4(41-33\omega)}\rho_s\alpha_s\sqrt{\theta_s\pi}\left[1 + \frac{12}{5}\omega^2(4\omega - 3)\alpha_s g_{o,ss} + \frac{16}{15\pi}(41 - 33\omega)\omega\alpha_s g_{o,ss}\right] \quad (10)$$

where $\omega = 1/2(1 + e_{ss})$; d is the biomass particle diameter; s is the solid phase.

The granular energy dissipation can be computed by using the expression derived by Lun et al.[21] When the granular flow has a smaller volume fraction than the maximum possible value, a solid pressure is considered for the pressure gradient term in the momentum equation, which includes a kinetic term and a particle collision term:

$$p_{s=\alpha_s}\rho_s\theta_s + 2\rho_s(1 + e_{ss})\alpha_s^2 g_{o,ss}\theta_s \quad (11)$$

The radial distribution function allows the different levels of compressibility. It works as a correction factor that gives the probability of collisions when the granular phase goes to denser states. Ansys Fluent provides empirical relations for the radial distribution function when there is one solid phase.

3.5. Chemical Reactions Model. *3.5.1. Devolatilization.* Devolatilization is a process where moisture and volatile matters are driven out from biomass by heat. No devolatilization process is included in Ansys/Fluent considering the Eulerian−Eulerian method. To develop a reliable gasification model, it is necessary to include a devolatilization model in the Fluent code.

Biomass is thermally decomposed into volatiles, char, and ash, in agreement with the following equation:

$$\text{biomass} \rightarrow \text{char} + \text{volatiles} + \text{steam} + \text{ash} \quad (12)$$

Note that ash appears for illustration only; the simulation does not consider ash content in the solid phase.

In the present work, the volatile matter is composed of the following species:

$$\text{volatiles} \rightarrow \alpha_1\text{CO} + \alpha_2\text{CO}_2 + \alpha_3\text{CH}_4 + \alpha_4\text{H}_2 \quad (13)$$

The biomass mixture composition is determined based on the proximate and elemental analysis shown in Table 2.

Since there are no data on the exact distribution of the volatiles in biomass, the single-rate model developed by Badzioch and Hawsley[22] was adopted. The single-rate model produced moderate and reliable devolatilization rates with little computational effort. Additionally, a demoisturization equation was also considered. These two pseudo-heterogeneous reactions were modeled with a single reaction rate in agreement with the Arrhenius law.

3.5.2. Homogeneous Gas-Phase Reactions. The modeling of the homogeneous gas-phase reactions should consider both the kinetic and the turbulent mixing rate effects.[23] The gas phase is conditioned by the effect caused by the chaotic fluctuations of the solid particles. This turbulent flow leads to velocity and pressure fluctuations on the gaseous species. Fluent provides the finite-rate/eddy-dissipation model, which considers both the Arrhenius and the eddy-dissipation reaction rates. The water gas shift reaction and the CO, H_2, and CH_4 combustion reactions were considered, respectively:

$$\text{CO} + \text{H}_2\text{O} \leftrightarrow \text{CO}_2 + \text{H}_2 \quad (14)$$

$$\text{CO} + 0.5\text{O}_2 \rightarrow \text{CO}_2 \quad (15)$$

$$\text{H}_2 + 0.5\text{O}_2 \rightarrow \text{H}_2\text{O} \quad (16)$$

$$\text{CH}_4 + 2\text{O}_2 \rightarrow \text{CO}_2 + 2\text{H}_2\text{O} \quad (17)$$

The Arrhenius rates for each one of these reactions can be expressed as follows, respectively:

$$r_{\text{CO combustion}} = 1.0 \times 10^{15}\exp\left(\frac{-16\,000}{T}\right)C_{\text{CO}}C_{\text{O}_2}^{0.5} \quad (18)$$

$$r_{\text{H2combustion}} = 5.159 \times 10^{15}\exp\left(\frac{-3430}{T}\right)T^{-1.5}C_{\text{O}_2}C_{\text{H}_2}^{1.5} \quad (19)$$

$$r_{\text{CH4combustion}} = 3.552 \times 10^{14}\exp\left(\frac{-15\,700}{T}\right)T^{-1}C_{\text{O}_2}C_{\text{CH}_4} \quad (20)$$

$$r_{\text{water gas shift}} = 2780\exp\left(\frac{-1510}{T}\right)\left[C_{\text{CO}}C_{\text{H}_2\text{O}} - \frac{C_{\text{CO}_2}C_{\text{H}_2}}{0.0265\exp\left(\frac{3968}{T}\right)}\right] \quad (21)$$

The eddy dissipation reaction rate can be expressed using the following equation:

$$r_{\text{eddy dissipation}} = \alpha_{i,r}M_{w,i}A\rho\frac{\varepsilon}{k}\min\left(\min_R\left(\frac{Y_R}{\alpha_{R,r}M_{w,R}}\right), B\frac{\sum_p y_p}{\sum_i^N \alpha_{i,R}M_{w,i}}\right) \quad (22)$$

The minimum value of these two contributions can be defined as the net reaction rate.

3.5.3. Species Transport Equations. The local mass fraction of each specie Y is computed by using a convection-diffusion equation as follows:

$$\frac{\partial}{\partial t}(\rho Y_i) + \nabla(\rho Y_i\vartheta) = -\nabla\cdot J_i + R_i + S_i \quad (23)$$

where J_i is the diffusion flux of species i due to concentration gradients, R_i is the net generation rate of species i due to homogeneous reaction, and S_i is a source term related to the species i production from the solid heterogeneous reaction. The diffusion flux was computed as a function of the turbulent Schmidt number.

3.5.4. Heterogeneous Reaction Rate. Char is the solid devolatilization residue. Heterogeneous reactions of char with the gas species such as O_2 and H_2O are complex processes that involve balancing the rate of mass diffusion of the oxidizing chemical species to the surface of biomass particles with the surface reaction of these species with the char. The overall rate of a char particle is determined by the oxygen diffusion to the particle surface and the rate of surface reaction, which depend on the temperature and composition of the gaseous environment and the size, porosity, and temperature of the particle. The commonly simplified reaction models consider the following overall reactions, char combustion (eq 24), H_2O (eq 25) and CO_2 char gasification (eq 26):

$$\text{C} + \text{O}_2 \rightarrow \text{CO}_2 \quad (24)$$

dx.doi.org/10.1021/ef500570t | Energy Fuels 2014, 28, 5766−5777

$$C + H_2O \rightarrow CO + H_2 \quad (25)$$

$$C + CO_2 \rightarrow 2CO \quad (26)$$

r

The heterogeneous reactions are influenced by many factors, namely, reactant diffusion, breaking up of char, interaction of reactions, and turbulence flow. To include both diffusion and kinetic effects the kinetic/diffusion surface reaction model (KDSRM)[24,25] was applied. This model weights the effect of the Arrhenius rate and the diffusion rate of the oxidant at the surface particle. The diffusion rate coefficient can be defined as

$$D_0 = C_1 \frac{[(T_p + T_\infty) \div 2]^{0.75}}{d_p} \quad (27)$$

where d_p means particle diameter.

The Arrhenius rate can be defined as follows:

$$r_{\text{Arrhenius}} = Ae^{-\left(\frac{E}{R_{T_p}}\right)} \quad (28)$$

The final reaction rate weights both contributions and is defined as follows:

$$\frac{d_{m_p}}{d_t} = -A_p \frac{\rho R T_\infty Z_{ox}}{M_{w,ox}} \frac{D_0 r_{\text{Arrhenius}}}{D_0 + r_{\text{Arrhenius}}} \quad (29)$$

This model was included in the CFD framework by using the UDF tool.

At biomass and air inlets the mass flow rate was prescribed, while at the outlet the atmospheric pressure level was assigned. At the walls the materials (steel and insulation) and corresponding thicknesses and heat conduction coefficients were prescribed, as well as the ambient temperature conditions (25 °C).

All materials (gas species, solid bio mass particles) were assigned appropriate properties from standard thermodynamic tables. The properties of the gas species (density ρ, viscosity μ, thermal conductivity k, and specific heat capacity C_p) were allowed to vary with local main phase temperature, and the mixture value was calculated from its local composition and available Fluent laws (ideal gas law for ρ and mass-weighted mixing law for μ, k, and C_p).

3.6. Energy Conservation. To describe the energy conservation the following energy conservation equation must be solved for each phase:

$$\frac{\partial(\alpha_q \rho_q h_q)}{\partial t} + \nabla \cdot (\alpha_q \rho_q \vec{u}_q h_q) = -\alpha_q \frac{\partial(p_q)}{\partial t} + \overline{\tau}_q : \nabla(\vec{u}_q) - \nabla \cdot \vec{q}_q + S_q + \sum_{p=1}^{n} (\vec{Q}_{pq} + \dot{m}_{pq} h_{pq} - \dot{m}_{pq} h_{pq}) \quad (30)$$

The rate of energy transfer is assumed as a function of the temperature difference between phases:

$$Q_{pq} = h_{pq}(T_p - T_q) \quad (31)$$

Provided convection is the main heat transfer mechanism within the reactor, the heat transfer coefficient is related to the Nusselt number of phase q by

$$h_{pq} = \frac{6k_p \alpha_q \alpha_p Nu_q}{d_p^2} \quad (32)$$

3.7. Numerical Procedure. The problem under consideration is solved by using Fluent, a finite volume method-based CFD solver. Mesh was built using GAMBIT software, and the reactor schematic is depicted in Figure 3. Quadrilateral cells of uniform grid spacing were used. The grid is chosen to be sufficiently fine to capture the steep gradients in the vicinity of the inlet and outlet of the gasifier. Several simulations were performed considering different sized quadrilateral cells. The optimal size was found when no meaningful differences were obtained considering syngas composition, temperature, velocity and turbulence profiles. The selected size is about 12 times larger than the particle size, which, as found in literature,[26] can capture effectively the hydrodynamics in fluidized bed reactors.

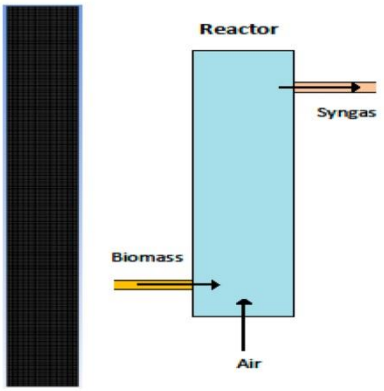

Figure 3. Schematic of the mesh and corresponding bubbling fluidized bed gasifier.

The second order upwind scheme is used to discretize the convective terms in the momentum and energy equations. The SIMPLE scheme is used for solving the pressure−velocity coupling. The system of algebraic equations is solved using the Gauss−Seidel point-by-point iterative method in conjunction with the algebraic multigrid method solver. Relative convergence criterion of 10^{-8} for residuals of the continuity and momentum equations and of 10^{-14} for residual energy equation were prescribed in this work. To find a stable solution, gas−solid flow is previous solved without using the chemical reactions. After finding the established flow pattern, the chemical reactions were included, and the full system was solved.

4. DISCUSSION AND RESULTS

4.1. Experimental Runs and Model Validation. To the best of our knowledge there are limited data regarding syngas obtained from biomass substrates using a pilot scale thermal gasification plant. The majority of the literature shows syngas compositions obtained in a laboratory or small-scale gasifier. Large-scale systems are expensive, and their inherent logistical difficulties are easily understandable. However, there is a large difference between the laboratory and semi-industrial results due to phenomena of complex nonlinear hydrodynamic behavior, the chaotic nature and complicated reactions that strongly impact the gas−solid flow behavior. Additionally, there are no studies comparing the quality of syngas based on different indices for a gasification process by using biomasses

dx.doi.org/10.1021/ef500570t | Energy Fuels 2014, 28, 5766−5777

Table 3. Experimental Operating Conditions and Syngas Analysis

experimental conditions	forest residues			coffee husk			vine-pruning residues		
temperature (°C)	815	815	790	815	790	790	790	790	815
admission biomass (kg/h)	63	74	63	28	28	41	25	55	55
air flow rate (Nm^3/h)	94	98	98	75	72	80	52	40	40
syngas flow rate (Nm^3/h)	106	94	100	106	88	116	107	108	102
syngas fraction (dry basis)									
H_2	8.2	8.4	7.6	12.4	7.6	7.5	5.1	10.4	12.7
CO	18.6	18.0	17.9	11.4	11.1	10.6	8.3	11.7	14.1
CH_4	4.6	4.4	4.4	1.6	2.4	2.4	1.1	2.4	2.3
CO_2	16.7	17.1	17.1	18.7	17.0	18.5	16.5	20.1	17.9
N_2	48.0	48.2	49.2	52.3	54.2	55.2	56.4	51.2	49.1
syngas NHV									
MJ/Nm^3	5.16	5.02	4.93	3.34	3.20	3.07	1.99	3.46	4.02

largely available in Portugal. The present model was calibrated and validated using experimental data and operating information from a pilot-scale fluidized bed gasifier.

Table 3 shows the experimental operating conditions and the syngas analysis in three different gasification runs for the three different studied biomasses. The net heat values (NHV) were computed considering the syngas basis composition determined by gas chromatography and using the standard combustion heats of the compounds obtained at 25 °C. An increase in gasification temperature promoted the formation of a syngas with higher hydrogen and carbon monoxide contents (the major contributors to the calorific value of syngas) and, consequently, higher NHV of the syngas. Generically, the results obtained with the different biomasses show a relation between the biomass calorific value and the calorific value of the syngas obtained: higher biomass calorific value (Table 2) results in higher calorific syngas production. In fact, it turns out that the syngas formed with the highest calorific value was obtained by gasification of forest residues, a more energetic material. This relationship between the biomass calorific content and the syngas NHV can be explained considering first that the biomass calorific value is related to the amount of carbon and hydrogen present in the biomass, that is, an increased amount of carbon and hydrogen lead to higher calorific value, and second, a larger amount of these two elements allows production of larger quantities of hydrogen and carbon monoxide, the major contributors for the calorific value of the syngas. Analysis of the dependence of producer gas properties on conditions of biomass admission seems to show that for all gasification runs studied there is a decrease in syngas calorific value with increasing quantity of biomass admitted. Because the syngas NHV is also dependent on the air flow rate, different biomass feeding rates were simulated keeping the other operating conditions constant to verify the former assumption. It was observed that increasing the biomass feeding rate leads to lower syngas NHV (for all the studied biomasses). These results are in agreement with the literature.[27] This is consistent with the fact that a faster feeding of biomass to the reactor reduces the extent of the reactions. From the experimental gasification runs, it can be observed that the vine-pruning residues lead to the highest generation of hydrogen, while forest residues promote the highest content of CO.

Figure 4 gives the experimental and numerical results for coffee husks gasification runs described in Table 3. It can be verified that the numerical results show a good agreement with those obtained from the experimental runs carried out in a

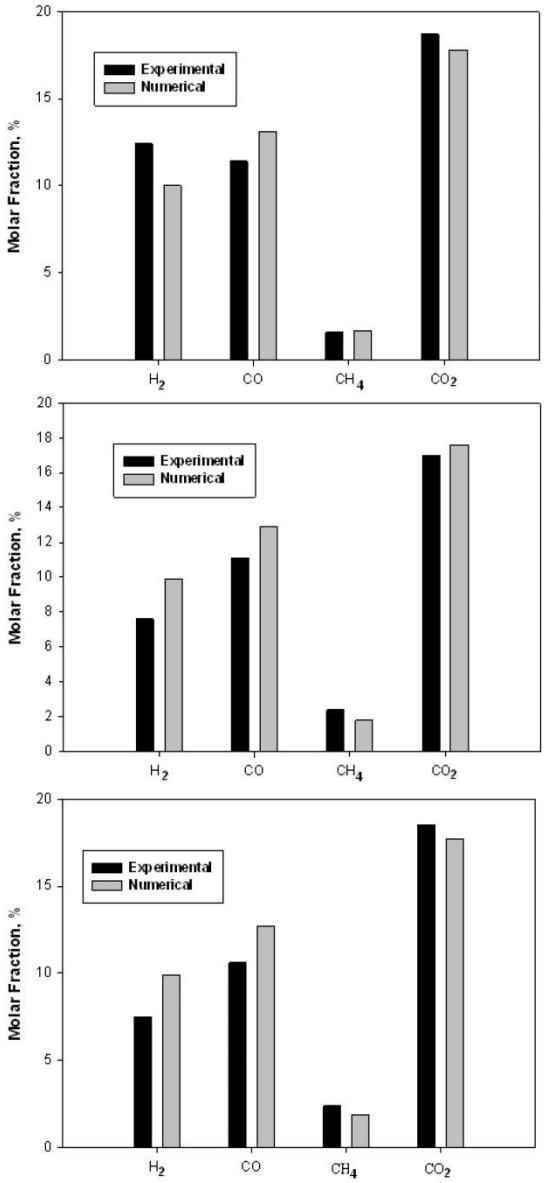

Figure 4. Experimental and numerical molar syngas composition (obtained from coffee husks) considering the operating conditions from (a) run 1, (b) run 2, and (c) run 3.

dx.doi.org/10.1021/ef500570t | *Energy Fuels* 2014, 28, 5766−5777

pilot-scale bubbling fluidized bed gasifier. Considering all simulations (for the three different biomasses), the maximum obtained error was about 20%. The simulations also predict the species molar fraction behavior at different runs with similar trends considering the increasing or decreasing of species at different operating conditions. The numerical code was applied successfully to the three biomasses. These errors are very reasonable for a complex system such as biomass gasification in a pilot-scale reactor. Differences can be found due to some simplifying assumptions followed by our developed model. Proximate analysis and kinetics (some data are relative to coal particles) were taken from literature. Ash and some light hydrocarbons were not considered. Also, a 2-D approach was followed. A more detailed devolatilization approach should be attempted, and tar decomposition should also be treated. These simplifications should be properly treated in future papers.

4.2. Model Performance. The thermal biomass gasification process involves a set of complex chemical reactions that lead to the formation of three fractions: syngas, ashes (chars), and condensates. The most important fraction, amounting to more than 70% (by weight) consists of light gases, namely, CO, H_2, CH_4, CO_2, and N_2. Figure 5 shows the contours of H_2 and CO_2, CH_4, and N_2 molar fractions in the gas mixture (obtained from coffee husks), respectively. The higher values for H_2 are located immediately above the air inlets, while at a greater height for CO_2. The water−gas shift reaction is exothermic, and the decrease of temperature in the upper zones makes the H_2 values increase and makes the opposite effect for CO. CO_2 and H_2 acquire their exit values very quickly below the free board area. At the bottom of the gasifier there is a large amount of unconverted carbon, which becomes reduced along the gasifier height. On the other hand, the volatile combustion also leads to increased amounts of CO_2 at higher positions in the gasifier. The amount of CH_4 is higher in the inlet region of the gasifier as a result of devolatilization. N_2 shows the higher amounts in the low region of the gasifier and then decreases for upper zones. Similar pattern distributions were found for forest and vine-pruning residues.

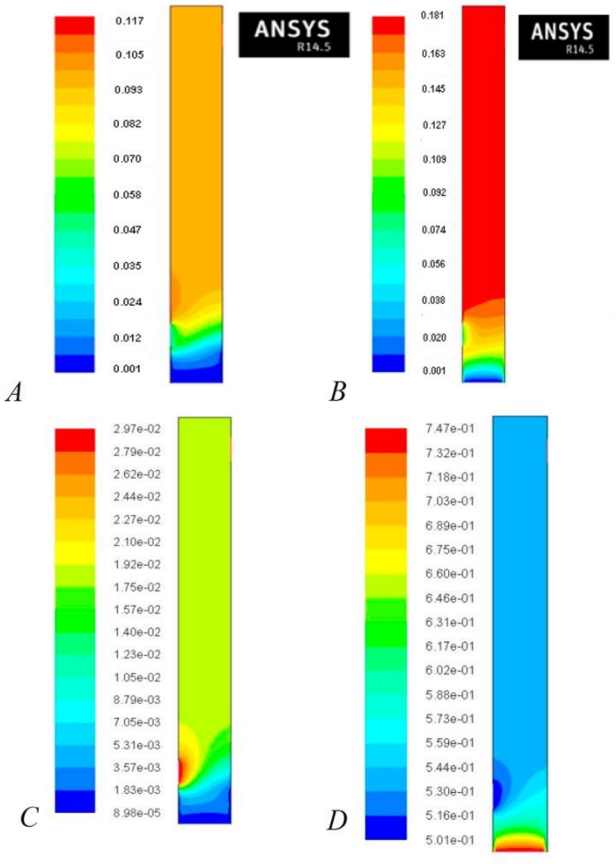

Figure 5. Countours of the (a) H_2, (b) CO_2, (c) CH_4, and (d) N_2 molar fractions in the gas mixture (run 1 for coffee husks).

The developed model was also applied to different operating conditions, namely, testing the effect of the gasification temperature and the steam-to-biomass ratio (SBR) on the syngas molar fractions. Figure 6 depicts the syngas molar fraction as a function of the gasification temperature. From Figure 6 it can be seen that the increase of the gasification temperature promotes the formation of a syngas with higher hydrogen and carbon monoxide content and consequently higher syngas NHV, as stated in the experimental data. Both hydrogen and carbon monoxide seem to increase up to asymptotic values. On the other hand, the CH_4 and CO_2 contents follow an opposite trend. CH_4 decreases as a function of the temperature because the methane reaction formation is exothermic. These results are in agreement with the literature.[28] According to Le Chatelier's principle, higher temperatures favor products in endothermic reactions. Therefore, the endothermic reaction in eq 15 was strengthened leading to an increase in the hydrogen content.

Figure 7 shows the syngas H_2/CO molar ratio as a function of the temperature. The main application for a syngas with high H_2/CO ratio is related to the fuel cell technology. In general, syngas generated from biomass tends to have a relatively low H_2/CO ratio (<1). It can be observed that vine-pruning and coffee husks residues show the higher H_2/CO ratios with values ranging approximately from 0.7 to 0.8. On the other hand, and due to the higher values of CO, forest residues show H_2/CO ratios nearer to 0.4 and approximately constant along the selected temperature range.

For domestic purposes, it is preferable to obtain a syngas with higher CH_4/H_2 ratios. Figure 8 depicts the syngas CH_4/H_2 molar ratio as a function of the temperature for the three studied biomasses. All the studied biomasses show a similar pattern with a decrease of the CH_4/H_2 molar ratio as the temperature increases. Once again, both coffee husks and vine-pruning residues show similar ratio values. The higher values are found for forest residues.

The carbon conversion defines the fraction of carbon from biomass converted to carbon in syngas components:

$$\text{carbon conversion} = \frac{12 \times M}{X_C \times m} \tag{33}$$

where M is the total molar flow of carbon in the syngas components, X_C is carbon fraction in the biomass (obtained from the ultimate analysis), and m is the biomass flow into the gasifier.

From Figure 9, it can be seen that higher carbon conversions are obtained by using forest residues as substrate, with a maximum value of 97.9% at 1073 K. Typical values in a gasification reactor vary between 70% and 90%. On the other hand, gasification using coffee husks only leads to carbon conversions up to 80%. From literature there are no clear trends of carbon conversion evolution as a function of the temperature and SBR.[29] Surprisingly, it was found that carbon

dx.doi.org/10.1021/ef500570t | Energy Fuels 2014, 28, 5766−5777

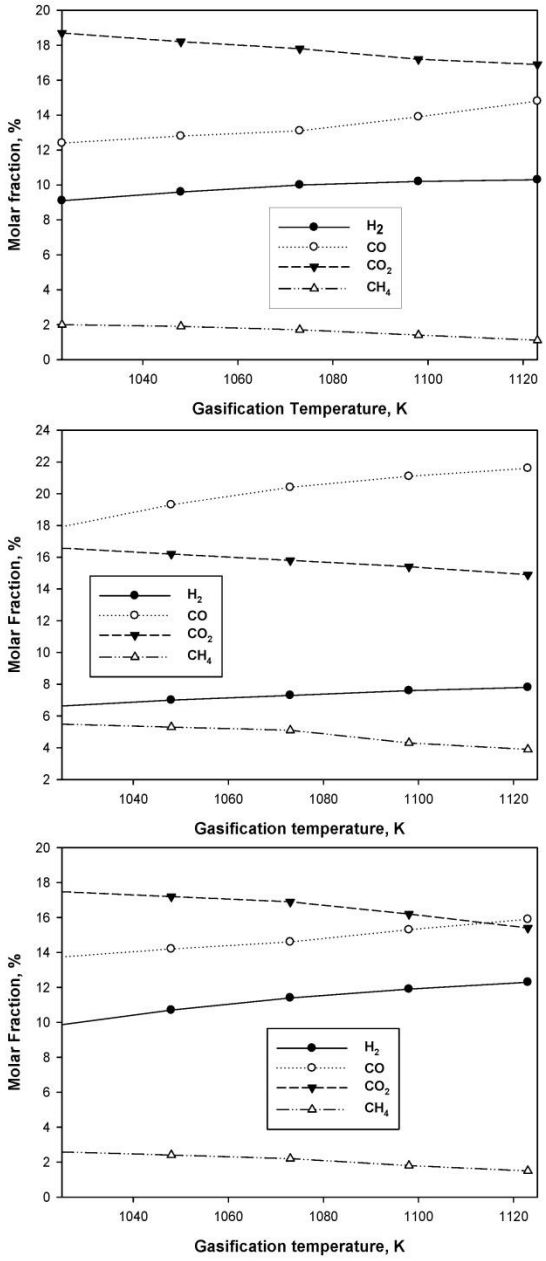

Figure 6. Syngas molar fractions as a function of the gasification temperature for (a) coffee husks, (b) forest residues, and (c) vine-pruning residues (operating conditions from run 1—coffee husks).

conversion is a very weak function of temperature. Indeed, data found in the literature are extremely scattered. From our numerical simulation, it was observed that the carbon conversion changes only slightly with the temperature, and depending on the substrate a slight increase or decrease is found. These results confirm the main conclusions drawn from the literature.

The CGE is defined as the percentage of the heating value of biomass converted into the heating value of the product gas (HHV). It can be computed as follows:

$$\mathrm{CGE} = \frac{\text{gas yield} \times \text{HHV of product gas}}{\text{HHV of fuel} + \text{heat addition}} \quad (34)$$

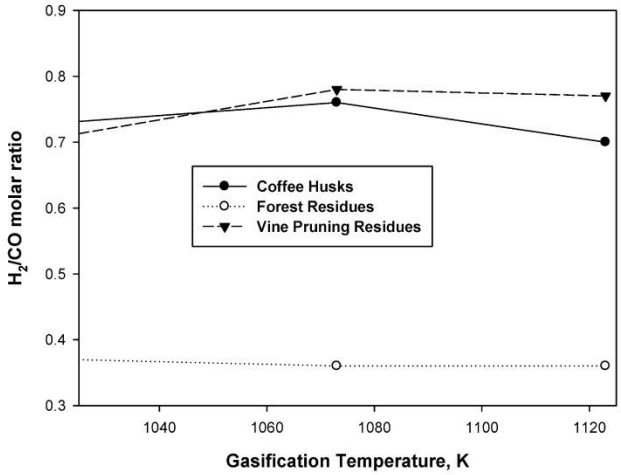

Figure 7. Syngas H_2/CO molar ratio as a function of the temperature (operating conditions from run 1—coffee husks).

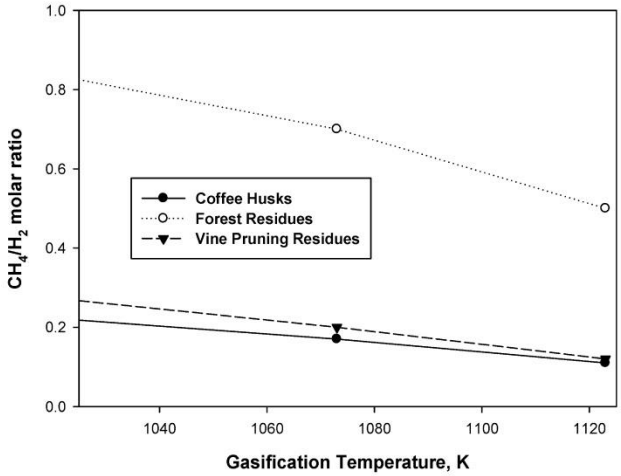

Figure 8. Syngas CH_4/H_2 molar ratio as a function of the temperature (operating conditions from run 1—coffee husks).

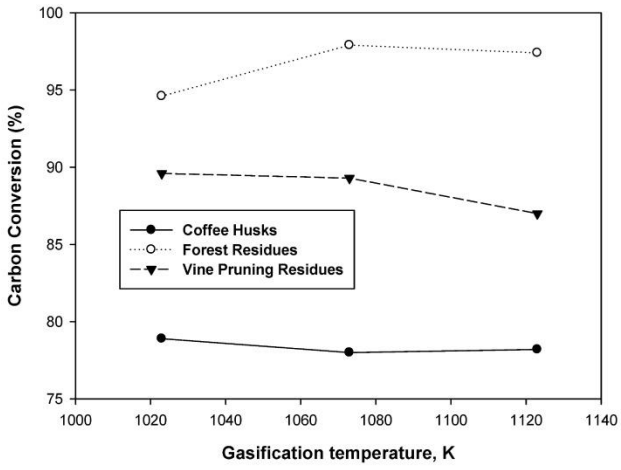

Figure 9. Carbon conversion as a function of the temperature (operating conditions from run 1—coffee husks).

From Figure 10, it can be verified that the CGE increases with the gasification temperature and that the vine-pruning residues show the higher efficiencies. High gas efficiencies are

dx.doi.org/10.1021/ef500570t | Energy Fuels 2014, 28, 5766—5777

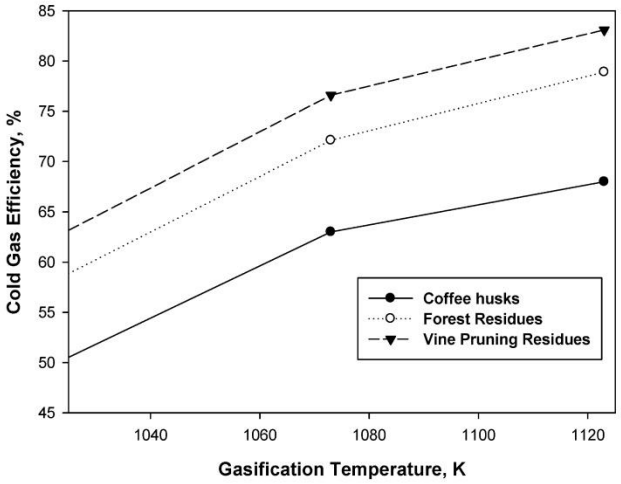

Figure 10. Cold gas efficiency as a function of the gasification temperature (operating conditions based in run 1—coffee husks).

suitable for integrated gasification combined cycles (IGCC) applications.

The SBR can be defined as the steam mass flow rate divided by the fuel mass flow rate (dry basis). The SBR was varied over a range of values from 0 to 1.5 by holding the other variables constant. Figure 11 shows the syngas molar fractions as a function of the SBR.

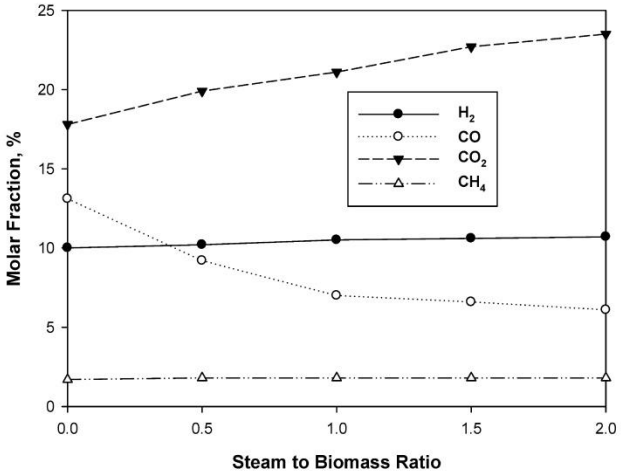

Figure 11. Syngas molar fractions as a function of the steam to biomass ratio for coffee husks (other operating conditions from run 1—coffee husks).

It can be observed that, with the increase of SBR, the content of hydrogen and CO_2 showed an increasing trend, while that from CO decreased, in agreement with literature.[28,30] At low values of SBR both carbon and methane are reformed leading to the formation of H_2 with its concentration increase. At SBRs higher than 1, the hydrogen increases slowly, and after 1.5 there is no increase effect. This implies that the surplus of steam is not reacting and that adding more steam is not efficient. Similar trends were observed for forest and vine-pruning residues. The effect of the SBR on the different indices for the syngas quality is depicted in Table 4.

The H_2/CO ratio in volatile matter is constant, so this ratio increase is related to the chemical reactions that are being developed along the gasification process and favor the H_2 generation and CO consumption (water/gas shift reaction).The H_2/CO ratio increases as a function of the SBR. Higher SBRs lead to the generation of H_2, and consequently this ratio increases. Considering the CH_4/H_2 ratio, it was verified that the SBR effect was very slight. The carbon conversion shows a minimum at middle SBR values and then starts again to increase slightly. Finally, the CGE decreases with the SBR.

The developed model predicts with reasonable accuracy the syngas composition at different operating conditions on a pilot scale, showing the effective trend of each one of the light gases. Other syngas quality indices can also be computed. This is a powerful tool for designing large-scale systems that may be dominant in a near future. The adopted simplifications are identified and will be the subject of analysis in future papers.

5. CONCLUSIONS

A multiphase 2-D model was developed under the Fluent framework to simulate the gasification of three large available Portuguese biomasses: coffee husks, forest residues, and vine-pruning residues. An Eulerian—Eulerian approach exchanging mass, energy, and momentum coupled with homogeneous and heterogeneous reactions was used. The model was calibrated and validated using experimental data and operating information from a pilot-scale fluidized bed gasifier. The experimental data obtained for large-scale systems are crucial to better understanding the gasification phenomenon and to better predict final syngas compositions. Numerical results are in good agreement with the experimental data obtained at three different operating conditions and for all the studied biomasses. The numerical model also predicted the effect of the gasification temperature and SBR on the final syngas composition, as well as the CGE, carbon conversion, and H_2/CO and CH_4/H_2 ratios.

Differences were observed mainly due to some simplifications that were included in the numerical simulation development; specifically, proximal analysis and reaction kinetic data were taken from the literature, light hydrocarbons and ash were not treated, and a 2-D geometry was adopted.

The different indices are very useful to select the best biomass as a function of the gasification application. Among the

Table 4. Steam-to-Biomass Ratio Effect on H_2/CO Ratio, CH_4/H_2 Ratio, Carbon Conversion, and Cold Gas Efficiency for All the Studied Biomasses

experimental conditions	forest residues			coffee husk			vine-pruning residues		
SBR	0	0.75	1.5	0	0.75	1.5	0	0.75	1.5
H_2/CO molar ratio	0.36	0.48	0.56	0.76	1.30	1.60	0.78	1.19	1.32
CH_4/H_2 molar ratio	0.70	0.70	0.71	0.17	0.17	0.18	0.19	0.20	0.21
carbon conversion (%)	97.9	92.2	92.9	78.0	72.2	74.1	89.3	83.9	84.3
cold gas efficiency (%)	72.1	67.2	65.1	63.0	52.9	50.0	76.6	67.2	65.1

dx.doi.org/10.1021/ef500570t | Energy Fuels 2014, 28, 5766—5777

three biomasses, it was concluded that coffee husks and vine-pruning residues show better H_2/CO ratios, which are especially suitable for fuel cell integration purposes. Considering domestic applications, a typical index is the CH_4/H_2 ratio where the highest values were obtained by using the forest residues. The highest CGEs were obtained by using the vine-pruning residues. The obtained data are crucial to describe scenarios concerning the potential use of biomass as a source of energy in Portugal.

AUTHOR INFORMATION

Corresponding Author

*E-mail: rouboa@utad.pt. Phone: 351 259350317. Address: Quinta de Prados, Apartado 1013,5001-801 Vila Real. Fax: +351 259 350 356.

Author Contributions

The manuscript was written through contributions of all authors. All authors have given approval to the final version of the manuscript.

Notes

The authors declare no competing financial interest.

ACKNOWLEDGMENTS

We would like to express our gratitude to the Portuguese Foundation for Science and Technology (FCT) for the support given to Grant No. SFRH/BPD/71686 and to Project PTDC/AAC-AMB/103119/2008 and ALTERCEXA-POCTEC Program.

NOMENCLATURE

A, B = calibration constants
$C_{1\varepsilon}$, $C_{2\varepsilon}$, $C_{3\varepsilon}$ = constants
C_p = specific heat capacity
D_0 = diffusion rate coefficient
e_{ss} = restitution coefficient
$g_{o,ss}$ = radial distribution function
G_k = generation of turbulence kinetic energy due to the mean velocity gradients
G_b = generation of turbulence kinetic energy due to buoyancy
h_{pq} = heat transfer coefficient between the fluid phase and the solid phase
k = thermal conductivity
M_c = molecular weight
$M_{w,i}$ = molecular weight of i component
p = gas pressure
$\vec{q}_q$ = heat flux
q^{th} = specific enthalpy
R = universal gas constant
R_c = reaction rate
S_k = user-defined source terms
S_q = source term due to chemical reactions
S_ε = user-defined source terms
T = temperature
U = mean velocity
v = instantaneous velocity
Y = mass fraction
Y_M = contribution of the fluctuating dilatation in compressible turbulence to the overall dissipation rate

Other Symbols

α = volume fraction
ρ = density
ϕ_{ls} = energy exchange between the fluid phase and the solid phase
$k_{\Theta a}$ = diffusion coefficient
$k_{\Theta a}\nabla(\Theta_s)$ = diffusion energy
$(-P_s\bar{I} + \bar{\tau}_s)$: $\nabla(\vec{v}_s)$ = generation of energy by the solid stress tensor
$\gamma_{\Theta a}$ = collisional dissipation of energy
τ = tensor stress
μ = viscosity
γ_c = stoichiometric coefficient

Subscripts

g = gas phase
s = solid phase
i = component

REFERENCES

(1) Ciferno, P.; Marano, J. *Benchmarking Biomass Gasification Technologies for Fuels, Chemicals and Hydrogen Production;* U.S. Department of Energy, National Energy Technology Laboratory, 2002. Available from: http://www.netl.doe.gov/technologies/coalpower/gasification/pubs/pdf/BMassGasFinal.pdf, last accessed 29th January, 2013.

(2) Jenkins, B.; Baxter, L.; Miles, T., Jr; Miles, T. Combustion properties of biomass. *Fuel Proc. Technol.* **1998**, *54*, 17−46.

(3) Ferreira, S.; Moreira, N.; Monteiro, E. Bioenergy overview for Portugal. *Biomass Bioenergy* **2009**, *33*, 1567−1576.

(4) Fiori, L.; Florio, L. Gasification and Combustion of Grape Marc: Comparison Among Different Scenarios. *Waste Biomass Valorization* **2010**, *1*, 191.

(5) Kırtay, E. Recent advances in production of hydrogen from biomass. *Energy Convers. Manage.* **2011**, *52*, 1778−89.

(6) Spiegel, C. *Designing & Building Fuel Cells;* McGraw-Hill; 2007.

(7) *The hydrogen economy: a non-technical review;* United Nations Environment Programme, 2006.

(8) Rosen, M. A. Thermodynamic investigation of hydrogen production by steam−methane reforming. *Int. J. Hydrogen Energy* **1999**, *16*, 207−17.

(9) Levin, D.; Chahine, R. Challenges for renewable hydrogen production from biomass. *Int. J. Hydrogen Energy* **2010**, *35*, 4962−69.

(10) Ahmed, T.; Ahmad, M.; Yusup, S.; Inayat, A.; Khan, Z. Mathematical and computational approaches for design of biomass gasification for hydrogen production: A review. *Renewable Sustainable Energy Rev.* **2012**, *16*, 2304−15.

(11) Xie, J.; Zhong, W.; Jin, B.; Shao, Y.; Liu, H. Simulation on gasification of forestry residues in fluidized beds by Eulerian−Lagrangian approach. *Bioresour. Technol.* **2012**, *121*, 36−46.

(12) Xue, Q.; Fox, R. Multi-fluid CFD modeling of biomass gasification in polydisperse fluidized-bed gasifiers. *Powder Technol.* **2014**, *254*, 187−198.

(13) Xue, Q.; Dalluge, D.; Heindel, T.; Fox, R.; Brown, R. Experimental validation and CFD modeling study of biomass fast pyrolysis in fluidized-bed reactors. *Fuel* **2012**, *97*, 757−769.

(14) Gungor, A.; Yildirim, U. Two dimensional numerical computation of a circulating fluidized bed biomass gasifier. *Comput. Chem. Eng.* **2013**, *48*, 234−250.

(15) Knowlton, T.; Karri, R.; Issangya, A. Scale-up of fluidized-bed hydrodynamics. *Powder Technol.* **2005**, *150*, 72−77.

(16) Eaton, M.; Smoot, D.; Hill, C.; Eatough, N. Components, formulations, solutions, evaluation, and application of comprehensive combustion models. *Prog. Energy Combust. Sci.* **1999**, *25*, 387−436.

(17) Bridgewater V.; Evans D. *An assessment of thermochemical conversion systems for processing biomass and refuse;* Energy technology support unit (ETSU) on behalf of the Department of Trade, ETSU B/T1/00207/REP; 1993.

(18) Wilson, L.; John, G.; Mhilu, C.; Yang, W.; Blasiak, W. Coffee husks gasification using high temperature air/steam agent. *Fuel Process. Technol.* **2010**, *91*, 1330−37.

(19) Launder, B.; Spalding, B. *Lectures in Mathematical Models of Turbulence;* Academic Press: London, England, 1972.
(20) Syamlal, M.; Rogers, T. J. *MFIX documentation: Vol. 1. Theory Guide;* National Technical Information Service: Springfield, VA, 1993. DOE/METC-9411004, NTIS/DE9400087.
(21) Lun, C.; Savage, S. B.; Jeffrey, D.; Chepurniy, N. Kinetic theories for granular flow: Inelastic particles in couette flow and slightly inelastic particles in a general flow field. *J. Fluid Mech.* **1984**, *140*, 223−256.
(22) Badzioch, S.; Hawsley, P. G. W. Kinetics of Thermal Decomposition of Pulverized Coal Particles. *Ind. Eng. Chem. Process Des. Dev.* **1970**, *4*, 521−30.
(23) Yu, L.; Lu, J.; Zhang, X.; Zhang, S. Numerical simulation of the bubbling fluidized bed coal gasification by the kinetic theory of granular flow. *Fuel* **2007**, *86*, 722−34.
(24) Baum, M.; Street, P. Predicting the behavior of coal particles. *Combust. Sci. Technol.* **1971**, *3*, 231−43.
(25) Field, M. A. Rate of combustion of size-graded fractions of char from a low rank coal between 1200K-2000K. *Combust. Flame* **1969**, *13*, 237−252.
(26) Gelderbloom, S. J.; Gidaspow, D.; Lyczkowski, R. W. CFD simulations of bubbling/collapsing fluidized beds for three geldart groups. *AIChE J.* **2003**, *49*, 844−58.
(27) Miao, Q.; Zhu, J.; Barghi, S.; Wu, C.; Yin, X.; Zhou, Z. Modeling Biomass gasification in Circulating Fluidized Beds: Model Sensitivity analysis. *Int. J. Energy Power Eng.* **2013**, *2*, 57−63.
(28) Turn, S.; Kinoshita, C.; Zhang, Z.; Ishimura, D.; Zhou, J. An experimental investigation of hydrogen production from biomass gasification. *Int. J. Hydrogen Energy* **1998**, *23*, 641−48.
(29) Timmer K. Carbon conversion during bubbling fluidized bed gasification of biomass. Ph.D. Thesis, Iowa University, 2008.
(30) Silva, V.; Rouboa, A. Using a two-stage equilibrium model to simulate oxygen air enriched gasification of pine biomass residues. *Fuel Process. Technol.* **2013**, *109*, 111−17.